

GAC-MAC
WINNIPEG
2013



AT THE
CENTRE OF
THE CONTINENT

AU
CENTRE DU
CONTINENT



Pirate Island - Paint Lake by Nancy-lynn Hughes

PROGRAM • PROGRAMME
with abstracts
volume 36

GAC[®]-MAC
AGC[®]-AMC

Joint Annual Meeting
Congrès annuel conjoint





Discover the potential
in one of Canada's most unexplored
Archean greenstone gold belts.

www.sangold.ca



TSX: SGR | OTCQX: SGRCF

Located in Eastern Manitoba

Welcome! Bienvenue!

**GAC-MAC
WINNIPEG
2013**



**AT THE
CENTRE OF
THE CONTINENT**

**AU
CENTRE DU
CONTINENT**

TABLE OF CONTENTS

Thank you to our Sponsors	2
Welcome to Winnipeg 2013	3
Local Organizing Committee	4
Delegate Information	5
Technical Information for Presenters	7
Convention Centre Floor Plan	8
Meeting at a Glance	9
Technical Program at a Glance	10
Plenary and Special Addresses	12
Special Events	13
Award Events	16
Business Meetings	18
Exhibitors	19
Exhibit Floor Plan	21
Field Trips	22
Short Courses	24
Outreach - Earth Science Awareness	25
Wednesday Technical Program	28
Wednesday Poster Session	36
Thursday Technical Program	39
Thursday Poster Sessions	47
Friday Technical Program	51
Abstracts	59
Author Index	205

TABLE DES MATIÈRES

Merci aux commanditaires	2
Bienvenue à Winnipeg 2013	3
Comité organisateur local	4
Renseignements généraux	5
Avis aux présentateurs	7
Plan d'étage du Centre des congrès	8
Aperçu du congrès	9
Programme en un coup d'oeil	10
Interventions plénières et particulières	12
Activités spéciales	13
Remise des prix	16
Séances de travail	18
Exposants	19
Plan de l'étage des expositions	21
Excursions	22
Cours intensifs	24
Sensibilisation aux sciences de la Terre	25
Programme du mercredi	28
Session d'affiches de mercredi	36
Programme du jeudi	39
Session d'affiches de jeudi	47
Programme du vendredi	51
Abstracts	59
Index des auteurs	205

Thank you to our Sponsors / Merci aux commanditaires

PLATINUM / PLATINE (\$15,000+)

HUDBAY

GOLD / OR (\$10,000+)

GOLDCORP
RED LAKE GOLD MINES

SAN GOLD



SILVER / ARGENT (\$5,000+)



Natural Resources
Canada

Ressources naturelles
Canada



UNIVERSITY
OF MANITOBA

Clayton H. Riddell Faculty of
Environment, Earth, and Resources

BRONZE (\$2,000+)

APEGM



**RED BEDS
RESOURCES LIMITED**

VALE



**NORTHERNSHIELD
RESOURCES INC.**

IRON / FER (\$1,000+)

Claude Resources Inc.
Discovering. Developing. Delivering.

Franklin Geosciences



GEOSCIENTISTS
GÉOSCIENTIFIQUES CANADA

**Manitoba Prospectors and
Developers Association**

**VMS
VENTURES INC.**

SUPPORTER / PARTISAN (<\$1,000)

amec

**Thank You to Supporters of the Winnipeg 2013 Organizing Committee
Merci aux bienfaiteurs du comité organisateur**



**THE MANITOBA
MUSEUM**
encouraging Discovery



UNIVERSITY
OF MANITOBA

Department of Geological Sciences



**THE UNIVERSITY OF
WINNIPEG**

Welcome to Winnipeg 2013 / Bienvenue à Winnipeg 2013

On behalf of the Winnipeg 2013 Organizing Committee, we welcome you to the Prairies and to our city for the Joint Annual Meeting of the Geological Association of Canada and the Mineralogical Association of Canada. Winnipeg 2013 is being held in the ancestral gathering place for many First Nations and Métis at the confluence of the Red and Assiniboine Rivers. However, our chosen motto, “At the Centre of the Continent”, refers not only to the geographic location of Winnipeg at the historic crossroads and near the longitudinal centre of North America, but also to the convergence of the geoscience community to share our latest research findings, to discuss topical issues, and to raise awareness of these issues among the public. Thanks to the consolidated efforts of our Committee and especially the Technical Program team, the Meeting offers a wide spectrum of sessions, symposia and lectures spanning the gamut of Earth science research and teaching in Canada and internationally. Beyond the three days of the Meeting, our program includes two short courses and seven field trips that will explore a 3-billion-year cross-section of Manitoba geology, from Precambrian basement rocks to Holocene sediments, and provide a fresh perspective on the diverse natural resources found in the Province. Our outreach activities were designed to raise awareness of the Earth processes and resources among teachers, students, science enthusiasts and the public at large. These activities include a teachers’ workshop and field trip, a First Nations’ geoscience forum, and a public lecture on the history of Lake Agassiz and its lasting effects on the Prairies.

Winnipeg is renowned for its cosmopolitan arts, culture and cuisine, and is once again the home of the Winnipeg Jets hockey team. The Manitoba Museum, Assiniboine Park, Leo Mol Sculpture Garden and The Forks National Historic Site are just a few of the city’s numerous cultural attractions. If you are arriving early or staying an extra day, consider going on a bison safari at FortWhyte Alive, or catching a glimpse of French Impressionists at The Winnipeg Art Gallery. Or just kick back after a long day of talks in the blooming midst of the English Gardens in Assiniboine Park! Also, we are delighted to offer you social events that reflect the life and hospitality of the Prairies. Join us on Thursday for the Prairie Roundup, featuring a scenic railway ride and a country-style BBQ banquet, and head down to The Forks on Friday for the Wind-up Evening and, perhaps, some souvenir shopping at the local Market and Johnston Terminal.

We hope that our program and events will keep you busy and entertained for the entire duration of the Meeting, and look forward to helping you make it a fulfilling cultural experience. Thank you for joining us at Winnipeg 2013.

Nancy Chow, Chair
Anton Chakhmouradian, Co-Chair

Au nom du comité organisateur, nous vous souhaitons la bienvenue dans les Prairies et, particulièrement, chez nous à Winnipeg, à l’occasion du congrès annuel conjoint de l’Association géologique du Canada et de l’Association minéralogique du Canada, tenu au confluent des rivières Rouge et Assiniboine, lieu de rassemblement ancestral des Premières nations et des Métis. Pourtant, la devise (Au centre du continent) renvoie non seulement à la position géographique de Winnipeg, situé au carrefour historique près du centre longitudinal de l’Amérique du Nord, mais aussi à la convergence des membres de la collectivité des sciences de la Terre venus communiquer les conclusions des recherches les plus récentes, discuter de questions particulières et en sensibiliser le public. Grâce à l’effort collectif du comité, particulièrement de l’équipe du Programme technique, une variété de séances, de symposiums et de cours au sujet de l’ensemble des recherches et de l’enseignement en matière de géosciences au Canada et à l’échelle internationale vous est offerte. Outre les trois journées de congrès, le programme prévoit deux cours intensifs et sept excursions pour explorer la géologie du Manitoba en coupe transversale de trois milliards d’années, du socle rocheux précambrien aux sédiments holocènes, et poser un regard neuf sur les ressources naturelles provinciales. Nos activités de promotion, conçues pour sensibiliser l’enseignant, l’étudiant, le mord du des sciences et le public en général au sujet des ressources et des méthodes scientifiques, comprennent un atelier et une excursion pédagogique destinés aux enseignants, un forum des Premières nations sur les sciences de la Terre, et une conférence ouverte au public sur l’histoire du lac Agassiz et ses effets durables sur les Prairies.

Winnipeg, synonyme d’arts, de culture et de cuisine cosmopolites, est aussi de nouveau le domicile de l’équipe de hockey des Jets. Le Musée du Manitoba, le parc Assiniboine, le jardin de sculptures Leo Mol et le lieu historique national de La Fourche sont quelques uns de ses nombreux attraits. Si vous arrivez tôt ou que vous restiez un jour de plus, allez observer les bisons au centre FortWhyte Alive ou jeter un coup d’œil sur l’œuvre d’impressionnistes français à la Galerie des beaux-arts de Winnipeg. Ou bien, après une grande journée de conférences, détendez-vous parmi les inflorescences des Jardins anglais du parc Assiniboine. Quant aux activités sociales typiques de la vie et de l’hospitalité des Prairies, voici : jeudi, montez à bord d’un train d’époque à destination d’un BBQ de campagne; vendredi, amenez-vous à la Fourche où aura lieu une soirée décontractée de fin de congrès, une occasion aussi de magasiner au terminus Johnston et au marché.

Nous espérons que le programmes et les activités vous tiendront occupés et vous divertiront. Nous serions heureux que le congrès ait été pour vous une expérience culturelle des plus enrichissantes. Merci d’avoir accepté notre invitation.

Nancy Chow, présidente
Anton Chakhmouradian, co-président

Local Organizing Committee

Comité organisateur local



General Chair/Présidente	Nancy Chow	University of Manitoba
Co-Chair/Co-président	Anton Chakhmouradian	University of Manitoba
Accommodations/Hébergement	Alfredo Camacho	University of Manitoba
Exhibits/Expositions	Bill Buhay	University of Winnipeg
Field Trips/Excursions	Scott Anderson	Manitoba Geological Survey
Finance	Norman Halden	University of Manitoba
Outreach Program/Sensibilisation	Jeff Young	University of Manitoba
Publications	Andrew Frederiksen	University of Manitoba
Publicity/Publicité	Graham Young	The Manitoba Museum
Registration/Inscription	Elena Sokolova	University of Manitoba
Short Courses/Cours intensifs	Ian Ferguson	University of Manitoba
Special Events/Activités spéciales	Karen Ferreira	University of Manitoba
Sponsorship	Chris Beaumont-Smith Kelly Gilmore	Manitoba Geological Survey Consultant
Technical Program/ Programme technique	Christian Böhm Mostafa Fayek	Manitoba Geological Survey University of Manitoba
Technical Services/Services techniques	Neil Ball	University of Manitoba
Transportation/Transport	Chris Couëslan	Manitoba Geological Survey



Delegate Information

Renseignements généraux

You will find the Registration and Help Desks on the main floor of the Convention Centre, in Meeting Room MR5 (see map p. 8), where tourism information will be available.

Parking

Parking will be available in the Convention Centre parkade for a cost of \$16.00 per day (4-12 hours). Additional parking may also be available in nearby surface parking lots and parkades, as well as at metered on-street locations.

Registration

The Registration Desk is located in MR5 on the main floor of the Convention Centre.

Hours: Tuesday, May 21: 1:00 – 8:00 p.m.

Wednesday, May 22: 7:00 a.m. – 5:00 p.m.

Thursday, May 23: 8:00 a.m. – 5:00 p.m.

Friday, May 24: 8:00 a.m. – 1:00 p.m.

Speaker Ready Room

Delegates scheduled to give an oral presentation have access to a small number of computers in the Speaker Ready Room, located in the VIP Salon on the main floor of the Convention Centre, to ensure their presentation displays correctly on a Windows PC. **Delegates must load their talk in their session 30 minutes prior to the start of the session.**

Internet Café

The Internet Café is located in the VIP Salon on the main floor of the Convention Centre.

Presentation Theatre

No food or drink is permitted in the Presentation Theatre on the second floor of the Convention Centre.

Food and Refreshments

Coffee will be available daily in the Exhibits Hall on the second floor of the Convention Centre, starting at 9:00 a.m. and during the morning refreshment breaks.

A cash bar will be available in the Exhibits Hall during the Icebreaker Reception on Tuesday evening (7:00-10:00 p.m.) and the poster sessions on Wednesday and Thursday afternoon (4:00-6:00 p.m.).

Lunch can be purchased at the Centre Place Café on the second floor of the Convention Centre or from the many nearby restaurants and food outlets.

Le bureau d'inscription et le bureau d'aide sont situés au local MR5 de l'étage principal du Centre des congrès, où il y a aussi de l'information touristique (voir le Plan d'étage, p. 8).

Stationnement

Les frais de stationnement dans le garage du Centre des congrès sont de 16 \$ par jour (pour 4 à 12 heures). Il existe aussi des parcs de stationnement et des garages aériens à proximité du Centre, ainsi que des places dans les rues, à tarif à la durée.

Inscription

Le bureau d'inscription est situé au local MR5 de l'étage principal du Centre des congrès.

Heures d'accueil : le mardi 21 mai de 13 h à 20 h;

le mercredi 22 mai de 7 h à 17 h;

le jeudi 23 mai de 8 h à 17 h;

le vendredi 24 mai de 8 h à 13 h.

Local des présentateurs

Les congressistes prévoyant donner une présentation orale ont accès à un petit nombre d'ordinateurs dans le Local des présentateurs du Salon VIP, à l'étage principal du Centre des congrès pour s'assurer que leurs documents s'affichent correctement dans l'environnement Windows. **Les présentateurs doivent charger leur matériel de présentation 30 minutes avant le début de la séance.**

Café Internet

Le Café Internet est situé dans le Salon VIP, à l'étage principal.

Salle des conférences

Aucune consommation de nourriture ou de boisson n'est permise dans la salle des conférences située au deuxième étage du Centre des congrès.

Rafrâichissements

Des rafraîchissements seront servis dans le salon des expositions du deuxième étage à partir de 9 h et pendant les pauses du matin.

Il y aura un bar payant dans le même salon le mardi entre 19 h et 22 h, dans le cadre de la séance d'accueil, et les mercredi et jeudi entre 16 h et 18 h, dans le cadre des séances de communications affichées.

Le dîner peut être pris au Centre Place Café, situé au deuxième étage du Centre des congrès, ou dans les nombreux restaurants et comptoirs à proximité.

Delegate Information

Renseignements généraux



Office

The Local Organizing Committee will have an office located in the Executive Conference Centre, next to the lobby on the main floor of the Convention Centre.

Press Room

VIP Salon on the main floor of the Convention Centre.

Hours: Wed-Thurs, 7:00 a.m. – 6:00 p.m.

Fri, 7:00 a.m. – 2:00 p.m.

Liability

The registration fees do not include insurance for participants. Neither the Winnipeg Convention Centre, nor the Local Organizing Committee, is responsible for any loss, injury or damage to persons or belongings, however caused.

Bureau du comité organisateur

Le comité organisateur occupe un bureau dans le Centre exécutif, situé à côté du vestibule, sur l'étage principal du Centre des congrès.

Salle de presse

Salon VIP, étage principal du Centre des congrès.

Heures d'accueil : les mercredi et jeudi de 7 h à 18 h;

le vendredi de 7 h à 14 h.

Dispense de responsabilité

Le paiement des droits d'inscription ne procure pas d'assurance. Le Centre des congrès de Winnipeg et le Comité organisateur du congrès annuel conjoint se dégagent de la responsabilité d'éventuels préjudices à la personne, pertes de biens ou dommages, peu importe la cause.



Technical Information for Presenters

Avis aux présentateurs

Oral Presentation Guidelines

20 minutes have been allotted for each paper; ~15 minutes for the presentation and ~5 minutes for questions. Please stay within these limits.

Each presentation room is equipped with a Microsoft Windows PC (running Windows 7), and the presentations will be displayed using Microsoft PowerPoint 2010. For delegates who have created their presentations on a different operating system (e.g. Mac OS), we request that you make sure that your presentation displays correctly on a Windows 7 system. We also recommend that presenters visit the speaker ready room, located in the VIP Salon on the main floor of the Convention Centre, to verify that their presentation works correctly.

Delegates scheduled to give an oral presentation are required to load their PowerPoint file in the room where their presentation is scheduled, and on the day they are to speak, a minimum of 30 minutes before the session is to begin. There will be an assistant in each presentation room available to help with this task. It is the responsibility of each presenter to bring their talk on either a memory key (preferred) or CD/DVD, and to make sure that their talk is uploaded in good time before the start of the session. To ensure the sessions run smoothly and on time, presentations will not be uploaded during sessions, nor will it be possible for personal laptops to be attached to the projecting equipment.

Poster Session Guidelines

Each presenter will be provided with a poster board with a display area 1.2 metres (4 ft) high by 1.8 metres (6 ft) wide, and a choice of pushpins or Velcro to affix their posters to the poster boards.

Poster board assignments will be on display at the Registration Desk and in the poster display area in 2FGH on the second floor of the Convention Centre. Presenters are encouraged to hang their posters between 1:00 and 8:00 p.m. on Tuesday, May 21st, or before 2:00 p.m. on Wednesday, May 22nd. Although posters will remain up for the duration of the meeting, poster sessions are from 4:00 to 6:00 p.m. on Wednesday, May 22nd and Thursday, May 23rd, and poster presenters are expected to be at their posters throughout this two-hour period on their allotted day. Official designated time for removal of posters is Friday, May 24th, 4:00-6:00 p.m.

Directives concernant les présentations orales

La durée de chaque communication est fixée à 20 minutes, soit plus ou moins 15 minutes consacrées à la présentation et 5 minutes consacrées aux questions. Veuillez respecter ces limites.

Chaque salle de présentation est munie d'un ordinateur à système d'exploitation Windows 7 de Microsoft avec PowerPoint 2010. Les présentateurs ayant produit leur communication au moyen d'un autre système, p. ex., sur Mac OS, devraient s'assurer de la compatibilité en matière d'affichage. Il est recommandé qu'ils se présentent au local de vérification du fonctionnement de leur médium de présentation, situé dans le salon VIP (rez-de-chaussée du Centre des congrès).

Les présentateurs doivent mettre leur fichier PowerPoint (clé USB, préférablement, ou CD-DVD) à la disposition du préposé de la salle de présentation au moins 30 minutes avant la séance, le jour de la prestation. Il incombe à chaque présentateur de veiller à ce que le contenu de sa présentation soit installé en temps opportun dans le système avant le début de la séance. Pour le bon déroulement de la séance et pour respecter l'horaire, aucune installation ne se fera pendant la présentation. Il ne sera pas possible non plus de faire usage d'un portable personnel joint au système de projection.

Directives concernant les présentations par affiches

Un tableau d'affichage d'une superficie d'étagage de 1,2 mètre (4 pi) de haut, sur 1,8 mètre (6 pi) de large, ainsi qu'un assortiment de punaises ou de velcro pour le fixage d'affiches, seront mis à la disposition de chaque présentateur.

L'assignation du lieu de présentation est affichée au bureau d'inscription ainsi qu'au deuxième étage du Centre des congrès, dans la salle prévue pour les présentations (2FGH). Les présentateurs devraient installer leur tableau entre 13 h et 20 h le mardi 21 mai ou avant 14 h le mercredi 22 mai. Les séances de présentations se déroulent le mercredi 22 mai et le jeudi 23 mai entre 16 h et 18 h. Les présentateurs devraient être en poste pendant toute la séance. Le démontage des tableaux est prévu pour le vendredi 24 mai entre 16 h et 18 h.

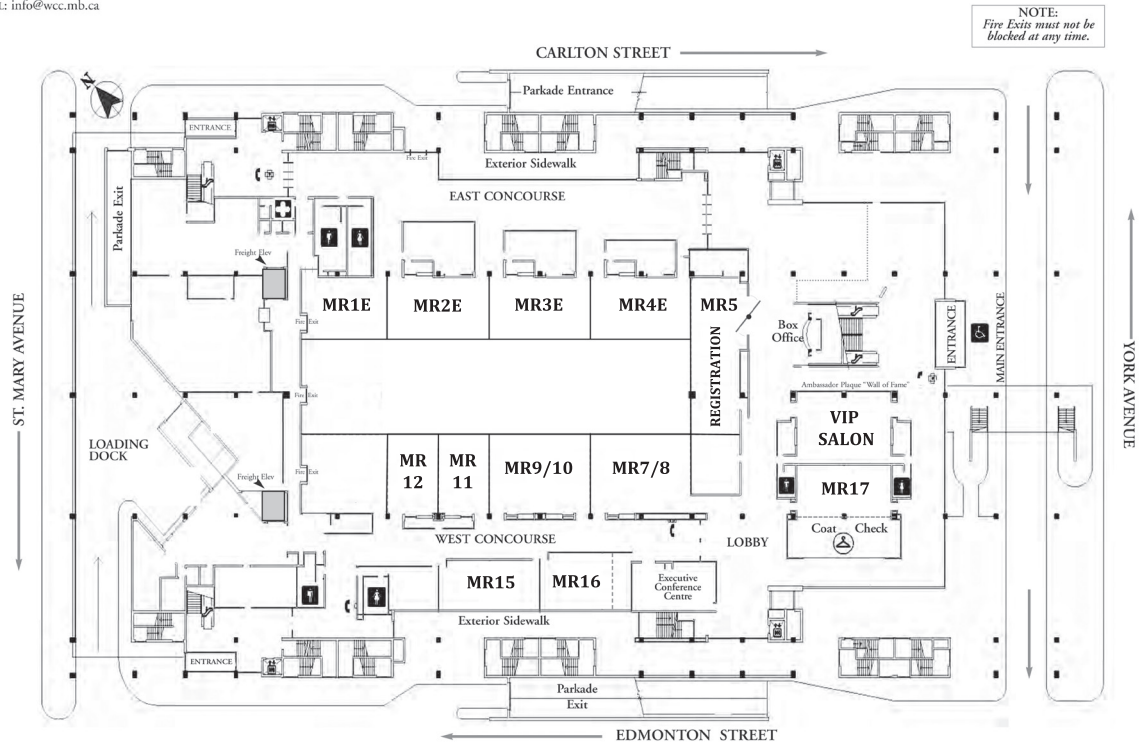
Convention Centre Floor Plan / Plan d'étage du Centre des congrès



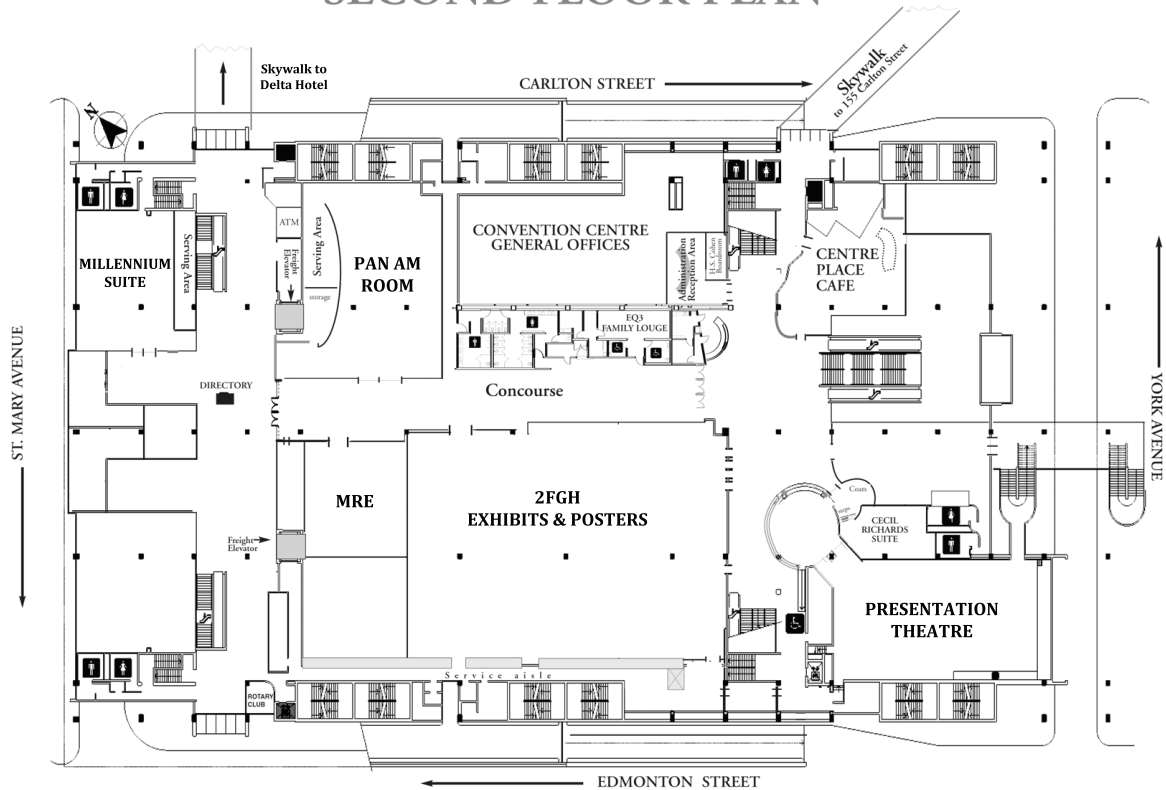
**WINNIPEG
CONVENTION
CENTRE**

375 YORK AVENUE, WINNIPEG, MANITOBA, CANADA R3C 3J3
PHONE: (204) 956-1720 FAX: (204) 943-0310
TOLLFREE: 1-800-565-7776 EMAIL: info@wcc.mb.ca
www.wcc.mb.ca

GROUND FLOOR PLAN



SECOND FLOOR PLAN





Meeting at at Glance

Aperçu du congrès

	Monday, May 20	Tuesday, May 21	Wednesday, May 22	Thursday, May 23	Friday, May 24	
7:00						7:00
7:20						7:20
7:40						7:40
8:00			Onsite Registration MRS (7am-5pm) Speaker Ready / Internet Cafe VIP Salon (7:00am-6:00pm)	Onsite Registration MRS (8am-5pm) Speaker Ready / Internet Cafe VIP Salon (7:00am-6:00pm)	Onsite Registration MRS (8am-1pm) Speaker Ready / Internet Cafe VIP Salon (7:00am-2:00pm)	8:00
8:20						8:20
8:40						8:40
9:00						9:00
9:20						9:20
9:40						9:40
10:00						10:00
10:20						10:20
10:40						10:40
11:00						11:00
11:20						11:20
11:40						11:40
12:00						12:00
12:20						12:20
12:40						12:40
13:00						13:00
13:20						13:20
13:40						13:40
14:00						14:00
14:20						14:20
14:40						14:40
15:00						15:00
15:20						15:20
15:40						15:40
16:00						16:00
16:20						16:20
16:40						16:40
17:00						17:00
17:20						17:20
17:40						17:40
18:00						18:00
18:20						18:20
18:40						18:40
19:00						19:00
19:20						19:20
19:40						19:40
20:00						20:00
20:20						20:20
20:40						20:40
21:00						21:00
21:20						21:20
21:40						21:40
22:00						22:00
22:20						22:20
22:40						22:40
23:00						23:00

Technical Program at a Glance / Programme en un coup d'oeil

		Presentation Theatre	MR2E	MR3E	MR4E	MR7/8	MR9/10
W E D N E S D A Y	8:20	SS5 Uranium: Cradle to Grave	SS7 Rare Metals and VMS	SY1 Earth Materials (Hawthorne)	SS2 Assembly of North America	SS6 REEs in Melts	SS9 Ni-Cu-PGE-Cr
	10:00	Refreshment Break / Pause-santé					
	10:20	SS5	SS7	SY1	SS2	SS6	SS9
	10:40	Uranium: Cradle to Grave	Rare Metals and VMS	Earth Materials (Hawthorne)	Assembly of North America	REEs in Melts	Ni-Cu-PGE-Cr
	11:00						
	11:20	GAC® PRESIDENTIAL ADDRESS: <i>Trend Spotting in the Geosciences</i> Peter Bobrowsky, Geological Survey of Canada (President of GAC®), Presentation Theatre, Winnipeg Convention Centre, 11:20 am - 12:00 pm					
	12:00	GAC LUNCHEON - Pan-Am Room, Winnipeg Convention Centre, 12:00 - 1:40 pm / STUDENT NETWORKING LUNCHEON - Meeting Room 1E, Winnipeg Convention Centre, 12:00 - 1:40 pm					
	13:40	SS5 cont.	SS7 cont.	SY1 cont.	SS2 cont.	SS6 cont.	SS9 cont.
	14:40	Uranium: Cradle to Grave	Rare Metals and VMS	Earth Materials (Hawthorne)	Assembly of North America	REEs in Melts	Ni-Cu-PGE-Cr
	15:00						
2 2 M A Y	15:20						
	15:40						
		POSTERS (Exhibits Hall - 4-6 pm): SY1, SS2, SS5, SS6, SS7, SS9, SS16, GS2, GS6, GS7					
	19:00	GEOSCIENCE IN OUR LIVES PUBLIC LECTURE: <i>The drowning and draining of Manitoba: from Lake Agassiz to today</i> James T. Teller, Department of Geological Sciences, University of Manitoba Presentation Theatre, Winnipeg Convention Centre, 7:00 pm					
		Presentation Theatre	MR2E	MR3E	MR4E	MR7/8	MR9/10
	8:20	SY1 cont. Earth Materials (Hawthorne)	SY2 Granitic Pegmatites (Černý)	SS5 cont. Uranium: Cradle to Grave	SS3 Superior Province	SY3 & Intro Phanerozoic Seas (Ludvigsen)	SS9 cont. Ni-Cu-PGE-Cr
	9:40						
	10:00	Refreshment Break / Pause-santé					
	10:20	SY1 cont. Earth Materials (Hawthorne)	SY2 Granitic Pegmatites (Černý)	SS5 cont. Uranium: Cradle to Grave	SS3 Superior Province	SY3 Phanerozoic Seas (Ludvigsen)	SS8 Layered Mafic Int.
	11:00						
2 3 M A Y	11:20	PLENARY ADDRESS: <i>The Origin of Laurentia</i> Paul F. Hoffman, Harvard University & University of Victoria Presentation Theatre, Winnipeg Convention Centre, 11:20 - 12:00 pm					
	12:00	MAC LUNCHEON - Pan-Am Room, Winnipeg Convention Centre, 12:00 - 1:40 pm					
	13:40	SY1 cont. Earth Materials (Hawthorne)	SY2 cont. Granitic Pegmatites (Černý)	SS5 cont. Uranium: Cradle to Grave	SS3 cont. Superior Province	SY3 cont. Phanerozoic Seas (Ludvigsen)	SS8 cont. Layered Mafic Intrusions
	15:00						
	15:20						
	15:40						
		POSTERS (Exhibits Hall - 4-6 pm): SY2, SS1, SS3, SS4, SS8, SS11, SS12, SS13, SS14, SS18, SS23, GS1, GS3, GS4, GS5					
	17:30	PRAIRIE ROUNDUP: <i>Rural Train Ride and BBQ Dinner</i> at the Hitch 'n Post Ranch, 5:30 pm					
		Present. Theatre	MR2E	MR3E	MR4E	MR7/8	MR9/10
	8:20	SY4 Stirring the Pot (Hoffman)	SY2 cont. Granitic Pegmatites (Černý)	SS5 cont. Uranium: Cradle to Grave	SS3 cont. Superior Province	SS4 Diamonds	SS23 IOCG and Porphyry
F R I D A Y	9:20						
	9:40						
	10:00	Refreshment Break / Pause-santé					
	10:20	SY4 Stirring the Pot (Hoffman)	SS1 Geoscience, Northern Frontiers	SS20 Research & Environmental Decisions	SS3 cont. Superior Province	SS4 Diamonds	SS23 IOCG and Porphyry
	11:00						
	11:20	PLENARY ADDRESS: <i>The Science and the Discovery of Volcanogenic Massive Sulphide Deposits</i> Harold Gibson, Laurentian University Presentation Theatre, Winnipeg Convention Centre, 11:20 am - 12:00 pm					
	12:00	MDD LUNCHEON - Pan-Am Room, Winnipeg Convention Centre, 12:00 - 1:40 pm					
	13:40	SY4 cont.	SS1 cont.	SS20 cont.		SS4 cont.	SS23 cont.
	14:40	Stirring the Pot (Hoffman)	Geoscience, Northern Frontiers	Research & Environmental Decisions		Diamonds	IOCG and Porphyry
	15:00						
2 4 M A Y	15:20						
	15:40						

Technical Program at a Glance / Programme en un coup d'oeil

	MR11	MR12	MR15	MR16		Exhibits Hall	
8:20		GS2 Petrology & Volcanology	SS16 Impact Cratering	GS6 Quaternary Geology			
10:00	Refreshment Break / Pause-santé						
10:20		GS2 Petrology & Volcanology	SS16 ...	GS6 ...			
10:40							
11:00							
11:20	GAC® PRESIDENTIAL ADDRESS: <i>Trend Spotting in the Geosciences</i> Peter Bobrowsky, Geological Survey of Canada (President of GAC®), Presentation Theatre, Winnipeg Convention Centre, 11:20 am - 12:00 pm						
12:00	GAC LUNCHEON - Pan-Am Room, Winnipeg Convention Centre, 12:00 - 1:40 pm / STUDENT NETWORKING LUNCHEON - Meeting Room 13, Winnipeg Convention Centre, 12:00 - 1:40 pm						
13:40	SS19 Geoscience Articles	GS2 cont. Petrology & Volcanology	SS15 Geomicrobiology	GS7 GIS & Remote Sensing	Field Trip FT-B1 Geology of Manitoba Legislative Building (1:30-5:30)		
14:40							
15:00							
15:20							
15:40							
	POSTERS (Exhibits Hall - 4-6 pm): SY1, SS2, SS5, SS6, SS7, SS9, SS16, GS2, GS6, GS7					Posters	
19:00	GEOSCIENCE IN OUR LIVES PUBLIC LECTURE: <i>The drowning and draining of Manitoba: from Lake Agassiz to today</i> James T. Teller, Department of Geological Sciences, University of Manitoba Presentation Theatre, Winnipeg Convention Centre, 7:00 pm						
	MR11	MR12	MR15	MR16	MRE (2 nd Floor)	Exhibits Hall	
8:20	SS12 Adv. in Exploration Techniques	SS10 Metamorph. in the Ore Environment		SS17 Planetary Geology & Astrobiology	SS22 (8:30) First Nations Geoscience		
9:40							
10:00	Refreshment Break / Pause-santé						
10:20	SS12 Adv. in Expl. Techniques	SS10 Metamorph. in the Ore Environment	GS3 Geochem and Geochron	SS17 Planetary Geology & Astrobiology	SS22 (8:30) First Nations Geoscience & Discussion		
11:00							
11:20	PLENARY ADDRESS: <i>The Origin of Laurentia</i> Paul F. Hoffman, Harvard University & University of Victoria Presentation Theatre, Winnipeg Convention Centre, 11:20 - 12:00 pm						
12:00	MAC LUNCHEON - Pan-Am Room, Winnipeg Convention Centre, 12:00 - 1:40 pm						
13:40	SS14 Prairie Hydrology	SS10 cont. Metamorph. in the Ore Environ.	GS3 cont. Geochem and Geochron	SS18 Astromaterials	SS22 cont. (1:20) First Nations Geoscience & Discussion		
15:00							
15:20							
15:40							
	POSTERS (Exhibits Hall - 4-6 pm): SY2, SS1, SS3, SS4, SS8, SS11, SS12, SS13, SS14, SS18, SS23, GS1, GS3, GS4, GS5					Posters	
17:30	PRAIRIE ROUNDUP: <i>Rural Train Ride and BBQ Dinner</i> at the Hitch 'n Post Ranch, 5:30 pm						
	MR11	MR12	MR15	MR16	Millennium Suite	Exhibits Hall	
8:20	SS21 Geoscience Professionalism	SS11 Prior to Pangea	SS13 Williston Basin	GS4 Structural Geology	(8:30)		
9:20					Teacher Workshop		
9:40							
10:00	Refreshment Break / Pause-santé						
10:20	SS21 Geoscience Professionalism	SS11 Prior to Pangea	SS13 Williston Basin	GS4 Structural Geology	Teacher Workshop		
11:00							
11:20	PLENARY ADDRESS: <i>The Science and the Discovery of Volcanogenic Massive Sulphide Deposits</i> Harold Gibson, Laurentian University Presentation Theatre, Winnipeg Convention Centre, 11:20 am - 12:00 pm						
12:00	MDD LUNCHEON - Pan-Am Room, Winnipeg Convention Centre, 12:00 - 1:40 pm						
13:40	GS1 Mineralogy & Crystallography	SS11 cont. Prior to Pangea	SS13 cont. Williston Basin	(1:00) MRE (2 nd Floor) Teacher Workshop Senior	(1:00) Teacher Workshop Junior		
14:40							
15:00							
15:20							
15:40							

Plenary and Special Addresses

Interventions plénières et particulières



Wednesday, May 22

GAC® Presidential Address

Trend Spotting in the Geosciences

by Dr. Peter Bobrowsky, Geological Survey of Canada (President of GAC®),

Room / Salle: **Presentation Theatre**, Winnipeg Convention Centre, 11:20 a.m. – 12:00 p.m.

Free Public Lecture: *Geoscience in Our Lives*

The Drowning and Draining of Manitoba: from Lake Agassiz to Today

by Dr. James T. Teller, University of Manitoba

Room / Salle: **Presentation Theatre**, Winnipeg Convention Centre, 7:00 p.m.

Sponsored by the Clayton H. Riddell Faculty of Environment, Earth, and Resources



UNIVERSITY
OF MANITOBA

Clayton H. Riddell Faculty of
Environment, Earth, and Resources

Thursday, May 23

Plenary Address

The Origin of Laurentia

by Dr. Paul F. Hoffman, Harvard University and University of Victoria

Room / Salle: **Presentation Theatre**, Winnipeg Convention Centre, 11:20 a.m. – 12:00 p.m.

Friday, May 24

Plenary Address

The Science and the Discovery of Volcanogenic Massive Sulphide Deposits

by Dr. Harold Gibson, Laurentian University

Room / Salle: **Presentation Theatre**, Winnipeg Convention Centre, 11:20 a.m. – 12:00 p.m.

No food or drink is permitted in the Presentation Theatre / Nourriture et boissons interdits dans la salle Presentation Theatre.



Special Events Activités spéciales

Tuesday, May 21, 2013

Icebreaker Welcome Reception

Winnipeg welcomes you! Come to meet and greet colleagues, visit the exhibit booths and posters, and enjoy complimentary snacks. Free attendance to all registrants. Cash bar.

Time: 7:00-10:00 p.m. – Exhibits Hall (Rooms 2FGH), Winnipeg Convention Centre

Sponsored by Goldcorp Inc.



Mardi 21 mai 2013

Séance d'accueil

Winnipeg vous souhaite la bienvenue! Rencontrez les collègues (d'anciens, d'actuels ou de nouveaux collègues), prenez connaissance des stands et des posters tout en dégustant quelques grignotines. Bar payant. Toute personne inscrite au congrès est admise sans frais.

De 19 h à 22 h – Salle d'expositions (Salles 2FGH), Centre des congrès de Winnipeg

Parrainé par Goldcorp Inc.



Wednesday, May 22, 2013

Fun Run

Meet in the lobby of the Delta Hotel ready to go for a run to get your day off to a good start with some fresh air and exercise. No registration necessary. Free for everyone who wants to join in the fun.

Time: Leaving at 6:30 a.m. from the Delta Hotel lobby.

GAC Annual Luncheon

Following Peter Bobrowsky's Presidential Address, the Geological Association of Canada will enjoy their annual luncheon. The Logan Medal, the W.W. Hutchison Medal, the J. Willis Ambrose Medal and the E.R. Ward Neale Medal will be presented. Cash bar. \$55 (students \$35) incl. tax

Time: Noon. – Pan Am Room, Winnipeg Convention Centre

Student Networking Luncheon

Come join us for an insightful Student Networking Lunch for both undergraduate and graduate students who seek career advice, answers to their career questions, and tips for finding a job in your field. \$10 for students (professionals \$35) incl. tax

Time: Noon – Meeting Room 1E, Winnipeg Convention Centre

Mercredi 22 mai 2013

Diverticourse

Joignez-vous à un groupe de congressistes en manque d'air frais et d'exercice, et faites un circuit de jogging pour bien commencer la journée. Sans frais, tous sont invités, aucune inscription nécessaire.

Heure : Départ à 6 h 30 de l'entrée de l'hôtel Delta

Dîner annuel de l'Association géologique du Canada

Le dîner de l'Association géologique du Canada fera suite au message annuel du président, en l'occurrence Peter Bobrowsky. On y décernera la médaille Logan, la médaille W.W. Hutchison, la médaille J. Willis Ambrose et la médaille E.R. Ward Neale.

Bar payant. 55 \$ (étudiants 35 \$) toutes taxes comprises

Heure : midi – Salle Pan Am, Centre des congrès de Winnipeg

Dîner de réseautage pour étudiants

Le dîner s'adresse aux étudiants prédiplômés et aux étudiants diplômés en quête de conseils sur la profession, de réponses à leurs questions et d'indices par rapport au décrochage d'un emploi. 10 \$ étudiants (35 \$ professionnels) toutes taxes comprises

Heure : midi – Salle de réunion 1E, Centre des congrès de Winnipeg

Special Events

Activités spéciales



Wednesday, May 22, 2013

Reception to Honour Robert F. Martin, Editor of *The Canadian Mineralogist* 1978-2013

Please come to a reception to celebrate and honour the service contribution of Robert F. Martin to the Canadian mineralogical community. Bob is retiring as editor of the *Canadian Mineralogist*, a post that he has held since 1978. During this time he personally edited 2500 manuscripts and 10 special publications.

Time: 5:00-7:00 p.m. – Millennium Suite, Winnipeg Convention Centre

Manitoba Night

The Department of Geological Sciences of the University of Manitoba invites our alumni, along with our staff and students, to attend Manitoba Night. Share your stories over some traditional Manitoba social fare. Cash bar.

Time: 8:00 p.m. – Millennium Suite, Winnipeg Convention Centre

Thursday, May 23, 2013

MAC Annual Luncheon

Join your fellow mineralogists at your special luncheon! The Mineralogical Association of Canada will present its Young Scientist Award, the Peacock Medal, the Hawley Medal, among other special presentations. \$55 (students \$35) incl. tax

Time: Noon – Pan Am Room, Winnipeg Convention Centre

Tour: Manitoba Museum

Guided tour of the award-winning Manitoba Museum. The 1.5 hour tour will tell the story of Manitoba through the ages, from the Arctic coast to the prairie grasslands, with particular focus on the Earth science aspects of the Museum (i.e., new Ancient Seas and refurbished Earth History galleries). Admission, transportation, tour guide and applicable taxes included. \$30 incl. tax

Time: Bus boards at 1:45 p.m. in front of the Winnipeg Convention Centre (York Ave. entrance). Return approx. 4:45 p.m.

Mercredi 22 mai 2013

Réception en l'honneur de Robert F. Martin, réviseur de 1978 à 2013 au *Canadian Mineralogist*

Une célébration est prévue pour le mercredi 22 mai, de 17 h à 19 h, dans le salon Millennium du Centre des congrès, pour reconnaître Robert F. Martin et souligner sa contribution à la communauté minéralogique canadienne à titre de réviseur de la revue de l'Association minéralogique du Canada depuis 1978. Jusqu'à sa retraite en 2013, Bob aura révisé 2500 manuscrits et 10 publications spéciales.

De 17 h à 19 h – Salle Millenium, Centre des congrès de Winnipeg

Soirée manitobaine

Le département des sciences de la Terre de l'Université du Manitoba tiendra une réunion des anciens. Venez rencontrer des membres du personnel, des professeurs à la retraite et des étudiants à l'occasion d'une soirée de socialisation avec partage d'histoires et d'expériences. Bar payant.

Heure: 20 h – Salle Millenium, Centre des congrès de Winnipeg

Jeudi 23 mai 2013

Dîner annuel de l'Association minéralogique du Canada

Retrouvez vos collègues minéralogistes au dîner annuel de votre association! Entre autres présentations, on y décernera le Prix du jeune scientifique, la médaille Peacock et la médaille Hawley. 55 \$ (étudiants 35 \$) toutes taxes comprises

Heure : midi – Salle Pan Am, Centre des congrès de Winnipeg

Visite guidée du Musée du Manitoba

La visite guidée du prestigieux Musée du Manitoba vous fait traverser les périodes géologiques et passer de la côte Arctique à la prairie herbeuse vallonnée. Les aspects du Musée ayant trait aux sciences de la Terre sont particulièrement mis en évidence, p. ex., la nouvelle galerie des mers anciennes et la galerie réaménagée de l'Histoire de la terre. Frais de la visite guidée : 30 \$ (transport, entrée, guide touristique et taxes compris).

Heure : Embarquement à 13 h 45 devant le Centre des congrès de Winnipeg (avenue York), retour prévu pour 16 h 45.



Special Events Activités spéciales

Thursday, May 23, 2013

Prairie Roundup

All aboard! Ride on the Prairie Dog Central Railway, one of the oldest regular scheduled vintage trains in Canada. We'll take you to the Hitch 'n Post Ranch at Grosse Isle for a prairie-style barbecue that will satisfy even the hungriest geologist! After dinner, enjoy the ranch grounds and kick up your heels to the music of the Jenifer Scott Band. Cash bar. Casual attire. Bring a light jacket and a big appetite. \$95 incl. tax

Time: Buses board at 5:30 p.m. in front of the Winnipeg Convention Centre (York Ave. entrance). Return approx. 11:30 p.m.

Jeudi 23 mai 2013

Party de prairie

Tout le monde à bord! Empruntez le Prairie Dog Central, l'un des trains d'époque les plus anciens du Canada à rouler selon un horaire fixe, pour vous rendre au ranch Hitch 'n Post, à Grosse Isle, où un barbecue à la mode des prairies saura satisfaire le géologue des plus affamés. La soirée se poursuivra par une balade sur les lieux et une danse à la musique de l'ensemble de Jenifer Scott. Bar payant. Tenue de détente. Manteau recommandé. 95 \$ toutes taxes comprises

Heure : Embarquement à 17 h 30 devant le Centre des congrès de Winnipeg (avenue York), retour prévu pour 23 h 30.

Friday, May 24, 2013

MDD Annual Luncheon

Enjoy the final luncheon of the conference with your colleagues of the Mineral Deposits Division of the GAC. The Duncan R. Derry Medal and William Harvey Gross Award will be presented. \$55 (students \$35) incl. tax

Time: Noon – Pan Am Room, Winnipeg Convention Centre

Wind-up Evening

Time to unwind! Join us on the lower patio of the Beachcomber Restaurant on the banks of the Red River at The Forks National Historic Site for a bite to eat and a drink or two. You can stroll along the riverwalk and shop for a few souvenirs in The Forks Market and Johnson Terminal. Cash bar. Casual attire. Bring a light jacket. \$35 (incl. tax)

Time: 7:00-9:30 p.m. – The Beachcomber Restaurant, The Forks

Vendredi 24 mai 2013

Dîner annuel de la Division des gîtes minéraux

Profitez du dernier dîner en commun du congrès en compagnie de vos collègues de la Division des gîtes minéraux. On y décernera la médaille Duncan R. Derry et le prix William Harvey Gross. 55 \$ (étudiants 35 \$) toutes taxes comprises

Heure : midi – Salle Pan Am Room, Centre des congrès de Winnipeg

Soirée de fin de congrès

Rassemblement sur la terrasse inférieure du restaurant Beachcomber, au confluent des rivières Rouge et Assiniboine, lieu historique national de la Fourche. Promenez-vous sur le sentier riverain, magasiner quelques souvenirs dans le terminus Johnson et le Marché de la Fourche. Bar payant. Tenue de détente. Manteau recommandé. 35 \$ toutes taxes comprises

Heure : de 19 h à 21 h 30 – restaurant Beachcomber, à la Fourche

Award Events

Remise des prix



GAC® Awards

The following awards will be presented during the GAC® Luncheon on Wednesday May 22, Noon, Pan Am Room, Winnipeg Convention Centre

The Logan Medal

The highest award of the Geological Association of Canada is awarded to an individual for sustained distinguished achievement in Canadian Earth Science. The award will be presented to **Dr. George Pemberton** of the University of Alberta.

The W.W. Hutchison Medal

This medal is awarded to a young individual for recent exceptional advances in Canadian Earth Science research. The award will be presented to **Dr. Duane Froese**, of the University of Alberta.

The J. Willis Ambrose Medal

This medal is awarded to an individual for sustained dedicated service to the Canadian Earth Science community. The award will be presented to **Dr. Simon Hammer**, retired from Geological Survey of Canada in Ottawa.

The E.R. Ward Neale Medal

This award recognizes outstanding efforts to communicate and explain geoscience to the public through one or more of the following vehicles: public lectures, print or electronic media articles, school visits, elementary and secondary school educational materials, field trips, science fairs, and other public communications. The award will be presented to **Dr. Murray Roed**, Geological/Engineering Consultant in Kelowna, BC.

MAC Awards

The following awards will be presented during the MAC Luncheon on Thursday May 23, Noon, Pan Am Room, Winnipeg Convention Centre

Peacock Medal

The Peacock Medal, formerly the Past-Presidents' Medal, is awarded to a scientist who has made outstanding contributions to the mineral sciences in Canada. There is no restriction regarding nationality or residency. The award will be presented to **Dr. David R. M. Pattison** of the University of Calgary.

Prix de l'AGC®

Les prix suivants seront décernés durant le dîner de l'AGC®, mercredi le 22 mai, midi, Salle Pan Am, Winnipeg Convention Centre

La médaille Logan

Le prix le plus prestigieux de l'Association géologique du Canada est décerné à une personne pour son œuvre remarquable en sciences de la Terre au Canada. La médaille sera décernée au **Dr. George Pemberton** de l'Université de l'Alberta.

La médaille W.W. Hutchison Medal

Cette médaille est décernée à une jeune personne pour une découverte exceptionnelle récente dans le domaine de la recherche en sciences de la Terre au Canada. La médaille sera décernée au **Dr. Duane Froese** de L'Université de l'Alberta.

La médaille J. Willis Ambrose

Cette médaille est décernée à une personne pour son dévouement exceptionnel à la communauté canadienne des sciences de la Terre. La médaille sera décernée au **Dr. Simon Hammer**, en retraite de la Commission géologique du Canada, Ottawa.

La médaille E.R. Ward Neale

Ce prix veut souligner les efforts exceptionnels pour diffuser et expliquer les géosciences au public par l'un ou plusieurs des moyens suivants: conférences grand public, articles papiers ou électroniques, visites scolaires, production de matériel éducatif scolaire à l'élémentaire ou au secondaire, excursions de terrain, expo-sciences, et autres moyens de communication publique. La médaille sera décernée à **Dr. Murray Roed**, consultant en géologie et ingénierie, Kelowna, C.-B.

Prix de l'AMC

Les prix suivants seront présentés durant le dîner de l'AMC, jeudi le 23 mai, midi, Salle Pan Am, Winnipeg Convention Centre

Médaille Peacock

La médaille Peacock, jadis la médaille du président sortant, est décernée à un scientifique qui a contribué de manière exceptionnelle aux sciences minérales au Canada. Il n'y a aucune restriction concernant le statut de nationalité ou de résidence. La médaille sera décernée au **Dr. David R. M. Pattison** de l'Université de Calgary.



Award Events

Remise des prix

Young Scientist Award

This award is given to a young scientist who has made a significant international research contribution in a promising start to a scientific career. The award will be presented to **Dr. Kimberly Tait** of the Royal Ontario Museum.

Hawley Medal

The Hawley Medal is awarded to the authors of the best paper to appear in *The Canadian Mineralogist* in a given year. The award will be presented to **B. Lalinská-Voleková, J. Majzlan, T. Klimko, M. Chovan, G. Kučerová, J. Michňová, R. Hovorič, J. Göttlicher** and **R. Steininger** for their paper: “*Mineralogy of weathering products of Fe-As-Sb mine wastes and soils at several Sb deposits in Slovakia*” published in *The Canadian Mineralogist*, 2012, v.50, p.481-500.

Mineral Deposits Division (MDD) of GAC®

The following awards will be presented during the MDD Luncheon on Friday, May 24, at 12:00 Noon, Pan Am Room, Winnipeg Convention Centre

The William Harvey Gross Award

This award is bestowed to a geoscientist less than 40 years of age who has made a significant contribution to the field of Economic Geology in a Canadian context. The award will be presented to **Dr. Michel Houlé** of the Geological Survey of Canada.

The Duncan R. Derry Medal

This medal is awarded to an outstanding economic geologist who has made contributions to the science of Economic Geology in Canada. The award will be presented to **Dr. Alan Galley** of the Canadian Mining Innovation Council, previously of the Geological Survey of Canada.

Prix jeune scientifique

Ce prix est décerné à un jeune chercheur qui a contribué de manière significative à une recherche internationale en début de carrière scientifique prometteuse. Cette année, le prix sera remis au **Dr. Kimberly Tait** du Musée royal de l'Ontario.

Médaille Hawley

La médaille Hawley est décerné aux auteurs du meilleur article à paraître dans le *Canadian Mineralogist* d'une année donnée. Le prix sera remis à **B. Lalinská-Voleková, J. Majzlan, T. Klimko, M. Chovan, G. Kučerová, J. Michňová, R. Hovorič, J. Göttlicher** et **R. Steininger** pour leur article: «*Mineralogy of weathering products of Fe-As-Sb mine wastes and soils at several Sb deposits in Slovakia*» publié dans *The Canadian Mineralogist*, 2012, v.50, p.481-500.

Prix de la Division des dépôts minéraux (DDM) de l'AGC®

Les prix suivants seront décernés lors du dîner de la DDM, vendredi le 24 mai, midi, Salle Pan Am Room, Winnipeg Convention Centre

Le prix William Harvey Gross

Ce prix est décerné à un géoscientifique de moins de 40 ans qui a contribué de manière significative au domaine de la géologie économique dans un contexte canadien. Le prix sera décerné au **Dr. Michel Houlé** de la Commission géologique du Canada.

La médaille Duncan R. Derry

Cette médaille est décernée à un spécialiste de stature remarquable en géologie économique et qui a contribué de manière exceptionnelle à la science de la géologie économique au Canada. La médaille sera décernée au **Dr. Alan Galley** du Canadian Mining Innovation Council, retraité de la Commission géologique du Canada.

Business Meetings

Séances de travail



Association/Meeting Association/séance	Date Date	Time Heure	Venue/Room Endroit/salle
<i>Geological Association of Canada</i>			
Outgoing Council Meeting	May 20	9:30-5:00 p.m.	Delta Hotel
Outgoing Council Meeting	May 21	8:30-5:00 p.m.	Delta Hotel
Annual Business Meeting	May 22	5:00-6:00 p.m.	WCC MR16
Planetary Sciences Div. Meeting	May 22	5:00-6:00 p.m.	WCC MR15
President's Breakfast Meeting	May 23	7:00-8:30 a.m.	WCC Millennium Suite
Precambrian Division Annual Meeting	May 23	12:00-1:00 p.m.	WCC MR16
Canadian Sedimentary Research Grp.	May 23	3:30-4:30 p.m.	WCC MR7/8
Mineral Deposits Division AGM	May 23	4:00-5:00 p.m.	WCC MR11
Volcanology/Igneous Petrology Div.	May 23	4:00-5:00 p.m.	WCC MR16
Structural Geology/Tectonic Div.	May 23	4:30-5:30 p.m.	WCC MR12
Joint GAC-MAC Exec. Breakfast Mtg.	May 24	7:00-9:00 a.m.	WCC MR17
Geophysics Division Meeting	May 24	12:00-1:00 p.m.	WCC MR16
Incoming Council Meeting	May 24	4:00-6:00 p.m.	WCC MR17
<i>Mineralogical Association of Canada</i>			
Member AGM Meeting	May 23	4:30-5:00 p.m.	WCC MR15
IMA Council Meeting	May 23	4:00-7:00 p.m.	WCC MR12
<i>Canadian Geological Foundation</i>			
Meeting	May 25	8:30-5:00 p.m.	Room 315, Wallace Bldg, University of Manitoba, 125 Dysart Road, Winnipeg
<i>Canadian Geoscience Education Network</i>			
Annual General Meeting	May 21	1:00 to 5:00 p.m.	Millennium Library, Buchwald Room
<i>Canadian Journal of Earth Sciences</i>			
Editorial Board Meeting	May 23	12:00-2:00 p.m.	WCC MR17
<i>Canadian Nuclear Safety Commission</i>			
Information Session	May 22	12:00-1:30 p.m.	Delta Hotel
Information Session	May 22	6:00-9:00 p.m.	Delta Hotel
<i>Energy Frontiers</i>			
Business Meeting	May 19	8:00-6:30 p.m.	WCC Pan Am Room
<i>Natural Sciences and Engineering Research Council of Canada</i>			
Information Session	May 22	4:00-6:00 p.m.	WCC MR4E
WCC = Winnipeg Convention Centre			



Exhibitors Exposants

Booth/Kiosque 1**Isomass Scientific Ltd.**

#140, 5700-1 St. SW
Calgary, AB T2H 3A9

Phone/Tél: 403-255-6631 **Fax/Télec:** 403-255-6958

E-mail/Courriel: Peter.stow@isomass.com

Contact: Peter Stow

Booth/Kiosque 2**Department of Geology****Brandon University**

2nd Floor, J. R. Brodie Science Centre
270-18th St. Brandon, MB R7A 6A9

Phone/Tél: 204-727-9680 **Fax/Télec:** 204-728-7346

E-mail/Courriel: lir@brandonu.ca

Contact: Rong-Yu Li

Booth/Kiosque 3 & 4**Geological Association of Canada (GAC)**

c/o Department of Earth Sciences
300 Prince Phillip Drive
Memorial University of Newfoundland
St. John's, NL A1B 3X5

Phone/Tél: 709-864-7660 **Fax/Télec:** 709-864-2532

E-mail/Courriel: gac@mun.ca

Contact: Karen Dawe

Booth/Kiosque 5**Actlabs Ltd.**

1336 Sandhill Dr.
Ancaster, ON L9G 4V5

Phone/Tél: 905-648-9611 **Fax/Télec:** 905-648-9613

E-mail/Courriel: stacy@actlabs.com

Contact: Stacey Russell

Booth/Kiosque 6**Acme Analytical Labs**

Suite 1201-700 West Pender St.
Vancouver, BC V6C 1G8

Phone/Tél: 604-253-3158

E-mail/Courriel: Lisa.Melton@acmelab.com

Contact: Lisa Melton

Booth/Kiosque 7 & 8**Mineralogical Association of Canada (MAC)**

490 rue de la Couronne
Quebec City, QC G1K 9A9

Phone/Tél: 418-653-0333 **Fax/Télec:** 418-653-0777

E-mail/Courriel: jcaron@mineralogicalassociation.ca

Contact: Johanne Caron

Booth/Kiosque 9**Geosciences Laboratory**

933 Ramsey Lake Road
Sudbury, ON P3E 6B5

Phone/Tél: 705-670-5644 **Fax/Télec:** 705-670-3047

E-mail/Courriel: Merilla.clement@ontario.ca

Contact: Merilla Clement

Booth/Kiosque 10**Nunavut Arts and Crafts Association**

PO Box 1539, Iqaluit, NU X0A 0H0

Phone/Tél: 867-979-7808 **Fax/Télec:** 867-979-6880

E-mail/Courriel: mbeauregard@gov.nu.ca

Contact: Mike Beauregard

Booth/Kiosque 11**Manitoba Geological Survey**

360-1395 Ellice Avenue
Winnipeg, MB R3G 3P2

Phone/Tél: 204-945-6549 **Fax/Télec:** 204-945-1406

E-mail/Courriel: Christian.bohm@gov.mb.ca

Contact: Christian Bohm

Booth/Kiosque 12**GAC-MAC 2014****Dept. of Earth Sciences****University of New Brunswick**

Box 4400, 2 Bailey Drive
Fredericton, NB E3B 5A3

Phone/Tél: 506-447-3190

E-mail/Courriel: dlentz@unb.ca

Contact: David Lentz

Booth/Kiosque 13**Elemental Controls – Niton XRF**

3230 Wharton Way
Mississauga, ON L4X 2C1

Phone/Tél: 866-544-9974

Fax/Télec: 905-282-9519

E-mail/Courriel: kgrattan@elementalcontrols.com

Contact: Keith Grattan

Booth/Kiosque 14**Living Sky Geophysics Inc.**

31 McCully Cr.
Saskatoon, SK S7L 5L8

Phone/Tél: 306-249-2800

E-mail/Courriel: David.bingham@livingskygeophysics.ca

Contact: David Bingham

Exhibitors Exposants



Booth/Kiosque 15

**Department of Geography
University of Winnipeg**

515 Portage Avenue

Winnipeg, MB R3B 2E9

Phone/Tél: 204-786-9451

Fax/Télec: 204-774-4134

E-mail/Courriel: m.vachon@uwinnipeg.ca

Contact: Marc Vachon

Booth/Kiosque 16

Olympus Canada

25 Leek Cr.

Richmond Hill, ON L4B 4B9

Phone/Tél: 289-269-0160

E-mail/Courriel: Laura.boccia@olympus.com

Contact: Laura Boccia

Booth/Kiosque 17

Canadian Science Publishing

Building M-55

1200 Montreal Road

Ottawa, ON K1A 0R6

Phone/Tél: 613-998-6913 **Fax/Télec:** 613-952-7656

E-mail/Courriel: Kelly.bogh@nrcresearchpress.com

Contact: Kelly Bogh

Booth/Kiosque 18

GNS Scientific/Rafter Radiocarbon

30 Gracefield Road

PO Box 31312

Lower Hutt 5040

New Zealand

Phone/Tél: +64 4570 4123

E-mail/Courriel: m.sim@gns.cri.nz

Contact: Mike Sim

Booth/Kiosque 19

Department of Earth Sciences

Laurentian University

935 Ramsey Lake Road

Sudbury, ON P3E 2C6

Phone/Tél: 705-675-1151 **Fax/Télec:** 705-675-4898

E-mail/Courriel: ntardif@laurentian.ca

Contact: Nicole Tardif

Booth/Kiosque 20

Department of Geological Sciences

University of Manitoba

240 Wallace Bld.

125 Dysart Road

Winnipeg, MB R3T 2N2

Phone/Tél: 204-474-9371 **Fax/Télec:** 204-474-7623

E-mail/Courriel: Ij_ferguson@umanitoba.ca

Contact: Ian Ferguson

Booth/Kiosque 21

Carl Zeiss Canada Ltd.

45 Valleybrooke Drive

Toronto, ON M3B 2S6

Phone/Tél: 800-387-8037

E-mail/Courriel: darryl.dyck@zeiss.com

Contact: Darryl Dyck

Booth/Kiosque 22

The Manitoba Museum

190 Rupert Avenue

Winnipeg, MB R3B 0N2

Phone/Tél: 204-956-2830 **Fax/Télec:** 204-924-3679

E-mail/Courriel: gyoung@manitobamuseum.ca

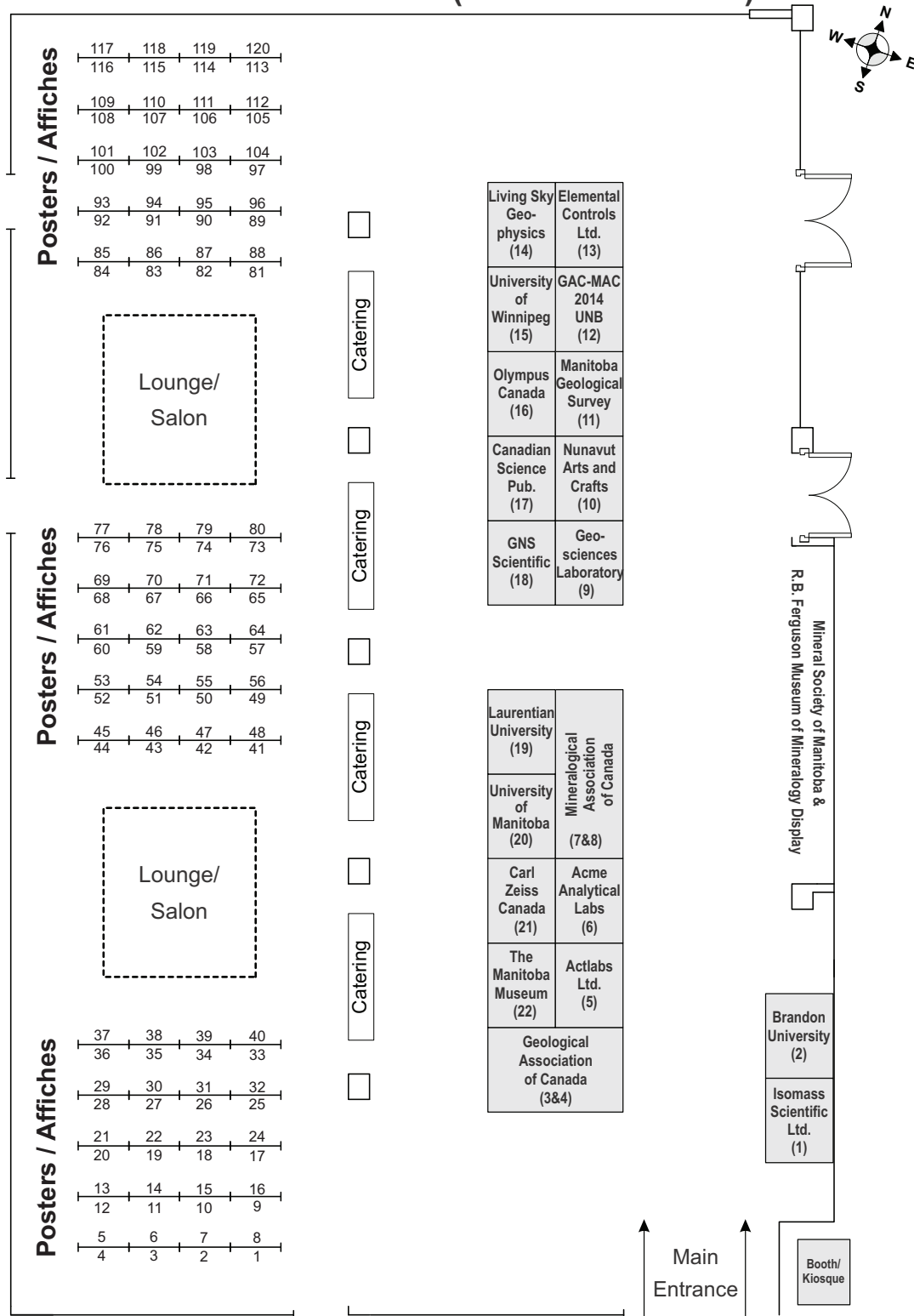
Contact: Graham Young



Exhibit Floor Plan

Plan de l'étage des expositions

Exhibitors/Exposants Posters/Affiches (Room/Salle 2FGH)



Field Trips Excursions



Pre-meeting

FT-A1: The Rice Lake Mine Trend, Manitoba: Regional Setting, Host Rock Stratigraphy and Structural Evolution of a Classical Archean Orogenic Lode-Gold System

Scott Anderson and Doug Berthelsen (trip dates: May 18–21, 2013)

Sponsored by the Mineral Deposits Division, GAC®

FT-A2: Volcanological and Structural Setting of Paleoproterozoic VMS and Gold Deposits at Snow Lake, Manitoba

Al Bailes, Simon Gagné, Kate Rubingh and Craig Taylor (trip dates: May 18–21, 2013)

Sponsored by the Mineral Deposits Division, GAC®

FT-A3: Stratigraphy and Ore Deposits in the Thompson Nickel Belt, Manitoba

Chris Couëslan and Josef Macek

(Cancelled)

FT-A4: Upper Cretaceous and Paleocene Stratigraphy, Gas Shale and Industrial Minerals of the Pembina Mountain and Turtle Mountain Areas

Jim Bamburak and Michelle Nicolas

(Cancelled)

FT-A5: Mars Analogues in Manitoba: The Lake St. Martin Impact Structure and East German Creek Hypersaline Springs

Ed Cloutis and Gordon Osinski

(Cancelled)

During meeting

FT-B1: Geology of the Manitoba Legislative Building

Jeff Young and Graham Young (trip date: May 22, 2013)

Post-meeting

FT-C1: The Tanco Mine: Geological Setting, Internal Zonation and Mineralogy of a World-Class Rare Element Pegmatite Deposit

Tania Martins, Paul Kremer and Peter Vanstone (trip dates: May 24–25, 2013)

Sponsored by the Mineral Deposits Division, GAC®

Excursions pre-congrès

FT-A1: La configuration de la minéralisation de la mine du lac Rice, Manitoba : contexte régional, stratigraphie des roches hôtes et évolution structurale d'un système aurifère filonien classique d'un orogène archéen

Scott Anderson, Doug Berthelsen (18 au 21 mai, 2013)

Parrainé par la Division des dépôts minéraux, AGC®

FT-A2: Contexte volcanologique et structural des gisements de SMV et d'or au lac Snow, Manitoba

Al Bailes, Simon Gagné, Kate Rubingh, Craig Taylor (18 au 21 mai, 2013)

Parrainé par la Division des dépôts minéraux, AGC®

FT-A3: Stratigraphie et gisements de minerai dans la bande nickélifère Thompson au Manitoba

Chris Couëslan, Josef Macek

(Annulé)

A4: Stratigraphie du Crétacé supérieur et du Paléocène, schiste gazéifère et minéraux industriels des régions des collines Pembina et Turtle

Jim Bamburak, Michelle Nicolas

(Annulé)

A5: Les sources du ruisseau East German et de la carrière Mafeking

Ed Cloutis, Gordon Osinski

(Annulé)

Excursion durant le congrès

FT-B1: Géologie de l'édifice du parlement du Manitoba

Jeff Young, Graham Young, Bill Brisbin (22 mai, 2013)

Excursions post-congrès

FT-C1: La mine Tanco : contexte géologique, zonation et minéralogie d'un gisement pegmatitique d'éléments rares de classe mondiale

Tania Martins, Paul Kremer, Peter Vanstone (24 et 25 mai, 2013)

Parrainé par la Division des dépôts minéraux, AGC®



Field Trips Excursions

FT-C2: Neoproterozoic Mafic-Ultramafic Intrusions in the Bird River Greenstone Belt: Tectonic Setting and Economic Significance

Paul Gilbert, James Scoates, Jon Scoates, Eric Yang, Caroline Mealin, Michel Houllé and Carey Galeschuk (trip dates: May 24–27, 2013)

Sponsored by the Mineral Deposits Division, GAC®

FT-C3: The Volcanological and Structural Evolution of the Paleoproterozoic Flin Flon Mining District: The Anatomy of a Giant VMS System

Harold Gibson, Bruno Lafrance, Sally Pehrsson, Michelle DeWolfe, Kelly Gilmore and Renée-Luce Simard (trip dates: May 25–29, 2013)

Sponsored by the Mineral Deposits Division, GAC®

FT-C4: Metamorphosed Alteration Zones and Regional Metamorphism: Examples from the Trans-Hudson Orogen

Chris Couëslan, Doug Tinkham, Al Bailes and Simon Gagné
(Cancelled)

FT-C5: Ordovician-Silurian Boundary Interval in the Williston Basin Outcrop Belt of Manitoba: A Record of Global and Regional Environmental and Biotic Change

Bob Elias and Graham Young (trip dates: May 25–27, 2013)
Sponsored by the Paleontology Division, GAC®

FT-C6: Quaternary Geology, Geomorphology and Sedimentology to Inform Watershed Science Across the Pembina Escarpment

David Lobb and Geneviève Ali
(Cancelled)

FT-C2: Intrusions mafiques-ultramafiques néoarchéennes de la bande de roches vertes de la rivière aux Oiseaux : contexte tectonique et importance économique

Paul Gilbert, James Scoates, Jon Scoates, Eric Yang, Caroline Mealin, Michel Houllé, Carey Galeschuk (24 au 27 mai, 2013)

Parrainé par la Division des dépôts minéraux, AGC®

FT-C3: L'évolution volcanologique et structurale du district minier paléoprotérozoïque de Flin Flon : l'anatomie d'un système géant de SMV

Harold Gibson, Bruno Lafrance, Sally Pehrsson, Michelle DeWolfe, Kelly Gilmore, Renée-Luce Simard (25 au 29 mai, 2013)

Parrainé par la Division des dépôts minéraux, AGC®

FT-C4: Zones d'altération métamorphiques et métamorphisme régional : exemples tirés de l'orogène trans-hudsonien

Chris Couëslan, Doug Tinkham, Al Bailes, Simon Gagné
(Annulé)

FT-C5: Intervalle de la limite Ordovicien-Silurien dans la bande d'affleurements du bassin de Williston au Manitoba : une archive des changements environnementaux et biotiques régionaux et globaux

Bob Elias, Graham Young (25 au 27 mai, 2013)
Parrainé par la Division de paléontologie, AGC®

FT-C6: Données de géologie du Quaternaire, de géomorphologie et de sédimentologie nécessaires à la compréhension des systèmes hydrographiques recoupant l'escarpement de Pembina

David Lobb, Geneviève Ali
(Annulé)

Short Courses

Cours intensifs



MAC-1: Uranium - Cradle to Grave

Peter Burns and Ginger Sigmon

Sponsored by Mineralogical Association of Canada

GAC-1: Petrography of Mafic Layered Intrusions

James Scoates and Jim Miller

Sponsored by Geological Association of Canada, Volcanology and Igneous Petrology Division; Geological Association of Canada, Mineral Deposits Division

GAC-2: Impact Cratering: Processes And Products

Sponsored by Geological Association of Canada, Planetary Sciences Division

Gordon Osinski

(Cancelled)

MAC-1: Uranium du Berceau au Tombeau

Peter Burns, Ginger Sigmon

Parrainé par l'Association minéralogique du Canada

GAC-1: Pétrographie des Intrusions Stratifiées Mafiques

James Scoates, Jim Miller

Parrainé par l'Association géologique du Canada, division de la volcanology et de la pétrologie ignée; l'Association géologique du Canada, division des dépôts minéraux

GAC-2: Formation de Cratères d'Impact : un Processus Géologique

Gordon Osinski

Parrainé par l'Association géologique du Canada, division des sciences planétaires

(Annulé)



Outreach - Earth Science Awareness

Sensibilisation aux sciences de la Terre

The outreach program features events designed to raise awareness of the Earth Sciences to the general public, teachers and their students. Featured events include a teacher workshop and field trip, the Geoscience in Our Lives public presentation, and a special session entitled First Nations Geoscience Forum.

Le programme de sensibilisation comprendra des activités relatives aux sciences de la Terre et conçues pour le grand public, les enseignants et leurs élèves. Parmi ces activités figurent un atelier et une excursion pour enseignants, une conférence publique et une session spéciale intitulée Forum des Premières nations sur les sciences de la Terre.

Outreach Program Information:

EdGEO Teacher Workshop and Field Trip

The Canadian Geoscience Education Network (CGEN) presents the Winnipeg 2013 EdGEO Teacher Workshop. It is designed to help grades four and seven teachers from across Manitoba to meet the specific learning outcomes of the science curriculum. Professional Earth science educators from across Canada will deliver this program using “hands-on” activities and sharing their ideas and approaches to Earth science education. Teachers will receive instruction linked to lesson plans, classroom activities and a resource package that can be used to deliver workshop activities in their classroom. The Winnipeg 2013 EdGEO Teacher Workshop received generous financial support from the Canadian Geological Foundation and EdGEO, the Canadian Earth Science Teacher Workshop Program.

EdGEO Teacher Workshop

Date and time: Friday, May 24th, 8:30 a.m. to 3:45 p.m.
Location: Millennium Suite, Second Floor, Winnipeg Convention Centre

Teachers will have the opportunity to explore the geology of southern Manitoba with professional Earth science educators. We will go back in time to examine and discuss the evolution of Manitoba's landscape by visiting areas shaped by inland seas and continental glaciers during periods of climatic warming and cooling.

EdGEO Teacher Field Trip

Date and time: Saturday, May 25th, 8:30 a.m. to 5:00 p.m.
Departure: Wallace Building, University of Manitoba

First Nations Geoscience Forum

The First Nations Geoscience Forum brings Indigenous Elder knowledge holders together with professional Earth science educators and teachers to share their perspectives and explore



Programme de sensibilisation:

Atelier et excursion EdGEO pour enseignants

The Canadian Geoscience Education Network (CGEN) présente l'atelier EdGEO pour enseignants Winnipeg 2013. Il est conçu pour aider les enseignants des 4e au 7e années à atteindre des résultats d'apprentissages spécifiques du programme d'études manitobain en sciences de la nature. Des pédagogues spécialisés en sciences de la Terre, provenant de partout au Canada, animeront une journée d'activités pratiques et de partage d'idées et d'approches. Les enseignants participant à l'atelier recevront une trousse de matériel qui aidera à mener des activités semblables dans leur classe. L'atelier EdGEO pour enseignants Winnipeg 2013 a reçu un appui financier généreux du Canadian Geological Foundation et du EdGEO, le Canadian Earth Science Teacher Workshop Program.

Atelier EdGEO pour enseignants

Date : Vendredi, le 24 mai, de 8h30 à 15h45.
Lieu : Millennium Suite, deuxième étage, Winnipeg Convention Centre.

Les enseignants auront la possibilité d'explorer la géologie du sud du Manitoba accompagnés d'éducateurs professionnels spécialisés en sciences de la Terre. Nous remonterons le temps pour examiner et discuter l'évolution du paysage manitobain en visitant des endroits que des mers intérieures et des glaciers continentaux ont façonnés pendant des périodes de réchauffement et de refroidissement climatiques.

Excursion EdGEO pour enseignants

Date : Samedi, le 25 mai, de 8h30 à 17h00.
Point de départ : Wallace Building, Université du Manitoba

Forum des Premières nations sur les sciences de la Terre

Le Forum des Premières nations sur les sciences de la Terre réunira des anciens (éducateurs traditionnels autochtones), des

Outreach - Earth Science Awareness

Sensibilisation aux sciences de la Terre



the design of Earth science outreach and teaching programs. Participants will receive Indigenous teachings provided by First Nations elders on ancestral knowledge of Earth processes and a better understanding of how Earth science education is currently delivered in Manitoba. Breakout learning circles will allow participants to engage in refining common goals with the potential for positive outcomes in science education and future geoscientists in the Indigenous community.

Sponsored by Vale.

Date and time: Thursday, May 23rd, 8:40 a.m. to 3:45 p.m.
Location: MRE, Second Floor, Winnipeg Convention Centre



membres de la collectivité géologique et des agents d'éducation en matière scientifique pour communiquer leurs perspectives et se pencher sur la conception de programmes de promotion et d'enseignement des sciences de la Terre. Les participants recevront de la part des anciens des enseignements sur les connaissances ancestrales concernant les processus géologiques et seront ainsi mieux informés par rapport à l'éducation dispensée à l'échelle provinciale et nationale en matière de géosciences. Ils se joindront ensuite à des petits groupes de discussion pour préciser des objectifs communs qui pourraient mener à des résultats positifs sur les plans de l'éducation en sciences et de la formation de scientifiques parmi les membres de la collectivité autochtone.

Parrainé par Vale.

Date : Jeudi, le 23 mai, de 8h40 à 15h45.
Lieu : MRE, deuxième étage, Winnipeg Convention Centre.

EdGEO Teacher Workshop

Room: Millennium Suite (Second Floor)

Sponsored by: Canadian Geoscience Education Network (CGEN)

8:40 **Murphy, L.** (*Manitoba Geological Survey*) Connecting indigenous culture and science education

9:00 **Williams, J.** (*Mining Matters*) and **Halfkenny, B.** (*Carleton U.*) Rocks and minerals in your classroom and beyond, part I

10:00 Refreshments

10:20 **Williams, J.** (*Mining Matters*) and **Halfkenny, B.** (*Carleton U.*) Rocks and minerals in your classroom and beyond, part II

11:00 **Young, J.** (*U Manitoba*) Snippets of time: the geology of Manitoba classroom version

EdGEO Teacher Workshop Junior

Room: Millennium Suite

Sponsored by: Canadian Geoscience Education Network (CGEN)

13:00 **Hymers, L.** (*Ontario Mining Association*) and **Bank, C.** (*U Toronto*): Landscape development, soils and erosion.

15:00 **Nowlan, G.** (*Geological Survey of Canada*) The importance of Earth science literacy and planetary citizenship

EdGEO Teacher Workshop Senior

Room: MRE (Second floor)

Sponsored by: Canadian Geoscience Education Network (CGEN)

13:00 **Murray, J.** (*Manitoba Innovation, Energy and Mines*) Plate Tectonics - A Scientific Revolution for Our Geologic Time

13:30 **Danko, J.** (*Argyle Alternative High School*) Discovering Earth Science Through Inquiry using LwICT (Literacy with Information and Communications Technology) and Formative Assessment

14:00 **Williams, E.** (*École Riverside Secondary School*) Connecting resources to the real world

14:30 **Young, J.** (*U Manitoba*) Earth structure for the classroom

15:00 **Nowlan, G.** (*Geological Survey of Canada*) The importance of Earth science literacy and planetary citizenship (Note: presentation is in the Millennium Suite)

Geoscience in Our Lives

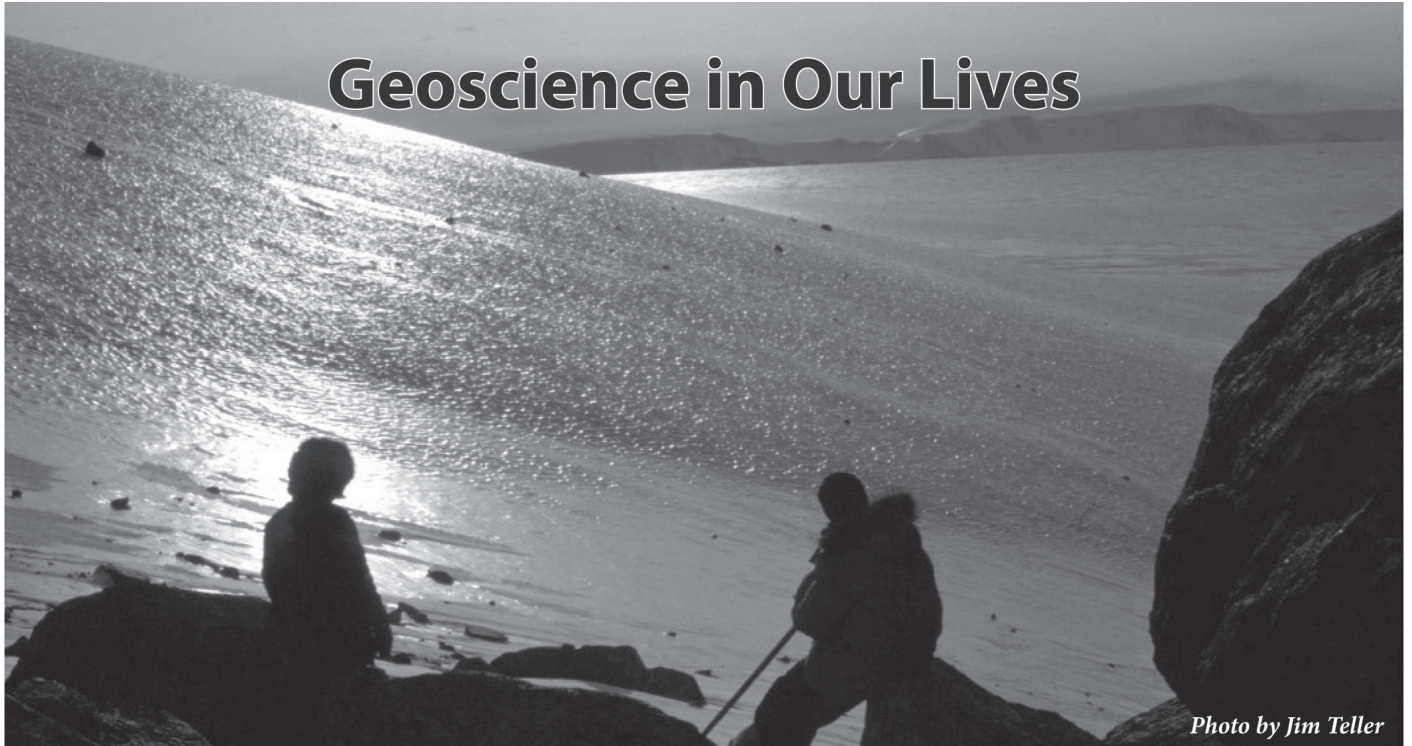


Photo by Jim Teller

The Drowning and Draining of Manitoba: From Lake Agassiz to Today

James T. Teller, Department of Geological Sciences, University of Manitoba

The Red River Lowlands have been repeatedly flooded since retreat of the Laurentide Ice Sheet about 12,000 years ago. Initially that ice sheet formed a dam that prevented drainage of the Canadian Prairies and Northern Great Plains of the U.S. from reaching Hudson Bay. The largest lake in the world, Lake Agassiz, was ponded in front of the glacier for nearly 5000 years, inundating most of southern Manitoba and parts of northwestern Ontario, Saskatchewan, North Dakota, and Minnesota. Sandy beaches formed around the shorelines of the lake when it was at different levels, and clay was deposited in the deeper waters of the basin. Overflow from Lake Agassiz during its life was through several different routes: (1) south into the Mississippi River and Gulf of Mexico, (2) east into the Great Lakes to the St. Lawrence Valley and North Atlantic Ocean, and (3) northwest into the Mackenzie River and the Arctic Ocean. The lake finally drained away into Hudson Bay about 8400 years ago, after which modern drainage patterns were established across central Canada. Each change in routing of Lake Agassiz overflow was accompanied

by a catastrophic burst of water; when that burst reached the oceans it changed the way they circulated and, in turn, caused global cooling.

After Lake Agassiz drained away, the modern Red River was established on the floor of the old lake bed. Because of the low gradient of the river and low relief of the lake plain, flooding has repeatedly occurred along the river, inundating large areas during spring runoff; major floods in the 19th century were recorded in 1826, 1852, and 1861. Saturated ground conditions in the fall, early freezing of the ground, high precipitation, and rapid and late snow melt in the spring commonly have led to spring flooding. In recent years, such as 1979, 1996, 1997, 1999, 2006, and 2009, large floods have occurred. Only construction of the 48-km-long Red River Floodway in 1968 around the city of Winnipeg has prevented flood disasters in the city of Winnipeg like the one in 1950; the Floodway prevented an estimated \$10 billion in flood damage in 2009.



UNIVERSITY
OF MANITOBA

Clayton H. Riddell Faculty of
Environment, Earth, and Resources

sponsored by Clayton H. Riddell Faculty of Environment, Earth, and Resources

**7:00 p.m., Wednesday, May 22nd
Presentation Theatre at the Winnipeg Convention Centre
Everybody Welcome**

Wednesday Technical Program

Programme du mercredi



	Present. Theatre	MR2E	MR3E	MR4E	MR7/8	MR9/10	MR11	MR12	MR15	MR16		Exhibits Hall
8:20	SS5 Uranium: Cradle to Grave	SS7 Rare Metals and VMS	SY1 Earth Materials (Hawthorne)	SS2 Assembly of North America	SS6 REEs in Melts	SS9 Ni-Cu- PGE-Cr		GS2 Petrology & Volcanology	SS16 Impact Cratering	GS6 Quaternary Geology		E X H I B I T S
10:00	Refreshment Break / Pause-santé											
10:20	SS5 Uranium: Cradle to Grave	SS7 Rare Metals and VMS	SY1 Earth Materials (Hawthorne)	SS2 Assembly of North America	SS6 REEs in Melts	SS9 Ni-Cu- PGE-Cr		GS2 Petrology & Volcanology	SS16 ...	GS6 Quaternary Geology		
10:40												
11:00												
11:20	GAC® PRESIDENTIAL ADDRESS: <i>Trend Spotting in the Geosciences</i> Peter Bobrowsky, Geological Survey of Canada (President of GAC®), Presentation Theatre, Winnipeg Convention Centre, 11:20 am - 12:00 pm											
12:00	GAC Luncheon - Pan-Am Room, Winnipeg Convention Centre, 12:00 - 1:40 pm Student Networking Luncheon - Meeting Room 1E, Winnipeg Convention Centre, 12:00 - 1:40 pm											
13:40	SS5 <i>cont.</i> Uranium: Cradle to Grave	SS7 <i>cont.</i> Rare Metals and VMS	SY1 <i>cont.</i> Earth Materials (Hawthorne)	SS2 <i>cont.</i> Assembly of North America	SS6 <i>cont.</i> REEs in Melts	SS9 <i>cont.</i> Ni-Cu- PGE-Cr	SS19 Geoscience Articles	GS2 <i>cont.</i> Petrology & Volcanology	SS15 Geomicro- biology	GS7 GIS & Remote Sensing	Field Trip FT-B1 Geology of Manitoba Legislative Building (1:30-5:30)	
14:40												
15:00												
15:20												
15:40												
POSTERS (Exhibits Hall): SY1 (7), SS2 (5), SS5 (14), SS6 (5), SS7 (5), SS9 (8), SS16 (4), GS2 (5), GS6 (3), GS7 (1)												Posters 4-6 pm
19:00	GEOSCIENCE IN OUR LIVES PUBLIC LECTURE: <i>The drowning and draining of Manitoba: from Lake Agassiz to today</i> James T. Teller, Department of Geological Sciences, University of Manitoba Presentation Theatre, Winnipeg Convention Centre, 7:00 pm											

Presentations are listed for each Symposium, Special Session and General Session. For oral presentations, the speaker is indicated with an asterisk. Poster presenters for the sessions shown must be in attendance between 4:00 p.m. and 6:00 p.m. to discuss their poster with conference attendees. A cash bar will be available in the Exhibits Hall at this time.

Les présentations sont listées pour chaque symposium, session spéciale et session générale. Pour les présentations orales le(la) conférencier(ère) est indiqué(e) avec un astérisque. Les présentateurs des affiches pour les sessions indiquées doivent être sur place entre 16h00 et 18h00 pour discuter du contenu de leur présentation. Un bar payant sera disponible dans la salle d'exposition des affiches. Aucune nourriture ni boisson n'est permise au Presentation Theatre.

Wednesday, May 22 - Morning

SYMPOSIA

SY1 EARTH MATERIALS, PETROLOGICAL AND GEOCHEMICAL PROCESSES (IN HONOUR OF FRANK C. HAWTHORNE)

Room / Salle: MR3E

Supported by / Soutenue par: MAC / AMC

Organizers / Organisateurs: Elena Sokolova, Norman Halden

Chairs / Présidents: Norman Halden and Elena Sokolova

08:20 Shannon, R.D.* and Fischer, R.X. Keynote (40 min): Empirical electronic polarizabilities in oxides, hydroxides, oxyfluorides and oxychlorides

09:00 Longstaffe, F.J.* and Léveillé, R.J. Stable isotopic compositions of kerolite from microbial deposits in basaltic caves, Kauai, Hawaii

09:20 Welch, M.D.* and Mitchell, R.H. Topological possibilities for carpholite-like structures: A new double-chain silicate $K Ba Fe^{3+} Mg_7 Si_8 O_{22} (OH)_2 (OH,F)_6$

09:40 Peterson, R.C. Crystal chemistry of hydrous magnesium sulfates and hydrous magnesium carbonates: Implications for the Martian surface

10:00 *Refreshment Break / Pause-santé*

10:20 Maresch, W.V.*, Schertl, H-P. and Hertwig, A. Fluid-precipitated jadeitites and jadeite-lawsonite-quartz rocks from the Dominican Republic: Novel records of aqueous fluids in an intra-oceanic subduction zone

10:40 Alexandre, P.*, Kyser, K. and Uvarova, Y. The significance of the chemical composition of natural uraninite

11:00 Calas, G.*, Allard, T., Balan, E., Cormier, L., Galois, L. and Juhin, A. Crystal chemistry of transition elements and defects in minerals and glasses: A unifying perspective

SPECIAL SESSIONS

SS2 ASSEMBLY OF NORTH AMERICA: A TECTONIC AND METALLOGENIC REAPPRAISAL

Room / Salle: MR4E

Supported by / Soutenue par: GAC Precambrian Division; GAC Volcanology and Igneous Petrology Division; GAC Planetary Sciences Division; GAC Mineral Deposits Division

Organizers / Organisateurs: Andrey Bekker, Sally Pehrsson, Natasha Wodicka, Christian Böhm

Chairs / Présidents: Andrey Bekker and Sally Pehrsson

08:20 Ootes, L.*, Davis, W.J. and Jackson, V.A. Keynote (40 min): Whence came Hottah Terrane?

09:00 Delpech, E.*, Jebrak, M., Lulin, J-M. and Stevenson, R. Polymetallic mineralization in the context of Minto Subprovince crustal evolution, Nunavik, Québec, Canada

09:20 Lodge, R.W.D.*, Gibson, H.L., Stott, G.M., Hudak, G.J. and Jirsa, M.A. Geochronology and geochemistry of Neoproterozoic Timiskaming-type assemblages in the Shebandowan and Vermilion greenstone belts, Wawa subprovince, Superior Craton

09:40 Partin, C.A. *, Bekker, A., Sylvester, P.J., Wodicka, N., Stern, R.A., Chacko, T. and Heaman, L.M. Examining the apparent 2.45 to 2.2 Ga magmatic gap using the record of U-Pb, Hf, and O isotopes in magmatic and detrital zircon from the Canadian Shield

10:00 *Refreshment Break / Pause-santé*

10:20 Wodicka, N.*, Corrigan, D., Whalen, J.B., Sanborn-Barrie, M. and St-Onge, M.R. Did a proto-ocean basin form along the southeast Rae margin during the Paleoproterozoic? Evidence from U-Pb geochronology, Nd isotope data, geochemistry, and tectonostratigraphy

10:40 Adetunji, A., Ferguson, I.* and Jones, A. Resistivity structures of the Precambrian Superior-Grenville margin defined by the magnetotelluric method as part of the POLARIS project

SS5 URANIUM: CRADLE TO GRAVE

Room / Salle: Presentation Theatre

Supported by / Soutenue par: GAC Environmental Sciences Division

Organizers / Organisateurs: Peter Burns, Ginger Sigmon

Chairs / Présidents: Peter Burns and Ginger Sigmon

08:20 Navrotsky, A. From uraninite to clusters to uranyl minerals - Thermochemical studies

08:40 Ushakov, S.V.*, Shvareva, T.Y. and Navrotsky, A. Applications of gas adsorption calorimetry for surface characterization: Water on UO_2 and other examples

09:00 McGrail, B.T.*, Jouffret, L.J., Lussier, A.J. and Burns, P.C. Spectroscopy and supramolecular assembly of uranyl peroxide cage clusters

09:20 Vlaisavljevich, B.*, Miro, P., Hu, S., Dzubak, A., Spezia, R., Cramer, C.J. and Gagliardi, L. Molecular dynamics simulations of uranyl-peroxide nanocapsules in aqueous solution

09:40 Johnson, R.L.*, Ohlin, C.A., Pellegrini, K., Burns, P.C. and Casey, W.H. Using ^{31}P NMR to probe the solution dynamics of a large uranyl-peroxo cluster

10:00 *Refreshment Break / Pause-santé*

Wednesday, May 22 - Morning

- 10:20** **Lussier, A.J.*, McGrail, B.T., Dzik, E.A., Na, C. and Burns, P.C.** Interactions between uranyl peroxo nanoclusters and solid surfaces in aqueous environments
- 10:40** **Becker, U.*, Yuan, K., Gebarski, B., Ewing, R.E. and Renock, D.** Redox mechanisms of uranyl and uranium nanocluster reactions on minerals surfaces
- 11:00** **Ashton, K.E.*, Normand, C., Chi, G., LeGault, T. and McFarlane, C.R.M.** The Beaverlodge vein-type uranium deposits revisited
- SS6** **RARE EARTH ELEMENTS IN MELTS, FLUIDS AND CRYSTAL STRUCTURES**
Room / Salle: MR7/8
Supported by / Soutenue par: MAC / AMC
Organizers / Organismes: Anton Chakhmouradian, Ian Coulson
Chairs / Présidents: Ian Coulson and Anton Chakhmouradian
- 08:20** **Smith, E.M.* and Kopylova, M.G.** A fresh look at Eu anomalies: The effect of Cl-rich fluids
- 08:40** **Moore, B.T.*, Hanchar, J.M., Chafe, A. and Fournelle, J.** Rare earth element substitution and charge balancing in synthetic apatite
- 09:00** **Chakhmouradian, A.R.* and Reguir, E.P.** Monticellite: A neglected rare-earth host in mantle-derived undersaturated rocks and its significance for magma evolution
- 09:20** **Mitchell, R.H.* and Mariano, A.N.** Rare earth element-bearing perovskites in slags formed by the aluminothermic reduction of pyrochlore
- 09:40** **Ushakov, S.V.* and Navrotsky, A.** Measurements of fusion enthalpies of rare earth oxides, perovskites and pyrochlores
- 10:00** *Refreshment Break / Pause-santé*
- 10:20** **Harper, C.T.*, Pandur, K. and Pearson, J.G.** New REE discoveries at Great Western Minerals Group's Hoidas Lake property, northwest Saskatchewan
- 10:40** **Pandur, K.*, Ansdell, K., Kontak, D., Creighton, S., Harper, C., Pearson, J. and Halpin, K.** Allanites, melt and fluid inclusions in the Hoidas Lake REE deposit, Saskatchewan, Canada: Constraints on a complex magmatic-hydrothermal system
- 11:00** **Dalsin, M.L.* and Groat, L.A.** Rare earth element mineralogy of the Wiccheeda carbonatite complex, central British Columbia, Canada

- SS7** **PRECIOUS AND RARE METALS IN THE VOLCANOGENIC MASSIVE SULFIDE ENVIRONMENT**
Room / Salle: MR2E
Supported by / Soutenue par: GAC Mineral Deposits Division
Organizers / Organismes: Patrick Mercier-Langevin, Harold Gibson, Simon Gagné
Chairs / Présidents: Patrick Mercier-Langevin, Harold Gibson and Simon Gagné
- 08:20** **Mercier-Langevin, P.*, Lafrance, B., Bécu, V., Dubé, B., Kjarsgaard, I., Guha, J. and Ross, P-S.** Geology, alteration and mineralization of the Lemoine auriferous VMS deposit, Chibougamau camp, Abitibi greenstone belt, Québec, Canada: Geologic evidence for a magmatic input
- 08:40** **Monecke, T., Gibson, H.*, McNicoll, V., Dubé, B. and Hannington, M.** Volcanological setting of the Archean world-class gold-rich Horne and Quemont VMS deposits, Blake River Group, Abitibi Greenstone Belt, Canada
- 09:00** **Dubé, B.*, Mercier-Langevin, P., Kjarsgaard, I., Hannington, M., Bécu, V., Côté, J., Moorhead, J., Legault, M. and Bédard, N.** The Bousquet 2-Dumagami world-class Archean Au-rich volcanogenic massive sulphide deposit, Abitibi: Metamorphosed submarine advanced argillic alteration footprint and genesis
- 09:20** **Yergeau, D.*, Mercier-Langevin, P., Dubé, B., Malo, M., Bernier, C., Savoie, A. and Simard, P.** Synvolcanic Au-Cu ± Ag-Zn-Pb massive sulphides, veins and disseminations of the Westwood deposit, Abitibi greenstone belt, Québec
- 09:40** **Wartman, J., Morton, R. and Hudak, G.*** Physical volcanology and hydrothermal alteration at the Rainy River gold project, NW Ontario
- 10:00** *Refreshment Break / Pause-santé*
- 10:20** **Bailes, A.H.*, Galley, A.G., Janser, B.W. and Simms, D.H.** Anatomy of a large syn-volcanic alteration zone in the stratigraphic footwall to the Au-rich Zn-Cu VMS deposit at Lalor Lake, Manitoba, Canada
- 10:40** **Caté, A.V.*, Mercier-Langevin, P., Ross, P-S., Duff, S., Hannington, M., Dubé, B. and Gagné, S.** The Paleoproterozoic Lalor VMS deposit, Snow Lake, Manitoba: Observations on the nature and architecture of the gold and base metal-rich ore zones and associated alterations

Wednesday, May 22 - Morning

SS9 MAGMATIC NI-CU-PGE-CR DEPOSITS: ORE-FORMING PROCESSES WITH IMPLICATIONS FOR EXPLORATION

Room / Salle: MR9/10

Sponsored by / Parrainé par: Northern Shield Resources Inc.

Supported by / Soutenue par: GAC Mineral Deposits Division

Organizers / Organismes: Michel Houlé, Valérie Bécu, Doreen E. Ames, Xue-Ming (Eric) Yang, Paul Gilbert

Chairs / Présidents: Michel Houlé and Paul Gilbert

08:20 Peck, D.C. Keynote (40 min): Mafic and ultramafic magmatic provinces: Deposit types, mineral endowment, prospectivity and exploration approaches

09:00 Heggie, G.*, MacTavish, A., Johnson, J. and Hollings, P. PGE-Ni-Cu versus Ni-Cu-PGE deposits: Contrasting sulphur abundance in the Midcontinent Rift

09:20 Dunlop, M.*, Ripley, E.M. and Li, C. Geochemistry and sulfur isotope characteristics of mafic dikes and intrusions associated with the Eagle magmatic Ni-Cu-PGE deposit, Upper Michigan

09:40 Smoke, R.*, Linnen, R., Samson, I., Good, D. and Shahabi-far, M. Analysis of fluid inclusions from the Marathon Cu-Pd deposit: The role of hydrothermal fluids in mineralization

10:00 *Refreshment Break / Pause-santé*

10:20 Houlé, M.G.*, McNicoll, V.J., Bécu, V., Yang, X-M. and Gilbert, H.P. New age for the Mayville Intrusion: Implication for a large mafic-ultramafic event in the Bird River greenstone belt, southeastern Manitoba

10:40 Yang, X-M.*, Gilbert, H.P., Houlé, M.G., Bécu, V., McNicoll, V.J. and Corkery, M.T. The Neoproterozoic Mayville mafic-ultramafic intrusion in the Bird River greenstone belt, southeastern Manitoba: Geological setting, geochemical variation and the implications for Cu-Ni-PGE-Cr mineral exploration

11:00 Knox, B.* and Ashton, K.E. Details from a belt of magmatic Ni-Cu occurrences and deposits preserved in a granulite facies terrain, Dodge Domain eastern Rae craton margin

SS16 IMPACT CRATERING: A GEOLOGICAL PROCESS

Room / Salle: MR15

Supported by / Soutenue par: GAC Planetary Science Division

Organizers / Organismes: Gordon Osinski, Richard Grieve

Chairs / Présidents: Gordon Osinski and Livio Tornabene

08:20 Buhlmann, E. Searching for a giant impact structure in the Flin Flon-Snow Lake area, Manitoba

08:40 Osinski, G.R.*, Abou-Aly, S., Francis, R., Marion, C.L., Pickersgill, A.E., Tornabene, L.L. and Hansen, J. Canada's newest confirmed meteorite impact structure: The Prince Albert impact structure, NWT, Canada

09:00 Deptuck, M.E.* and Campbell, D.C. Widespread margin-collapse triggered by the ~51 Ma Montagnais marine bolide impact, offshore Nova Scotia

09:20 MacDonald, W.D.* and Crosta, A. Anisotropy of magnetic susceptibility (AMS) studies in two impact structures in Parana basin basalts, Brazil

09:40 Pickersgill, A.E.*, Flemming, R.L. and Osinski, G.R. Shock metamorphism in plagioclase from the Mistastin Lake impact structure, Canada

10:00 *Refreshment Break / Pause-santé*

10:20 Marion, C.L.*, Osinski, G.R. and Linnen, R.L. Hydrothermal mineralization at the Prince Albert impact structure, Victoria Island, Canada

GENERAL SESSIONS

GS2 IGNEOUS AND METAMORPHIC PETROLOGY AND VOLCANOLOGY

Room / Salle: MR12

Supported by / Soutenue par: MAC / AMC

Organizers / Organismes: Ekaterina Reguir, Ryan Kressall

Chairs / Présidents: Ekaterina Reguir and Ryan Kressall

08:20 DeWolfe, M.Y.* and Pittman, N. Heterolithic breccia containing both fluidal- and cored-'scoria' clasts, Flin Flon, Manitoba: Evidence of submarine fire fountaining

08:40 Jugo, P.J. Sulfur partitioning between silicate melts and volatile phases: A better way to understand the "sulfur solubility minimum"?

09:00 Stewart, R.C.*, Kontak, D.J. and Ames, D.E. Petrography and fluid inclusions reflect a history of pervasive fluid-mediated metasomatism in the Granophyre Unit of the 1.85 Ga Sudbury Igneous Complex, Ontario

09:20 Jørgensen, T.R.C.*, Leshner, C.M. and Tinkham, D.K. Major and trace element geochemistry of the Elsie Mountain Formation volcanic rocks, Southern Province, Canada: Implications for contact metamorphism along the southern margin of the Sudbury Igneous Complex

Wednesday, May 22 - Morning

09:40 Chudy, T.C.* and Groat, L.A. A cathodoluminescence study of calcite-dolomite microstructures and Cal-Dol geothermometry in highly metamorphosed carbonatites: An example from the Fir carbonatite, east-central British Columbia, Canada

10:00 *Refreshment Break / Pause-santé*

10:20 Webster, E.R.* and Pattison, D.R.-M. Polyphase deformation and metamorphism in the southern Kootenay Arc and Purcell Anticlinorium, southeastern British Columbia

10:40 Fillmore, J.A.* and Coulson, I. Adakite volcanism in Canada: Petrological and geochemical constraints on the origin of the Garibaldi Volcanic Complex, southwestern British Columbia, Canada

11:00 Hébert, R.*, Guilmette, C., Dostal, J., Lesage, G., Bezard, R. and Wang, C. Miocene post-colisional shoshonites and their crustal xenoliths, Yarlung Zangbo Suture Zone, southern Tibet; Geodynamic significance

GS6 QUATERNARY GEOLOGY

Room / Salle: MR16

Organizers / Organismes: Michelle Trommelen, Roger Paulen

Chairs / Présidents: Michelle Trommelen and Roger Paulen

08:20 Paulen, R.C.*, McClenaghan, M.B., Hicken, A.K., Layton-Matthews, D., Duso, G. and Sader, J. Ice-flow history and glacial dispersal from the Izok Lake Zn-Cu-Pb-Ag volcanogenic massive sulphide deposit, Nunavut

08:40 Trommelen, M.S.*, Ross, M. and Campbell, J.E. A spatial mosaic of overprinting and inheritance within the till sheet of northeastern Manitoba

09:00 Lett, R.E. Mining a till geochemical database for new mineral prospects in British Columbia

09:00 Gao, C.*, McAndrews, J.H., Wang, X., Menzies, J., Turton, C.L., Wood, B.D., Pei, J. and Kodors, C. Late Neogene deposits and sedimentary conditions in the James Bay Lowland, Canada

09:40 McCarthy, F.M.G.*, Krueger, A.M., Danesh, D., Volik, O., Drljepan, M., Roy, H. and Hubeny, J.B. Palynological proxies of anthropogenic impact in North American lakes

10:00 *Refreshment Break / Pause-santé*

10:20 Adekanmbi, O.H. Vegetation history of the Lagos lagoon coastal environments southwestern Nigeria: A palynological approach

Wednesday, May 22 - Afternoon

SYMPOSIA

SY1 EARTH MATERIALS, PETROLOGICAL AND GEOCHEMICAL PROCESSES (IN HONOUR OF FRANK C. HAWTHORNE)

Room / Salle: MR3E

Supported by / Soutenue par: MAC / AMC

Organizers / Organismes: Elena Sokolova, Norman Halden

Chairs / Présidents: Elena Sokolova and Norman Halden

01:40 Cámara, F.* and Sokolova, E. (40 min) From chemical composition to structure topology in Ti silicates: Prediction of new structure topologies

02:20 Belley, P.M.*, Grice, J.D., Poirier, G. and Rowe, R. Serendibite from the Portage-du-Fort marble, Pontiac County, Québec

02:40 Grice, J.D.* and Kristiansen, R. Hydrogen in the Gugiaite Structure

03:00 Haring, M.* and McDonald, A. On the crystal structure of UK 79, a potentially new mineral from Mont Saint-Hilaire, QC

03:20 McDonald, A.A. On the crystal structure of UK77, a potentially new mineral from Mont Saint-Hilaire, QC: Pushing the limits of 'routine' Single-crystal X-ray Diffraction (SXRD) analyses

03:40 Martin, R.F.* and De Vito, C. The fall and rise of calcium in a granitic pegmatite, and the explanation of mixed NYF-LCT assemblages at Anjanabonoina, Madagascar

SPECIAL SESSIONS

SS2 ASSEMBLY OF NORTH AMERICA: A TECTONIC AND METALLOGENIC REAPPRAISAL

Room / Salle: MR4E

Supported by / Soutenue par: GAC Precambrian Division; GAC Volcanology and Igneous Petrology Division; GAC Planetary Sciences Division; GAC Mineral Deposits Division

Organizers / Organismes: Andrey Bekker, Sally Pehrsson, Natasha Wodicka, Christian Böhm

Chairs / Présidents: Natasha Wodicka and Christian Böhm

Wednesday, May 22 - Afternoon

- 01:40** Syme, E.C. **Keynote (40 min):** Tectonic evolution of the Paleoproterozoic Flin Flon Belt and regional setting of volcanogenic massive sulphide deposits
- 02:20** Pehrsson, S.J.*, Ramaekers, P., Fayek, M., Eglington, B.E., Rainbird, R.H. and St-Onge, M. Extent and metallogenic significance of the Racklan-Forward orogen in Canada
- 02:40** Medig, K.P.R.*, Thorkelson, D.J., Davis, W.J., Rainbird, R.H., Gibson, H.D., Turner, E.C. and Marshall, D.D. Evidence of the Laurentia-Australia connection? Detrital zircons from Mesoproterozoic strata in Yukon, Canada
- 03:00** van Nostrand, T.S. Evolution and deformation of the Mesoproterozoic Seal Lake Group in central Labrador
- 03:20** McLeish, D.F.*, Johnston, S.T., Friedman, R.M. and Mortensen, J.K. Stratigraphy and U-Pb zircon-titanite geochronology of the Aley carbonatite complex, Northeast British Columbia: Evidence for Antler-aged orogenesis in the Foreland Belt of the Canadian Cordillera
- SS5** **URANIUM: CRADLE TO GRAVE**
Room / Salle: Presentation Theatre
Supported by / Soutenue par: GAC Environmental Sciences Division
Organizers / Organismes: Peter Burns, Ginger Sigmon
Chairs / Présidents: Peter Burns and Ginger Sigmon
- 01:40** McKechnie, C.L.*, Annesley, I.R. and Ansdell, K.M. Petrogenetic model for U-Th-REE mineralized granitic pegmatites in the high-grade metamorphic rocks of the Wollaston Domain, Saskatchewan: Evidence from Fraser Lakes Zone B
- 02:00** Annesley, I.R.*, McKechnie, C.L., Mercadier, J., Armitage, A., Sexton, A. and Bogdan, T.S. Economic potential (?) for U-Th-REE-mineralized granitic pegmatites in the Wollaston Domain, northern Saskatchewan, Canada: Evidence from a resource estimate at Fraser Lakes Zone B
- 02:20** Parsons, M.B.*, Friske, P.W.G., Ford, K.L. and LeBlanc, W.K.G. Transport and fate of uranium, rare earth elements, and radionuclides from decommissioned tailings at the historical Bicroft Uranium Mine, Ontario
- 02:40** Laidlow, A.M.*, Parsons, M.B., Jamieson, H.E. and Gault, A.G. Characterization of uranium and REE mobility downstream of a uranium tailings impoundment near Bancroft, Ontario
- 03:00** Fuchs, S.*, Schumann, D., Williams-Jones, A. and Vali, H. Hydrocarbons: A source of uranium and titanium in the Witwatersrand, South Africa
- 03:20** Sharpe, R.W.*, Fayek, M., Quirt, D. and Jefferson, C.W. A genetic model for the Bong uranium deposit, Thelon Basin, Nunavut, Canada
- 03:40** Othmane, G.*, Allard, T., Morin, G., Sélo, M., Llorens, I., Chen, N., Brest, J., Fayek, M. and Calas, G. Uranium-bearing phases in mill tailings from Gunnar, Canada
- SS6** **RARE EARTH ELEMENTS IN MELTS, FLUIDS AND CRYSTAL STRUCTURES**
Room / Salle: MR7/8
Supported by / Soutenue par: MAC / AMC
Organizers / Organismes: Anton Chakhmouradian, Ian Coulson
Chairs / Présidents: Anton Chakhmouradian, Ian Coulson
- 01:40** Purdy, C.J.K.* and Jamieson, H.E. Rare earth elements in tailings leachate from Nechalacho, Northwest Territories: Are they truly dissolved?
- 02:00** Feng, Y.* and Samson, I. Character of mineralizing fluids in the T-Zone, Thor Lake rare-element deposit: Implications for HFSE mobility and mineralization
- 02:20** Timofeev, A.* and Williams-Jones, A. Niobium and tantalum mineralization in the Nechalacho REE deposit, NWT, Canada
- 02:40** Moore, M.A.*, Chakhmouradian, A.R., Sidhu, R., Yang, P., Mariano, A.N. and Spencer, E.A. Rare-earth mineralization in the Bear Lodge alkaline complex, Wyoming: Mineralogical and isotopic characteristics
- SS7** **PRECIOUS AND RARE METALS IN THE VOLCANOGENIC MASSIVE SULFIDE ENVIRONMENT**
Room / Salle: MR2E
Supported by / Soutenue par: GAC Mineral Deposits Division
Organizers / Organismes: Patrick Mercier-Langevin, Harold Gibson, Simon Gagné
Chairs / Présidents: Patrick Mercier-Langevin, Harold Gibson, Simon Gagné
- 01:40** Lam, J.*, Tinkham, D.K. and Gibson, H.L. Identification of metamorphic assemblages and textures associated with gold mineralization at the Lalor deposit, Snow Lake, MB
- 02:00** Engelbert, M.S.*, Gibson, H.L. and Lafrance, B. Gold enrichment in the auriferous Photo Lake deposit, Snow Lake, Manitoba

Wednesday, May 22 - Afternoon

02:20 Totenhagen, C.F.*, Hudak, G.J., Morton, R.L. and Quigley, T.O. Stratigraphy and physical volcanology associated with the Paleoproterozoic Back Forty VMS deposit, Menominee County, Michigan

02:40 Pilote, J-L.*, Piercey, S.J., Pilgrim, L. and Legrow, P. Volcano-stratigraphic relationships, lithogeochemistry, and structural analysis of the 1807 zone, Ming Mine, Baie Verte Peninsula, Newfoundland

03:00 Lode, S.*, Piercey, S.J., Devine, C.A., Layne, G.D. and Piercey, G. Lithogeochemistry and sulfur isotopic composition of hydrothermal mudstones associated with the Lemarchant volcanogenic massive sulfide (VMS) deposit, Tally Pond belt, central Newfoundland

03:20 McClenaghan, S.H. Rare earth elements in volcanogenic massive sulfides: Evidence for their origin from hydrothermal gangue minerals

03:40 Lalonde, E.* and Beaudoin, G. The metallogeny of the Turgeon deposit: A middle Ordovician volcanogenic massive sulfide (VMS) deposit in Belledune, New Brunswick

SS9 MAGMATIC NI-CU-PGE-CR DEPOSITS: ORE-FORMING PROCESSES WITH IMPLICATIONS FOR EXPLORATION

Room / Salle: MR9/10

Sponsored by / Parrainé par: Northern Shield Resources Inc.

Supported by / Soutenue par: GAC Mineral Deposits Division

Organizers / Organismes: Michel Houlié, Valérie Bécu, Doreen E. Ames, Xue-Ming (Eric) Yang, Paul Gilbert

Chairs / Présidents: Eric Yang and Valérie Bécu

01:40 Lesher, C.M. Keynote (40 min): The roles of local incorporation, *in-situ* segregation, and physical transport in the genesis of magmatic sulfide and oxide deposits

02:20 Laarman, J.E.*, Barnett, R.L., Duke, N.A. and Weston, R.L. Petrogenesis and mineral chemistry of the McFaulds Lake chromite deposits

02:40 Carson, H.J. E.*, Lesher, M., Houlié, M.G., Metsaranta, R.T. and Shinkle, D.A. Komatiite-associated Cr and Ni-Cu-(PGE) mineralization in the Black Thor – Black Label ultramafic intrusion, McFaulds Lake greenstone belt, Canada

03:00 Franchuk, A.*, Lightfoot, P. and Kontak, D. High tenor Ni-PGE sulfide mineralization in the South Managan ultramafic intrusion, Thompson Nickel Belt, Manitoba

03:20 Manor, M.J.*, Scoates, J.S., Nixon, G.T. and Ames, D.E. Ultramafic intrusions in orogenic terrains: Late Cretaceous Ni-Cu-(PGE) mineralization at the Giant Mascot sulfide deposit, Hope, B.C.

03:40 Jackson-Brown, S.*, Scoates, J.S., Nixon, G.T. and Ames, D.E. Orogenic Ni-Cu-PGE deposits: Cu-PGE mineralization in the DJ/DB Zone of the Turnagain Alaskan-type intrusion, north-central British Columbia, Canada

SS15 GEOMICROBIOLOGICAL AND BIOGEOCHEMICAL ADVANCES IN ENVIRONMENTAL SYSTEMS

Room / Salle: MR15

Supported by / Soutenue par: GAC Environmental Earth Science Division

Organizers / Organismes: Ian Power, Lachlan MacLean

Chairs / Présidents: Ian Power and Lachlan MacLean

01:40 Lindsay, M.B.J. Keynote (40 min): Long-term biogeochemistry of mine tailings amended with organic carbon for managing water quality

02:20 Fortin, D.*, Najem, T. and Cotroneo, S. Characterization of fresh and aged biogenic iron oxides (BIOS)

02:40 Gault, A.G. *, Jamieson, H.J., Sherriff, B.L., Londry, K.L., Johnson, B.C., Davidson, S. and Harrington, J.M. Mechanisms of natural Zn attenuation in No Cash Creek, Yukon, Canada

03:00 Weisener, C.G. Investigating the development of biogeochemical redox gradients in Alberta oil sands tailings ponds

03:20 Power, I.M.*, Harrison, A.L., Dipple, G.M., Wilson, S.A. and Southam, G. Microbially and biochemically facilitated carbon sequestration

SS19 FEATURED ARTICLES IN GEOSCIENCE CANADA

Room / Salle: MR11

Organizers / Organismes: Brendan Murphy

Chairs / Présidents: Michelle Nicolas and Derek Armstrong

01:40 Rainbird, R.*, Behnia, P. and Harris, J.R. Remote predictive geological mapping utilizing high resolution satellite imagery, western Minto Inlier, Victoria Island, NWT

02:00 Ootes, L.*, Gleeson, S., Turner, E., Rasmussen, K., Gordey, S., Falck, H., Martel, E. and Pierce, K. Keynote (40 min): Metallogenic evolution of the Mackenzie and eastern Selwyn mountains of Canada's northern Cordillera, Northwest Territories: A compilation and review

02:40 Boggs, K.J.E.*, Dordevic, M.M. and Shipley, S.T. Keynote (40 min): Grotto Creek, Front Ranges, Canadian Cordillera; a Google Earth® Model with COLLADA and Wxazygy® Transparent Interface.

Wednesday, May 22 - Afternoon

03:20 Keppie, D.F. Keynote (40 min): A tale of two triple junctions

GENERAL SESSIONS

GS2 IGNEOUS AND METAMORPHIC PETROLOGY AND VOLCANOLOGY

Room / Salle: MR12

Supported by / Soutenue par: MAC / AMC

Organizers / Organisateurs: Ekaterina Reguir, Ryan Kressall

Chairs / Présidents: Ryan Kressall and Ekaterina Reguir

01:40 McCarron, T.* and Gaidies, F. Coupling garnet growth modeling and *in situ* LA-ICP-MS monazite geochronology: Unraveling the Grenvillian orogeny in the Mazinaw Domain of southeastern Ontario

02:00 Timmermans, A.C.*, Cousens, B.L. and Henry, C.D. Geochemistry and geochronology of Tertiary magmatism from the north-central Great Basin, Nevada, to the Ancestral Cascade Arc, California

02:20 Pathak, V.*, Patil, S.K. and Shrivastava, J.P. Low field AMS and rock magnetic studies on the lava flows from Mandla lobe of the eastern Deccan volcanic province, India

02:40 Papoutsas, A.*, Pe-Piper, G. and Piper, D. Variation in REE-enrichment of A-type granites in complex shear zones, Cobequid Highlands, Nova Scotia

03:00 Nair, R.*, Chacko, T., Verwimp, J. and McDowell, K. Did komatiites contribute to TTG formation in the Archean?

GS7 GIS AND REMOTE SENSING

Room / Salle: MR16

Organizers / Organisateurs: Wool Moon

Chairs / Présidents: Wool Moon

01:40 Shelat, Y., Harris, J.R.*, LaRocque, A., Leblon, B., Jefferson, C., Lentz, D. and Tschirhart, V. Mapping lineaments in Nunavut using multi-beam RADARSAT-2 polarimetric SAR and LANDSAT7-ETM+ images

02:00 Harris, J.R.*, Behnia, P. and Rainbird, R. Remote predictive geological mapping of western Minto Inlier, Victoria Island, NWT: Application of quantitative classification techniques

02:20 Lee, S.K.Y.*, Lenton, M. and Keller, G. GeoCapture – Geological and geochemical database management system for drill hole and surface data

Poster Session I – Wednesday, May 22, 2013

- SY1 EARTH MATERIALS, PETROLOGICAL AND GEOCHEMICAL PROCESSES (IN HONOUR OF FRANK C. HAWTHORNE)**
Supported by / Soutenue par: MAC / AMC
Organizers / Organiseurs: Elena Sokolova, Norman Halden
- SY1-P1 Tait, K.T.*, Chu, K. and Abdu, Y.** Garyansellite and kryzhanovskite from Rapid Creek, Yukon, Canada
- SY1-P2 Reusser, D.*, Elliott, W.S., Casey, W.H. and Navrotsky, A.** Aluminum hydroxide molecular clusters to minerals - Comparison of the thermochemistry of solid ϵ -GaAl₁₂ and flat-Al₁₃ to ϵ -Al₁₃ Keggin compounds
- SY1-P3 Lussier, A.J.* and Hawthorne, F.C.** Structural isomerism in minerals based on octahedral [M^{VI}O₄] chains
- SY1-P4 Škoda, R., Novák, M.*, Havránek, V. and Lens, C.** Solid solutions between silicate and phosphate minerals of the olivine structure type: Example from Pøibyslavice metagranite, Czech Republic
- SY1-P5 Clark, C.M.*, Cymes, B.A., Guzelaydin, E. and Badgerow, C.J.** Occupancy of the X-site in povondraite
- SY1-P6 Tweedale, F., Hanley, J., Kontak, D.* and Rogers, N.** Evaporate mound analysis of quartz-hosted fluid inclusions by SEM/EDS: Evaluation and application of method to assess granitoid metal fertility
- SY1-P7 Bosi, F.* and Andreozzi, G.B.** Site preference of Fe²⁺ and Mn²⁺ in tourmaline: Considerations on the inductive effects of and on mean bond distances
- SS2 ASSEMBLY OF NORTH AMERICA: A TECTONIC AND METALLOGENIC REAPPRAISAL**
Supported by / Soutenue par: GAC Precambrian Division; GAC Volcanology and Igneous Petrology Division; GAC Planetary Sciences Division; GAC Mineral Deposits Division
Organizers / Organiseurs: Andrey Bekker, Sally Pehrsson, Natasha Wodicka, Christian Böhm
- SS2-P1 Pavlova, G.G.*, Borisenko, A.S., Lebedev, V.I., Tretiakova, I.G. and Prokopiev, I.R.** Cobalt and silver mineralization of Central Asia
- SS2-P2 Daoudene, Y.*, Tremblay, A., Goutier, J. and Ruffet, G.** Tectono-metamorphic relationships of the Abitibi greenstone belt and the Opatika plutonic belt: Insights from the lac-au-Goéland area, northern Québec
- SS2-P3 Seifert, T.* and Sandmann, D.** The giant Beaver Brook antimony deposit, central Newfoundland, Canada
- SS2-P4 Harris, L.B.*, Bédard, J.H. and Dufréchoy, G.** SCLM rifting in the SE Superior Craton – Implications for deformation and mineralization in the Abitibi and Grenville Province and tectonic reconstructions
- SS2-P5 Bryksin, A.*, Frederiksen, A.W., Zaporozan, T., Darbyshire, F.A., Snyder, D. and Van der Lee, S.** Project NA13: Towards an updated tomographic model of the Canadian lithosphere
- SS5 URANIUM: CRADLE TO GRAVE**
Supported by / Soutenue par: GAC Environmental Sciences Division
Organizers / Organiseurs: Peter Burns, Ginger Sigmon
- SS5-P1 Adelani, P.O.* and Burns, P.C.** Base and solvent-driven formation of hybrid uranyl nanocages
- SS5-P2 Liu, Y.*, Jouffret, L., Szymanowski, J.E. S. and Burns, P.C.** Sequestration of uranium in mesoporous silica SBA-15 as uranyl clusters
- SS5-P3 Wylie, E.M.*, Phillip, W.A. and Burns, P.C.** New filtration methods for the aqueous separation of uranyl peroxoclusters from simulated used nuclear fuel
- SS5-P4 Sejkora, J., Plasil, J.*, Hlousek, J. and Skoda, R.** Unusual supergene U⁴⁺ minerals from the Geschieber vein, Jáchymov, Czech Republic
- SS5-P5 Turner, K.M.*, Zhang, F. and Ewing, R.C.** High pressure structural response of U60
- SS5-P6 Tiwari, S.* and Maginn, E.** Stabilities of actinyl ion complexes in aqueous phase
- SS5-P7 Liang, R.*, Chi, G., Ashton, K. and Normand, C.** Characterization of fluids associated with uranium mineralization in the Beaverlodge area, northern Saskatchewan
- SS5-P8 Nelson, A-G.D.*, Albrecht-Schmitt, T. and Ewing, R.** Hydrothermal synthesis, crystal structure, and characterization of three silver uranium diphosphonate and a 3D thorium carboxylate
- SS5-P9 Park, S.** Computational study of plutonium (VI) and uranium (VI) complex reduction on quartz surface (100)
- SS5-P10 Pellegrini, K.L.*, Martinez, N., Jouffret, L.J., Fein, J.B. and Burns, P.C.** Dissolution studies of autunite minerals

Poster Session I – Wednesday, May 22, 2013

- SS5-P11** **Solomon, J.M.*, Alexandrov, V., Shvarevac, T.Y., Sadigh, B., Navrotsky, A. and Asta, M.** Computational study of energetics and defect-ordering tendencies for Y and La in UO_2
- SS5-P12** **Guo, X.*, Tavakoli, A.H., Shvareva, T. and Navrotsky, A.** Synthesis and energetics of lanthanide and actinide substituted garnet
- SS5-P13** **Shabaga, B.M.*, Fayek, M., Guo, W. and Zhanjiu, W.** Petrography and uranium mineralogy of the BaiYangHe volcanic-hosted uranium deposit, Xinjiang Autonomous Region, China
- SS5-P14** **Oh, G.N.* and Burns, P.C.** Chemistry of the uranyl – sulfide systems
- SS6** **RARE EARTH ELEMENTS IN MELTS, FLUIDS AND CRYSTAL STRUCTURES**
Supported by / Soutenue par: MAC / AMC
Organizers / Organiseurs: Anton Chakhmouradian, Ian Coulson
- SS6-P1** **Coulson, I.M.** Rare earth elements and their (sub) economic redistribution: An example from the North Qôroq nepheline syenite centre of South Greenland
- SS6-P3** **Olinger, D.A.** Hydrothermal remobilization of rare earth elements in a carbonatite-hosted rare earth element deposit, Bear Lodge Mountains, Wyoming
- SS6-P4** **Feng, Y.* and Samson, I.** Mobilization and precipitation of HFSE in the T-Zone, Thor Lake rare-element deposit: Insights from mass balance calculations
- SS6-P5** **Elliott, R.*, Ansdell, K.M., Harper, C.T., Pandur, K. and Pearson, J.G.** Field relationships, petrography and geochemistry of lamprophyre dykes from the Hoidas Lake area, Zemplin Domain, Saskatchewan
- SS6-P6** **Souza Neto, J.A.* and Santos, E.J.** HREE and Y anomalies in U-mineralized granites of the São José de Espinharas deposit, northeastern Brazil: Evidence of the composition of ore-forming metasomatic fluids
- SS7** **PRECIOUS AND RARE METALS IN THE VOLCANOGENIC MASSIVE SULFIDE ENVIRONMENT**
Supported by / Soutenue par: GAC Mineral Deposits Division
Organizers / Organiseurs: Patrick Mercier-Langevin, Harold Gibson, Simon Gagné
- SS7-P1** **Pilchin, A.* and Pilchin, M.** Sulfur generations, formation of sulfide deposits and their association with platinum group elements
- SS7-P2** **Gill, S.B.*, Piercey, S.J., Devine, C.A. and Copeland, D.A.** Mineralogy and styles of barite-rich Zn-Pb-Ba-Ag-Au mineralization in the Lemarchant volcanogenic massive sulfide (VMS) deposit
- SS7-P3** **Mercier-Langevin, P.*, Hannington, M., Dubé, B., McNicoll, V., Goutier, J. and Monecke, T.** Geodynamic influences on the genesis of Archean world-class gold-rich VMS deposits: Examples from the Blake River Group, Abitibi greenstone belt, Canada
- SS7-P4** **Duff, S.*, Hannington, M., Caté, A., Mercier-Langevin, P., Kjarsgaard, I., Dubé, B. and Gagné, S.** Major ore types of the Lalor gold-rich massive sulfide deposit, Snow Lake, Manitoba
- SS7-P5** **Lima, A.M.C.*, Rodrigues, B.C., Oliveira, A. and Guimaraes, F.** Recent research on indium from The Lagoa Salgada orebody, Iberian Pyrite Belt, Portugal
- SS9** **MAGMATIC NI-CU-PGE-CR DEPOSITS: ORE-FORMING PROCESSES WITH IMPLICATIONS FOR EXPLORATION**
Sponsored by / Parrainé par: Northern Shield Resources Inc.
Supported by / Soutenue par: GAC Mineral Deposits Division
Organizers / Organiseurs: Michel Houllé, Valérie Bécu, Doreen E. Ames, Xue-Ming (Eric) Yang, Paul Gilbert
- SS9-P1** **Turchiaro, F.* and Brennan, J.** Experimental investigation of Pt and Rh solubility in basalt-rhyolite mixtures
- SS9-P2** **Meghji, I.*, Linnen, R., Samson, I., Ames, D. and Good, D.** The character and distribution of Cu-PGE mineralization at the Geordie Lake deposit within the Coldwell Complex, Ontario
- SS9-P3** **Meal, C.A.*, Linnen, R.L., Lin, S., Theyer, P. and Corkery, M.** Bird River Intrusive Complex in the western Superior Province, Manitoba: Evidence for a conduit model and controls on Ni-Cu-PGE and Cr mineralization
- SS9-P5** **MacInnis, L.M.*, Kontak, D.J., Ames, D.M. and Rayner, N.M.** Unraveling the nature and origin of the Grey Gabbro unit, host to the Podolsky Cu-Ni-PGE deposit, Sudbury, Ontario
- SS9-P6** **Bécu, V.*, Houllé, M.G., McNicoll, V.J., Yang, X.M. and Gilbert, P.H.** New insights from textural, petrographic and geochemical investigation of the gabbroic rocks of the Bird River Intrusive Event within the Bird River greenstone belt, southeastern Manitoba

Poster Session I – Wednesday, May 22, 2013

- SS9-P7** **Cafagna, F.* and Jugo, P.J.** Experimental study on the mobility of highly siderophile elements complexed with Te, Bi, and As
- SS9-P8** **Adibpour, M.*, Jugo, P.J. and Ames, D.E.** Trace element distribution in sulfide assemblages from the Levack-Morrison ore system, Sudbury, Ontario: Looking for chemical fingerprints of ore processes
- SS16** **IMPACT CRATERING: A GEOLOGICAL PROCESS**
Supported by / Soutenue par: GAC Planetary Science Division
Organizers / Organiseurs: Gordon Osinski, Richard Grieve
- SS16-P1** **Craig, M.A.*, Flemming, R.L., Osinski, G.R., Cloutis, E.A., Anderson, J., Izawa, M.R., Sapers, H.M. and Marion, C.L.** XRD patterns of glassy impactites: Correlating composition and origin via cluster variation analysis and implications for Mars
- SS16-P2** **Tornabene, L.L.*, Ling, V., Osinski, G.R., Boyce, J.M., Harrison, T.N. and McEwen, A.S.** A revised global depth-diameter scaling relationship for Mars based on pitted impact melt-bearing craters
- SS16-P3** **Abou-Aly, S.*, Osinski, G., Marion, C., Hansen, J., Pickersgill, A. and Francis, R.** Preliminary magnetic study of the newly discovered Prince Albert impact structure
- SS16-P4** **Glombick, P.*, Schmitt, D., Xie, W. and Bown, T.** Bow City, Alberta: A possible new impact structure?
- GS2** **IGNEOUS AND METAMORPHIC PETROLOGY AND VOLCANOLOGY**
Supported by / Soutenue par: MAC / AMC
Organizers / Organiseurs: Ekaterina Reguir, Ryan Kressall
- GS2-P1** **Greenfield, A-M.R., Ghent, E.D.* and Russell, J.K.** Geothermobarometry of spinel peridotites from southern British Columbia: Implications for the thermal conditions in the upper mantle
- GS2-P2** **Hastie, E.C.G.*, Gagnon, J.E. and Samson, I.M.** Toward an integrated geologic, geochemical, and structural model for formation of the MacLellan Au-Ag and related mineral deposits, Lynn Lake, Manitoba
- GS2-P3** **Lafrance, S.* and Jébrak, M.** Gold mineralisations in the Duquesne-Ottoman property, Abitibi greenstone belt, Quebec, Canada
- GS2-P4** **Groulier, P-A.*, Ohnenstetter, D., Andre-Mayer, A-S., Solgadi, F., Mouhksil, A. and El Basbas, A.** Pegmatitic nepheline syenitic dyke swarm in the Crevier alkaline intrusion (Quebec)
- GS2-P5** **Glendenning, M.W.P.*, Gagnon, J.E. and Polat, A.** The MacLellan Au-Ag deposit, Lynn Lake, Manitoba: Characterization of host rock lithologies using field relationships, petrography, and lithogeochemistry
- GS6** **QUATERNARY GEOLOGY**
Organizers / Organiseurs: Michelle Trommelen, Roger Paulen
- GS6-P1** **Nguyen, M.K.*, Hicock, S.R. and Barnett, P.J.** Quaternary glaciation and stratigraphy of the Ridge River area, northern Ontario
- GS6-P2** **Fenton, M.M.*, Waters, J.E., Pawley, S.M., Atkinson, N., Utting, D.J. and McKay, K.** Map 601 the first surficial geology map of Alberta: Creation and content
- GS6-P3** **Charbonneau, R.* and Cayer, A.** Brecciation of preglacial alterite and injection of diamictic debris: A sharp contrast in rheological behaviour between two unconsolidated materials in the subglacial environment, Montviel carbonatite complex, Abitibi, Québec
- GS7** **GIS AND REMOTE SENSING**
Organizers / Organiseurs: Wooil Moon
- GS7-P1** **Raisuddin, I.*, Wolfe, R. and Bank, C.** Geophysical applications for non-invasive forensic searches

Poster Sessions I and II are sponsored by HudBay Minerals Inc.

The logo for HudBay, featuring the word "HudBay" in a bold, sans-serif font. The "H" and "B" are significantly larger and more prominent than the other letters, with the "u" and "a" nestled between them. The "y" is also large and extends downwards.



Thursday Technical Program

Programme du jeudi

	Present. Theatre	MR2E	MR3E	MR4E	MR7/8	MR9/10	MR11	MR12	MR15	MR16	(2 nd Floor) MRE	Exhibits Hall
8:20	SY1 <i>cont.</i> Earth Materials (Hawthorne)	SY2 Granitic Pegmatites (Černý)	SS5 <i>cont.</i> Uranium: Cradle to Grave	SS3 Superior Province	SY3 & Intro Phanerozoic Seas (Ludvigsen)	SS9 <i>cont.</i> Ni-Cu- PGE-Cr	SS12 Adv. in Exploration Techniques	SS10 Metamorph. in the Ore Environment		SS17 Planetary Geology & Astrobiology	SS22 (8:30) First Nations Geoscience	E X H I B I T S
9:40												
10:00	Refreshment Break / Pause-santé											
10:20	SY1 <i>cont.</i> Earth Materials (Hawthorne)	SY2 Granitic Pegmatites (Černý)	SS5 <i>cont.</i> Uranium: Cradle to Grave	SS3 Superior Province	SY3 Phanerozoic Seas (Ludvigsen)	SS8 Layered Mafic Int.	SS12 Adv. in Explor. ...	SS10 Metamorph. in the Ore Environment	GS3 Geochem and Geochron	SS17 Planetary Geology ...	SS22 First Nations Geoscience Discussion	
11:00												
11:20	PLENARY ADDRESS: <i>The Origin of Laurentia</i> Paul F. Hoffman, Harvard University & University of Victoria Presentation Theatre, Winnipeg Convention Centre, 11:20 - 12:00 pm											I B I T S
12:00	MAC LUNCHEON - Pan-Am Room, Winnipeg Convention Centre, 12:00 - 1:40 pm											
13:40	SY1 <i>cont.</i> Earth Materials (Hawthorne)	SY2 <i>cont.</i> Granitic Pegmatites (Černý)	SS5 <i>cont.</i> Uranium: Cradle to Grave	SS3 <i>cont.</i> Superior Province	SY3 <i>cont.</i> Phanerozoic Seas (Ludvigsen)	SS8 <i>cont.</i> Layered Mafic Intrusions	SS14 Prairie Hydrology	SS10 <i>cont.</i> Metamorph. in the Ore Environment	GS3 <i>cont.</i> Geochem and Geochron	SS18 Astro- materials	(1:20) SS22 <i>cont.</i> First Nations Geoscience & Discussion	
15:00												
15:20												
15:40												
	POSTERS (Exhibits Hall): SY2 (10), SS1 (2), SS3 (3), SS4 (2), SS8 (2), SS11 (1), SS12 (1), SS13 (9), SS14 (2), SS18 (3), SS23 (2), GS1 (6), GS3 (3), GS4 (4), GS5 (2)											Posters 4-6 pm

Presentations are listed for each Symposium, Special Session and General Session. For oral presentations, the speaker is indicated with an asterisk. Poster presenters for the sessions shown must be in attendance between 4:00 p.m. and 6:00 p.m. to discuss their poster with conference attendees. A cash bar will be available in the Exhibits Hall at this time.

Les présentations sont listées pour chaque symposium, session spéciale et session générale. Pour les présentations orales le(la) conférencier(ère) est indiqué(e) avec un astérisque. Les présentateurs des affiches pour les sessions indiquées doivent être sur place entre 16h00 et 18h00 pour discuter du contenu de leur présentation. Un bar payant sera disponible dans la salle d'exposition des affiches. Aucune nourriture ni boisson n'est permise au Presentation Theatre.

Thursday, May 23 - Morning

SYMPOSIA

SY1 EARTH MATERIALS, PETROLOGICAL AND GEOCHEMICAL PROCESSES (IN HONOUR OF FRANK C. HAWTHORNE)

Room / Salle: Presentation Theatre

Supported by / Soutenue par: MAC / AMC

Organizers / Organisateurs: Elena Sokolova, Norman Halden

Chairs / Présidents: Elena Sokolova and Norman Halden

08:20 Williams, P.A. (40 min) The supergene geochemistry of antimony and bismuth

09:00 Uvarova, Y. and Kyser, K.* Applied mineralogy using short-wave infrared reflectance spectroscopy to define temperatures of clay alteration around ore deposits

09:20 Oberti, R.*, Boiocchi, M., Welch, M.D. and Zema, M. Towards a model for HT behaviour of (orthorhombic and monoclinic) amphiboles

09:40 Henry, D.J.*, Mogk, D.W., Mueller, P.A., Foster, D.A., Wooden, J.L. and Dutrow, B.A. Upper-to-middle level exposure of a 2.8 Ga continent in the northern Wyoming Province, USA: Petrologic-mineralogical evidence

10:00 *Refreshment Break / Pause-santé*

10:20 Schindler, M. Rock coatings: Forensic tools for atmospheric compositions

10:40 Fayek, M.* and Hawthorne, F.C. Fingerprinting turquoise and tourmaline using isotopic techniques

11:00 Hughes, J.M.* and Nekvasil, H. Solid solution in the (F, OH, Cl) apatite ternary system

SY2 GRANITIC PEGMATITES - FROM FASCINATING CRYSTALS TO HIGH-TECH ELEMENTS (IN HONOUR OF PETR ČERNÝ)

Room / Salle: MR2E

Supported by / Soutenue par: MAC / AMC

Organizers / Organisateurs: Milan Novák

Chairs / Présidents: Milan Novák

08:20 London, D. Keynote (40 min): Petrologic assessment of zonation within granitic pegmatites

09:00 Maneta, V.* and Baker, D.R. Developing pegmatitic textures in a Li-rich granitic system - an experimental perspective

09:20 Kremer, P.D.*, Davis, D.W., Lin, S. and Linnen, R.L. Syn-deformational emplacement of the Bernic Lake pegmatite group, Bird River greenstone belt, southeastern Manitoba

09:40 Bynoe, L.*, Linnen, R., Jiang, D., Davis, D. and Woulfe, J. Factors controlling the emplacement of the giant Whabouchi lithium pegmatite, Quebec, Canada

10:00 *Refreshment Break / Pause-santé*

10:20 Grew, E.S.*, Maas, R. and Carson, C.J. Isotopic constraints on the source of pegmatites with boron and beryllium minerals in the Larsemann Hills, Prydz Bay, Antarctica

10:40 Magna, T., Novák, M.* and Janoušek, V. Lithium isotopes in giant pegmatite bodies – implications for their sources and evolution

11:00 Burns, M.G.G.*, Kontak, D.J., McDonald, A., Groat, L.A. and Kyser, K.T. Implications of stable isotopes ($\delta^{18}\text{O}$, δD , $\delta^{13}\text{C}$) for magma and fluid sources in an LCT pegmatite swarm in the NWT, Canada: Evidence for involvement of multiple fluid reservoirs

SY3 LIFE AND TIMES OF PHANEROZOIC SEAS (IN HONOUR OF ROLF LUDVIGSEN)

Room / Salle: MR7/8

Supported by / Soutenue par: GAC Paleontology Division

Organizers / Organisateurs: Brian Pratt, Nigel Hughes, Ed Landing, Godfrey Nowlan, Dave Rudkin, Steve Westrop, Graham Young

Chairs / Présidents: Steve Westrop and Brian Pratt

08:20 Steve Westrop *Rolf Ludvigsen: The Man and His Science*

08:40 Pratt, B.R.* and Zhang, X-g. The Ediacaran Doushantuo microbiota: Animal, mineral or vegetable?

09:00 Hughes, N.C.*, Balint, M.B. and Caron, J-B. Evaluating the degree of transport and time averaging among Burgess Shale fossil assemblages via taphonomic analysis of the trilobite *Elrathina cordillerae*

09:20 Kimmig, J.* and Pratt, B.R. A new middle Cambrian Burgess Shale-type Lagerstätte from the Middle Cambrian of the Mackenzie Mountains, Northwest Territories, Canada

09:40 Young, G.A.*, Rudkin, D.M., Dobrzanski, E.P., Cuggy, M.B., Robson, S.P., Demski, M.W., Thompson, D.P. and Stewart, L.A. The edge of a warm sea: Harmonious progression of facies and biotas at the Ordovician William Lake Lagerstätte, Manitoba

10:00 *Refreshment Break / Pause-santé*

10:20 Rudkin, D.M. The green book – A Ludvigsen legacy

10:40 Boyce, W.D. *Bathyrus perplexus* Billings, 1865, not so perplexing

11:00 Westrop, S.R.*, Amati, L., Carlucci, J.R. and Brett, C.E. Foreland basin formation, environmental change and trilobite paleoecology, Late Ordovician of eastern Laurentia

Thursday, May 23 - Morning

SPECIAL SESSIONS

SS3 TECTONIC EVOLUTION AND METALLOGENY OF THE SUPERIOR PROVINCE: NEW INSIGHTS FROM THE NORTH CARIBOU TERRANE, THE "RING OF FIRE", AND BEYOND

Room / Salle: MR4E

Supported by / Soutenu par: GAC Precambrian Division; GAC Volcanology and Igneous Petrology Division; GAC Mineral Deposits Division
Organizers / Organismes: Scott Anderson, Christian Böhm, Tim Corkery, Peter Hollings
Chairs / Présidents: Peter Hollings

08:20 Harris, L.B.* and Bédard, J.H. Keynote (40 min): Crustal evolution and deformation of the Abitibi Subprovince, Superior Craton, Canada in a non-plate tectonic Archean Earth – comparisons with Venus

09:00 Bédard, J.H.* and Harris, L.B. Keynote (40 min): Disaggregation and reassembly of the Superior Craton on a subductionless, stagnant-lid Archean Earth

10:00 Refreshment Break / Pause-santé

10:20 Percival, J.A. Keynote (40 min): Superior Province: The orogenic context

SS5 URANIUM: CRADLE TO GRAVE

Room / Salle: MR3E

Supported by / Soutenu par: GAC Environmental Sciences Division
Organizers / Organismes: Peter Burns, Ginger Sigmon
Chairs / Présidents: Peter Burns and Ginger Sigmon

08:20 Albrecht-Schmitt, T.E. The strange structures and unusual properties of actinide borates

08:40 Plasil, J. Broadening the knowledge of the crystal chemistry of zirconite-group minerals

09:00 Gurchiy, V.V.*, Krivovichev, S.V. and Tananaev, I.G. Crystal chemistry of uranyl selenates

09:20 Kovrugin, V.*, Gurchiy, V. and Krivovichev, S. Application of the principle of dimensional reduction to uranyl oxysalts with monovalent cations

09:40 Balboni, E.* and Burns, P.C. Inorganic controls on the incorporation of Np(V) and U(VI) in carbonate, sulfate and borate minerals

10:00 Refreshment Break / Pause-santé

10:20 Walker, S.M.* and Becker, U. A first-principles study of uranyl and neptunyl incorporation into sulfate minerals

10:40 Koeman, E.C.*, Simonetti, A., Bellucci, J., Wallace, C. and Burns, P.C. Deciphering the origin of red inclusions within trinitite using *in-situ* chemical and isotopic (Pb & U) evidences

11:00 Corrales, L.R. Solubility and partitioning of actinide complexes in aqueous alkane Bi-phasic systems

SS8 LAYERED INTRUSIONS: NEW PARADIGMS AND APPROACHES TO UNDERSTANDING MAGMATIC PROCESSES

Room / Salle: MR9/10

Supported by / Soutenu par: MAC / AMC
Organizers / Organismes: James S. Scoates, Jim Miller
Chairs / Présidents: Jim Miller and James Scoates

10:00 Refreshment Break / Pause-santé

10:20 Maier, W.D.*, Barnes, S-J. and Groves, D.I. Keynote (40 min): Petrogenesis of the Bushveld Complex and its PGE-Cr-V deposits

SS9 MAGMATIC NI-CU-PGE-CR DEPOSITS: ORE-FORMING PROCESSES WITH IMPLICATIONS FOR EXPLORATION

Room / Salle: MR9/10

Sponsored by / Parrainé par: Northern Shield Resources Inc.
Supported by / Soutenu par: GAC Mineral Deposits Division
Organizers / Organismes: Michel Houllé, Valérie Bécu, Doreen E. Ames, Xue-Ming (Eric) Yang, Paul Gilbert
Chairs / Présidents: Doreen Ames and Paul Gilbert

08:20 Dare, S.A. S.*, Ames, D., Lightfoot, P.C., Barnes, S-J. and Beaudoin, G. Trace elements in Fe-oxides from fertile and barren igneous complexes: Investigating their use as an exploration tool for Ni-Cu-PGE deposits

08:40 Pagé, P.* and Barnes, S-J. Chromite composition by LA-ICP-MS: Upgraded petrogenetic and provenance tools, the new generation

09:00 Méric, J.*, Pagé, P., Barnes, S-J. and Houllé, M. Trace element and PGE content of chromites from komatiites in the Alexo area (Abitibi, Ontario) and implication for exploration: A LA-ICP-MS study

09:20 Hiebert, R.S.*, Bekker, A., Houllé, M.G., Leshner, C.M. and Wing, B.A. Multiple sulfur isotopes and the Hart komatiite-hosted Ni-deposit, Abitibi Greenstone Belt, Ontario: Evaluating and tracing the signature of contamination in komatiite

09:40 Brennan, J.M. Effect of sulfur on the solubility of platinum in molten silicate: Preliminary results

10:00 Refreshment Break / Pause-santé

Thursday, May 23 - Morning

SS10 METAMORPHISM IN THE ORE ENVIRONMENT

Room / Salle: MR12

Supported by / Soutenue par: GAC Mineral Deposits Division, Society of Economic Geologists, GAC Volcanology and Igneous Petrology Division

Organizers / Organismes: Chris Couëslan, Doug Tinkham, David Pattison, Simon Gagné

Chairs / Présidents: Doug Tinkham and Chris Couëslan

08:20 Spry, P.G.*, O'Brien, J.J., Heimann, A., Teale, G.S., Jackson, S.E. and Rogers, D. Keynote (40 min): The chemistry of gahnite and garnet in lode horizon rocks as exploration guides to Broken Hill-type mineralization, Broken Hill area, Australia

09:00 Pattison, D.R.M. Metamorphic minerals as vectors to mineralization

09:20 Zulu, J.D.S.*, McFarlane, C.R.M. and Lentz, D.R. Structural and metamorphic evolution of the Key Anacon Zn-Pb-Cu-Ag deposit, Bathurst Mining Camp, Canada

09:40 Tinkham, D.K. A model for metamorphic devolatilization in the Lalor deposit alteration system, Snow Lake, MB

10:00 Refreshment Break / Pause-santé

10:20 Hindemith, M.* and Indares, A. The petrographic and geochemical study of hydrothermally altered metavolcanics, metamorphosed at granulite-facies conditions from the Canyon domain in the central Grenville Province of Quebec, Canada

10:40 Bailes, A.H.*, Galley, A.G., Paradis, S. and Taylor, B. Variation in large synvolcanic alteration zones at Snow Lake, Manitoba, Canada, with proximity to associated VMS deposits

11:00 Fagan, A.J.* and Groat, L.A. Metamorphism and the formation of ruby and pink sapphire deposits in SW Greenland

SS12 ADVANCES IN EXPLORATION TECHNIQUES

Room / Salle: MR11

Supported by / Soutenue par: GAC Mineral Deposits Division

Organizers / Organismes: Julie Palich

Chairs / Présidents: Julie Palich

08:20 Somarin, A.K. Application of portable XRF in ore exploration and mining: Examples from Mexico, Colombia and South Africa

08:40 Makvandi, S.*, Beaudoin, G., Ghasemzadeh-Barvarz, M. and McClenaghan, B. Developing indicator mineral methods; Application of iron oxides in discovery of VMS deposits

09:00 Müller, A.*, Wanvik, J.E. and Ihlen, P.M.

Petrological and chemical characterization of high-purity quartz deposits with examples from Norway

09:20 Poulin, R.S.*, McDonald, A.M., Kontak, D.J. and McClenaghan, B.M. A crystal-chemical investigation of the suitability of scheelite as a discriminator for different ore-forming settings: Initial results from cathodoluminescence studies

09:40 Power, M.J.*, Hattori, K.H., Sorba, C., Kotzer, T., Pinti, D.L. and Potter, E.G. Surface media expressions above buried uranium: The Phoenix & Millennium deposits, Athabasca Basin

10:00 Refreshment Break / Pause-santé

10:20 Ross, P-S.*, Bourke, A. and Fresia, B. Multi-sensor logging of exploration drill cores – Why? How? Any case studies?

10:40 Shales, A. The GRYPHON multi-parameter airborne platform: The future of regional exploration

SS17 TERRESTRIAL ANALOGUES FOR COMPARATIVE PLANETARY GEOLOGY AND ASTROBIOLOGY

Room / Salle: MR16

Supported by / Soutenue par: GAC Planetary Science Division, MAC

Organizers / Organismes: Ed Cloutis, Gordon Osinski

Chairs / Présidents: Gordon Osinski and Ed Cloutis

08:20 Cloutis, E.A.*, Whyte, L., Qadi, A., Anderson-Trocme, L., Bell III, J., Berard, G., Boivin, A., Ellery, A., Greenberger, R. and Haddad, E. How to search for methane on Mars: Results of rover field trials at Mars analogue sites

08:40 French, J.E. Questioning the textural evidence for microbial bioalteration of volcanic glass and its robustness as a terrestrial analog biosignature for Mars astrobiology

09:00 Peterson, R.C.* and Tait, K. Terrestrial analogues of the Martian surface: Comparison of three distinctive sites in the Canadian Arctic

09:20 Stromberg, J.M.*, Barr, E., Slater, G., Cloutis, E.A., Flemming, R., Harris, R. and Banerjee, N.R. Characterization of the ~2.7 Ga ankerite at the Dome Mine, Timmins, Ontario: Implications for understanding Martian paleoenvironments and biomarker preservation

09:40 Harris, L.B.* and Bédard, J.H. New tectonic models for Venus and Earth aided by comparative studies

10:00 Refreshment Break / Pause-santé

Thursday, May 23 - Morning

- 10:20 Schumann, D.*, Andersen, D.T., Sears, S.K. and Vali, H.** HRTEM investigation of the mineral assemblages associated with cryptoendolithic communities in Beacon Sandstone, University Valley, Antarctica
- 10:40 Battler, M.M.*, Osinski, G.R., Banerjee, N.R. and Cloutis, E.** Comparison of XRD and reflectance spectroscopy data from saline perennial cold spring mineral deposits at Wolf Spring, and implications for detecting spring deposits on Mars
- SS22 FIRST NATIONS GEOSCIENCE**
Room / Salle: MRE
Sponsored by / Parrainé par: Vale
Organizers / Organismes: Jeff Young, Linda Murphy
Chairs / Présidents: Linda Murphy and Jeff Young
- 08:30 Murphy, L.A. and Young, J.** *Introduction and Opening Remarks*
- 08:40 Sinclair, Elder K.* and Murphy, L.A.** **Keynote (40 min):** Grandmother teaching Earth Science
- 09:20 Laramée, Elder M.L.* and Robinson-Settee, Elder H.** Animating Mother Earth
- 09:40 Pruden, G.** First Nations, Metis and Inuit perspectives
- 10:00** *Refreshment Break / Pause-santé*

- 10:20 Discussion** (10:20 – 11:20)
- 11:20 Summary** (10 min)

GENERAL SESSIONS

- GS3 GEOCHEMISTRY AND GEOCHRONOLOGY**
Room / Salle: MR15
Supported by / Soutenu par: MAC / AMC
Organizers / Organismes: Christian Böhm, Alfredo Camacho
Chairs / Présidents: Christian Böhm and Alfredo Camacho
- 10:00** *Refreshment Break / Pause-santé*
- 10:20 Cates, N.L.*, Mojzsis, S.J., Caro, G., Bleeker, W., Hopkins, M.D., Guitreau, M., Blichert-Toft, J., Trail, D. and Abramov, O.** Component geochronology of the 3960 Ma Acasta Gneiss
- 10:40 Rios, D.C.*, Davis, D.W., Conceicao, H., Santos, I.P.L. and Rosa, M.d.S.** New insights into Serrinha Nucleus evolution: The Quijingue Archean megacryst anorthosite
- 11:00 Easton, R.M.** 50 million years of syenite magmatic evolution and related metasomatism along the Central Metasedimentary Belt Boundary thrust zone, western Grenville Orogen

Thursday, May 23 - Afternoon

SYMPOSIA

- SY1 Earth Materials, Petrological and Geochemical Processes (in Honour of Frank C. Hawthorne)**
Room / Salle: Presentation Theatre
Supported by / Soutenu par: MAC / AMC
Organizers / Organismes: Elena Sokolova, Norman Halden
Chairs / Présidents: Elena Sokolova and Norman Halden
- 01:40 Burns, P.C. (40 min)** Recent advances in nanoscale uranium materials in the Energy Frontier Research Center “Materials Science of Actinides”
- 02:20 Groat, L.A.*, Pieczka, A., Evans, J.R., Grew, E.S., Ma, C. and Rossman, G.R.** The structure and crystal chemistry of dumortierite I. A new classification of the dumortierite group as a supergroup
- 02:40 Evans, R.J.* and Groat, L.A.** The structure and crystal chemistry of dumortierite II. Structure and topology of the dumortierite supergroup and dumortierite-like materials
- 03:00 Della Ventura, G.*, Bellatreccia, F., Marcelli, A. and Radica, F.** FTIR imaging of geological materials
- 03:20 Krivovichev, S.V.** Structural complexity and metastable crystallization
- 03:40 Hawthorne, F.C.** The state of mineralogy: The present and the future
- SY2 GRANITIC PEGMATITES - FROM FASCINATING CRYSTALS TO HIGH-TECH ELEMENTS (IN HONOUR OF PETR ČERNÝ)**
Room / Salle: MR2E
Supported by / Soutenu par: MAC / AMC
Organizers / Organismes: Milan Novák
Chairs / Présidents: David London
- 01:40 Linnen, R.L.*, Aseri, A., Che, X., Botcharnikov, R., Holtz, F. and Thibault, Y.** **Keynote (40 min):** The importance of fluorine in pegmatite melts
- 02:20 Krejsek, S.* and Kynický, J.** Dolní Bory pegmatite field - New evolution concept
- 02:40 Snook, B.*, Müller, A., Williamson, B. and Wall, F.** Towards exploration tools for high purity quartz in the Bamble-Evje pegmatite belt, south Norway

Thursday, May 23 - Afternoon

- 03:00** **Anderson, M.O.***, **Lentz, D.**, **McFarlane, C.R.M.**, **Falck, H.** and **Hall, D.C.** Trace-element geochemistry of muscovite as petrogenetic indications of pegmatite evolution in the Moose II lithium-tantalum pegmatite deposit, Northwest Territories, Canada
- 03:20** **Wise, M.A.** Crystallization conditions of epidote in granitic pegmatites
- 03:40** **Cempírek, J.*** and **Groat, L.A.** Mineralogy of the mixed-family Rau I pegmatite, Yukon Territory
- SY3** **LIFE AND TIMES OF PHANEROZOIC SEAS (IN HONOUR OF ROLF LUDVIGSEN)**
Room / Salle: MR7/8
Supported by / Soutenue par: GAC Paleontology Division
Organizers / Organiseurs: Brian Pratt, Nigel Hughes, Ed Landing, Godfrey Nowlan, Dave Rudkin, Steve Westrop, Graham Young
Chairs / Présidents: Dave Rudkin and Graham Young
- 01:40** **Amati, L.***, **Westrop, S.R.**, **Brett, C.E.**, **Swisher, R.E.** and **Carlucci, J.R.** Integrating sequence stratigraphy, biostratigraphy and chemostratigraphy: An example from the Katian (Late Ordovician) reference section, central Oklahoma
- 02:00** **Mángano, M.G.***, **Buatois, L.A.**, **Wilson, M.A.** and **Droser, M.L.** Ichnologic signatures of the Ordovician radiation
- 02:20** **Cuggy, M.B.***, **Rudkin, D.M.** and **Young, G.A.** The life and times of a new Ordovician eurypterid from the William Lake Lagerstätte, Manitoba
- 02:40** **Zhang, S.*** and **Pell, J.** Conodonts from carbonate xenoliths in Chidliak kimberlites confirm the previous existence of Lower Paleozoic cover on Hall Peninsula, Nunavut and provide temperature estimates
- 03:00** **Lapenskie, K.D.*** and **Jin, J.** Paleogeographic differentiation of the Early Silurian Virgiana brachiopod fauna in Laurentia

SPECIAL SESSIONS

- SS3** **TECTONIC EVOLUTION AND METALLOGENY OF THE SUPERIOR PROVINCE: NEW INSIGHTS FROM THE NORTH CARIBOU TERRANE, THE "RING OF FIRE", AND BEYOND**
Room / Salle: MR4E
Supported by / Soutenue par: GAC Precambrian Division; GAC Volcanology and Igneous Petrology Division; GAC Mineral Deposits Division
Organizers / Organiseurs: Scott Anderson, Christian Böhm, Tim Corkery, Peter Hollings
Chairs / Présidents: Tim Corkery

- 01:40** **Thurston, P.C.*** and **Kamber, B.S.** Testing the relationship between LIPs, BIF, and VMS deposits in the Abitibi greenstone belt
- 02:00** **Beakhouse, G.P.** Implications of the plutonic record for the thermal and tectonic evolution of the Abitibi Subprovince
- 02:20** **Lodge, R.W.D.***, **Gibson, H.L.**, **Stott, G.M.** and **Franklin, J.T.** Rapid development and subsidence of a Neoproterozoic volcanic arc hosting the Winston Lake VMS ore bodies, Wawa subprovince, Superior Craton
- 02:40** **Maier, W.D.*** and **Vaillancourt, C.** PGE mineralization in the Highbank Lake layered intrusion, northern Ontario, Canada
- 03:00** **Sappin, A-A.***, **Houlé, M.G.**, **Vaillancourt, C.**, **Leshner, C.M.** and **McNicoll, V.J.** Mafic and ultramafic intrusions in the eastern Uchi Domain of the Superior Province, Northern Ontario: New insights from mineralogical and geochemical analysis
- 03:20** **Metsaranta, R.T.*** and **Houlé, M.G.** Geological investigations in the McFaulds Lake greenstone belt ("Ring of Fire"), Oxford-Stull domain, Superior Province
- 03:40** **Houlé, M.G.***, **Leshner, C.M.**, **Metsaranta, R.T.**, **Goutier, J.**, **McNicoll, V.** and **Gilbert, H.P.** Temporal and spatial distribution of magmatic Ni-Cu-PGE/Cr-PGE/Fe-Ti-V deposits in the Bird River/Uchi/Oxford-Stull/La Grande-Eastmain superdomain: A new metallotect within the Superior Province
- SS5** **URANIUM: CRADLE TO GRAVE**
Room / Salle: MR3E
Supported by / Soutenue par: GAC Environmental Sciences Division
Organizers / Organiseurs: Peter Burns, Ginger Sigmon
Chairs / Présidents: Peter Burns and Ginger Sigmon
- 01:40** **Lesbros, M.*** and **Beaudoin, G.** Hydrothermal alteration and uranium mineralization at the Camie River prospect (Otish Basin, Québec)
- 02:00** **Galoisy, L.***, **Calas, G.**, **Cormier, L.**, **Delaye, J-M.**, **Peugot, S.** and **Jollivet, P.** Molecular scale origin of nuclear glass properties during elaboration, alteration, and aging under irradiation
- 02:20** **Reid, K.D.***, **Ansdell, K.** and **Guoxiang, C.** Preliminary investigation of fluids associated with Mackenzie dykes in the Centennial deposit area, south-central Athabasca Basin, Saskatchewan
- 02:40** **Millar, R.***, **Annesley, I.R.**, **Rudnick, R.L.**, **Liu, X.** and **Ansdell, K.** Li and B isotopic composition of basement rocks from multiple sites of the Eastern Athabasca Basin, Saskatchewan, implications as a possible vectoring tool?

Thursday, May 23 - Afternoon

03:00 Hobbs, D.T.*, Rudisill, T.S. and Denham, M.E.
Perspectives on the uranium life cycle at the Savannah River Site

SS8 LAYERED INTRUSIONS: NEW PARADIGMS AND APPROACHES TO UNDERSTANDING MAGMATIC PROCESSES

Room / Salle: MR9/10

Supported by / Soutenu par: MAC / AMC

Organizers / Organiseurs: James S. Scoates, Jim Miller

Chairs / Présidents: James Scoates and Jim Miller

01:40 Miller, J.D. The Layered Series at Duluth – Evidence for magmatic venting from a shallow mafic layered intrusion

02:00 Mealin, C.A.*, Leshner, C.M., Bedard, J., Hryciuk, M. and Wing, B. Archean sulfur records the arrested development of a Proterozoic igneous complex

02:20 Milidragovic, D.* and Francis, D. Constraining magma compositions for the ultramafic cumulate rocks of the Ungava Craton's Q-suite (2.7 Ga) ~ using the program MELTS

02:40 Hunt, E.J.*, Finch, A.A. and Donaldson, C.H. Magmatic layering in a peralkaline intrusion: An example from Layer 0, Ilímaussaq Complex, S. Greenland

03:00 Wall, C.J.*, Scoates, J.S., Friedman, R.M. and Meurer, W.P. Identifying unconformities, unconformities, and "rockbergs" within the Stillwater Complex using high-precision U-Pb zircon geochronology

SS10 METAMORPHISM IN THE ORE ENVIRONMENT

Room / Salle: MR12

Supported by / Soutenu par: GAC Mineral Deposits Division, Society of Economic Geologists

Organizers / Organiseurs: Chris Couëslan, Doug Tinkham, David Pattison, Simon Gagné

Chair / Présidente: David Pattison

01:40 Tomkins, A.G. Keynote (40 min): The critical role of deformation in metamorphic sulfide melting

02:20 McFarlane, C.R.M.* and McKeough, M. Anatexis of phosphatic metalliferous shales as an ingredient in unusual pegmatite-hosted monazite-apatite-ilmenite occurrences

02:40 Jeanneret, P.*, Goncalves, P., Trap, P., Durand, C., Marquer, D. and Quirt, D. Deformation and partial melting as critical processes for the remobilization of uranium: Example of Mudjatik-Wollaston Transition Zone (Saskatchewan, Canada)

SS14 PRAIRIE HYDROGEOLOGY

Room / Salle: MR11

Supported by / Soutenu par: IAH CNC (International Association of Hydrogeologists - Canadian National Chapter)

Organizers / Organiseurs: Jeff Bell, Graham Phipps

Chairs / Présidents: Jeff Bell

01:40 English, C.B.* and Ali, G. Required steps and recurring challenges in the dual hydrological and geological classification of Prairie watersheds

02:00 Toop, D.C. Unconventional origins of the Spiritwood Buried Valley aquifer in Manitoba

02:20 Bell, J.J. Groundwater resource evaluations of buried valley aquifers

02:40 Zaporozan, T.* and Ferguson, I. Electromagnetic imaging of the Spiritwood Valley buried aquifer near Cartwright, Manitoba, Canada

03:00 Toop, D.C. Application of hydrogeology and glacial geology to native orchid conservation in Manitoba

03:20 Lobb, D.A.*, Koiter, A.J., Owens, P.N., Tiessen, K.H.D. and Li, S. Assessment of soil erosion and sedimentation in South Tobacco Creek using radiochemistry and geochemistry as tracers

SS18 ASTROMATERIALS: METEORITES AND MORE

Room / Salle: MR16

Supported by / Soutenu par: GAC Planetary Science Division, MAC

Organizers / Organiseurs: Chris Herd

Chairs / Présidents: Chris Herd and Katrina van Drongelen

01:40 Flemming, R.L.*, Tait, K., Schmidt, M.E., Cloutis, E.A., Herd, C.D.K., Sylvester, P.J., Kissin, S.A., Brown, P.G., Osinski, G.R. and Banerjee, N.R. ASTRO – Astromaterials Training and Research Opportunities CSA Cluster

02:00 Izawa, M.R.M.*, Cloutis, E.A., Pompilio, L., Reddy, V., Hiesinger, H., Nathues, A., Mann, P., Le Corre, L., Palomba, E. and Bell III, J.F. Modal mineralogy of Howardite, Eucrite and Diogenite (HED) meteorites by Rietveld refinement of X-ray diffraction data

02:20 van Drongelen, K.D.* and Tait, K.T. Polymict eucrite Northwest Africa 5232: The compositional and textural diversity of clasts and a previously undescribed Na-rich eucrite lithology

02:40 Herd, C.D.K.*, Bryden, C.D., Pearson, D.G. and Duke, M.J.M. The Tissint Martian meteorite: Petrologic comparisons to other shergottites

Thursday, May 23 - Afternoon

- 03:00** **Abdu, Y.*, Hawthorne, F., Varela, M.E. and Duley, W.** Nanodiamonds and amorphous carbon in carbonaceous-chondrite xenoliths in the Kapoeta meteorite: Astrophysical implications
- 03:20** **Ibrahim, M.*, McCausland, P.J.A., Brown, P.G., Umoh, J. and Holdsworth, D.W.** Micro-Porosity Distribution in the Tagish Lake C2 carbonaceous chondrite
- SS22** **FIRST NATIONS GEOSCIENCE**
Room / Salle: MRE
Sponsored by / Parrainé par: Vale
Organizers / Organisateurs: Jeff Young, Linda Murphy
Chairs / Présidents: Linda Murphy and Jeff Young
- 01:20** **Ouellette, R.F.** Merging Indigenous and Western Science
- 01:40** **Ferris, K.K.** Mining Movie Making Youth Camp
- 02:00** **Mihychuk, M.** Building bridges and positive results: The Manitoba Mineral Resources Training Program - An example of industry and First Nation collaboration
- 02:20** **Discussion** (2:20 – 3:30)
- 03:30** **Summary** (10 min)

GENERAL SESSIONS

- GS3** **GEOCHEMISTRY AND GEOCHRONOLOGY**
Room / Salle: MR15
Supported by / Soutenue par: MAC / AMC
Organizers / Organisateurs: Christian Böhm, Alfredo Camacho
Chairs / Présidents: Alfredo Camacho and Christian Böhm
- 01:40** **Cutts, J.A.*, Easton, R.M. and Carr, S.D.** *Circa* 1060-1090 Ma syn- to post-orogenic plutonism in the Grenville Province of Ontario: Insights from major, trace element and isotope geochemistry
- 02:00** **Wolczanski, H.E.*, Lee, J.K.W. and Camacho, A.** Thermal history of the Flinton Group, Mazinaw Domain, Grenville Province, Ontario
- 02:20** **Fortin, M-A.* and Baker, D.R.** The effect of water on sulphur solubility in natural melts
- 02:40** **Power, I.M.*, Harrison, A.L., Dipple, G.M., Kenward, P.A., Wilson, S.A., McCutcheon, J. and Southam, G.** A depositional model for hydromagnesite-magnesite playas

Poster Session II – Thursday, May 23, 2013

- SY2 GRANITIC PEGMATITES - FROM FASCINATING CRYSTALS TO HIGH-TECH ELEMENTS (IN HONOUR OF PETR ČERNÝ)**
Supported by / Soutenue par: MAC / AMC
Organizers / Organisateurs: Milan Novák
- SY2-P1 Dittrich, T.*, Schulz, B., Seifert, T., Hagemann, S. and Gutzmer, J.** Application of combined SEM, BSE and EDX techniques to the mineralogical and geochemical characterization of granitic-pegmatites
- SY2-P2 Shirose, Y.* and Uehara, S.** Compositional variation and paragenesis of Li tourmaline from Nagatare, Fukuoka Prefecture, Japan
- SY2-P3 Novák, M.*, Gadas, R., Galiová Vašíňová, M. and Pezzotta, F.** Compositional variations in Cs,Li,Mg-rich beryl from exocontact of the complex Manjaka pegmatite, Sahatany Valley, Madagascar
- SY2-P4 Sánchez-Muñoz, L.*, Modreski, P.J., Zagorsky, V., Frost, B.R. and De Moura, O.J.M.** Relationships between the twin patterns of perthitic K-feldspars from granitic pegmatites and their geotectonic setting during the subsolidus stage
- SY2-P5 Anderson, A.J.*, Rhede, D. and Wirth, R.** The occurrence and alteration of (Y, REE, U, Th)-(Nb, Ta, Ti) oxide minerals near the footwall contact of the Greenbushes pegmatite, Western Australia
- SY2-P6 Hetherington, C.J.* and Husdal, T.** 400 Ma dates in a rare element NYF-pegmatite from Stetind, Nordland, Norway: Recrystallized Proterozoic assemblages or A-type pegmatite-emplacement in overly-thickened crust at a continental margin?
- SY2-P7 Výravský, J.*, Novák, M., Škoda, R., Johan, Z. and Šrein, V.** Pretulite ScPO_4 from the Dolní Bory pegmatite, Czech Republic and its miscibility with zircon and xenotime
- SY2-P8 Pires, F.R.M.*, Amorim, H.S. and Silva, L.L.F.** Gormanite distribution and equilibrium conditions in pegmatite from Corrego Frio fields, Galileia, Minas Gerais, Brazil
- SY2-P9 Chakhmouradian, A.R.*, Reguir, E.P., Ballantine, N.G., Yang, P. and Mumin, H.** Evolution of granitic pegmatites at Eden Lake (northern Manitoba): Evidence from accessory rare-earth-bearing minerals
- SY2-P10 Mendes, L.U.D.S., Lima, A.M.C.* and Noronha, F.** Mineral geochemistry of granites and pegmatites from Seixoso-Vieiros pegmatite field, northern Portugal
- SS1 GEOSCIENCE AND RESOURCES AT CANADA'S NORTHERN FRONTIERS: CHALLENGES AND OPPORTUNITIES**
Supported by / Soutenue par: GAC Precambrian Division; GAC Mineral Deposits Division
Organizers / Organisateurs: John Percival, John Ketchum, Luke Ootes, Dave Mate, Mostafa Fayek
- SS1-P1 Mathieu, J.*, Kontak, D.J. and Turner, E.C.** Phanerozoic diagenesis and associated economic potential of Proterozoic and Paleozoic dolostones on Victoria Island (NWT and NU)
- SS1-P2 Baldwin, G.J., Turner, E.C.* and Kamber, B.S.** Geochemical and geochronological evidence against direct LIP influence on deposition of the Rapitan iron formation, Canada
- SS3 TECTONIC EVOLUTION AND METALLOGENY OF THE SUPERIOR PROVINCE: NEW INSIGHTS FROM THE NORTH CARIBOU TERRANE, THE "RING OF FIRE", AND BEYOND**
Supported by / Soutenue par: GAC Precambrian Division; GAC Volcanology and Igneous Petrology Division; GAC Mineral Deposits Division
Organizers / Organisateurs: Scott Anderson, Christian Böhm, Tim Corkery, Peter Hollings
- SS3-P1 Ola, O.B.*, Frederiksen, A.W., Deniset, I. and Toni, D.** Variations in shear-wave splitting across the Mid-Continent Rift
- SS3-P2 Therrien, S.J., Conly, A.G.* and Moore, L.C.** Mineralogical and geochemical assessment of possible iron formations at the Red Lake gold mine
- SS3-P3 McLeod, J.*, Ferguson, I.J., Craven, J. and Jones, A.G.** Assessment of the electrical resistivity structure of the northwest Superior craton and adjacent Trans Hudson Orogen using the magnetotelluric method
- SS4 DIAMOND: FROM BIRTH IN THE MANTLE TO EMPLACEMENT IN KIMBERLITE**
Supported by / Soutenue par: MAC / AMC
Organizers / Organisateurs: Maya G. Kopylova, Yana Fedortchouk
Chairs / Présidents:
- SS4-P1 Cookenboo, H.O.* and Benitez, L.** Severely corroded diamonds from the foliated Salvador 1 Kimberlite compared to alluvial populations in the Espinhaço Mountains
- SS4-P2 Fedortchouk, Y.*, Skvortsova, V.L. and Zhang, Z.** A review of experimental data of diamond dissolution with the focus on morphological features

Poster Session II – Thursday, May 23, 2013

- SS8 LAYERED INTRUSIONS: NEW PARADIGMS AND APPROACHES TO UNDERSTANDING MAGMATIC PROCESSES**
Supported by / Soutenue par: MAC / AMC
Organizers / Organiseurs: James S. Scoates, Jim Miller
- SS8-P1 Fourny, A.*, Weis, D. and Scoates, J.S.**
 Determining accurate and precise isotopic compositions of reference materials to investigate isotopic heterogeneity in mafic layered intrusions
- SS8-P2 Venturi, C. and Greenough, J.D.*** Size and source matter: New information on the giant, Proterozoic, Suwar/Wadi Qutaba layered mafic intrusion in Yemen
- SS11 PALEOGEODYNAMICS OF THE EARTH BEFORE PANGAEA**
Supported by / Soutenue par: GAC Geophysics Division IGCP project 597: "Amalgamation and Breakup of Pangaea: the type example of the supercontinent cycle"
Organizers / Organiseurs: Phil McCausland, Brendan Murphy, Joe Hodych, Rob Rainbird, Ken Buchan, Richard Ernst
- SS11-P1 Jin, J., Harper, D.A.T., Cocks, R.M., McCausland, P.J.A.*, Rasmussen, C.M.Ø. and Sheehan, P.M.**
 Biofacies constraints on the Ordovician equator in Laurentia: A test of Early Paleozoic geomagnetic field geometry
- SS12 ADVANCES IN EXPLORATION TECHNIQUES**
Supported by / Soutenue par: GAC Mineral Deposits Division
Organizers / Organiseurs: Julie Palich
- SS12-P1 Falck, H.*, Day, S., Pierce, K., Ootes, L. and Watson, D.** Regional metallogeny patterns as revealed by the distribution of heavy minerals in stream sediments from the Mackenzie Mountains, NWT
- SS13 WILLISTON BASIN AND OTHER INTRACRATONIC BASINS - SEDIMENTOLOGY, STRATIGRAPHY, PALEONTOLOGY AND RESOURCES**
Sponsored by / Parrainé par: Red Beds Resources Ltd.
Supported by / Soutenue par: GAC Canadian Sedimentology Research Group
Organizers / Organiseurs: Michelle Nicolas, Pamela Fulton-Regula, James Bamburak, Nancy Chow
- SS13-P1 Zhang, L.* and Buatois, L.A.** Sedimentary facies, depositional environment and sequence stratigraphy of the Upper Devonian-Lower Carboniferous Bakken Formation in the southeastern corner of Saskatchewan
- SS13-P2 Haidl, F.M.*, Jensen, G.K.S. and Yang, C.** Economic potential of Red River strata in Saskatchewan: Drilling deeper for additional resources
- SS13-P3 Chabanole, L.E.* and Buatois, L.A.**
 Sedimentology and stratigraphy of the Bakken Formation, west-central Saskatchewan & east-central Alberta
- SS13-P4 Gilbert, M.M.*, Buatois, L. and Renaut, R.**
 Regional stratigraphy and sedimentology of the Belly River Group (Campanian) in southwestern Saskatchewan, Canada
- SS13-P5 Törö, B.*, Pratt, R.B. and Renaut, W.R.** Soft-sediment deformation as indicators of paleoseismic activity in lacustrine deposits (Green River Formation, Eocene, USA)
- SS13-P6 Nicolas, M.P.B.*, Bamburak, J.D., Sosseininejad, S. and Pedersen, P.K.** Mineralogy, geochemistry and facies variations of a potential shallow shale gas play within the Cretaceous Carlile and Favel formations, southwestern Manitoba
- SS13-P7 McWhirter, B.R.*, Lobb, D.A., Bamburak, J., Nicolas, M., Sheng, L. and Ali, G.** Determination of the bedrock stratigraphy of the South Tobacco Creek area in the Pembina Hills portion of the Manitoba Escarpment using field investigation, LIDAR and photo imagery
- SS13-P8 McCracken, A.D.*, Armstrong, D.K., Lavoie, D., Brunton, F.R. and Nicolas, M.** Conodont biostratigraphy of the Hudson Bay and Moose River basins, Ontario and Manitoba
- SS13-P9 Prior, G., Hathway, B., Glombick, P.*, Pana, D., Banks, C., Hay, D., Schneider, C., Grobe, M., Elgr, R. and Weiss, J.** New bedrock geology map of Alberta
- SS14 PRAIRIE HYDROGEOLOGY**
Supported by / Soutenue par: IAH CNC (International Association of Hydrogeologists - Canadian National Chapter)
Organizers / Organiseurs: Jeff Bell, Graham Phipps
- SS14-P1 Petzold, H.*, McWhirter, B.R., Lobb, D.A., Ali, G., Owens, P.N., Brancourt, J. and Liu, C.** Channel morphology of the Tobacco Creek watershed in southern Manitoba

Poster Session II – Thursday, May 23, 2013

- SS14-P2** Dale, J.E.*, Swetlow, J., Kelimu, W., Lafond, G., Morris, E., Sunley, S. and Tant, C. Improving the accuracy of soil conductivity measurements
- SS18** **ASTROMATERIALS: METEORITES AND MORE**
Supported by / Soutenu par: GAC Planetary Science Division, MAC
Organizers / Organiseurs: Chris Herd
- SS18-P1** van Drongelen, K.D.*, Tait, K.T. and Dera, P. Phosphorus-bearing Fe,Ni-sulphide in Murchison and carbonaceous chondrite clasts in polymict eucrite NWA 5232
- SS18-P2** Muir, S.L.* and Solferino, G.F. D. Olivine grain growth in a Fe-S matrix. A tool to interpret formation of Pallasite meteorites
- SS18-P3** Applin, D.M.*, Cloutis, E.A. and Izawa, M.R.M. Spectral reflectance properties of common metal-oxalates exposed to simulated Mars surface conditions
- SS23** **MAGMATIC-HYDROTHERMAL DEPOSITS: PORPHYRY, IOCG AND EPITHERMAL SYSTEMS (DEDICATED TO THE MEMORY OF ROBERT KERRICH)**
Organizers / Organiseurs: Hamid Mumin, Jeremy Richards, Louise Corriveau
- SS23-P1** Wang, R.W-R.*, Richards, J., Hou, Z. and Yang, Z. Increased magmatic water content — the key to late-collisional porphyry Cu \pm Mo \pm Au formation in the Oligo-Miocene Gangdese belt, Tibet
- SS23-P2** Millonig, L.J.*, Groat, L.A., Linnen, R.L. and O'Brien, D.O. The epithermal Engineer Mine gold deposit, British Columbia
- SS23-P3** Ghorbani, M.A.*, Alirezaei, S. and Alimohammadi, M. The role of NW dextral transpressional deformation on magma ascent and associated porphyry style alteration-mineralization in Daralu-Hanza area, Kerman copper belt, SE Iran
- GS1** **MINERALOGY, CRYSTALLOGRAPHY AND MINERAL CHEMISTRY**
Supported by / Soutenu par: MAC / AMC
Organizers / Organiseurs: Yana Fedortchouk, Olivier Gagné, Zhihai Zhang
- GS1-P1** Macek, I.* and Novák, M. Fluorine-rich tourmalines from a classical topaz locality Schneckenstein, Vogtland, Germany
- GS1-P2** Járóka, T. and Seifert, T.* Characterization of cassiterite parageneses in metasomatic altered meta-mafic rocks of the “Felsitzone”, Großschirma - Freiberg mining district, Erzgebirge, Germany
- GS1-P3** Kovrugin, V.*, Colmont, M., Mentré, O. and Krivovichev, S. Crystal structures of two novel compounds in the PbO–NiO–SeO₂ system
- GS1-P4** Brzozowski, M.*, Samson, I., Gagnon, J., Linnen, R. and Good, D. Variation in fracture mineralogy and mineral chemistry around the Marathon Cu-PGE deposit, Ontario
- GS1-P5** Seifert, T. Late- and post-Variscan vein-type silver mineralization in the Erzgebirge-Krušné hory, Germany and Czech Republic
- GS1-P6** Tomes, H.*, Tait, K.T. and Nicklin, I. Phosphate nodules from Big Fish River, Yukon, Canada
- GS3** **GEOCHEMISTRY AND GEOCHRONOLOGY**
Supported by / Soutenu par: MAC / AMC
Organizers / Organiseurs: Christian Böhm, Alfredo Camacho
- GS3-P1** Thomson, D.M.*, Rainbird, R.H., Bekker, A. and Prince, J. Paired organic carbon and carbonate carbon isotope records from the Tonian-Cryogenian Shaler Supergroup, Victoria Island, NWT
- GS3-P2** Steffen, A.L.*, Lewis, A.R., Zamora, F. and Saini-Eidukat, B. Chemical weathering of Miocene sediments from the Dry Valleys, Antarctica
- GS3-P3** Steffen, A.L.*, Hopkins, D.G., Saini-Eidukat, B. and Breker, J.S. Use of a GIS/stratigraphic model to predict zones of elevated trace element concentrations in soils derived from Cretaceous Pierre Shale on the Pembina Escarpment, Cavalier County, North Dakota
- GS3-P4** Kellett, D.A.*, Rogers, N., McNicoll, V. and van Staal, C. Relationships between pluton emplacement, mineralization and deformation at the Gander/Avalon boundary, Newfoundland from a geochronological and thermochronological perspective
- GS4** **STRUCTURAL GEOLOGY AND TECTONICS**
Organizers / Organiseurs: Scott Anderson, Paul Kremer
- GS4-P1** Zsámboki, L., Dehler, S.A. and Barr, S.M.* Geophysical modeling of pre-Carboniferous “basement” rocks in the Cabot Strait area: Implications for geological correlations and terrane accretion in the northern Appalachian orogen
- GS4-P2** White, C.E.* and MacHattie, T.G. The eastern Cobequid Highlands, northern mainland Nova Scotia, Canada: An enigmatic piece of the Avalonian puzzle
- GS4-P3** Backeberg, N.R.* and Rowe, C.D. The deformation history of the Finlayson Lake greenstone belt: Implications for greenstone belt geometry

Poster Session II – Thursday, May 23, 2013

- GS4-P4** **From, R.* and Larson, K.** A cryptic tectonometamorphic discontinuity in the Greater Himalayan sequence, Likhu Khola study area, east-central Nepal
- GS5** **PALEONTOLOGY**
Organizers / Organisateurs: Robert Elias
- GS5-P1** **Boulding, R.*, Dale, J.E. and Tokaryk, T.** Biohorizons of the Upper Cretaceous Eastend Formation near Eastend, Saskatchewan
- GS5-P2** **Shahkarami, S., Mangano, M.*, Buatois, L.A. and Siab Ghodsi, A.** Ichnology of the Ediacaran-Cambrian Soltanieh Formation of northern Iran: Reconstructing animal-substrate interactions during the Cambrian explosion

Poster Sessions I and II are sponsored by HudBay Minerals Inc.





Friday Technical Program

Programme du vendredi

	Present. Theatre	MR2E	MR3E	MR4E	MR7/8	MR9/10	MR11	MR12	MR15	MR16	Millennium Suite	Exhibits Hall
8:20	SY4 Stirring the Pot (Hoffman)	SY2 <i>cont.</i> Granitic Pegmatites (Černý)	SS5 <i>cont.</i> Uranium: Cradle to ...	SS3 <i>cont.</i> Superior Province	SS4 Diamonds	SS23 IOCG and Porphyry	SS21 Geoscience Profession- alism	SS11 Prior to Pangea	SS13 Williston Basin	GS4 Structural Geology	Teacher Workshop	E X H I B I T S
9:20												
9:40												
10:00	Refreshment Break / Pause-santé											
10:20	SY4 Stirring the Pot (Hoffman)	SS1 Geoscience, Northern Frontiers	SS20 Research & Environmental Decisions	SS3 <i>cont.</i> Superior Province	SS4 Diamonds	SS23 IOCG and Porphyry	SS21 Geoscience Profession- alism	SS11 Prior to Pangea	SS13 Williston Basin	GS4 Structural Geology	Teacher Workshop	
11:00												
11:20	PLENARY ADDRESS: <i>The Science and the Discovery of Volcanogenic Massive Sulphide Deposits</i> Harold Gibson, Laurentian University Presentation Theatre, Winnipeg Convention Centre, 11:20 am - 12:00 pm											
12:00	MDD LUNCHEON - Pan-Am Room, Winnipeg Convention Centre, 12:00 - 1:40 pm											
13:40	SY4 <i>cont.</i> Stirring the Pot (Hoffman)	SS1 <i>cont.</i> Geoscience, Northern Frontiers	SS20 <i>cont.</i> Research & Environmental Decisions		SS4 <i>cont.</i> Diamonds	SS23 <i>cont.</i> IOCG and Porphyry	GS1 Mineralogy & Crystal- lography	SS11 <i>cont.</i> Prior to Pangea	SS13 <i>cont.</i> Williston Basin	Teacher Workshop	Teacher Workshop	
14:40												
15:00												
15:20												
15:40												

Presentations are listed for each Symposium, Special Session and General Session. For oral presentations, the speaker is indicated with an asterisk. Poster presenters for the sessions shown must be in attendance between 4:00 p.m. and 6:00 p.m. to discuss their poster with conference attendees. A cash bar will be available in the Exhibits Hall at this time.

Les présentations sont listées pour chaque symposium, session spéciale et session générale. Pour les présentations orales le(la) conférencier(ère) est indiqué(e) avec un astérisque. Les présentateurs des affiches pour les sessions indiquées doivent être sur place entre 16h00 et 18h00 pour discuter du contenu de leur présentation. Un bar payant sera disponible dans la salle d'exposition des affiches. Aucune nourriture ni boisson n'est permise au Presentation Theatre.

Friday, May 24 - Morning

SYMPOSIA

SY2 GRANITIC PEGMATITES - FROM FASCINATING CRYSTALS TO HIGH-TECH ELEMENTS (IN HONOUR OF PETR ČERNÝ)

Room / Salle: MR2E

Supported by / Soutenue par: MAC / AMC

Organizers / Organismes: Milan Novák

Chairs / Présidents: Milan Novák

08:20 Pires, F.R.M.* and Silva, L.L.F. New approach in the phosphate mineral study, topology, equilibrium conditions and pegmatite emplacement in the Galileia fields, Minas Gerais, Brazil

08:40 Sánchez-Muñoz, L.*, Sobrados, I., Sanz, J., Van Tendeloo, G., Ke, X., Cremades, A., Rodriguez, M.Á., del Campo, A. and Gan, Z.H. Amazonitic lead-rich orthoclase from Broken Hill, Australia

09:00 Pires, F.R.*, Fonseca, M.A. and Silva, L.F. Regional zoning and topology for the chrysoberyl and alexandrite mineralizations at the Oriental Pegmatite province of Minas Gerais, Brazil

SY4 STIRRING THE POT: GEOSCIENCE CANADA SYMPOSIUM (IN HONOUR OF PAUL F. HOFFMAN)

Room / Salle: Presentation Theatre

Supported by / Soutenue par: Geoscience Canada / Geoscience Canada

Organizers / Organismes: Brendan Murphy, Galen Halverson

Chairs / Présidents: Brendan Murphy and Galen Halverson

08:20 van Staal, C.*, Chew, D., Zagorevski, A., McNicoll, V., Hibbard, J., Skulski, T., Castonguay, S., Escayola, M. and Sylvester, P. Keynote (40 min): Evidence for hyper-extension during Late Ediacaran-Early Cambrian opening of the Iapetus Ocean in the northern Appalachians and British Caledonides

09:00 St-Onge, D. From glacial lake Coppermine rhythmities to the olistostrome of the Sleigh Creek Formation

09:20 Halverson, G.P.*, Macdonald, F.A., Kunzmann, M., Strauss, J.V., Théou-Hubert, L. and Cox, G.M. Keynote (40 min): Neoproterozoic record of Rodinia breakup, eukaryotic evolution, and biogeochemical change in Yukon, Canada

10:00 Refreshment Break / Pause-santé

10:20 Cox, G.M.*, Halverson, G., Minarik, W., Le Heron, D., Stevenson, R., Poirier, A., Macdonald, F., Bellefroid, E. and Strauss, J. Cryogenian iron formation: A definitive link to mafic magmatism and weathering of mafic crust

10:40 Maloof, A.C.* and Rose, C.V. Entry into the end-Cryogenian glaciation of South Australia

11:00 Rose, C.V.* and Maloof, A.C. Exit from the end-Cryogenian glaciation of South Australia

SPECIAL SESSIONS

SS1 GEOSCIENCE AND RESOURCES AT CANADA'S NORTHERN FRONTIERS: CHALLENGES AND OPPORTUNITIES

Room / Salle: MR2E

Supported by / Soutenue par: GAC Precambrian Division; GAC Mineral Deposits Division

Organizers / Organismes: John Percival, John Ketchum, Luke Ootes, Dave Mate, Mostafa Fayek
Chairs / Présidents: Luke Ootes and John Percival

10:00 Refreshment Break / Pause-santé

10:20 Percival, J.A.*, Pehrsson, S.J., Berman, R.G., Wodicka, N., Harris, J.R., Kellett, D., Davis, W.J., Nadeau, L. and Bethune, K. Geo-mapping Frontiers: A new look at some underexplored parts of mainland Nunavut and Northwest Territories

10:40 Harris, J.R.*, Russell, H. and Percival, J. Remote predictive mapping – Progress in geological mapping in Canada's North

11:00 Hamilton, B.M.*, Sanborn-Barric, M., Rayner, N., Pattison, D.R.M., Berman, R.G. and Young, M.D. Andalusite-bearing supracrustal rocks reveal insights into early Paleoproterozoic metamorphism and deformation on Cumberland Peninsula, eastern Baffin Island, Nunavut

SS3 TECTONIC EVOLUTION AND METALLOGENY OF THE SUPERIOR PROVINCE: NEW INSIGHTS FROM THE NORTH CARIBOU TERRANE, THE "RING OF FIRE", AND BEYOND

Room / Salle: MR4E

Supported by / Soutenue par: GAC Precambrian Division; GAC Volcanology and Igneous Petrology Division; GAC Mineral Deposits Division

Organizers / Organismes: Scott Anderson, Christian Böhm, Tim Corkery, Peter Hollings
Chair / Présidente: Scott Anderson

08:20 Duguet, M.* and Beakhouse, G.P. Metamorphism in the Bending Lake area, western Wabigoon Subprovince, Ontario

08:40 Kontak, D.J. The Archean Côté gold Au(-Cu) deposit, northern Ontario, Canada: A large tonnage, low-grade Au deposit centred on a 2740 Ma magmatic-hydrothermal diorite complex

Friday, May 24 - Morning

- 09:00** **Zhou, X.*, Lin, S. and Anderson, S.D.** Lithology, alteration and structure of the Ogama-Rockland gold deposit in the southeast margin of the Ross River pluton, Rice Lake greenstone belt, Superior Province, Manitoba
- 09:20** **Duff, J., Hattori, K.*, Schneider, D., Biczok, J. and McFarlane, C.** Timiskaming-type sedimentary rocks near the Musselwhite gold mine in the North Caribou greenstone belt, Western Superior Province of Canada
- 09:40** **McNicoll, V.J.*, Dubé, B., Biczok, J., Castonguay, S., Oswald, W., Mercier-Langevin, P., Skulski, T. and Malo, M.** The Musselwhite gold deposit, North Caribou greenstone belt, Ontario: New high-precision U-Pb ages and their impact on the geological and structural setting of the deposit
- 10:00** *Refreshment Break / Pause-santé*
- 10:20** **Lin, S.*, Zhang, J., Linnen, R. and Martin, R.** Young-Davidson and Hemlo gold deposits in the Superior Province, Ontario: Contrasting styles of mineralization of common tectonic origin?
- 10:40** **Bleeker, W.** Major faults, synorogenic clastic deposits, and gold mineralization in Archean cratons: syn-orogenic extension followed by thick-skinned thrust burial, and final strike-slip
- 11:00** **Frederiksen, A.W.*, Bollmann, T., Darbyshire, F.A. and Van der Lee, S.** A seismic image of the lithosphere beneath the western Superior Province and the Mid-Continent Rift
- SS4** **DIAMOND: FROM BIRTH IN THE MANTLE TO EMPLACEMENT IN KIMBERLITE**
Room / Salle: MR7/8
Supported by / Soutenu par: MAC / AMC
Organizers / Organismes: Maya G. Kopylova, Yana Fedortchouk
Chair / Présidente: Maya Kopylova
- 08:20** **Wirth, R.* and Yang, J.** Sources of diamond formation revealed by nano-inclusions in diamond
- 08:40** **Smith, E.M.*, Kopylova, M.G., Frezzotti, M.L. and Afanasiev, V.P.** Nitrogen bubbles in the mantle: Evidence from diamond inclusions
- 09:00** **Nichols, K.*, Stachel, T., Stern, R.A., Pell, J. and Mate, D.** Diamond sources beneath the Hall Peninsula, Nunavut: A preliminary assessment based on micro-diamonds
- 09:20** **Hunt, L.*, Stachel, T., Pearson, D.G., Stern, R., Muehlenbachs, K. and McLean, H.** Multi-stage evolution of non-gem diamonds at the Diavik diamond mine, Canada
- 09:40** **Stachel, T.*, Harris, J.W., Hunt, L., Muehlenbachs, K. and EIMF,** Diamonds from the Argyle lamproite (Western Australia): Different from any other mine?
- 10:00** *Refreshment Break / Pause-santé*
- 10:20** **Osovetskii, B.M., Reguir, E.P.*, Chakhmouradian, A.R., Veksler, I.V., Yang, P., Kamenetsky, V.S. and Camacho, A.** Trace-element analysis and U-Pb geochronology of perovskite and its importance for tracking unexposed rare-metal and diamond deposits
- 10:40** **Kressall, R.D.* and Fedortchouk, Y.** Major- and trace-element composition of Fe-Ti oxides from the Lac de Gras kimberlites
- 11:00** **Ene, V-V.* and Schulze, D.J.** Chemical characterization of ilmenite suites from the Kimberley diamond mines, South Africa
- SS5** **URANIUM: CRADLE TO GRAVE**
Room / Salle: MR3E
Supported by / Soutenu par: GAC Environmental Sciences Division
Organizers / Organismes: Peter Burns, Ginger Sigmon
Chairs / Présidents: Peter Burns and Ginger Sigmon
- 08:20** **Boulerice, A.R.* and Hattori, K.** Major and minor compositions of alteration minerals associated with the uranium mineralization at Phoenix and Millennium deposits, Athabasca Basin, in northern Saskatchewan
- 08:40** **Quirt, D.H.** Other commodities of interest in unconformity-type uranium deposits
- 09:00** **Li, Z.*, Bethune, K., Chi, G., Bosman, S. and Card, C.** Preliminary 3D modelling and structural interpretation of the southeastern Athabasca basin
- 09:20** **Haixia, C.* and Guoxiang, C.** Petrographic and geochemical studies of bleaching diagenesis and implications for unconformity-type uranium mineralization in the Athabasca Basin
- SS11** **PALEOGEODYNAMICS OF THE EARTH BEFORE PANGAEA**
Room / Salle: MR12
Supported by / Soutenu par: GAC Geophysics Division IGCP project 597: "Amalgamation and Breakup of Pangaea: the type example of the supercontinent cycle"
Organizers / Organismes: Phil McCausland, Brendan Murphy, Joe Hodych, Rob Rainbird, Ken Buchan, Richard Ernst
Chairs / Présidents: Phil McCausland, Brendan Murphy and Rob Rainbird
- 08:20** **Eglington, B.M.*, Pehrsson, S.J. and Evans, D.** Visualising Precambrian plate motions and the timing of crustal response to geodynamic processes: An example from the Kalahari Craton, southern Africa

Friday, May 24 - Morning

- 08:40 Pehrsson, S.J.*, Buchan, K.L., Eglington, B.E., Berman, R.L. and Whalen, J.** Did plate tectonics shutdown in the Paleoproterozoic? A global-spatial assessment
- 09:00 Buchan, K.L.** The global database of primary paleomagnetic poles from precisely-dated rock units and its application to Paleoproterozoic and Mesoproterozoic continental reconstructions
- 09:20 Hodych, J.P.* and Buchan, K.L.** Testing for rapid true polar wander in the Ediacaran using paleomagnetic data from Avalonia
- 09:40 Cleven, N.R.*, Lin, S., Davis, D. and Xiao, W.** Elucidating Paleozoic tectonic events from conglomerate clast-detrital zircon geochronology of the Hongliuhe Group in the southern Central Asian Orogenic Belt, northwest China
- 10:00 Refreshment Break / Pause-santé**
- 10:20 Murphy, J.B.*, Braid, J.A., Dahn, D., Gladney, E., Dupuis, N. and Quesada, C.** An eastern Mediterranean analogue for the Late Palaeozoic evolution of the Pangaeian suture zone in SW Iberia
- 10:40 Hynes, A. Keynote (40 min):** How difficult was subduction in the Archean?
- 09:20 Nowlan, G.S.*, Elias, R.J., Young, G.A., Demski, M.W., Stewart, L.A., Wheadon, B.J. and Dobrzanski, E.P.** The Late Ordovician conodont extinction event in the context of carbon isotopic data and interpretation of the Ordovician - Silurian boundary in the Hudson Bay and Williston basins
- 09:40 Demski, M.W.*, Stewart, L.A., Elias, R.J., Young, G.A., Nowlan, G.S. and Dobrzanski, E.P.** Mass extinction in Manitoba: Biotic change and stratigraphy associated with the Ordovician-Silurian boundary interval
- 10:00 Refreshment Break / Pause-santé**
- 10:20 Bates, K.* and Chow, N.** Lithofacies analysis and reservoir quality of the Upper Devonian Duperow Formation, southwestern Manitoba
- 10:40 Eggie, L.* and Chow, N.** Diagenetic controls on the petroleum reservoir quality of the middle unit of the Wymark Member (Upper Devonian Duperow Formation), southwestern Manitoba
- 11:00 Rainbird, R.H.*, Thomson, D., Prince, J. and Krapez, B.** The Amundsen Cratonic Basin of northwestern Canada: Remnant of supercontinent Rodinia's interior
- SS13 WILLISTON BASIN AND OTHER INTRA-CRATONIC BASINS - SEDIMENTOLOGY, STRATIGRAPHY, PALEONTOLOGY AND RESOURCES**
Room / Salle: MR15
Sponsored by / Parrainé par: Red Beds Resources Ltd.
Supported by / Soutenue par: GAC Canadian Sedimentology Research Group
Organizers / Organismes: Michelle Nicolas, Pamela Fulton-Regula, James Bamburak, Nancy Chow
Chairs / Présidents: Michelle Nicolas and Derek Armstrong
- 08:20 Nicolas, M.P.B.*, Lavoie, D. and Armstrong, D.K.** Oil shale and reservoir rocks of the Hudson Bay Lowland, northeastern Manitoba
- 08:40 Pietrus, E.*, Chow, N. and Nicolas, M.** Sedimentological analysis and reservoir potential of the Lower Silurian Ekwon River Formation, Hudson Bay Basin, northeastern Manitoba
- 09:00 Armstrong, D.K.*, Lavoie, D., McCracken, A.D., Asselin, E. and Galloway, J.M.** Stratigraphy and source rocks of the Hudson Platform in northern Ontario
- SS20 DOES GEOLOGICAL RESEARCH AFFECT ENVIRONMENTAL DECISIONS?**
Room / Salle: MR3E
Organizers / Organismes: Heather Jamieson, Barbara Sherriff
Chairs / Présidents: Heather Jamieson and Barbara Sherriff
- 10:00 Refreshment Break / Pause-santé**
- 10:20 Parsons, M.B. Keynote (40 min):** Turning geoscience research into environmental outcomes at the Geological Survey of Canada
- 11:00 Langenberg, W.** Global carbon capture and storage (CCS) to mitigate climate change: Is it worth the price?
- SS21 GEOSCIENCE PROFESSIONALISM: ISSUES, RESPONSIBILITIES AND INFORMATION - WHAT DO YOU NEED TO KNOW?**
Room / Salle: MR11
Sponsored by / Parrainé par: Association of Professional Engineers and Geoscientists of the Province of Manitoba (APEGM)
Supported by / Soutenue par: Geoscientists Canada, Association of Professional Engineers and Geoscientists of the Province of Manitoba (APEGM)
Organizers / Organismes: Tim Corkery, Oliver Bonham, Greg Vogelsang
Chairs / Présidents: Tim Corkery and Greg Vogelsang

Friday, May 24 - Morning

- 08:20 Bonham, O.J.H.* and Corkery, M.T.** The IUGS Task Group on Global Geoscience Professionalism (TGGGP) - the birth of a global forum for professional affairs in geoscience
- 08:40 Bobrowsky, P.T.*, VanDine, D. and Couture, R.** Technical landslide guidelines for Canadian professional geoscientists
- 09:00 Reichelt, R.A.S.** Ethical responsibilities of geoscientists in environmental geology
- 09:20 Bank, C.* and Ryan, A.M.** Ethics in geosciences - what ethical dilemmas can we expect and how can we formally teach ethical behaviour?
- 09:40 Van der Flier-Keller, E.E.** Communicating Earth Science with the public: Part of our professional responsibility
- 10:00 Refreshment Break / Pause-santé**
- 10:20 Kirkham, G.D.** NI43-101 mineral resource estimation and the role and responsibilities of the qualified person
- 10:40 MacLachlan, K.K.*, Bonham, O.J.H., Broster, B.E. and Johnson, K.K.** Developing a competencies profile for the profession of geoscience
- 11:00 Ansdell, K.M.* and Stanley, C.** Geoscience knowledge requirements for Professional Registration: A primer for students as to the use of the GKE document
- SS23 MAGMATIC-HYDROTHERMAL DEPOSITS: PORPHYRY, IOCG AND EPITHERMAL SYSTEMS (DEDICATED TO THE MEMORY OF ROBERT KERRICH)**
Room / Salle: MR9/10
Organizers / Organismes: Hamid Mumin, Jeremy Richards, Louise Corriveau
Chairs / Présidents: Hamid Mumin, Jeremy Richards and Louise Corriveau
- 08:20 Richards, J. Keynote (40 min):** Subduction-zone magmatism as a source for lithospheric metallogeny
- 09:00 Mumin, A.H.* and Richards, J.P.** Evolution of magmatic-hydrothermal ore systems in response to secular changes in sulphur, oxygen, biospheric processes, and geothermal gradients from the Archean to the present
- 09:20 Alirezaei, S.** Variations in porphyry copper deposits; Case studies from the southern part of the Cenozoic Urumieh-Dokhtar magmatic belt, Iran
- 09:40 Hollings, P.*, Cooke, D. and Wolfe, R.** Miocene and Pliocene tectonic evolution of Northern Luzon, Philippines: Implications for porphyry mineralization
- 10:00 Refreshment Break / Pause-santé**

- 10:20 Alimohammadi, M.* and Alirezaei, S.** Distribution of hydrothermally altered rocks in the Raziabad-Madin area, southern part of the Kerman Copper belt, south Iran, based on spectral analysis of ASTER data
- 10:40 Einali, M.M.E.*, Bakker, R.S.A. and Alirezaei, S.R.B.** Darrehzar porphyry copper deposit, southeast Iran: Fluid inclusion and stable isotope evidence for a hydrothermal system dominated by magmatic fluids
- 11:00 Alirezaei, S.*, Borhanzadeh, F. and Sabouri, M.** Alteration-mineralization in the Miduk porphyry Cu-Au deposit; Cenozoic Urumieh-Dokhtar magmatic belt, Iran

GENERAL SESSIONS

- GS4 STRUCTURAL GEOLOGY AND TECTONICS**
Room / Salle: MR16
Organizers / Organismes: Scott Anderson, Paul Kremer
Chairs / Présidents: Paul Kremer
- 08:20 Wood, C.*, Bethune, K.M., McEwan, B., Carlson, A., McLintock, K. and Skanderbeg, B.** Journey to the centre of Santoy: Structural study of the auriferous Santoy shear zone, northeastern Glennie domain, Saskatchewan
- 08:40 Rubingh, K.E.*, Lafrance, B. and Gibson, H.L.** Structural geology of the McLeod Road-Birch Lake thrust panel with emphasis on the importance of structures relating to gold mineralisation, Snow Lake, Manitoba
- 09:00 Mendoza, F.* and Giraldo, K.** Definition of structural controls on formation of lode deposits of associated to mayor OTU shear zone fault system at El Limon Au vein, Zaragoza - Antioquia, Colombia
- 09:20 Pierre, S.*, Jébrak, M., Faure, S. and Roy, G.** Perseverance Mine, a deformed Archean volcanogenic massive sulphide deposit, Matagami mining camp, Quebec, Canada
- 09:40 Duguet, M.*, Magnus, S.J. and Ratcliffe, L.** Structural geology of the Mazinaw Domain, Admaston-Horton area, northeastern Central Metasedimentary Belt, Grenville Province, Ontario
- 10:00 Refreshment Break / Pause-santé**
- 10:20 White, S.E.* and Waldron, J.W.F.** Structure and deformation history of the Appalachian thrust front in western Newfoundland
- 10:40 White, J.C.** The role of fault-related fluids and nano-precipitates in establishing architecturally suitable mineralization zones, Kiggavik region, Nunavut

Friday, May 24 - Afternoon

SYMPOSIA

SY4 STIRRING THE POT: GEOSCIENCE CANADA SYMPOSIUM (IN HONOUR OF PAUL F. HOFFMAN)

Room / Salle: Presentation Theatre

Supported by / Soutenu par: Geoscience Canada / Geoscience Canada

Organizers / Organismes: Brendan Murphy, Galen Halverson

Chairs / Présidents: Galen Halverson and Brendan Murphy

01:40 Easton, R.M. Paleoproterozoic rift-drift transition along the southern margin of the Superior craton: a renewed look at the tectonic record preserved by the Huronian Supergroup

02:00 Higgins, J.A.*, Schrag, D.P., Swart, P.K., Miller, N.R., Macdonald, F.A., Maloof, A. and Hoffman, P.F. Keynote (40 min): Magnesium isotopes and the origin of dolomite

02:40 Hoffman, P.F. Keynote (40 min): The Great Oxidation Event (GOE) and a Siderian Snowball Earth: MIF based correlation of early Paleoproterozoic glaciations

SPECIAL SESSIONS

SS1 GEOSCIENCE AND RESOURCES AT CANADA'S NORTHERN FRONTIERS: CHALLENGES AND OPPORTUNITIES

Room / Salle: MR2E

Supported by / Soutenu par: GAC Precambrian Division; GAC Mineral Deposits Division

Organizers / Organismes: John Percival, John Ketchum, Luke Ootes, Dave Mate, Mostafa Fayek

Chairs / Présidents: John Percival and John Ketchum

01:40 Beauregard, M.A. Nunavut Carving Stone Deposit Evaluation Program: Establishing grade, tonnage and composition for the carving stone arts industry

02:00 Turner, E.C.*, Kamber, B.S., Kontak, D.J., Long, D.G.F., Hnatyshin, D., Creaser, R., Morden, R. and Hahn, K. Spatial and temporal constraints on base-metal distribution in the Mesoproterozoic Borden Basin (Nanisivik District), NU

02:20 Hahn, K.E.* and Turner, E.C. Regional deposition of giant deep-water carbonate seep mounds in the Mesoproterozoic Borden Basin (NU)

02:40 Bédard, J.H.*, Hayes, B., Hryciuk, M., Wing, B., Beard, C., Dell'Oro, T., Weis, D., Scoates, J., Williamson, N. and Cousens, B. The Neoproterozoic Franklin Large Igneous Province on Victoria Island

03:00 Whelan, S.C.*, Gleeson, S.A., Stern, R.A. and Buchanan, C. Au mineralization at 3Ace, south-east Yukon

03:20 Sack, P.J.*, Danyushevsky, L.L., Gilbert, S., Large, R.R. and Gregory, D. Diagenetic pyrite, a source of gold in sediment-hosted gold deposits? Examples from the Selwyn basin, Yukon

SS4 DIAMOND: FROM BIRTH IN THE MANTLE TO EMPLACEMENT IN KIMBERLITE

Room / Salle: MR7/8

Supported by / Soutenu par: MAC / AMC

Organizers / Organismes: Maya G. Kopylova, Yana Fedortchouk

Chairs / Présidents: Thomas Stachel

01:40 Hilchie, L.*, Pell, J., Scott Smith, B.H. and Russell, J.K. The CH-6 kimberlite, Canada: Textural and mineralogical features and their relevance to volcanic facies and magma batch interpretation

02:00 Zhang, Z.*, Fedortchouk, Y. and Hanley, J.J. Pressure effect on diamond resorption morphology

02:20 Cookenboo, H.O.* and Benitez, L. Visual characteristics of Vargem Bonita diamonds compared to indicator mineral compositions from the Canastra 1 Kimberlite

02:40 Benitez, L.* and Cookenboo, H.O. Diamond populations and diamond-associated indicator minerals point to one or more local sources within the Alto Paranaíba Diamond Province in western Minas Gerais State, Brazil

03:00 Kopylova, M.M. G.* and Beausoleil, Y.Y.L. Distribution of eclogites in the Slave mantle: The effect of subduction and metasomatism

03:20 Creighton, S.* and Read, G.H. Metasomatic overprinting of the lithospheric mantle of the Archean Sask Craton

03:40 Flemming, R.L.*, Weiss, T.L.C. and Dean, B. Quantifying strain-related mosaicity in mantle olivine by μ XRD: Examples from kimberlites and mantle xenoliths.

Friday, May 24 - Afternoon

SS11 PALEOGEODYNAMICS OF THE EARTH BEFORE PANGAEA

Room / Salle: MR12

Supported by / Soutenu par: GAC Geophysics Division IGCP project 597: "Amalgamation and Breakup of Pangaea: the type example of the supercontinent cycle"

Organizers / Organisateurs: Phil McCausland, Brendan Murphy, Joe Hodych, Rob Rainbird, Ken Buchan, Richard Ernst

Chairs / Présidents: Phil McCausland, Brendan Murphy and Rob Rainbird

01:40 Waldron, J.W.F.*, Schofield, D.I. and Murphy, J.
Geodynamics of Iapetus Ocean closure in the Appalachian-Caledonide orogen

02:00 Johnston, S.T. Keynote (40 min): Assembling Pangea: Not a linear process

SS13 WILLISTON BASIN AND OTHER INTRACRATONIC BASINS - SEDIMENTOLOGY, STRATIGRAPHY, PALEONTOLOGY AND RESOURCES

Room / Salle: MR15

Sponsored by / Parrainé par: Red Beds Resources Ltd.

Supported by / Soutenu par: GAC Canadian Sedimentology Research Group

Organizers / Organisateurs: Michelle Nicolas, Pamela Fulton-Regula, James Bamburak, Nancy Chow

Chairs / Présidents: Michelle Nicolas and Derek Armstrong

01:40 Hatcher, J.* and Bamburak, J.D. A new lectostratotype locality of the Millwood Member of the Upper Cretaceous Pierre Shale in Manitoba

02:00 Bingham-Koslowski, N.*, Tsujita, C. and Jin, J.
Tectonic arch control on the distribution of black shales in Paleozoic epeiric seas: A case study from southwestern Ontario

02:20 Wach, G.D.*, Kidston, J., Pelkey, R., Pothier, H. and Watson, N. Depositional environments, petrography and provenance of the mid-Cretaceous Dina and Cummings formations, Alberta

02:40 Bamburak, J.D.*, Nicolas, M.P.B. and Hatcher, J. A visual system of correlating bentonite seams in the Pembina Member of the Upper Cretaceous Pierre Shale in the Pembina Hills area of Manitoba and North Dakota

SS20 DOES GEOLOGICAL RESEARCH AFFECT ENVIRONMENTAL DECISIONS?

Room / Salle: MR3E

Organizers / Organisateurs: Heather Jamieson, Barbara Sherriff

Chairs / Présidents: Heather Jamieson and Barbara Sherriff

01:40 Brown, J.L.*, Nguyen, S.T., Lange, K. and Su, G.
The role of geoscience in the long term storage of radioactive wastes - Current Canadian perspective and regulatory oversight

02:00 Frempong, V.E., Flemming, R.L.*, Yanful, E.K. and Kuma, J.S. Soil characterization for landfill site selection in Tarkwa-Nsuaem municipality, Ghana

02:20 Sherriff, B.L.*, Johnson, B., Eary, T., Harrington, J., Davidson, S., Jamieson, H., Gault, A. and Londry, K. Natural attenuation of metals from the No Cash 500 mine adit discharge, Keno Hills Mining District, Yukon Territory, Canada

02:40 Jamieson, H.E.*, Buckwalter-Davis, M.J., Dongas, J. and Fenwick, L. Research on the prediction of mine drainage and the colloidal transport of metals

03:00 Sherriff, B.L.* and Mihychuk, M. The arsenopyrite stockpile at Snow Lake Manitoba: An example of university research leading to remediation by industry

03:20 Sealey, H.N.*, Gault, A.G. and Jamieson, H.E. Arsenic mobility and attenuation in a natural wetland at Terra Mine, Silver Bear, Northwest Territories

SS23 MAGMATIC-HYDROTHERMAL DEPOSITS: PORPHYRY, IOCG AND EPITHERMAL SYSTEMS (DEDICATED TO THE MEMORY OF ROBERT KERRICH)

Room / Salle: MR9/10

Organizers / Organisateurs: Hamid Mumin, Jeremy Richards, Louise Corriveau

Chairs / Présidents: Hamid Mumin, Jeremy Richards and Louise Corriveau

01:40 Dare, S.A. S.*, Barnes, S-J., Beaudoin, G., Méric, J. and Boutroy, E. Are the magnetite "lava flows" of El Laco (Chile) magmatic? Comparison of trace elements in magnetite with magmatic Fe-oxide deposits

02:00 Somarin, A.K.* and Mumin, H. Thermometric studies of the Mag Hill IOCG system, Contact Lake belt, Northwest Territories, Canada

02:20 Kontak, D.J.*, Dubé, B., McNicoll, V., Creaser, R. and Kyser, K. The Upper Beaver Au-Cu deposit, Kirkland Lake, Ontario, Canada: An Archean IOCG analogue or just an intrusion-related iron oxide copper gold deposit (?)

Friday, May 24 - Afternoon

- 02:40 Forslund, N. and Kissin, S.A.*** Alteration and fluid characteristics of the Hamlin Lake IOCG occurrence, northwestern Ontario
- 03:00 Corriveau, L.*, Montreuil, J-F., Hayward, N., Enkin, R., Davis, B., Potter, E., McMartin, I. and Normandeau, P.X.** Exploration technologies and models for IOCG and affiliated iron oxide alkali-altered deposits with case examples from the Great Bear magmatic zone, Canada
- 03:20 Rowins, S.M.* and Howarth, L.N.** Intrusive rocks associated with the Neoarchean Troilus Au-Cu deposit, Frotet-Evans greenstone belt, Quebec
- 03:40 Fayol, N.* and Jébrak, M.** The Lac Bachelor gold deposit (Abitibi, Québec)

GENERAL SESSIONS

GS1 MINERALOGY, CRYSTALLOGRAPHY AND MINERAL CHEMISTRY

Room / Salle: MR11

Supported by / Soutenue par: MAC / AMC

Organizers / Organismes: Yana Fedortchouk, Olivier Gagné, Zhihai Zhang

Chairs / Présidents: Yassir Abdu and Olivier Gagné

- 01:40 Roper, A.J.*, Leverett, P. and Williams, P.A.** Towards a comprehensive geochemical model for antimony in the oxidized environment
- 02:00 Murphy, T.*, Leverett, P. and Williams, P.** Bismuth dispersion in the supergene zone
- 02:20 Shahabi Far, M.*, Samson, I., Gagnon, J., Linnen, R. and Good, D.** Textural character and chemistry of plagioclase and apatite in the Marathon Cu-PGE deposit, Ontario: Implications for mineralizing processes
- 02:40 MacNeil, L.*, Peterson, R., Färber, G., Groat, L. and Witzke, T.** Mineralogical studies of a low-temperature hydrothermal barium-rich skarn deposit, Gunn Claim, Yukon Territory
- 03:00 Gagné, O.C.* and Hawthorne, F.C.** Bond lengths in the solid state: A comprehensive survey
- 03:20 Rani, N.*, Shrivastava, J.P. and Bajpai, R.K.** Deccan Traps associated Obsidian and its suitability for radioactive waste disposal in geological repository

**Nanodiamonds and amorphous carbon in carbonaceous-chondrite xenoliths in the Kapoeta meteorite: Astrophysical implications**

Abdu, Y.A.¹, Hawthorne, F.C.¹, Yassir, Abdu@ad.umanitoba.ca, Varela, M.E.² and Duley, W.W.³, ¹Department of Geological Sciences, University of Manitoba, Winnipeg, MB R3T 2N2; ²Instituto de Ciencias Astronómicas de la Tierra y del Espacio (ICATE), Av España 1512 Sur, CP J5402DSP, San Juan, Argentina; ³Department of Physics, University of Waterloo, Waterloo, ON N2L 3G1

Interstellar or presolar nanodiamonds, with a mean crystallite size of 1-3 nm, were discovered by Lewis *et al.* (1987) in the acid-treated residues of carbonaceous chondrites. These nanodiamonds contain isotopically anomalous noble gases, particularly Xe-HL anomaly, which is enriched both in the heavy (H) and the light (L) isotopes of Xe. The origin and the process by which these presolar nanodiamonds have formed is still debated; however many authors favor formation from a process similar to chemical-vapor-deposition (CVD). Kapoeta is an achondrite meteorite characterized as a gas-rich polymict breccia with a light-dark structure. It belongs to the howardite group, which together with eucrites and diogenites constitute the HED meteorites, with 4 Vesta as a probable parent asteroid. Kapoeta contains mm-sized dark inclusions that are described as carbonaceous chondrite (CC) materials; these are believed to have been incorporated into the HED parent body by carbonaceous meteorite impactors at a later stage of its formation. Here, we present results from a Fourier-transform infrared (FTIR) and Raman spectroscopy study on CC material from the Kapoeta meteorite.

The KBr-pellet FTIR spectrum of the CC material (4000-400 cm⁻¹) shows absorption bands attributable to silicates (the dominant band) and aliphatic CH₂ and CH₃ groups. The C-H stretching region of the spectrum (3100-2600 cm⁻¹) is dominated by a strong CH₂ absorption band at ~2922 cm⁻¹, very similar to that observed in IR spectra of organic matter in carbonaceous chondrites and the diffuse interstellar medium. Very weak bands indicative of C-H stretching vibrations in aromatic hydrocarbons were also observed. Nanodiamonds, as evidenced by micro-Raman spectroscopy, were found as aggregates of micro- to submicrometer particles forming clusters that scatter in and around a dark region (~400 µm in size) in the KBr-pellet. Micro-Raman spectroscopy indicates that these nanodiamonds coexist with an amorphous carbon phase(s). Micro-FTIR spectra, collected from the diamond-enriched region are radically different from the KBr-pellet spectrum, and their C-H stretching region is dominated by a strong and broad absorption band at ~2886 cm⁻¹ that may be assigned to tertiary CH groups, in accord with the IR absorption spectra of hydrocarbon dust in dense interstellar clouds. Our results will be discussed in connection with the IR spectroscopic features of interstellar nanodiamonds and the different scenarios proposed for their formation. (SS18; Thurs. 3:00)

Vegetation history of the Lagos lagoon coastal environments southwestern Nigeria: A palynological approach

Adekanmbi, O.H., Department of Botany, University of Lagos, Akoka, Yaba, Lagos, Nigeria, sholaadekanmbi2000@yahoo.com

Vegetation history and distribution of swamp forest in Lagos lagoon coastal environments were reconstructed by means of pollens derived from surface sediments collected from eight lagoonal communities. The palynomorphs identified in the studied samples represent the pollen and spore deposition over the past few years, derived mainly from the local and to a lesser extent from regional vegetation. These materials are good reflection of vegetation, environmental condition and extent of the lagoon in the recent past. The palynofacies recovered are made up of mixed ecological zones due to regular inundation by freshwater, although the pollen of dominant ecological zone was distinct. Several species that were prominent in the vegetation were well represented in the pollen spectrum and such include *Laguncularia racemosa* (0.93%), *Avicennia germinans* (1.45%), *Alchornea cordifolia* (1.8%), *Rauwolfia vomitoria* (0.41%), *Alstonia boonei* (0.58%), *Cleistopholis patens* (0.29%), *Ceraptoteris cornia* (0.17%), *Acrostichum aureum* (0.41%), *Elaeis guineensis* (0.99%) and *Aracaceae* pollen (1.45%). This implies

that the vegetation that existed in this community in recent past is very similar to what exist in the present day. Furthermore, even though some of the sampled sites seem undisturbed at present, the recovery of *Elaeis guineensis*, the pollen of trees common in cleared and secondary forest and weeds of cultivated and waste ground such as *Aspilia africana* and *Chromola odorata* indicates the disturbance of this site sometimes in the past. (GS6; Wed. 10:20)

Base and solvent-driven formation of hybrid uranyl nanocages

Adelani, P.O. and Burns, P.C., Department of Civil & Environmental Engineering & Earth Sciences, University of Notre Dame, Notre Dame, IN 46556 USA, padelani@nd.edu

The lack of coordination along the axial position of the uranyl ion favors the formation of one-dimensional chains or two-dimensional sheets that normally result from linkage of uranyl bipyramids. Synthesis of well-organised nanospherical uranyl structures is extremely difficult, especially when planar aromatic ligands are employed. One way to circumvent this is by using pliable oxoanions to introduce curvature in uranyl polyhedra. The central issue we intend to address in ongoing studies is to incorporate transition metals and lanthanide cations in nanoscale uranyl cages, so that we can probe further their structural variations and electronic properties. Hydrogen peroxide has been used extensively for the formation of nanoscale uranyl cage clusters; current research efforts are focused on using organic moieties as secondary linkers in order to incorporate transition metals. However, while the nanospheric topology is common in polyoxometalate-based uranyl containing clusters, it is exceptionally rare in uranyl-organic coordination nanocages. This presentation highlights results of recent studies with peroxide-carboxyphosphonates and arsonates. (SS5; Wed. Poster)

Resistivity structures of the Precambrian Superior-Grenville margin defined by the magnetotelluric method as part of the POLARIS project

Adetunji, A., demlad@gmail.com, Ferguson, I.J., Department of Geological Sciences, University of Manitoba, Winnipeg, MB R3T 2N2, and Jones, A.G., Dublin Institute of Advanced Studies, Dublin, Ireland

The Archean Superior province shares a tectonic boundary with the Proterozoic Grenville province. The lithosphere beneath the Superior-Grenville margin, in southern Ontario, was investigated with a northwest-southeast oriented, 650 km long profile of magnetotelluric (MT) data. The profile consists of 40 broadband MT sites from Portable Observatories for Lithospheric Analysis and Research Investigating Seismicity (POLARIS) and the earlier LITHOPROBE Abitibi-Grenville transect. It crosses the Abitibi and Pontiac subprovinces of the Superior province as well as the Central Gneiss and Central Metasedimentary Belts of the Grenville province. The Grenville Front Tectonic Zone separates the Grenville province from the Superior province and the Central Metasedimentary Belt Boundary Zone separates the two belts in the Grenville province.

Geoelectric strike analysis results show that the strike azimuth varies both along the profile and with depth. Dominant strike azimuths of N45°E and N85°E were defined for the crust and the lithospheric mantle respectively. An azimuth of N68°E determined for asthenospheric depths (200-400 km) is parallel to the hotspot reference model of absolute plate motion in the area. The 2-D inversion model for the crust shows that the Grenville Front Tectonic Zone and the Central Metasedimentary Belt Boundary Zone extend with a southeast dip throughout the crust. It also shows a predominantly conductive Central Metasedimentary Belt. A 2-D inversion model for the whole lithosphere defines a resistive zone dipping southeast from a location beneath the Central Gneiss Belt. The resistive zone extends beneath the Central Metasedimentary Belt where it lies between 100 km and 260 km depth. It is interpreted to be modified lithosphere formed by mantle depletion and/or emplacement of subducted Archean lithosphere. A deep conductor is observed extending across the northwest and central part of the profile. Beneath the southwest Superior province its top is



approximately horizontal and lies at a depth of about 160 km. The conductivity of the feature increases beneath the Pontiac subprovince, where it is overlain by a shallower mantle conductor. Further to the southeast, the feature dips downwards beneath the Grenville province, with its top reaching a depth of 300 km. The conductor is interpreted to be the lithosphere-aesthenospheric boundary and the part with higher conductivity beneath the Pontiac subprovince as representing a refertilized mantle scar. The scar, which has survived a series of tectonic events, was left by an Archean thermomechanical event and was last refertilized by the Cretaceous Great Meteor hotspot plume. (SS2; Wed. 10:40)

Trace element distribution in sulfide assemblages from the Levack-Morrison ore system, Sudbury, Ontario: Looking for chemical fingerprints of ore processes

Adibpour, M.¹, mx_adibpour@laurentian.ca, Jugo, P.J.¹, and Ames, D.E.², ¹Department of Earth Sciences, Laurentian University, Sudbury, ON P3E 2C6; ²Geological Survey of Canada, 601 Booth St., Ottawa, ON K1A 0E8

The Levack-Morrison system is one of the few ore deposits associated with the Sudbury Igneous Complex (SIC) where there is continuity between contact Ni-Cu ores and footwall Cu-PGE (platinum group elements) ore types. The magmatic origin of high-Ni, low-PGE contact type deposits is reasonably well established. These deposits are thought to result from the segregation of immiscible sulfide melts that accumulated along the floor of the SIC during cooling of the impact melt sheet that generated it. In contrast, the origin of mineralization within the footwall is not well understood, in part because of the various styles of mineralization. Some authors have emphasized the significance of magmatic processes whereas others have favoured hydrothermal or metamorphic processes in remobilizing elements. In the Morrison deposit the footwall ores are divided into three different subtypes: a transition zone between contact and footwall type ores (Morrison Upper Zone, Ni \approx Cu), chalcopyrite veins associated with pentlandite and quartz (Morrison Middle Zone, Cu-PGE-Ni), and disseminated low-sulfide, high-PGE ores (Morrison Lower Zone, PGE-Cu). To determine if chemical fingerprints can be established for each deposit type, laser ablation ICP-MS element distribution maps were created on sulfide assemblages from samples of each deposit type. Preliminary results have not detected any significant differences in trace element distribution for the major sulfides (pyrrhotite, pentlandite, and chalcopyrite). However, pyrite (when present) shows significant variability in trace element content and distribution. In the Levack contact type deposit, relatively large euhedral pyrite grains (up to 1 mm) exhibit complex zoning in Co, As, and Se, commonly associated with detectable zoning in Ru, Rh, Os, and Ir, variations (mostly as nuggets invisible to SEM imaging) in Au, Pd, Pt, as well as discrete inclusions of galena (visible under reflected light). In the Morrison footwall deposits, rare anhedral pyrite (up to 0.5 mm) of the Upper Zone assemblages and rare anhedral to euhedral pyrite of the Lower Zone (up to 0.03 mm) also show abundant Co, but without the complex Co zoning seen in pyrite from contact ores. However, with the exception of Bi, pyrite from footwall ores has no detectable trace elements. The documented variations of trace elements in pyrite from contact ores is consistent with models suggesting that this pyrite formed from cooling of immiscible sulfide liquid. Additional work on bornite-millerite veins and maps with larger beam diameters (lower detection limits) on major sulfides is planned. (SS9; Wed. Poster)

The strange structures and unusual properties of actinide borates

Albrecht-Schmitt, T.E., Florida State University, 95 Chieftan Way, Tallahassee, FL, 32303 USA

Periodic trends across the actinide series from thorium to californium will be developed in regard to the formation of atypical borate materials. These material display unusual oxidation states, redox chemistry, coordination environments, and are remarkably resistant to radiation damage. (SS5; Thurs. 8:20)

The significance of the chemical composition of natural uraninite

Alexandre, P., Kyser, K., Queen's University, Kingston ON K7L 3N6, alexandre@geol.queensu.ca, and Uvarova, Y., SCIRO CESRE, 26 Dick Perry Ave, Kensington WA 6151, Australia

The chemical composition of natural uraninite is relatively well known with regards to major elements, from electron microprobe analyses, and REE, from recent laser ablation ICP-MS studies. However, the amount and variability of trace elements has not been well studied, nor has the variability of uraninite chemistry as function of deposit type. In the present work, the chemical composition of uraninites from five deposit types (unconformity, tabular, metasomatic, intrusive, and vein) is compiled, based on literature data (electron microprobe), new electron microprobe data, and new laser ablation ICP-MS data.

The results underline the extreme chemical variation of natural uraninite, with concentrations for any element, U excepted, varying between below detection limit and several weight percent. This variability is due to different conditions of uraninite formation and alteration and suggests, in addition to the non-stoichiometric nature of uraninite, that it might not be possible to define a single uraninite chemical composition. The approximate overall median concentrations of natural uraninites are 2.5 wt% Th, 2.1 wt% Ca, 1.0 wt% REE, 0.6 wt% Mn, 0.5 wt% Si, 0.5 wt% Y, 0.4 wt% V, 0.3 wt% Fe, 0.3 wt% As, 1500 ppm W, 800 ppm Mg, 400 ppm Bi, 350 ppm Ti, 300 ppm Sb, and 280 ppm Sr, with another dozen elements (Ag, Ba, Cu, Ga, Ge, Hf, Mo, Nb, Sc, Sn, Zn, and Zr) rarely exceeding 100 ppm individually and totalling 350 ppm.

Uraninite from sandstone-hosted deposits (tabular, unconformity) is characterized by negligible Th, low Y and REE, high "substitution" elements (SiO₂+CaO+FeO of 5.3 wt% for tabular and 3.0 wt% for unconformity-related uraninite), and high "trace" elements (total of 10 wt% for tabular and 3 wt% for unconformity-related uraninite). Additionally, the REE of unconformity-related uraninite exhibit strongly pronounced bell-shaped spectra, clearly different from those in tabular uraninites, which are LREE-enriched. Inversely, the magmatic and metasomatic-related uraninites have high Th (4.7 and 7.1 wt%, respectively), high Y (1.4 and 0.26 wt%), and high SREE (2.4 and 1.4 wt%); and low "substitution" and "trace" elements, with the exception of Ca, which can reach 10 wt% in intrusive-related uraninite. Additionally, the REE exhibit a clear Eu anomaly, most pronounced in the Na-metasomatism-related uraninites. (SY1; Wed. 10:40)

Distribution of hydrothermally altered rocks in the Raziabad-Madin area, southern part of the Kerman Copper belt, south Iran, based on spectral analysis of ASTER data

Alimohammadi, M. and Alirezaei, S., Faculty of Earth Sciences, Shahid Beheshti University, Tehran, Iran, M_Alimohammadi@sbu.ac.ir, PO Box 15875-4731

The Cenozoic Urumieh-Dokhtar Magmatic Belt (UDMB) of Iran is a major host to porphyry Cu±Mo±Au deposits (PCDs). Most known PCDs in the UDMB occur in the southern section of the belt, also known as the "Dehaj-Sardoeieh belt", or "Kerman Copper belt". The PCDs are commonly associated with well-developed potassic, phyllic, propylitic, and less commonly, argillic alterations, with phyllic alteration being dominant, and the prime target in exploration using satellite imagery. The alterations are variably developed in the PCDs, and no consistent patterns can be established.

Phyllic alteration, as commonly represented by abundant sericite, is missing, or only locally developed, in some PCDs, particularly those in the Jebal-Barez Mountains to the south of the Kerman copper belt, and Cu anomalies are, at least partly, associated with silicified zones.

An Advanced Space-borne Thermal Emission and Reflection Radiometer (ASTER), with three visible and near infrared (VNIR) bands, six shortwave infrared (SWIR) bands, and five thermal infrared (TIR) bands, was used to identify the distribution of the alteration minerals (assemblages) associated with copper mineralization in the Raziabad-Madin area, which is one of the few copper deposits known in Jebal-Barez. The area is covered by Upper Cretaceous-Eocene sedimentary, volcanic and plutonic rocks intruded by younger plutonic



and subvolcanic bodies of felsic-intermediate compositions.

Alteration-mineralization covers an area ~ 2 km², and appears to be mostly associated with a porphyritic quartz-diorite.

The research includes ASTER data pre-processing, processing and field and petrographic studies. Various image processing techniques, including different ratio images, relative band depths, minimum noise fraction, pixel purity index, and matched filter processing were used to delineate and generate a hydrothermal alteration map. VNIR+SWIR relative reflectance spectral analysis was used for detecting and mapping sericitic, argillic and propylitic alterations, which were found to be of limited exposures. Silicified rocks could not be distinguished in the 9 VNIR-SWIR bands, due to the lack of diagnostic spectral absorption features in quartz in this wavelength region. Areas of quartz stockworks and silicified rocks were successfully mapped in the 5 thermal-infrared (TIR) bands, as demonstrated by follow-up field and petrographic studies. The silicified rocks and quartz stockworks in Raziabad-Madin are characterized by abundant magnetite, pyrite and minor chalcopyrite.

The Raziabad-Madin area provides an example of porphyry-style mineralization associated with silicic alteration, and not necessarily with extensive phyllic and/or argillic alterations. Results from this study suggest that silicic alteration can be conveniently inspected and targeted, and this should be considered as a promising tool for exploration for PCDs in Jebel-Barez and likely in other areas of potential PCDs. (SS23; Fri. 10:20)

Variations in porphyry copper deposits; Case studies from the southern part of the Cenozoic Urumieh-Dokhtar magmatic belt, Iran

Alirezaei, S., Faculty of Earth Sciences, Shahid Beheshti University, Evin, Tehran, Iran, PO Box 15875-4731

Cenozoic was a time of active magmatism in Iran, represented by three major magmatic belts in west, known as Urumieh-Dokhtar, north-northwest, known as Alborz-Azarbaijan, and East Iran. The magmatism led to the formation of a wide range of hydrothermal ores, including porphyry-type Cu±Mo±Au, and epithermal base and precious metals deposits. The majority of the known PCDs occur in the southern section of the Urumieh-Dokhtar, known as Dehaj-Sardoieh, or Kerman, belt.

The PCDs share some key features, such as association with shallow intrusions, ore formation by saline, hot fluids, extensive hydrothermal alteration and alteration zoning, and simple hypogene ore mineralogy, dominated by pyrite-chalcopyrite ± bornite ± molybdenite. Mineralization occurs variably in the parent intrusions as well as the enclosing rocks. Most intrusions occur as steep-walled stocks, circular to elliptical in plan view, <500 m. to 3000 meters in diameters. They vary in composition from diorite to quartz-diorite, quartz-monzodiorite, quartz-monzonite, and granodiorite. They are metaluminous to slightly peraluminous, high-K calc-alkaline, and display distinct enrichments in LREE relative to HREE, high Sr/Yb ratios, and slightly positive Eu anomalies. Most PCDs formed in middle-upper Miocene, consistent with the final stages of the Neotethyan subduction and early stages of continental collision. In spite of the similarities, distinct variations exist in details from one deposit to the other, complicating the exploration trends. The variations arise from both primary hypogene (endogenous), and secondary supergene (exogenous) processes. The main primary factors include:

- Source effects (magma source, and conditions of melting and storage);
- Evolution of the parent magma (equilibration and separation from the source or storage, the size or volume of the melt batch, simple vs. complex intrusions, wall rock contamination);
- Depth of emplacement, cooling rate, and timing of hydrothermal fluid exsolution; and
- Composition and permeability of the host rocks. The primary factors set major controls over the composition (water/volatile contents, ore elements) and oxidation states of the magmas and

fluids, hypogene ore/alteration assemblages, tonnage/grade, and the mode of ore formation (stockwork vs. disseminated).

The PCDs have been variably affected by post-ore uplift/exhumation and supergene processes, leading to variable development of leached, oxide, and supergene enriched zones. The main controls include climate, permeability (drainage), topography, and exposure level that in turn control the composition and buffering capacity of the altered-mineralized host rocks, pyrite content and pyrite/chalcopyrite (bornite) ratio, and remobilization-precipitation of Cu. (SS23; Fri. 9:20)

Alteration-mineralization in the Miduk porphyry Cu-Au deposit; Cenozoic Urumieh-Dokhtar magmatic belt, Iran

Alirezaei, S., Shahid Beheshti University, Evin, Tehran, Iran, s-alirezaei@sbu.ac.ir, Borhanzadeh, F. and Sabouri, M., Parsolang Engineering Company, No. 16, Alley 40 Markazi, Allameh South, Tehran, Iran

The Miduk porphyry Cu-Mo-Au deposit lies in the southern part of the Cenozoic Urumieh-Dokhtar magmatic belt, Iran. The mineralization is associated with a Miocene shallow quartz-diorite to quartz-monzodiorite body intruded into Paleocene-Eocene intermediate-mafic volcanic and pyroclastic rocks. The intrusion consists of plagioclase, biotite, and subordinate K-spar, hornblende and quartz phenocrysts in a quartz-feldspar matrix. The country rocks vary from andesite to basaltic andesite, basalt, and various tuffs.

Hydrothermal alteration in Miduk is distinguished by a proximal potassic assemblage, dominated by biotite and K-spar. Biotite occurs as a newly-formed phase in the matrix, as well as replacing earlier magmatic hornblende and biotite. K-spar occurs as anhedral grains and grain aggregates preferably replacing magmatic plagioclase, and in quartz-K-spar veinlets. Gypsum and magnetite are common, and locally abundant, occurring as scattered grains and in veinlets with, or without, quartz and sulfides. The potassic alteration grades outward into phyllic alteration, where the earlier potassic assemblages, and magmatic minerals left intact from potassic alteration, are increasingly replaced by sericite and minor chlorite. Phyllic alteration covers large areas and appears to be, at least partly, of overprint nature. Phyllic alteration has drastically altered the original features, rendering the identification of the original rocks extremely difficult. There is chemical, mineralogical and textural evidence that the overprint phyllic alteration was associated with extensive redistribution of copper, and possibly gold. A propylitic halo, distinguished by the occurrence of chlorite, epidote, and carbonates, is well developed in the enclosing volcanic rocks.

Mineralization occurs in quartz-sulfide stockworks and as disseminated sulfide grains, in the parent intrusion and the host volcanic rocks. Chalcopyrite is the main hypogene copper mineral, associated with abundant pyrite, and subordinate bornite and molybdenite. Supergene processes led to the development of a high-grade supergene enriched blanket over a thick leached cap. Oxide minerals, dominated by malachite, are locally abundant above the enriched blanket. Several late- and post-ore hornblende-diorite dykes, some containing recoverable copper assays, occur in the deposit.

The recent deep diamond drill holes by the National Iranian Copper Industries have indicated that the ore body extends vertically for over 1000 meters, and that the central potassic zone contains significantly higher copper and gold assays. A characteristic feature, with increasing depth, in the central part of the deposit, is the scarcity of pyrite, and the common occurrence of bornite. A significant correlation exists between the abundance of gold and the occurrence of bornite. (SS23; Fri. 11:00)

Integrating sequence stratigraphy, biostratigraphy and chemostratigraphy: An example from the Katian (Late Ordovician) reference section, central Oklahoma

Amati, L.¹, amatilm@potdam.edu, Westrop, S.R.², Brett, C.E.³, Swisher, R.E.² and Carlucci, J.R.⁴, ¹SUNY Potsdam, Potsdam, NY, USA 13676; ²University of Oklahoma, Norman, OK, USA



73072; ³University of Cincinnati, Cincinnati, OH, USA 45221-0013; ⁴Midwestern State University, Wichita Falls, TX, USA 76308

The Katian Stage (Late Ordovician) reference section is a roadcut through mostly inner to mid-ramp Viola Formation at Highway 99 near Fittstown, Oklahoma. Recent work on conodont biostratigraphy and carbon isotope stratigraphy results in the novel interpretation that this section is entirely older (M5 sequence of eastern Laurentia) than the well-known, mostly deep ramp Viola successions of the south flank of the Arbuckle Mountains along I-35 (M6 and younger sequences). The sequence stratigraphy and trilobite faunas of the Viola and the Kimmswick Subgroup in Missouri offer a different perspective. The Viola of the reference section is composed mostly of shallow subtidal facies with diverse trilobite faunas. A record of the graptolite *Diplacanthograptus spiniferus* at 35 m above the base of the Viola shows that the upper half of the section is no older than M6. This is supported by the associated trilobites, which include several species recorded from the Kimmswick Subgroup (M6 and younger). The base of M6 can, in fact, be identified at about 18 m above base of the Viola in the reference section, where it is marked by a TST of coarse, cross-bedded bioclastic grain- to rudstone facies that appears to correlate with the base of Kimmswick in the St. Louis area. Under this interpretation, the carbon isotope excursion reported from the upper half of the reference section as the GICE may be the same excursion identified as the KOPE near the base of the Viola in the I-35 section. It also implies that the conodont *Belodina confluens* makes a relatively "late" entry into the succession at the reference section. Although the I-35 section overlaps with the reference section, there remains a larger break beneath the Viola in the former, with cut-out of part of M4 and most, if not all, of M5. The conflicting interpretations of these sections underscore the need to consider all available evidence, including sequence stratigraphy and biostratigraphy, preferably with multiple faunal groups, when dating and correlating isotope excursions. (SY3; Thurs. 1:40)

The occurrence and alteration of (Y, REE, U, Th)-(Nb, Ta, Ti) oxide minerals near the footwall contact of the Greenbushes pegmatite, Western Australia

Anderson, A.J., St. Francis Xavier University, Antigonish, NS B2G 2W5, aanderso@stfx.ca, Rhede, D. and Wirth, R., Helmholtz Centre Potsdam, GFZ German Research Centre for Geosciences, Telegrafenberg, D-14473 Potsdam, Germany

The (2.527 Ga) Greenbushes rare-element pegmatite in Western Australia is an important source of lithium and tantalum. The pegmatite, which was emplaced syntectonically into the Donnybrook-Bridgetown shear zone within the Yilgarn Craton, consists of five distinct petrologic zones. Columbite-tantalite-, euxenite-, pyrochlore-, and aeschynite-group minerals were examined in samples collected from the albite zone of the pegmatite and in granoblastic metamorphic rocks from its footwall contact. Electron microprobe analysis (EMPA) of (Y, REE, U, Th)-(Nb, Ta, Ti) oxide minerals in polished thin sections, and transmission electron microscope (TEM) investigations of thin foils extracted from selected regions in a single grain, reveal varying degrees replacement and crystallinity. Alteration of rare metal oxides is characterized by loss of heavy rare earth elements (HREEs) and Nb, and the addition of Al, Si, P, Ca, Fe, As, La, and Ce. The occurrence of tantalum oxide minerals in metamorphic host rocks and as thin veins within grain boundaries of recrystallized quartz and albite in the albite zone suggest that tantalum and niobium in primary phases was remobilized by hydrothermal fluids at the time of deformation. (SY2; Thurs. Poster)

Trace-element geochemistry of muscovite as petrogenetic indications of pegmatite evolution in the Moose II lithium-tantalum pegmatite deposit, Northwest Territories, Canada

Anderson, M.O.¹, Anderson.geology@gmail.com, Lentz, D.¹, McFarlane, C.R.M.¹, Falck, H.² and Hall, D.C.¹, ¹University of

New Brunswick, Fredericton, NB E3B 5A3; ²Northwest Territories Geoscience Office, Yellowknife, NT X1A 2R3

The internal evolution of the Late Archean rare-metal-bearing Moose II pegmatite, NWT, was examined using the trace-element geochemistry of muscovite. Historically, this deposit was mined for both lithium and tantalum (1946 – 1954) and represents the most notable LCT pegmatite in the Slave pegmatite field. The pegmatite is 430 m long, up to 61 m wide, and is discordantly hosted within polydeformed metatubidites of the Archean Yellowknife Supergroup. This dyke is characterized by an irregular spatial zonation of mineral assemblages, consisting of a narrow border zone, a fine-grained wall zone, three megacrystic intermediate zones, massive quartz and amblygonite-montebrasite core zones, saccharoidal albite zones, and muscovite-rich replacement zones.

The geochemistry of primary muscovite by laser ablation ICP-MS adds some constraints to the degree of evolution and progressive fractionation in the Moose II pegmatite. Trace-element contents (n=39) show elevated Li (avg. 221 ± 63 ppm), Cs (avg. 149 ± 57 ppm), Ta (avg. 76 ± 13 ppm), and Nb (avg. 67 ± 8 ppm). An increase in Li contents in muscovite is correlated with the occurrence of spodumene, with the highest concentration in the second intermediate zone (avg. 502 ± 48 ppm Li, n=7). The sequence of fractionation between the mineralogical zones progresses from the margins inwards, beginning with the wall zone, and followed by the intermediate zone 1, 3, and then 2; the fractionation patterns exhibit predictable elemental and key element ratio changes in each mineralogical zone. The change in the major mineralogy of the inward succession of zones in the Moose II pegmatite broadly correspond to the calculated phase relations at high pressures (500 MPa) for the well-studied Li-rich Harding pegmatite, New Mexico. The distribution of mineralogical zones suggests that the northern exposure of the pegmatite is more fractionated than the southern exposures.

Analyses of fine-grained (secondary-late) muscovite (n=44) formed by hydrolysis of feldspars throughout the pegmatite show distinct geochemical signatures compared to the coarse-grained primary muscovite crystals, with higher concentrations of B (avg. 79 ± 5 ppm), Zn (avg. 113 ± 17 ppm), Sn (avg. 278 ± 50 ppm), and Nb (avg. 183 ± 8 ppm), and decreased concentrations of Ta (avg. 38 ± 5 ppm). A late, Nb-rich metasomatizing fluid also resulted in Nb-rich overgrowths and patchy replacements on primary columbite-tantalite crystals. Therefore, at subsolidus conditions, Nb is evidently considerably more mobile than Ta. These results emphasize the need for further experimental work on niobium versus tantalum solubility. (SY2; Thurs. 3:00)

Economic potential (?) for U-Th-REE-mineralized granitic pegmatites in the Wollaston Domain, northern Saskatchewan, Canada: Evidence from a resource estimate at Fraser Lakes Zone B

Annesley, I.R.¹, jnrirvine@gmail.com, McKechnie, C.L.¹, Mercadier, J.², Armitage, A.³, Sexton, A.³ and Bogdan, T.S.⁴, ¹Department of Geological Sciences, University of Saskatchewan, 114 Science Place, Saskatoon, SK S7N 5E2; ²GeoResources, Université de Lorraine, CNRS-CREGU, Boulevard des Aiguillettes B.P. 70239, Vandoeuvre-les-Nancy, France; ³GeoVector Management Inc., 10 Green St., Napean, ON K2J 3Z6; ⁴JNR Resources Inc., 204-315 22nd St. East, Saskatoon, SK S7K 0G6

The Way Lake Uranium Project is located in the eastern Wollaston Domain, northern Saskatchewan. Active uranium exploration by JNR Resources Inc. (JNR), until recently, targeted low-grade, high-tonnage granitic intrusive-style U-Th-REE-type deposits, with potential to discover basement-hosted unconformity-type uranium deposits. Exploration involved airborne and ground geophysics, ground-based prospecting and drilling programs, drill core geochemistry, and detailed petrological studies. Fraser Lakes Zone B was discovered by a prospecting and drilling program in 2008. This style of primary uranium mineralization associated with intrusive magmatic rocks is commonly referred to as 'Rössing type'. At Zone B, U-Th-REE-mineralized granitic pegmatites/leucogranites intrude the deformed



contact between Paleoproterozoic metasedimentary gneisses of the Wollaston Group and Archean orthogneisses. The mineralization is mixed in origin; both magmatic and xenocrystic, and occurs mainly within fresh to altered granitic pegmatite comprising uraninite, uranoan thorite, monazite, and/or zircon; accompanied by varying degrees of chlorite, hematite, fluorite, sericite, and clay mineral alteration. It is associated with anomalous pathfinder elements: zirconium, cobalt, copper, nickel, molybdenum, lead, and zinc.

An initial resource estimate and an associated technical report for the Fraser Lakes Zone B were prepared by GeoVector Management Inc. for JNR, in compliance with the requirements of NI 43-101. The Fraser Lakes Zone-B deposit, using a base case cut-off grade (COG) of 0.01% U_3O_8 , is currently estimated to contain an inferred resource totaling 6,960,681 lbs of U_3O_8 within 10,354,926 tonnes at an average grade of 0.030% U_3O_8 . There are also significant quantities of thorium and rare earth element oxides, specifically La_2O_3 , Ce_2O_3 , Yb_2O_3 , and Y_2O_3 . Using the same base case COG, the inferred resource includes 5,339,219 lbs of ThO_2 at an average grade of 0.023%. The resource was determined from a database of 1,283 assay results in 32 drill holes totaling 5,694 meters of drilling. The drill holes are spaced primarily 75 to 250 meters apart along a strike length of approximately 1,400 meters, and tested mineralization to a vertical depth up to 175 meters. Mineralization varies in thickness from 2 to >20 meters. This resource estimate is categorized as "Inferred", as defined by the Canadian Institute of Mining and Metallurgy guidelines.

Presently, there is no certainty that this mineral resource will be converted into mineable reserves once economic considerations are applied. However, it is a significant low-grade high-tonnage deposit within a small "postage-stamp" area. This raises the question: what is the possibility of discovering economic deposits of Rössing type in the Wollaston Domain? (*SS5; Wed. 2:00*)

Geoscience knowledge requirements for Professional Registration: A primer for students as to the use of the GKE document

Ansdeell, K.M., Dept. of Geological Sciences, University of Saskatchewan, Saskatoon, SK S7N 5E2, kevin.ansdeell@usask.ca, and Stanley, C., Dept. of Earth and Environmental Sciences, Acadia University, Wolfville, NS B4P 2R6

A goal for many geoscience (geology, geophysics, environmental geoscience) undergraduate and graduate students being trained in Canada is to eventually become a Professional Geoscientist in order to practice what they have learned in their future career. Part of the requirement for professional registration is knowledge of appropriate aspects of geoscience. In 2008, the Canadian Geoscience Standards Board, a committee of Geoscientists Canada, developed a document called "Geoscience Knowledge and Experience Requirements for Professional Registration in Canada", informally called the "GKE", which provides a comprehensive summary of the foundation and elective science and geoscience curricula considered to be appropriate background, and the type of experience necessary to become a Professional Geoscientist. This presentation outlines how students and regulators across Canada should use this document.

The fundamental assumption in the GKE is that the necessary geoscience knowledge is gained through the equivalent of a 4-year B.Sc. degree in Canada, which normally includes 9 courses in "foundational" science (e.g. chemistry, physics, mathematics), and 18 courses in geoscience, which includes some subject areas that are considered foundational for all types of geoscientists. The hope is that all university curricula allow students to meet these requirements, and this is typically the case. Engineering programs at universities are formally accredited, whereas geoscience programs are not. Thus, regulators develop a list of courses, in consultation with university faculty, that are available at universities in their province that cover the subject areas. This set of courses is used as a check list for each individual applicant, including those trained internationally. Unfortunately, there are, at present, some subject areas in science or geoscience that are required in some provinces and not in others. These are highlighted in this presentation. It is also important to note that

students who might not have majored in geoscience originally, but who have since taken the necessary courses, either in graduate school or some other program, can satisfy the requirements for registration. In addition, the time in a graduate program counts, at least in part, to the experience in geoscience requirement for registration.

A new 2-year project is underway to outline the skills or competencies that a Professional Geoscientist should have by the time of registration. Some of these may require the completion of a particular course or set of courses during a B.Sc. program; others may be demonstrated via specific work experience. The development of these competency requirements provides another tool for geoscience regulators to properly and fairly evaluate the credentials and abilities of applicants to the profession of geoscience, especially those applicants who are internationally-trained. (*SS21; Fri. 11:00*)

Spectral reflectance properties of common metal-oxalates exposed to simulated Mars surface conditions

Applin, D.M., daniel.m.applin@gmail.com, Cloutis, E.A. and Izawa, M.R.M., University of Winnipeg, Winnipeg, MB R3B 2E9

Metal-oxalates are the only geologically stable minerals of any organic acid, so the likelihood of their presence on Mars, if life exists or existed, is high.

The difference in atmospheric pressure and composition, and ultraviolet flux on Mars may lead to molecular instability, and hence the destruction of the biomarker or the inheritance of a different spectral signature from molecular rearrangement.

We have conducted a spectroscopic study of whewellite ($CaC_2O_4 \cdot H_2O$) and glushinskite ($MgC_2O_4 \cdot 2H_2O$) under simulated Mars surface conditions with HOSERLab's mini Mars Environment chamber for 30 days.

In situ reflectance spectra from 0.35-2.5 μm were collected with an ASD FieldSpec Pro HR spectrometer. Spectra were acquired at $i=0^\circ$ and $e=0^\circ$ using a bifurcated reflectance probe. Spectra from 2-5.2 μm were collected with D&P Model 102F FT infrared spectrometer at $i \sim 30^\circ$ and $e=0^\circ$.

Spectra from 0.35-2 μm show that whewellite shows no decrease in intensity of the OH and H_2O absorption bands at 1.5 and 2 μm . The only observable changes are the development of a colour center at 0.58 μm and a slight reddening of the slope into the UV. Glushinskite shows a decrease in intensity of the OH and H_2O absorption bands near 1.5 and 2 μm and has also developed a sharp reddening into the UV.

Spectra from 2-5.2 μm show that the characteristic CO overtones for whewellite at 2.4 and 2.5 μm are subdued, but nevertheless observable. The probable C-O overtones/combinations between 3 and 4 μm , and the O-C=O bending overtone near 4.4 μm is very subdued. The glushinskite spectrum appears radically different from day zero. The C-O stretch overtone at $\sim 2.42 \mu m$ has lost most of its intensity and has slightly shifted to a longer wavelength. The 3-4 μm bands are again unrecognizable. The O-C=O bending overtone near 4.4 μm has either disappeared or shifted to a longer wavelength, and there appears to be new absorption bands at $\sim 4.6 \mu m$.

Both glushinskite and whewellite undergo dehydration when exposed to simulated Mars surface conditions. Glushinskite has lost much water, whewellite less so. The spectral changes associated with the oxalate anion are interesting, and planned additional spectral measurements will clarify these changes.

Our results suggest that Ca and Mg oxalate biominerals become damaged by Mars surface conditions. We do, however, still observe C-O bonds, so the oxalate has not decomposed. This raises the possibility that carbon could be present in the Martian regolith as dehydrogenated oxalate. (*SS18; Thurs. Poster*)

Stratigraphy and source rocks of the Hudson Platform in northern Ontario

Armstrong, D.K.¹, derek.armstrong@ontario.ca, Lavoie, D.², McCracken, A.D.³, Asselin, E.² and Galloway, J.M.³, ¹Ontario



Geological Survey, 933 Ramsey Lake Rd., Sudbury, ON P3E 6B5; ²Geological Survey of Canada, 490 rue de la Couronne, Québec, QC; ³Geological Survey of Canada, 3303-33rd Street NW, Calgary, AB

This study is undertaken as part of the Geological Survey of Canada's Hudson and Foxe Basins GEM (Geoscience Mapping for Energy and Minerals) Project. Archival petroleum and mineral exploration cores and new mineral exploration cores were logged, sampled and analyzed for a number of parameters including: biostratigraphy (conodonts and chitinozoans), Rock EvalTM6, chemostratigraphy ($\delta^{13}\text{C}$ and $\delta^{18}\text{O}$), petrology, and major and trace element geochemistry. These new data are assisting in refining the stratigraphic framework and geology maps. Limited reconnaissance scale field mapping was also undertaken.

One petroleum exploration well has been drilled in the Hudson Bay Lowlands (HBL) in Ontario, the 1969 Aquitaine Sogepet *et al* Pen No. 1. It cored over 800 m of Upper Ordovician to Middle(?) Devonian strata. The Ordovician records large scale transgressive-regressive cycles, within which are well developed metre- to decimetre scale evaporitic cycles. The Lower Silurian section is dominated by less well developed evaporitic cycles. These are disconformably overlain by biostromal and biohermal limestones of the Llandovery Ekwan River and Attawapiskat formations. Disconformably(?) overlying these are evaporite-bearing dolomudstones, red mudstones and brecciated dolostone, traditionally assigned to the Wenlock to Lower Devonian Kenogami River Formation without biostratigraphic control. Biostratigraphic evidence from off-shore wells suggests these latter strata are mainly Middle Devonian.

Two mineral exploration cores in the HBL have yielded significant intersections of Upper Ordovician source rock, the Boas River Formation (up to 9.5 m of up to 13% TOC) and an isolated occurrence of Cenozoic lacustrine sediments. Thin horizons of organic-rich shale about the same stratigraphic level as the Boas River occur in core 90 km to the northwest (9.24% TOC) and 140 km to the southeast (1.20% TOC). The uppermost 4 m of Boas River Formation (TOC up to 8%) was discovered in outcrop along the Asheweig River.

Significantly more mineral exploration cores are available for the James Bay Lowlands (JBL), especially from the last two decades with the discovery of diamond-bearing kimberlites in the Attawapiskat River area and of chromium, nickel and other metals in the "Ring of Fire" area near the erosional edge of the Paleozoic west of Attawapiskat. No significant occurrences of Ordovician source rock have been found in these cores. They have been useful in documenting thinning and changing nature of units from the Hudson Bay to Moose River basins and in revising geology maps for this area. (SS13; Fri. 9:00)

The Beaverlodge vein-type uranium deposits revisited

Ashton, K.E.¹, Ken.Ashton@gov.sk.ca, Normand, C.¹, Chi, G.², LeGault, T.² and McFarlane, C.R.M.³, ¹Saskatchewan Geological Survey, 200-2101 Scarth Street, Regina, SK S4P 2H9; ²Department of Geology, University of Regina, 3737 Wascana Parkway, Regina, SK S4S 0A2; ³Department of Geology, University of New Brunswick, PO Box 4400, Fredericton, NB E3B 5A3

The past-producing Beaverlodge uranium district, situated immediately adjacent to the northern margin of the Athabasca Basin, produced more than 65 million pounds of U_3O_8 at an average grade of about 0.2% U. The vein-type deposits are mainly hosted by anatectic leucogranites produced during a *ca.* 1.93 Ga amphibolite-facies metamorphic event and older amphibolite belonging to the 2.33-1.93 Ga Murmac Bay group, but deposits also occur in Murmac Bay group quartzites, 2.33 Ga granite, and in mafic volcanic rocks associated with the unconformably overlying *ca.* 1.82 Ga Martin group redbeds.

The leucogranites that host much of the mineralization contain abundant xenoliths of Murmac Bay group supracrustal rocks and have been variably sheared, leading previous workers to misinterpret them as argillites. Least-deformed examples of the leucogranite contain higher uranium concentrations than average granites, but strongly deformed equivalents are significantly depleted, suggesting that uranium released

as a result of leucogranite deformation may have contributed to the mineralization. Regional alteration includes kilometre-scale, along-strike networks of hematized and albitized leucogranites. In the resulting albitites, metamorphic plagioclase and K-feldspar have been replaced by hydrothermal albite. Chlorite-leucoxene pseudomorphs of biotite, previously formed by metamorphic retrogression, have been replaced by the hydrothermal assemblage albite-rutile-specular hematite-carbonate, which also fills the voids left by quartz dissolution. A preliminary *ca.* 1.8 Ga age for rutile suggests that albitization took place about 100 Ma after leucogranite emplacement; however, it is unclear whether it was coeval with uranium mineralization or rather acted as ground preparation. Many of the deposits are also spatially related to the Martin group unconformity. The nature of the inferred genetic link is unclear but the Martin group could have provided a source of metals, oxidized fluids, heat, and/or structural control.

Uranium mineralization is mainly in the form of pitchblende and generally occurs in fault zones, fractures, and within carbonate and quartz veins. Previously determined *ca.* 1.8 Ga uraninite ages, along with the widespread albitite alteration (as opposed to lower-temperature, clay-dominated alteration), suggest that these deposits predate the *ca.* 1.6 Ga unconformity-type deposits related to the 1.75-1.50 Ga Athabasca Group. (SS5; Wed. 11:00)

The deformation history of the Finlayson Lake greenstone belt: Implications for greenstone belt geometry

Backeberg, N.R. and Rowe, C.D, McGill University, Montreal, QC H3A 0E8, nils.backeberg@mail.mcgill.ca

The structural geometry of Archean greenstone belts is key to understanding the evolution and tectonic framework of the oldest preserved continental fragments in the Earth's stable cratons. We present a detailed structural study of the 2.931 - 3.003 Ga Finlayson Lake greenstone belt, which is located in the south-central Wabigoon Subprovince of the Superior Province. The Finlayson belt is situated between three TTG gneiss domes of similar ages: the 3.002 Ga Marmion gneiss; the 2.982 Ma Eye-Dashwa gneiss; and the 2.936 Ga Hardtack gneiss.

Previous work documented tectonic foliation and way-up indicators with variable lithological and chronological boundary interpretations, suggesting that the Finlayson belt either forms a synformal keel between the TTG gneiss domes (Stone and Kamineni 1989), or is comprised of three fault- bounded metamorphic and chronologically different sub-belts: eastern-, central- (or Witch Bay) and western belt (Stone 2008, *pers. comm.* D. Stone). Nearly all lithological boundaries and structural features in the Finlayson belt (except those on the western margin) lie approximately parallel to the eastern boundary with the Marmion gneiss.

Using stratal paleo-up indicators including graded bedding and pillows, we assessed the possibility for an overall synformal geometry for the greenstone belt. Way-up indicators are generally consistent across the central belt (southeast facing) and the western belt (northwest facing). Local way-up reversals are explained by small scale ccw folds and together with the steeply plunging fold axes do not conform to the synformal keel structure of the belt as presented in Stone and Kamineni (1989). We have been able to define two compressional events: An older lower-amphibolite facies, sinistral transpression event with a NNW sub-horizontal shortening axis, overprinted by a retrogressive greenschist facies event with a SE sub-horizontal shortening axis. We find that the older deformation accommodated most of the shortening and is best preserved in the western belt, becoming more cryptic towards the east, due to the increasing intensity of the overprinting fabrics closer to the boundary with the Marmion gneiss. The deformation history is common across the entire Finlayson Belt and there is no evidence for separate allochthonous sub-belts. Structural data for the Finlayson belt support a single volcanic basin that experienced early extension, sinistral transpression and pure flattening retrogression events with predominantly sub horizontal principle stress axes. (GS4; Thurs. Poster)

**Anatomy of a large syn-volcanic alteration zone in the stratigraphic footwall to the Au-rich Zn-Cu VMS deposit at Lalor Lake, Manitoba, Canada**

Bailes, A.H.¹, bailesgeoscience@mts.net, Galley, A.G.², Janser, B.W.³ and Simms, D.H.⁴, ¹Bailes Geoscience, 6 Park Grove Drive, Winnipeg, MB R2J 3L6; ²Exploration Research Director, CMIC, 2-250-155 Queens Street, Ottawa, ON; ³HudBay Minerals Inc., Box 1500, Flin Flon, MB R8A 0A2; ⁴HudBay Minerals Inc., Box 130, Snow Lake, MB R0B 1M0

Studies of the mineralogy and geochemistry of fossil hydrothermal systems have traditionally centered on discordant footwall alteration zones directly beneath VMS deposits. Less completely studied are regionally extensive subconcordant and semiconformable zones of alteration that occur within VMS-hosting stratigraphies. Those that formed at depth are considered important as they may represent high temperature domains where metal leaching occurred and mineralized/ore generating hydrothermal fluids were formed.

The mineralogy, chemistry and isotopic characteristics of a large (9 × 2 km) alteration zone, which occurs stratigraphically beneath the Au-rich VMS deposit at Lalor Lake, is the subject of this presentation. This laterally extensive zone of alteration, which is largely confined to volcanoclastic units 1-2 km beneath the VMS deposit, merges with disconformable zones of alteration that can be traced up section to not only the Au-rich Lalor Lake Zn-Cu deposit but also a number of smaller Zn-Cu VMS deposits, including the Chisel Lake deposit. A thick accumulation of permeable, volcanoclastic rocks in the stratigraphic footwall is speculated to have played an important role in not only the hydrology of the hydrothermal system but also to the generation of metals now resident in the overlying VMS deposits. The Chisel Lake area VMS deposits were host to 10.34 million tonnes of ore grading 10.21% Zn, 0.50% Cu, 1.44 g/tonne Au and 38.55 g/tonne Ag. The Lalor Lake deposit, which began production in August 2012, is inferred to contain 18.1 million tonnes of Zn-Cu ore (8.97% Zn, 0.64% Cu, 0.64 g/tonne Au and 25.24 g/tonne Ag) and 5.4 million tonnes of Cu-Au ore (0.46% Zn, 0.47% Cu, 4.7 g/tonne Au and 30.6 g/tonne Ag).

The alteration zone beneath the Lalor Lake VMS deposit developed in two stages. The first produced a semi-conformable zone of silicification, albitization and epidotization, which is spatially related to areas with abundant synvolcanic dykes and intrusions. Many of the dykes are feeders for overlying extrusive volcanic rocks and were intruded into unconsolidated, water-saturated volcanic tuff and tuff breccia. The second stage produced a sub-concordant zone manifest as metamorphic mineral assemblages rich in staurolite, garnet, amphibole, biotite, chlorite and/or muscovite. In drill core the sub-concordant alteration zone includes kyanite, cordierite, anthophyllite and gahnite, and merges with sulphide-rich footwall alteration (disconformable alteration) directly below the deposit. Carbonate-tremolite-chlorite/talc rich rocks are common in proximity to the sulphide mineralization at the Lalor Lake VMS deposit. The extensive aluminosilicate-sericite alteration, abundance of carbonate sediments and high precious metal content of the sulphide zones and stringers suggest shallow water hydrothermal activity with probable subcritical phase separation (boiling) of the hydrothermal fluids. (SS7; Wed. 10:40)

Variation in large synvolcanic alteration zones at Snow Lake, Manitoba, Canada, with proximity to associated VMS deposits

Bailes, A.H.¹, bailesgeoscience@mts.net, Galley, A.G.², Paradis, S.³ and Taylor, B.⁴, ¹Bailes Geoscience, 6 Park Grove Drive, Winnipeg, MB R2J 3L6; ²Exploration Research Director, CMIC, 2-250-155 Queens Street, Ottawa, ON; ³GSC, Box 9860, West Saanich Road, Sidney, BC V8L 4B2; ⁴GSC, 601 Booth Street, 7th Floor, Room 702, Ottawa, ON K1A 0E8

Due to its rich mineral endowment, excellent outcrop exposure and large domains of hydrothermally altered rocks, the juvenile 1.89 Ga Snow Lake arc volcanic assemblage is an important natural laboratory for testing applicability of modern volcanogenic massive sulphide (VMS) models to ancient deposits that are well exposed in cross section. For 25 years, a series of multidisciplinary investigations

examined regionally metamorphosed products of sub-seafloor hydrothermal events at Snow Lake, Manitoba. This presentation summarizes some of the important findings of these studies, including those from the recently-discovered Au-rich Lalor Lake VMS deposit, and suggests a stratigraphic-hydrothermal model incorporating all of the VMS deposits.

The Snow Lake area is characterized by laterally extensive zones with anomalous 1.82 Ga mineral assemblages, including porphyroblasts of garnet, staurolite, amphibole, biotite, gahnite and/or kyanite produced by regional metamorphism of rocks altered during pre-metamorphic, 1.89 Ga, synvolcanic, hydrothermal fluid-rock interaction. Three separate episodes of hydrothermal alteration are recognized that span the evolution of host volcanic rocks from a primitive (Anderson sequence) to mature arc (Chisel sequence) geotectonic setting. The geological, geochemical, mineralogical and stable isotope attributes of various alteration zones indicate that they include both VMS-related and VMS-unrelated, were produced at high- and low- temperatures, and developed in seafloor and sub seafloor (intra-stratal) environments.

Large, laterally extensive alteration zones at Snow Lake are up to 20 km in strike length and 2 km wide. Their large exploration 'footprint', compared to associated disconformable alteration zones and VMS deposits, means that such zones provide useful targets that can vector in exploration for VMS depositional settings within volcanic belts. The VMS-related, laterally extensive alteration zones at Snow Lake display diagnostic variations in intensity and style of alteration along strike towards VMS deposits, are stratigraphically underlain by altered portions of synvolcanic intrusions, are cut by discordant zones of more intensely altered rocks, and can be demonstrated to have formed by interaction with high temperature (>350°C) hydrothermal fluids. (SS10; Thurs. 10:40)

Inorganic controls on the incorporation of Np(V) and U(VI) in carbonate, sulfate and borate minerals

Balboni, E., Department of Civil and Environmental Engineering and Earth Sciences, 156 Fitzpatrick Hall, Notre Dame, IN 46556, USA

The interaction of radionuclides with mineral phases strongly affects their mobility and sequestration in the subsurface. A key uncertainty is associated with the high mobility of Np(V)O₂²⁺ and U(VI)O₂²⁺ released into the environment. The environmental behavior of the actinyl ions is, to a large extent, controlled by sorption reactions such as inner- and outer- sphere complexation, ion exchange and coprecipitation/structural incorporation.

Here we perform a comparative study to assess how ligand strength, symmetry of the crystal structure and nature of the cation sites present in the mineral phase affect incorporation and adsorption of Np(V)O₂²⁺ and U(VI)O₂²⁺ in carbonate, sulfate and borate minerals that form at low temperature. Np(V)O₂²⁺ and U(VI)O₂²⁺ are expected to behave differently owing to their different charge, size and complexation behavior. (SS5; Thurs. 9:40)

Geochemical and geochronological evidence against direct LIP influence on deposition of the Rapitan iron formation, Canada

Baldwin, G.J., geoff.j.baldwin@gmail.com, Turner, E.C., Department of Earth Sciences, Laurentian University, Sudbury, ON P3E 2C6, and Kamber, B.S., Department of Geology, Trinity College Dublin, Dublin, Ireland

The emplacement of Large Igneous Provinces (LIPs) has been suggested as a possible trigger for the late Neoproterozoic "snowball Earth" glaciations, which in turn drove deposition of glacially associated iron formation, such as the Rapitan iron formation of the northern Canadian Cordillera. This proposal is largely based on observed chronological relationships among stratigraphic units thought to be correlative with the Rapitan iron formation, and the assumption that large-scale hydrothermal activity, such as would be associated with LIP emplacement, would be required to deposit large volumes of iron formation. This assumption has led to misinterpretation of REE+Y data



from Neoproterozoic iron formation, specifically the absence of the positive Eu anomaly, which is incompatible with this theory. Recent detrital zircon U-Pb geochronology results indicate that the Rapitan iron formation had a maximum depositional age of 711.33 ± 0.25 Ma, which is significantly younger than established ages for the Franklin LIP, which has been attributed to triggering the “snowball Earth”. The significant time gap (between 5 and 12 m.y. long) suggests that it is improbable that the emplacement and weathering of this LIP, under the so-called “Fire and Ice” model, was directly responsible for “snowball Earth”. Furthermore, this timing disparity between LIP emplacement and iron formation deposition makes the implication of hydrothermally sourced iron for the Rapitan iron formation less plausible, particularly in the absence of the positive Eu anomaly, the sole conclusive indicator for hydrothermal influence in Archean and Paleoproterozoic iron formations. Thus, the emplacement of the Franklin LIP did not directly cause “snowball Earth”, nor did it supply the iron for the Rapitan iron formation. A broader role of the mantle plume event associated with the Franklin LIP should not, however, be dismissed. This episode of mantle plume activity is spatially and temporally associated with continental rifting and break-up of the supercontinent Rodinia, which has been suggested as the cause of “snowball” glaciations. Given that the available evidence indicates that glacial cover drove the build-up of dissolved iron in Rapitan basin water, it is not unreasonable to conclude that, whereas a Neoproterozoic mantle plume event did lead to “snowball” glaciation and coeval iron formation deposition, it was strictly through continental rifting, rather than through LIP emplacement and associated hydrothermal activity. (*SS1; Thurs. Poster*)

A visual system of correlating bentonite seams in the Pembina Member of the Upper Cretaceous Pierre Shale in the Pembina Hills area of Manitoba and North Dakota

Bamburak, J.D., james.bamburak@gov.mb.ca, Nicolas, M.P.B., Manitoba Geological Survey, 360-1395 Ellice Avenue, Winnipeg, MB R3G 3P2, and Hatcher, J., Canadian Fossil Discovery Centre, 111-B Gilmour Street, Morden, MB R6M 1N8

The Pembina Member of the Cretaceous Pierre Shale outcrops along the southern extent of the Manitoba Escarpment and within the Pembina River Valley of southwestern Manitoba and northeastern North Dakota. The member is characterized by at least 17 buff nonswelling calcium montmorillonite (altered volcanic ash) seams found interbedded with variable thicknesses of marine black carbonaceous, pyritic shale, near the base of the member. The ash is believed to have originated from multiple eruptions of the Elkhorn Mountains of western Montana about 80 million years ago. The seams range in thickness from <1.0 cm to ~30 cm. The first reported visual correlation of Pembina Member bentonite seams in the Pembina Hills area of southern Manitoba was done in 1940; and utilized the relative position of the thickest (~30 cm) seam in a ~0.75 m thick vertical succession of four bentonite seams (Quartet beds) separated by black shale. This sequence can be used as a diagnostic barcode-like signature to identify and correlate overlying and underlying bentonite beds from site to site in the Pembina Hills, where there is significant exposure.

The Quartet beds form the upper portion of a 1 metre thick black shale interval containing 6 or 7 bentonite seams that were quarried by the former operator, Pembina Mountain Clays Limited from 1939 to 1990, at approximately 21 sites in the Pembina Hills of Manitoba. The crushed, dried and acid-activated product (not produced anywhere else in Canada) was mainly sold as an adsorbant to decolourize or remove impurities from vegetable oils; and for engine oil recycling. Recognition of the Quartet beds in the outcrop belt of the Pembina Member in Manitoba and North Dakota is vital to any resource estimation of potential nonswelling calcium bentonite resources; and to the future development of this unique commodity.

In addition, knowledge of the correct stratigraphic sequence of the bentonite seams during sampling will be valuable as a control for radiometric age dating of the seams; for biostratigraphic correlation of foraminifera, molluscs and fossil palynomorphs within the intervening

black shales; and for placing large vertebrate marine fossils within their proper stratigraphic context. (*SS13; Fri. 2:40*)

Ethics in geosciences - what ethical dilemmas can we expect and how can we formally teach ethical behaviour?

Bank, C., Department of Earth Sciences, University of Toronto, Toronto, ON M5S 3B1, charly.bank@utoronto.ca, and Ryan, A.M., Department of Earth Sciences and Department of Environmental Science, Dalhousie University, 1459 Oxford St., Halifax, NS B3H 4R2

Earth scientists can no longer ignore the impact of their science on the societal and political realm, and society can no longer ignore the role of the earth sciences in today's world. At this time we lack a clear understanding of the range of ethics dilemmas an earth scientist may face in her/his career, and how the education of earth scientists may include the formal teaching of ethical behaviour. Our study aims to shed light on both aspects; we anticipate that the results gained through an anonymous questionnaire and follow-up interviews with self-identified individuals will be useful in summarizing the current state of ethics education in Canadian earth science and providing ideas for a way forward. (*SS21; Fri. 9:20*)

Lithofacies analysis and reservoir quality of the Upper Devonian Duperow Formation, southwestern Manitoba

Bates, K.B. and Chow, N., Department of Geological Sciences, University of Manitoba, 125 Dysart Road, Winnipeg, MB R3T 2N2

The Upper Devonian (Frasnian) Duperow Formation in the subsurface of the Williston Basin is part of the discontinuity-bounded Saskatchewan-Beaverhill sequence. The formation was deposited in the intracratonic Elk Point Basin and consists of cyclical successions of limestones, dolostones and evaporites. The Duperow Formation in Manitoba reaches a thickness of 122 to 195 m and thins laterally to the east. The formation is divided into three members on the basis of laterally continuous marker beds: Saskatoon Member (7-14 m thick), Wymark Member (80-108 m thick; subdivided into lower, middle and upper units) and Seward Member (49-58 m thick).

The Duperow Formation is a proven hydrocarbon producer in Saskatchewan, Montana and North Dakota, and is stratigraphically equivalent to the economically important Leduc Formation in the Alberta Basin. Limited geological knowledge of the formation in Manitoba has resulted in low exploration activity and no commercial production within Manitoba.

On the basis of core and thin section examination, three lithofacies associations, representing a restricted interior platform setting, are recognized in the Duperow Formation in Manitoba. The subtidal lithofacies association (LA 1) consists of six lithofacies: (A) skeletal wackestone-packstone; (B) skeletal framestone-rudstone; (C) intraclast wackestone-packstone; (D) mottled to nodular lime mudstone; (E) stromatoporoid-coral floatstone; and (F) stromatoporoid framestone. The intertidal lithofacies association (LA 2) consists of 2 lithofacies: (G) massive dolomudstone; and (H) laminated lime mudstone. The supratidal lithofacies association (LA 3) consists of 4 lithofacies: (I) intraclast rudstone; (J) interlaminated dolostone and anhydrite; (K) massive anhydrite; and (L) patterned dolostone. Cyclicity in the Duperow Formation is on the scale of meters and displays shoaling-upward trends.

Facies-controlled dolomitization appears to be the primary influence on reservoir quality. Lithofacies G (massive dolostone) in the middle unit of the Wymark Member has the highest intercrystalline and microvuggy porosity (15-20%). Pores are locally occluded by anhydrite cement. Lithofacies H (laminated lime mudstone) is also recognized as a potential reservoir lithology; partial dolomitization has resulted in dolomite-rich laminae with good intercrystalline porosity (15%). Live-oil staining was observed in all three members of the Duperow Formation but appears to be most pervasive in the middle and upper units of the Wymark Member. (*SS13; Fri. 10:20*)

**Comparison of XRD and reflectance spectroscopy data from saline perennial cold spring mineral deposits at Wolf Spring, and implications for detecting spring deposits on Mars**

Battler, M.M., mbattler@uwo.ca, Osinski, G.R., Banerjee, N.R., Western University, London, ON, and Cloutis, E., University of Winnipeg, Winnipeg, MB

Several features hypothesized to be spring deposits have been discovered on Mars. A limited number of spring systems exist in Mars environmental analogue settings on Earth and of those, few have been thoroughly investigated for mineralogy. In order to anticipate and confirm spectral signatures of martian spring deposits, it is useful to compare terrestrial laboratory quality XRD data to spectral data from a suitable Mars analogue spring site. This study focuses on analyses of mineral crusts deposited by Wolf spring on Axel Heiberg Island, NV, Canada. WS is a cold, saline, perennial spring, flowing through 400–600 m of permafrost in an area of diapiric uplift. Wolf spring represent a good depositional and environmental analogue to potential past, or perhaps recent, aqueous environments on Mars. Mineralogy is dominated by halite (NaCl), thenardite (Na₂SO₄), mirabilite (Na₂SO₄•10H₂O), and gypsum (CaSO₄•2H₂O). WS samples were analysed using XRD and reflectance spectroscopy, and WS sample spectra were compared to linear mixtures of the dominant WS minerals. Analyses of linear mixtures facilitate the qualitative approximation of mineral abundances in the WS samples. Results indicate that gypsum and mirabilite are more readily detectable by reflectance spectroscopy than most other minerals over a wider range of spectra and even in very small quantities. Halite is nearly invisible spectrally in the 0.3 to 2.5 µm range, but has strong features in the 2.5 to 25 µm range. These features can still be seen when halite is mixed with gypsum and thenardite. Thenardite has weak spectral features which can be masked even by small quantities of gypsum in the 0.3 to 2.5 µm range, but has strong features in the 2.5 to 25 µm range, which are still visible when thenardite is mixed with gypsum. The strongest features are between 4 and 5 µm, however, which is beyond the range of the CRISM spectrometer, and which can be obscured by CO₂ features in the lower resolution OMEGA spectra. In the search for spring deposits on Mars, gypsum-dominated features will be easier to identify from orbit, but thenardite-dominated features may also be seen when not masked by other sulfates. (SS17; Thurs. 10:40)

Implications of the plutonic record for the thermal and tectonic evolution of the Abitibi Subprovince

Beakhouse, G.P., Ontario Geological Survey, 933 Ramsey Lake Road, Sudbury, ON P3E 6B5, gary.beakhouse@ontario.ca

Intermediate to felsic intrusive rocks within the Abitibi Subprovince are subdivided into 5 suites. The pre-tectonic suite is synvolcanic (2750–2695 Ma), characterized by high-Al TTG petrogenetic affinity (eclogitic to mafic garnet granulitic residue), occurs predominantly in large belt-bounding batholithic complexes and is the most voluminous component of the Abitibi plutonic record. The volumetrically-subordinate early syntectonic suite (2691–2685 Ma) is synchronous with “Krist” volcanism and consists predominantly of high-level porphyry units with high-Al TTG petrogenetic affinity (mafic garnet granulitic residue). The syntectonic suite (2686–2676 Ma) is approximately synchronous with Porcupine assemblage sedimentation, has a transitional sanukitoid to high-Al TTG petrogenetic affinity and occurs as moderate-sized plutons within folded Tisdale assemblage units and within large belt-bounding batholithic complexes. The late-tectonic suite is synchronous with Timiskaming assemblage volcanism and sedimentation (2680–2668 Ma) and characterized by a strongly alkalic, mantle-derived petrogenetic affinity. A minor post-tectonic to late-tectonic suite (~2676 Ma) is interpreted to originate by intracrustal melting of the pre-tectonic suite. These suites record a temporal change from voluminous, early melting of mafic crust at lower crustal to upper mantle depths that abruptly (at ~2685 Ma) transitions to melting of a metasomatized ultramafic (mantle) source. This process is interpreted within a modified uniformitarian tectonic model, with early magmas generated by partial melting of subducted/subcreted mafic crust and

with later magmas generated by partial melting of the subduction-modified mantle wedge and intracrustal melting.

The pre-tectonic batholithic complexes record paleopressures of 500 to 700 MPa and structurally underlie the lower metamorphic grade (maximum paleopressures ~350 MPa) greenstone belt, resulting in an inversely density-stratified crustal configuration that persisted throughout the pre-tectonic stage, suggesting the crust was relatively rigid and characterized by low average geothermal gradients. Heating of the crust at approximately 2682 ± 5 Ma modified the rheology of the midcrust permitting density inversion with the more buoyant, midcrustal plutonic substrate tectonically emplaced to higher crustal levels in regional structural culminations represented by the large batholithic (Kenogamissi and Round Lake) complexes. This process incorporated regional-scale detachment faults at the base of and within the greenstone belt and regional folding that is largely responsible for the observed crustal architecture of the Abitibi Subprovince. The trigger for this range of processes is interpreted to be the introduction of hot asthenospheric mantle into the previously cool mantle wedge attendant with subduction termination, resulting in late, mantle-derived intermediate to felsic magmatism and extensional orogenic collapse. (SS3; Thurs. 2:00)

Nunavut Carving Stone Deposit Evaluation Program: Establishing grade, tonnage and composition for the carving stone arts industry

Beauregard, M.A., Resident Geologist, Mineral & Petroleum Resources, Department of Economic Development & Transportation, Government of Nunavut, PO Box 289, Arviat, NU X0C 0E0

The 2010-2013 Nunavut Carving Stone Deposit Evaluation Program is a collaborative project between the Government of Nunavut, Economic Development & Transportation and the Canada-Nunavut Geoscience Office. The primary goal of this program is to verify the quality and size of carving stone deposits throughout Nunavut. To date, seventy-five sites within reach of nineteen communities in the Qikiqtaaluk (eastern) and Kivalliq (central) regions have been examined. Sites in the Kitikmeot (western) region will be assessed in 2013.

Systematic evaluation has doubled the total number of important carving stone deposits in Canada's Arctic. Forty-five deposits have been defined, of which nine quarries and nine undeveloped sites contain substantial resources of high-quality soft stone. These findings suggest that Nunavut overall will have sufficient carving stone resources for many years. However, six of nineteen hamlets visited remain impoverished for local carving stone resources. Additionally, access and marine transportation are infrastructure challenges facing future development of good-grade, large-tonnage deposits.

All deposits have been categorized by stone quality, tonnage and composition. Community consultation-derived partnerships between local carvers and project personnel generated carving-suitability and deposit parameters during site visits. Serpentinite is the territorial-wide carving stone of choice gathered from hydrated ultramafic intrusives, which are rarely large enough to be mapped. Minor usage is made of marble, argillite and limestone.

Gathering of carving stone is a legislated Inuit right in Nunavut. Stone is hand-mined without use of explosives and transported by skidoo or small boat. Sites vary in size from individual use to community quarries. A ‘small’ deposit would provide 100 tonnes (50 cubic yards). An example of a large regional supplier is the tidewater site accessed by southeast Baffin Island communities. This exceptional quarry at Korok Inlet near Cape Dorset has produced 500 tonnes per annum of excellent-quality stone for 60 years. Recently confirmed ‘major’ deposits (hosting up to one million tonnes) are 100 times larger in size than any present-day community quarry. Major deposits are associated with the Archean Prince Albert Group, part of a 1000-km long supracrustal succession extending northeast from the Kivalliq region to Baffin Island.

Geoscientific research of selected deposits is being conducted by the University of Manitoba. Thorough characterization of the various



rock types will assist in creating exploration and exploitation 'tool kits' for artisan-suitable carving stone. (*SSI; Fri. 1:40*)

Redox mechanisms of uranyl and uranium nanocluster reactions on minerals surfaces

Becker, U., Yuan, K., Gebarski, B., Ewing, R.C., University of Michigan, Earth and Environmental Sciences, 2534 CC Little, Ann Arbor, MI 48109 USA, ubecker@umich.edu, and Renock, D., Department of Earth Sciences, Dartmouth College, Hanover, NH 03755, USA

One common way to immobilize actinides in the environment is to reduce them, typically to their 4+ state, in order to precipitate actinide oxides on naturally occurring minerals or on corrosion products of waste containers. However, little is known about the actual reaction mechanism, *i.e.* the role of the redox potential, the nature of the reductant, the importance of minerals in terms of providing catalytic surfaces, the role of anions in solution that polarize a mineral surface to promote or inhibit electron transfer, and the activated states that may slow down the kinetics of the redox process.

To learn more about redox mechanisms at the atomic scale and the thermodynamics and kinetics are affected, we have performed electrochemical studies using a micropowder electrode technique, a quantum-mechanical approach. The electrochemical approach allows us to determine the specific redox potential of actinide reduction on a given mineral surface. For example, uranyl reduction takes place at -0.22 V on hematite, -0.17 V on magnetite, and at -0.14 V on pyrite. By varying the sweep rate of the through the electrochemical regime, the diffusion-controlled part of the reaction (*i.e.*, diffusion of the actinide complex through the Stern layer) can be separated from the electron transfer kinetics of the redox reaction.

Mineral surfaces can often lower activation energies, such as stripping of water molecules from the reactants in order to allow them to form inner sphere complexes and moderate potential spin transitions and orbital incompatibilities that reductant and oxidant may have in solution. Our calculations show that the energy gain of the co-adsorption of hydroquinone (as an analogue for microbial reduction) and uranyl is on the order of 0.5 eV (≈ 50 kJ/mol) as compared to the separate adsorption of uranyl and hydroquinone. Similar co-adsorption on FeS (mackinawite) reveals that Fe(II) cations in the mineral surface become high spin (Fe(II) in bulk mackinawite is low spin), thereby increasing its potential for electron transfer. In addition, molecular orbital maps show that there are highly delocalized orbitals that connect the reductant through the mineral surface to the oxidant allowing electrons to travel easily back and forth within the same orbital.

Preliminary results show the potential of deriving a comprehensive database containing a high number of combinations of reductants, actinyl complexes, mineral surfaces, and polarizing agents (anions) in solutions that may have a significant influence on actinide redox thermodynamics and kinetics in the environment. (*SS5; Wed. 10:40*)

New insights from textural, petrographic and geochemical investigation of the gabbroic rocks of the Bird River Intrusive Event within the Bird River greenstone belt, southeastern Manitoba

Bécu, V.¹, vabecu@nrcan.gc.ca, Houlé, M.G.¹, McNicoll, V.J.², Yang, X.M.³ and Gilbert, P.H.³, ¹Geological Survey of Canada, GSC-Québec, 490 Couronne Street, Québec, QC G1K 9A9; ²Geological Survey of Canada, GSC-Ottawa, 601 Booth Street, Ottawa, ON K1A 0E8; ³Manitoba Geological Survey, 360-1395 Ellice Avenue, Winnipeg, MB R3G 3P2

Numerous mafic and ultramafic intrusions are widely distributed within both arms of the Neoarchean Bird River greenstone belt (BRGB) in southeastern Manitoba. These intrusions occur over a strike length of ~75 km, and host significant Ni-Cu-(PGE) magmatic sulphide and chromite deposits/occurrences. In the southern arm, several of these are interpreted to belong to the Bird River magmatic event including, from east to west, Bird Lake, Maskwa-Dumbarton, Page, Peterson, Chrome,

and National Ledin. Each of these intrusions is characterized by a lower ultramafic and an upper mafic zone of variable relative proportions. The Coppermine Bay intrusion (CBI), located close to the western end of the southern arm, is interpreted to be related to volcanic rocks of the Northern-MORB formation, although similar, in part, to some rocks of the Bird River magmatic event. In the BRGB northern arm, there are additional intrusions interpreted to belong to the Bird River magmatic event, including (from east to west) Euclid Lake (ELI), New Manitoba, Mayville East, and Mayville intrusions. The mafic-ultramafic intrusions within both arms contain significant Cr and Ni-Cu-(PGE) deposits/occurrences. In this contribution we report detailed field, textural, petrographic and geochemical observations on two of these intrusions, the CBI and the ELI, located within the southern and northern arms respectively.

The CBI is dominantly mafic and composed largely of gabbro, leucogabbro, anorthositic gabbro, and rare pyroxenite. Two styles of mineralization occur within the CBI: 1) PGE±Ni±Cu mineralization associated with disseminated sulphides and 2) thin chromitite seams; these are both associated with gabbroic, melanocratic phases of the intrusion.

The ELI is a mafic-ultramafic body that consists of a lower ultramafic zone characterized by alternating peridotite and chromitite layers, and an upper mafic zone composed of variable proportions of gabbro, leucogabbro, anorthositic gabbro, and rare olivine-rich pyroxenite. The only significant mineralization observed in the ELI consists of chromitite seams within the ultramafic zone. The historic resource estimate is 4.16 Mt of ore grading 6.42% Cr₂O₃.

Preliminary results from this study suggest that the CBI exhibits textural and petrographic characteristics very similar to the ELI, and furthermore that both intrusions are comparable to the Mayville intrusion, supporting their proposed linkage with the Bird River magmatic event. This interpretation, as well as the similar styles of mineralization among the CBI, ELI and other mafic-ultramafic intrusions, strongly suggests that the potential for Ni-Cu-PGE-Cr mineralization extends well beyond the traditionally explored areas within the Bird River Sill and the Mayville intrusion. (*SS9; Wed. Poster*)

Keynote (40 min): Disaggregation and reassembly of the Superior Craton on a subductionless, stagnant-lid Archaean Earth

Bédard, J.H., Geological Survey of Canada, 490 de la Couronne, Québec, QC G1K 9A9, jbedard@nrcan.gc.ca, and Harris, L.B., INRS-ETE, 490 de la Couronne, Québec, QC G1K 9A9

The S&W Superior craton is considered to be a tectonic collage, with diachronous (between ~2.72 and ~2.68 Ga) collisional orogenesis propagating systematically from N to S, with an average interval of ~10 my between collisions. Most tectonic models assume that terrane accretion was mediated by uniformitarian plate tectonics (arcs, ridges). However, most 'terrane' are interpreted to have had long histories of 'arc' magmatism, which requires corresponding intervals of subduction and consumption of wide oceanic tracts. As a result, it becomes difficult to rationalize the uniform collision polarity and short intervals between collisions of these tiny terranes with such a model. Furthermore, the rarity or absence of Archaean ophiolites, overprinting thrust and fold belts, high-pressure rocks and paired metamorphic belts, orogenic andesites, and diagnostic source-metasomatic trace element signatures in putative arc rocks casts doubt on the very existence of Archaean subduction. Evidence from Venus implies that continental drift and Himalayan style indentation and escape tectonics can occur on telluric planets without arcs or ridges, probably as a result of basal mantle traction on deep, stiff, cold, buoyant sub-continental mantle keels. Application of such a model to the S&W Superior would involve southward drift of the Hudson's Bay Terrane / Northern Superior Superterrane (which has the deepest keel in the Superior), with sequential accretion of these small, closely spaced 'terrane' to the leading edge of the drifting craton. Although most of the S&W Superior 'terrane' are interpreted to have been independent fragments prior to their assembly, many share a similar geological history, with



older (pre-2.8Ga) basement and abundant Neo-Archaeon magmatism. We propose that most of these 'terranes' originally belonged to an older Superior (I) craton that was partly disaggregated by the arrival and southward flow of large mantle plumes at ~2.75-2.7 Ga. The lithospheric mantle beneath zones of maximum extension like the Abitibi and Wabigoon were largely destroyed or attenuated by necking, and so only juvenile magmas erupted in these newly oceanized areas. NE-directed flow from the same plume system would have triggered the paroxysmal TTG magmatism of the NE-Superior, and extended its crust to generate the observed NNW fabrics. (*SS3; Thurs. 9:00*)

The Neoproterozoic Franklin Large Igneous Province on Victoria Island

Bédard, J.H.¹, jbedard@nrcan.gc.ca, Hayes, B.², Hryciuk, M.³, Wing, B.³, Beard, C.^{4,5}, Dell'Oro, T.⁵, Weis, D.⁵, Scoates, J.S.⁵, Williamson, N.⁶, Cousens, B.⁶, Naslund, H.R.⁷, MacDonald, W.⁷ and Nabelek, P.⁸, ¹Geol. Survey of Canada, QC; ²Cardiff University, UK; ³McGill University, Montreal, QC; ⁴University of Bristol, UK; ⁵PCIGR, University of British Columbia, Vancouver, BC; ⁶Carleton University, Ottawa, ON; ⁷SUNY Binghamton, USA; ⁸U Missouri, USA

Large parts of the Proterozoic Minto Inlier of Victoria Island have been remapped as part of the GEM program. Proterozoic platform rocks of the Shaler Supergroup and capping basalts of the Neoproterozoic (ca. 716 Ma) Franklin Large Igneous Province that formed during the breakup of Rodinia are unconformably overlain by a nearly flat-lying Paleozoic platform sequence. All rocks are cut by NE-trending block faults. The Natkusiak continental flood basalts (≤1 km thick) are preserved as 2 lobes (NE & SW) in a shallow syncline. They are the only known extrusive phase of the Franklin event, and erupted onto quartz-rich fluvial sandstones of the Kujjua Fm. that pinches out towards the NE. The lowermost extrusive unit (ca 50-100 m thick) is a primitive basalt (7-11 wt% MgO) characterized by LREE-LILE-enrichment, high L/HREE, and moderately enriched isotopic signatures (e.g. ^{87/86}Sr_i up to 0.70791); suggesting an enriched source. A hiatus in eruptive activity is marked by deposition of red-weathering volcanoclastic lahars or damburst deposits that fill palaeovalleys. Laterally extensive basaltic (10-6% MgO) sheet flows overlie the volcanoclastics and show several up-section differentiation cycles. The sheet flow basalts are less enriched in LREE and have lower ^{87/86}Sr_i (0.70251-0.70605) than basal basalts, suggesting a gradation to a more depleted source with time. The sheet flow basalts in the two lobes are isotopically distinct, indicating regional-scale isotopic heterogeneity in the source and/or contaminants of these lavas; with a completely compartmentalized plumbing system. The exposed plumbing system is dominated by sills, with localized fault-guided NW trending dykes which were sites of preferential wall rock assimilation and metamorphism. AMS fabrics in dykes confirm that these were upflow zones. Two sill populations are present. Diabasic sills have trace element signatures like those of sheet flows, whilst older, more LREE-enriched, more primitive sills resemble the basal lavas. Some sills show evidence of recharge by olivine-rich slurries. Localized sulphide immiscibility was triggered by assimilation of S-rich host rocks, suggesting that there exists a potential for magmatic NiS deposits in the area. The upper contacts of sills are locally marked by hydrothermal Fe-Oxide pods, some of which are enriched in Pt-Pd. All of the sills examined so far have isotopic signatures that match the NE lobe basalts, even those that are directly beneath the lavas. The feeder system for the SW lobe lavas is not exposed within the Inlier. (*SS1; Fri. 2:40*)

Groundwater resource evaluations of buried valley aquifers

Bell, J.J., B.Sc. (G.E.), P.Eng., Friesen Drillers Limited, 307 PTH 12 N Steinbach, MB R5G 1T8, jeff@friesendrillers.com

Within the Canadian prairies, buried valley aquifers serve as water supply for many communities and industries. The hydrogeology and recharge characteristics of these aquifers are typically very complex. Due to the Province of Manitoba's location on the eastern fringe of the

Western Canadian Sedimentary Basin, buried valley aquifer investigations have not been warranted as frequently as in other areas of the Canadian Prairies. Most of the Province of Manitoba has an abundance of overburden and bedrock aquifers throughout the most populated areas. In the western areas of Manitoba, access to major surface water and shallow groundwater sources has limited historical exploration for groundwater in buried valley aquifers.

Well hydraulics and safe well yield calculations have traditionally been challenging in Buried Valley Aquifers. Often, the analysis becomes very complex, and critical aspects of the geology and hydrogeology are difficult to incorporate. The analysis can be further complicated by the fact that in many cases, the geological characterization of the aquifer is not well defined. In many cases, the bedrock surface is highly undulating, and the presence of other buried valleys entering the area is not known.

In this paper, a case study of the hydraulic analysis of the Brandon Channel Aquifer is discussed. The long term observation well network installed on this aquifer was of critical importance in the hydraulic parameter analysis. Using the historical data of the aquifer response to pumping changes assists in the analysis and prediction of response to new pumping increases. Environmental isotopes were also utilized extensively in the aquifer characterization and analysis.

Buried Valley Aquifers represent a major water supply source for some parts of the Canadian Prairies. Careful evaluation and assessment is required, along with an understanding of the peculiar hydraulics of bounded aquifers. (*SS14; Thurs. 2:20*)

Serendibite from the Portage-du-Fort marble, Pontiac County, Québec

Belley, P.M., Dept. of Earth Sciences, University of Ottawa, Ottawa, ON K1N 6N5, pbel063@uottawa.ca, Grice, J.D., Poirier, G. and Rowe, R., Canadian Museum of Nature, PO Box 3443, Station D, Ottawa, ON K1P 6P4

A 10-15 cm band of serendibite-bearing calc-silicate rock occurs in Portage-du-Fort Group dolomitic marble and serpentine marble in the Central Metasedimentary Belt of the Grenville Province. The composition of this serendibite is Ca_{1.9}Na_{0.1}Mg_{2.6}Al_{5.0}B_{1.5}Si_{2.8}O₂₀ (B calculated on the basis of 20 oxygen sites). It occurs as subhedral to euhedral crystals up to 4 cm in length, frequently altered to a mixture of tourmaline, spinel, ± phlogopite. This alteration is absent to moderate in diopside-dominated portions of rock, but extensive in calcite-filled pockets. Three major phases of mineralisation can be observed: (1) the primary assemblage of serendibite and aluminous diopside; (2) an alteration assemblage of tourmaline, spinel and phlogopite after serendibite, and pargasite after diopside; and (3) a fine-grained, muscovite alteration of scapolite in pockets with tourmaline and phlogopite. Magnesian tourmaline, both uvite and dravite, occurs in the calc-silicate rock and in the bordering metasomatized marble (carbonate-silicate rock). In the calc-silicate rock, tourmaline occurs as: (A) A blue-grey alteration product of serendibite, or as late-stage, euhedral to subhedral, crystals that differ in physical properties; (B) honey-brown stubby crystals, or (C) pale blue to green prismatic crystals, or (D) dark brown to dark green stubby crystals. These varieties form three distinct populations with respect to the Ca/(Ca + Na) fraction: (1) 0.30 includes (C) and part of (A); (2) 0.49 includes (B) and (D); and (3) 0.80 as part of (A). Direct associations (overgrowth) suggest initial forms as (B), followed by (C) and then (D). In the carbonate silicate zone, tourmaline varieties have Ca/(Ca + Na) fractions of 0.50 and 0.62. (*SY1; Wed. 2:20*)

Diamond populations and diamond-associated indicator minerals point to one or more local sources within the Alto Paranaíba Diamond Province in western Minas Gerais State, Brazil

Benitez, L., Universidade Federal do Espírito Santo, Departamento de Gemologia, Av. Fernando Ferrari, 514, Goiabeiras, CEP 29075-910, Vitória, ES, Brazil, leilabenitez@gmail.com, and Cookenboo, H.O., 278 West 5th Street, North Vancouver, BC V7M 1K1



Numerous very large gems have been recovered from a 5 km stretch of the Santo Antonio do Bonito river, in near Coromandel in western Minas Gerais State, Brazil. Among these large gem diamonds are at least 9 stones >300 carats apiece, according to historical and government records including the largest gem ever reported from Brazil: the “Getúlio Vargas” weighing 726.6 carats and discovered in 1938. The diamond population is dominated by large crystals of rhombododecahedron and irregular morphology, with an elevated percentage of stones showing significant dissolution and cleaved broken surfaces. The population includes uncolored, uncolored-yellow and fancy colors (pink, yellow and blue). The concentration of very large diamonds from a short stretch of the river points to a proximal origin. Similar visual features characterize diamond populations from the surrounding Alto Paranaíba Diamond Province, where 450 stones have been classified visually.

Diamond associated indicator minerals have been recovered upstream from this concentration of very large diamonds in the Santo Antonio do Bonito river. Among the recovered diamond associated minerals are Cr-rich pyrope, Cr-rich chromite, and Na-enriched (Ti-poor) eclogite. Kimberlites and closely related intrusive rocks also occur upstream of the concentration of large diamonds.

A diamond population that is somewhat more clear and shows less dissolution than in the Coromandel area occurs in the Bagagem River near the western margin of the Alto Paranaíba Diamond Province. A pink diamond named “Estrela do Sul” weighing 261.38 carats was recovered in this river, as well as numerous other stones in excess of 100 carats. Heavy minerals recovered from the Bagagem River include magnetite, ilmenite, staurolite, and minor proportions of limonite, tourmaline, rutile, zircon, pyrope garnet, diopside and sapphire, but as of yet no kimberlite or diamond associated minerals have been identified.

The concentration of large diamonds in a short stretch of the Santo Antonio do Bonito river, with diamond associated indicator minerals recovered upstream, point to a proximal source of some important diamonds in the Alto Paranaíba Diamond Province. The Estrela do Sul population featuring diamonds that are more clear and show less dissolution may point to another source area near the western margin of Alto Paranaíba Diamond Province. (SS4; Fri. 2:40)

Tectonic arch control on the distribution of black shales in Paleozoic epeiric seas: A case study from southwestern Ontario

Bingham-Koslowski, N., nbingham@uwo.ca, Tsujita, C. and Jin, J., University of Western Ontario, London, ON

Organic-rich mudrocks, or black shales, have been considered hallmarks of anoxic, deep-water marine conditions. However, recent studies have demonstrated their deposition in a range of aquatic environments from deep to shallow water. This has raised questions regarding both the nature and scale of causative factors of large-scale anoxia, as recorded by black shales. The accumulation and preservation of black shales require an abundant source of organic matter and the development of anoxic conditions, but the relative significance of, and nature of interplay between, these factors in black shale deposition is poorly understood. To better comprehend the conditions and mechanisms necessary for shallow-water black shale deposition, this study investigates one of the largest, stratigraphically continuous, black shale deposits in Ontario; The Kettle Point Formation. The Kettle Point Formation can be subdivided into three distinct lithofacies: greyish-green mudstones, interlaminated black shales, and non-interlaminated black shales. Greyish-green mudstones occur interbedded with interlaminated black shales and alternate with thick packages of non-interlaminated black shales.

The Kettle Point Formation occurred syndepositionally with the Acadian orogeny where fine-grained siliciclastics were deposited in an epeiric sea. The formation is paleogeographically situated between the Appalachian and Michigan Basins, in the Chatham Sag, and bounded by the Algonquin and Findlay arches. The overall thickness and the spatio-temporal facies continuity of the Kettle Point Formation was largely controlled by the presence of these arches. Detailed core analysis and geophysical data correlation exposes three arch-related

trends. (1) The thickness of the Kettle Point Formation increases towards the deepest sections of the Chatham Sag and thins towards the northeast and southwest with increasing proximity to the arches; (2) The abundance of greyish-green mudstones is greatest towards the arches; and (3) greyish-green units become thicker and more continuous archwards.

These trends, coupled with paleontological and sedimentological data, are here interpreted to reflect changing paleoenvironmental conditions, especially regarding the onset and intensification of anoxia. Periods of maximum, basin-wide anoxia, correspond to thick, continuous packages of non-interlaminated black shales, whereas increases in the abundance, thickness and continuity of greyish-green mudstones are inferred to represent dysoxic conditions. Black shales are not limited to southwestern Ontario but are found globally throughout the Paleozoic. This suggests that in addition to local elements, such as the presence of tectonic arches and orogenies, large-scale, global factors influenced the formation and deposition of black shales, potentially including sluggish marine circulation that could have rendered Paleozoic epeiric seas prone to frequent anoxia. (SS13; Fri. 2:00)

Application of Late Quaternary processes and history to the investigation of seabed geohazards on the outer shelf and upper slope of the Canadian Beaufort Sea

Blasco, S.¹, PO Box 1006, Dartmouth, NS, B2Y 4A2, sblasco@nrcan.gc.ca, Hughes-Clarke, J.², Woodworth-Lynas, C.³, Rankin, S.⁴ and MacKillop, K.¹, ¹Geological Survey of Canada, PO Box 1006, Dartmouth, NS B2Y 4A2; ²University of New Brunswick, PO Box 4400, Fredericton, NB E3B 5A3; ³Fugro Geosurveys Inc., 25 Pippy Place, St John's, NL A1B 3X2; ⁴Canadian Seabed Research Ltd., 341 Myra Road, Porters Lake, NS B3E 1G2

(Cancelled)

Major faults, synorogenic clastic deposits, and gold mineralization in Archean cratons: syn-orogenic extension followed by thick-skinned thrust burial, and final strike-slip

Bleeker, W., Geological Survey of Canada, 601 Booth Street, Ottawa, ON K1S 2S7, wbleeker@nrcan.gc.ca

Lode gold deposits or “orogenic gold deposits” have generally been understood in the context of terrane accretion, thrusting, crustal shortening and an attendant metamorphic cycle. In recent years there has been a growing recognition, however, in moderately eroded Archean greenstone belt environments, that synorogenic extension likely played a critical role (e.g., Bleeker *et al.*, 2008, GAC Abstract; Blewett *et al.*, 2010, Prec. Research). Looking at terranes across the Superior craton there are a number of observations that are indeed puzzling in light of an accretion and shortening-only model:

- Fold-thrust systems are characterized by a network of upward-branching faults; why would they focus fluid flow en route to the upper crust?
- Why are shallow crustal levels and low-grade, or even sub-greenschist facies rocks and vein systems preserved?
- And why are the synorogenic clastic basins preserved and not quickly eroded off the top during general post-orogenic uplift?
- Why do some of these basins show a rapid transition to deep water facies?
- Why was there a sudden flare-up of alkaline magmatism, overlapping in time with these late basins?

Crustal thickening would lead to a delayed lower crustal metamorphic cycle and a peak in metamorphic fluid production tens of millions of years after accretion. Yet, some age constraints on gold deposits do indicate relatively early ages close in time to that of synorogenic basins and associated magmatism. Although local explanations could probably account for some of these observations at any particular locality, a distinct synorogenic phase of extension (differential uplift, basin formation and deepening), followed by thick-



skinned thrust inversion (deep burial and preservation) can explain all these observations in a single coherent model (Bleeker, 2012, OGS Open File Report 6280).

The general structural complexity of most Archean terranes, compounded by imperfect exposure, is the main reasons why this synorogenic phase of extension has been slow to be fully recognized. Such structural histories typically involve: 1) an early phase of folding and thrusting and, on the larger scale, terrane imbrication—all predating the extensional phase; 2) then the sharp phase of synorogenic extension; 3) a later phase of thick-skinned thrusting that inverted the extensional architecture; 4) further shortening and steepening of all structures; and finally, 5) transpression and degeneration to and overprinting by strike-slip deformation. The major “breaks” of these terranes, now steepened thrusts, and overprinted by final strike slip, thus originated as major synorogenic extensional faults, not as early high-level thrust structures. (SS3; Fri. 10:40)

Technical landslide guidelines for Canadian professional geoscientists

Bobrowsky, P.T.¹, pbobrows@nrca.gc.ca, VanDine, D.² and Couture, R.¹, ¹Geological Survey of Canada, 601 Booth St., Ottawa, ON K1A 0E8; ²VanDine Geological Engineering, 267 Wildwood Ave., Victoria, BC V8S 3W2

Professionals in all disciplines frequently rely on specialized documentation that provides examples of “best practice” for its practitioners. Occasionally such documents are prescriptive, regulatory and obligatory in the legal sense, but more frequently they are timely and extensive compilations (guidelines) by the peer community that illustrate current philosophies of practice, successful examples of application and consensus opinions on various methods and techniques relevant to the discipline in question. Professional geologists, geotechnical engineers and others in Canada will soon have access to a national best practices volume focusing specifically on landslides to be issued by the Government of Canada that will address a variety of key landslide topics affecting the health and safety of Canadians. The aim of this volume is to provide a state of the art synthesis on issues such as a lexicon of specialized terminology, a review of methods and techniques for landslide hazard identification and monitoring, analyses of the contributing and triggering factors, descriptions of mitigative options and many other aspects. The Geological Survey of Canada coordinated contributions from respected Canadian experts representing government, academia and the private sector as advisors, editors, authors and reviewers to the various volume chapters. Besides the landslide volume the Geological Survey of Canada is also publishing other volumes on seismic site characterization and space weather phenomena. The significance and role of adequate representation by the professional community practicing in various sectors, importance of collaboration and dialogue, need for endorsement by learned societies and other lessons learned in this exercise will be outlined and reviewed in this presentation. The guidelines effort by the GSC provides an excellent example of a successful program and strategy that best serves both the professional geoscience community and the public at large on a number of geo-issues of value to all participants. (SS21; Fri. 8:40)

Keynote (40 min): Grotto Creek, Front Ranges, Canadian Cordillera; a Google Earth® Model with COLLADA and Wxazygy® Transparent Interface.

Boggs, K.J.E.¹, kboggs@mtroyal.ca, Dordevic, M.M.² and Shipley, S.T.³, ¹Mount Royal University, Mount Royal Gate sw, Calgary, AB T3E 6K6; ²Old Dominion University, Elkhorn Avenue, Norfolk, VA, 23529 USA; ³WxAnalyst, Ltd., Oakdale Crescent Court, Fairfax, VA, 22030 USA

Using virtual globes, such as Google Earth®, it is now possible for students to explore the entire Earth, the Moon and Mars; while combining multiple 2-D images into one 3-D image with topography. Here an introductory field school student geological map and cross-sections are presented that provide some interactive components useful for creating virtual field trips (VFTs). This Grotto Creek project

represents the final four-day mapping project of this two week course, taught before the second year geology courses. The Grotto Creek map area is located in the McConnell Thrust Sheet in the Front Ranges of the Canadian Cordillera, across the Trans-Canada Highway between Calgary and Banff, Alberta. Due to time constraints, the region between the East Grotto Creek thrust fault and the Lac des Arcs thrust fault were not visited, requiring students to extrapolate the geology across a portion of the field area. The geological map was digitized and then draped over topography in Google Earth. Two custom sliders were created using SketchUp, COLLADA, JavaScript and Google Earth® Application Program Interface (API) to elevate the cross-sections above topography and to reconstruct folding and faulting. The Wxazygy® transparent interface was used to create a queryable *in situ* cut-away cross-section embedded into topography. Such Google Earth models are beneficial for education purposes as they are more intuitive through the elimination of distractions by irrelevant features, internal versus external views, and Krathwohl’s affective domain. Here, the ultimate goal starting with this pilot Google Earth® Model, is to create a series of 3-D interactive VFTs through the Canadian Cordillera. It is hoped that these VFTs employed as supplemental introductions to real field experiences will greatly decrease the overwhelming nature of first field experiences. Google Earth®, SketchUp, COLLADA, JavaScript and Google Earth® APIs were used because they are supported by multiple platforms, widely available, free, relatively simple to use and well integrated with each other. This abstract summarizes the first article in the Google Earth series of Geoscience Canada (October 2012) by these authors. (SS19; Wed. 2:40)

The IUGS Task Group on Global Geoscience Professionalism (TGGGP) - the birth of a global forum for professional affairs in geoscience

Bonham, O.J.H., Geoscientists Canada, 200-4010 Regent St., Burnaby, BC V5C 6N2, obonham@ccpg.ca, and Corkery, M.T., Geoscientists Canada, Winnipeg, MB R3M 3M6

At the 34th International Geological Congress in Brisbane, Australia, in August 2012, the International Union of the Geological Sciences (IUGS) created a new Task Group. The IUGS Task Group on Global Geoscience Professionalism (“TGGGP”) now provides a single global forum for interchange on professional affairs in geoscience worldwide.

Because of the unique and vital services that geoscience offers to all of society, geoscientists are increasingly being relied upon to directly serve the public by providing expert services and opinions upon which others rely for key decision-making. This has resulted in geoscience evolving across the world into a true “professional calling”, in addition to the scientific endeavor that it has always been.

Professional geoscience organizations around the world are increasingly being looked to by governments and by society: to assist with the setting of standards for communication of geoscience information relevant to public safety, sustainable development and capital investment; and to set standards and content of academic training and experience required for safe and competent geoscience practice. This is in addition to fulfilling their core mandate to safeguard the public’s interest: by maintaining up to date and openly accessible registers of competent practitioners; by setting codes of conduct and ethics; and by self-regulating practice.

This emergent dimension in geoscience has global implications, which is increasing in importance as mankind worldwide increases its demands for Earth resources (minerals and Earth materials, extractable energy, water, and soil) and its need to understand, use, manage and conserve Earth’s surface and subsurface.

The IUGS Task Group on Global Geoscience Professionalism ensures that the geoscience community - across all its differing specialties and across all legal traditions and jurisdictions – going forward, will be fully engaged in this transformation of its profession.

This contribution will present the rationale behind the formation of the new IUGS Task Group on Global Geoscience Professionalism, introduce the national and international organizations that are already involved, and explain the evolving role that Geoscientists Canada is



playing in the Task Group on behalf of Canada's profession. (SS21; Fri. 8:20)

Site preference of Fe²⁺ and Mn²⁺ in tourmaline: Considerations on the inductive effects of and on mean bond distances

Bosi, F., ferdinando.bosi@uniroma1.it, and Andreozzi, G.B., gianni.andreozzi@uniroma1.it, Department of Earth Sciences, Sapienza University of Rome, Italy

Tourmalines are well known as valuable indicator minerals that can provide information on the compositional evolution of their host rocks, chiefly due to their ability to incorporate a large number of elements.

Recently, limitations of Fe²⁺ and Mn²⁺ occupancy at the Z site and model concerning variation in bond distance as a function of and have been proposed. However, on the basis of information from crystal-structure refinements, Mössbauer spectroscopy, optical absorption spectroscopy, bond-valence theory, ionic radius concept and the literature inspection, the proposed limitations result to be weakly based.

In particular, we show that the possibility of Fe²⁺ occurrence at the Z site of the tourmaline structure to a detectable degree is well supported. Conversely, existing experimental data does not provide undisputable evidence for the occurrence of Mn²⁺ at the Z site. Notwithstanding, there exists no solid foundation for the proposed inductive effects of YMn²⁺ on , and the proposed effects must merely be regarded as speculative models. Statistical analysis shows that the Z average value is 1.906(2) Å, which is consistent with the observed values of Z at the 99% confidence limit (within 3σ) in tourmalines with the Z site fully occupied by Al. Consequently, the proposed inductive effect of and on can be ruled out. (SY1; Wed. Poster)

Biohorizons of the Upper Cretaceous Eastend Formation near Eastend, Saskatchewan

Boulding, R., Dale, J.E., Dept. of Geology, University of Regina, Regina, SK S4S 0A2, janis.dale@uregina.ca, and Tokaryk, T., Royal Saskatchewan Museum Fossil Research Station, Eastend, SK S0N 0T0

This project examines the stratigraphy and biohorizons of the Upper Cretaceous Eastend Formation at two sites near Eastend, Saskatchewan. Stratigraphic sections and fossil identification were made at the 30 m high Road Cut Site located on the south-east side of highway 13 (49°29.958' N, 108°50.761' W) and at the Humphrey Site, a north-west section of valley wall (49°31.589' N, 108°49.288' W). The fossil collections made in this study are compared with the taxa described by L. S. Russell in 1943 to create an updated faunal list for the formation. In total, 55 fossil specimens were collected from a fossil layer at the Humphrey site and surface material from the Road Cut site. This study identified the first vertebrate material to be recognized in the Eastend Formation including mosasaur vertebrae, a piece of turtle shell, fish vertebrae and numerous shark teeth. In addition, collections were made of bivalves, gastropods, scaphopods, and wood fragments exhibiting varying degrees of weathering. At the Humphrey site, fossils were found in the Lower Eastend Formation in a biohorizon within a bed of massive sands. Most of the Lower Eastend Formation sediments are interpreted to form in a low energy environment with planar laminated sands and clay/silt layers. In addition, examination of bivalve and scaphopod shells revealed they were infilled with clays indicating previous burial. The diversity and disarticulated nature of the fossils in the massive sands, coupled with the infilling of invertebrate shells, indicate that they were exhumed and transported to their current site during higher energy conditions likely indicative of storm action. All fossils collected at the two sites were found below the Lower to Upper Eastend transition zone characterized by increased coarsening of sediments and increasing thickness of beds. Additional exposures of the Eastend Formation will be explored to find new biohorizons, to help elucidate the original source of the fossil material. (GS5; Thurs. Poster)

Major and minor compositions of alteration minerals associated with the uranium mineralization at Phoenix and Millennium deposits, Athabasca Basin, in northern Saskatchewan

Boulerice, A.R., aboul032@uottawa.ca, and Hattori, K., khattori@uottawa.ca, University of Ottawa, Ottawa, ON K1N 6N5

Uranium deposits in the Athabasca Basin occur mainly along the unconformity between the crystalline basement rocks and the overlying mid-Proterozoic Athabasca sandstone. The uranium mineralization is accompanied by extensive alteration forming kaolinite, illite, chlorite and dravitic tourmaline. In addition, the rocks have undergone paleoweathering of the basement rocks and diagenesis of sandstones before the mineralization. To constrain the origin of fluids, we examined major and minor elements including halogens of alteration minerals associated with uranium deposits at the Denison Mine's Phoenix deposit and the Cameco's Millennium deposit. The Phoenix deposit, with 52.3 million lb of U₃O₈, occurs along the unconformity at a depth of 400 m, and the Millennium deposit, with 46.8 million lbs of U₃O₈, along a basement fault at a depth of 750 m.

Samples are representative alteration minerals around the two uranium deposits. Millennium samples are graphitic pelites and pegmatite collected from DDH CX055 at depths from 590.7m to 659.6m. Phoenix samples are sandstones (one at a depth of 168.7m) and basement samples near the deposits. Tourmaline occurs as bluish veinlets in pervasively altered rocks at Millennium and forms coarse grains, up to 10 micrometers. The minerals examined are tourmaline, sudoite from the Millennium deposit, muscovite from both deposits, kaolinite and clinocllore from the Phoenix deposit. Tourmaline from the Millennium deposit is all magnesiofoitite with an average formula of (A_{0.73}Na_{0.24})(Mg_{1.89}Fe_{0.047}Al_{0.65})(Si_{5.84}Al_{0.15})O₁₈(OH_{3.94}F_{0.051}Cl_{0.0068}) where A stands for a vacancy. Muscovite has an average formula of (K_{1.61}Na_{0.027})(Al_{3.60}Mg_{0.37}Fe_{0.13})(Si_{6.54}Al_{1.44}Ti_{0.023})O₂₀(OH_{3.90}F_{0.099}Cl_{0.0054}) and those from Millennium has slightly higher MgO (2.27 wt%) and lower FeO (0.93wt%) than that of Phoenix (1.43 wt%MgO; 1.43 wt%FeO), but the overall compositions are similar, suggesting the fluids responsible for muscovite crystallization were similar at two deposits. Clinocllore has an average formula of (Mg_{4.53}Al_{3.17}Fe_{3.78})(Si_{5.70}Al_{2.30})O₂₀(OH_{15.9}F_{0.052}Cl_{0.0092}) with sudoite having an average formula of (Mg_{2.8}Al_{6.3}Fe_{0.095})(Si_{6.88}Al_{1.12})O₂₀(OH_{15.5}F_{0.059}Cl_{0.0059}), which is distinguished from clinocllore by having a higher Al, lower Fe and lower Mg contents. The contents of Cl in all samples are surprisingly low, mostly 0.04 wt% and up to 0.08 wt% in muscovite and illite. The atomic ratios of F/Cl are overall high, up to 750 and the averages are 7.9 for magnesiofoitite, 58 for muscovite, 13 for illite, 13 for sudoite, 15 for clinocllore and 10 for kaolinite. The evidence suggests significant F in hydrothermal fluids. (SS5; Fri. 8:20)

Bathyrus perplexus Billings, 1865, not so perplexing

Boyce, W.D., Geological Survey, Newfoundland and Labrador Department of Natural Resources, PO Box 8700, St. John's, NL A1B 4J6

The type specimen of *Bathyrus perplexus* Billings, 1865 is a pygidium (GSC 632) from faulted limestones exposed in East Arm, Bonne Bay in western Newfoundland's Gros Morne National Park. Because of the lack of other sclerites, some workers have regarded it as a junior subjective synonym of *B. extans* (Hall, 1847); others have compared it to *Acidiphorus pseudobathyrus* Ross, 1967. The discovery of additional sclerites (cranidia, librigenae, thoracic segments, pygidia) confirms its distinctness.

Bathyrus perplexus is widespread in western Newfoundland, though it has a restricted stratigraphic range. It normally occurs in the uppermost Aguathuna Formation (St. George Group). At Table Point, however, it ranges into the basal bed of the Spring Inlet Member of the Table Point Formation (Table Head Group).

Bathyrus perplexus Billings typically occurs as part of a low diversity assemblage, along with the leperditiid ostracod *Bivia*. This is



characteristic of the nearshore Bathyrus biofacies. (*SY3; Thurs. 10:40*)

Effect of sulfur on the solubility of platinum in molten silicate: Preliminary results

Brenan, J.M., University of Toronto, 22 Russell St, Toronto, ON, brenan@es.utoronto.ca

Past work on platinum-group element (PGE) solubility in mafic magmas has largely focussed on the role of oxygen fugacity and temperature, whereas the effect of dissolved sulfur has remained uncharacterized. Such information is clearly essential, however, when evaluating the possible role of alloys on affecting PGE behaviour during melting and igneous differentiation. The effect of dissolved sulfur on the solubility of Pt in molten basalt has been measured in experiments done at 1200°C and 1 atm with f_{S_2} controlled using solid sulfide buffers (Pt-PtS, Ru-RuS₂; log f_{S_2} of -0.4 and -1.7, respectively) and f_{O_2} estimated from a calibration using the Cr-content of run-product glasses. A synthetic basalt was employed with 10 wt% FeO, with added sulfide melt (FeS + 1 wt% each of Cu and Ni) containing 15 wt% Pt. Glass + sulfide were packed in crucibles made from natural chromite, then loaded, along with the sulfide buffer, in silica ampoules, which were evacuated, then sealed. Samples were held for 1 and 4 days at temperature, then quenched. The samples equilibrated for 1 day were then subject to an additional hour at 500g using a centrifuge furnace. Run-product glasses were measured for trace elements using LA-ICPMS. Experiments produced at the Ru-RuS₂ buffer contained sulfide + silicate melt and Fe-Pt alloy, whereas those done at Pt-PtS yielded sulfide + silicate melt, but are alloy-undersaturated. Glasses are relatively free of metal or sulfide contamination, as evidenced by uniform, and low time-resolved signals for Pt. The Pt content of run-product glasses produced at log f_{S_2} of -0.4 and -1.7 are 0.19 and 0.024 ppm, respectively, which are 600- and 900-fold higher than values measured at the same f_{O_2} under sulfur-free conditions. Pt alloy solubility will therefore be significantly enhanced in the presence of dissolved sulfur, thus maintaining Pt in solution until the onset of saturation in immiscible sulfide liquid. Results are also relevant to recent estimates of the sulfide-silicate melt partitioning of Pt based on separate metal solubility estimates in sulfide and sulfur-free silicate. Values of D_{sulfide-silicate} estimated from that work for the f_{O_2} - f_{S_2} conditions of this study are 10⁹ to 10¹⁰, but reduce to 10⁶ to 10⁷ if the effect of dissolved sulfur in the silicate melt is taken into account. Such results are in much better agreement with values for D_{sulfide-silicate} of ~10⁶ measured directly from the Pt solubility experiments. (*SS9; Thurs. 9:40*)

The role of geoscience in the long term storage of radioactive wastes - Current Canadian perspective and regulatory oversight

Brown, J.L., Nguyen, T.S., Lange, K. and Su, G., Canadian Nuclear Safety Commission, Ottawa, ON K1P 5S9, julie.brown@cnscccsn.gc.ca

Within the next decade, the Canadian Nuclear Safety Commission (CNSC) expects to receive an application for the long term management of spent nuclear fuel. Currently, Ontario Power Generation is proposing to construct a deep geological repository for low and intermediate level wastes within Ordovician limestone at a depth of ~680 m, near the Bruce nuclear power plant. Their application is currently being assessed in terms of meeting safety requirements. These types of repositories rely on the host rock and engineered barriers that are intended to contain and isolate radioactive wastes from the biosphere for geologically long periods of time.

To date, CNSC's research program in support of the geological disposal concept has focussed on sedimentary rocks, to obtain more information about the suitability of the proposed DGR near Bruce. Four studies funded through CNSC's Coordinated Assessment and Research Program (CARP) examine features that will aid in the assessment of sedimentary rocks as an effective host for the long term containment and isolation of radioactive wastes:

1. Natural tracer profiles from limestone formation porewaters show that chlorine and bromine increase together from low concentrations in shallow waters, through a mixing zone, attaining constant saline compositions at a depth of around 450 m, >200 m above the proposed repository horizon. The study shows that deep groundwaters have remained isolated from shallow meteoric waters for the last ~100 My.
2. The impact of past and future glacial cycles on a potential repository was evaluated using a Thermal-Hydraulic-Mechanical-Chemical (THMC) model, which reconstructed past rock response and made predictions about rock behaviour during future glacial events.
3. Another THMC model is being developed to model the excavation disturbed zone (EDZ) created during repository construction.
4. Modelling gas generation from waste degradation and container corrosion is a work in progress.

The CNSC is anticipating an application for the long term management of spent fuel; a site selection process has already been initiated. In preparation, CNSC has recently formed a geoscience working group to access currently untapped Canadian expertise. The treatment of technical issues along the lines of dealing with uncertainties, how to model geological conditions and contaminant transport over extremely long time scales, and identifying knowledge gaps in relations to the geoscientific characterization of a potential site are key issues that will aid in the evaluation of the Safety Case: the collection of arguments in support of long term safety. (*SS20; Fri. 1:40*)

Project NA13: Towards an updated tomographic model of the Canadian lithosphere

Bryksin, A.¹, fater.gs@gmail.com, Frederiksen, A.W.¹, Zaporozan, T.¹, Darbyshire, F.A.², Snyder, D.³ and Van der Lee, S.⁴, ¹Department of Geological Sciences, University of Manitoba, Winnipeg, MB R3T 1K6; ²Centre GEOTOP, Université du Québec à Montréal, Montréal, QC H3C 3P8; ³Geological Survey of Canada, Natural Resources Canada, 601 Booth St., Ottawa, ON K1A 0E8; ⁴Department of Earth and Planetary Sciences, Northwestern University, Evanston, IL 60208-3130, USA

Large-scale lithospheric structure in continental regions is dominated by the deep roots of Precambrian terranes, and records evidence of past tectonic activity; an understanding of the lithosphere is thus helpful in tectonic reconstructions that assist in targeting mineral exploration. More directly, Precambrian continental roots contain the conditions necessary for diamond formation. We are in the progress of developing an improved continental-scale image of the lithosphere using surface waves from distant earthquakes. Existing continental-scale models are primarily based on single-station analyses, which provide constraints on individual event-station paths and so are limited by the available seismicity in the study area; as much of Canada is essentially aseismic, such models have had limited resolution. Instead, we employ two-station measurement, in which seismograms from global earthquakes are compared between pairs of instruments; phase changes in the seismogram record structure along the path between the two stations and cancel out the contribution of the earthquake itself. We have developed a software suite that allows for efficient two-station phase velocity analysis, and will present preliminary results showing differing surface-wave dispersion responses between tectonic environments. These measurements will ultimately be incorporated into continental-scale dispersion maps and three-dimensional models of mantle structure. (*SS2; Wed. Poster*)

Variation in fracture mineralogy and mineral chemistry around the Marathon Cu-PGE deposit, Ontario

Brzozowski, M.¹, brzozowm@uwindsor.ca, Samson, I.¹, Gagnon, J.¹, Linnen, R.² and Good, D.³, ¹University of Windsor, Windsor, ON N9B 3P4; ²University of Western Ontario, London, ON N6A 5B7; ³Stillwater Canada Inc., Marathon, ON P0T 2E0



The Marathon Cu-PGE deposit is hosted by the Two Duck Lake Intrusion (TDLI), a late-stage phase of the Eastern Gabbro, in the Coldwell Complex, Ontario. The most abundant sulfide minerals are chalcopyrite and pyrrhotite, with lesser bornite, pentlandite, and pyrite, which occur as disseminated to semi-massive mineralization. Late-stage chlorite \pm calcite veins are present throughout the Marathon deposit and indicate the sub-solidus movement of fluids through the host sequence. This allows the possibility that metals, such as Ni, Cu, and Co, were mobilized out of the mineralized TDLI and into the comparatively unmineralized Eastern Gabbro. Such movement may be recorded in the chemistry of the vein minerals.

Samples of chlorite and calcite, as well as patchy chlorite alteration, were obtained from drill holes that represent variable amounts of mineralization, and different parts of the deposit. Chlorite occurs as fine-grained, bladed crystals in massive, radiating, or aligned aggregates. Raman spectroscopy and energy-dispersive spectroscopy (EDS) were used to identify the chlorite species as chamosite and clinocllore ($Mg\# = 0.02$ to 0.68). Calcite is less abundant than chlorite and occurs as fine-grained, anhedral crystals. It is found as aggregates, isolated crystals, and as the dominant mineral in portions of some veins.

Preliminary laser ablation ICP-MS analyses demonstrate that a variety of trace elements are detectable in all of the chlorite analyzed. Transition elements (Ti, V, Mn, Co, Ni, Cu, Zn, Cd) showed the highest concentrations, ranging from 0.04 ppm for Cd, to 3111 ppm for Mn. Precious metals (Pd, Pt, Au, Ag) have concentrations that were generally below the detection limits, but in a few samples, Pt, Au, and Ag have concentrations up to 0.01 ppm, 0.03 ppm, and 0.04 ppm, respectively. Metalloids (As, Sb, Pb, Bi) have concentrations intermediate between those of the transition and precious metals, ranging from a minimum of 0.01 ppm for Bi to a maximum of 1 ppm for As, with Sb and Pb falling within this concentration range. No systematic variations in major element concentrations were observed between rock types (Two Duck Lake Gabbro vs Eastern Gabbro), however, variations in trace element concentrations were observed between drill holes. Future work will determine the nature of spatial variations in chlorite chemistry in order to assess the utility of chlorite chemistry as an exploration vector for Cu-PGE mineralization. (**GS1; Thurs. Poster**)

The global database of primary paleomagnetic poles from precisely-dated rock units and its application to Paleoproterozoic and Mesoproterozoic continental reconstructions

Buchan, K.L., Geological Survey of Canada, 601 Booth Street, Ottawa, ON K1A 0E8, kbuchan@nrcan.gc.ca

There are many hundreds of Paleoproterozoic and Mesoproterozoic paleomagnetic poles whose interpretation has yielded numerous (often conflicting) apparent polar wander paths, and continent or supercontinent reconstructions, as well as proposals for very rapid continental drift or true polar wander. Unfortunately, most of these paleopoles are derived from poorly dated rock units, with ages that often have uncertainties of tens or hundreds of millions of years. In addition, most paleopoles are not demonstrated primary and hence may bear no relationship to the age of the rock unit from which they are obtained. Here, the small but growing number of primary paleopoles from precisely-dated rock units (mainly mafic dykes and sills) is identified. Their use in reliably testing whether plate tectonic processes were active, charting the drift of continents and testing continental reconstructions is described. This 'key pole' database is now sufficient to demonstrate that (1) continents drifted throughout the period, (2) they drifted with respect to one another (presumably as a result of plate tectonic processes) at least as early as the middle Paleoproterozoic, and (3) Laurentia and Baltica drifted together (with northern Norway adjacent to northeastern Greenland) through the early Mesoproterozoic. In addition, key poles for a number of other blocks, including the Superior, Slave, Dharwar and North China cratons, Siberia, Kaapvaal, Kalahari and Amazonia provide some constraints on elements of continental reconstructions. However, the key pole data set is still far too small to (1) demonstrate the existence of supercontinents

(comprising most of the earth's landmass) in the Paleoproterozoic or Mesoproterozoic, (2) test models of large amalgamations of Archean cratonic blocks in the early-middle Paleoproterozoic, or (3) test proposals of true polar wander. (**SS11; Fri. 9:00**)

Searching for a giant impact structure in the Flin Flon-Snow Lake area, Manitoba

Buhlmann, E., Northern Manitoba Mining Academy, 4 Hart Avenue, Flin Flon, MB R8A 1N4, banya1nc@hotmail.ca

A 140×100 km ellipsoidal area centered on Elbow Lake, 65 km northeast of Flin Flon, Manitoba, comprises the Flin Flon – Snow Lake VMS mining district including 29 past and currently producing mines. The deposits are arranged in two major clusters near Flin Flon and Snow Lake and two smaller 'clusters' near Sherridon and Reed Lake.

The district is unique by reason of its mineral wealth in tonnage and grade of the copper – zinc – gold ores (past production and present resources 200 million tonnes). An ore-generating natural process would have had to process close to 300 tonnes of country rock with an average crustal copper abundance of 70 g/tonne to produce one tonne of ore. The gigantic amounts of focused energy to accomplish this can readily be supplied by an impact event, singular or clustered. To identify such an event would be a very challenging task because the impact would have been in offshore volcanic terrain. Up to the present no such events have been identified. But there are indirect pointers that leave much room for an impact event in the district. A specific volcanic rock type like icelandite tends to be spatially associated with VMS deposits. It is not clear if the icelandite formed in upper crustal magma chambers or from an impact melt.

A reconnaissance of numerous locations east and northeast of Flin Flon, around Sherridon and Elbow Lake was carried out. At Elbow Lake a circular area was defined on topographic maps and aerial photographs. It has a diameter of 3.8 km and encompasses the main Elbow shear zone under Elbow Lake. A microbreccia of granodioritic rock on Elbow Lake shows granophyric quartz feldspar intergrowth and a microbreccia sample returned a 2.5 ppb iridium anomaly. Near Flin Flon, several gabbroic breccias show a possible melt rock matrix. Hematization is common along the Missi/Amisk contact. Injections of melt or microbreccia into volcanic sediments were observed in at least two areas. Numerous volcanic sediments show intense striations, reminiscent of shatter cones but not definite enough.

The Flin Flon – Sherridon – Snow Lake – Reed Lake area is well suited to show if and how normal volcanic processes can be separated from impact related processes. It can show if the immense energy of a major impact can result in ore-forming processes, how such processes work and how impact related ore bodies can be located. (**SS16; Wed. 8:20**)

Implications of stable isotopes ($\delta^{18}O$, δD , $\delta^{13}C$) for magma and fluid sources in an LCT pegmatite swarm in the NWT, Canada:

Evidence for involvement of multiple fluid reservoirs

Burns, M.G.G.¹, mg_burns@laurentian.ca, Kontak, D.J.¹, McDonald, A.¹, Groat, L.A.² and Kyser, T.K.³, ¹Department of Earth Sciences, Laurentian University, 935 Ramsey Lake Rd, Sudbury, ON P3E 2C6; ²Department of Earth, Ocean and Atmospheric Sciences, University of British Columbia, Vancouver, BC V6T 1Z4; ³Department of Geological Sciences and Geological Engineering, Kingston, ON K7L 3N6

The 82 Ma Little Nahanni Pegmatite Group (LNPG), located on the NWT-Yukon border, consists of several hundred, cm- to m-scale, sub-vertical LCT-type pegmatites and dikes covering a 15 km strike length. The dikes intrude siliciclastic and calcareous units of the Precambrian to Lower Cambrian Yusezyu and Narchilla formations. Varying degrees of albitization and phyllic (Qtz-Ms) alteration of the dikes are associated with ore-grade Ta-Nb and Sn-W mineralization. Fluid inclusion studies indicate distinct CO_2 - H_2O and H_2O fluids, both of low-salinity (<1 - 2 wt. % eq. NaCl), were involved during pegmatite evolution. Whereas conventional $\delta^{18}O$ and δD data for primary and secondary assemblages (Qtz, Kf, Alb) has been used to broadly assess



source reservoirs and the nature of mineralization and alteration, Raman spectroscopy (examining the peak shift of vibrational modes for O-T-O bonds), the first application to pegmatite studies, has been related to micro-scale variation of $\delta^{18}\text{O}$ in feldspars and assessment of dissolution:precipitation processes. Results from mass spectrometry indicate that $\delta^{18}\text{O}$ for Qtz = 10.2‰ to 14.9‰, Kf = 6.8‰ to +13.8‰, Alb = 0.4‰ to 14.9‰, and Ms = 9.6‰ to 13.2‰, with δD for Ms = -182‰ to -67‰, and $\delta^{13}\text{C}$ (VPDB) = -24.7 to -9.2‰ for fluid inclusion extracts. These data are consistent with: (1) a metasedimentary protolith for the pegmatite melts (*i.e.*, $\delta^{18}\text{O}_{\text{source}} \sim 8\text{--}12\text{‰}$); (2) involvement of different fluid reservoirs (magmatic, metamorphic, and meteoric) during subsolidus cooling of the pegmatites ($\delta^{18}\text{O}_{\text{H}_2\text{O}}$ @ 400°C -2 to +12‰) and; (3) a biogenic source for the C. Results for Raman spectroscopy indicate a greater degree of peak shift ($\Delta\omega$) for Alb (7.2 cm) relative to Kf (4.0 cm), this being proportional to the ranges obtained for $\delta^{18}\text{O}$ data. Results also correlate with texture: saccharoidal Alb is both similar to and depleted in $\delta^{18}\text{O}$ relative to Kf, but cleavelanditic Alb is consistently depleted relative to Kf. The results of this study indicate the post-crystallization history of the pegmatite involved interaction with several fluid reservoirs and that fluid-mediated alteration, coincident with some rare-metal mineralization, involved ingress of meteoric water. Integration of Raman spectroscopic data with feldspar textures demonstrates that it is possible to correlate micro-scale textural evolution in pegmatites with fluid types which, in this case, indicate that both growth of cleavelandite and saccharoidal Alb replacement of primary Kf coincided with incursion of meteoric water. (SY2; Thurs. 11:00)

Recent advances in nanoscale uranium materials in the Energy Frontier Research Center "Materials Science of Actinides" (40 min)

Burns, P.C., University of Notre Dame, 156 Fitzpatrick Hall, Notre Dame, IN, 46556 USA, pburns@nd.edu

In honor of Frank C. Hawthorne, I will present recent findings of the Energy Frontier Research Center concerning nanoscale uranium materials. Approximately 80 distinct clusters built from uranyl polyhedra have been synthesized and characterized. These have diameters in the 1.5 to 3.5 nanometer range, and contain as many as 124 uranyl polyhedra. Potential applications in an advanced nuclear energy system will be explored. (SY1; Thurs. 1:40)

Factors controlling the emplacement of the giant Whabouchi lithium pegmatite, Quebec, Canada

Bynoe, L.¹, lbynoe@uwo.ca, Linnen, R.¹, Jiang, D.¹, Woulfe, J.¹ and Davis, D.², ¹The University of Western Ontario, Department of Earth Sciences, 1151 Richmond St., London, ON N6A 5B7; ²University of Toronto, 27 King's College Circle, Toronto, ON M5S

This project addresses the factors responsible for the emplacement of the Whabouchi pegmatite and also defines the extent of Li mineralization on the property. The Whabouchi lithium pegmatite is located approximately 280 km north-northwest of Chibougamau and 40 km east of the Cree Nation of Nemaska, Quebec. The Whabouchi pegmatite is enclosed in a transpressional high-strain zone of metabasites in a metamorphosed volcano-sedimentary belt. There is a well-developed subvertical transposition foliation and a subvertical stretching lineation in the high-strain zone. Shear sense indicators, best observed on horizontal sections, include rotated clasts with tails, asymmetrical boudins, and asymmetrical folds. These suggest a dextral sense of shear. As high-strain zone fabrics do not extend to the surrounding granitoids along or across strike of the zone, the shear zone deformation must have been fairly localized. The main body of the Whabouchi pegmatite is parallel to the transposition foliation and practically undeformed, but branching veinlets from the main body have been folded and boudinaged by the shear zone deformation. These observations suggest that the Whabouchi pegmatite intruded syn-kinematically during the deformation of the shear zone. Previous work on the Whabouchi pegmatite gave a zircon age of 2577 ± 14 Ma. In

this study, muscovite-garnet pegmatites south along strike of the Whabouchi pegmatite gave a monazite age of 2595 ± 14 Ma. Biotite-garnet pegmatites 3 km to the north contain highly damaged zircon that showed late Archean resetting but spot analyses on unaltered domains gave a consistent age of 2819 ± 13 Ma. Granite to the southwest of the Whabouchi pegmatite gave a zircon age of 2704 ± 5.3 Ma, while one to the northeast containing complex monazite gave an age of 2647 ± 19 Ma. All ages were determined using the U-Pb system measured by LA-ICPMS. These ages provide a constraint for the timing of deformation within the shear zone responsible for the late-stage pegmatite intrusion event around 2595 to 2577 Ma during which, the Whabouchi pegmatite was emplaced.

The second tier of the project involved the analysis of the geochemistry and mineralogy of the metasomatic aureole – a useful exploration tool – surrounding the Whabouchi pegmatite. Generally, with increased distance from the Whabouchi pegmatite, Li (with Rb and Cs) content decreases. However, approximately 500 m northeast of the mineralized pegmatite along strike, there is an increase in Li content of the 1 km diameter aureole, possibly marking an extension of the spodumene-rich Whabouchi pegmatite. (SY2; Thurs. 9:40)

Experimental study on the mobility of highly siderophile elements complexed with Te, Bi, and As

Cafagna, F. and Jugo, P.J., Laurentian University, Dept. Earth Sciences, 935 Ramsey Lake Rd., Sudbury, ON P3E 2C6, fx_cafagna@laurentian.ca

Platinum Group Elements (PGE: Ru, Rh, Pd, Os, Ir, Pt) and Highly Siderophile Elements (HSE: PGE, plus Re and Au) are often associated with magmatic Cu-Ni sulfide deposits. PGE and Au can be found in solid solution within sulfides or as discrete minerals (Platinum Group Minerals, PGM) together with ligands such as Te, Bi, and As. In the Sudbury District, Ontario, PGM are present both in massive Ni-Cu sulfide ores near to the contact of the igneous complex and in low-sulfide mineralization associated with footwall deposits. The mechanism by which HSE are separated from the contact ores into the footwall is often attributed to Cl-bearing hydrothermal fluids. However, Te, Bi, and As can complex with HSE and transport these elements away from the contact ores. To understand if and how these semimetals can transport HSE, experiments were performed using a synthetic mixture of sulfides that produced troilite, pentlandite, bornite, and chalcopyrite. A mixture of HSE was added to the sulfides in a mass proportion of 1:50 (with HSE mixed in a molar proportion of 1:1 to each other). The starting materials were alternately doped with one semimetal. A parallel set of experiments, containing MgOH (designed to reproduce the traits of hydrothermal fluids) instead of semimetals, was performed for comparison with the semimetal-bearing experiments. The starting materials were inserted into graphite capsules and then sealed in Pt capsules. Experiments were performed with piston-cylinder presses, at a pressure of 0.5 GPa and at temperatures between 500 °C and 900 °C. Run products were analyzed with Scanning Electron Microscope (SEM), using Energy Dispersive Spectroscopy (EDS). Results show that Au, Pd, and Pt-bearing minerals formed a halo within the walls of the graphite capsule, around the chamber containing the sulfides. This is evidence that the semimetals, especially Te and Bi, are effective carriers for Au, Pd and, to a lesser extent, Pt. None of the other HSE were involved in the process, although Rh, that was sometimes detected in the dispersion halo. Tellurium transported Au and Pd down to 550 °C but Pt only down to 800 °C whereas As transported the three metals down to 800 °C and Bi down to 600 °C. These results indicate that Au, Pd, and Pt can be transported into the footwall by semimetals, at temperatures compatible with the cooling of magmatic sulfides, without the presence of hydrothermal fluids. (SS9; Wed. Poster)

Crystal chemistry of transition elements and defects in minerals and glasses: A unifying perspective

Calas, G., georges.calas@upmc.fr, Allard, T., Balan, E., Cormier, L., Galoisy, L., Juhin, A. and Morin, G., Institut de Minéralogie et



Physique des Milieux Condensés, Université Pierre & Marie Curie, 75252 Paris, France

Minerals provide a large wealth of information on their formation conditions and further evolution, through substituted trace and minor elements/isotopes and structural defects. These impurities also give specific properties to industrial minerals, such as their coloration. Spectroscopic approaches are the basis of chemically selective crystal chemistry. They provide an unified view on the behavior of these minor elements in systems of geological, industrial or environmental interest.

The first part of the talk will be devoted to recent information on element location in crystal lattice, including oxidation state, charge compensation and relaxation processes. This information is possible by combining a large diversity of spectroscopic, diffraction and microscopic techniques and simulation tools. Application to the location of Cr and V in various colored minerals (spinel, garnets, corundum...) will be presented, in relation with their formation conditions and the origin of their color.

Similar information will be presented on the speciation of transition elements in silicate glasses (quenched melts). Recent information from a broad range of spectroscopic and scattering methods has provided a unique harvest of results of scientific and technological significance: unusual coordination numbers, distribution of site geometry, sensitivity to the chemical bond, medium-range organization, heterogeneous spatial distribution. This provides a unique structural perspective of glass structure, which can be described with a polyhedral approach.

A last example will concern radiation-induced defects, used to trace short-lived uranium daughter elements in transition element-free minerals such as quartz and clay minerals. The high specific area of clays makes them sensitive to ground-level radiation doses. By an adequate experimental calibration, it is possible to trace the past transfer of radionuclides in the geosphere, helping to model uranium-bearing fluid migration during U-deposit formation or for the investigation of natural analogues of geologic repositories for nuclear wastes. (SYI; Wed. 11:00)

From chemical composition to structure topology in Ti silicates: Prediction of new structure topologies (40 min)

Cámara, F.^{1,2}, fernando.camaraartigas@unito.it, and Sokolova, E.¹, ¹Dept. of Geological Sciences, University of Manitoba, Winnipeg, MB; ²Dipartimento di Scienze della Terra, Università di Torino, Italy

Sokolova (2006) developed general structural principles and established the relation between structure topology and chemical composition for 24 Ti disilicate minerals containing the TS (titanium-silicate) block, which is composed of a central trioctahedral (O) sheet and two adjacent (H) sheets of [5-7]-coordinated polyhedra and Si₂O₇ groups. The general formula of the TS block is AP₂BP₂MH₂MO₄(Si₂O₇)₂X_{4+n}, where MH₂ and MO₄ = cations of the H and O sheets; MH = Ti, Nb, Zr, Mn, Ca + REE, Ca; MO = Ti, Zr, Nb, Fe²⁺, Mg, Mn, Ca, Na; AP and BP = cations at the peripheral (P) sites = Na, Ca + REE, Ca, Ba, Sr, K; X = anions = O, OH, F, H₂O; X_{4+n} = XO₄ + XP_n, n = 0, 1, 2, 1.5, 4. The stoichiometry of core part of the TS block, MH₂MO₄(Si₂O₇)₂XO₄, is invariant. All structures consist of a TS block and an I (intermediate) block that comprises atoms between two TS blocks. The I block consists of alkali and alkaline-earth cations, oxyanions (PO₄)³⁻, (SO₄)²⁻ and (CO₃)²⁻, and H₂O groups. Structures of TS-block minerals fall into four groups, each characterized by the topology and stereochemistry of the TS block: Groups I, II, III and IV, with Ti = 1, 2, 3 and 4 apfu, respectively.

Here we introduce the concept of basic and derivative structures for 32 TS-block minerals. Basic TS-block structure contains one type of TS and I blocks (or TS blocks link directly, additional cations do not occur and the I block is absent) and is characterized by one type of self-linkage of TS blocks; the two H sheets of one TS block are invariably identical. Derivative TS-block structure contains one or more types of TS and I blocks, is characterized by one or more types of self-linkage of

TS blocks and is related to a number of basic structures of the same Group. Basic and derivative structures occur in 28 and 4 TS-block minerals (Groups II and III), respectively. Based on established relationships between derivative and basic structures, possible atomic arrangements have been predicted for (1) 2 basic structures (Groups III and IV) and (2) 12 derivative structures (Groups II and III). Each derivative structure has been derived by adding structural fragments (which represent related basic structures) via sharing the central O sheet of the TS blocks of adjacent structural fragments. (SYI; Wed. 1:40)

Komatiite-associated Cr and Ni-Cu-(PGE) mineralization in the Black Thor – Black Label ultramafic intrusion, McFaulds Lake greenstone belt, Canada

Carson, H.J.E.¹, hcarson@laurentian.ca, Leshner, C.M.¹, Houle, M.G.^{2,1}, Metsaranta, R.T.³ and Shinkle, D.A.⁴, ¹Mineral Exploration Research Centre, Department of Earth Sciences, Laurentian University, Sudbury, ON P3E 2C6; ²Geological Survey of Canada, Québec, QC G1K 9A9; ³Ontario Geological Survey, Sudbury, ON P3E 6B5; ⁴Cliffs Natural Resources, Thunder Bay, ON P7B 6M8

The Black Thor – Black Label ultramafic intrusion is part of the regionally-extensive 'Ring of Fire' ultramafic-mafic intrusive suite in the Neoproterozoic McFaulds Lake greenstone belt of northwestern Ontario. The intrusion is ~1.5 km thick and ~2.6 km long, and can be subdivided into three main zones: 1) a lower zone of accumulative-mesocumulate komatiitic dunite locally containing disseminated/semi-massive/massive Ni-Cu-PGE-bearing sulfides, 2) a middle zone of chromite-bearing heterocumulate-mesocumulate dunite/peridotite and heterocumulate-mesocumulate chromitite, and 3) an upper zone of mesocumulate-orthocumulate komatiitic peridotite/pyroxenite. Cr mineralization occurs in the middle zone and is comprised of lower magmatically brecciated ores (Black Label), and upper thick-laminated to thick-bedded disseminated/ net-textured/semi-massive ores (Black Thor). The intrusion locally contains inclusions of underlying granitoids, appears to be younger than overlying metavolcanic rocks, and is cross cut by a pyroxenite that disrupts Black Label. Multiple phases of gabbros and ferrogabbros overlie and locally cross cut the intrusion. All rocks have been metamorphosed to lower greenschist facies, but relict olivine and pyroxene are locally preserved. Chromite grains, regardless of rock texture, are 0.05-0.15 mm and euhedral with almost no evidence of recrystallization.

The genesis of the Ni-Cu-(PGE) mineralization is not yet clear, but the mineralogy (pyrrhotite-pentlandite-chalcocopyrite ± PGMs) and textures suggests that it is magmatic. Minor chalcocopyrite-rich veins appear to represent residual sulfide melts derived by fractional crystallisation of Fe-Ni-rich Cu-poor monosulfide solid solution. The occurrence of sulfides along the lower contact of the intrusion and in associated feeder dikes suggests that at least some of the sulfides have been transported into their present locations. The genesis of the Cr mineralization is even less well constrained at this stage, but several models are being investigated including: physical transportation of slurries of finely-dispersed chromite with or without magmatic slumping, and *in-situ* crystallisation associated with oversaturation of chromite with oxidation, wallrock contamination, and/or magma mixing. The overwhelmingly cumulate nature of the ores and olivine-rich host rocks suggests an open (flow-through) magmatic system similar to most other mineralised komatiitic systems. (SS9; Wed. 2:40)

The Paleoproterozoic Lalor VMS deposit, Snow Lake, Manitoba: Observations on the nature and architecture of the gold and base metal-rich ore zones and associated alterations

Caté, A.¹, antoine.cate@ete.inrs.ca, Mercier-Langevin, P.², Ross, P.-S.¹, Duff, S.³, Hannington, M.³, Dubé, B.² and Gagné, S.⁴, ¹Institut national de la recherche scientifique – Centre Eau, Terre et Environnement, 490 rue de la Couronne, Québec, QC G1K 9A9; ²Geological Survey of Canada, 490 rue de la Couronne, Québec, QC G1K 9A9; ³Department of Earth Sciences, University of Ottawa, Ottawa, ON K1N 6N5; ⁴Manitoba



Geological Survey, 360-1395 Ellice Ave., Winnipeg, MB R3G 3P2

Lalor is a recently discovered Au-Zn-rich volcanogenic massive sulphide (VMS) deposit. It is located in the Paleoproterozoic Snow Lake arc assemblage, host to numerous past producing Cu-Zn and Zn-Cu VMS deposits.

Lalor is the largest deposit of the Snow Lake camp and also the richest in gold with reserves of 14.4 Mt at 1.86 g/t Au, 24 g/t Ag, 0.6 wt.% Cu and 7 wt.% Zn and resources estimated at 12.6 Mt at 3.85 g/t Au, 27.3 g/t Ag, 0.9 wt.% Cu and 2.3 wt.% Zn, for a total size of approximately 27 Mt and potentially containing 75 t Au. It consists of distinct Zn-Cu-Pb±Au-Ag semi-massive to massive sulphide lenses and zones of Au-Ag-Pb-Cu disseminated sulphides. The ore zones are stratigraphically and/or structurally stacked in a complexly deformed and metamorphosed succession of intensely hydrothermally altered rocks attributed to the Chisel mature arc sequence that host other Zn-rich VMS deposits.

Preliminary results indicate that the footwall is composed of at least three distinct but highly altered mafic to felsic volcanic (and perhaps sedimentary) units. The alteration of the footwall is both extensive and intense. At least 11 distinct alteration assemblages have been defined based on the distribution and relative abundance of specific metamorphic minerals such as amphiboles, chlorite, cordierite, biotite, muscovite, pyrite, staurolite, garnet, kyanite, sillimanite, diopside and epidote. The variations in alteration assemblages are possibly in part due to varying protolith composition, but also probably due to the superposition of several hydrothermal events. The hanging wall does not show any extensive alteration and could be in structural contact with the deposit as proposed earlier. At least five ore types can be defined. They include Zn±Cu-rich massive sulphide lenses and three distinct ore types that carry significant gold: (1) Cu-rich massive sulphides; (2) low sulphide calc-silicates zones with high Ag-Pb-Cu±As-Se-Te and; (3) anthophyllite-rich alteration zones with traces of finely disseminated pyrrhotite.

These numerous alteration assemblages and the variety in ore styles result from a complex hydrothermal history and possible modifications during deformation and metamorphism. The important gold endowment of the deposit, its size and its distinctive features compared to known anomalous and gold-rich VMS deposits make Lalor an ideal site to document and better understand gold enrichment processes in the VMS environment, which is one of the main objectives of the current project. (SS7; Wed. 11:00)

Component geochronology of the 3960 Ma Acasta Gneiss

Cates, N.L.¹, cates@colorado.edu, Mojzsis, S.J.¹, Caro, G.², Bleeker, W.³, Hopkins, M.D.¹, Guitreau, M.¹, Blichert-Toft, J.⁵ and Abramov, O.⁶, ¹University of Colorado, Boulder, CO, 80302 USA; ²Université de Lorraine, 15 rue Notre Dame des Pauvres, Vandoeuvre-les-Nancy, France; ³Geological Survey of Canada, 601 Booth Street, Ottawa, ON K1A 0E8; ⁴University of New Hampshire, 56 College Road, Durham, NH, 03824 USA; ⁵Université Claude Bernard Lyon 1, CNRS UMR 5276, 46 Allée d'Italie, 69007 Lyon, France; ⁶United States Geological Survey, 2255 N. Gemini Drive, Flagstaff, AZ, 86001 USA

Compiled U-Pb zircon ages of the oldest parts of the Acasta Gneiss Complex (AGC) in the Northwest Territories span about 4050-3850 Ma; yet older 4200 Ma xenocrystic U-Pb zircon ages have also been reported for this terrane. The AGC has at least 50 km² of outcrop exposure, but only a small subset has been documented in the detail required to investigate a complex history. To better understand this history, ion microprobe zircon geochronology was combined with whole-rock and zircon rare earth element compositions and Ti-in-zircon thermometry from a sub-divided ~60 cm² slab of an Acasta banded gneiss, and compared to other nearby variably deformed AGC granitoid gneiss samples. Micro-sampling by this method reveals components with distinctive geochemical characteristics that are correlative with separate U-Pb zircon age populations and whole-rock compositions, but not with ¹⁴⁷Sm-¹⁴³Nd isotope systematics.

Melts that formed the oldest lithological components of the Acasta gneisses thus far identified have distinctive trace element compositions that include strong positive Eu anomalies. Lattice-strain theory, Ti-in-zircon thermometry, zircon saturation temperatures and other trace element criteria all reconcile these melts with a ca. 3920 Ma U-Pb zircon population. However, the AGC does preserve a legacy of older crustal material in the form of common preservation of ca. 4020 Ma zircons. The trace-element chemistry of these older (pre-4000 Ma) zircons is incompatible with the rock that hosts them and must represent inheritance, suggesting that they are sourced from incomplete assimilation of older crust. Modeling also shows that the magmas that gave rise to the oldest domains formed at contemporary oxygen fugacities. Based on our analysis of U, Yb and Y zircon trace element discrimination diagrams and partition modeling with natural rock samples, we conclude that a good candidate for the protolith of the pre-4000 Ma inherited zircons is a mafic to intermediate rock with only moderate LREE/HREE enrichment and no positive Eu anomaly. Because the ancient zircon component seems to be widespread in the Acasta gneisses, searches for pre-4000 Myr old rocks should be undertaken in the vicinity of the AGC. (GS3; Thurs. 10:20)

Mineralogy of the mixed-family Rau I pegmatite, Yukon Territory

Cempirek, J.^{1,2}, and Groat, L.A.¹, ¹Department of Earth, Ocean and Atmospheric Sciences, University of British Columbia, Vancouver, BC V6T 1Z4; ²Department of Mineralogy and Petrography, Moravian Museum, 65937 Brno, Czech Republic.

The Rau pegmatite field is located in the SE part of the Rau gold property, located approx. 100 km NE of Mayo, Yukon Territory. Multiple fluorine-rich barren and mixed-family pegmatites are hosted in limestone and dolomite of the Bouvette Formation. Origin of the pegmatites can probably be related to the nearby Rackla pluton which is a biotite-muscovite granite with aplitic phases near the margins.

The Rau I pegmatite is geochemically the most evolved pegmatite dyke of the field. Its thickness ranges from 0.1 to 0.5 m. The pegmatite is hosted in dolomite-rich limestone; its exocontact contains common F-rich tremolite, fluoborite, norbergite, Rb-bearing fluorophlogopite, F-rich talc, pyrite, chalcophyrite, arsenopyrite, and calcite prevails over rare dolomite. The pegmatite border zone contains common uvitic tourmaline, F-rich tremolite, F,Rb-rich phlogopite and fluorite. The pegmatite wall and intermediate zones are characterized by common F-rich schorl, muscovite, apatite, and rare beryl. The centre of the pegmatite contains common amazonite, albite, pink and blue tourmaline, muscovite, siderite and fluorite. Primary accessory minerals enclosed in albite include common U,Th-rich zircon (Zr/Hf ~ 15-18, locally up to 1.7), thorite, monazite, and columbite-group minerals. Secondary Ta,Nb-oxide minerals, scheelite and uraninite are common, and rare calcioancylite-(Ce) after monazite has been identified.

Columbite-group minerals (CGM) show primary compositional trend from manganocolumbite to manganotantalite with Mn/(Fe+Mn) ~ 0.95, Ta/(Nb+Ta) between 0.05 and 0.5, and minor (FeTa) → (ScTi) substitution. Secondary CGM feature dissolution-precipitation textures and significant iron enrichment resulting in Mn/(Fe+Mn) ~ 0.2; their Ta/(Nb+Ta) ratios and Sc,Ti contents are similar to the primary CGM. Secondary CGM are accompanied by F-dominant microlite, scheelite, and by rare Ta,Nb-rich cassiterite, wadginitite and Sc,W,Ti-rich ixiolite/wodginite.

Tourmaline-group minerals (TGM) exhibit extreme variability from Ca-rich dravite and uvite in the border zone via schorl-foitite in the wall and intermediate zones to zoned crystals with fluor-schorl and fluor-elbaite composition rimmed by fluor-dravite and dravite in the pegmatite core.

The Rau I pegmatite is a textbook example of *in-situ* pegmatite contamination. Formation of a B,F-rich exocontact skarn zone and high contents of Ca, Mg, carbonates and sulphides result from the interchange of mass and fluids between the cooling pegmatite body and the dolomite host rock. (SY2; Thurs. 3:40)



Sedimentology and stratigraphy of the Bakken Formation, west-central Saskatchewan & east-central Alberta

Chabanole, L.E., luc999@mail.usask.ca, and Buatois, L.A.,
University of Saskatchewan, 114 Science Place, Saskatoon, SK
S7N 5E2

The Upper Devonian-Lower Mississippian Bakken Formation of West-Central Saskatchewan, located in the West Canadian Sedimentary Basin (WCSB) is often overlooked due to the current popularity of its southeastern counterpart.

The Bakken in West-Central Saskatchewan (Ranges 19W3 to 29W3 and Townships 27 to 37 in this study) is part of a complex stratigraphic succession not in that it is unconformably underlain by the Upper Devonian Big Valley Formation of the Three Forks Group, but more so due to the fact that it can be conformably overlain by the Mississippian Madison Group carbonates or unconformably overlain by the Jurassic-Cretaceous Success S2 clastics or the Cretaceous Manville clastics.

At a glance, West-Central Bakken is similar to Southeastern Bakken in that it is comprised of a heterogeneous middle sandstone/siltstone member, located between the lower and upper black shale members. However, upon closer observation the middle sandstone/siltstone member differs from its southeastern equivalent.

Preliminary results from detailed core analysis have led to the recognition of five broad units. Two units are assigned to the upper and lower black shales that occur at the bottom and the top of the sedimentary succession, respectively. The middle member has been subdivided into three units: the lowermost is a lag deposit primarily composed of crinoid ossicles and brachiopod fragments, overlain by interbedded/laminated sandstone, siltstone, and mudstone, which is in turn overlain by a bioturbated siltstone/sandstone unit. Initial analysis of the middle member suggests deposition in a shallow-marine environment displaying a complex interplay of wave and tidal influence, as revealed by the association of hummocky cross-stratification, wave-ripple cross-lamination, flaser and wavy bedding, and mudstone drapes. (SS13; Thurs. Poster)

Monticellite: A neglected rare-earth host in mantle-derived undersaturated rocks and its significance for magma evolution

Chakhmouradian, A.R. and Reguir, E.P., University of Manitoba,
125 Dysart Road, Winnipeg, MB R3T 2N2

Monticellite (ideally CaMgSiO_4) is a common groundmass phase in kimberlites, and also occurs in some carbonatites and ultramafic lamprophyres as (micro)phenocrysts or in the groundmass. In lesser quantities, this mineral occurs in some ultramafic plutonic rocks associated with carbonatites. Despite its obvious petrologic significance, virtually nothing is known about the trace-element chemistry of monticellite from any of these rocks, or on how it affects the evolution of mantle-derived Ca-rich ultrabasic magmas (~20-25 wt.% SiO_2 , 12-15 wt.% MgO and 22-28 wt.% CaO). Assessment of the petrochemical role of monticellite has so far been hindered by the common occurrence of earlier-crystallized olivine (+/- other minerals) in the same rock. Our data demonstrate that monticellite is an important host for rare-earth elements in such magmas commonly containing several hundred ppm REE, and showing a clear preference for heavy lanthanides (chondrite-normalized $\text{La/Yb} = 0.02-0.5$). Monticellite-groundmass partition coefficients, calculated for unperpetinized subvolcanic ultramafic lamprophyre from Kontozero (northwestern Russia), range from 0.01 (La) to ~20 (Lu), indicating that this mineral serves as the principal repository for heavy REE in kimberlites and related rocks. Interestingly, the Y/Ho ratio in this mineral is consistently superchondritic (28-50); the Y partition coefficient is about 1.5 times higher than the Ho value. The preferential uptake of heavy REE and Y by this mineral contrasts with the partitioning behavior of perovskite in the same magma types (Chakhmouradian *et al.* 2013). Our calculations also indicate a much greater compatibility of Co in monticellite relative to Ni ($D = 0.9$ and 0.05 , respectively). To summarize, fractionation of monticellite from Ca-rich ultrabasic magmas will lead to derivative melts enriched in

light REE, but showing anomalously low Y/Ho and Co/Ni ratios ($<< 28$ and 0.05 , respectively), and to monticellite-rich (disaggregated) cumulates showing a complementary trace-element signature. (SS6; Wed. 9:00)

Reference:

Chakhmouradian, A.R., Reguir, E.P., Kamenetsky, V.S., Sharygin, V.V. and Golovin, A.V. (2013) Trace-element partitioning in perovskite: Implications for the geochemistry of kimberlites and other mantle-derived undersaturated rocks. *Chemical Geology* (*in press*).

Evolution of granitic pegmatites at Eden Lake (northern Manitoba): Evidence from accessory rare-earth-bearing minerals

Chakhmouradian, A.R., chakhmou@cc.umanitoba.ca, Reguir, E.P., Ballantine, N.G., Yang, P., University of Manitoba,
Winnipeg, MB R3T 2N2, and Mumin, A.H., Brandon University,
Brandon, MB R7A 6A9

At Eden Lake (northern Manitoba, Canada), granitic pegmatites intrude alkali feldspar syenites and calcite carbonatites of Paleoproterozoic age. The age of pegmatite emplacement is estimated as 1750 Ma, based on U-Pb data for isotopically re-equilibrated titanite from the wall-rock syenites. The pegmatites are mineralogically simple (quartz + alkali feldspars), but contain relatively abundant euhedral crystals of black andradite and dark purple fluorite confined to the marginal and axial (quartz-rich) zones of pegmatite veins, respectively. Andradite is extremely rare in granitic rocks, and the conditions of its crystallization are poorly understood. The abundance of this mineral in the Eden Lake pegmatites is undoubtedly due to contamination of the parental felsic melts by carbonate material. Our thermodynamic calculations show that, in the presence of Fe, andradite will be stable to much higher levels of $f(\text{CO}_2)$ relative to any Ca silicate regardless of P and T. At $T < 600^\circ\text{C}$, the stability of andradite is constrained by its breakdown to Fe oxides, quartz and calcite, whereas above 600°C , the limiting $f(\text{CO}_2)$ values are defined by equilibrium andradite + quartz \leftrightarrow calcite + hedenbergite. Both andradite and fluorite are the major repositories for rare-earth elements (REE) in the pegmatites [up to 4000 and 250 ppm Y+(La...Lu), respectively]. The andradite crystals are strongly zoned, showing a core-rim pattern of REE variation generally consistent with the published partition coefficients for these elements (*i.e.*, decreasing proportion of heavy lanthanides toward the rim). However, this trend is accompanied by a decrease in heavy-REE content an increase in Y/Ho ratio (from 31-33 to 48-59), which cannot be explained by crystal-chemical controls. Zoned fluorite records further loss of REE and enrichment in Y relative to Ho (leading to Y/Ho = 156 in the rim of some crystals). We interpret these mutually consistent trends to indicate the release of a fluid (carbonate-rich?) phase from the contaminated pegmatite. This fluid preferentially scavenged heavy REE from the system, producing the observed trace-element distribution patterns. It is feasible that the expelled fluid gave rise to at least some of the late carbonate-bearing vein assemblages common at Eden Lake. (SY2; Thurs. Poster)

Brecciation of preglacial alterite and injection of diamictic debris: A sharp contrast in rheological behaviour between two unconsolidated materials in the subglacial environment, Montviel carbonatite complex, Abitibi, Québec

Charbonneau, R., Inlandsis Consultants, 7667 avenue
Chateaubriand, Montréal, QC H2R 2M2, remi@inlandsis.ca, and
Cayer, A., Ressources GéoMégA Inc, 475 rue Victoria, St-
Lambert, QC J4P 2J1

Glacial sedimentary structures, enhanced by a neat color contrast between an unconsolidated dark alterite and an overlying light-grey diamict (basal till), show a network of light grey dykes intruding brecciated alterite at their contact. Higher up in the profile, a few angular alterite fragments became embedded into the light-grey diamict. These observations suggest the following series of subglacial events: (1) fracturation of the alterite (2) injection of light-grey matrix into the fractures, (3) dilatation of the "subglacial breccias" and (4) entrainment



of alterite as ghost clasts, higher into the basal debris zone. This peculiar exposure was observed from mechanical trenching performed to characterized surficial sediments for the development of the Montviel REE Deposit in the Abitibi Geological Sub-Province of northwestern Quebec. The exposed structures suggest a sharp rheological contrast between brittle deformation for the dark alterite and fluid behaviour for the light-grey diamict, which appears to have been injected into thin fractures. This contrast may reflect thermal conditions whereby unfrozen fluid subglacial debris was injected into fractures of the frozen and brittle alterite. Another interpretation relies to interstitial water pressure which may control rheology by reducing friction between mineral grains, thus making the subglacial debris deformable under ice weight pressure. In this case, the fine pores of the diamictic debris may allow the buildup of an interstitial pressure to produce a highly-fluid material. In contrast, the sand-sized granular alterite has large pores and a high conductivity which may have caused the interstitial water to escape towards lower pressure zone, leaving a nondeformable and brittle material. However, the close intermixing of high and low interstitial water pressure appears unlikely, which favor the first interpretation based on contrasting thermal conditions. According to this later interpretation, the brecciation process is likely to have taken place at the beginning of the glacial event and must have been preserved for its duration, until the final deglaciation. (**GS6; Wed. Poster**)

Petrographic and geochemical studies of bleaching diagenesis and implications for unconformity-type uranium mineralization in the Athabasca Basin

Chu, H.X., University of Regina, 3737 Wascana Parkway,
Regina, SK S4S 0A2, chu207@uregina.ca

The Proterozoic Athabasca basin in northern Saskatchewan and Alberta, which hosts the largest high-grade uranium deposits in the world, is generally considered as an oxidizing basin that provided oxidizing fluids to extract uranium either from the basin or the basement to form deposits near the sub-Athabasca unconformity. Inspection of drill cores from different parts of the basin indicates that a significant portion of the reddish strata was bleached to a variety of pale white-grey colors. The contacts between the reddish and bleached rocks vary from irregular-gradational to straight-sharp, suggesting that the bleaching process may have taken place in diagenetic environments ranging from shallow to deep burial (after significant solidification). The bleaching phenomenon, observed in sandstones far away from mineralization in the barren middle of the basin, share some similarities with bleaching associated with uranium mineralization near the margin of the basin.

In order to better understand the nature of the bleaching and its potential significance for uranium mineralization, petrographic and geochemical studies of 22 paired reddish and bleached sandstones from the DV10-001 drill core in the central part of the Athabasca basin were carried out in this study. The petrographic studies indicate that the reddish part contains more iron oxides and matrix, while the bleached part contains more illite and quartz overgrowths. Geochemical analyses and mass balance calculations show that K, Mg, and U were gained, and Si and Fe were lost during the bleaching diagenesis. It is proposed that a small portion of the uranium contained in the oxidizing fluids permeating in the reddish sandstones was reduced by reducing fluids during the bleaching process and “fixed” in the bleached rocks, whereas most of the uranium in the fluids remained in the oxidized status and was carried further to favorable sites near the unconformity to form uranium deposits. Based on mass balance calculation, a minimum of 1.1 million tons of uranium is estimated to have been “fixed” or “dispersed” in the basin through the bleaching diagenesis, suggesting that the oxidizing basinal fluids may have carried sufficient amounts of uranium to account for the uranium accumulation in the deposits. (**SS5; Fri. 9:20**)

A cathodoluminescence study of calcite-dolomite microstructures and Cal-Dol geothermometry in highly metamorphosed carbonatites: An example from the Fir carbonatite, east-central British Columbia, Canada

Chudy, T.C. and Groat, L.A., University of British Columbia,
2020 - 2207 Main Mall, Vancouver, BC V6T 1Z4,
tchudy@eos.ubc.ca

The Fir carbonatite system is located in the Monashee Mountains of east-central British Columbia and has been subjected to multiple episodes of deformation with peak conditions of amphibolite facies (*i.e.*, 620 °C at 6-7 kbar) metamorphism. The carbonatites contain a range of microstructures such as various exsolution lamellae that can be either magmatic or metamorphic in origin. The distinction between the two potential scenarios is necessary in the context of the petrogenesis of these rocks and can be only achieved by a detailed examination of the relation of the carbonates and their compositions, and careful application of the Cal-Dol geothermometer.

This study examines the carbonate matrix of three texturally and/or compositionally different calcite carbonatite samples including a gneissic carbonatite, a phoscoritic carbonatite, and a dynamically recrystallized carbonatite. These are compared to two regional metacarbonate rocks (impure dolomitic marbles) that are expected to have the same deformational history.

In all samples at least two calcite generations can be distinguished based on the CL characteristics and mineral composition. The earliest calcite has the darkest CL colours and contains a wide range of dolomite inclusions of which some are interpreted as exsolution lamellae (*e.g.*, stubby, oriented or vermicular to irregular) and others as microclasts that stem from larger clasts. A second calcite generation has brighter CL characteristics and is always replacing the first one but does not immediately affect the dolomite inclusions. This calcite is very inhomogeneous, porous and inclusion-rich in the regional rocks where it occasionally occurs between amphiboles and dolomite grains. The second calcite in the carbonatites is similar but it is always characterized by significant amounts of very fine-grained dolomite exsolution features that form spectacular symplectite-like structures and clouds.

Based on this distinction the temperatures were calculated with consideration of the observed amount of exsolved dolomite. Maximum temperatures of 650 °C were obtained for the regional metacarbonate rocks and slightly higher values of up to 700 – 750 °C in the carbonatites. The former are in agreement with regional metamorphic temperatures whereas the latter very likely reflect magmatic conditions. Retrograde calcite formation is estimated to have occurred at around 430 °C in the marbles and at only marginally higher temperatures in the calcite carbonatite suite.

This study shows that careful and detailed petrographic examination can help to unravel the petrogenetic history of strongly deformed and metamorphosed carbonatites and that magmatic features can be preserved despite amphibolite-facies metamorphism. (**GS2; Wed. 9:40**)

Occupancy of the X-site in povondraite

Clark, C.M., Cymes, B.A., Guzelaydin, E., and Badgerow, C.J.,
Dept. of Geography and Geology, Eastern Michigan University,
Ypsilanti, MI, USA 48197, christine.clark@emich.edu

Povondraite is the most iron-rich tourmaline known, with the end-member formula $\text{NaFe}^{3+}_3(\text{Fe}^{3+}_4\text{Mg}_2)(\text{Si}_6\text{O}_{18})(\text{BO}_3)_3(\text{OH})_3\text{F}$. While tourmaline with a povondraite component is reported from a number of locales, the species itself is quite rare, with a limited set of published crystal-chemical data. The X-site in povondraite, predominantly occupied by Na (+ K), is unlike many other tourmalines in that there seems to be very little vacancy. Reported chemical compositions from multiple researchers are well-behaved with analytical totals that approach 100 wt% for ideal amounts of B_2O_3 and H_2O , but normalization by standard methods results in X-site sums greater than 1 *apfu*. Past research has examined a number of potential problems, including the possibility of overlapping peaks, interstitial K,



mobilization of alkalis during analysis, $\text{Fe}^{2+}/\text{Fe}^{3+}$ ratios, ^{41}B and $\text{OH}+\text{F}$ sums, with no obvious answer to the over-population of the X -site. The impossibly high values of alkalis reported for povondraite is not easily explained by errors in chemical analysis or missing constituents. In order to better understand povondraite, we are collecting additional crystal structure and chemical data on samples. To further constrain the possibility of alkali mobilization, we are using aegirine in addition to albite and jadeite as a Na standard. We are also exploring the published bond-lengths of all cation sites for evidence of either unreported vacancy or occupancy by Na in a site beyond X . (*SY1; Wed. Poster*)

Elucidating Paleozoic tectonic events from conglomerate clast-detriral zircon geochronology of the Hongliuhe Group in the southern Central Asian Orogenic Belt, northwest China

Cleven, N.R.¹, ncleven@uwaterloo.ca, Lin, S.¹, Davis, D.² and Xiao, W.J.³, ¹University of Waterloo, 200 University Avenue West, Waterloo, ON N2L 3G1; ²University of Toronto, 22 Russell Street, Toronto, ON M5S 3B1; ³Institute of Geology and Geophysics, Chinese Academy of Science, No. 19 Beitucheng West Road, Beijing 100029, China

The Hongliuhe Group is located in Northwest China, as a final syn-orogenic clastic deposit created just prior to termination of orogeny in the Central Asian Orogenic Belt. It is a thrust imbricated sedimentary sequence that fines upward from thick conglomerate packages at the base to turbidites at the top. The conglomerate clast lithotypes vary from being metamorphic and very heterogeneous at the base to nearly monomictic granitoids up-section, providing an unroofing profile of the provenance. Granitoid clasts with compositions ranging from granitic to tonalitic, and with varying states of pre-depositional metamorphism or deformation were sampled from two stratigraphic levels. The clast samples were divided into groups based on their degree of deformation: as undeformed, slightly deformed (showing any degree of alignment or foliation) and deformed (strong tectonic foliation). Each group was used as a detrital geochronology sample, and each set of three was complemented with a sandstone detrital sample taken meters above or below the same stratigraphic level. Geochronological analyses were performed using LA-ICPMS U-Pb dating techniques on separated zircon grains, and preliminary results show that the clast-detriral samples have much more diverse age representations than the sandstone samples. All data assembled together shows three orogenic peaks, at 315 Ma, 395 Ma, and 450 Ma, with a period of quiescence separating the final from the earlier two. The sandstone detrital samples have single orogenic peaks of activity centered at 450 Ma. The basal clast-detriral sample shows a timing sequence of the deformed clasts having the oldest age, the undeformed the youngest, and the slightly deformed having both age peaks. The mid-stratigraphic set of clast-detriral samples differs: the undeformed clast sample has both the 395 Ma peak and the oldest peak of the set, at 460 Ma; the slightly deformed clast sample peaks at 410 Ma, and the deformed clast sample peaks at 400 Ma, with no older grains. This may mean that in this provenance strain localized into the youngest granitoid bodies over the oldest; the simplest explanation being that youngest intrusion was syn-tectonic. Though not the only possibility, this inference is backed by ages of three late-syn-tectonic dykes in granitoids, sampled from the surrounding crustal-scale shear zones. Such interpretation leads to conclusions that there was a significant tectonic event that ended orogenesis and spanned the Early Devonian epoch. Any later deformation of granitoid bodies is not significantly represented or preserved in the sedimentary record of the Hongliuhe Group. (*SS11; Fri. 9:40*)

How to search for methane on Mars: Results of rover field trials at Mars analogue sites

Cloutis, E.A.¹, Whyte, L.², Qadi, A.³, Anderson-Trocme, L.², Bell III, J.F.⁴, Berard, G.¹, Boivin, A.³, Ellery, A.³, Greenberger, R.⁵, Haddad, E.⁶, Jamroz, W.⁶, Kruzelecky, R.⁶, Mann, P.¹, Mustard, J.⁵, Olsen, K.⁷, Perrot, M.⁸, Popa, D.², Ralchenko, M.³, Rhind, T.¹, Samson, C.³, Sharma, R.¹, Stromberg, J.¹, Strong, K.⁷, Tremblay,

?⁸ and Wing, B.⁹, ¹University of Winnipeg, Winnipeg, MB R3B 2E9; ²McGill University, Ste Anne de Bellevue, QC H9X 3V9; ³Carleton University, Ottawa, ON K1S 5B6; ⁴Arizona State University, Tempe, AZ, 85287-1404 USA; ⁵Brown University, Providence, RI, 02912 USA; ⁶MPBC Inc., Pointe Claire, QC H9R 1E9; ⁷University of Toronto, Toronto, ON M5S 1A7; ⁸UQAM, Montreal, QC H3C 3P8; ⁹McGill University, Montreal, QC H3A 2A7

The search for signs of past or extant life on Mars is a high priority for future Mars exploration, and will involve both landed and orbital missions. The CSA supported an analogue mission designed to simulate a Mars micro-rover mission geared toward identifying and characterizing the sources of methane emissions on Mars. This analogue mission included two rover deployments, in the summers of 2011 and 2012.

The analogue sites were in the Appalachian ophiolites in Quebec. This region was chosen because of the expectation that methane is being produced in serpentinized terrains (albeit at low levels), and because putative detections of methane on Mars coincide with areas that have surficial serpentine. Two primary sites were selected: the Jeffrey and Norbestos mines, near Asbestos, QC.

The instruments included in the deployments consisted of "core" and "non-core" investigative instruments. The core instrument suite included a stereo colour camera, reflectance, UV-induced fluorescence and Raman point spectrometers, and a methane detector. The non-core instruments included a visible region hyperspectral imager, an electromagnetic induction sounder, and a UV-vis imager.

For the first deployment, the adopted search strategy involved measuring methane concentrations during a pre-planned traverse, and if enhanced methane were detected, to try and follow concentration gradients to the source.

This first deployment, and subsequent field testing, demonstrated that methane seepages show very strong vertical gradients (smokestack effect). It was also found that even in the presence of winds, methane plumes disperse very little laterally to wind direction. These results demonstrated that methane concentrations decline to background levels within ~1 metre of a point sources and that methane detection based on intercepting a plume would have little chance of success unless a plume was inadvertently intercepted.

As a result, the June 2012 deployment at the Norbestos site utilized a search strategy based on utilizing colour imagery to identify the most promising targets for methane emissions, specifically fractures and joints. Target prioritization was based on categorizing these structural elements in terms of width, lateral persistence, evidence of iron oxyhydroxide staining or other discolouration around the structure, and water seepage.

After target prioritization the rover was directed to the highest priority targets to conduct more detailed measurements, including methane measurements, Raman and reflectance point spectroscopy, and in-fracture UV fluorescence measurements.

Our rover trials demonstrated that methane search strategies based on image analysis rather than methane "sniffing" are a viable and preferred search strategy for future. (*SS17; Thurs. 8:20*)

Visual characteristics of Vargem Bonita diamonds compared to indicator mineral compositions from the Canastra 1 Kimberlite

Cookkenboo, H.O., 278 West 5th Street, North Vancouver, BC V7M 1K1, hcookenboo@gmail.com, and Benitez, L., Universidade Federal do Espírito Santo, Departamento de Gemologia, Av. Fernando Ferrari, 514, Goiabeiras, Vitória, ES, CEP 29075-910, Brazil

Visual characteristics of diamond populations vary in different parts of Brazil. In some locales, diamond populations are tied to kimberlite sources with their own characteristic indicator mineral chemical signature. Comparing the visual characteristics of diamond populations with their probable source kimberlite indicator mineral signature provides insight into emplacement and local mantle conditions.



Diamonds from Vargem Bonita, which is located near the sub-surface margin of the Sao Francisco Craton, are an example of a visually distinct population associated with a particular kimberlite source. The Vargem Bonita diamonds are mined from alluvial deposits of the Sao Francisco River where it debouches from steep mountains onto a broader alluvial plain. The diamondiferous and deeply eroded Canastra 1 Kimberlite is located in those steep mountains directly upstream from Vargem Bonita and is almost certainly a source for the Vargem Bonita diamonds.

The Vargem Bonita diamonds are dominated by well-formed, intact crystals that are mostly colorless (~60%) and colorless-yellowish (~25%). Fancy colors are absent, as are green coats. Most stones are very clear, and only occasionally have a few small inclusions. Octahedra shapes (~60%) dominate, with dodecahedras occurring (~10%) less commonly. Resorption is almost absent. Small crystals are most abundant (~70%) are between 0.01-0.60 carats but occasionally stones larger than 4 carats are found. Most stones are intact and of excellent gemological quality. Bort crystals (~25%) are common, which is consistent with a proximal kimberlitic source, as are most of the other features. This indicates that although the Vargem Bonita diamonds are recovered from alluvial deposits, they were not transported far. These clues reinforce the primary source being the diamondiferous Canastra 1 kimberlite.

The Canastra 1 Kimberlite indicator minerals are characterized by a small population (<1%) of Cr-rich, sub-calcic pyropes (G10s) consistent with sampling mantle from the diamond stability field. However, the kimberlite lacks the very sub-calcic harburgitic Cr-pyropes typical of many diamond-bearing kimberlites elsewhere which are likely to have sampled depleted mantle. Other indicator minerals from Canastra 1 include chromium-rich chromites, forsterite olivine and abundant Mg-ilmenite and Cr-diopside.

The abundance of Cr-diopside (rich in calcium) and Mg-ilmenite (rich in titanium) suggests the mantle was re-fertilized by melt before emplacement of the kimberlite. The mantle melt re-fertilization event may be associated with craton margin processes, and possibly with growth of the diamonds shortly before emplacement, given the lack of diamond resorption. (SS4; Fri. 2:20)

Severely corroded diamonds from the foliated Salvador 1 Kimberlite compared to alluvial populations in the Espinhaço Mountains

Cookkenboo, H.O., 278 West 5th Street, North Vancouver, BC V7M 1K1, hcookenboo@gmail.com, and Benitez, L., Universidade Federal do Espírito Santo, Departamento de Gemologia, Av. Fernando Ferrari, 514, Goiabeiras, Vitória, ES, CEP 29075-910, Brazil

Severely corroded diamonds characterize the Salvador 1 Kimberlite and surrounding Chapada Velha alluvial deposits. These severely corroded diamond populations have highly irregular morphologies that are distinct from diamonds elsewhere in the Espinhaço Mountain range of east-central Brazil. Commonly, the severe corrosion is restricted to only one side of an individual stone. The Chapada Velha diamonds include fancy colors, which are absent from most of the region.

Indicator minerals from the Salvador 1 Kimberlite are limited to chromite, which reaches chrome-rich compositions in excess of 64.00% Cr₂O₃. Silicate indicator minerals are absent. The Salvador 1 Kimberlite is foliated in some phases parallel to the elongate extension of the kimberlite body by post-emplacement metamorphism due to regional compression. The kimberlite intruded the west side of the Chapada Diamantina mountains in central Bahia State, in contact with the Tombador Formation paleoconglomerate. Field relations suggest that Tombador depositional system eroded the kimberlite. The Tombador paleoconglomerate is diamondiferous at the Salvador 1 Kimberlite, and is the presumed sources of diamonds for alluvial deposits on the eastern side of the Chapada Diamantina. However, diamond populations from the east side of Chapada Diamantina are distinct from the corroded populations near Salvador 1, although

closely comparable to other populations mined along the Espinhaço Mountains south into Minas Gerais State.

Diamonds from several Espinhaço Mountain range populations in Minas Gerais (Diamantina, Grão Mogol and Jequitai areas) have been classified visually. The populations are predominantly less than 2 carats, and the stones are typically colorless-yellow. However, an exceptional population occurs in the Grão Mogol area with a considerable number of yellow crystals accompanying the colorless-yellow stones. The most commonly occurring shape is rhombododecahedral. Overall, the diamonds of the Espinhaço show good clarity. Inclusions are few and small, if seen at all. The degree of dissolution is very low; crystal breaks and irregular shapes are rare. The presence of a green coat is very characteristic in these stones. Notably, yellow/brown coats also occur in the Jequitai region.

The Salvador 1 Kimberlite is unusual because of its metamorphic foliation, lack of silicate indicator minerals, and severely corroded diamonds (which are distinct from other populations in the Espinhaço Mountains). Dissolution of diamond occurs in the mantle and during kimberlite emplacement (possibly by CO₂ enriched fluids). The severe corrosion common to Salvador 1 diamonds suggests that diamond dissolution may occur after emplacement in the unusual case of a metamorphosed kimberlite. (SS4; Fri. Poster)

Solubility and partitioning of actinide complexes in aqueous alkane Bi-phasic systems

Corrales, L.R., The University of Arizona, Tucson, AZ, lrcorral@email.arizona.edu

Molecular dynamics simulation methods are applied to detail the molecular mechanisms that control solubility and partitioning thermodynamics of actinide chelate complexes across aqueous – alkane interfaces. Solubility properties and partitioning are characterized by determining the Helmholtz energy (*a.k.a.* the free energy) difference using potential of mean force (PMF) trajectory calculations. The employed PMF method captures the bulk solubility differences, hence the partition coefficient, while characterizing the interfacial role in impeding or facilitating transport. Fundamental beta-diketonates ligands typically used in extraction and separation processes are compared with respect to their constituents that provide different interactions with solvents. This study is based on partitioning complex heterogeneous systems into simpler basic system so as to apply dilute approximations in characterizing solubility and partitioning thermodynamics. The goal is to gain an understanding of the non-ideal contributions that control the solute sensitivity to solvent response so as to gain a molecular-level understanding of the factors that control solubility and partitioning. The overall study focuses on trivalent actinide ions to understand how to best remove such species from raffinate solutions of spent fuels, and on why higher valence ions respond differently to these chelating agents. In this presentation, the employed fundamental methods will be presented with respect to why they are useful to gain a better understanding of solvation properties and transport mechanisms of actinide metal complexes in aqueous – alkane heterogeneous solvent systems. (SS5; Thurs. 11:00)

Exploration technologies and models for IOCG and affiliated iron oxide alkali-altered deposits with case examples from the Great Bear magmatic zone, Canada

Corriveau, L.¹, lcorriveau@nrcan.gc.ca, Montreuil, J-F.², Hayward, N.³, Enkin, R.⁴, Davis, W.⁵, Potter, E.⁵, McMartin, I.⁵ and Normandeau, P.X.⁶, ¹Geological Survey of Canada, 490 de la Couronne, Québec, QC G1K 9A9; ²INRS-ETE, 490 de la Couronne, Québec, QC G1K 9A9; ³Geological Survey of Canada, Vancouver, BC; ⁴Geological Survey of Canada, Sidney, BC; ⁵Geological Survey of Canada, Ottawa, ON; ⁶McGill University, Montréal, QC

Polymetallic, 1.87 Ga iron oxide alkali-altered (IOAA) systems and iron oxide copper-gold (IOCG) deposits in the Great Bear magmatic zone (Canada) stand upright, are tilted or gently folded, differentially exhumed, and/or transcurrent faulted, exposing the metasomatic



footprints of IOAA systems from upper crustal source regions to deposits. Each system exhibits similar regional space-time evolution of metasomatic alteration, veins and breccias from least-altered precursors (plutonic, volcanic, sedimentary and metamorphic) to deposits. Once the metasomatic mineral parageneses are unified under their key chemical elements (e.g., Na, Ca-Fe, K-Fe), diagnostic metasomatic facies emerge, each with distinct chemical characteristics largely inherited from the fluids and formed under different temperature regimes. Element speciation, mobility and redistribution across the metasomatic facies and associated brecciation are of a magnitude beyond that of any other deposit type. Such activity and their intensity account for an extraordinary range of deposit types including iron oxide-apatite, specialized metal, magnetite- to hematite-group IOCG and albitite-hosted uranium deposits, with continuum to epithermal and porphyry deposits. The ideal prograde alteration sequence represents a conceptual IOAA alteration vector-to-deposit model. Though presented as unidirectional, each metasomatic facies can be permuted or repeated to adapt to transition, juxtaposition, superimposition and cyclical build-up of alteration tied to faulting, brecciation, differential exhumation, and magma emplacement. In the field or during core logging, inferences can be drawn about incoming and outgoing fluids/metals for each alteration observed and used to highlight components of the system that remain to be discovered. Tested under the Geomapping for Energy and Minerals (GEM) program, the model has demonstrable predictive exploration capabilities in the field. Moreover, the distinctive composition of each metasomatic facies facilitates the use of discrimination diagrams and geochemical alteration profiling (e.g., molar concentration profiles) to prognosticate fertility of IOAA systems and develop exploration targets. Multivariate signatures of pathfinder and alteration-related elements also enhance effectiveness of exploration based on till geochemistry whereas chemical/physical distinctiveness of a selection of minerals (*i.e.* apatite, magnetite) show potential for the indicator mineral exploration method in glaciated terrain. Rock physical properties and radiometric attributes are also distinctive. Alteration mapping aided by portable gamma-ray spectrometers and magnetic-susceptibility meters, and new geophysical potential field techniques enhance rapid targeting of prospective areas at local and regional scales. Finally, in examples where IOAA systems have been entrained in orogenesis and metamorphosed to high-grade, attributes of their metamorphosed metasomatic facies remain diagnostic though some exploration methods will have to be adapted to these environments to remain efficient. (SS23; Fri. 3:00)

Rare earth elements and their (sub)economic redistribution: An example from the North Qôroq nepheline syenite centre of South Greenland

Coulson, I.M., Solid Earth Studies Laboratory, Department of Geology, University of Regina, Regina, SK S4S 0A2, ian.coulson@uregina.ca

In addition to their scientific value, and in the unravelling of petrological processes, the rare earth elements (REE) have come to be essential constituents in nearly everything around us, be they cars, computers or lasers. The public realisation and awareness of the importance of REE, coupled with a restricted supply, has brought their exploration to a principal level. That REE are found in peralkaline igneous rocks and carbonatites has long been recognised, but the necessary processes that can result in economic concentrations of these rare elements and host minerals are poorly understood. Moreover, the mobility of so-called 'immobile' trace elements that include REE requires explanation. To this end, this study presents the results of investigations into the occurrence and redistribution of REE and other high-field strength elements found in the North Qôroq centre, Gardar Province (Mesoproterozoic) of South Greenland.

Investigation of nepheline syenites and country-rocks to the North Qôroq centre has demonstrated the variable chemistry and nature of REE and HFSE and their derivative minerals. Extensive fractional crystallisation produced rocks ranging from augite syenite to peralkaline lujavrite; this compositional range is displayed in the varied

mineralogy and chemistry. Coupled with this fractionation is an increase in incompatible elements resulting, in the most evolved rocks, with the crystallisation of eudialyte.

Extensive metasomatism accompanied the emplacement of syenite units within the North Qôroq centre. Early fluid activity was dominantly Na-Cl rich and pervasive, whereas later fluids, often seen to overprint this alkali-metasomatism, were dominated by $\text{Ca} - (\text{CO}_3)^{2-} - (\text{F}) - (\text{PO}_4)^{3-}$. This may, however, reflect the activity of one fluid changing in response to external conditions. Evidence suggests that fluids modified the pre-existing rock chemistry and mineralogy, resulting in local enrichment (or scavenging) of country-rock (metasediments and granite-gneiss) and metasomatised syenite. Metasomatic mineralogy is dominated by phases such as apatite, zircon and rare-earth fluorocarbonate that were likely transported in the form of complexes of $(\text{F})^-$ and $(\text{CO}_3)^{2-}$, and $(\text{PO}_4)^{3-}$.

The source of fluid activities relates to the evolution of syenite magma, with early expulsion of an aqueous (Cl-rich) fluid, that resulted in extensive albitisation. Continued fractionation led to incompatible element enrichment and residual magmas that were peralkaline and $(\text{F})^-$, $(\text{CO}_3)^{2-}$ and $(\text{PO}_4)^{3-}$ enriched. Aggressive fluids emanating from these highly evolved magmas were responsible for the element redistribution seen in the metasomatised rocks that include earlier syenite intrusions and their country rocks. (SS6; Wed. Poster)

Cryogenian iron formation: A definitive link to mafic magmatism and weathering of mafic crust

Cox, G.¹, Halverson, G.¹, Minarik, W.¹, Le Heron, D.², Stevenson, R.³, Poirier, A.³, Macdonald, F.⁴, Bellefroid, E.¹ and Strauss, J.⁴,
¹McGill University, Montreal, QC; ²Royal Holloway, University of London, UK; ³GEOTOP/UQAM, Montreal, QC; ⁴Harvard University, MA, USA

The reappearance of Iron Formation (IF) during the Cryogenian (850 Ma-625 Ma) and their close association with glaciogenic sediments has led them to be viewed as a direct result of "Snowball Earth" conditions and a return to ferruginous ocean basins. In this paper we show using major element geochemistry combined with Nd isotopes that while glaciation is no doubt the best explanation for anoxia, the explanation for the reappearance of IF is widespread mafic volcanism, its associated hydrothermal input and crucially the significant weathering of mafic rocks. This results in $\text{Fe}^{2+}:\text{S}^{2-}$ ratios that are greater than unity allowing ferruginous conditions to dominate over euxinic conditions. While such a model does not uniquely require "Snowball Earth" conditions, it does provide an explanation for the association of iron formation with the earlier Sturtian glacial epoch and the absence of iron formation associated with the younger Marinoan glaciation. Furthermore, the limited data available for Archean and Paleoproterozoic BIF's would suggest this model may be applicable to these older IF occurrences. (SY4; Fri. 10:20)

XRD patterns of glassy impactites: Correlating composition and origin via cluster variation analysis and implications for Mars

Craig, M.A.¹, mrcraig44@uwo.ca, Flemming, R.L.¹, Osinski, G.R.¹, Cloutis, E.A.², Anderson, J.³, Izawa, M.R.M.², Sapers, H.M.⁴ and Marion, C.L.¹,
¹Western University, Department of Earth Sciences/Centre for Planetary Science and Exploration, 1151 Richmond St., London, ON N6A 5B7; ²University of Winnipeg, Department of Geography/Hyperspectral Optical Sensing for Extraterrestrial Reconnaissance Laboratory, 515 Portage Ave., Winnipeg, MB R3B 2E9; ³PANalytical, 117 Flanders Rd., Westborough, MA, USA 01581; ⁴McGill University, Department of Natural Resource Sciences, 2111 Lakeshore Rd., Ste. Anne de Bellevue, QC H9X 3V9

Impact cratering may well have been the dominant geological process that shaped the surface of Mars. Researchers have speculated about the volume of, and the areal extent to which, amorphous phases, specifically glassy phases, cover the Martian surface. Reflectance and emission spectra from laboratory studies of glassy and highly shocked materials have provided plausible matches with remotely sensed spectra



from both the Mars Global Surveyor and the Mars Reconnaissance Orbiter. These studies have suggested amorphous materials could comprise a significant portion of the upper-most regolith. The Phoenix lander found what may have been amorphous material and the Mars Science Laboratory (MSL) Curiosity Rover has now definitively identified amorphous material in the first sample analyzed by the Chemistry and Mineralogy (CheMin) instrument aboard MSL.

The X-Ray Diffraction (XRD) pattern collected by CheMin is of a sample that may contain up to 50% amorphous material. Conventional wisdom suggests that the amorphous component is volcanic glass and/or the nano-crystalline weathering products of volcanic glass. This is the most likely conclusion given that the crystalline components include Forsterite and Andesine which are consistent with basaltic glass, but the composition alone may not be able to tell us whether the glass is extrusive and quickly quenched resembling obsidian, pyroclastic, or impact produced. When CheMin comes across amorphous samples such as these, or those where little or no crystalline components are found, could one use the XRD pattern of amorphous materials alone to identify an origin?

It is plausible that one could compare XRD patterns with exemplars from terrestrial sources of amorphous glassy materials, *i.e.* extrusive basaltic glasses, pyroclastics, and terrestrial impactites, and come up with reasonable matches that point to origin and composition. There are a few methods one could use to compare XRD patterns and derive associations: fitting the amorphous halo (or the 'hump') to derive its maxima in 2 theta or d-spacing, Fourier analysis of the collected XRD pattern, and cluster variation analysis of either the full pattern or the isolated amorphous halo.

Preliminary results of a multivariate cluster analysis of XRD patterns collected from a suite of exemplars including: impact glasses from the Haughton, Ries and Mistastin Lake impact structures, and non-impact glasses including obsidian, fulgurite, Trinitite and others, illustrate the similarities and differences between these glassy materials suggesting that comparative analysis of XRD patterns could potentially remotely identify the formation mechanism or origin of amorphous phases. (*SS16; Wed. Poster*)

Metasomatic overprinting of the lithospheric mantle of the Archean Sask Craton

Creighton, S., Saskatchewan Research Council, 125-15 Innovation Blvd, Saskatoon, SK S7N 2X8, creighton@src.sk.ca, and Read, G.H., Shore Gold Inc., 300-224 4th Ave South, Saskatoon, SK S7K 5M5

The Sask Craton is a remnant Archean microcontinent in east-central Saskatchewan that presents an interesting challenge to the major paradigms in diamond exploration. Firstly, despite being of Archean heritage, it was extensively reworked during the Trans Hudson Orogeny (THO) approximately 1.85 billion years ago. Thus, in terms of tectonic history, the Sask Craton has more in common with Proterozoic cratons than "true" Archean cratons *e.g.* the Slave and Kaapvaal cratons. Secondly, it was largely assumed that the lithospheric mantle beneath the Sask Craton was either removed or completely modified by thermal and/or chemical overprinting during the THO effectively eliminating any diamonds that it may have held. A corollary to the thermal-metasomatic overprinting of the Sask cratonic lithospheric mantle is a paucity of harzburgitic (G10) garnets. Indeed, in a relatively large population of 1316 peridotitic garnet xenocrysts recovered during exploration, only 62 (4.7%) classify as G10 or G10D whereas 548 (42%) classify as G9. The low relative abundance of G10 garnets is at odds with typical garnet populations derived from diamondiferous kimberlites in Archean cratons.

Trace-element characteristics of G9 and G10 garnets indicate that despite the strong metasomatic overprint, the Sask lithospheric mantle preserves a remnant of its Archean heritage. Some of the garnets that classify as G9 and G10 have sinusoidal to moderately sinusoidal REE_N patterns indicative of a two-stage history of depletion and re-enrichment in highly incompatible elements. These garnets have Y and Zr concentrations consistent with "depleted" and fluid metasomatized

garnets and are likely the closest representatives to the original composition of the Sask cratonic lithospheric mantle. The majority of G9 garnets analyzed have normal REE_N patterns and Zr-Y concentrations suggestive of metasomatism by melts enriched in elements more compatible in the garnet structure. The maximum TiO₂ concentration of the garnets increases with increasing temperature suggesting that the degree of metasomatic re-enrichment increases with increasing depth. This observation is consistent with intense melt metasomatism derived, presumably, from subducting slabs during the THO.

Clinopyroxene grains from garnet lherzolite xenoliths from the Sask craton also attest to a pervasive metasomatic overprint – zoning in all major and minor elements. Because of the inherent randomness in xenocryst preservation, single crystal clinopyroxene thermobarometry gives erratic and unreliable results. Therefore, a set of filters has been developed to eliminate clinopyroxene grains that are compositionally invalid for thermobarometry. These filters can be used for all mantle-derived clinopyroxene databases to improve the reliability of single-crystal thermobarometry. (*SS4; Fri. 3:20*)

The life and times of a new Ordovician eurypterid from the William Lake Lagerstätte, Manitoba

Cuggy, M.B.¹, michael.cuggy@usask.ca, Rudkin, D.M.² and Young, G.A.³, ¹Department of Geological Sciences, University of Saskatchewan, Saskatoon, SK S7N 5E2; ²Department of Natural History (Palaeobiology), Royal Ontario Museum, Toronto, ON M5S 2C6; ³Geology and Paleontology, The Manitoba Museum, Winnipeg, MB R3B 0N2

Upper Ordovician (Richmondian) dolomudstones of the William Lake Lagerstätte, central Manitoba, are yielding exceptionally preserved remains of a wide range of soft-bodied and weakly sclerotized organisms associated with a sparse shelly fauna. These sediments were deposited in restricted, shallow, and very low-energy conditions in marginal marine environments. The fauna includes a variety of non-biomineralized arthropods, among them many specimens of a new species of eurypterid. Most eurypterid fossils at William Lake are small and probably represent juveniles. Many of the smallest individuals occur higher in the shallowing-upward cycle, suggesting that they lived in the shallowest conditions. Recent discoveries of larger individuals have predominately been made lower in the section, representing deeper water that was closer to normal marine conditions. This pattern of size distribution has also been reported in Upper Silurian eurypterids of the Welsh Borderlands. Concentrations of smaller eurypterids in shallow water environments have previously been regarded as 'nurseries' where juveniles could develop with less competition.

The greatest diversity of eurypterids is recorded in Silurian and Lower Devonian Lagerstätten of Europe and North America. Occurrences of pre-Silurian eurypterids are extremely limited, with only a few species so far reported from Canada and just six genera described worldwide. Their early evolutionary history is obscure, and any new material from this interval is potentially significant. These new finds will aid in elucidating the initial Ordovician radiation of eurypterids. Preliminary analysis of the available material reveals a new taxon that does not easily fit into any of the established clades within the Eurypterida. It has a mixture of characteristics typical of a number of different superfamilies, as well as unique characters not seen anywhere else in the Order. This suggests that the poorly known record of Ordovician eurypterids may be obscuring a more complicated evolutionary history than has been previously suggested. (*SY3; Thurs. 2:20*)

Circa 1060-1090 Ma syn- to post-orogenic plutonism in the Grenville Province of Ontario: Insights from major, trace element and isotope geochemistry

Cutts, J.R.¹, jamiecutts@cmail.carleton.ca, Easton, R.M.² and Carr, S.D.¹, ¹Ottawa-Carleton Geoscience Centre, Department of Earth Sciences, Carleton University, Ottawa, ON K1S 5B6;



²Precambrian Geoscience Section, Ontario Geological Survey,
933 Ramsey Lake Road, Sudbury, ON P3E 6B5

The Kensington-Skootamatta ultrapotassic plutonic suite was emplaced throughout the eastern Composite Arc Belt and Frontenac-Adirondack belt of the Grenville province during the onset of Ottawan-phase orogenesis (~1060-1090 Ma). The deep crustal, more highly metamorphosed Mazinaw Terrane, however, remained devoid of such magmatism during this period. Despite the ongoing Himalayan-scale collisional tectonics, the plutons remained unmetamorphosed, undeformed, and cross-cut the regional fabric. Characterisation of the petrography, geochemistry, and geochronology of select plutons from the Kensington-Skootamatta suite in the Sharbot Lake, Grimsthorpe, and Frontenac terranes in Ontario has been undertaken to further refine the tectonic evolution of the western Grenville Province and to provide insight into the geochemistry of post-orogenic alkaline plutonism.

Petrography and geochemistry reveal 2 sub-groups; an early syenite to monzonite suite and a late granite to alkali feldspar granite suite. Major element geochemistry indicates that both are shoshonitic and dominantly ferroan; however the syenites are strongly alkalic (miaskitic) and metaluminous whereas the granites are alkalic to alkali-calcic, and metaluminous to peraluminous. These characteristics are typical of a within-plate/anorogenic to post-orogenic tectonic setting. In contrast, trace element profiles uniformly show depletions in Nb, Ti, Sr and P with negative REE slopes, and relative HREE enrichments that are typical of magmatism in a subduction-zone setting. Isotope data (average $Sr_{initial} \sim 0.703$; $\epsilon_{Nd} \sim +3-4$) suggest derivation from a relatively primitive source with little contamination from continental crust.

Preliminary interpretation indicates generation of the source melt at depths shallower than the garnet stability field. Extension and thinning of the lithospheric crust, followed by upwelling and replacement of the lithospheric mantle by previously metasomatised asthenosphere led to a basaltic underplate in a collisional (within-plate) setting. Subsequent melting and fractionation of the basalt underplate may have produced an early syenite melt which was further fractionated to generate the late granite suite. (GS3; Thurs. 1:40)

Improving the accuracy of soil conductivity measurements

Dale, J.¹, Swetlow, J.², Kelim, W.¹, Lafond, G.³, Morris, E.², Sunley, S.² and Tant, C.², ¹Dept. of Geology, University of Regina, Regina, SK S4S 0A2; ²EcoTech Research Ltd. 1717 13th Avenue, Regina, SK S4P 0V4; ³Agriculture and Agri-Food Canada, Indian Head Research Farm, RR#1 Gov Rd. Box 760, Indian Head, SK S0G 2K0

These research results are part of an ongoing interdisciplinary Saskatchewan Agricultural Development Fund project (ADF #20090323) that includes estimating several soil properties from ground conductivity measurements. Moisture content and salinity are just some of these properties. Our purpose was to estimate soil moisture content from ground conductivity readings at AESB sites in Indian Head and Swift Current, Saskatchewan. Conductivity is measured in the laboratory from soil samples using standard laboratory techniques that measure electrical conductivity. A second method involves towing a ground conductivity meter developed by EcoTech Inc. over the fields. This instrument indirectly measures salinity levels by measuring the electrical conductivity of the soil. When a greater concentration of salts is encountered, higher conductivity readings are observed. This method of salinity assessment is well established, and makes it possible to quickly survey a field and locate high salinity areas. However, recent studies suggest that common methods of measuring soil conductivity and salt content from soil samples may underestimate the level of salinity (Amakor, X.N., *et al.* 2010). In our studies, we discovered a moderate correlation between conductivity values and soil moisture at soil depths between 30 to 60 cm below the surface and 60 to 91 cm below the surface. pH of soil samples in the A horizon from 1 to 7 cm depths were found to weakly correlate with conductivity where lower pH values correspond with higher conductivity readings. Most surprising was a strong correlation between conductivity readings and the type of crop that had been harvested. On further analysis we

discovered that the type of crop controls the range of conductivity values and the range of soil moisture. The type of previously harvested crop is a better predictor of soil moisture than conductivity. Current studies are looking at how the root structure of previous field crops affects the relationship between conductivity measurements and other soil properties including soil texture and organic content. (SS14; Thurs. Poster)

Rare earth element mineralogy of the Wicheeda carbonatite complex, central British Columbia, Canada

Dalsin, M.L., mdalsin@eos.ubc.ca, and Groat, L.A., Department of Earth, Ocean and Atmospheric Sciences, University of British Columbia, Room 2020, 2207 Main Mall, Vancouver, BC V6T 1Z4

Carbonatites are rare magmatic rocks composed of greater than 50% carbonate minerals. They are generally associated with continental rift related tectonic settings. Carbonatites are commonly enriched in REE's, Nb, and P. The Wicheeda carbonatite complex, located 80 km northeast of Prince George, has been historically explored for its REE potential but until recently there has been very little extensive exploration or scientific study. Work has begun to determine the geology, mineralogy, geochemistry and geochronology of the Wicheeda carbonatite. The rare earth mineralogy of the Wicheeda carbonatite is complex and is being defined through the use of classical petrography, scanning electron microscopy, electron probe microanalysis, and single crystal X-ray diffraction. The REE mineralogy consists of Ca-REE-fluorocarbonates (including bastnäsite-(Ce), parisite-(Ce), and synchysite-(Ce)), Ba-REE-fluorocarbonates (including cordylite-(Ce), kukharenkoite-(Ce), cebaite-(Ce), huangnoite-(Ce), and qaqarsukite-(Ce)), ancylite-(Ce), monazite, euxenite and silicates; the majority of which are LREE rich. Understanding carbonatites and the mineralogy of REE deposits is important to designing a successful exploration strategy and determining whether a deposit is economic or not, and work on the Wicheeda complex could assist in exploration for other REE deposits in the Rocky Mountain Rare Element Belt as a whole. (SS6; Wed. 11:00)

Tectono-metamorphic relationships of the Abitibi greenstone belt and the Opatika plutonic belt: Insights from the lac-au-Goéland area, northern Québec

Daoudene, Y.¹, daoudene@gmail.com, Tremblay, A.¹, Goutier, J.² and Ruffet, G.³, ¹Université du Québec à Montréal, Montréal, QC H2X 3Y7; ²Ministère de Ressources naturelles et de la Faune du Québec, Val-d'Or, QC J9P 3L4; ³University de Rennes 1 UMR CNRS 6118, 35042 Rennes Cedex, France

The Archean Superior Province is made up of several subprovinces and/or terranes that amalgamated during the Kenoran orogeny between 2.72 and 2.68 Ga. Although the overall geology of these terranes is commonly well-documented and understood, the nature of the terrane boundaries still remains poorly constrained in several cases. The boundary between the Abitibi greenstone belt (AGB) and the Opatika plutonic belt (OPB), for instance, is currently interpreted as surficial trace of a paleo-subduction zone on the basis of seismic data. However, additional structural and metamorphic data from such contact zones are necessary to debate about crustal tectonics in the region during the Archean.

This study presents new structural data gathered along the Abitibi-Opatika contact zone in a region located close to the lac-au-Goéland, at ~90 km East of Matagami. Amphibolite-grade metavolcanic and metasedimentary rocks of the AGB there overly plutonic rock, dominantly tonalitic, belonging to the OPB. The volcanic rocks of the AGB are generally characterized by steeply dipping foliations that are consistent with those observed in the OPB, and both the AGB and the OPB are affected by NW-SE to East-West trending tight folds. The intensity of regional deformations seems to be stronger in the vicinity of the Abitibi-Opatika contact zone and when present, shear-sense criteria suggest top-to-the-south motions although the nature and kinematic of the contact zone deformation still remains to be precisely constrained.



Microstructural observations of oriented rocks samples on both sides of the contact zone indicate the predominance of sub-solidus fabrics developed at the amphibolite facies. Also, the occurrence of abundant syn-kinematic tonalitic dykes and tonalitic-dioritic plutons (2696-2693 Ma) intruding the AGB close to the contact with the OPB is indicative of widespread magmatic activity during deformation and suggests synorogenic partial melting at depth.

The structural characteristics of the Abitibi and Opatika contact zone suggest that these two crustal belts formed a single structural unit during regional deformation. Metamorphic grade of rocks in the studied area, in comparison with that documented farther south in the AGB further suggests that the contact zone with the OPB, besides corresponding to a major corridor of ductile deformation, clearly exposed a deeper crustal level. To better constrain the timing of deformation, the amphibolite- and greenschist-grade regional metamorphism that characterizes these rocks will be dated using $^{40}\text{Ar}/^{39}\text{Ar}$ thermochronology. (SS2; Wed. Poster)

Trace elements in Fe-oxides from fertile and barren igneous complexes: Investigating their use as an exploration tool for Ni-Cu-PGE deposits

Dare, S.A.S.¹, sasdare@hotmail.com, Ames, D.², Lightfoot, P.C.³, Barnes, S.-J.¹ and Beaudoin, G.⁴, ¹Université du Québec à Chicoutimi (UQAC), Chicoutimi, QC G7H 2B1; ²Geological Survey of Canada, Ottawa, ON K1A 0E8; ³Vale, Brownfield Exploration, Sudbury, ON P0M 1N0; ⁴Université Laval, Québec, QC G1V 0A6

Magmatic Ni-Cu-PGE sulfide deposits are hosted towards the base of ultramafic and mafic igneous complexes and formed by efficient accumulation of immiscible sulfide liquids that scavenged chalcophile metals from the host silicate magma. An efficient tool in the exploration of Ni-Cu-PGE deposits is the depletion of highly chalcophile metals in host intrusions, as recorded by whole rock ratios (e.g., Cu/Zr, Cu/Pd, Ni/Ni*) and Ni depletion in olivine. Magmatic Fe-oxides (magnetite and/or ilmenite) commonly crystallize from mafic and intermediate magmas and contain several chalcophile elements in trace abundance. This TGI4 project investigates whether Fe-oxides record evidence of sulfide saturation in order to provide an indicator mineral vector towards Ni-Cu-PGE deposits at depth. A suite of 25 trace elements were determined in magnetite and ilmenite, by laser ablation ICP-MS at LabMaTer (UQAC), from a variety of barren and fertile igneous complexes, including two of Canada's largest Ni-deposits: the 1.85 Ga Sudbury Igneous Complex (Ontario) and 1.34 Ga Voisey's Bay (Newfoundland). Barren igneous complexes studied comprise layered mafic intrusions (Bushveld, South Africa and Sept Iles, Quebec) and anorthosite suites (Saguenay-Lac-St-Jean, Quebec) that host Fe-Ti-V-P deposits, some of which contain trace amounts of magmatic sulfides but no Ni-Cu-PGE deposits. Mafic rocks of the 1.33 Ga Newark Island layered intrusion (Newfoundland) were also studied as they are similar in composition and setting to Voisey's Bay but barren of Ni-Cu-PGE deposits. In sulfide-undersaturated magmas Cu, Sn, Mo and Zn are incompatible during fractionation and thus increase in concentration in both magnetite and ilmenite. Upon sulfide saturation and the formation of a trace amount of sulfide, Cu is depleted in the silicate magma relative to the other incompatible elements. Cu depletion as recorded by Fe-oxides is a sensitive indicator of sulfide saturation but it is not diagnostic of whether a Ni-bearing sulfide deposit formed. In contrast, Ni and Co are compatible during fractionation, partitioning into olivine, orthopyroxene and where present sulfide, and their concentration steadily decreases in the Fe-oxides together with Cr. Fe-oxides from barren complexes plot on a single Ni-Cr trend but Fe-oxides from fertile complexes, hosting Ni-Cu-PGE deposits, plot on a parallel Ni-Cr trend displaced to lower Ni concentration. Ni depletion is therefore recorded in Fe-oxides and has the potential to identify intrusions with buried Ni-sulfide mineralization. The advantages of using Fe-oxides as an exploration tool include their resistance to post-magmatic processes such as

alteration and their preservation and easy recovery in glacial till. (SS9; Thurs. 8:20)

Are the magnetite "lava flows" of El Lago (Chile) magmatic? Comparison of trace elements in magnetite with magmatic Fe-oxide deposits

Dare, S.A.S.¹, sasdare@hotmail.com, Barnes, S.-J.¹, Beaudoin, G.², Méric, J.¹ and Boutroy, E.², ¹Université du Québec à Chicoutimi (UQAC), Chicoutimi, QC G7H 2B1; ²Université Laval, Québec, QC G1V 0A6

Magnetite forms under a wide variety of conditions, crystallizing at high temperature from silicate magmas or precipitating at lower temperatures from hydrothermal fluids or seawater. Due to a large number of minor and trace element substitutions into magnetite its trace element composition should reflect the differences in these conditions. As such the chemical 'fingerprint' of magnetite is used in petrogenetic and provenance studies with a growing interest as an indicator mineral in the exploration of ore deposits. We have analyzed magnetite in magmatic massive Fe-oxide deposits (Ti-rich magnetite, ilmenite, ± apatite) from layered intrusions and a massif-type anorthosite, by laser ablation ICP-MS at UQAC, in order to study how magmatic processes affect the trace element compositions. Trace element data from the enigmatic magnetite "lava flows" from El Lago, Chile, was also collected in order to consider whether these magnetites are indeed of igneous origin (Fe-rich melt) or formed by hydrothermal alteration of andesite lava flows.

Magnetite from layered intrusions records the evolution of the fractionating silicate liquid. Magnetite layers at base of the sequence contain magnetite richer in compatible elements (Cr, Ni, Mg and V) whereas those found higher in the sequence are richer in incompatible elements (e.g., Ti, Nb and Ta), having crystallized from a more evolved melt (together with apatite). Magnetite from the anorthosite shows similar compositions to those from layered intrusions. Fresh andesite host rocks at El Lago contain phenocrysts of Ti-rich magnetite, of typical magmatic composition, with apatite and rare ilmenite. However, magnetite from the El Lago massive ore "lava flows" are distinctly different to any known magmatic magnetite: 1) it is depleted in many elements but in particular those considered relatively immobile in hydrothermal fluids (e.g., Ti, Al, Cr, Zr, Hf and Sc), 2) magnetite is enriched in elements that are highly incompatible into magnetite (REE, Si, Ca and P) and normally in very low abundance in magmatic magnetite, 3) behaviour of Ni-Cr is decoupled with ratios > 1, typical of magnetite from IOCG, IOA and skarns, and 4) oscillatory zoning of Si, Ca, Mg and REE in El Lago magnetite is similar to that found in skarn magnetite. Furthermore, magnetite of clear secondary origin in the altered host rock has the same composition as magnetite from the El Lago massive ore. Thus the chemical fingerprint of magnetite from the El Lago "lava flows" supports the hydrothermal model of alteration of andesite lava rather than a magmatic origin. (SS23; Fri. 1:40)

FTIR imaging of geological materials

Della Ventura, G.¹, dellaven@uniroma3.it, Bellatreccia, F.¹, Marcelli, A.² and Radica, F.¹, ¹Università Roma Tre, Largo S. Leonardo Murialdo 1, 00146 Roma; ²INFN - Laboratori Nazionali di Frascati, Via E. Fermi 40, 00044 Frascati (Roma), Italy

There are three possible experimental set-ups in FTIR microscopy: (1) point detector analysis in a confocal layout, (2) FTIR mapping done by integrating the signal from successive locations of the specimen surface, (3) FTIR imaging, performed with bi-dimensional arrays such as focal plane array (FPA) detectors. In the FTIR mapping mode one measures the infrared spectrum at each in-plane point and then uses peak heights, peak areas, the integer performed in a defined spectral region or other criteria to visualize the distribution of the target molecule. This experimental set-up can be coupled to a confocal set-up to achieve a high SNR (signal-to-noise-ratio). In the FPA imaging mode, one obtains the whole image in a single data collection thanks to a multichannel detection similar to the concept of recording images



with charge-coupled devices (CCDs) in optical microscopy. The number of pixels (the "detectors") and their effective size will depend on the FPA type. Typical arrays range from the 64×64 channels, providing 4096 individual spectra, to 256×256 or 1024×1024 channels, allowing imaging of large areas. Such arrays are coupled with 15× or 36× objectives, so that a single pixel corresponds to a physical dimension in the range 2.5 to 5 µm.

H-C-O functional groups are characterized by highly polar bonds and absorb infrared radiation with high efficiency, therefore FTIR micro-spectroscopy coupled with imaging possibilities may be used to qualitatively and quantitatively measure these molecular arrangements in geological materials with a spatial resolution close to the diffraction limit. For Earth science materials, the new imaging capabilities of FTIR detectors have been so far used to address features such as zoning of volatile species across the sample or possible configurational changes of structurally-bound carbon molecular species (e.g., CO₂ vs. CO₃) during the crystal growth. Such features, which are barely accessible with conventional micro-analytical techniques, may provide constraint in terms of physico-chemical parameters relating to the conditions of formation of the samples, and important information on the evolution of geological systems vs. time. In this talk, some recent studies done in our FTIR laboratory, in particular aimed at characterizing the distribution of hydrogen and carbon in rock-forming microporous minerals such as feldspaths and cordierite, will be presented. The use of FTIR imaging to study experimental products, notably cordierite and beryl doped with carbon dioxide under different P and T conditions, as well as tests to monitor dehydration processes in real time, will finally be discussed. (SY1; Thurs. 3:00)

Polymetallic mineralization in the context of Minto Subprovince crustal evolution, Nunavik, Québec, Canada

Delpech, E.¹, Jebrak, M.¹, delpech.emilie@courrier.uqam.ca, Lulin, J.M.³ and Stevenson, R.^{1,2}, ¹Earth and Atmospheric Sciences Department/²GEOTOP, University of Quebec at Montreal, PO Box 8888, succursale Centre-Ville, Montréal, QC H3C 3P8; ³Exploration Azimut Inc. 110 De La Barre Street, Suite 214, Longueuil, QC J4K 1A3

The metallogenic evolution of Nunavik is still poorly understood. Recent discoveries made by Azimut Exploration Inc., about 140 km east of Hudson Bay, provide an opportunity to conduct new research on the subject. The region of interest forms a 330-km by approximately 30 to 50-km north-oriented corridor called the Rex Trend. This area is contained within the Qalluvituuq-Payne and Lac Minto domains, near the boundary with the Utsalik Domain, within the Minto Subprovince of the Archean Superior Province. The regional geological framework is dominated by plutonic rocks (essentially granites and TTG series) and volcano-sedimentary rocks. It also comprises ultramafic and alkaline intrusions.

Some of the previous regional studies have described diverse types of mineralization, late metasomatism and deep crustal structures. These data need to be re-assessed in light of the recently acquired new information.

The currently identified mineralized systems can be classified as: QWPre- to syn-orogenic:

1. Sulphide-hosted Au-Ag-Cu mineralization associated with faults, dominantly in metavolcanic rocks;
2. Sulphide-hosted Au mineralization in banded iron formations (BIF);
3. Porphyry-type Cu-Mo mineralization associated with granodioritic intrusions along a NNW-SSE trending corridor;

Post-orogenic:

4. IOCG-type Cu-(Co) mineralization as stockworks and quartz-chlorite-magnetite breccias associated with NNW-SSE faults;
5. Intrusion-related Ag-Au-Bi-Cu, W-Sn and Rb-Cs-Li-(Ta) mineralization associated with a large monzogranite intrusion;
6. Nb-REE-Y-P mineralization related to alkaline magmatism;
7. Sc concentrations in serpentinized ultramafics.

Some of these types are common to Archean greenstone belts (1, 2) and common to Precambrian cratons (3, 6), whereas others are totally new to the Northern Superior Province (4, 5, 7). The IOCG-type (4) appears as a late hydrothermal event crosscutting the regional foliation. The occurrence of a major hydrothermal event along the Rex Trend and the presence of widespread alkaline rocks suggest the presence of a significant N-S lithospheric suture in the craton. Such a structure could have channelled magmas and fluid(s) that propagated along local NNW-SSE faults to form the veins, breccias and stockworks that constitute these mineralized systems. (SS2; Wed. 9:00)

Mass extinction in Manitoba: Biotic change and stratigraphy associated with the Ordovician-Silurian boundary interval

Demski, M.W.¹, matthewdemski@gmail.com, Stewart, L.A.¹, Elias, R.J.¹, Young, G.A.², Nowlan, G.S.³ and Dobrzanski, E.P.², ¹Department of Geological Sciences, University of Manitoba, Winnipeg, MB R3T 2N2; ²Geology and Paleontology, The Manitoba Museum, Winnipeg, MB R3B 0N2; ³Geological Survey of Canada, 3303 33rd Street NW, Calgary, AB T2L 2A7

The first of five major mass extinctions in the Phanerozoic Era occurred near the end of the Ordovician Period (Hirnantian Age), approximately 445 million years ago. This event led to the demise of approximately 85% of marine species. The Late Ordovician extinction is widely accepted to be the result of global environmental change associated with extensive glaciation in south-polar Gondwana. Fauna that thrived in pre-extinction greenhouse conditions were devastated by abrupt cooling and the loss of marine habitats as a result of sea-level drop. Glacio-eustatic regression was particularly significant in epicontinental seas (such as in the Williston Basin of central Laurentia), where endemic species could not escape to the open ocean. The major pulse of glaciation was restricted to the Hirnantian (~1 m.y.), with conditions returning to a pre-Hirnantian state in the Early Silurian.

Strata exposed at two areas in west-central Manitoba (Grand Rapids Uplands and Cormorant Hill) record an interval across the Ordovician-Silurian (O-S) boundary, which includes evidence of the Late Ordovician mass extinction. Recent studies have focused on age determination of the uppermost Ordovician strata and precise positioning of the O-S boundary using lithostratigraphy, carbon-isotope chemostratigraphy (i.e. recognition of the Hirnantian Isotopic Carbon Excursion, or HICE), and biostratigraphy based on conodont microfossils. Employing these methods, it has been determined that strata of Hirnantian age are present in west-central Manitoba and, by extension, the rest of the Williston Basin. The position of the O-S boundary has been raised to the top of the Upper Ordovician Stonewall Formation.

Macrofossils collected in these areas record biotic change near the margin of a fluctuating epicontinental sea during the extinction interval. A period of glacio-eustatic regression and subaerial exposure separated a highly diverse, coral-dominated, pre-extinction fauna in the lower Stonewall Formation from a lower diversity fauna preserved in uppermost Stonewall, Hirnantian-aged strata. This latter fauna shares similarities with other, similar-aged assemblages in North America (e.g. Edgewood Assemblage of the east-central United States), and strengthens the interpretation of a Hirnantian age for uppermost Stonewall strata in the study area. This fauna was succeeded by a third, highly diverse fauna in the Lower Silurian Fisher Branch Formation, immediately overlying the Stonewall Formation, which represents the Early Silurian recovery of marine faunas. (SS13; Fri. 9:40)

Widespread margin-collapse triggered by the ~51 Ma Montagnais marine bolide impact, offshore Nova Scotia

Deptuck, M.E., Canada-Nova Scotia Offshore Petroleum Board, 1791 Barrington St., Halifax, NS B3J 3K9, mdeptuck@cnsopb.ns.ca, and Campbell, D.C., Geological Survey of Canada (Atlantic), Bedford Institute of Oceanography, PO Box 1006, Dartmouth, NS B2Y 4A2

The ~51 Ma Montagnais impact crater on the outer Scotian Shelf is well known, but the potential effects from the impact event on the slope



and rise seaward of the crater have, until now, remained poorly understood. Through detailed seismic stratigraphic correlation and ties to available wells, we define a three-fold seismic stratigraphic subdivision for Upper Cretaceous to Eocene strata on the shelf and slope, calibrated to the most recent biostratigraphic results. Using this framework, we identify a number of depositional and erosional products that are temporally-consistent with a late Ypresian impact event (within the limits of seismic and biostratigraphic resolution). We link a series of prominent failure scarps on the outer shelf and upper slope to a single widespread mass transport deposit (MTD) on the lower continental slope, rise and abyssal plain. Failed material amassed in a large debris field referred to here as the 'Montagnais MTD'. It covers an area of ~93 000 km² and travelled up to 580 km from the impact site where its distal termination onlaps the New England Seamounts, making it one of the largest known debris avalanches on Earth. We interpret these deposits, and the associated pattern of erosion landward of them, as products of widespread margin collapse caused by a combination of ground shaking and ensuing tsunamis triggered by the Montagnais impact event. This study provides insight into the potential effects of outer-shelf marine impact events immediately down slope from impact sites, and their diminished effects with increasing distance along the margin. (*SS16; Wed. 9:00*)

Heterolithic breccia containing both fluidal- and cored-'scoria' clasts, Flin Flon, Manitoba: Evidence of submarine fire fountaining

DeWolfe, Y.M. and Pittman, N., Mount Royal University, 4825 Mount Royal Gate SW, Calgary, AB T3E 6K6, mdewolf@mtroyal.ca

A unique heterolithic breccia containing rounded, cored 'scoria' clasts occurs as a discrete bed (~25 m thick) within a Paleoproterozoic submarine volcanic succession in the area of the Schist Lake and Mandy volcanogenic massive sulphide (VMS) deposits. The Schist Lake and Mandy deposits are located approximately 4 km southeast of the town of Flin Flon, Manitoba.

The heterolithic breccia is crudely bedded, containing lithic clasts of amygdaloidal basalt, laminated mafic tuff, and rhyolite. Lithic clasts range in size from 1 cm to 100 cm and are angular to round in shape. Some lithic clasts are mantled by <1 cm to 8 cm of amygdaloidal basalt, forming cored 'scoria' clasts. In addition to the lithic, and cored 'scoria' clasts, the unit contains fluidal, amygdaloidal basalt clasts, ranging in size from 1 cm to 50 cm, with formerly glassy rims. Petrographic and chemical analyses of the fluidal basalt clasts and the basaltic rims on the cored 'scoria' clasts show they have identical compositions. Changes in clast size and the relative percentages of each clast type define crude beds, ranging from 1 m to 4 m in thickness, within the breccia.

The fluidal basaltic clasts within the unit are interpreted to be a result of submarine fire fountaining of relatively low-viscosity lava. The cored 'scoria' clasts are interpreted to be a result of wall rock fragments being entrained in the magma and erupted with an adhering rim of basaltic melt. The lithic clasts are interpreted to be wall rock fragments erupted without an adhering rim of basaltic melt. Recognition of the heterolithic breccia as a product of fire fountaining constrains both vent proximity (within tens of metres) and the environment of deposition, both important factors in determining the potential for more VMS-style mineralization in the area. (*GS2; Wed. 8:20*)

Application of combined SEM, BSE and EDX techniques to the mineralogical and geochemical characterization of granitic-pegmatites

Dittrich, T.¹, Thomas.Dittrich@mineral.tu-freiberg.de, Schulz, B.¹, Seifert, T.¹, Hagemann, S.², Gutzmer, J.^{1,2}, ¹Department of Economic Geology and Petrology, Institute of Mineralogy, TU Bergakademie Freiberg, Brennhaugasse 14, D-09596 Freiberg/GERMANY; ²Centre of Exploration Targeting, The University of Western Australia, 35 Stirling Highway, Crawley,

Perth, Western Australia 6009; ³Helmholtz Institute Freiberg for Resource Technology, Halsbrücker Str. 34, D-09599 Freiberg/Germany

Rapid technological development within the past decade has resulted in a sharply increasing demand for various speciality metals such as Nb, Ta, Li, Be, Cs and others. Economically feasible natural concentrations of these metals are found, among others, in pegmatites. However, in most cases, the metals are contained in high concentrations only in minerals that are of minor to trace abundance in mineralised pegmatites. Identifying and tracing of such economically relevant minerals in pegmatites places particular challenges on exploration and exploitation. New exploration tools are needed to swiftly and reliably identify pegmatites with high economic potential. Because of the very coarse crystal size and the heterogeneous and variable zoning of pegmatite bodies this screening can rarely be achieved by geochemical analysis. Instead, multi-faceted ore-characterization and the development of new evaluation techniques are needed.

Coarse-grained granitic pegmatites bearing heterogeneously distributed lithium-caesium-tantalum minerals (LCT) may serve as an example of the problem of representative sampling for geochemical and mineralogical characterisation. Bulk samples are usually taken for bulk rock geochemical characterisation. To allow for rapid screening, we propose the following procedure: The samples are crushed to grain sizes < 0.5 mm, homogenised and subdivided into subsamples with an individual weight of about 200g. In this manner, the bottleneck of representativity is effectively overcome. A part of the granular sample is embedded to form a grain mount and then polished and carbon-coated for automated SEM-EDS mineral liberation analysis (MLA). Another sample fraction is ground to analytical fineness and prepared for XRF, XRD and ICPMS bulk chemical and mineralogical analysis. Bulk chemical analysis is suitable to acquire the composition of the sample, but it is not suitable for identification of particular minerals hosting the target elements; XRD, on the other hand, is limited by the fact that minerals occurring in concentrations smaller than 1 wt% cannot reliably be identified. SEM-EDS-based mineral liberation analysis (MLA), on the other hand, can identify all rare minerals present, but fails in the detection of Be and Li and also, to some extent, in the correct distinction of members of solid solution series (e.g. mica). The technique was applied to pegmatite ores from the greenstone hosted Neo- to Meso-Archean Londonderry and Catlin Creek LCT-pegmatite deposits of the Yilgarn Craton in Western Australia. Results emphasize that the advantages and disadvantages of each analytical method may be balanced by a combined approach. (*SY2; Thurs. Poster*)

The Bousquet 2-Dumagami world-class Archean Au-rich volcanogenic massive sulphide deposit, Abitibi: Metamorphosed submarine advanced argillic alteration footprint and genesis

Dubé, B.¹, bdube@nrnc.gc.ca, Mercier-Langevin, P.¹, Geological Survey of Canada, 490 rue de la Couronne, Québec, QC G1K 9A9, Kjarsgaard, I.², Hannington, M.³, Bécu, V.¹, Côté, J.⁴, Moorhead, J.⁵, Legault, M.⁶ and Bédard, N.⁴, ¹Geological Survey of Canada, 490 rue de la Couronne, Québec, QC G1K 9A9; ²Consulting Mineralogist, 15 Scotia Place, Ottawa, ON K1S 0W2; ³University of Ottawa, 140 Louis Pasteur, Ottawa, ON K1N 6N5; ⁴Agnico-Eagle Mines Ltd, Lapa mine Division, 299, Boulevard St-Paul N. Route 117 Rivière Heva, QC J0Y 2H0; ⁵Ministère des Ressources naturelles et de la Faune, 420 boul. Lamaque, Val-d'Or, QC J9P 3L4; ⁶Agnico-Eagle Mines Ltd, 145 King Street East, Suite 400, Toronto, ON M5C 2Y7

The Bousquet 2-Dumagami deposit is an Archean Au-rich volcanogenic massive sulphide deposit (VMS) with a total production of ~4 Moz Au. The deposit is located within the Doyon-Bousquet-LaRonde mining camp in northwestern Quebec and hosted by the 2704-2695 Ma Blake River Group, the world's most productive volcanic assemblage for Au-rich VMS deposits. The deposit consists of stacked, deformed and transposed semimassive to massive pyrite-rich lenses, breccia zones and associated sulphide veins and stringer zones hosted by the upper member of the Bousquet Formation. The main ore zone is



known as the Massive Hangingwall Zone or as Zone 5. Another semimassive to disseminated pyrite-rich auriferous zone with coarsely recrystallized massive pyrite is present in the footwall. The Massive Hangingwall Zone is a Au-Ag-Cu-Zn sheet-like, semimassive to massive, pyrite-rich sulphide lens intermixed with vein and breccia zones. The dominant ore type consists of Au-Cu mineralization, but its upper and eastern parts are enriched in Zn. The ore consists of a complex assemblage of sulphides, sulphosalts and native gold, including abundant pyrite, sphalerite, a few percent of chalcopyrite, bornite, and galena, with some visible gold. The Massive Hangingwall Zone was formed by subsea-floor replacement of footwall calc-alkaline dacitic volcanoclastic rocks and hanging-wall blue quartz-phyrlic rhyolite.

Despite significant N-S shortening and metamorphism, which was responsible for transposition, flattening, folding and recrystallization, a number of different metamorphic mineral assemblages can be mapped over several tens of meters from distal to proximal to the ore: (1) quartz-muscovite±Mn-garnet±biotite±chlorite; (2) quartz-muscovite±pyrite; (3) quartz-muscovite-andalusite-pyrophyllite-pyrite with topaz and diaspore; (4) massive quartz-pyrite. All metamorphosed alteration assemblages are characterized by strong progressive Na₂O depletion. Gains in MnO, Fe₂O₃T, MgO, and CaO are recorded in the quartz-muscovite ± Mn-garnet ± biotite ± chlorite assemblage. In the quartz-muscovite-andalusite-pyrophyllite-pyrite and the proximal massive quartz-pyrite assemblages all oxides, except SiO₂, Fe₂O₃T and TiO₂, were strongly to almost entirely leached. The andalusite-kyanite-pyrophyllite-bearing aluminous assemblages are interpreted to represent metamorphosed equivalents of synvolcanic advanced argillic-style alteration, whereas the massive quartz-pyrite assemblage is similar to the massive silicic alteration. Gold emplacement is considered synvolcanic, coeval with the formation of the sulphide zones, and similar to the age of the host rhyolite (2697.8 Ma) and overlying felsic volcanic rocks (2697.5 Ma). The major Au endowment of the Doyon-Bousquet-LaRonde mining camp may be related to favourable source rock or Au reservoirs specific to the lower crust or upper mantle beneath the eastern Archean Blake River Group. (SS7; Wed. 9:00)

Timiskaming-type sedimentary rocks near the Musselwhite gold mine in the North Caribou greenstone belt, Western Superior Province of Canada

Duff, J.¹, duff.jason00@gmail.com, Hattori, K.¹, khattori@uottawa.ca, Schneider, D.¹, Biczok, J.² and McFarlane, C.³, ¹University of Ottawa, Ottawa, ON K1N 6N5; ²Musselwhite Mine, Goldcorp Inc., PO Box 7500, Thunder Bay, ON P7B 6S8; ³University of New Brunswick, Fredericton, NB E3B 5A3

Timiskaming-type sedimentary rocks are the youngest lithological unit overlying most rocks in Archean greenstone belts, and are common in the central and southern Superior Province of Canada. These immature sedimentary rocks are important in unravelling the evolution of the Superior Province as they were deposited along major crustal shear deformation zones and are spatially associated with large gold deposits, such as the Porcupine and Kirkland Lake gold camps.

The North Caribou Superterrane (NCS) is considered to have been the nucleus of the Archean Superior Province of Canada during accretionary growth of the continent as it contains old, ~ 3.0 Ga, supracrustal rocks. The North Caribou Greenstone belt (NCGB) is in the north-central part of the NCS and it contains a ~ 3.0 Ga sedimentary sequence including quartz arenites (Donaldson & De Kemp, 1998). The NCGB is also the host of the major orogenic gold deposit at Musselwhite, which occurs in banded iron-formation, <20 km from clastic rocks of the Zeemal-Heaton assemblage (ZHA). This assemblage occur in the northern margin of the greenstone belt near the east-trending Totogan-North Caribou Shear Zone, the major shear deformation along the boundary between the North Caribou Terrain and the Island Lake Domain to the north. New U-Pb zircon ages from the ZHA show that at least parts of the sedimentary rocks were deposited at

around 2680 Ma. The quartzofeldspathic arenite from the Heaton Lake area (~ 40 km east of Musselwhite) yielded concordant zircon ages ranging from 2681-2712 My. Sublithic arenites farther east ~ 7 km at Obabigan Lake yielded ages of 2723 -2745 My. The data suggest episodic development of basins and/or the change in the provenances in a basin along the deformation zone. In either case, the data proves the deposition of Timiskaming-type sedimentary rocks along the Totogan-North Caribou Shear Zone. Considering a Sm-Nd hydrothermal garnet age of 2690 Ma at the Musselwhite mine reported by Biczok *et al.* (2012), the new data suggest that the mineralization was likely synchronous with the crustal-scale shear deformation and the deposition of the Timiskaming-type sedimentary rocks. (SS3; Fri. 9:20)

Major ore types of the Lalor gold-rich massive sulfide deposit, Snow Lake, Manitoba

Duff, S.¹, sduff@uottawa.ca, Hannington, M.¹, Caté, A.², Mercier-Langevin, P.³, Kjarsgaard, I.⁴, Dubé, B.³ and Gagné, S.⁵, ¹Department of Earth Sciences, University of Ottawa, Ottawa, ON K1N 6N5; ²Institut national de la recherche scientifique – Centre Eau, Terre et Environnement, 490 rue de la Couronne, Québec, QC G1K 9A9; ³Geological Survey of Canada, 490 rue de la Couronne, Québec, QC G1K 9A9; ⁴Mineralogical Consultant, 15 Scotia Place, Ottawa, ON K1S 0W2; ⁵Manitoba Geological Survey, 360-1395 Ellice Ave., Winnipeg, MB R3G 3P2

The Lalor deposit is a recently opened (August 2012) Au-Cu-Zn VMS deposit located in Snow Lake, Manitoba, at the east end of the Paleoproterozoic Flin Flon-Snow Lake greenstone belt within a tectonostratigraphic sequence known as the Snow Lake Arc (SLA) assemblage. At an estimated 27 Mt, (reserves plus resources) it is the largest deposit within the SLA assemblage. Eleven ore zones have been identified: 6 base metal-rich zones and 5 gold zones. During the summer of 2012, 150 drill core samples were selected from 7 ore zones (3 base metal zones and 4 gold zones) to better establish the mineralogical and trace element associations of the different ore types. Four main gold-rich ore types and metal associations have been identified: Type 1 massive sulfide (Au-Zn±Cu±Ag), Type 2 carbonate-chlorite-schist (Ag-Au±Pb±Zn), Type 3 semi-massive chalcopyrite (Au-Cu), and Type 4 low-sulfide ore (Au±Ag). Type 1 massive sulfide ore (average 7.5 ppm Au, 46.9 ppm Ag, 1.3% Cu, 8.5% Zn, 0.3% Pb, n= 34 samples) comprises mainly pyrite with interstitial sphalerite and minor calcite/dolomite. Chalcopyrite is present but discontinuous, and pyrrhotite occurs locally. Gahnite also occurs with sphalerite. Type 2 mineralization (14.8 ppm Au, 90.2 ppm Ag, 0.6% Cu, 2.2% Zn, 1.0% Pb, n=34) contains abundant disseminated galena and less common sphalerite in a chlorite and carbonate matrix; Cu-Fe sulfides are present locally but never the dominant sulfides. Type 3 semi-massive chalcopyrite ore (12.1 ppm Au, 37.4 ppm Ag, 2.8% Cu, 0.8% Zn, <0.01% Pb, n=27) occurs with quartz, biotite, and anthophyllite and commonly contains coarse garnet and staurolite. Type 1 mineralization is restricted to three upper lenses (#40, 10 and 20). Type 2 mineralization (#21 and 25 lenses) occurs at intermediate depths. Type 3 mineralization is found at the base of lens #27, which is the deepest known ore lens. Type 4 low-sulfide ore (19 ppm Au, 57.2 ppm Ag, 1.3% Cu, 0.6% Zn, 0.1% Pb, n=19) forms isolated zones within lenses #21, #25 and #27, in which gold occurs as rounded grains of electrum associated with tetrahedrite and galena. Intensive recrystallization and annealing is seen in all ore types. Polyphase deformation (F1 through F4) and amphibolite facies metamorphism have had a major impact on the ore-hosting assemblages. A goal of the present study is to determine the paragenesis of the precious metals in the different ore zones and, in particular, how hydrothermal alteration and metamorphism have influenced the distribution of gold in the deposit. (SS7; Wed. Poster)

Metamorphism in the Bending Lake area, western Wabigoon Subprovince, Ontario

Duguet, M., manuel.duguet@ontario.ca, and Beakhouse, G., Ontario Geological Survey, Earth Resources and Geoscience



Mapping Section, 933 Ramsey Lake Road, Sudbury, ON P3E 6B5

The Archean Bending Lake area in the western Wabigoon Subprovince displays dome-and-kneel structural pattern with the Revell Batholith being surrounded by supracrustal rocks and was affected by at least two metamorphic events.

For the M_1 metamorphic event, calculated metamorphic conditions by multiequilibrium thermobarometry (THERMOCALC v3.33 with the internally consistent thermodynamic database tcds55) on the south flank of the Revell batholith yielded temperatures between 595 and 650°C with pressure ranging from 5.7 to 7 kilobars. On the northern margin of the Revell batholith, a single garnet-staurolite-bearing metasedimentary sample yielded a temperature of 638°C and a pressure of 7.8 kilobars. These metamorphic conditions match those calculated for the 2734 Ma-old Revell batholith.

In order to reconstruct the P-T path of the M_1 metamorphism, isochemical sections (P-T diagram) were built on garnet-bearing rocks in the system MnNCKFMASHTi using the software Perple_X v6.6 and the internally consistent thermodynamic data set hp04ver translation for Perple_X of the database tcds55s. Garnet-core isopleths were plotted on the diagram and consistently crosscut each other at a high angle at 527°C and 5.2 kilobars very close to the garnet-in reaction. Compared with the multiequilibrium thermobarometry and considering the garnet zoning pattern, the investigated samples experienced a temperature increase of 130°C for a moderate pressure increase of 0.5 to 2 kilobars.

The M_2 event is characterised by much lower P-T (3 and 4.7 kilobars for temperature ranging from 400 to 600°C). Similar pressures were found within all the late-tectonic to post-tectonic (2695 to 2700 Ma) sanukitoid plutons indicating they were emplaced at higher crustal levels than the earlier plutons and that the associated uplift followed the onset of regional metamorphism. Similar timing of sanukitoid plutonism relative to regional metamorphism and uplift has been described from other portions of the Superior Province.

Some questions remain concerning the timing of this early M_1 event, its relationships with deformation and plutonism, its geodynamical context and its regional extent. In the Upper Manitou Lake area, 40 km to the west, a garnet-bearing metasedimentary rock sample yielded a pressure of 5.9 kilobars for a temperature of 509°C. Between the Bending Lake area and the Upper Manitou Lake area, the greenstone belt is mostly composed of mafic volcanic and plutonic rocks which were metamorphosed under greenschist-facies conditions. Such greenschist mineral assemblages are commonly thought to have developed under comparatively low-pressure conditions, but the results presented here suggest that this interpretation should be re-evaluated. (SS3; Fri. 8:20)

Structural geology of the Mazinaw Domain, Admaston-Horton area, northeastern Central Metasedimentary Belt, Grenville Province, Ontario

Duguet, M.¹, manuel.duguet@ontario.ca, Magnus, S.J.² and Ratcliffé, L.³, ¹Ontario Geological Survey, Earth Resources and Geoscience Mapping Section, 933 Ramsey Lake Road, Sudbury, ON P3E 6B5; ²Ottawa-Carleton Geoscience Centre, Department of Earth Sciences, Carleton University, Ottawa, ON K1S 5B6; ³1664 Bruce Rd. 9, Warton, ON N0H 2T0

The Mazinaw Domain in the Admaston-Horton area is composed of mafic volcanic plutonic rocks, siliciclastic and volcanoclastic rocks and calcite marbles belonging to the Grenville Supergroup. These units were intruded by several plutonic rock suites between 1229 and 1211 Ma. These older units were unconformably overlain by arenites, pelites and calc-silicates assigned to the Flinton Group. Maximum deposition age of the Flinton Group in this area is estimated at ca 1150 Ma (UPb on detrital zircons). All these supracrustal units were subsequently metamorphosed under upper amphibolite facies conditions during the Grenville Orogeny.

Early structural history in Mazinaw Domain is characterised by thrusting. This event was highly reworked by further tectonic events and its timing is still a matter of debate.

The Admaston-Horton area then underwent a major sinistral strike-slip deformational event that was responsible for the formation of shear zones associated with NE-trending upright to NW-verging folds in the area. This strike-slip event is coeval with the emplacement of pegmatitic syenite and syenogranite bodies. Further west, this sinistral strike-slip tectonic disappears and is replaced by top-to-the NW thrusting which is coeval with emplacement of syenite and syenogranite bodies. The fabric in these intrusive rocks was acquired at the supra-solidus stage when they were emplaced parallel to the main deformational fabric. The age of these synkinematic bodies is under investigation, but by comparison with other areas, is bracketed between 1080 and 1020 Ma. This switch in structural style also seems to mark the western boundary of the Mazinaw Domain. NE-trending structures such as fold axes and stretching and mineral lineations are absent in the western domain. Instead, the stretching lineation of the western domain is consistently plunging to the SE.

The Admaston-Horton area was also affected by another ductile deformation event that has not been previously noted. In the north part of the Mazinaw Domain, on a map scale, all of the NE-trending structures are consistently transposed into a NW-trend, and local NW-trending shear zones crosscut the earlier regional fabric. Within these shear zones, asymmetric boudinage of pegmatitic veins gives a dextral shear sense, consistent with the clockwise rotation of the structures on a map-scale view. These structures, likely Grenvillian in age, are perpendicular to the general trend of the domain. Such orthogonal structures are observed in younger orogens such as the Himalayas, where they have been recently described and discussed. (GS4; Fri. 9:40)

Geochemistry and sulfur isotope characteristics of mafic dikes and intrusions associated with the Eagle magmatic Ni-Cu-PGE deposit, Upper Michigan

Dunlop, M., mdunlop@umail.iu.edu, Ripley, E.M. and Li, C., Indiana University, 1001 E 10th Street, Bloomington, IN 47405 USA

The Baraga Basin in northern Michigan contains an Archean igneous basement overlain by Paleoproterozoic meta-sedimentary rocks that host a number of mafic intrusions and dikes, including the Eagle sulfide ore-bearing intrusion (1107.3 ± 3.7 Ma). The Eagle intrusion hosts a high grade Ni-Cu-PGE ore deposit, and is part of a belt of mafic intrusive bodies extending from northwest to southeast across the basin. This belt is bracketed to the north and south by similar-trending Cu-depleted mafic dikes. A large number of Cu-enriched mafic dikes (of the Baraga Dike Swarm) are present within the basin, and are oriented northeast-southwest. Also present is a series of Cr- and Ni-enriched mafic dikes which trend northwest-southeast.

The Boulderdash and Roland Lake intrusions show cumulate textures and have trace element and REE patterns very similar to that of Eagle. A comparison of Boulderdash and Roland Lake shows that the two intrusions have similar Pt/Pd and Pd/Ir ratios, but with Boulderdash being more depleted in all PGE. Additionally, Roland Lake appears to be related to a more primitive parental magma, crystallizing olivines ranging from Fo₇₅ to Fo₈₅, while olivines in the Boulderdash intrusion range from Fo₆₁ to Fo₆₉. Boulderdash also shows a small population of Fo₅₅ olivine crystals, suggesting a possible mixing of two different magmas.

PGE and trace element analyses show that the Cu-depleted dikes are strongly depleted in Ni, Au, and PGE relative to primitive mantle and strongly depleted in Cu relative to all other dikes and intrusions in the region. Furthermore, a plot of Th/Ta vs. La/Sm shows that the Cu-depleted dikes are very strongly contaminated with lithospheric material. This suggests that the Cu-depleted dikes experienced a sulfide saturation event triggered by contamination with sulfur from either the crust or subcontinental lithospheric mantle; a $\delta^{34}\text{S}$ value of 1‰ is non-unique and may indicate either crustal or mantle sulfur. By comparison, a plot of Th/Ta vs La/Sm for a dike located beneath the Eagle this intrusion indicates almost no contamination except at the dike margins. This fact suggests that contamination occurred more or



less *in situ*. Sulfide minerals sampled from the dike margin show a $\delta^{34}\text{S}$ of 11.7‰, a value that is consistent with contamination by the immediate country rocks. (*SS9; Wed. 9:20*)

50 million years of syenite magmatic evolution and related metasomatism along the Central Metasedimentary Belt Boundary thrust zone, western Grenville Orogen

Easton, R.M., Ontario Geological Survey, Earth Resources and Geoscience Mapping Section, B7064, 933 Ramsey Lake Road, Sudbury, ON P3E 6B5, mike.easton@ontario.ca

1:50 000 scale mapping, geochemical and geochronological studies in the Lake Clear area of Ontario have led to improved understanding of the origin of alkalic syenite, fenite and 'carbonatitic' rocks (~1090 to 1035 Ma) in the hanging wall of the Central Metasedimentary Boundary thrust zone (CMBBTz). Syenitic rocks in the western Grenville have been previously assigned to several lithodemic units, including the Nepheline Syenite, Kensington-Skootamatta and Fenite-Carbonatite suites. The results presented herein suggest that these suites may represent a continuum of syenitic magmatism spanning roughly 50 million-years, rather than discrete events.

From relative age relationships, there are at least 3 periods of syenite emplacement. 1) Older, igneous-textured ovoid syenite plutons (Burns Lake, Mt. St. Patrick) and newly-identified alkalic gabbro (Woermke, Highland) plutons and alkalic mafic dikes. The older syenites correspond to the Kensington-Skootamatta Suite, and were emplaced between 1088 and 1073 Ma (age of the Woermke gabbro). 2) During the medial period, linear-trending (90° or 20-45°) heterogeneous bodies of monzodiorite, syenite and nepheline-syenite (Wolfe, Eleanor plutons) were emplaced, with non-foid bearing intrusions being more common. Some correspond to the Nepheline Syenite Suite, but are much younger than previously suggested (~1050 Ma not ~1290 Ma). Their linear-shape suggests greater tectonic control on emplacement. Also, the medial intrusions are spatially restricted to 40 km of the CMBBTz, whereas the ovoid syenites occur throughout the Central Metasedimentary Belt. 3) The youngest magmatism produced a diverse package of rocks ('Fenite-Carbonatite' Suite). Syenites of this age are texturally and compositionally diverse on outcrop and regional scales, and associated with pyroxene- and/or calcite-bearing metasomatic rocks variously referred to as skarns, fenites and 'carbonatites'. Local differences in the younger syenites (km scale) may be related to host composition.

The origin of all the syenites is attributed to an influx of fluids and heat from 1090 and 1035 Ma resulting from upwelling of asthenospheric mantle due to crustal delamination. This resulted in an initial, voluminous, regional scale pulse of syenite and alkali basalt magmatism (1090-1070 Ma) forming discrete low U-Th, magnetic syenite plutons, alkalic gabbros and mafic dikes. Subsequently, reduced degrees of partial melting and increased tectonism led to emplacement of the medial syenites and foid-syenites (~1050 Ma, low U-Th, magnetic) along the CMBBTz. Finally, during the last gasp of magmatic activity, the fluid-rich late syenites (~1040 Ma) were emplaced which interacted extensively with their host rocks. This progression may reflect decreasing depth to the mantle source and increased interaction with the lower crust during the Ottawa stage of the Grenville orogeny. (*GS3; Thurs. 11:00*)

Paleoproterozoic rift-drift transition along the southern margin of the Superior craton: a renewed look at the tectonic record preserved by the Huronian Supergroup

Easton, R.M., Ontario Geological Survey, Earth Resources and Geoscience Mapping Section, B7064, 933 Ramsey Lake Road, Sudbury, ON P3E 6B5, mike.easton@ontario.ca

The Proterozoic history of the southern margin of the Superior craton in the upper Great Lakes region remains enigmatic, despite the fact that the oft-forgotten Huronian Supergroup contains a record of over 1.5 billion years of earth's history, from the end of the Archean to the final stages of the Grenville orogeny. Although individual tectonic elements have long been established, how they fit together in a coherent

evolutionary fashion remains unclear, and is the focus of this presentation.

From 2500 to 2220 Ma, the depositional history of the Huronian Sgp (and correlative strata in the Wyoming and Baltic cratons) preserves a tale of rift-drift transition remarkably similar to that preserved in the Paleoproterozoic Wopmay Orogen. Similarities include the presence of a well-defined plume centre with a radial dike swarm (Matachewan-Hearst), an early mafic magmatic pulse followed by bimodal magmatism, a potential failed arm (Wanapitei magnetic anomaly) and a transition from rift to shelf sedimentation. A key difference is the apparent absence of shelf-founding, which may indicate that a large ocean never developed to the south. The emplacement of Nipissing gabbro sills at 2220-2210 Ma can be interpreted as magmatic injection into a platform similar to the Wopmay example; alternatively, it could reflect an initial phase in the subsequent break-up of Superior-Baltica-Wyoming that culminated at 2120 Ma. Determining the amount of deformation and metamorphism in the Huronian Sgp related to Nipissing sill emplacement is key to understanding this period (2220-2120 Ma). The Marquette Range Sgp to the south may represent a second rift-drift transition, which did flounder, as indicated by deposition of the Animikie fore-deep succession. Both the Huronian and Marquette Range sgps were subsequently affected by the Penokean orogeny (~1835 Ma) related to collision with juvenile arc-terrains to the south, although the amount of Penokean deformation in the Huronian is uncertain. Coincident with Penokean orogenesis was the Sudbury meteorite impact (1850 Ma). Subsequent uplift of the Penokean served to drive K- and Na-rich basinal fluids north into the Huronian Sgp at ~1700 Ma. After Penokean collision, a series of arcs developed in succession along the southern flank of the craton, including the Killarney (Yavapai) (1740) belt and a 1450-1350 Andean-type arc now largely preserved within the Grenville Province. Renewed mafic magmatism occurred at 1240 Ma (Sudbury dike swarm) and 1140-1085 Ma (Midcontinent Rift). Northwest- migrating Grenville orogenesis from 1085 to 980 Ma had little direct effect on the Huronian Sgp, but may have utilized older structures, such as the Murray fault system. (*SY4; Fri. 1:40*)

Diagenetic controls on the petroleum reservoir quality of the middle unit of the Wymark Member (Upper Devonian Duperow Formation), southwestern Manitoba

Eggie, L.A. and Chow, N., University of Manitoba, Dept. of Geological Sciences, University of Manitoba, Winnipeg, MB R3T 2N2, lauren_eggie@hotmail.com

The Upper Devonian Duperow Formation is a widespread carbonate-evaporite succession present in the subsurface of the Williston Basin. The Duperow Formation formed in the Elk Point Basin during Frasnian time and represents the back-reef environment of a rimmed shelf in the southern part of the basin. In southwestern Manitoba, the formation is 122-195 m thick and thins eastward. The Duperow Formation in Manitoba is of economic interest, as it is a proven oil producer in Saskatchewan, North Dakota, and Montana; however, relatively little geologic work has been done on the formation in Manitoba. The middle unit of the Wymark Member (herein referred to as the middle Wymark Member) has been identified as the most prospective reservoir rock in the Duperow Formation on the basis of the good porosity and numerous oil shows in this unit. The middle Wymark Member is composed of subtidal, intertidal and supratidal lithofacies associations which are arranged into meter-scale, shallowing-upward cycles. The lithofacies associations are interpreted to have been deposited in an arid peritidal setting.

Potential reservoir units in the middle Wymark Member consist of packages of subtidal and intertidal lithofacies associations, up to 14 m thick, which are capped by nonporous evaporite lithofacies of the supratidal/sabkha lithofacies association, up to 3.5 m thick. The fossiliferous wackestone-packstone, stromatoporoid framestone, laminated mudstone, and dolostone lithofacies are characterized by 10-35% intercrystalline, interparticle, and microvuggy porosity, 0.1-210 mD permeability, and up to 19.6% oil saturation. Porosity in these



lithofacies was controlled primarily by marine and burial diagenesis. Marine diagenetic features include nonferroan radial-fibrous and radial-fibrous calcite cements which partially or completely fill primary interparticle porosity. Burial diagenetic features include intercrystalline and microvuggy porosity associated with pervasive dolomitization, as well as compacted and dissolved skeletal allochems. Dolomitization partially or pervasively affected all lithofacies and is interpreted to have formed due to evaporative pumping and seepage reflux associated with sabkha environments. Nonferroan blocky calcite, anhydrite and gypsum cements variably occlude intercrystalline and microvuggy porosity and reduce permeability in the reservoir units. Localized occurrences of dedolomite and intracrystalline porosity are tentatively attributed to late-stage meteoric diagenesis. (SS13; Fri. 10:40)

Visualising Precambrian plate motions and the timing of crustal response to geodynamic processes: An example from the Kalahari Craton, southern Africa

Eglinton, B.M.¹, bruce.eglinton@usask.ca, Pehrsson, S.J.² and Evans, D.³, ¹University of Saskatchewan, Saskatoon, SK S7N 5E2; ²Geological Survey of Canada, Ottawa, ON; ³Yale University, New Haven, NC, USA

Recent enhancements to Precambrian plate reconstructions utilising the Paleogis plug-in for ArcMap and GPlates software provide animated views of plate motion. Data (geochronology, ore deposits, dyke swarms), mostly derived from the DateView and StratDB databases, are superimposed on the moving plates to assess geodynamic models and investigate the age and setting of mineralisation.

Addition of polygon information for lithostratigraphic units, symbolised according to the classifications developed for the IGCP 509 project, provides additional insights into the timing and nature of the geodynamic processes. Models such as these are only possible where lithostratigraphic units are available as GIS polygons for which the geodynamic settings and environments of formation have been defined and linked to age. Such information is available for southern Africa.

The timing of collision of the Kaapvaal and Zimbabwe Cratons along the Limpopo Belt is contentious. One model has collision in the Archaean (~2.65 Ga) with subsequent trans-current reactivation in the Palaeoproterozoic (~2.02 Ga). The second has collision exclusively in the Palaeoproterozoic at ~2.02 Ga. A third model introduces substantial post-1.875 Ga transpression. The spatial distribution of lithologies, their geodynamic settings, and environments of deposition, all superimposed on continuous plate reconstructions, facilitates assessment of the different models. Several constraints appear to favor the second model in which collision of the Zimbabwe and Kaapvaal Cratons only occurred in the Palaeoproterozoic at about 2.02 Ga, although the Central Zone of the Limpopo Belt may have been part of one of the cratons much earlier. Major indicators that this was the case are:

- 1) the Zimbabwe Craton does not appear to have been a rigid, robust block prior to 2.63 Ga, thus is too young for supposed collision at ~2.65 Ga
- 2) close proximity of the collision zone to extensive Neoarchaean carbonate sediments of the lower Transvaal Supergroup and the absence of significant coeval molasse-type sediments is at odds with extensive exhumation of the Limpopo collision zone at ~2.65 Ga
- 3) the sub-linear and orogen-parallel distribution of coarse detrital Waterberg and Soutpansberg sediments just south of the Limpopo Belt is more consistent with collision at ~2.02 Ga

Substantial post-1.875 Ga transcurrent motion between the Kaapvaal and Zimbabwe Cratons, suggested by paleomagnetic data, appears inconsistent with ages of sedimentation and shearing, and instead may be due to rapid apparent (true?) polar wander.

Mineralisation in the region can be tied to the motions of the major plates. (SS11; Fri. 8:20)

Darrehzar porphyry copper deposit, southeast Iran: Fluid inclusion and stable isotope evidence for a hydrothermal system dominated by magmatic fluids

Einali, M.¹, M_Einali@sbu.ac.ir, Bakker, R.², bakker@unileoben.ac.at, and Alirezai, S.³, S-Alirezai@sbu.ac.ir, ¹Shahid Beheshti University, Evin, Tehran, Iran; ²Department of Applied Geosciences and Geophysics, University of Leoben, 8700 Leoben, Austria; ³Faculty of Earth Sciences, Shahid Beheshti University, PO Box 15875-4731, Tehran, Iran

The Darrehzar porphyry copper deposit (PCD) in the southern part of the Cenozoic Urumieh-Dokhtar magmatic belt, Iran, is associated with two shallow diorite and granodiorite intrusions. Alteration assemblages and mineralization typical of PCDs are developed in the intrusions and the volcanic host rocks. Four types of veinlets are distinguished: quartz-pyrite-chalcopyrite (Type-1); quartz-pyrite-molybdenite-chalcopyrite (Type-2); quartz-pyrite-chalcopyrite (Type-3); quartz-anhydrite-pyrite (Type-4).

Heating-freezing experiments were conducted on a Linkam MDS-600 stage in the Department of Applied Geosciences and Geophysics, Leoben University, Austria. O-H isotope analyses were performed in the Western Ontario University isotope laboratories.

Four types of fluid inclusions were identified on the basis of phases present at room temperatures: liquid-rich; vapor-rich; polyphase halite-bearing; and polyphase halite-sylvite bearing. Type-1 veinlets contain all four types of inclusions. The TH and salinities for the liquid-rich and vapor-rich inclusions vary between 220-260°C, 10-14, and 369-560°C, 8-17 mass% NaCl eq., respectively. The polyphase halite-bearing and sylvite-bearing inclusions homogenized by vapor disappearance at 275-425°C and 300-350°C, respectively; salinities vary between 35-42.5 and 27.6–43.8 mass% NaCl eq.; dissolution of sylvite occurred between 139-321°C.

Type-2 veinlets contain three types of inclusions. The TH and salinities for liquid-rich and vapor-rich inclusions vary between 176-304°C, 4.3-15, and 500-520°C, 6-8 mass% NaCl eq., respectively. The polyphase, halite-bearing inclusions homogenized by vapor disappearance at 325-400°C; salinities vary between 35-40 mass% NaCl eq.

Type-3 veinlets contain liquid-rich, vapor-rich, and polyphase, halite-bearing inclusions. The TH and salinities for the first two inclusion types vary between 147-156°C, 3.7-14.6, and 400-420°C, 4-6 mass% NaCl eq., respectively. The third inclusion type homogenized by vapor disappearance at 300-350°C; salinities vary between 32.5-42.5 mass% NaCl eq.

Type-4 veinlets contain liquid-rich, vapor-rich and polyphase halite-bearing inclusions. The TH and salinities for the first two inclusion types vary between 157-226°C, 5-10.6, and 400-440°C, 6-8 mass% NaCl eq., respectively. The third type homogenized by vapor disappearance at 375-425°C; salinities vary between 32.5-42.5 mass% NaCl eq.

The hydrothermal system evolved with separation of magmatic fluids from crystallizing magma at high temperatures (500-560°C) to produce potassic alteration. The fluid then separated into two immiscible phases including a low-salinity vapor, and a high-salinity brine (6-8 and 35-40 mass% NaCl equivalent, respectively) at temperatures 420- 450°C. The phyllic alteration formed by a hot (375-400°C), saline (32.5-42.5 mass% NaCl eq.) fluid. A cooler (150-220°C) and low-salinity (5-10 mass% NaCl eq.) fluid affected the porphyry system at final stages.

The $\delta^{18}\text{O}$ values for two hydrothermal biotite concentrates are 6.48 and 5.17 permil. Three sericite concentrates yielded $\delta^{18}\text{O}$ values between 7.70-8.20 permil and δD values between -72 to -77 permil. The $\delta\text{D}-\delta^{18}\text{O}$ values calculated for the fluids are consistent with a magmatic source. (SS23; Fri. 10:40)

**Field relationships, petrography and geochemistry of lamprophyre dykes from the Hoidas Lake area, Zemlak Domain, Saskatchewan**

Elliott, R.¹, rwe259@mail.usask.ca, Ansdell, K.M.¹, Harper, C.T.², Pandur, K.¹ and Pearson, J.G.³, ¹Department of Geological Sciences, University of Saskatchewan, Saskatoon, SK S7N 5E2; ²Harper Geological Consulting & Exploration, 2411 Cross Place Regina, SK S4S 4C8; ³Great Western Minerals Group Ltd., 219 Robin Crescent, Saskatoon, SK S7L 6M8

The Hoidas Lake area is located northeast of Uranium City, northern Saskatchewan, and is host to numerous LREE-enriched veins that cut amphibolite grade gneissic rocks of the Zemlak Domain, Rae Province. The mineralized veins are sub-parallel to the Nisikkatch-Hoidas Shear Zone, which is considered a splay off the northeast-trending regional Black Bay Fault. Several lamprophyre dykes occur in a kilometer-wide zone west of the main mineralized zones and extends for several kilometers along the same structural trend. The host rocks record multiple episodes of ductile deformation, whereas the lamprophyres only exhibit minimal late stage deformation. The lamprophyres were emplaced after the peak metamorphism at ca. 1910 – 1900 Ma, but appear to postdate mineralization. They are interpreted to be approximately the same age as the alkali basalts in the Martin Group, near Uranium City, which have been dated at ca. 1818 Ma.

Two distinct varieties of lamprophyre identified in the field were collected: 1) a light brown to pinky-brown weathered variety, and 2) a grey to grey-brown variety. Both types are porphyritic with the groundmass consisting mostly of alkali feldspars with phenocrysts ranging from 25 – 40% and dominated by biotite and/or phlogopite. Amphiboles are also present, although the grey variety has higher amphibole content. The mineral assemblage, and preliminary geochemical data are compatible with the minette class of calc-alkaline lamprophyres. Some dykes exhibit later alteration, with primary biotite replaced by chlorite, along with groundmass alteration to actinolite. A common secondary alteration is the development of hematite rims on magnetite grains, which have grown along cleavage planes of biotite, likely due to, and synchronous with, fluid movement related to late cross-cutting quartz-carbonate veinlets in the area.

The lamprophyres contain elevated barium, up to 4850 ppm, compared to other large ion lithophile elements. Ba enrichment is also observed in many of the mineralized veins and hyalophane-bearing pegmatites throughout the area. Barium enrichment is commonly associated with alkaline magmatism, which suggests that the lamprophyres are closely related to the events that led to the development of the REE mineralization. The melting of a metasomatized mantle lithosphere below this part of the Rae Province may have generated the lamprophyres, but also played a role in developing the carbonatitic/alkali magmatic-hydrothermal system with which the REE vein systems and hyalophane pegmatites may be linked. (SS6; Wed. Poster)

Chemical characterization of ilmenite suites from the Kimberley diamond mines, South Africa

Ene, V.-V. and Schulze, D.J., Department of Earth Sciences, University of Toronto, Mississauga, ON L5L 1C6

We have undertaken an electron microprobe study of ilmenites from Kimberley, South Africa, to understand better the mantle sources of ilmenite xenocrysts that are key indicator minerals in kimberlite exploration. Among mantle xenoliths from Kimberley mines, ilmenite occurs in the following rock types: MARID (Mica–Amphibole–Rutile–Ilmenite–Diopside), metasomatised peridotites, Granny Smith glimmerites (cpx–phlogopite–ilmenite), rutile–ilmenite rocks, dunites (olivine–ilmenite) and phlogopite orthopyroxenites. Using major and minor elements we have created a preliminary classification scheme for Kimberley ilmenites.

Our data only allow distinction between three broad suites: MARID/metasomatised peridotite, Granny Smith/dunite/rutile and orthopyroxenites. MARID and metasomatised peridotite ilmenites have the lowest MgO (5.3–8.1 wt%) and Al₂O₃ (<0.05 wt%) and highest Fe₂O₃ (6.6–23.4 wt%) values and those from the Granny

Smith/dunite/rutile suite have the highest MgO, in the narrow range (13.0–14.9 wt%), with Al₂O₃ in the range 0.2–0.6 wt% and lowest Fe₂O₃ (4.9–6.7 wt%). Ilmenites from orthopyroxenites mostly have intermediate MgO, Al₂O₃ and Fe₂O₃ contents (10.8–10.9 wt%, 0.1–0.4 wt% and 9.8–10.4 wt%, respectively). The range of Nb₂O₅ contents of the Granny Smith/dunite/rutile ilmenites is very restricted (0.07–0.14 wt%) whereas those of MARID/peridotite and orthopyroxenites are in a much wider range (0.03–1.44 wt% Nb₂O₅). The three suites can be distinguished on the basis of plots of MgO vs. Cr₂O₃, Al₂O₃ vs. Nb₂O₅ and FeO vs. Fe₂O₃ (calculated from stoichiometry).

We have applied these distinctions to a suite of ilmenite xenocrysts from the Wesselton Mine in Kimberley. We can tentatively classify their source rocks as 83% from the Granny Smith/dunite/rutile cluster, 15% from the MARID/metasomatic peridotites and 2% from phlogopite orthopyroxenites. Subdivision of the Granny Smith/rutile/dunite suite will require additional geochemical data. (SS4; Fri. 11:00)

Gold enrichment in the auriferous Photo Lake deposit, Snow Lake, Manitoba

Engelbert, M.S., Gibson, H.L. and Lafrance, B., Mineral Exploration Research Centre, Department of Earth Sciences, Laurentian University, Sudbury, ON P3E 2C6, mengelbert@laurentian.ca

Volcanogenic massive sulfide (VMS) deposits are traditionally mined for base metals (e.g. Cu, Zn, Pb) and precious metals are byproducts; however, some VMS deposits are also a significant Au resource. The Photo Lake deposit at Snow Lake, Manitoba, is a Cu–Zn–Au–Ag VMS deposit that occurs within the Chisel sequence of the Snow Lake arc assemblage of the Paleoproterozoic Trans-Hudson Orogen. With an average Au grade of 4.9 g/t, which is significantly higher than other VMS deposits in the Chisel sequence (Chisel, Chisel North, Lost and Ghost deposits; average gold grades of 0.4 to 1.8 g/t), it is classified as an auriferous VMS deposit. While all of the other VMS deposits within the Chisel sequence occur approximately 2 km above the base of the sequence at the contact between the Lower and Upper sequences, the Photo Lake deposit occurs within a thick section of rhyolite in the Upper Chisel sequence. The Photo Lake deposit may be a product of a younger VMS-forming event, or the deposit and host rhyolite may represent a thrust fault repetition of the underlying Chisel sequence. Field mapping in 2012 indicates that the deposit occurs within an isoclinally folded rhyolite flow complex rather than within a homoclinal rhyolitic succession. This is significant as the Photo Lake horizon may represent a relatively unexplored productive VMS interval. As such, an understanding of the processes responsible for Au enrichment at Photo Lake is critical for further exploration in the area.

We will use trace element geochemistry in conjunction with petrography, SEM and LA-ICP-MS to constrain the processes responsible for Au enrichment in the Photo Lake deposit. Primary base metal zonation at Photo Lake has been overprinted by remobilization of metals during deformation associated with peak, middle almandine–amphibolite facies, regional metamorphism. Gold grades exhibit a strong positive correlation with Cu, indicating that Cu and Au may have been deposited and/or remobilized together. Significant Au mineralization also occurs in quartz–carbonate–albite veins that contain acicular epidote, chalcocite and up to 25% galena. The association of quartz–carbonate veins with Au, chalcocite and galena, and the association of Au with Cu-rich massive sulfide intervals has also been recognized at the Au-rich Lalor deposit, which is located at the contact between the Lower and Upper Chisel sequences. (SS7; Wed. 2:00)

Required steps and recurring challenges in the dual hydrological and geological classification of Prairie watersheds

English, C.B. and Ali, G., University of Manitoba, Department of Geological Sciences, Winnipeg, MB R3T 2N2, umengli8@cc.umanitoba.ca

Assessing similarities and dissimilarities in watershed-scale runoff is a critical step towards process understanding and water resources



management in any region. This is particularly true in prairie landscapes where runoff generation and routing are often controlled by sheet flow on frozen ground, water losses in high infiltration capacity soils, slough and wetland connectivity, and enhanced drainage via man-made structures. Strong regional differences in runoff generation processes and flow statistics exist in the prairies and are thought to be influenced by different geological settings; however, it is unclear how established geology-driven classifications of prairie landscapes could be used as proxies for watershed hydrological regimes. We explored that question using a dataset of more than five hundred watersheds spreading across southern Manitoba, as well as draining creeks, streams, and rivers downstream of Lake Winnipeg. The study region is a heterogeneous landscape with various types of bedrock geology and surficial deposits, near-level agricultural fields, topographic escarpments, hummocky terrain and potholes which are likely to be associated with very different runoff generation processes. Flow statistics were first derived to illustrate the hydrological regime and runoff dynamics prevailing at the outlet of each watershed. Stepwise multiple regressions were then used to explore the relationships between those flow statistics and the relative proportions of bedrock geology types (*e.g.*, sedimentary, metamorphic, *etc.*) and surficial deposits types (*e.g.*, alluvium, colluvium, till) present in each watershed. Non-parametric tests were also run to evaluate whether different geological formations were associated with different hydrological regimes. Results show that variables such as the proportion of a watershed underlain by till veneer are critical for the prediction of high-flow conditions. In contrast, there were few significant correlations between low-flow statistics and the relative proportions of bedrock geology types and surficial deposit types. Geological formations alone could not explain the spatial variability in hydrological regimes unless they were coupled with surface drainage characteristics. Therefore, this work therefore suggests that specific combinations of surficial geology and surface drainage characteristics can be useful towards a better understanding and prediction of prairie watershed hydrological regimes. (SS14; Thurs. 1:40)

Linking porphyry deposit geology to geophysics via physical properties: Six porphyry deposits in British Columbia, Canada

Enkin, R.J., Geological Survey of Canada, PO Box 6000, Sidney, BC V8L 4B2, renkin@nrcan.gc.ca, and Mitchinson, D.E., 409 Granville Street, Vancouver, BC V6C 1T2, diannem@mirageosscience.com

(Withdrawn)

The structure and crystal chemistry of dumortierite II. Structure and topology of the dumortierite supergroup and dumortierite-like materials

Evans, R.J., rjamesevans@gmail.com, and Groat, L.A., Department of Earth, Ocean and Atmospheric Sciences, University of British Columbia, 2020-2207 Main Mall, Vancouver, BC V6T 1Z4

Dumortierite, $c. (Al, \square)Al_6BSi_3O_{16}(OH)_2$, has a strongly pseudo-hexagonal orthorhombic structure based on two kinds of rod-like double-chains of Al octahedra in a framework based on the {6·4·3·4} semiregular planar tiling. The large hexagonal channels contain chains of face-sharing Al octahedra (containing the Al1 site) attached to the framework by rings of SiO_4 tetrahedra. Smaller triangular channels contain planar BO_3 groups.

In addition to the minerals of the dumortierite supergroup, the minerals ellenbergerite, $c. (Mg, Ti, Zr, \square)Mg_3(Al, Mg)_3(Si, P)_4O_{14}(OH)_5$, phosphoellenbergerite, $c. (Mg, Fe, \square)Mg_6(PO_4, PO_3OH, AsO_4)_3(PO_3OH, CO_3)(OH)_3$, and ekatite, $c. (Fe^{3+}, Fe^{2+}, Zn)_6(AsO_3)_3(AsO_3, SiO_3OH)(OH)_3$, as well as a number of synthetic materials, possess a hexagonal structure similar to the dumortierite structure with a framework constructed of only one kind rod-like double-chains of octahedra. Many of these materials, like ellenbergerite, possess tetrahedral or triangular-pyramidal groups in

their triangular channels instead of planar groups. We group these hexagonal materials together with the minerals of the dumortierite supergroup as dumortierite-like materials. These materials can be described with a formula containing both chemical and structure-topological information called a structure generating function.

The underlying planar tiling and assemblage of the structures' rod-like components place constraints on the unit cell parameters and possible variations of the structure. By examining components of the structure of dumortierite-like materials, decomposed in different ways, we can compare chemically very different materials and identify similarities with other structure types. (SY1; Thurs. 2:40)

Metamorphism and the formation of ruby and pink sapphire deposits in SW Greenland

Fagan, A.J., afagan@eos.ubc.ca, and Groat, L.A., groat@mail.ubc.ca, University of British Columbia, Vancouver, BC

Historical studies of gem corundum (ruby and sapphire) deposits have been sporadic and have concentrated on the 'classic' producing areas (Burma, India, Sri Lanka *etc.*). This new study highlights the Greenland gemstone district, and the possibility that this could become a major supplier of gem-grade ruby and pink sapphire.

On Greenland, the host rocks for the gemstones are a highly metamorphosed layered mafic intrusion. We believe the crystals to be metamorphic/metasomatic in origin; and delineating the fluid composition, temperature/pressure of formation, isotopic composition will be the key to unravelling how this style of gem deposit is formed.

For this preliminary study a total of 40 ruby or pink sapphire crystals from the Greenland deposits were analyzed for their oxygen isotopic composition using whole crystal laser fluorination and major/trace element composition using electron microprobe. Results show there are geochemical differences between the ten different deposits analysed in this study. This may represent changes in the metamorphic grade across the 10 km area, or may represent changes in the crystallizing fluids over time. Since the gems are hosted in a phlogopite-corundum matrix (90% phlogopite), we surmise that this represents the physical form of the last metamorphic/metasomatic fluids that were generated during the last regional metamorphic event. The ruby deposits themselves show distinct structural affinities and all lie in the same series of low-strain zones (fold nose, parasitic folds) along regional fold structures. These fluid conduits most likely represent the place where the geochemistry, structure and metamorphism allowed the formation of gem-grade corundum crystals. (SS10; Thurs. 11:00)

Regional metallogeny patterns as revealed by the distribution of heavy minerals in stream sediments from the Mackenzie Mountains, NWT

Falck, H.¹, hendrik_falck@gov.nt.ca, Day, S.², Pierce, K.¹, Ootes, L.¹ and Watson, D.¹, ¹Northwest Territories Geoscience Office, Yellowknife, NT; ²Geological Survey of Canada, Ottawa, ON

Regional stream sediment surveys have been carried out over much of the Canadian Cordillera using the National Geochemical Reconnaissance (NGR) methodology. Traditionally, these government-run surveys have collected a grab sample of silt-sized stream sediment, and a corresponding water sample, at a target sample density of one sample per 13 km². With the increased interest in diamonds, the collection of coarser-grained and volumetrically-larger samples for heavy indicator minerals has been incorporated into the NGR sample suite. Heavy mineral concentrate (HMC) samples are picked for kimberlite indicator mineral (KIM) grains, magmatic massive sulphide indicator minerals, and gold grains. A one hundred grain count is also carried out on each sample and KIM and low chrome-diopside grains are electron microprobed to obtain their chemistry.

Since 2003, a silt, water and bulk stream sediment survey has been conducted throughout the Mackenzie Mountains by the Northwest Territories Geoscience Office and the Geological Survey of Canada, collecting material and observations from over 9000 sites including nearly 1300 HMC samples. Field observations and concentrate data



were compiled from annual status reports. The results derived from heavy mineral picking and chemical data are interpreted in this poster by comparing the elemental and mineralogical data with the established regional metallogeny.

The results have been examined for mineral deposit types commonly found in other parts of the Mackenzie Mountains including: redbed-associated Cu; carbonate-hosted Zn-Pb (Irish-type, minor Mississippi Valley-type); intrusion-related base metal and tungsten skarns; and, shale-hosted SEDEX Zn-Pb. Many showings within the survey area have been previously found or recognized on the basis of anomalous silt and water chemistry, but several styles of mineralization known to be present in the area (e.g. carbonate-hosted Zn-Pb) show up poorly in the silt chemistry data. However, this latter group of showings can be recognized using the bulk sampling results. Intriguing results include anomalous samples containing suites of minerals including gold and sapphire grains that are inconsistent with the known showing types, suggesting that further exploration for different mineralization styles is required in this area. (*SS12; Thurs. Poster*)

Fingerprinting turquoise and tourmaline using isotopic techniques

Fayek, M. and Hawthorne, F.C., Univ. of Manitoba, Dept. Geological Sciences, Winnipeg, MB R3T 2N2, fayek@cc.umanitoba.ca

Prices of gemstones vary by several orders of magnitude depending on their quality, color, clarity and provenance, and effective provenance tools are becoming more and more important in modern Gemology. Here, we present a summary of some isotopic SIMS techniques recently developed by Hawthorne, Fayek, and their students and collaborators that can be used to identify the provenance of gem materials such as turquoise and tourmaline.

Former Ph.D. student Sharon K. Hull and Research Associate Yassir Abdu, together with Fayek and Hawthorne, have developed a relatively non-destructive technique for sourcing turquoise that uses the *in-situ* micro-analytical capabilities of SIMS to analyze the isotope ratios of hydrogen ($^2\text{H}/^1\text{H}$) and copper ($^{65}\text{Cu}/^{63}\text{Cu}$) in turquoise. SIMS is capable of accurate (i.e., ‰ to sub-‰), *in-situ* isotopic measurement on solid samples as small as 50 micrometers. This small sample size and *in-situ* nature of the technique is particularly advantageous for analyzing rare or valuable archaeological artifacts as it produces little or no discernible perturbation to the artifact. Moreover, for turquoise, it allows us to avoid inclusions and altered spots which can cause scatter in the data (this is common where bulk analytical techniques are used on powdered samples). Over 20 mines in six historic and prehistoric mining districts throughout the southwestern US were characterized, and provenance plays an important role in tracing trade routes throughout the region.

Cu-bearing elbaite from Paraíba (Brazil) is a highly-prized gem fetching up to \$20,000 per ct. Gemstones of similar quality from Mozambique and Nigeria are now on the market, and reliable provenance tools are required to distinguish Paraíba tourmaline from blue varieties of Cu-bearing tourmaline from Africa. Research by undergraduate student Brandi Shabaga, supervised by Fayek and Hawthorne, and in collaboration with T. Ludwig and P.A.E. Pogge von Strandmann (Institute of Earth Sciences, Heidelberg University) and H.R. Marschall (Department of Earth Sciences, University of Bristol; now at the Department of Geology & Geophysics, Woods Hole Oceanographic Institution) have developed Li and B isotopic techniques that can fingerprint Cu-bearing elbaite from all three localities. This work has shown the suitability of these isotope systems as a provenance tool for gem tourmaline. Isotopic profiles across chemically zoned grains revealed homogenous B and Li isotopic compositions, illustrating their major advantage as a provenance tool over major-, minor- or trace-element signatures that often show extremely strong spatial zoning. Li and B isotopes of all investigated samples of Cu-bearing elbaite from the three localities have Li and B isotopic compositions within the ranges previously found for tourmaline from granitic pegmatites. (*SY1; Thurs. 10:40*)

The Lac Bachelor gold deposit (Abitibi, Québec)

Fayol, N., noemiefayol@gmail.com, and Jébrak, M., Département des sciences de la Terre et de l'Atmosphère - Université du Québec à Montréal (UQAM), CP 8888 Suc Centre-ville, Montréal, QC H3C 3P8

The Lac Bachelor gold deposit (Métanor Resources Inc.) is located along the Desmaraisville basin, in the Abitibi Greenstone Belt about 120 km WSW of Chapais. It is characterized by a volcano-sedimentary assemblage, mafic and felsic intrusions, and regional NE-SW faults. The Auger and Lac Bachelor sedimentary sequences respectively occur SE of the Coniagas mine and NW of the Bachelor mine. The Lac Bachelor sedimentary rocks belong to the Haïry Formation dated at 2692 ± 3 Ma in the Chapais region which represents the northern Abitibi equivalent of the Timiskaming sequences.

The gold mineralisation is located on the margin of the O'Brien stock which intrudes a volcanic sequence, mainly composed of andesite and tuff. The O'Brien is a quartz-syenite intrusion. This alkaline intrusion is polyphased and display two main textures, porphyritic and equigranular. Injections of aplitic dykes represent late events. The O'Brien stock is mainly composed of sodic and potassic feldspars, quartz and mafic minerals. Purple fluorite is present both disseminated in the syenite and in quartz-fluorite-pyrite veins that appears as comagmatic.

The Lac Bachelor gold deposit is characterized by several mineralized zones among which the Main zone (ZP) and the B zone (ZB) are the most economically important. A porphyry-type mineralisation is also observed in the stock with quartz, quartz-magnetite, quartz-fluorite, and pyrite stockwork. Subhorizontal quartz-fluorite veins extend into the host rocks proximal to the stock. The Main and B zones are mainly localized at the edges of the pluton, in the tuff, and follow pre-existing discontinuities. Both the ZP and the ZB are striking 110° to the north, however, as the ZP is plunging 55° to the south west, the ZB is subvertical. Gold occurs in association with disseminated pyrite. The other metallic minerals are magnetite, hematite and rare chalcopyrite. In the ZP and lesser in the ZB, the magnetite is oxidized into hematite. Therefore, gold is present in highly altered (hematite, carbonates) zones associated with disseminated pyrite. Free gold is rare. The ZB seems to be less hematized than the ZP, which is consistent with the timing. Indeed, structural relations between these zones suggest that the ZB was in place first and the ZP occurred after. The B zone is dominated by the magnetite event.

The hydrothermal event is clearly related to the intrusion of the O'Brien syenite. However fluids appear to have followed pre-existing discontinuities that focused the mineralization. Results illustrate the complementary role of magmatic and structural controls during the mineralization processes. (*SS23; Fri. 3:40*)

A review of experimental data of diamond dissolution with the focus on morphological features

Fedortchouk, Y.¹, yana@dal.ca, Skvortsova, V.L.² and Zhang, Z.¹, ¹Dalhousie University, 1459 Oxford Street, PO Box 15000, Halifax, NS B3H 4R2; ²Moscow State University, Lenin Hills, GSP-1, Moscow, Russia, 119991

Diamonds originate in the depths of the Earth's mantle, reside in different lithologies of subcratonic lithospheric mantle, and transported to the Earth's surface by the deep-seated magmas, kimberlite and lamproites. Fluids play a major role in the formation and preservation of diamond and in mantle metasomatism leading to kimberlite magmatism. Experiments show that diamond resorption morphology is sensitive to the composition and conditions of the oxidizing fluids and can help to examine volatiles in the subcratonic mantle and in kimberlite magmas. The diversity of resorption features on natural diamonds provides a wealth of information on the fluid environment in the mantle and in the ascending kimberlite. However, the existing experimental data while extensive is still random and allows different interpretations of the effect of individual parameters on the resorption morphology and origin of specific resorption features on natural diamonds. This work is an attempt to compile experimental data on



diamond dissolution in order to identify the effects of different parameters and to determine the conditions of diamond resorption in nature.

We consider three possible environments of diamond resorption: mantle (5-7 GPa), kimberlite ascent (1-3 GPa), and kimberlite pipe emplacement (0.1 MPa). The two criteria for selecting experimental data are: (1) clear description of the experimental conditions and the composition of the run start mixtures and products; and (2) detailed data on the resorption morphology. The selected studies examine diamond resorption in fluid-bearing systems (H_2O , CO_2 , $\text{CO}_2\text{-CO}$, CO-CH_4 , $\text{H}_2\text{O-Cl}$), in "dry" and volatile-bearing silicate, carbonate, and hydroxides melts, natural compositions (kimberlites, lamproites, alkali basalt), and in the presence of metal ions in a large range of temperatures and oxygen fugacity. The summary of diamond morphological changes shows tendency for development of tetrahedral forms with ditrigonal {111} faces in H_2O -bearing systems, and dodecahedron forms with trigonal {111} faces in CO_2 -bearing systems. Morphology of trigonal and square etch pits developed respectively in [111] and [100] directions also shows dependence on volatiles where flat-bottom trigons and point-bottom squares form in H_2O -bearing systems, and are opposite in CO_2 -systems. We further examine the presence and orientation of the striation on resorbed octahedra, presence of circular pits (in H_2O -fluid below 1 GPa), and accompanying development of surface graphitization. Our results show the prevailing effect of volatile composition over the intensive variables (temperature, f_{O_2} , pressure) while the development of certain resorption features only within limited range of conditions makes it possible to examine crystallization conditions of kimberlite magma. (SS4; Fri. Poster)

Mobilization and precipitation of HFSE in the T-Zone, Thor Lake rare-element deposit: Insights from mass balance calculations

Feng, Y., fengl@uwindsor.ca, and Samson, I.M.,
ims@uwindsor.ca, University of Windsor, Windsor, ON N9B 3P4

Although high field strength elements (HFSE) have been long considered to be immobile in most geologic environments, there is now a substantial body of evidence showing that HFSE can be mobilized in hydrothermal systems. The Thor Lake rare-element (Y-REE-Nb-Ta-Zr-Be) deposit, NWT, Canada, is a world-class peralkaline pluton-related HFSE mineral deposit and consists of two main mineralized zones; the Nechalacho deposit and the T-Zone. The T-Zone is a zoned pegmatite with a strong hydrothermal overprint that provides an excellent opportunity to investigate HFSE mobility during hydrothermal alteration. The granite that hosts the T-Zone sequentially underwent biotite-chlorite alteration, fluorite alteration, and then silicification. The earliest alteration recognized in the T-Zone pegmatite is silicification of feldspar, aegirine, and an unknown prismatic pegmatitic phase that was accompanied by the precipitation of Fe and Ti oxides and HFSE-bearing minerals. A quartz-oxide unit represents the most intense expression of this alteration. This assemblage was subsequently overprinted by polythionite alteration (Li metasomatism) and then by phenakite alteration (Be metasomatism). Component ratio diagrams and ISOCON analysis reveal that HFSE were remobilized and geochemical twins (e.g., Zr-Hf, Nb-Ta and Ho-Y) were decoupled to different extents during the various stages of hydrothermal alteration. The common occurrence of pseudomorphs suggests that there was minimal volume change during alteration. Development of the quartz-oxide unit (relative to least altered pegmatite) was accompanied by significant loss of LREE, Al, Na, and K, and addition of Fe, Mg, Ca, Ti, Nb, Ta, Zr, Hf and HREE. During polythionite alteration of the quartz-oxide unit, addition of LREE, Li, Al, and K was accompanied by removal of Ti, Nb, Ta, Zr, Hf, HREE, Fe, and Ca. Phenakite alteration subsequently resulted in addition of Al, Ca, K, Be, and HREE, and removal of Li, Nb, Ta, Zr, Hf and LREE, with conservation of SiO_2 . LREE and HREE appear to have behaved differently in the various alteration events (addition vs depletion). Enrichment of Ti, Nb, Ta, Zr, Hf and HREE was

accompanied by addition of Fe and Mg. Similar changes have been observed in the Nechalacho deposit at Thor Lake, where secondary HFSE assemblages are associated with a mafic alteration assemblages (mainly biotite, magnetite and hematite). (SS6; Wed. Poster)

Character of mineralizing fluids in the T-Zone, Thor Lake rare-element deposit: Implications for HFSE mobility and mineralization

Feng, Y., fengl@uwindsor.ca, and Samson, I.M., University of Windsor, 401 Sunset Avenue, Windsor, ON N9B 3P4,
ims@uwindsor.ca

The world-class Thor Lake rare-element deposit is hosted by the Blatchford Lake Complex, Northwest Territories, Canada. The T-Zone at Thor Lake is a zoned pegmatite comprising, from rim to core, a Wall Zone, Lower Intermediate Zone (LIZ), Upper Intermediate Zone (UIZ), and Quartz Core Zone, and has been subjected to a strong hydrothermal overprint. The principal high field strength element (HFSE) minerals, comprising bastnäsite-group minerals (bastnäsite, synchysite, parisite), zircon, columbite, xenotime, thorite and phenakite, are mostly present in pseudomorphs in massive quartz in the UIZ and Quartz Core Zone, and are considered hydrothermal. Many pseudomorphs are defined by the presence of primary fluid inclusions within and at the boundary of the pseudomorphs. Primary (P) and pseudosecondary (PS) fluid inclusions also occur in growth zones in quartz enclosing the pseudomorphs, and elongate inclusions in bastnäsite lying parallel to the c-axis of the host are also likely primary. The P and PS inclusions are dominated by liquid-rich, liquid-vapor (LV) inclusions or liquid-vapor-solid (LVS) inclusions. Most solids are trapped solids: they have inconsistent phase ratios, do not dissolve during heating, and have been identified using Raman spectroscopy to be the same as solid phases in the host pseudomorphs, namely zircon, rutile, and anatase. Raman spectroscopy also reveals that the LV±S inclusions contain minor CO_2 , and in some inclusions, CH_4 . Microthermometric measurements show that two fluids were involved in alteration and HFSE-mineral formation: one characterized by moderate salinity (~20 to 25 wt% NaCl eq.) and low homogenization temperature (~100 to 150°C) and the other by lower salinity (~5 to 10 wt% NaCl eq.) and higher homogenization temperature (~250 to 300 °C). SEM-EDS analysis of decrepitated of the primary inclusions show that in both fluid types, the principal dissolved components are Na and Cl, but that S and REE are present in minor to trace amounts. Fluorine and Ca, which are commonly considered to be important for the transport and precipitation of HFSE, respectively, were generally not detected, and only were present in trace amounts in a small number of decrepitated. Thus, chloride is likely to have been the predominant complexing agent for HFSE in the hydrothermal fluids in the T Zone at Thor Lake, and a model for precipitation that involved mixing with Ca-rich fluids are unlikely to have been important for the assemblages studied. (SS6; Wed. 2:00)

Map 601 the first surficial geology map of Alberta: Creation and content

Fenton, M.M., Waters, E.J., Pawley, S.M., Atkinson, N., Utting, D.J. and McKay, K., Alberta Geological Survey, Alberta Energy Resources Conservation Board, 4th Floor, Twin Atria Building, 4999-94 Avenue, Edmonton, AB T6B 2X3

This map portrays a generalized compilation of the surficial geology of Alberta (1:1 000 000 scale) using published Alberta Geological Survey, Geological Survey of Canada and Environment Canada maps, university theses, as well as new data. Data sources comprise 63 preexisting maps (scales 1:50 000 to 1:500 000; earliest 1960) along with project specific mapping of the few unmapped areas (1:500,000 to 1:1 000 000 scale). All were incorporated into a seamless provincial mosaic. Map boundary discrepancies were largely resolved during the reclassification process, with only limited remapping. The mosaic was then generalized using Geoscaler software. The resulting surficial geology layer was overlaid on a hill-shaded Shuttle Radar Topographic



Mission digital elevation model. This map is available at http://www.ags.gov.ab.ca/in_raster/pdf_and_digital_form.

The Surficial Geology Map of Alberta indicates the sediment types to be expected in the upper few metres. The relative abundance of the map units is: moraine undifferentiated (24%), moraine fluted (7%), moraine stagnant ice (19%), moraine glacially thrust (2%), glaciolacustrine (18%), organic deposits (10%), colluvial (5%), fluvial (4%), glaciofluvial (4%), eolian (3%), bedrock (3%), lacustrine (1%), preglacial fluvial (0.1%).

Moraine is widespread across uplands in northern Alberta and benchlands that parallel the Rocky Mountain and Foothills. Stagnant ice moraine is extensive in north-central Alberta and uplands within the Alberta Plains. Fluted moraine is present in low-relief corridors extending south between Edmonton and Calgary to the east and west of Red Deer, and southeast from Lac La Biche. Thrust or glaciotectionic moraine is locally present, the Neutral Hills for example.

Late Pleistocene glaciolacustrine deposits are the most widespread surficial geological unit associated with the retreating glaciers. They extend distally along the axes of a number of major river valleys in the province and fill basins in the southern half of Alberta. Glaciofluvial deposits represent a minor late Pleistocene unit. They form linear or irregularly shaped bodies, along meltwater channels, and extensive deposits occur around Muskeg Mountain, south of Lake Athabasca.

Eolian deposits, late Pleistocene to Holocene, are generally situated adjacent to glaciofluvial units, and to modern fluvial terraces and flood plains. Colluvium, Holocene, is significant on the slopes of the Rocky Mountains and Foothills, the Swan Hills, and the Birch and Caribou mountains, and along major valley systems. Lacustrine deposits are rare. Preglacial fluvial deposits (Paleogene to Neogene) form gravel-capped uplands including Cypress Hills, Hand Hills, Swan Hills and the Pelican Mountains. (GS6; Wed. Poster)

Mining Movie Making Youth Camp

Ferris, K.K., Noront Resources Ltd., 110 Yonge Street, Suite 400, Toronto, ON M5C 1T4, kaitlyn.ferris@norontresources.com

Noront Resources is a junior mining company with a deposit located in the Ring of Fire in the James Bay Lowlands of Northern Ontario. Noront is currently focused on the development of their Eagle's Nest nickel/copper Project that is located on the traditional territory of three First Nation communities.

Noront has an active Community Outreach program that is focused on working to support and create new and innovative ways to spark and capture community member interest specifically focused on the youth in geology, mining and earth science as a potential future career path.

Noront created the "Mining Movie Making Youth Camp" concept, a 3 day in community high school aged youth camp to help facilitate the youth to create their own submissions for the Ontario Mining Association's So You Think You Know Mining Video competition while introducing them to:

- mining education,
- geological education,
- film education,
- arts education.

A partnership was established between the OMA, Noront, Engage Learn, and DAREarts to bring camps to Webequie First Nation, Marten Falls First Nation and Long Lake #58 First Nation, all of which are communities that are surrounded by the Ring of Fire exploration and development.

During each 3 day camp the youth created, filmed and edited their own 2-3 minute video submission profiling what mining and geology mean to them and their community. The youth were asked to create their own interpretations of the benefits of mining based on their traditions and the knowledge from community members and Elders. At the end of each camp the youth were asked if they had new interests in geology and mining:

- Webequie – over 35% had a new interest,

- Marten Falls First Nation – over 55% had a new interest,
- Long Lake #58 – around 50% had a new interest.

The camp's success was based around the ability to draw in youth who were interested in the film and arts portion of camp and give them an introduction to geology, mining and earth science. The camp has the ability to reach a demographic that would not participate and sign up in a typical mining workshop.

This program exemplifies how important it is to find new and innovative ways to expose youth to the exciting career paths of geological and earth science. (SS22; Thurs. 1:40)

Adakite volcanism in Canada: Petrological and geochemical constraints on the origin of the Garibaldi Volcanic Complex, southwestern British Columbia, Canada

Fillmore, J.A., fillmorj@uregina.ca, Coulson, I., Solid Earth Studies Laboratory, Department of Geology, University of Regina, Regina, SK S4S 0A2

The Garibaldi Volcanic Complex (GVC) is located in southwestern British Columbia, Canada. It comprises two volcanic fields: the Garibaldi Lake Volcanic Field (GLVF) in the north and the Mount Garibaldi Volcanic Field (MGVF) in the south. Petrographical and geochemical studies on volcanic rocks collected from the GVC have determined that they exhibit adakitic characteristics; these intermediate rocks range from andesite to dacite represented mainly by lava flows and domes, and minor pyroclastic material. All examined samples are porphyritic, with approximately 10 to 20 % phenocrysts of plagioclase, hornblende and augite. The lavas from all the investigated volcanoes exhibit evidence of magma mixing, which include sieve textured crystals, dehydration reaction textures, differently sized phenocryst populations, xenocrysts and xenoliths. The geochemistry of the GVC magmas have several adakitic indicators which include high Sr/Y (>40), Mg# (~51), Al₂O₃ (>15 wt. %), low K₂O/Na₂O (~0.2), low Yb (<1.9 ppm) and fractionated rare earth element (REE) compositions (La/Yb(N)~8). The GVC magmas can be further divided into low silica adakites (LSA), which occur in the GLVF and MGVF, and high silica adakites (HSA), which are identified in the MGVF only. HSA contain > 60 wt. % SiO₂, lower MgO (0.5 to 4 wt. %), total CaO and Na₂O < 11 wt. %, and Sr contents < 1100 ppm. In contrast, LSA have < 60 wt. % SiO₂, 4-9 wt. % MgO, > 10 wt. % CaO+Na₂O and Sr in excess of 1000 ppm. Adakites were first described as the product of subducted slab melts within the garnet stability field. The subdivision of LSA and HSA reflects a different source region, where HSA are primary slab melts with an assimilated mantle wedge peridotite component and LSA are mantle wedge partial melts that have been modified by slab-derived magmas. Interpretation of these results suggests that the rocks of the GVC are adakites or adakite-like but limited data precludes rigorous geochemical characterisation; subsequent petrological models are, therefore, speculative. Further work is on-going to more fully elucidate the origins of the GVC. (GS2; Wed. 10:40)

Quantifying strain-related mosaicity in mantle olivine by μ XRD: Examples from kimberlites and mantle xenoliths.

Flemming R.L., Weiss, T. and Dean, B., Department of Earth Sciences, The University of Western Ontario, 1151 Richmond St., London, ON N6A 5B7, rflemmin@uwo.ca

Olivine in kimberlites and mantle xenoliths can exhibit spectacular undulatory extinction and subgrain formation. This has been well documented for mantle olivine using optical methods, and is attributed to dislocation creep during plastic deformation (Poirier and Nicolas 1975; Harte 1977). Migration of edge dislocations to form domain walls produces subgrains which can be slightly to highly misoriented with respect to each other, forming what crystallographers call 'mosaic blocks' (Klug and Alexander 1962). Strain-related mosaicity in minerals can be observed, and quantified, by two-dimensional X-ray diffraction methods (Hörsz and Quade 1973; Vinet *et al.* 2011).

We have performed *in situ* two-dimensional micro X-ray diffraction (μ XRD) on olivines from the Diavik Kimberlite, Lac de Gras, Canada, and mantle xenoliths from Bultfontein kimberlite,



Kimberley, South Africa. Our Diavik samples are from coherent kimberlite dykes A154N and A21, which have been previously studied by Brett *et al.* (2009). In the Diavik kimberlite, we examine the macrocrystic population of large, rounded to sub-rounded olivine grains (1-10 mm). These olivines exhibit a range of strain-related mosaicity. The mantle xenoliths from Kimberley, South Africa, have been previously reported by Creighton *et al.* (2009) and represent both coarse and porphyroclastic textures.

Subgrain development has been described optically and by μ XRD for olivine grains *in situ* in thin section. Mosaicity was quantified by the degree of angular dispersion or 'streaking' of the X-ray reflection along the Debye ring or chi dimension ($^\circ\chi$). Olivine grains exhibiting smooth undulatory optical extinction showed smooth homogeneous streaks by XRD (domain size $< 5 \mu\text{m}$), from which streaking was measured as full width at half maximum along chi (FWHM χ). Development of subgrains was also monitored by μ XRD, because as subgrain size exceeds 10-15 μm , the originally-homogeneous dispersion of X-rays (streak) appears as rows of X-ray spots (asterism) along chi. This coincides with optical recognition of subgrains. Asterism enables quantification of the angular rotation between the misoriented subgrains. This technique may prove useful in the study of deformation in mantle olivine. (SS4; Fri. 3:40)

Brett, R.C. *et al.* (2009) *Lithos*, **112S**: 201-212.

Creighton, S. *et al.* (2009) *Contrib. Mineral. Petrol.* **157**: 491-504.

Harte, B. (1977) *J. Geology*, **85**: 279-88.

Hörz, F. and Quaide, W. (1973) *Earth, Moon, and Planets*, **6**, 45-82.

Klug, H.P. and Alexander, L.E. (1962) *X-ray diffraction procedures*, 3rd ed., 716 p. Wiley, NY.

Poirier, J.P. and Nicolas, A. (1975) *J. Geology*, **83**: 707-720.

Vinet, N. *et al.* (2011) *American Mineralogist*, **96**: 486-497.

ASTRO – Astromaterials Training and Research Opportunities CSA Cluster

Flemming, R.L.¹, rflemmin@uwo.ca, Tait, K.², Schmidt, M.E.³, Cloutis, E.A.⁴, Herd, C.D.K.⁵, Sylvester, P.J.⁶, Kissin, S.A.⁷, Brown, P.G.⁸, Osinski, G.R.¹, Banerjee, N.R.¹, Webb, E.A.¹, Moser, D.E.¹ and McCausland, P.J.A.¹, ¹Earth Sciences, Western University, London, ON N6A 5B7; ²Royal Ontario Museum, Toronto, ON M5S 2C6; ³Earth Sciences, Brock University, St. Catharines, ON L2S 3A1; ⁴Geography, University of Winnipeg, Winnipeg, MB R3B 2E9; ⁵Earth and Atmospheric Sciences, University of Alberta, Edmonton, AB T6G 2E3; ⁶Earth Sciences, Memorial University, St. John's, NL A1B 3X5; ⁷Geology, Lakehead University, Thunder Bay, ON P7B 5E1; ⁸Physics & Astronomy, Western University, London, ON N6A 3K7

Astromaterials research encompasses the study of meteorites, returned samples from solar system bodies, impact-related rocks, and also manufactured materials which have been used in space. The Astromaterials Training and Research Opportunities (ASTRO) Cluster is a three-year partnership between researchers at seven Universities and funded by the Canadian Space Agency, to foster the development of Canadian expertise in the Tier 1 high priority strategic area of "Astromaterials analysis and curation." The core purpose of the ASTRO program is to promote astromaterials research capability in Canada by training the next generation of astromaterials researchers using our existing expertise and premier analytical facilities, coupled with opportunities for international collaboration. The functional components of the ASTRO program are: 1) a yearly short course for astromaterials training, held in May to maximize the impact for new students; 2) travel bursaries for student collaborative astromaterials research and conference participation; 3) support of undergraduate summer student research opportunities with astromaterials researchers, and; 4) the coordination of Canadian astromaterials research and training, including the linking of relevant resources (sample curation and availability, instrument availability, course and website development). The ASTRO program got underway with the Astromaterials Short Course hosted by the Royal Ontario Museum on May 22-23, 2012. The course had 40 participants, many of whom

proceeded to do astromaterials research during the summer as undergraduate and graduate students. The second annual ASTRO Short Course will be held at Western University in May 2013. Also in 2013, six undergraduates will be awarded ASTRO summer research positions and 10 graduate students will receive funding for conference or research travel. Development of web-based resources for astromaterials training and sample curation is also underway.

The final measure of the effectiveness of the ASTRO program will be the increase in Canadian competency and credibility in astromaterials research, such that the following goals are achieved: 1) An improvement in Canadian science capabilities and sample handling protocols to take advantage of analysis opportunities arising from upcoming exploration and sample-return missions; 2) An increase in the number, quality and diversity of meteorites in Canadian collections via meteorite recovery and typing; 3) Development of teaching materials aimed at senior undergraduate and graduate planetary science students; 4) Increased collaboration between ASTRO co-investigators, through trainee-related contact; and, 5) Increased Canadian participation in international Astromaterials curation and research. (SS18; Thurs. 1:40)

Alteration and fluid characteristics of the Hamlin Lake IOCG occurrence, northwestern Ontario

Forslund, N., Sabina Gold & Silver Corporation, 601 Squier Street, Thunder Bay, ON P7B 4A7, NForslund@sabinagoldsilver.com, and Kissin, S.A., Department of Geology, Lakehead University, Thunder Bay, ON P7B 5E1, sakissin@lakeheadu.ca

The Hamlin Lake IOCG occurrence is located approximately 120km southwest of Thunder Bay, Ontario, in the Shebandowan greenstone belt of the Archean Wawa Subprovince of the Superior Province. Chalcopyrite, molybdenite and gold, as well as magnetite, pyrite and pyrrhotite characterize the mineralogy of the occurrence. The timing of six styles of alteration, sodic, early potassic, calcic(iron), late potassic, carbonate and silicic, were determined on the basis of textural relationships. Sodic alteration, characterized by extensive albitization, accompanied brecciation of the host rocks. This phase of alteration may transition to potassic alteration, both of which are barren. The early potassic phase consists of biotite and magnetite in the matrix of the breccia, which is cut by epidote and sphene of the calcic(iron) alteration. Chalcopyrite-magnetite-pyrite were deposited in association with late potassic alteration. These episodes of alteration were designated as stage I mineralization. Stage I was succeeded by carbonate alteration, followed by vuggy quartz breccia that accompanied stage II mineralization. Stage II mineralization produced the highest chalcopyrite concentrations accompanied by pyrite and minor hematization.

Fluid inclusions in vuggy quartz from stage II mineralization yielded homogenization temperatures ranging from 271 to 180°C in the NaCl-H₂O-CO₂ system with salinities ranging from 12.4 to 11.0 wt % NaCl. Temperatures of 304 and 283°C for stage I mineralization were obtained from chalcopyrite-pyrite geothermometry based on sulfur isotopic compositions. Isotopic compositions of sulfides ranged from $\delta^{34}\text{S} = -6.9$ to $+1.8\text{‰}$, the source of which is unclear. Oxygen isotopic composition of water depositing magnetite in stage I ranged from $\delta^{18}\text{O} = +8.90$ to $+10.94\text{‰}$, consistent with a magmatic or deep-seated metamorphic source. Chlorite from stage II yielded δD - $\delta^{18}\text{O}$ relationships suggesting mixing of surficial water with magmatic or metamorphic water in stage I, with $\delta^{18}\text{O} = +0.4$ to $+5.9\text{‰}$. The two stages of mineralization differ in that stage I is associated with potassic alteration and iron oxide deposition, whereas stage II is associated with quartz and has a lack of massive iron oxides. The precursor albitization and stage I mineralization is consistent with general alteration patterns observed in magnetite-group IOCG deposits world-wide. The onset of carbonate alteration, followed by vuggy quartz with moderate- to high-sulfidation assemblages of stage II, is more typical of a transition to epithermal mineralization. (SS23; Fri. 2:40)



Characterization of fresh and aged biogenic iron oxides (BIOS)

Fortin, D., University of Ottawa, 140 Louis Pasteur, Ottawa, ON K1N 6N5, dfortin@uottawa.ca

Biogenic iron oxides, known as BIOS, have recently been the subject of several studies because of their potential role in contaminant sorption in natural environments. Other studies have also looked at the microbial population diversity of BIOS and at the key chemical factors controlling their formation and occurrence. Fresh natural BIOS were collected in a groundwater seepage area from pH-neutral Cu-Zn-Pb mine tailings in Québec, Canada. The amount of soluble Fe (II) and Fe total in the stream where BIOS formed decreased with distance from the source of the seepage area and the surface waters in contact with BIOS contained lower levels of heavy metals than waters collected at a BIOS-free site. Chemical digestion of the BIOS samples indicated that all heavy metals were sequestered by the matrix of cells and iron oxides, while X-ray diffraction analyses showed that ferrihydrite was a common component of all BIOS samples, but trace amounts of goethite and lepidocrocite were also detected. SEM imaging revealed that they were essentially composed of small particles of iron oxides in close association with tube-like structures reminiscent of Leptothrix cells, a well known neutrophilic iron oxidizing bacterium.

BIOS from another site, *i.e.*, a wetland in Chalk River, Ontario, were aged at 4 °C for a period of 5 years in the dark in order to simulate diagenesis. X-ray diffraction of the fresh material indicated that ferrihydrite was the main iron oxides in contact with the cells, but aged BIOS were far more crystalline. Microbial reduction of the aged BIOS showed that the rates of reaction were very slow when compared to those of the original fresh BIOS, suggesting the aged BIOS was for more crystalline, as indicated by X-ray diffraction. Our results indicate that fresh and aged BIOS are efficient sorbents of metal contaminants and that upon ageing, they are capable of retaining more metals into their structures, as the poorly ordered ferrihydrite transforms into more crystalline iron oxides. (SS15; Wed. 2:20)

The effect of water on sulphur solubility in natural melts

Fortin, M-A. and Baker, D.R., McGill University, 3450 rue University, Montréal, QC H3A 0E8, marc-antoine.fortin@mail.mcgill.ca

Sulphur plays an important role in many magmatic processes and a greater knowledge of its behaviour provides a means to understand and constrain a multitude of igneous mechanisms. A better understanding of the storage and transport of sulphur would improve our modelling of the formation of platinum-group element ore deposits and allow us to better monitor volcanoes, with the long-term goal of predicting their eruptions. Our understanding of the global sulphur cycle could also greatly benefit from a better quantification of its magmatic component. Previous studies investigated various temperatures, pressures, melt compositions, as well as oxygen and sulphur fugacities, but at anhydrous conditions almost exclusively. Despite the fact that almost all magmas contain measurable water, only limited work has been conducted at hydrous conditions. Our goal is to model how water affects the solubility of sulphides (FeS) in natural melts. We are experimentally determining the sulphur concentration at sulphide saturation (SCSS) using a piston-cylinder apparatus mimicking deep crustal pressures, 1 GPa, and magmatic temperatures, 1250 °C. We run each experiment for 6 hours, until equilibrium is reached as shown by Liu *et al.* (2007)¹. We conducted experiments on MORB and Etna basaltic melt compositions saturated in sulphide of pyrrhotite (FeS) composition; the same compositions used by Liu *et al.* (2007)¹. Oxygen fugacity in the experiments is controlled by the graphite-CO₂ (CCO) buffer, by using graphite in platinum capsules to hold the samples. We incrementally added up to ~4 wt% water to both basalt compositions. Preliminary results, using measured amounts of added water, show at most a small increase in the SCSS with increasing water-concentration, which contrasts with the decreasing trend observed by Liu *et al.* (2007)¹. Indeed, our experiments of MORB at anhydrous conditions display a SCSS of 1119 ± 40 ppm, and a SCSS of 1409 ± 38 ppm when we added 4.1 wt% water. We seek to further confirm the

relationship between water concentration and the SCSS by applying Raman spectroscopy to our samples to more accurately determine their water concentrations. Furthermore, we are currently investigating the effect of water on more felsic compositions (andesitic and rhyolitic) in order to revise and improve the model of Liu *et al.* (2007)¹.

¹Geochimica et Cosmochimica Acta **71** (2007) 1783–1799. (GS3; Thurs. 2:20)

Determining accurate and precise isotopic compositions of reference materials to investigate isotopic heterogeneity in mafic layered intrusions

Fourny, A., Weis, D. and Scoates, J.S., Pacific Centre for Isotopic and Geochemical Research, Department of Earth, Ocean & Atmospheric Sciences, University of British Columbia, Vancouver, BC V6T 1Z4, afourny@eos.ubc.ca

Recent studies show isotopic heterogeneities (Sr-Nd-Pb) in coexisting minerals from mafic layered intrusions such as the Bushveld Complex in South Africa; the Skaergaard intrusion, Greenland; the Kiglapait intrusion, Canada; and the Stillwater Complex of Montana, USA. These different initial isotopic ratios are not directly correlated to secondary alteration or to subsequent metamorphism, except for Pb isotopes in sulphides from the Stillwater Complex, and their presence has been variably interpreted to indicate that different minerals in cumulates crystallized from magmas of different compositions or that they originate from late-stage magmatic processes. Accurate and precise isotopic ratios of minerals are needed to resolve these differences. To achieve such high precision, reference materials with similar matrices to the samples need to be analyzed by MC-ICP-MS. In the case of ultramafic samples, where there are typically very low abundances of the elements of interest, isotopic compositions of reference materials have yet to be determined. With this aim, we have undertaken an analysis of Pb, Hf, Nd and Sr isotopic compositions using MC-ICP-MS from single rock digests for a wide range of mafic to ultramafic reference materials, including five basalts (BHVO-2, BIR-1, JB-3, BE-N, GSR-3), one anorthosite (AN-G), a diabase (W-2), a dolerite (DNC-1), a peridotite (JP-1), a serpentinite (UB-N), a pyroxenite (SARM-5), a norite (SARM-4) and a dunite (SARM-6). We report here preliminary results (all ±2SD) on these reference materials. The leached powder of BHVO-2 shows isotopic values in agreement with earlier studies (Weis *et al.*, 2006, 2007, G3) with an external precision (2SD) below 332 ppm for Pb isotopic ratios and 41 ppm for Hf. In contrast to BHVO-2, the reproducibility for BIR-1 is better for the unleached samples. Previous studies have shown a wide range of Pb isotopic values for BIR-1; our results are in agreement with Baker *et al.* (2004, Chemical Geology) with an average (n=7) of $^{208}\text{Pb}/^{204}\text{Pb} = 38.4965 \pm 0.0058$, $^{207}\text{Pb}/^{204}\text{Pb} = 15.6592 \pm 0.0021$, $^{206}\text{Pb}/^{204}\text{Pb} = 18.8497 \pm 0.0032$. We report Pb isotope ratios for W-2 (n=10) of $^{208}\text{Pb}/^{204}\text{Pb} = 38.6293 \pm 0.0150$, $^{207}\text{Pb}/^{204}\text{Pb} = 15.6621 \pm 0.0033$, $^{206}\text{Pb}/^{204}\text{Pb} = 18.7507 \pm 0.0083$ with an average of $^{176}\text{Hf}/^{177}\text{Hf} = 0.282736 \pm 0.000006$. We present, to our knowledge, the first Pb isotopic composition of DNC-1 (n=10): $^{208}\text{Pb}/^{204}\text{Pb} = 38.3726 \pm 0.0123$, $^{207}\text{Pb}/^{204}\text{Pb} = 15.6481 \pm 0.0030$, $^{206}\text{Pb}/^{204}\text{Pb} = 18.6891 \pm 0.0118$ with an average $^{176}\text{Hf}/^{177}\text{Hf} = 0.282849 \pm 0.000036$ (n=6). The mafic and ultramafic reference materials analyzed in this study to date provide an essential new dataset to investigate the extent and significance of isotopic heterogeneity between minerals within mafic layered intrusions. (SS8; Thurs. Poster)

High tenor Ni-PGE sulfide mineralization in the South Managan ultramafic intrusion, Thompson Nickel Belt, Manitoba

Franchuk, A.¹, anatoliy.franchuk@vale.com, Lightfoot P.C.², and Kontak, D.J.³, ¹Vale Brownfield Exploration, Thompson, MB R8N 1S4; ²Vale Brownfield Exploration, Copper Cliff, ON P0M 1N0; ³Department of Earth Sciences, Laurentian University, Sudbury, ON P3E 2C6

The South Managan ultramafic intrusion (SMUI), in the Proterozoic Thompson Nickel Belt (TNB), contains both PGE- and Ni- enriched



disseminated sulfide mineralization with a high metal tenor compared to other ultramafic-hosted deposits in the TNB. New whole-rock geochemical data, modal mineralogy, mineral chemistry, and quantitative element distribution obtained from drill-core samples through the SMUI are used to assess the relative roles of primary magmatic processes versus subsequent serpentinisation and deformation relevant to metal distribution. The intrusion is a steeply dipping, sill-like body 1200 m long and 125 m wide with a minimum depth extent of 1000 m. The intrusion is dominated by unaltered dunite with serpentine and carbonate alteration most intense against the Ospwagan Group metasedimentary rocks. The Ni-PGE mineralization occurs as a disseminated, intercumulus-textured sulphide phases of primary and secondary origin. In weakly altered dunite, the assemblage is dominated by interstitial pentlandite intergrown with accessory pyrite, but in the more altered parts the pentlandite-pyrite assemblage assumes a platy morphology and is intergrown with chlorite and serpentine. Where most tectonized and chlorite-carbonate altered, the dunite contains pyrrhotite with pentlandite eyes. Nickel grades range from 0.3 to 1.7% and TPMs ($\Sigma \text{Pt} + \text{Pd} + \text{Au}$) range from 0 to 1.3 ppm. The disseminated sulfides are not only enriched in Ni relative to most other TNB deposits (e.g. Ni tenors in SMUI are 5-36 wt.% versus 4-6 in Pipe sulfides), but also show strong enrichment in PGEs (e.g. Pd tenors in SMUI 36ppm per 100% sulfide versus 3 ppm per 100% sulfide in Pipe sulfides). The primary magmatic sulfides are interpreted to have formed at a high R factor by equilibration of crustal S with a komatiitic parental magma. The observed pentlandite-pyrite assemblage in the less altered part of the SMUI is inferred to represent an intercumulus sulfide assemblage generated through immiscible phase separation of a sulfide melt enriched in Ni and PGE. The appearance of pyrrhotite within sheared and reworked lithologies is attributed to sulfurization of the pentlandite-pyrite assemblage during chlorite-carbonate alteration. PGE mineralization shows a strong correlation with Ni-sulfides that survives metamorphic alteration. Modification of the sulphide assemblage during serpentinisation and deformation has altered the whole rock chemistry in systematic ways and the textures of the sulphides can be reconciled with a multi-phase evolution which helps establish processes governing the mineralogical and compositional diversity in other ultramafic hosted mineralization in the TNB. (SS9; Wed. 3:00)

A seismic image of the lithosphere beneath the western Superior Province and the Mid-Continent Rift

Frederiksen, A.W.¹, frederik@cc.umanitoba.ca, Bollmann, T.², Darbyshire, F.³ and Van der Lee, S.², ¹Department of Geological Sciences, University of Manitoba, Winnipeg, MB R3T 2N2; ²Department of Earth and Planetary Sciences, Northwestern University, Evanston, IL, 60208-3130 USA; ³Centre GEOTOP, Université du Québec à Montréal, Montreal, QC H3C 3P8

The assembly of Laurentia by Precambrian accretion is also believed to have formed the underlying lithosphere. Accretionary signatures are detectable by seismic observations, but subject to modification by later processes, e.g. orogeny, rifting, and plumes. We examine the lithosphere of the Archean Superior Province (SP) and environs using a set of teleseismic P-wave arrivals from Canadian and American instruments, including instruments from the Earthscope Transportable Array, the Manitoba Teleseismic Array, and the Canadian National Seismograph Network, as well as past temporary experiments. The resulting 3-D tomographic model has high resolution beneath the Dakotas and Minnesota, provides a first look at the lithosphere beneath Manitoba, and sharpens previously-documented features in Ontario. From the model and previous anisotropy observations, we detect: (i) a large high-velocity feature beneath the western SP, associated with elevated lithospheric anisotropy. The high-velocity feature does not match crustal boundaries; notably, its western edge lies ca. 200 km east of the contact with the Proterozoic Trans-Hudson Orogen (THO). (ii) A low-velocity channel-shaped feature strikes northwest through Minnesota and the Dakotas, associated with weakening anisotropy. (iii) High velocities southwest of (ii), beneath the Minnesota River Valley

terrane (MRVT), associated with low anisotropy. We interpret (i) to be accretionary, and contemporaneous with Superior assembly; similar velocity but weaker anisotropy of the MRVT is consistent with vertical-tectonic mechanisms. The inboard location of the THO contact may indicate modification of the Superior root. The low-velocity channel has no obvious crustal expression, but connects to an offset in the Proterozoic Mid-Continent Rift (MCR) and may be rift-related. The main axis of the MCR is not well-imaged by this data set, but will be examined via the temporary Superior Province Rifting Earthscope Experiment, currently in progress. (SS3; Fri. 11:00)

Soil characterization for landfill site selection in Tarkwa-Nsuaem municipality, Ghana

Frempong, V.E.¹, vfrempon@uwo.ca, Flemming, R.L.², rflemmin@uwo.ca, Yanful, E.K.³ and Kuma, J.S.⁴, ¹Mineral Engineering Department, University of Mines and Technology, Tarkwa PO Box 237, Ghana; ²Department of Earth Sciences, The University of Western Ontario, London, ON N6A 5B7; ³Civil and Environmental Engineering, The University of Western Ontario, London, ON N6A 5B7; ⁴Geological Engineering Department, University of Mines and Technology, Tarkwa PO Box 237, Ghana

We are characterizing candidate soils for the design and construction of the first engineered landfill for Tarkwa-Nsuaem Municipality in the Western Region of Ghana, as commissioned by the Municipal Assembly. Soil samples were taken from the proposed site which is located in the Kaware lithology of the Tarkwaian Group in Ghana for analysis. We have determined the bulk geochemistry by XRF and ICP-OES, mineralogy by XRD and geotechnical properties on the same samples. The soils are silty clayey sand (SM-CS), have a liquid limit of 22.1 and a plasticity index of 5.64. The average field moisture content is about 16.7% and the maximum Proctor compaction dry unit weight is 18.7 kN/m³, at an optimum moisture content of 11.6%. The saturated hydraulic conductivity, K_s, is 1×10^{-7} cm/s which is the maximum acceptable permeability for a landfill liner in Ghana. The major oxides from the XRF analysis are SiO₂ (78.76%) followed by Al₂O₃ (10.3%) and Fe₂O₃ (3.2%). This gives a silica-sesquioxide (S-S) ratio of 5.84, classifying it as a lateritic soil. The major mineralogy is quartz, muscovite and kaolinite, which are consistent with a lateritic soil profile. The soil was permeated with landfill leachate during the hydraulic conductivity experiment for 11 days. The break through curves indicate that most cations were initially desorbed from the soil into solution and later adsorbed towards the end of the permeation except for K⁺ and Mg²⁺ ions which gave the reverse result. The municipality is facing a lot of criticism from communities hosting waste dumps, because the dumps are not engineered and the resulting leachate flow has polluted both surface and ground water in the area. The municipality is therefore waiting for the results and recommendations of this research to locate and construct the first ever engineered landfill in the municipality. In order to meet the stipulations in the Ghana Landfill Guidelines, our recommended soil-based landfill liner design must reduce potential environmental contaminants to acceptable levels. (SS20; Fri. 2:00)

Questioning the textural evidence for microbial bioalteration of volcanic glass and its robustness as a terrestrial analog biosignature for Mars astrobiology

French, J.E., Department of Earth and Atmospheric Sciences, University of Alberta, 1-26 Earth Science Building, Edmonton, AB T6G 2E3, jef@ualberta.ca

The pervasive corrosion of submarine volcanic glasses on planet Earth has resulted in the widespread occurrence of complex alteration/dissolution microtextures in basaltic glasses within the *in situ* oceanic crust, ophiolites, and greenstone belts dating back to ~3.5 Ga. Over the last 20 years, the consensus has been that these complex corrosion microtextures along fractures in basaltic glass (so called 'granular' palagonite and 'tubular' etch-tunnels) are the direct result of microbial 'bioalteration' of basaltic glass. Here I demonstrate—with a



case study of Early Cretaceous basaltic glasses from Deep Sea Drilling Project (DSDP) Hole 418A—that these two varieties of alteration microtexture are not biological origin, but instead appear to form by preferential corrosion (by seawater) of randomly distributed alpha-recoil tracks and fission tracks (*i.e.*, radiation damaged sites) in the glass (\pm pressure solution).

To determine their origin, I combine petrographic and SEM observations of corrosion microtextures at the glass–palagonite interface, considerations of the tectonic setting, measurement of U and Th concentrations (32–42 ppb U; 108–132 ppb Th) of fresh basaltic glass by ICP–MS, and theoretical modelling of present-day radiation damage in basaltic glass caused by radioactive decay of U and Th. Accordingly, the complex abiotic corrosion/palagonitization microtextures identified in these DSDP 418A glasses include: 1) An etch-tunnel zone (*i.e.*, ‘tubular’ texture), comprising a complex network of anastomosing, branching, typically ~ 120 nm wide (but sometimes wider) alpha-recoil track etch-tunnels, interconnected with rare ~ 1 – 2 μ m wide by ~ 8 μ m long fission track etch-tunnels; 2) Dense concentrations of ~ 0.6 μ m wide palagonite ‘granules’ (*i.e.*, ‘granular’ texture) formed by selective palagonitization of large numbers of randomly distributed alpha-recoil tracks in the glass.

The ‘abiotic’ driving mechanism: As the oceanic crust ages and moves away from the spreading ridge, basaltic glass accumulates radiation damage while also being subjected to incremental increases in hydrostatic pressure (in this case from ~ 29 to ~ 63 MPa) as it gradually subsides under a deepening ocean—thus becoming increasingly susceptible to the effects of both pressure solution and preferential corrosion of radiation damage as the Atlantic Ocean gradually squeezes/injects its way into the glass with microscopic etch-tunnelling ‘needles’ of seawater (or by incipient palagonitization).

On the surface of Mars, basalt, palagonite, and volcanic/impact glasses are probably quite widespread, and coupled with the abundant evidence for past action of liquid water, means that future astrobiology missions to Mars may discover analogous ‘abiotic’ corrosion microtextures in Martian glasses. (SS17; Thurs. 8:40)

A cryptic tectonometamorphic discontinuity in the Greater Himalayan sequence, Likhu Khola study area, east-central Nepal

From, R.^{1,2} and Larson, K.^{1,3}, ¹Department of Geological Sciences, 114 Science Place, University of Saskatchewan, SK S7N 5E2; ²(Present Address) Department of Geological Sciences, 125 Dysart Road, University of Manitoba, MB R3T 2N2; ³(Present Address) Earth and Environmental Sciences, 3333 University Way, University of British Columbia Okanagan, BC V1V 1V7

Recent advances in our understanding of the Himalaya and adjacent regions have changed our perception and knowledge of how large mountain belts form. Understanding how the exhumed mid-crustal core of the orogen, the Greater Himalayan sequence, has evolved is crucial to further our interpretations of orogenic processes. Targeted mapping and sample collection in the Likhu Khola study area was carried out across the majority of the Greater Himalayan sequence in east-central Nepal to evaluate the tectonometamorphic evolution of this region. Pervasively ductily deformed metamorphic rocks in the study area comprise an inverted metamorphic sequence ranging from upper greenschist to upper amphibolite grade up-structural section. Mantled porphyroclasts and *s/c/c'* fabrics consistently record top-to-the-south directed shear. Geothermobarometric analyses were conducted on eleven specimens at different structural positions. Metamorphic temperature estimates slightly increase up structural section in the lower part of the study area but are within error of each other in the upper portion of the study area. In contrast, metamorphic pressure estimates increase up structural section at lower levels followed by decreasing pressures towards higher levels. *In situ* U–Th–Pb monazite geochronology, with simultaneous trace element data analysis, was carried out on a subset of rocks from the upper portion of the study area analyzed for pressure-temperature estimates. Metamorphic ages range from 27.4 ± 0.4 Ma to 15.3 ± 0.2 Ma indicating a protracted period of

metamorphism. Monazite ages from structurally lower positions in adjacent regions indicate younger metamorphism (~ 10 Ma) with a much shorter history.

The inflections in the apparent temperature and pressure gradient and changes in monazite ages are interpreted to indicate a tectonometamorphic discontinuity separating two distinct domains with different structural, thermal and metamorphic histories. This cryptic discontinuity is not easily identified in the field, although it generally corresponds to a significant increase in anatexite above it. Similar tectonometamorphic discontinuities at comparable structural levels have been recently identified along the length of the Himalaya including areas in NW India, western Nepal, west-central Nepal, Eastern Nepal, and Sikkim. Data from structurally above the identified tectonometamorphic discontinuity are consistent with mid-crustal channel flow processes in the deeper the orogenic hinterland whereas data below the discontinuity are consistent with critical-taper wedge processes in the shallower orogenic foreland. The discontinuity, therefore, represents the transition between spatially and temporally distinct convergence accommodation processes. (GS4; Thurs. Poster)

Hydrocarbons: A source of uranium and titanium in the Witwatersrand, South Africa

Fuchs, S., Schumann D., William Jones, A.E., Department of Earth & Planetary Sciences, McGill University, 3450 University Street, Montreal, QC H3A 2A7, sebastian.fuchs@mail.mcgill.ca, and Vali, H., Facility for Electron Microscopy Research, McGill University, 3640 University Street, Montreal, QC H3A 2B2

The Witwatersrand is the largest gold deposit on Earth and a major source of uranium. The preferred model for the genesis of the uranium is that it was introduced into the basin as detrital uraninite. This is supported by the rounded shapes of the uraninite grains. The association of uranium with organic matter has been explained as resulting from radiolytic polymerisation and immobilization of liquid hydrocarbons. Recent experimental studies, however, have shown that significant concentrations of metals can be dissolved in liquid hydrocarbons. The presence of oil inclusions in overgrowths on quartz pebbles suggests that oil migrated through the Witwatersrand basin, and that may therefore have transported metals.

We have used a combination of HR-TEM, bright field imaging, HAADF-S/TEM and elemental EDS analyses to investigate the nature and composition of the pyrobitumen and associated uranium and titanium minerals in the Carbon Leader Reef (Witwatersrand Supergroup). High resolution TEM bright field imaging has shown that the pyrobitumen consists of 100 to 200 nm thick sheets of organic matter, and hosts single nano-crystals (~ 5 nm) and concretions (< 3 μ m) of uraninite. Although nano-crystals of uraninite represent the major mineral phase within these concretions, HAADF-S/TEM elemental EDS line scan analyses and HRTEM lattice fringe images indicate the presence of coffinite nano-crystals within a network of uraninite nano-crystals. Anatase occurs as 200 nm diameter euhedral crystals in the pyrobitumen either in isolation from the uraninite or within the uraninite concretions.

The presence of single nano-crystals of uraninite in the pyrobitumen demonstrates that not all the uranium in the Witwatersrand basin is of detrital origin. Some uraninite was clearly the product of *in-situ* growth in organic matter. Anatase crystals are commonly overgrown and enveloped by uraninite, which may have acted as nucleation sites for the uraninite. This suggests that U and Ti were both transported as metallo-organic complexes in organic matter and precipitated due to thermal maturation, which released and led to the decomposition of the organo-metallic complexes. The maturation of the organic matter may also have led to the oxidation of uranium to uraninite.

The pyrobitumen also contains fractures or pockets filled with muscovite. In the adjacent pyrobitumen, the networks of uraninite nano-crystals commonly contain scattered coffinite crystals. This suggests coffinitization of the uraninite by hydrothermal solutions that



entered the pyrobitumen after nano-fractures had opened during the maturation process. (*SS5; Wed. 3:00*)

Bond lengths in the solid state: A comprehensive survey

Gagné, O.C., umgagneo@cc.umanitoba.ca, and Hawthorne, F.C.,
University of Manitoba, 125 Dysart Road (Wallace Building),
Winnipeg, MB R3T 2N2

Since 1973, Mineralogy has seen the valence-sum rule of bond-valence theory used extensively in verifying structure models obtained by crystal-structure refinement. Here, a complete survey of bond lengths from the International Crystal Structure Database (ICSD) is presented for all atoms of the periodic table of elements, bonded to oxygen and in different oxidation states and coordination numbers. Five hundred and seven (507) different ion configurations and 34,080 coordination polyhedra (a total of 192,467 bond distances) passed a rigorous filtering process. The bondlength data, plotted as histograms for every element configuration, yields an immense amount of information. The observed bond-length ranges were converted into bond-valence ranges for every ion configuration, which readily finds two simple uses: (1) the study of solid solution: by knowing the bond-valence pattern of a structure type (through a priori bond-valence calculations), one can predict what atoms can occupy the sites; and (2) as an aid to the assignment of atoms to sites in a structure (both in terms of bond lengths and bond valences). Of particular interest is the visual aspect of the histograms as this may indicate subtleties in the bondlength configurations for specific ions and allow us to examine the underlying principles giving rise to these distributions. Statistical information of the shape of the distribution (*e.g.* skew, kurtosis) and trends across the periodic table for specific classes of data (*e.g.* family, oxidation state) were sought for the different element configurations, revealing phenomena that are less obvious in smaller-scale studies. Finally, a summary of all information derived from the bond-length histograms is hoped to yield insight into the unusual behaviour (particularly multimodal distributions of bondlengths) of certain atoms. To this end, Density Functional Theory (DFT) simulations using bond-length constraints is done for atoms showing such multimodal behaviour to examine the reasons for such behaviour and link it to the electronic structure of the constituent atoms. (*GS1; Fri. 3:00*)

Molecular scale origin of nuclear glass properties during elaboration, alteration, and aging under irradiation

Galoisy, L., Galoisy@impmc.upmc.fr, Calas, G., Cormier, L.,
IMPMC, University of Paris, CNRS and IGP, Case 115, 75252
Paris Cedex 05, France, Delaye, J-M., Peugeot, S. and Jollivet, P.,
CEA Valrhô-Marcoule, DEN/DTCD/SECM/LCLT, BP17171,
30207 Bagnols sur Cèze cedex, France

We present information provided by the structural properties of glasses on the molecular-scale mechanisms governing the quality and long-term stability of nuclear glasses. An overall picture is obtained by a comparison between simplified and multicomponent matrices and between glass surface and bulk structure and by complementing experimental approaches by numerical simulations. Matrix stability relies on the synergy between glass/gel components with a major role played by competition for local charge compensation. The peculiar behavior of limited -solubility fission products such as Mo will be first presented in regard to glass quality. During the first stages of alteration in near- or under-saturated conditions, molecular-scale modifications of the glass surface govern the glass-to-gel transformation. Short-term glass durability depends on specific elements such as Zr, which may occur under contrasted coordination geometries. Under saturated conditions, a protective gel is formed, with a local structure similar to that in glasses, which explains the chemical control of the initial alteration rate. Under open alteration conditions, the gel forms with a different structural organization, in relation with increasing glass dissolution rate. We will present spectroscopic evidence of the distinct speciation of some elements, such as U, in glasses and gels. During external irradiation, there is also direct evidence of a coordination change of glass components near the glass surface. Complementary

information on ballistic effects arising from displacement cascades is provided by molecular dynamics simulations, which lead to a local thermal quenching model consistent with experimental observations on the structure of borosilicate melts. (*SS5; Thurs. 2:00*)

Late Neogene deposits and sedimentary conditions in the James Bay Lowland, Canada

Gao, C.¹, george.gao@ontario.ca, McAndrews, J.H.^{2,3}, Wang, X.⁴,
Menzies, J.⁵, Turton, C.L.³, Wood, B.D.⁶, Pei, J.⁴ and Kodors, C.⁵,
¹Ontario Geological Survey, Sudbury, ON P3E 6B5; ²University
of Toronto, Toronto, ON M5S 3B2; ³Royal Ontario Museum,
Toronto, ON M5S 2C6; ⁴Chinese Academy of Geological
Sciences, Beijing, 100081; ⁵Brock University, St. Catharines, ON
L2S 3A1; ⁶De Beers Canada Inc., ON P4N 2K3

Pliocene deposits were found in a buried trench with a floor 192 m below the surface or 108 m below the sea level in Silurian carbonate bedrock, adjacent to De Beers' Victor diamond mine near the Attawapiskat River, northern Ontario (52°49.5'N 83°52.5'W). The 170 m-thick Pliocene succession consists of about 50 m of till and 120 m of overlying lacustrine deposits. The till is a non-calcareous, clayey to sandy diamict rich in kaolinite, containing occasional faceted pebbles. Facies and microtexture studies indicate a subglacial environment under which the till was formed. The till contains peat and organic-rich detrital mud with sporadic glaciolacustrine silt and clay horizons. The predominance in pebble lithology of vein quartz, chert and quartzite suggests a major source from the Jurassic and Cretaceous fluvial sediments in the region. The overlying lacustrine sequence is also non-calcareous and rich in kaolinite. It contains laminated sand and silt with peat. Cobble-sized lag clasts occur at the base of the sequence, probably resulting from melt water erosion in front of the retreating ice sheet. Woody peat ranging from 1 to 30 m in thickness occurs in the upper part of the lacustrine sequence. At the top of the lacustrine sequence, silt and clay with fine lamination contains debris of clustered coarse sand grains that probably derived from ice rafting. This fining-upward sequence as a whole suggests increasing water depth over time in a lake basin probably much larger than the current bedrock trench, and that the present sequence is the erosional remnant of a much thicker lacustrine succession. Magnetostratigraphy together with pollen-derived biostratigraphy constrains the Pliocene succession to a time span from 3.6 to 3.0 Ma. The till is direct evidence for continental glaciation in the James Bay Lowland at ~3.5 Ma (3.6 – 3.4 Ma). The ice that deposited the till would appear to have been possibly part of a surging ice stream emanating from James Bay. After glaciation, rapid warming permitted thermophilic trees now exotic to this area to grow, which include Quercus, Carya, Liquidambar, Nyssa, and Taxodium. Furthermore, pollen analysis indicates alternating Carolinian deciduous and boreal evergreen forests under a climate that oscillated and cooled gradually over a prolonged postglacial period from 3.5 to 3.0 Ma. (*GS6; Wed. 9:20*)

Mechanisms of natural Zn attenuation in No Cash Creek, Yukon, Canada

Gault, A.G.¹, gault@geol.queensu.ca, Jamieson, H.E.¹, Sherriff, B.L.², Londry, K.L.^{3,4}, Johnson, B.C.⁵, Davidson, S.⁶ and Harrington, J.M.⁷, ¹Dept. of Geological Sciences and Geological Engineering, Queen's University, 36 Union Street, Kingston, ON K7L 3N6; ²Sherriff Environmental Inc., 5394 Manson Avenue, Powell River, BC V8A 3P4; ³Edmonton Waste Management Centre of Excellence, 13111 Meridian Street, Edmonton, AB T6S 1G9; ⁴Dept. of Biological Sciences, University of Alberta, Edmonton, AB T6G 2E9; ⁵Interralogic Inc., 913 11th Street, Golden, CO 80401 USA; ⁶Access Consulting Group, #3 Calcite Business Centre, 151 Industrial Road, Whitehorse, YT Y1A 2V3; ⁷Alexco Environmental Group, 7720 East Bellevue Avenue Suite B-104, Greenwood Village, CO 80111 USA

The Keno Hill Ag-Pb-Zn district (Yukon, Canada) has been mined intermittently since 1913 and hosts numerous watercourses impacted by historical mine water drainage. Circumneutral drainage from the



abandoned No Cash mine, containing approximately 10 mg/L dissolved Zn, feeds into No Cash Creek where ca. 99% of the dissolved Zn is removed from solution over the 3 km stream reach. Scanning electron microscopy (SEM) and electron microprobe inspection of thin sections prepared from No Cash Creek sediments indicated that the Zn was primarily present as Mn-Zn-rich colloform coatings on lithic grains and organic fragments within the sediment. Authigenic sphalerite was observed in a few instances, exclusively associated with cellulose-type structures.

Based on the SEM inspection, a range of targets were imaged by synchrotron-based micro-X-ray fluorescence (μ -XRF) mapping, and spots ($5 \times 5 \mu\text{m}$) were selected for further analysis using micro-X-ray diffraction (μ -XRD), and Zn K-edge micro-X-ray absorption near edge structure (μ -XANES) spectroscopy. Multiple μ -XRD spot analyses identified hetaerolite (ZnMn_2O_4) in the Mn-Zn-rich particle coatings, while fitting of associated μ -XANES analyses to model Zn-bearing standards also commonly identified hetaerolite in the Mn-Zn-rich colloform coatings. Hydrozincite ($\text{Zn}_5(\text{CO}_3)_2(\text{OH})_6$) and Zn sorbed on (or co-precipitated with) ferrihydrite were other principal hosts of Zn that could be well fit to the μ -XANES data collected in the Zn-Mn rich grain coatings.

The identity of the sphalerite micro-spheres observed by SEM was further confirmed by μ -XRD and μ -XANES measurements. We hypothesize that labile organic matter sustains anaerobic micro-niches where microbial sulfate-reduction can precipitate such sphalerite. Sulfate reduction was also measured in microcosm experiments using No Cash Creek sediments. The addition of acetate or methanol greatly stimulated sulfide production, suggesting the sediments were deficient in readily-utilizable organic carbon sources. Sulfate reduction in sediment from the adit area of No Cash Creek was very limited, perhaps inhibited by the high metal concentrations or restricted by the lack of organic substrates.

The consistent detection of the Zn-bearing minerals hetaerolite (μ -XRD and μ -XANES) and hydrozincite (μ -XANES) in multiple spot analyses suggests that a significant proportion of Zn in these samples is structurally sequestered. These mineralogical data, coupled with 20 years of water monitoring showing consistent removal of dissolved Zn along the stream flow path, suggest that attenuation of Zn is an ongoing, stable process at No Cash Creek. (*SS15; Wed. 3:20*)

The role of NW dextral transpressional deformation on magma ascent and associated porphyry style alteration-mineralization in Daralu-Hanza area, Kerman copper belt, SE Iran

Ghorbani, M.A., Ghorbanite@gmail.com, Alirezaei, S. and Alimohammadi, M., Faculty of Earth Sciences, Shahid Beheshti University, Tehran, Iran, PO Box 15875-4731

The Cenozoic Urumieh-Dokhtar Magmatic Belt (UDMB) in west-central Iran is interpreted to be a subduction-related magmatic arc formed by the northeastward subduction of the Neotethyan oceanic plate underneath Central Iranian microcontinent. The UDMB is a linear belt of intrusive, extrusive and subordinate sedimentary rocks, thrust northeastward onto the associated retroarc/retroforeland deposits, and transected by a number of right-lateral strike-slip faults. The belt evolved from an island arc setting in late Cretaceous-Paleocene into a continental, subduction-related setting in Eocene-Miocene, and into a collisional setting in late Miocene-Quaternary where most Porphyry Copper Deposits (PCDs) formed. Most known PCDs in the UDMB occur in the southern section of the belt in the Kerman province, also known as "Dehaj-Sardoieh belt", or "Kerman Copper belt" (KCB). NW-SE trending, orogen-parallel structures that bound KCB are the most significant structures in the area. The present dextral transpressional deformation in the area corresponds to the structures responsible for the emplacement of porphyries.

The Daralu, Sarmeshk, and Bondar-Hanza PCDs in the southern section of the KCB occur in a NW-SE trending fault zone, 15 kilometers long, characterized by a series of granodiorite to quartz-diorite and tonalitic shallow intrusions intruded into Paleocene-Eocene volcanic-sedimentary rocks. Besides the three known PCDs, the fault

zone also embraces several other alteration-mineralization spots, some with signatures of PCDs, as indicated by Aster imagery and follow-up field works.

Strike-slip NW-SE trending faults, the most important structural features, are intersected and displaced by NE-SW trending faults that appear to be the second most significant structural features in the area. The NW-SE trending faults are dextral strike-slip with a compressional component that lead to a transpressional deformation system, as supported by the regional deformation patterns. It is also evident that the alteration-mineralization assemblages in area along of the main fault zone are affected by it and in fact the NW-SE trending structures appear to be the main structural controls over alteration and mineralization in the area. The NE-SW trending faults are associated with sinistral strike-slip displacements.

Dextral transpressional deformation seems to be the dominant deformation pattern in this part of the KCB, and possibly throughout the belt, and has played a major role in the emplacement of magma to high levels to produce the porphyry-style alteration-mineralization. Moreover, the occurrence of such extensional locations in such deformation systems with compressional components (transpressional), requires a special geometric array like fault steps, oversteps and fault intersections. (*SS23; Thurs. Poster*)

Plenary Address: The science and the discovery of volcanogenic massive sulfide deposits

Gibson, H.L., Department of Earth Sciences, Laurentian University, 935 Ramsey Lake Road, Sudbury, ON P3E 2C6

Volcanogenic massive sulphide (VMS) deposits formed at or immediately below the seafloor in spatial, temporal and genetic association with volcanism. They represent a significant source of Cu, Zn, and Pb; Au, Ag, as well other elements (e.g. Sn, In), are common by-products. A total of 155 VMS deposits have been mined in Canada and most of these are Archean and Paleoproterozoic in age. The episodic distribution of VMS deposits from the Paleoproterozoic onwards has been linked to periods of supercontinent assembly and the preferential preservation of arc environments during accretionary events (e.g. Nuna and VMS deposits of the Trans-Hudson orogen).

VMS deposits are, perhaps, the most thoroughly researched deposit type. Since recognition of their syngenetic origin in the mid-1950s and the discovery in 1979 of actively forming VMS deposits on the seafloor, ancient deposits and their modern seafloor analogues have been the focus of decades of intensive geological, geochemical, isotopic and geochronological research. This has resulted in the development of arguably one of the best genetic models for any deposit type, which along with the relatively high value and multi-metal nature of their ores has, up until the mid 90's, fuelled exploration for this deposit type. Exploration criteria and strategies have changed as the genetic model for these deposits continuously evolved over the last hundred years. In Canada, for the period from 1900 to present, distinct lows in VMS discovery rates correspond to periods of low metal prices (recessions) and less exploration. Most pre-1950 discoveries are attributed to prospecting using exploration criteria based on an epigenetic model. New technologies, particularly the onset of commercial airborne electromagnetic surveys in the 1950s to 60s, and subsequent new technologies (e.g. Input AEM in the 70s) resulted in a significant increase in the discovery rate. Smaller peaks followed widespread adoption of a syngenetic model in the 1970s and refinements to that model from research done on modern seafloor analogues. This is particularly true for exploration in established mining districts where continued discovery, often at increasingly greater depths, was guided by exploration criteria based on a refined syngenetic model coupled with the use of new technologies (borehole EM, lithgeochemistry). The steady decrease in VMS discovery rate since the mid 1970s and, in particular, since the mid 1990s reflects, in part, the challenges resulting from increasing depth of discovery, the extensive surficial cover of shield areas, and a shift by many primary base metal companies to explore for larger deposit types that are more amenable to open pit mining operations. Increasing energy costs and environmental concerns



associated with open pit mining may refocus exploration efforts on VMS deposits. However, future exploration will require new criteria based on the seamless integration of the geological, geophysical and geochemical attributes of a VMS ore system into a predictive, holistic model. (SS24; Fri. 11:20)

Regional stratigraphy and sedimentology of the Belly River Group (Campanian) in southwestern Saskatchewan, Canada

Gilbert, M.M., Buatois, L. and Renaut, R., University of Saskatchewan, 114 Science Place, Saskatoon, SK S7N 5E2, mmg163@mail.usask.ca

The Belly River Group comprises an eastward thinning paralic to non-marine Campanian clastic succession in the Western Canadian Sedimentary Basin. Three formations are formally recognized in the western Canadian Plains. In ascending order, these are the Foremost (paralic to non-marine), Oldman (alluvial to paralic), and the Dinosaur Park (alluvial, estuarine, and paralic) formations. Each formation is bound by a disconformity, and presents distinctive sedimentologic attributes and petrographic signatures reflecting tectonic control of sediment supply. The Foremost Formation interfingers with the underlying marine Lea Park Formation, and records a time of overall regression. Maximum regression of the Western Interior Seaway is displayed in the Oldman Formation, with the transgressive Dinosaur Park interfingering with sediments of the overlying marine Bearpaw Formation.

Regional surface and subsurface correlation of the Belly River Group confirms its presence throughout southwestern Saskatchewan. Outcrops of Belly River Group age, particularly along the South Saskatchewan River, have yielded vertebrate fossil remains which present significant paleoecological implications. Placing these deposits within a formational framework has yet to be explored thoroughly. Therefore, further paleoenvironmental analysis of these deposits and careful evaluation of their correlation with more inland Alberta outcrops, particularly those of Dinosaur Provincial Park, will be essential to understand the stratigraphic architecture of the Belly River Group. (SS13; Thurs. Poster)

Mineralogy and styles of barite-rich Zn-Pb-Ba-Ag-Au mineralization in the Lemarchant volcanogenic massive sulfide (VMS) deposit

Gill, S.B.¹, s.gill@mun.ca, Piercey, S.J.¹, Devine, C.A.², and Copeland, D.A.³, ¹Memorial University of Newfoundland, St. John's, NL; ²Canadian Zinc Corporation, St. John's, NL; ³Consulting Geologist, St. John's, NL

The Zn-Pb-Ba-Ag-Au Lemarchant volcanogenic massive sulfide (VMS) deposit is a recently discovered Kuroko-style VMS deposit located in the Central Mobile Belt, Newfoundland. The deposit has a geological resource (NI43-101 compliant) of 2.58 Mt at 0.49% Cu, 4.51% Zn, 1.01% Pb, 54.62 g/t Ag, and 1.00 g/t Au. Characteristic of the deposit is an upper barite-rich zone that contains abundant sulfides, sulfosalts, and anomalous precious metals. Notably, while much of the barite is massive, bladed aggregates of barite are locally observed. The ore mineral assemblage in this zone consists of barite, abundant low-Fe (white-yellow) sphalerite, and Pb-Sb-Ag-As-bearing sulfosalts, including tennantite, tetrahedrite, friebertite, bournonite, and jamesonite, that are intergrown with bornite, galena, and chalcocite. Elevated Au values are associated with the barite-rich layer. Although minor visible free gold is present in the barite of some drill holes, Au is rarely observed and exists either sub-microscopically or as inclusions in other ore minerals such as pyrite and arsenopyrite. Silver occurs primarily in tetrahedrite, and as stromeyerite associated with bornite and barite.

Observed precious metal and mineral associations indicate that deposition within the barite-rich mineralization was likely from low temperature (<300°C) hydrothermal fluids. The barite layer may have influenced the anomalously high Au-Ag grade found at Lemarchant, acting as an insulator or chemical trap when the system was active to prevent dissipation of Au-Ag in hydrothermal fluid. The presence of

large, tabular barite crystals associated with precious metals suggests fluid boiling at shallow water depths (<1500m). Further detailed mineralogical, mineral chemistry, sulfur isotope, and thermodynamic calculations are required to better understand the setting of mineralization at Lemarchant. (SS7; Wed. Poster)

The MacLellan Au-Ag deposit, Lynn Lake, Manitoba: Characterization of host rock lithologies using field relationships, petrography, and lithogeochemistry

Glendenning, M., glendenm@uwindsor.ca, Gagnon, J., Polat, A., Department of Earth and Environmental Sciences, University of Windsor, Windsor, ON N9B 3P4

Studies of the MacLellan Au-Ag deposit Main Zone, situated north east of the town of Lynn Lake Manitoba, have identified the mineralization as either: 1) syngenetic, stratiform and exhalative in origin, and hosted by intercalated ultramafic and mafic flows, sulphidic siltstones, and iron formation; or 2) epigenetic, variably-deformed, sulphide-bearing, quartz veins and replacement bodies with associated biotite ± garnet alteration, hosted within mafic to ultramafic metavolcanics. Consequently, provenance of the primary host rock to the Au-Ag mineralization remains equivocal and the entire host rock sequence is relatively poorly characterized. Presently, it is unclear whether host rocks to the Au-Ag mineralization within the MacLellan deposit and related occurrences represent primary lithologies or are altered mafic or ultramafic metavolcanics, and their petrogenesis and geodynamic environment of emplacement are undetermined. Accordingly, extrapolating beyond the immediate vicinity of the MacLellan Au-Ag deposit and associated occurrences for the purpose of identifying other potential environments of 'MacLellan-style' mineralization along the remainder of the North Belt of the Lynn Lake greenstone belt is currently impossible. Furthermore, lack of a petrogenetic and geodynamic model prevents correlation with rocks on a larger scale.

Preliminary results indicate that there are three primary lithologies within the MacLellan deposit host rock sequence: 1) amphibole-plagioclase schist, which can be geochemically classified as island arc basalts and gabbros and are characterized by hornblende, actinolite, and partially sericitized plagioclase; 2) biotite-plagioclase schist, which can be geochemically classified as island arc basalts and gabbros and are characterized by biotite, partially sericitized plagioclase, and minor amounts of quartz; and 3) amphibole-chlorite schist, which can be geochemically classified as picrites and are characterized by hornblende, actinolite, and chlorite with minor quartz. Least altered mafic metavolcanic units are characterized by low loss on ignition values, very minimal or lack of calcite and quartz and a Ce/Ce* value between 0.9 and 1.1. Immobile element discrimination diagrams indicate that the geochemical character of the metavolcanic units were erupted in an arc setting. A number of secondary alteration types have been identified including silicification, carbonatization, biotitization, sericitization, and garnet associated with metamorphism. (GS2; Wed. Poster)

Bow City, Alberta: A possible new impact structure?

Glombick, P.¹, paul.glombick@ercb.ca, Schmitt, D.R.², Xie, W.² and Bown, T.D.², ¹Alberta Geological Survey, #402, 4999 - 98 Ave, Edmonton, AB T6B 2X3; ²Department of Physics, CCIS 4-183, University of Alberta, Edmonton, AB T6G 2E1

A semi-circular structure, approximately 8 km in diameter with a central uplifted region, has been discovered in the shallow subsurface of southern Alberta. Geophysical well log data from oil and gas wells were used to map the internal stratigraphy and structure of the Belly River Group as well as underlying Cretaceous strata. Structure maps indicate the overall geometry of the structure is semi-circular with a central uplifted region surrounded by a semi-circular depression, or annulus. Isopach maps indicate localized thickening and thinning within the Belly River Group and underlying Pakowki Formation. Local repetition or removal of strata was identified using well log correlation. The difference in elevation between the central uplift and annulus decreases with increasing structural depth. Analysis of legacy



2D seismic data in the area confirms the geometry modelled using well data and reveals a series of normal faults within the annulus. Contorted bedding, faulting, and anomalously steeply dipping bedding were confirmed in outcrop. The maximum age constraint on the structure is estimated at *ca.* 70 Ma, based on the preservation of rocks of the lowermost Horseshoe Canyon Formation within the annulus. (**SS16; Wed. Poster**)

Geothermobarometry of spinel peridotites from southern British Columbia: Implications for the thermal conditions in the upper mantle

Greenfield, A.-M.R., Ghent, E.D., Dept. of Geoscience, U. of Calgary, Calgary, AB T2N 1N4, ghent@ucalgary.ca, and Russell, J.K., Department of Earth & Ocean Sciences, University of British Columbia, Vancouver, BC V6T 1Z4

Geothermobarometry of spinel peridotites from southern British Columbia: implications for the thermal conditions in the upper mantle. Spinel lherzolite xenoliths within alkali basalt volcanic rocks exposed at Rayfield River and Big Timothy Mountain, south-central British Columbia represent samples of the underlying lithospheric mantle. Electron microprobe analysis shows that most xenoliths comprise compositionally homogeneous grains of olivine, orthopyroxene, clinopyroxene and spinel. We applied the following geothermometers: orthopyroxene-clinopyroxene, spinel-orthopyroxene, and spinel-olivine to these rocks. Temperatures calculated using the Brey and Köhler calibration of two-pyroxene thermometry were constrained in pressure by being required to lie on a model geotherm developed for this region of B.C. following the methods of Harder and Russell. The geotherm is constrained to produce a temperature at the Moho (33 km) of $825 \pm 25^\circ\text{C}$ in order to match the lowest temperature peridotite xenoliths recovered in this study. The simultaneous solution of the model geotherm and the pressure-dependent Brey-Köhler two-pyroxene thermometry removed the need for adopting an arbitrary pressure - although the overall effect of pressure on the temperature calculations is negligible ($\sim 2^\circ\text{C}$ for 100 MPa). We take these temperatures to represent peak mantle lithosphere temperatures. Fourteen Rayfield River xenoliths return average two-pyroxene temperatures between 841 and 961°C corresponding to depths of 34-42 km. Orthopyroxene-spinel and olivine-spinel results are $889 \pm 60^\circ\text{C}$ and $825 \pm 88^\circ\text{C}$, respectively. Five Big Timothy xenoliths have two-pyroxene temperature that span 840 to 1057°C (Mean $970 \pm 64^\circ\text{C}$) corresponding to depths of 34-48 km. Orthopyroxene-spinel and olivine-spinel temperatures are $844 \pm 63^\circ\text{C}$ and $896 \pm 232^\circ\text{C}$, respectively. We argue that this range in temperatures does not represent closure temperatures imposed during cooling either in the mantle or during transport by the lavas. The temperature ranges are due to differences in calibration of the geothermometers or lack of equilibration in exchange reactions in dry rocks. Isochemical phase diagrams (pseudosections) constrain the P-T field in which spinel is stable. These diagrams suggest that the spinel assemblage was stable at pressures ranging from approximately 9.6 to 14 kbar (10 kbar = 1 GPa). (**GS2; Wed. Poster**)

Isotopic constraints on the source of pegmatites with boron and beryllium minerals in the Larsemann Hills, Prydz Bay, Antarctica

Grew, E.S.¹, esgrew@maine.edu, Maas, R.² and Carson, C.J.³,
¹University of Maine, 5790 Bryand Center, Orono, ME 04469, USA; ²University of Melbourne, Parkville, VIC, 3010, Australia;
³Geoscience Australia, PO Box 378, Canberra, ACT, 2601, Australia

The Brattstrand Paragneiss, a highly deformed Neoproterozoic granulite-facies metasedimentary sequence, is cut by three generations of ~ 500 Ma pegmatite. The earliest recognizable pegmatite generation, synchronous with D_{2-3} , forms irregular pods and veins up to a meter thick, which are either roughly concordant or crosscut S_2 and S_3 fabrics and are locally folded. Pegmatites of the second generation, D_4 , form planar, discordant veins up to 20-30 cm thick, whereas the youngest generation, post- D_4 , form discordant veins and pods. The D_{2-3} and D_4

pegmatites are abyssal class (BBc subclass) characterized by tourmaline + quartz intergrowths and boralsilite ($\text{Al}_{16}\text{B}_6\text{Si}_2\text{O}_{37}$); the borosilicates prismatine, grandidierite, werdingite and dumortierite are locally present. In contrast, post- D_4 pegmatites host tourmaline (no symplectite), beryl and primary muscovite, *i.e.*, beryl subclass of the rare-element class. Spatial correlations between B-bearing pegmatites and B-rich units in the host Brattstrand Paragneiss are strongest for the D_{2-3} pegmatites and weakest for the post- D_4 pegmatites, suggesting that D_{2-3} pegmatites may be closer to their source.

Initial $^{206}\text{Pb}/^{204}\text{Pb}$ and $^{207}\text{Pb}/^{204}\text{Pb}$ and $^{208}\text{Pb}/^{204}\text{Pb}$ ratios, measured in acid-leached alkali feldspar separates, vary considerably (17.71 – 19.97 , 15.67 – 15.91 , 38.63 – 42.84), forming broadly linear arrays well above global Pb growth curves. The D_{2-3} pegmatites contain the most radiogenic Pb while the post- D_4 pegmatites have the least radiogenic Pb; data for D_4 pegmatites overlap with both groups. The near-linear trends are interpreted in terms of two source components. Component 1 contains very radiogenic Pb and most likely represents old upper crust with high U/Pb and very high Th/Pb. Component 2 has a distinctive high-207/low-206 signature which evolved through dramatic lowering of U/Pb in crustal protoliths during the Neoproterozoic granulite-facies metamorphism. Component 1, represented in the locally-derived D_{2-3} pegmatites, could reside within the Brattstrand Paragneiss which contains a unit (Tassie Tarn Metaquartzite) with very high U/Pb and Th/Pb and detrital zircons up to 2.1 Ga old. Pb isotope component 2, represented in the “far-from-source” post- D_4 pegmatites resembles the Pb in Cambrian granites intrusive into the Brattstrand Paragneiss suggesting either they share the same or similar source, or that the post- D_4 pegmatites are differentiates of the Cambrian granites. (**SY2; Thurs. 10:20**)

Hydrogen in the Gugiaite Structure

Grice, J.D., Canadian Museum of Nature, PO Box 3443 Stn D, Ottawa, ON K1P 6P4, and Kristiansen, R., PO Box 32, N-1650 Sellesbakk, Norway

The Larvik Plutonic Complex (LPC) occupies the 50 km long and 20 km wide area in Norway between the Oslofjord in the east and the Langesundsford in the west and is the southern part of Oslo rift, which was formed by intracontinental magmatic activity in late Carboniferous and early Permian time. The LPC, and especially its western district, hosts a large number of pegmatites, penetrating the huge larvikite quarries, which are quarried for ornamental stone, an extensive export product. Some of the pegmatites show a rich assemblage of rare and unique minerals. The pegmatites in the LPC are unique in its extreme enrichment of late stage beryllium minerals, mainly silicates, presumably derived from the hydrothermal alteration of the primary Be-silicates leucophanite and meliphanite, and partly the Be-borate hambergite. Sixty-five percent of all Be-minerals known from alkaline rocks and syenite-pegmatites occur in the LPC.

One of the secondary minerals present is hydroxyl-bearing gugiaite (‘hydroxylgugiaite’); discovered in two different locations, approximately 7 km apart. It occurs as small, $\sim 100\ \mu\text{m}$, rod-like, pale yellowish crystals or as white or grey, anhedral grains and rarely as euhedral crystals, with a flattened pillow-shaped tetragonal dipyrmaid form. It is tetragonal $P4_21m$, $a\ 7.415(1)$, $c\ 4.961(2)\ \text{\AA}$, $V\ 272.9(1)\ \text{\AA}^3$ and $Z = 2$. The cell parameters are slightly smaller than gugiaite from other localities and the refractive indices $\omega\ 1.622(2)$, $\gamma\ 1.632(2)$ are lower. The chemical composition of ‘hydroxylgugiaite’ differs from gugiaite from the type locality in China. The average empirical formula is: $(\text{Ca}_{1.3\pm0.7})(\text{Si}_{0.9}\text{Be}_{0.1})(\text{Be}_{1.2}\text{Si}_{0.8})[\text{O}_5(\text{OH})_2]$ vs. ideal $\text{Ca}_2\text{BeSi}_2\text{O}_7$.

Crystal quality is poor with diffuse diffraction spots, but one data set refined to $R = 0.03$. The incorporation of H into the structure has interesting consequences. It partially occupies the Ca site. As there is only one O site that has an unshared vertex this is the only one suitable for the addition of a bonded H atom. Bond-valence compensation requires the OH to be part of a tetrahedron centred essentially by Be. This requires a reversal of the Be and Si sites from that observed in gugiaite. In ‘hydroxylgugiaite’ the Be site is now a (53) node and the



Si site a (54) node. The Be site (53) node is that found in the planar nets of leucophanite and meliphanite. (SY1; Wed. 2:40)

The structure and crystal chemistry of dumortierite I. A new classification of the dumortierite group as a supergroup

Groat, L.A.¹, groat@mail.ubc.ca, Pieczka, A.², Evans, R.J.¹, Grew, E.S.³, Ma, C.⁴ and Rossman, G.R.⁴, ¹University of British Columbia, Vancouver, BC V6T 1Z4; ²AGH-University of Science and Technology, Kraków 30-059, Poland; ³University of Maine, Orono, ME 04469-5790, USA; ⁴California Institute of Technology, Pasadena, CA 91125-2500, USA

Dumortierite, $c. (Al, \square)Al_6BSi_3O_{16}(OH)_2$, is second only to tourmaline-supergroup minerals as the most abundant B-bearing phase in metamorphosed pelitic and psammitic rocks, aluminous metasomatic rocks and granitic plutonic rocks. Dumortierite is known to incorporate significant quantities of the trace elements Ta, Nb, As and Sb in its structure, which is unusual among silicates in pegmatites and other deposits where these elements are concentrated. Each of these elements are incorporated in the wide (~ 7 Å in diameter) hexagonal channels in the dumortierite structure, with Ta^{5+} , Nb^{5+} replacing Al^{3+} in the face-sharing octahedra coordinating the Al1 site, and $As^{3+}O_3$ and $Sb^{3+}O_3$ groups replacing SiO_4 groups. The As and Sb sites are displaced farther into the channel than the corresponding Si sites to accommodate longer As-O and Sb-O bonds, and in some cases As and Sb are further split into separate sites. Vacancies at the Al1 site are created both by the substitution of Al by (Ta, Nb) in order to maintain charge balance and to separate highly-charged cations, and by the substitution of Si by (As, Sb) where coordinating oxygen atoms are lost due to lone pairs of electrons associated with the As^{3+} and Sb^{3+} cations. Under the recent reclassification of the dumortierite group as a supergroup (approved by the IMA Commission on New Minerals, Nomenclature and Classification, proposal 12-C, November 6, 2012), the newly constituted dumortierite group includes dumortierite, $AlAl_6BSi_3O_{18}$, and magnesiodumortierite, $MgAl_6BSi_3O_{17}(OH)$, as well as six Ti-, Fe- and OH-bearing end-members that are found as subordinate components in dumortierite and magnesiodumortierite.

The mineral holtite, which is largely found in pegmatites, was originally described as the isostructural (Ta, Nb)- and (As, Sb)-rich analogue of dumortierite. Subsequent analyses of dumortierite and holtite from several localities revealed a nearly continuous solid solution between them: $Al_{7-5x-4w-y}^{3+}(Ta, Nb)_xTi_w^{4+}\square_{(2x+w+y)}^{2+}BSi_{(3-y)}^{4+}(Sb, As)_yO_{18-y}$, assuming 1 B per formula unit and negligible OH, which raised the question whether holtite was a distinct mineral. Under the recent reclassification, a newly constituted holtite group comprises holtite, newly defined as $(Ta_{0.6}\square_{0.4})Al_6BSi_3O_{18}$, and two new minerals nioboholtite (IMA 2012-068), $(Nb_{0.6}O_{0.4})Al_6BSi_3O_{18}$, and titanoholtite (IMA 2012-69), $(Ti_{0.75}\square_{0.25})Al_6BSi_3O_{18}$.

A new mineral from the Szklary pegmatite, Lower Silesia, Poland, (As, Sb)Σszklaryite (IMA 2012-070), has $> Si$ and negligible Ta, Nb or Ti, defining a new end-member $\square Al_6BAS^{3+}_3O_{15}$ and a potential szklaryite group within the dumortierite supergroup. (SY1; Thurs. 2:20)

Pegmatitic nepheline syenitic dyke swarm in the Crevier alkaline intrusion (Quebec)

Groulier, P.A., pierre-arthur.groulier9@etu.univ-lorraine.fr, Ohnenstetter, D., Andre-Mayer, A.S., Université de Lorraine, laboratoire GéoRessources, 54000 Nancy, Lorraine, France, Solgadi, F., Moukhsil, A. and El Basbas, A., Bureau de l'exploration géologique du Québec, Ministère des Ressources naturelles du Québec, 400, boul. Lamaque, Val d'Or, QC J9P 3L4

The Crevier alkaline igneous complex is located in the Grenville province, north to the Lac Saint-Jean. The complex follows the Waswanipi-Saguenay corridor, part of the Saguenay graben which hosts the Saint-Honoré (Niobec) Nb-Ta deposit.

The main unit of the Crevier alkaline igneous complex is a massive nepheline syenite cut by dykes of layered nepheline syenite,

ijolite, biotite and biotite-carbonate bearing nepheline syenite, carbonatites and camptonites. Pegmatitic nepheline dykes swarm oriented N320° crosscut both previous units. The Nb-Ta mineralisation is mainly linked to the pegmatite dyke swarm. Detailed mapping of the mineralised dyke swarm show that the dykes are emplaced during dextral shearing, the dykes are generally symmetric with, from the margin fan, shaped large albite and nepheline crystals (up to 30cm long) open toward the centre of the dyke, the central part of the dyke is a medium to fine grained nepheline syenite. Two groups of pyrochlores occur: primary pyrochlores from magmatic events and secondary pyrochlores from hydrothermal process with re-mobilisation of some chemical elements. Large pyrochlores (≥ 1 mm) are associated with late sodalite rich nepheline syenitic veinlets. Magmatic pyrochlores are often associated with Sr bearing fluorapatites, and show always resorption and recrystallisation features which indicating that primary magmatic crystals underwent chemical changes with losses of Na-Ti-Nb and win of F-Si-K-Fe-Mn during interaction with a F rich fluid. The second group of pyrochlores are linked to a network of fractures, they are smallest but more homogeneous than the magmatic ones. They are spatially associated with fluorapatite, iron sulphides, Fe-Ti oxides and sometimes REE rich carbonates. Further geochemical analysis will bring new data on the different magmatic and mineralisation processes. U-Pb dating on zircon on both massive syenite and dyke swarm will bring geochronological constraints and will help to place the intrusion in a geodynamical context. (GS2; Wed. Poster)

Synthesis and energetics of lanthanide and actinide substituted garnet

Guo, X., xguo@ucdavis.edu, Tavakoli, A.H., Shareva, T. and Navrotsky, A., Peter A. Rock Thermochemistry Laboratory, University of California, Davis, CA

The garnet structure is a promising nuclear waste form due to its potential of accommodating various actinide elements. For better understanding of the immobilization mechanism in lanthanide- and actinide-substituted garnet, we have synthesized and studied the thermodynamic stability of yttrium iron garnet substituted with varying Ce and Th contents. Solid state and citrate-nitrate combustion synthesis methods have been used. Formation of the single phase indicate that a charge coupled substitution reaction involving Fe^{3+}/Fe^{2+} facilitates the incorporation of tetravalent cerium and actinide cations. The calorimetric measurements of the samples using oxide melt solution calorimetry demonstrate the stabilizing effect of Ce and Th incorporation into the garnet structure. Future work will be directed along the synthesis and thermodynamic study of U-substituted yttrium iron garnet. (SS5; Wed. Poster)

Crystal chemistry of uranyl selenates

Gurzhiy, V.V., vladgeo17@mail.ru, Krivovichev, S.V., St.Petersburg State University, University Emb. 7/9, 199034 St. Petersburg, Russia, and Tananaev, I.G., Frumkin Institute of Physical Chemistry and Electrochemistry RAS, Leninsky Av. 31-4, 119071, Moscow, Russia

Uranium compounds containing Se are of special importance from the environmental and mineralogical points of view, because ^{79}Se isotope is chemically and radiologically toxic fission product with the half life of 1.1×10^6 years (Burns *et al.*, 1999). In this work, we examine structural relations and systematics for uranyl selenates, i.e. uranyl compounds with tetrahedrally coordinated Se^{6+} cations. Analysis of uranyl selenate structures known at present demonstrates predominance of structural connectivities based upon corner-sharing coordination polyhedra. The most convenient method for the description of such structures is representation of their topologies in terms of bicolored graphs. Within this description, vertices correspond to coordination polyhedra, and the presence of an edge between the neighboring vertices complies with the presence of bridging O atom between the respective coordination polyhedra.



Nowadays, there are more than 100 structures known containing uranyl selenate complexes: 1 based upon finite clusters, 3 frameworks, 3 nanotubules, 25 chains and 77 layered compounds.

In the crystal structures of inorganic uranyl selenates, uranyl selenate complexes are linked via monovalent cations (K^+ , Na^+ , Rb^+ , etc.) or octahedrally coordinated divalent cations ($[Ni(H_2O)_6]^{2+}$, $[Zn(H_2O)_6]^{2+}$, $[Mg(H_2O)_6]^{2+}$, etc.). In the crystal structures of amine-templated uranyl selenates, structure formation is regulated by hydrogen bonding systems and by arrangement of hydrophobic and hydrophilic parts of molecules with voids and dense fragments of inorganic complexes. The basic structural principle of organic-inorganic uranyl composites templated by electroneutral molecules (such as crown ethers), is the translation of interactions between organic and inorganic components by means of protonated water molecule complexes (e.g., $H_3O_2^+$ and H_3O^+).

This work was supported by RFBR (grant 12-05-31344), Saint-Petersburg State University through the internal grant 3.37.84.2011. XRD study was carried out in the X-ray Diffraction Centre of St.Petersburg State University (*SS5; Thurs. 9:00*)

Regional deposition of giant deep-water carbonate seep mounds in the Mesoproterozoic Borden Basin (NU)

Hahn, K.E. and Turner, E.C., Department of Earth Sciences, Laurentian University, Sudbury, ON, kx_hahn@laurentian.ca

The Mesoproterozoic Borden Basin (NU) contains unusual deep-water carbonate rocks. Isolated dolostone mounds of the Ikpiarjuk Formation in the lower Bylot Supergroup are kms in diameter, hundreds of m thick, enclosed by 1.1 Ga black shale (Arctic Bay Formation), and centred over, and elongate parallel to, basin-scale, syndepositionally active faults. The mounds accumulated below storm wave-base and below the photic zone and are characterised by an unusual clotted texture. Ikpiarjuk Formation mounds faithfully record the chemistry of the seawater from which they were precipitated. Solution and *in situ* laser-ablation ICP-MS analysis of samples from a variety of lithofacies show normal Proterozoic REE patterns. All mounds formed in the anoxic zone of a stratified water column, which is evident in consistent, positive Ce anomalies throughout the basin and vertically through the mounds. Negative Eu anomalies toward the tops of mounds suggest that the basin became restricted late in the mounds' depositional history. Although carbonate buildups formed by seepage of groundwater or other fluids are not rare in the rock record, there are currently no other documented examples of Proterozoic seep-related carbonate mounds that formed in such deep-water, sub-photoc conditions. Phanerozoic seep deposits generally consist of carbonate buildups no larger than a few m thick, and commonly contain complex bacterial and metazoan communities that lived off the seep fluids. The Ikpiarjuk mounds probably formed through a combination of water-column and benthic precipitation that may have been mediated by a chemosynthetic microbial community. (*SS1; Fri. 2:20*)

Economic potential of Red River strata in Saskatchewan: Drilling deeper for additional resources

Haidl, F.M., Jensen, G.K.S. and Yang, C., Saskatchewan Ministry of the Economy, 201 Dewdney Avenue East, Regina, SK S4N 4G3, fran.haidl@gov.sk.ca

As of September 1, 2012, Red River reservoirs in southeastern Saskatchewan have yielded 4.14 million cubic metres (26 million bbls) of oil from 202 wells. These Upper Ordovician rocks, however, remain under-explored in this area.

Red River rocks in the Williston Basin are remnants of strata deposited in warm shallow seas that covered much of the North American craton during the Late Ordovician. In southeastern Saskatchewan these rocks are subdivided into the Yeoman Formation and the overlying Herald Formation. The Yeoman Formation is composed primarily of burrow-mottled fossiliferous lime mudstones and wackestones which have undergone varying degrees of dolomitization. The Herald Formation is composed of limestones, dolostones, and evaporites and is subdivided into, in ascending order,

the Lake Alma and Coronach members and the Redvers unit. It is difficult to consistently define the boundary between the Yeoman and the Lake Alma due to the variability of "transitional" facies that are found between the laminated to thinly-bedded, commonly argillaceous dolomudstones in the basal Lake Alma and burrow-mottled Yeoman strata. Oil is produced from dolomudstones in the Lake Alma Member of the Herald Formation, burrow-mottled dolostones in the upper one-third of the Yeoman Formation and from dolomitized "transitional" facies.

Precambrian basement structure played a major role in the development of Red River reservoirs and trapping mechanisms. Precambrian paleotopography associated with NW- and NE-trending structures controlled deposition of Deadwood strata as reflected in the NE and NW alignment of areas of thin to zero Deadwood strata. Subsequent differential compaction of these sediments coupled with episodic movement of basement structures in the Phanerozoic controlled Red River facies distribution and formation of low-relief small structural closures in which most Red River oil is trapped.

Complex dolomitization patterns often result in interbedding of dolostone reservoirs and non-reservoir limestones in producing areas. In addition, lateral and vertical variations in dolomitization create the potential for stratigraphic traps and for combined structural stratigraphic traps.

Use of 3-D seismic and horizontal well technology facilitates exploration for and development of these complex Red River reservoirs associated with small structures. (*SS13; Thurs. Poster*)

Keynote (40 min): Neoproterozoic record of Rodinia breakup, eukaryotic evolution, and biogeochemical change in Yukon, Canada

Halverson, G.P.¹, galen.halverson@mcgill.ca, Macdonald, F.A.², Kunzmann, M.¹, Strauss, J.V.², Théou-Hubert, L.¹ and Cox, G.¹, ¹McGill University, Montreal, QC H3A 2A7; ²Harvard University, Cambridge, MA, 02138 USA

Recent mapping, chemostratigraphy, geochronology, and sequence stratigraphic analysis of Neoproterozoic strata in Yukon, Canada have helped to elucidate the timing and geometry of basin formation related to Rodinia break-up in northern Laurentia. In the Coal Creek and Hart River inliers, the early Neoproterozoic Fifteenmile Group unconformably overlies the Pinguicula Group. The lower Fifteenmile Group (Gibben and Chandindu formations) is highly variable in thickness and fills half-grabens that originated during ca. 830 Ma continental extension, perhaps related to emplacement of the Guibei and Willouran large igneous provinces in neighboring China and Australia. The lower Fifteenmile Group is equivalent to the Hematite Creek and Katherine groups in the Wernecke Mountains. The upper Fifteenmile Group (Reefal assemblage and Craggy dolostone) represents a dominantly thermal phase of subsidence, intermittently interrupted by localized extension. The Reefal assemblage preserves NNW-prograding stromatolitic reef tracts developed over relic bathymetric highs and is geochronologically constrained by a U-Pb zircon age of 811 Ma near the top of the formation. Equivalent strata in the Tatonduk inlier, on the Alaska-Yukon border, contain the earliest known biomineralizing microfossils. The Reefal assemblage correlates with the Basinal assemblage of the basal Little Dal Group in the Wernecke and Mackenzie mountains. This correlation, coupled with the new chemostratigraphic and radiometric data permit a more accurate calibration of early Neoproterozoic carbonate and strontium isotope records. The Craggy dolostone, which is found only in the Coal Creek inlier, records establishment and progradation of a broad carbonate platform that was subsequently uplifted and beveled prior to deposition of the Callison Lake dolostone. This distinct unit is present only in the Coal Creek and Hart River inliers, where it comprises mostly stromatolitic carbonates, but also contains shaley intervals with sedimentary talc. Development of deeper water facies along the southern margin of the Coal Creek and Hart River inliers suggest the onset of N-S extension, presaging significant block faulting and 717 Ma volcanism associated with the overlying Mount Harper Group. The



Callison Lake dolostone is missing in the Wernecke Mountains, where an angular unconformity formed during the Corn Creek orogeny juxtaposes the lower Little Dal Group and middle Cryogenian strata. Correlation of underlying and overlying strata between Yukon and the Northwest Territories indicates that the Callison Lake dolostone occupies the same stratigraphic position as the Coates Lake Group in the Mackenzie Mountains. The roughly coeval occurrence of extension at this time suggests a transtensional-transpressional regime in northwest Canada *ca.* 720 Ma, at the same time that the Franklin large igneous province was emplaced. The full separation of northwest Canada from Rodinia did not occur until the late Ediacaran or early Cambrian, consistent with early Paleozoic subsidence records in the Cordillera. (*SY4; Fri. 9:20*)

Andalusite-bearing supracrustal rocks reveal insights into early Paleoproterozoic metamorphism and deformation on Cumberland Peninsula, eastern Baffin Island, Nunavut

Hamilton, B.M.¹, brett.hamilton@ucalgary.ca, Sanborn-Barrie, M.², Rayner, N.², Pattison, D.R.M.¹, Berman R.G.² and Young, M.D.³, ¹University of Calgary, 2500 University Dr. NW, Calgary, AB T2N 1N4; ²Geological Survey of Canada, 601 Booth Street, Ottawa, ON K1A 0E8; ³Dalhousie University, Edzell Castle Circle, Halifax, NS B3H 4J1

Supracrustal rocks of the Paleoproterozoic Hoare Bay group on Cumberland Peninsula preserve three metamorphic domains. There is a broad region of upper-amphibolite-facies rocks; local domains of granulite-facies assemblages adjacent to Qikiqtarjuaq plutonic suite intrusions; and a 120 by 15 km corridor of middle-amphibolite-facies rocks designated the Touak-Sunneshine metamorphic low (TSMML). The TSMML contains muscovite+sillimanite metapelite with the prograde growth sequence staurolite, andalusite, followed by sillimanite, which required a low-pressure pressure-temperature path that transected the staurolite+andalusite stability field at 3.3-4.1 kbar and approximately 560°C.

Three generations of tectonic structures are recognized in the TSMML. An early fabric (S₁), only visible in thin sections, is represented by aligned inclusions in porphyroblasts. The dominant schistosity (S₂), which is axial planar to open to isoclinal F₂ folds, is folded by approximately coaxial, outcrop- and map-scale F₃ folds.

Andalusite porphyroblasts are typically wrapped by S₂ and include a tectonic fabric that is straight in the core (S₁) and rarely curves at the rim (S₂). These microstructures indicate that the growth of andalusite cores post-dated D₁ and the growth of rims was synchronous with early D₂, but D₂ continued after andalusite growth ceased. Sillimanite defines a mineral lineation (L₂) in several localities in the TSMML supporting pre- to syn-D₂ sillimanite growth; however, outcrops with both andalusite and a mineral lineation are rare. Given that D₂ took place predominantly at sillimanite-stable conditions, it appears that andalusite only persisted in rocks that accumulated relatively little D₂ strain.

Andalusite-bearing rocks contain metamorphic monazites with ages that represent the oldest Paleoproterozoic monazite population from Cumberland Peninsula. One sample contains monazite as inclusions within andalusite and garnet that yielded a ²⁰⁷Pb/²⁰⁶Pb age of 1890±7 Ma. A nearby sample contains monazite inclusions in andalusite and S₁-parallel inclusions in garnet with an age of 1893±10 Ma, in addition to an 1880±8 Ma population that incorporates one S₂-parallel matrix grain. These age populations overlap with *ca.* 1.90-1.88 Ga U-Pb zircon ages from the Qikiqtarjuaq plutonic suite consistent with low-pressure metamorphism resulting from the advection of magmatic heat into the mid-crust. Deformation causing the development of a penetrative fabric in Hoare Bay group rocks appears to have been underway by 1893±10 Ma and this is thought to reflect the development of a compressive continental arc. Elsewhere on Cumberland Peninsula, Paleoproterozoic metamorphism and penetrative deformation are dated at *ca.* 1860 Ma, and thought to be a result of Trans-Hudson continental collision. (*SS1; Fri. 11:00*)

On the crystal structure of UK 79, a potentially new mineral from Mont Saint-Hilaire, QC

Haring, M., mx_haring@laurentian.ca, and McDonald, A.M., Department of Earth Sciences, Laurentian University, 935 Ramsey Lake Road, Sudbury, ON P3E 2C6

UK79 is a potentially new mineral discovered in vugs within sodalite syenite xenoliths. The mineral occurs in slightly radiating bundles of acicular crystals (avg. dimensions: 0.006 × 0.011 × 0.51 mm) associated with aegirine, eudialyte, nepheline, natrite, pyrrhotite and natrolite. UK79 crystallizes in the P-1(#2) with a 6.837(1), b 7.575(2), c 8.841(2) Å, α 99.91(3), β 102.19(3), γ 102.78(3)°, V 424.81(1) Å³, and Z = 4. The crystal structure of UK 79 was solved and refined to R = 1.69% for 2409 reflections (Fo > 4σFo). It contains one unique Na and B site, two Mn sites, and three Si sites. The SiO₄ tetrahedra are linked through shared corners to two adjacent SiO₄ tetrahedra to form single silicate chains. These silicate chains are linked through shared corners to BO₂(OH)₂ tetrahedra, forming single loop-branched silicate chains. These loop-branched silicate chains are linked through shared corners to bands of edge sharing MnO₆ octahedra, which share (OH) groups with the BO₂(OH)₂ tetrahedra. A series of channels, perpendicular to [100], result from the linkages between the loop-branched silicate chains and the MnO₆ bands are occupied by Na. UK79 has crystal structural similarities to scheuchzerite (Na(Mn,Mg)₉[VSi₉O₂₈(OH)](OH)₃) and saneroite (Na₂(Mn,Fe)₁₀(Si,V)₁₁O₃₄(OH)₄). All three minerals are single chain silicates, where the silicate chains in UK79 are loop-branched: scheuchzerite contains silicate chains with loop branches as well as open-branches, and saneroite contains silicate chains with open-branches. In the crystal structures of UK79, scheuchzerite, and saneroite, the silicate chains are linked together by bands of edge sharing MnO₆ octahedra. In all three mineral structures, bands of MnO₆ octahedra occur in alternating layers with the silicate chains, generating channels that are occupied by Na. Loop-branched silicate chains are more prevalent in minerals with large proportions of highly electronegative cations (*i.e.*, V, Nb, Zr, B). The presence of highly electronegative cations in a crystal structure reduces repulsion between SiO₄ tetrahedra resulting in shrinkage and bending of the silicate chain. The bends in the silicate chain may be bridged by an electronegative cation or additional SiO₄ tetrahedra. In the case of UK 79, which formed in an Si - poor environment, a BO₂(OH)₂ tetrahedra instead of SiO₄ bridges the bends in the silicate chain. (*SY1; Wed. 3:00*)

New REE discoveries at Great Western Minerals Group's Hoidas Lake property, northwest Saskatchewan

Harper, C.T.¹, ctharpergeology@gmail.com, Pandur, K.² and Pearson, J.G.³, ¹Harper Geological Consulting & Exploration, 2411 Cross Place, Regina, SK S4S 4C8; ²Department of Geological Sciences, University of Saskatchewan, Saskatoon, SK S7N 5E2; ³Great Western Minerals Group Ltd., 219 Robin Cres., Saskatoon, SK S7L 6M8

Great Western Minerals' Hoidas Lake REE property, located 60 km northeast of Uranium City, lies within the northeastern Zemplak Domain, 5 km west of Black Bay Fault, which marks the boundary between Zemplak and Train Lake domains. The major rock units include a tonalite gneiss complex of probable Archean age and granitic gneisses, mainly of Paleoproterozoic age. Minor rock units include: migmatitic metasedimentary gneisses, intermediate to mafic amphibolites, diorites, syenite, hyalophane-bearing pegmatites, unmineralized diopside-hyalophane veins and their REE mineralized forms, and lamprophyre dykes. The last four rock units have an alkaline magmatic affinity.

Concurrent radiometric prospecting helped discover several new REE showings, hosted in amphibolite, diorite, tonalite and granitic gneisses in three areas: (1) the amphibolite showings, (2) Hoidas North, and (3) New Hoidas South Showings. The amphibolite showings are predominantly diopside-allanite-hyalophane ±barite veins occupying northerly and westerly structures with grades locally up to 16.166% total rare earth elements (TREE). The Hoidas North showings occur in three parallel NE-trending zones comprising red and green apatite



breccias with allanite veins and intergrowths. The northwestern-most zone was traced for 110 m along strike and over a width of at least 6 m. Apatite breccia samples typically contain 3 to 5% TREE, and massive allanite samples up to 12% TREE. At Hoidas South three new showings, all beneath 30 to 40 cm of till, were found southeast and southwest of the original showing. They are predominantly coarse red apatite breccia, with up to 5% TREE. Geochemically, all showings are light REE dominant at >95% of TREE, and importantly Nd accounts for 17 to 27% of TREE. Apatite breccias have anomalous Y and HREE.

The REE mineralization truncates *ca.* 1970-1940 Ma composite D₁-D₂ foliation and *ca.* 1910-1900 Ma peak metamorphic mineral assemblages, but is locally affected by lower grade D₃ deformation associated with northeast shear zone (mylonitic) development. The mineralization predates emplacement of *ca.* 1820 Ma lamprophyre dykes, providing a narrow window for REE development. The growing evidence at Hoidas is that the complex REE mineralization originated from a pegmatitic-like alkaline/carbonatitic magmatic-hydrothermal system enriched in Ca, PO₄, Sr, Ba, REE, and F. This is further supported by presence of syenite, hyalophane pegmatites and lamprophyres. These enriched magmas and fluids used structural pathways associated with the Nisikkatch – Hoidas Shear Zone to be emplaced as pegmatitic-like diopside-hyalophane REE veins with their associated wall rock alteration. (*SS6; Wed. 10:20*)

Remote predictive mapping – Progress in geological mapping in Canada's North

Harris, J.R.¹, Russell, H. and Percival, J., Geological Survey of Canada, 601 Booth St, Ottawa, ON K1A 0E8, harris@nrcan.gc.ca

Due to its vast territory and world-class mineral and energy potential, efficient methods are required for upgrading the geoscience knowledge base of Canada's North. An important part of this endeavour involves updating geological map coverage. In the past, the coverage and publication of traditional geological maps covering only a limited region demanded multiple years of fieldwork. Presently more efficient approaches for mapping larger regions within shorter time spans are required. As a result, an approach termed Remote Predictive Mapping (RPM) has been implemented since 2004 in pilot projects by the Geological Survey of Canada. This project falls under the larger Geo-mapping for Energy and Minerals (GEMS) program initiated by Natural Resources Canada.

Remote pre-dictive mapping comprises the compilation and interpretation (visual or computer-assisted) of a variety of geoscience data to produce predictive maps containing structural, lithological, geophysical, and surficial information to support field mapping. Predictive geological maps may be iteratively revised and upgraded to publishable geological maps on the basis of evolving insight by repeatedly integrating newly acquired field and laboratory data in the interpretation process. The predictive map(s) can also serve as a first-order geological map in areas where field mapping is not feasible or in areas that are poorly mapped. The fundamental difference between RPM and traditional ground-based mapping is that in the latter, the compilation of units away from field control (current and legacy field observations) is largely based on geological inference while in RPM this geological inference is repeatedly tested and calibrated against remote sensing imagery.

Predictive geologic maps are derived from a variety of geoscience data including geophysical, geological, geochemical and remotely sensed as well as existing legacy and field data. A variety of quantitative and qualitative techniques using image analysis and Geographic Information (GIS) systems are employed to produce these predictive maps. This presentation summarizes the production of predictive maps of surficial materials from Baffin Island, Vitoria Island and Wager Bay focusing on quantitative classification techniques. Bedrock examples including both lithology and structure are shown from the Operation GEM project covering the central Churchill province. The production of bedrock predictive maps rely on primarily

visual interpretation of enhanced imagery (geophysical, optical, radar) employing a "heads-up" interpretation process using touch-screen technology. These interpretations are then integrated with legacy field data using a GIS to produce a prediction of rock units. Predictive maps of geologic structures are produced through a combination of visual interpretation of geophysical and optical data in concert with automated algorithms for extracting contacts, linear highs and lows from airborne magnetic data. (*SS1; Fri. 10:40*)

Remote predictive geological mapping of western Minto Inlier, Victoria Island, NWT: Application of quantitative classification techniques

Harris, J.R.¹, harris@nrcan.gc.ca, Behnia, P.² and Rainbird, R.¹, ¹Geological Survey of Canada, 601 Booth Street, Ottawa, ON K1A 0E8; ²Geofirma, 1 Raymond St., Ottawa, ON

Supervised classification (Robust Classification Method) of LANDSAT-7 and SPOT-5 data was used to analyze the bedrock geology of a part of the western Minto Inlier on Victoria Island, Canada. The Robust Classification Method was used as it provides a series of uncertainty measures for evaluating the classification results. Six bedrock classes including gabbro, basalt, carbonate of the Wynniatt Formation, quartz-arenite of the Kuujua Formation, evaporite of the Minto Inlet and Kilain Formations, and Paleozoic carbonate together with six surficial classes including vegetation, were defined as the training dataset. The resulting classified images derived from the LANDSAT and SPOT data were very similar in terms of the regional distribution of lithological classes, as reflected by fairly high classification accuracies for both image types. Diabase and basalt, despite having a similar mineralogical composition are spectrally distinct throughout most of the study area. Complicating spectral signatures of overlying glacial sediments and/or other overburden materials and spectral similarities between some of the lithologies caused poorer classification in some areas. Generally the LANDSAT imagery provided better spectral separability between most of the lithological units than the SPOT imagery. However, in certain areas where the spectral separation between different lithologies is not dependant on the SWIR-2 (band 7 on LANDSAT) and/or blue bands (band 1 on LANDSAT), the SPOT imagery provided a better classification because of higher spatial resolution. (*GS7; Wed. 2:00*)

Mapping lineaments in Nunavut using multi-beam RADARSAT-2 polarimetric SAR and LANDSAT-7-ETM+ images

Harris, J.R.¹, harris@nrcan.gc.ca, Shelat, Y.², LaRocque, A.³, Leblon, B.³, Jefferson, C.¹ (601 Booth St.), Lentz, D.² and Tschirhart, V.⁴, ¹Geological Survey of Canada, Natural Resources Canada, 615 Booth Street, Ottawa, ON K1A 0E8; ²Department of Earth Sciences, University of New Brunswick, Fredericton, NB E3B 5A3; ³Faculty of Forestry and Environmental Management, University of New Brunswick, Fredericton, NB E3B 5A3; ⁴MAGGIC, School of Geography & Earth Sciences, McMaster University, Hamilton, ON L8S 4K1

This study tested the use of multi-beam RADARSAT-2 polarimetric Synthetic Aperture Radar (SAR) data along with LANDSAT-7 Enhanced Thematic Mapper (ETM+) images for mapping lineaments in Umiujalik Lake area, Nunavut, Canada. The RADARSAT-2 polarimetric SAR images were acquired in three west-looking descending beam modes (FQ1, FQ12, and FQ20) with increasing respective incidence angles. We examined the effects of varying polarizations and incidence angles of RADARSAT-2 SAR data for lineament mapping. Lineaments were visually interpreted on LANDSAT-7 ETM+ principal component images, on RADARSAT-2 SAR single-polarized images, multi-polarized (HH, HV, and VV) RGB composites, and on polarimetric total power images. It was possible to identify more lineaments on RADARSAT-2 SAR images than on LANDSAT-7 ETM+ images. Polarization analysis suggests that regardless of the incidence angle, a higher number of lineaments were identified on the HH image than on the HV image, but the most lineaments were identified on the multi-polarized RGB composite.



Incidence angle effects also had an apparent influence on the number of delineated lineaments. More lineaments were identified on the FQ12 images than over the FQ1 or FQ20 images. The dominant lineaments trends are NW and NNW, which correspond to both the ice flow movement direction during the last glaciations of the area and a set of faults previously mapped in that direction. A smaller set of easterly lineaments is related to bedrock structures, such as faults and trends of prominent lithologic units. The study is a product of Geomapping for Energy and Minerals Program's Uranium and RPM projects. (**GS7; Wed. 1:40**)

Keynote (40 min): Crustal evolution and deformation of the Abitibi Subprovince, Superior Craton, Canada in a non-plate tectonic Archean Earth – comparisons with Venus

Harris, L.B., Institut national de la recherche scientifique, Centre - Eau Terre Environnement, 490 de la Couronne, Québec, QC G1K 9A9, lyal.harris@ete.inrs.ca, and Bédard, J.H., Commission géologique du Canada, Québec, 490 de la Couronne, Québec, QC G1K 9A9

Granite greenstone sequences in the southern Superior Craton in Canada were formed in a plume-related volcanic plateau-like setting during rifting of older cratonic lithosphere (N Superior Province - Minnesota River Valley domain) at ~2.75-2.7 Ga. Mantle plume activity led to necking, focussed thermal erosion, destruction and assimilation of ancient lithosphere, and formation of isotopically juvenile crust. 3D images of S-wave seismic tomographic data of the Superior Province show that the Abitibi Subprovince overlies a symmetrical rift in the sub-crustal lithospheric mantle (SCLM), with no evidence for 'fossil' subduction zones. Early rift structures localized subsequent deformation and hydrothermal fluid flow during N-S shortening and eastwards lateral escape in the ~2696 Ma Shebandowanian orogeny. Major gold deposits and kimberlites are located above rift-bounding faults in the SCLM. Enhanced aeromagnetic images of the central-northern Abitibi illustrate penetrative E-W dextral ductile shearing preceded formation of discrete, ductile to brittle-ductile, conjugate transcurrent and E-W reverse (\pm dextral) shear zones implying ~N-S bulk shortening. Offset and ductile deflection of dense, mafic crust along regional transcurrent shear zones in the Abitibi Subprovince and its continuation in the Grenville Province parautochthon is apparent on short wavelength Bouguer gravity. An Archaean sinistral, NE-striking shear zone (the proto-Grenville shear zone) is identified along the SE margin of the Abitibi and Opatca subprovinces.

Venus, a planet without plate tectonics, is presented as an analogue for a non-plate-tectonic Archean Earth. The geometry of reverse and strike-slip shear zones in the Abitibi Subprovince is similar to that of shear zones developed ahead of a rigid indenter. Displacement of 'craton-like' plana on Venus forming fold and thrust belts is attributed to mantle tractions and strong coupling between the lithosphere and mantle flow. Similarly, shortening, rift inversion, and regional deformation in the Abitibi is attributed to cratonic mobilization where southward displacement of the N Superior Province resulted from mantle flow acting upon its deep lithospheric keel. (**SS3; Thurs. 8:20**)

New tectonic models for Venus and Earth aided by comparative studies

Harris, L.B., Institut national de la recherche scientifique, Centre - Eau Terre Environnement, 490 de la Couronne, Québec, QC G1K 9A9, lyal.harris@ete.inrs.ca, and Bédard, J.H., Commission géologique du Canada, Québec, 490 de la Couronne, Québec, QC G1K 9A9

The high surface temperatures of Venus implies that structures imaged on its surface by radar imagery are comparable to mid-crustal structures on Earth, yet many previous interpretations of Venus are based on comparisons with upper, brittle crustal structures on Earth. Bouguer gravity of Venus acquired during Magellan missions has been previously used mainly for interpretation of lithospheric or crustal

thicknesses and for studies of mantle dynamics, and not for mapping regional, lithospheric-scale structures. In this study, concepts derived from the analysis of fold and thrust belts and transcurrent to transpressional brittle-ductile shear zones in metamorphic terrains on Earth and analogue modelling are applied to the interpretation of Magellan radar images. Venus Bouguer gravity data was enhanced using techniques applied for regional tectonic studies on Earth but (to our knowledge) not previously undertaken for Venus. The main outcomes are:

- Refolded folds and overprinting shear zones in the Ovda Regio area of Venus provide evidence for polyphase deformation, implying consistent changes in regional principal stress orientations over large areas of the planet's surface.
- Transcurrent shear zones are of far greater extent than previously mapped. 'Plate-like' horizontal displacements of several hundred kilometres on Venus occurred without the action of stresses due to 'ridge push', 'slab pull', and 'trench suction' proposed in the current plate tectonic paradigm for plate tectonics on Earth. Instead, lateral displacement of coronae and 'craton-like' plana on Venus result from mantle tractions at their base in a stagnant lid convection regime.

Venus is commonly proposed as an analogue for the Archean Earth. The presence of broad fold and thrust belts and regional transcurrent shear zones on Venus suggests that plate tectonics is not required to explain similar structures for an Archean Earth. Studies of Venus support a cratonic mobilism model for Earth where cratons are displaced due to mantle flow acting upon their deep lithospheric keels. (**SS17; Thurs. 9:40**)

SCLM rifting in the SE Superior Craton – Implications for deformation and mineralization in the Abitibi and Grenville Province and tectonic reconstructions

Harris, L.B.¹, lyal.harris@ete.inrs.ca, Bédard, J.H.², and Dufréchoy, G.^{1,3}, ¹Institut national de la recherche scientifique, Centre - Eau Terre Environnement (INRS-ETE), 490 de la Couronne, Québec, QC G1K 9A9; ²Commission géologique du Canada, Québec, 490 de la Couronne, Québec, QC G1K 9A9; ³(Present address) BRGM, BP 36009, 45060 Orléans Cedex 2, France

3D images of S-wave seismic tomographic data of the Superior Province illustrate that the Abitibi Subprovince overlies a symmetrical rift in the sub-crustal lithospheric mantle (SCLM) of older Archean lithosphere (N Superior Province and Minnesota River Valley domain). Whilst generally E-W-trending, the interpreted Archean rift changes to a NW-SE orientation in the easternmost Abitibi and Grenville Province parautochthon. The NW-SE trending rift in the SE margin to the Superior Province parallels the Belomorian Province separating the Kola and Karelian cratons that are placed against the Superior Province in tectonic reconstructions, providing a further argument for the relative position of these cratons in the Archean. The change in orientation by 120° suggests rifting may have occurred over a mantle plume. The NE segment of an Archean sinistral, NE-striking shear zone (the proto-Grenville shear zone) along the SE margin of the Abitibi and Opatca subprovinces similarly makes a 120° angle with the two rift segments and thus may follow an aulacogen in the rifted SCLM.

The displacement history and geometry of reverse and strike-slip shear zones in the Abitibi Subprovince is similar to that of structures developed during progressive lateral escape and indentation during impingement of a rigid body. We propose that southward migration of the old cratonic nucleus (N Superior Craton) in response to mantle flow acting upon its deep lithospheric keel, and not subduction-related processes, led to progressive southward accretion of crustal fragments and oceanic plateaux-like segments like the Abitibi, shortening and inverting the initial rift. Major epigenetic gold deposits are located above rift-bounding faults in the SCLM, suggesting that early rift structures localized subsequent deformation and hydrothermal fluid flow. The 1.1 Ga Desmaraisville and 0.55 Ga Otish kimberlite clusters also coincide with interpreted rift structures in SCLM.



NW-SE-striking structures in Archean basement to the Grenville Province (*i.e.* transverse to the Grenville orogen), formed during Paleoproterozoic rifting and reactivated during the Mesoproterozoic Grenville orogenic cycle, also correlate with SCLM rift margins. Our observations highlight the important role of ancient mantle structures on localizing deformation, hydrothermal fluid flow, emplacement of igneous bodies, and mineralization in the overlying crust.

Research was funded by Laurentian Goldfields, NSERC, Richmond Minerals, Fort Chimo Minerals, and DIVEX. The seismic tomographic database was provided by S. Godey. (**SS2; Wed. Poster**)

Toward an integrated geologic, geochemical, and structural model for formation of the MacLellan Au-Ag and related mineral deposits, Lynn Lake, Manitoba

Hastie, E.C.G., Gagnon, J.E. and Samson, I.M., University of Windsor, Department of Earth and Environmental Sciences, 401 Sunset Avenue, Windsor, ON N9B 3P4, hastie1@uwindsor.ca

The MacLellan Au-Ag deposit and related occurrences are located in the northern portion of the Paleoproterozoic Lynn Lake greenstone belt (LLGB) in northwest Manitoba. Historically, at least seven mineralized zones have been identified, including the former MacLellan Mine (Main, East and Nisku Zones), and the K, Dot, Rainbow, and West occurrences. Previous studies of the geology of the LLGB and the MacLellan Au-Ag deposit have largely focused on the regional geology, were reconnaissance in nature and discussed only some of the mineralized zones, or addressed in detail only limited areas or aspects of the MacLellan Au-Ag deposit. To date, a comprehensive study of the lithology, geochemistry, deformation, mineralization, and alteration across all of the properties that host the MacLellan Au-Ag deposit and related occurrences has not been completed.

Exploration activities undertaken since 2011 by Carlisle Goldfields Ltd. (drill programs, surface mapping, and assays) have substantially increased the size of the total Au-Ag resource and have provided new lithologic, structural, and geochemical data across all of the related occurrences. Historic and new data on lithology, mineralization, and deformation are being used to develop an integrated model for the MacLellan Au-Ag deposit and related occurrences.

Preliminary results indicate that: 1) the dominant, primary lithologies that host the Au-Ag mineralization are chlorite-hornblende schist (metapelite), porphyritic metabasalt/metagabbro (extrusive and intrusive equivalents), albite, and granite (Burge Lake), 2) quartz-biotite schists that were previously characterized as metasediments (*i.e.*, 'greywacke') are altered metabasalts, 3) alteration of the primary lithologies is associated with D₂ dextral shears, with Au-Ag mineralization occurring within structurally-controlled alteration haloes, 4) Au-Ag mineralization in the MacLellan deposit is associated with silicification and biotite ± garnet alteration. The alteration and deformation style appears to be relatively consistent across all of the seven Au-Ag occurrences, but the sulphide mineralogy varies along strike (*i.e.*, Au-Ag is predominantly associated with arsenopyrite in the western portion of the deposit, with pyrite and pyrrhotite in the centre, and with galena and sphalerite in the east), and 5) mineralized samples containing predominantly arsenopyrite and galena/sphalerite have low Au/Ag ratios (~1/20 and ~1/40, respectively), however, mineralized samples containing predominantly pyrite and pyrrhotite have high Au/Ag ratios (~9/1). (**GS2; Wed. Poster**)

A new lectostratotype locality of the Millwood Member of the Upper Cretaceous Pierre Shale in Manitoba

Hatcher, J., Canadian Fossil Discovery Centre, 111-B Gilmour Street, Morden, MB R6M 1N9, collections@discoverfossils.com, and Bamburak, J.D., Manitoba Geological Survey, 360-1395 Ellice Avenue, Winnipeg, MB R3G 3P2

The Millwood Member of the Upper Cretaceous Pierre Shale in Manitoba is composed of montmorillonite-rich non-calcareous olive-grey shale, interbedded with soft, calcareous shale, ironstone concretionary beds, and bentonite seams. The original type locality for the Millwood Member was chosen by Joseph Tyrrell in 1890 where the

Member was exposed in a series of railway-cuts in the Assiniboine River valley near the town of Millwood, Manitoba. However, a dispute arose during a cricket match between the owner of the local sawmill and the Superintendent of the Manitoba and North Western Railway (M&NWR) and as a result, the M&NWR chose to bypass the thriving village. The community survived for a short time, but gradually declined as businesses and residents moved away to other railway economic centers of the Province and today only a few scattered and abandoned buildings remain with Tyrrell's original type locality being overgrown. A neostratotype was selected in 1980 by McNeil and Caldwell in exposed road-cuts along PR 478, approximately 8 km south of Millwood, Manitoba. However, a recent trip to study the neostratotype proved fruitless as these road-cuts are now also overgrown, and therefore the need of a lectostratotype locality exists.

Within the SW ¼ Sec. 18-T4-R6, W 1st Mer. (abbreviated SW18-4-6-W1) within the Rural Municipality of Thompson, Manitoba, a large butte known as Mount Nebo is readily identifiable in the Second Prairie Level of Pembina Hills region on the Manitoba Escarpment. Composed of the olive-grey non-calcareous to calcareous shale and ironstone concretionary beds of the uppermost Millwood Member of the Pierre Shale, Mount Nebo is thus formally chosen to become the current Millwood lectostratotype locality. The butte is accessible directly on the north side of section road 20 N, 11 km west of PR 432. The Upper Cretaceous shale around the base of Mount Nebo has also produced many large vertebrate marine fossils housed at the Canadian Fossil Discovery Centre in nearby Morden, Manitoba. The landform is a sparsely vegetated rounded butte which is not likely to become overgrown and should serve as an adequate lectostratotype locality for many years to come. (**SS13; Fri. 1:40**)

The state of mineralogy: The present and the future

Hawthorne, F.C., Geological Sciences, University of Manitoba, Winnipeg, MB R3T 2N2

What is the theoretical framework that we use to interpret mineralogical data and the way that minerals behave in geological processes? We use *crystal chemistry* to systematize mineral properties and behaviour, classical *thermodynamics* to examine geological processes involving minerals, and *computational mineralogy* to derive properties of minerals, particularly where their stabilities are beyond the reach of current experimental techniques. Crystal chemistry, thermodynamics and computational mineralogy are very powerful, but they have tended to dictate the questions that we ask about minerals: We ask questions to which standard theory can give us an answer. There are many questions of scientific interest which are opaque to our current theoretical approaches. Such questions tend to be neglected because they are seen as intractable or even irrelevant to current issues of applied science. Why do minerals have the chemical formulae that they do? Why do they have their specific structural arrangements? Why are minerals stable over specific ranges of pH, Eh, temperature, pressure and activities of their various constituents, and what controls the salient ranges of these variables? What are the relations between crystal structure and enthalpy, entropy and Gibbs free energy of formation? These questions are fundamental to Mineralogy itself and yet have tended to be ignored in the past. Here, I will examine how we can address such questions from a theoretical perspective, and how we can incorporate process (*e.g.*, crystallization, dissolution) into these considerations, as distinct from using purely descriptive vehicles for minerals. The ideal is to develop an understanding of the atomic-scale factors that control the chemical compositions and structural arrangements of minerals, and to relate those atomic-scale factors to processes that affect minerals (*e.g.*, crystallization, dissolution, melting, alteration). Minerals can be very complicated entities, and the ideal approach should also be able to impart some intuitive understanding to the stability of minerals and their participation in geological processes. I will briefly consider *Bond Topology*, *Complexity of Information Content*, and aspects of *Evolutionary Mineralogy* as possible constituents of such a theoretical approach to Mineralogy *sensu lato*. (**SY1; Thurs. 3:40**)

**Miocene post-collisional shoshonites and their crustal xenoliths, Yarlung Zangbo Suture Zone, southern Tibet; Geodynamic significance**

Hébert, R.¹, rejean.hebert@ggl.ulaval.ca, Guilmette, C.², Dostal, J.³, Lesage, G.¹, Bezard, R.⁴ and Wang, C.S.⁵, ¹Université Laval, Avenue de la Médecine, Québec, QC G1V 0A6; ²University of Waterloo, Waterloo, ON; ³St. Mary's University, Halifax, NS B3H 3C3; ⁴Durham University, Sciences Labs, Durham, Great Britain, DH1 3LE; ⁵Beijing University of Geosciences, Xueyuan Road, Beijing, China, 100083

The convergence between the Indian plate and the southern margin of the Eurasian continent created an active continental margin from Late Jurassic until about 40 Ma ago, which then evolved to form the Himalaya and the Tibetan Plateau during the continental collision stage. Post-collisional magmatism in southern Tibet, north of the Yarlung Zangbo Suture Zone (YZSZ) has been active since 45 Ma and is related to normal faulting and extensional tectonism. To date no such magmatism was reported within the YZSZ itself. This paper reports on the discovery of Miocene shoshonites within the YZSZ. They are significant because the magma travelled, at least in part, through oceanic crust, thus limiting interaction with the continental crust to the mid-crustal level and which affected the post-collisional magmatic rocks occurring in the northern part of the subduction system. In addition, xenoliths and xenocrysts of crustal origin in these rocks constrain the nature of metamorphic rocks underlying the YZSZ at mid-crustal level. The geochemical signatures of the shoshonitic rocks, including Nd and Sr isotope systematics, indicate derivation from a garnet-bearing middle continental crustal source. Crustal imprint complicates modelling of the petrogenetic processes which occurred prior to mid-crustal ponding of the magma which took place between 11 and 17 Ma at depths of 40 to 50 km. The significant role of crustal contamination raises serious concerns about models proposed for similar magmatic activity elsewhere in the Himalaya and the Tibetan Plateau. (GS2; Wed. 11:00)

PGE-Ni-Cu versus Ni-Cu-PGE deposits: Contrasting sulphur abundance in the Midcontinent Rift

Heggie, G.J., MacTavish, A., Johnson, J., Panoramic PGMs Canada Ltd, Thunder Bay, ON, Geoff.Heggie@panres.com, and Hollings, P., Lakehead University, Thunder Bay, ON

The Paleoproterozoic Midcontinent Rift contains a number of orthomagmatic mineralized mafic-ultramafic intrusions with olivine as a dominant cumulate phase: Eagle, Tamarack, Thunder Bay North, and Seagull. The mineralization style and metal tenor of mineralization in these intrusions can be largely divided into massive Ni dominant (Eagle and Tamarack) and disseminated PGE dominant (Thunder Bay North and Seagull). With only subtle differences in parental magma compositions, the main difference between the two metal tenor groups is the host rocks. Nickel dominant systems are emplaced proximal to Paleoproterozoic sulphide-bearing black shale, whereas, PGE dominant systems are emplaced into sulphide-poor Archean granites and metasedimentary rocks.

Mechanisms leading to sulphur saturation in sulphur-rich settings are easily postulated. However, mechanisms and processes leading to mineralization in sulphur-poor settings are more ambiguous. Examination of mineralization, mineral chemistry, whole rock chemistry, and isotopic systems within the Seagull Intrusion and Thunder Bay North Complex provide sufficient data to numerically model and hypothesize on a deposit model for the formation of PGE dominant mineralized systems.

It is purported that sulphur-saturation within the Thunder Bay North Complex and Seagull Intrusion was a result of igneous fractionation, rather than an external S-source. Fractionation induced sulfur saturation results in only minor amounts of immiscible sulfide liquid. Chalcophile elements with high partition coefficients (PGE) are enriched over chalcophile elements with lower partition coefficients (Ni). The result is disseminated PGE-rich mineralization. Secondary physical dynamic processes within the systems can upgrade the

mineralization from an occurrence as documented at Seagull to a mineral deposit as defined within the Thunder Bay North Complex. (SS9; Wed. 9:00)

Upper-to-middle level exposure of a 2.8 Ga continent in the northern Wyoming Province, USA: Petrologic-mineralogical evidence

Henry, D.J.¹, glhenr@lsu.edu, Mogk, D.W.², Mueller, P.A.³, Foster, D.A.³, Wooden, J.L.⁴ and Dutrow, B.L.¹, ¹Louisiana State University, Baton Rouge, LA 70803, USA; ²Montana State University, Earth Sciences, Bozeman, MT, USA; ³University of Florida, Geological Sciences, Gainesville, FL, USA; ⁴Stanford University, Earth Sciences, Stanford, CA, USA

In his wide range of investigations Frank Hawthorne continually considers the chemical/crystallographic/isotopic relationship of minerals to their larger context of petrologic and geochemical problems. In turn, investigations of minerals in context (*i.e.* petrologic mineralogy) are key to addressing hypotheses that can include aspects of the tectonics evolution of a terrain. One such example is that of the petrologic-mineralogical evolution of a section of Archean crust in the northern Wyoming Province, USA.

The 2.8 Ga plutonic and metamorphic rocks in the northern portion of the Wyoming Province in Montana and Wyoming (USA) represent a continuum of crustal levels (~10-25 km) within a Mesoarchean continent. Although these rocks contain a diverse record of crustal evolution extending before 2.8 Ga (as early as ~4.0 Ga), it is the 2.8 Ga magmatic rocks (tonalite-trondhjemite-granodiorite *i.e.* TTG suite) that volumetrically dominate the region from the South Snowy Block (partially in Yellowstone National Park) to the Main Beartooth Massif (~110 km distance). Magmatic rocks in the westernmost area are dominated by undeformed bulbous, peraluminous, epizonal, quartz-monzonitic plutons that cut metasedimentary rocks with low-P assemblages *e.g.* andalusite-staurolite (~580°C, ~3.5 kbar). In contrast, in the eastern part of the area 2.8 Ga magmatism in the Long Lake magmatic complex (LL) includes a diverse series of meta-dioritic rocks to metaluminous TTG suite rocks. Each of the rock types do not exhibit consistent sequential field, geochemical or geochronologic relationships *i.e.* they are essentially coeval, but independent, magmatic units that are mixed in a ductile environment. In the easternmost area there are numerous xenoliths including aluminous migmatites with typical metamorphic assemblages of qtz + pl + K-fsp + bt + sil ± grt ± crd with peak metamorphic conditions of 750-800°C and 7-8 kbar. Between the west-east extremes, the plutonic rock transition to heterogeneous TTG plutons with intermediate P-T conditions. Through their minerals, these plutonic rocks are interpreted as belonging to a section of 2.8 Ga continental crust developed in response to subduction-zone processes and ultimately exposed at varying depths. (SY1; Thurs. 9:40)

The Tissint Martian meteorite: Petrologic comparisons to other shergottites

Herd, C.D.K.¹, herd@ualberta.ca, Bryden, C.D.¹, Pearson, D.G.¹ and Duke, M.J.M.², ¹Department of Earth and Atmospheric Sciences, 1-26 Earth Sciences Building, University of Alberta, Edmonton, AB T6G 2E3; ²SLOWPOKE Nuclear Reactor Facility, 2-51 South Academic Building, University of Alberta, Edmonton, AB T6G 2G7

The Tissint meteorite fell in Morocco July 18, 2011 and is the first fall of a meteorite from Mars since 1962. As a fresh fall into a desert environment, Tissint represents some of the most pristine Martian material available for study. Like other olivine-phyric shergottites, Tissint's petrogenesis included precipitation of olivine megacrysts at some depth, followed by groundmass crystallization upon eruption. Olivine megacrysts are at minimum cumulate, if not xenocrystic. We have determined the SiO₂ content of bulk powders of Tissint by Neutron Activation Analysis and carried out calculations of oxygen fugacity using the olivine-pyroxene-spinel oxybarometer. Based on the mismatch between bulk Mg# and Mg# of the melt in equilibrium with



olivine cores, we estimate that the rock contains approximately 5% cumulate olivine. On this basis, and using our determination of SiO_2 along with previously published whole-rock major and minor element values, we calculate a bulk parental melt composition that is comparable to that of the NWA 5789 picritic basalt, albeit with higher Fe. Assessment of olivine-pyroxene equilibrium indicates that the most Mg-rich low-Ca pyroxene ($\sim\text{Wo}_{55}\text{En}_{45}\text{Fs}_{25}$) came on the liquidus with olivine of Fo_{69} . The choice of chromite in equilibrium with these phases is equivocal; however, application of the Sack and Ghiorso oxybarometer using a range of low-Ti chromite compositions yields and oxygen fugacity within 0.5 log units of the iron-wustite buffer.

The low oxygen fugacity of Tissint is consistent with its depleted incompatible trace element composition (e.g., low La/Yb); Tissint appears to maintain the relationship between redox state and incompatible trace elements observed in many other shergottites, and is grouped with other reduced and depleted members along with several other olivine-phyric shergottites. As a test of the mineral-based oxybarometers, we assessed whether bulk V/Sc ratios of the shergottites correlate with oxygen fugacity; Lee *et al.* (2005) demonstrated the utility of V/Sc for “seeing through” the effects of fractional crystallization, magma ascent and differentiation for Earth basalts. If the oxygen fugacity estimates for the shergottites reflect the redox states of their mantle sources, as opposed to the overprinting effects of ascent/degassing, then V/Sc should correlate with oxygen fugacity. This does appear to be the case for the basaltic shergottites (those without olivine phenocrysts). However, Tissint and the other olivine-phyric shergottites group at low oxygen fugacity and high V/Sc, off the linear trend of the basaltic shergottites. We conclude that olivine-phyric and basaltic shergottites are derived from distinct mantle sources. (SS18; Thurs. 2:40)

400 Ma dates in a rare element NYF-pegmatite from Stetind, Nordland, Norway: Recrystallized Proterozoic assemblages or A-type pegmatite emplacement in overly-thickened crust at a continental margin?

Hetherington, C.J., Texas Tech University, Box 41053, Lubbock, TX, USA 79409-1053, callum.hetherington@ttu.edu, and Husdal, T., Veslefrikk 4, 8028 Bodø, Norway

The Stetind pegmatite is exposed in a small abandoned feldspar-quartz quarry on the north-western flank of Mt. Stetind, NE of Bodø. It is one of several pegmatite bodies that intrudes the ~ 1798 Ma Tysfjord Granite. The quarry exposes a vertically oriented pegmatite body with coarse-grained inter-locked feldspar and quartz and sheet-like aggregates of biotite. The pegmatite has sharply defined anisotropic mineralogical zones that trend towards a quartz-rich core. Besides quartz, albite and microcline, a broad assemblage of Nb-, Y-, F-, rare earth element (REE) and actinide-bearing minerals have been described leading to our classification of the body as a rare element NYF-pegmatite.

Many rare-element minerals occur in bands or crystal aggregates with subsets of the rare-element assemblage occurring as discrete sub-assemblages consistent with sequential crystallization. On the basis of textural relationships the general order of rare-element mineral crystallization is oxides and phosphates (excluding xenotime), silicates, carbonates, and lastly fluorides. In some instances there is also textural evidence of back-reaction between early crystallizing phases and the evolving fluid that was becoming richer in F. Examples include relict zircon with abundant inclusions of (yttrio)-fluorite and skeletal fergusonite. These reactions have led to the replacement of early crystallizing phases, typified by xenotime rims replacing and overgrowing apatite. There is no textural evidence of regional deformation in the pegmatite that may be attributed to Caledonian orogenesis and nappe emplacement.

Several actinide-bearing phases including zircon, allanite, uraninite, thorite, fergusonite and xenotime have been dated by ID-TIMS, LA-ICP-MS or total U-Th-Pb EPMA methods. U-Pb ID-TIMS analysis of allanite, uraninite, thorite and fergusonite give dates close to 400 Ma; a similar date for xenotime was obtained using EPMA

methods. Preliminary LA-ICP-MS data for zircon is complex and discordant with a loosely constrained lower intercept of ~ 400 Ma and a very poorly constrained upper intercept in the mid- to late-Proterozoic. We interpret the textures and dates to represent a period of rare-element NYF-pegmatite emplacement into orogenically thickened crust along the margin of Baltica that post-dates fabric development in the Tysfjord granite. The source of the pegmatite fluids is unknown, but compositional markers such as high F-abundances have been used to argue that the Tysfjord granite and the pegmatites are genetically related; this will be tested using Hf isotopes. (SY2; Thurs. Poster)

Multiple sulfur isotopes and the Hart komatiite-hosted Ni-deposit, Abitibi Greenstone Belt, Ontario: Evaluating and tracing the signature of contamination in komatiite

Hiebert, R.S.¹, russelhiebert@gmail.com, Bekker, A.¹, Houlé, M.G.², Leshar, C.M.³ and Wing, B.A.⁴, ¹University of Manitoba, 125 Dysart Road, Winnipeg, MB R3T 2N2; ²Geological Survey of Canada, 490 rue de la Couronne, Québec, QC G1K 9A9; ³Laurentian University, Sudbury, ON P3E 2C6; ⁴Department of Earth & Planetary Sciences, 3450 University St., Montreal, QC H3A 2A7

The Hart komatiite-hosted Ni-deposit is located in the ca. 2.7 Ga Abitibi Greenstone Belt approximately 30 km south of Timmins, Ontario. Komatiite-hosted Ni-deposits, such as the Hart deposit, are thought to have been formed by S-undersaturated magmas incorporating sulfur from underlying rocks through thermomechanical erosion to form an immiscible sulfide xenomelt. The addition of sulfur is required as melting of the mantle generates a S-undersaturated magma as it rises to surface due to increased solubility of sulfur in mafic and ultramafic melts as pressure decreases.

Photochemical reactions between UV radiation and sulfur dioxide in the Earth's early oxygen-free atmosphere resulted in mass-independent fractionation of sulfur isotopes. The photochemically fractionated sulfur compounds, elemental sulfur and sulfate, were delivered from the atmosphere to the oceans, biologically processed there, incorporated into sediments, and are now preserved in Archean sedimentary rocks. The sulfur from these compounds, with the unique signature of Archean atmospheric processing, would have been transferred to the Hart Ni-deposit when supracrustal rocks were melted by the komatiite flow to generate this deposit, and can help to identify the source of crustal contamination.

We have identified two footwall lithologies with significant sulfur content that had the potential to be sulfur sources for this deposit, graphitic argillite and an exhalite unit, which has in the past been described as iron formation but varies in along strike over distances of 10's of metres from banded Fe-oxide-chert iron formation to predominantly chert or massive pyrite. Both lithologies have somewhat overlapping multiple S isotope values typical of bacterial sulfate reduction in Archean rocks. In the exhalite, $\delta^{34}\text{S}$ and $\Delta^{33}\text{S}$ values range -11.4 to +7.6‰ (n = 23, avg -2.2‰) and -1.4 to -0.3‰ (avg -0.6‰) respectively. In the argillite, $\delta^{34}\text{S}$ and $\Delta^{33}\text{S}$ values range +1.6 to +5.0‰ (n = 3, avg +3.4‰) and -1.0 to -0.2‰ (avg -0.5‰), respectively.

In preliminary data from the sulfides in the komatiite have similar average values to those of the exhalite and $\delta^{34}\text{S}$ and $\Delta^{33}\text{S}$ values range -4.1 to -1.5‰ (n=5, avg -2.6‰), and -0.6‰, respectively. This, along with field relationships, suggests that the exhalite is the dominant source of sulfur for the deposit. An additional objective of our study is to determine how the sulfur isotope values of contaminated komatiite vary across the flow channel, from the proximal position to the mineralization to the flanks of the flows, and how the sulfur isotope values of contaminated komatiite flows differ from those of the overlying uncontaminated komatiite flows. (SS9; Thurs. 9:20)

Keynote (40 min): Magnesium isotopes and the origin of dolomite

Higgins, J.A.¹, jahiggin@princeton.edu; Schrag, D.P.², Swart, P.K.³, Miller, N.⁴, Macdonald, F.², Maloof, A.¹ and Hoffman, P.F.², ¹Princeton University, Princeton, NJ 08540 USA; ²Harvard University, Cambridge, MA 02138 USA; ³University



of Miami, Miami, FL 33149 USA; ⁴University of Texas at Austin, Austin, TX 78712 USA

In spite of 200 years of study, the origin of sedimentary dolomite (Mg,Ca)CO₃ remains enigmatic. A spectacular example of this are the shallow-water 'cap' dolostones deposited world-wide in the aftermath of the terminal Cryogenian glaciation. To better understand the origin of the 'cap dolostone' and dolomite more generally, we have measured the Mg isotopic composition of dolomite from a range of paleo-environments including Neogene examples from the Bahamas, the Monterey Formation, and Resolution Guyot (ODP 866A) and Neoproterozoic cap dolostones from Namibia, Mongolia, and Arctic Alaska. Measured $\delta^{26}\text{Mg}$ values range from ~ -1 to $\sim -3\%$. The variability in $\delta^{26}\text{Mg}$ values is largely systematic; some sites are characterized by a single homogenous $\delta^{26}\text{Mg}$ value whereas others are characterized by both local and regional excursions. We explore possible explanations for the observed variability, focusing on the role of fluid flow and magnesium supply (advection or diffusion?). We explore implications for geochemical records in dolomites and those in the Neoproterozoic cap dolostones in particular. (SY4; Fri. 2:00)

The CH-6 kimberlite, Canada: Textural and mineralogical features and their relevance to volcanic facies and magma batch interpretation

Hilchie, L.¹, Pell, J.², Scott Smith, B.H.³ and Russell, J.K.¹,
¹Department of Earth, Ocean and Atmospheric Sciences,
University of British Columbia, Vancouver, BC V6T 1Z4;
²Peregrine Diamonds Ltd., 201-1250 Homer St, Vancouver, BC
V6B 1C6; ³Scott-Smith Petrology Inc., 2555 Edgemont Blvd,
North Vancouver, BC V7R 2M9

The 64 kimberlites of the Chidliak and adjacent Qilaq projects on Baffin Island, Nunavut constitute the Chidliak Kimberlite Province. We present early results from the first detailed study of the CH-6 kimberlite, one of the bodies with economic potential. CH-6 is a pipe-like body (~ 0.9 Ha at surface; 150.1 ± 1.6 Ma) located ~ 120 km east of Iqaluit that crosscuts paragneisses of the Hall Peninsula Block, and contains xenoliths of since-eroded Paleozoic sedimentary carbonate cover. Previous core logging and petrographic studies report that the Chidliak kimberlites include textures ranging from typical coherent kimberlite to typical Fort à la Corne type pyroclastic kimberlite. The CH-6 pipe contains rocks with some comparable textures but most of the pipe exhibits characteristics for which volcanic facies assignment is not straightforward. In particular, some texturally ambiguous rocks with groundmass textures typical of coherent kimberlite have features more characteristic of pyroclastic processes. These features include reduced proportions of olivine microcrysts, broken macrocrysts, apparent melt selvages on olivine grains and xenoliths, and intimately mixed carbonate xenoliths derived from the since-eroded cover. These features suggest an extrusive origin for all or most of the CH-6 pipe infill, and may imply clastogenic origins. New descriptive megascopic to microscopic analyses of CH-6 drill core focusing on textures and mineralogy will be used to address the principal goals of this investigation, elucidating volcanic facies and discriminating between magma batches. (SS4; Fri. 1:40)

The petrographic and geochemical study of hydrothermally altered metavolcanics, metamorphosed at granulite-facies conditions from the Canyon domain in the central Grenville Province of Quebec, Canada

Hindemith, M., mafh88@mun.ca, and Indares, A., Memorial University of Newfoundland Department of Earth Sciences, 300 Prince Philip Drive, St. John's, NL A1B 3X5

Hydrothermally altered volcanic (HAV) rocks were recently recognized in the Canyon domain (central Grenville Province). These rocks occur in a 1.2 Ga layered bimodal felsic-mafic sequence inferred to represent the remnants of a volcanic belt formed within a crustal extension setting, and were subsequently metamorphosed under granulite-facies conditions during the Grenvillian orogeny. Characteristic components of the HAV rocks are garnetite layers and 'bleached' felsic gneisses

with aluminous nodules. Both rock types are in gradational contact with felsic gneisses of rhyolitic composition preserving recrystallized and corroded quartz megacrysts in a finer grained quartzofeldspathic matrix. Garnetites consist of $>50\%$ garnet, which is commonly spessartine and almandine rich (up to 16% and 73% respectively) with subordinate quartz and/or plagioclase. Aluminous nodules in felsic gneisses are mineralogically zoned; they consist of garnet, with sillimanite (and in some cases spinel and corundum) concentrated in the core of the nodules. The nodules are variably overgrown by biotite at their rims and are mantled by plagioclase becoming albitic towards the quartzofeldspathic matrix. In addition, some nodular gneisses have a matrix dominated by K-feldspar and contain disseminated sulphides and relics of bipyramidal quartz megacrysts. The 'bleached' felsic gneisses are generally enriched in potassium and aluminum relative to an "average" granite composition, which is consistent with argillic alteration types. REE patterns in the HAV rocks show slight depletion of LFSE and flat HREE signatures with negative anomalies for Eu, Nb, Ti, V and Cr. The absence of a peralkaline signature is consistent with VMS environments. HAV rocks contain >1000 ppm Ba, Sr and W with high counts of base metals which are interpreted to behave as mobile elements in hydrothermal VMS systems. This study shows that petrographic and geochemical characteristics of HAV rocks can be preserved at granulite-facies conditions. Volcanic belts formed in shallow-marine environments represent first-order targets for mineral exploration of VMS deposits. This study has implications on the economic potential of ancient volcanic belts in the Grenville Province. (SS10; Thurs. 10:20)

Perspectives on the uranium life cycle at the Savannah River Site

Hobbs, D.T., Rudisill, T.S. and Denham, M.E., Savannah River National Laboratory, Aiken, SC, USA 29860,
david.hobbs@srnl.doe.gov

The Savannah River Site located in South Carolina has served as one of the production sites for defense nuclear materials in the United States since the mid-1950s. The site featured a heavy water production facility, nuclear fuel and target production facilities, five heavy-water nuclear reactors and two reprocessing facilities. The reprocessing facilities recovered uranium, plutonium and other radioisotopes from the irradiated fuel and target materials. The recovered uranium was purified and enrichment adjusted for reuse in the production reactors. Separation processes were primarily based on PUREX chemistry, which uses tributyl phosphate to extract uranium and plutonium from nitric acid solutions.

Chemical residues from the reprocessing facilities, referred to as high-level nuclear waste (HLW), have been stored in large, underground tanks. Facilities have been built or are under construction to dispose of the legacy HLW. One of these facilities, the Defense Waste Processing Facility (DWPF), has been operating since 1996 to incorporate the HLW into a highly durable borosilicate glass wasteform. Pretreatment of HLW supernatant liquids occurs in the Actinide Removal Process (ARP) and Modular Caustic Side Solvent Extraction (MCU) facilities. The ARP facility removes Sr-90 and alpha-emitting radionuclides (U, Np, Pu, Am) from HLW supernatant liquids using an inorganic sorbent, monosodium titanate (MST). The MCU facility removes Cs-134/137 using a calixarene extractant. Since 2008, this pilot-scale facility has processed more than 3.8 million gallons of HLW. A larger facility, referred to as the Salt Waste Processing Facility (SWPF), will use the same separation technology as ARP/MCU and features an annual throughput of about 7.5 million gallons of HLW.

Uranium release to soil and groundwater at the Savannah River Site has occurred primarily at four locations – the fuel fabrication area, a pilot-scale testing facility near the Savannah River, and at two sets of seepage basins associated with the reprocessing facilities. At the fuel fabrication and pilot-scale testing locations, uranium was released into the surface waters. In contrast, uranium was released directly to the subsurface from seepage basins that received liquid low-level radioactive waste from the reprocessing facilities. This uranium is



migrating through groundwater discharging to a down-gradient stream. The only active remediation of uranium occurs in these groundwater plumes. This paper will discuss the nature of uranium at each of these waste units and remediation efforts at the seepage basins as well as details about the reprocessing and disposition of uranium from the nuclear production facilities. (SS5; Thurs. 3:00)

Testing for rapid true polar wander in the Ediacaran using paleomagnetic data from Avalonia

Hodych, J.P., Department of Earth Sciences, Memorial University of Newfoundland, St. John's, NL A1C 3X5, jhodych@mun.ca, and Buchan, K.L., Geological Survey of Canada, 601 Booth St., Ottawa, ON K1A 0E8

Ediacaran paleomagnetic data has been used to suggest that rapid true polar wander (TPW) moved Laurentia from equator to pole between ca. 615 and 590 Ma and back again between ca. 590 and 565 Ma (Mitchell *et al.*, 2011). Such a rapid cycle of oscillatory TPW is theoretically possible (e.g. Creveling *et al.*, 2012). However, its effects would be global and we shall discuss whether Ediacaran paleomagnetic results from Avalonia support the suggestion. In the Avalon zone of Newfoundland, the primary nature of the magnetization has been demonstrated using conglomerate tests in three studies of Ediacaran formations. The 605 ± 5 Ma Harbour Main Group volcanics near Colliers yield a paleolatitude of 39° ± 10° (Hodych and Buchan, 2012). The 583 ± 6 Ma Calmer Formation volcanics and sediments yield a paleolatitude of 35° ± 10° (McNamara *et al.*, 2001; omitting the Famine Back Cove basalt because it is very likely Devonian). The 570 ± 5 Ma Bull Arm Formation volcanics yield a paleolatitude of 19° ± 11° (Pisarevsky *et al.*, 2012). All three primary magnetizations have similar declinations and are consistent with Avalonia slowly moving ~20° towards the equator between ca. 605 and 570 Ma. These data do not show evidence of the large TPW oscillation cycle that Mitchell *et al.* (2011) infer for Laurentia in this period. The 596 ± 2 Ma Lynn-Mattapan volcanics of the Avalon zone near Boston also appear to pass conglomerate tests and yield a paleolatitude of 38° ± 8° (Thompson *et al.*, 2007), but have a magnetization declination that differs by ~6° from the Colliers and Calmer declinations. Assuming that the declination difference is due to later Ediacaran or early Paleozoic clockwise rotation of the Boston area relative to the Avalon zone of Newfoundland, the Lynn-Mattapan paleolatitude is consistent with the model of slow drift of Avalonia rather than rapid TPW. However, the possibility that the declination difference reflects a TPW oscillation cycle (between ca. 605 and 596 Ma and back between ca. 596 and 586 Ma) cannot be ruled out. This would require that Avalonia be located far from Laurentia near the axis of the rotation that caused the TPW, and would also require a much more complicated TPW pattern than that proposed by Mitchell *et al.* (2011) as the Avalonia oscillation cycle would not be matched in time with that postulated for Laurentia. (SS11; Fri. 9:20)

Plenary Address: The origin of Laurentia

Hoffman, P.F., 1216 Montrose Ave., Victoria, BC V8T 2K4, paulhoffman@gmail.com

Recent studies demonstrate the existence, age and subduction polarity of a collisional orogen between the Hearne and Rae cratons, the Snowbird tectonic zone. Now, the relative ages and tectonic polarities of all major Orosirian (2050-1800 Ma) collisions between the Archean cratons of proto-Laurentia are tentatively known. The oldest geosutures bound the Rae craton, which collided first with the Slave craton in 1.97 Ga, forming the Thelon orogen, and then with the Hearne craton in 1.92 Ga. Other Orosirian geosutures are younger than 1.90 Ga. The Rae craton was on the upper plate for both the 1.97 and 1.92 Ga collisions. After a stint within the lower plate for the 1.88 Ga arc-continent collision in Wopmay orogen, the Rae craton returned to the upper plate during 1.88 to 1.84 Ga subduction beneath the Great Bear magmatic arc and 1.86 to 1.83 Ga subduction beneath the Wathaman-Narsajuaq magmatic arc, the latter leading to 1.83-1.82 Ga collision with the Superior craton forming the Trans-Hudson orogen. Subduction and

mantle downflow existed beneath the Rae craton from the start of the Orosirian assembly of Laurentia. Geodynamically, this suggests that the Rae craton was the first to be captured in the mantle downwelling region, and thereafter served as a backstop for other incoming cratons and composite cratons. The Rae craton is the geodynamic origin around which proto-Laurentia (i.e. pre-Grenville Laurentia) was assembled. It remains to be determined if it was also the origin of Nuna, the medial Proterozoic supercontinent, within which it occupied a central location. (SS24; Thurs. 11:20)

Keynote (40 min): The Great Oxidation Event (GOE) and a Siderian Snowball Earth: MIF based correlation of early Paleoproterozoic glaciations

Hoffman, P.F., 1216 Montrose Ave., Victoria, BC V8T 2K4, paulhoffman@gmail.com

The Great Oxidation Event (GOE) is best defined by the disappearance of mass-independent fractionation (MIF) of S-isotopes in sedimentary sulfide and sulfate minerals, indicating an apparent irreversible rise in atmospheric O₂ above 10⁻³ PAL (2 ppm) at a point in Siderian (2.50-2.30 Ga) time. From a planetary atmosphere perspective, the GOE could have triggered a major glaciation through the destruction of reduced greenhouse gases (CH₄, H₂S, SO₂, H₂, etc.). However, existing correlations between early Paleoproterozoic successions divorce the low-latitude Makganyene glaciation in southern Africa from the GOE. They also imply a younger age for the GOE in southern Africa (~2.3 Ga) compared with North America (~2.4 Ga), which is physically implausible. A new correlation scheme is proposed in which the Makganyene glaciation (Griqualand West basin) is correlated with the second of three Huronian glaciations in North America (Bruce and lower Vagner formations), the one with postglacial cap-carbonates, with the Meteorite Bore Member (Turee Creek Group) in Western Australia, and with an erosion surface in the middle Duitschland Formation (Eastern Transvaal basin) across which the GOE occurs. The correlation is consistent with existing MIF and other atmospheric redox proxy data, as well as with U-Pb and Re-Os geochronology. In the new scheme, only three glaciations (the minimum allowable) are needed globally, all three are represented in southern Africa, and the second was a Siderian snowball Earth coincident with a globally synchronous GOE at ~2.4 Ga. (SY4; Fri. 2:40)

Miocene and Pliocene tectonic evolution of Northern Luzon, Philippines: Implications for porphyry mineralization

Hollings, P., Geology Department, Lakehead University, 955 Oliver Road, Thunder Bay, ON P7B 5E1, peter.hollings@lakeheadu.ca, Cooke, D.R. and Wolfe, R., CODES, ARC Centre for Excellence in Ore Deposits, Private Bag 126, Hobart, Tasmania 7001, Australia

Northern Luzon in the Philippines formed in a complex tectonic environment, and is currently sandwiched between two active subduction zones. However, the Miocene to Pliocene tectonic history of the region and the relationship to well developed porphyry and epithermal mineralisation is not well understood. Models for the Oligocene to Early Miocene of Northern Luzon have advocated a reversal from westward to eastward subduction, but volcanic rocks preserved in the Central Cordillera range and Cagayan Valley record a prolonged history of eastward subduction. In the Cagayan Valley potassic magmas associated with porphyry mineralization in the Didipio area formed in a back arc rift. Coeval rocks in the Baguio District of the Central Cordillera are predominantly calc alkaline volcanic rocks that formed in the main arc.

Eastward subduction continued into the Pliocene and Pleistocene where magmatic rocks of the Baguio District are spatially and temporally associated with mineralization. The district hosts >35 million ounces of gold and 2.7 million tonnes of copper in epithermal, porphyry and skarn deposits that formed in the last 3.5 million years. The Pliocene rocks in the Baguio area comprise a suite of intermediate to felsic low- to medium-K intrusions, some of which have adakitic affinities, and a second suite of mafic to intermediate, medium-K to



shoshonitic hornblende-phyric dikes. The onset of Pliocene magmatic activity is coeval with the initiation of subduction of the Scarborough Ridge along the Manila Trench and associated flattening and/or tearing of the downgoing slab.

Perturbations in the steady state tectonic environment from the Miocene to the Pleistocene in Northern Luzon, particularly slab flattening possibly linked to ridge subduction, can be linked to and possibly triggered, porphyry and epithermal mineralization events. (SS23; Fri. 9:40)

Temporal and spatial distribution of magmatic Ni-Cu-PGE/Cr-PGE/Fe-Ti-V deposits in the Bird River/Uchi/Oxford-Stull/La Grande-Eastmain superdomain: A new metalotect within the Superior Province

Houlé, M.G.¹, michel.houle@nrcan.gc.ca, Leshner, C.M.², Metsaranta, R.T.³, Goutier, J.⁴, McNicoll, V.⁵ and Gilbert, H.P.⁶, ¹Geological Survey of Canada, GSC-Québec, 490 Couronne Street, Québec, QC G1K 9A9; ²Mineral Exploration Research Centre, Department of Earth Sciences, Laurentian University, Sudbury, ON P3E 2C6; ³Ontario Geological Survey, 933 Ramsey Lake Rd, Sudbury, ON P3E 6B5; ⁴Géologie Québec, Ministère des Ressources naturelles, 70 avenue Québec, Rouyn-Noranda, QC J9X 6R1; ⁵Geological Survey of Canada, GSC-Ottawa, 601 Booth Street, Ottawa, ON K1A 0E8; ⁶Manitoba Geological Survey, 360-1395 Ellice Avenue, Winnipeg, MB R3G 3P2

The Superior Province is one of the largest coherent Archean cratons in the world, with a prolific mineral endowment that includes world-class orogenic lode Au deposits, world-class volcanogenic-associated massive Cu-Zn-(Pb) sulfide deposits, and economically significant magmatic Ni-Cu-(PGE) deposits. Cr and Fe-Ti-V mineralization in ultramafic-mafic intrusions was known from several areas of the province, but was considered to be only marginally significant until the discovery of the world-class Cr deposits and potentially significant Fe-Ti-V mineralization in the McFaulds Lake greenstone belt ("Ring of Fire") of northern Ontario.

Ni-Cu-(PGE), Cr-PGE, and Fe-Ti-V deposits/occurrences in the northern part of the Superior Province occur within supracrustal successions along the margins and within the interiors of the Bird River/Uchi/Oxford-Stull/La-Grande-Eastmain domains (BUOGE "superdomain"). Ni-Cu-PGE deposits occur across the superdomain and appear to range from Neoproterozoic to Mesoproterozoic, with the best examples occurring within the Bird River (e.g., Maskwa, Mayville), Uchi (e.g., Thierry, Norton Lake), Oxford-Stull (e.g., Eagle's Nest), Eastmain (e.g., Nisk), and La Grande (e.g., Gayot) domains. Cr-PGE deposits also occur across the superdomain and appear to be mainly Neoproterozoic in age, with the best examples occurring in the Bird River (e.g., Chrome), Oxford-Stull (e.g., Big Trout Lake, McFaulds Lake), and La Grande (e.g., Menarik) domains. Importantly, these Cr-bearing ultramafic-mafic intrusions also host significant Ni-Cu-(PGE) mineralization. Fe-Ti-V deposits/occurrences appear to be more spatially restricted and less abundant, and have been recognized only within the westernmost (e.g., Pipestone) and eastern (e.g., Butler, Thunderbird) parts of the Oxford-Stull domain.

The BUOGE superdomain defines a major Cr-PGE/Ni-Cu-PGE/Fe-Ti-V metalotect that appears to be fundamentally different in terms of magma composition (low-Mg komatiite/high-Mg tholeiite vs. high-Mg komatiite/tholeiite), volcanic-subvolcanic setting (ultramafic intrusions > lava flows vs. ultramafic intrusions < lava flows), and sedimentary environments (oxide facies iron formation > sulfide facies iron formation vs. oxide facies iron formation < sulfide facies iron formation) from the Ni-Cu-(PGE)-dominated systems in the Abitibi greenstone belt or the apparently relatively unmineralized North Caribou core, Island Lake, and Goudalie domains. Detailed studies of the tectonic, volcanic, and petrogenetic settings of key areas of the BUOGE superdomain are in progress and should provide light on why this metalotect is so different from those in the southern part of the Superior Province. (SS3; Thurs. 3:40)

New age for the Mayville Intrusion: Implication for a large mafic-ultramafic event in the Bird River greenstone belt, southeastern Manitoba

Houlé, M.G.¹, michel.houle@nrcan.gc.ca, McNicoll, V.J.², Bécu, V.¹, Yang, X.M.³ and Gilbert, H.P.³, ¹Geological Survey of Canada, GSC-Québec, 490 Couronne Street, Québec, QC G1K 9A9; ²Geological Survey of Canada, GSC-Ottawa, 601 Booth Street, Ottawa, ON K1A 0E8; ³Manitoba Geological Survey, 360-1395 Ellice Avenue, Winnipeg, MB R3G 3P2

Mafic-ultramafic intrusions occur throughout the southern (SA) and the northern arm (NA) of the Bird River greenstone belt (BRGB), located between the English River basins and the Winnipeg River Terrane within the southwestern part of the Superior Province. Several mafic-ultramafic components have been identified: (1) synvolcanic gabbroic rocks within MORB-type formations (SA, NA); (2) the ca. 2745 Ma Bird River Sill (BRS; SA); (3) the Mayville intrusion (MI; NA); (4) glomeroporphyritic gabbroic sills/dikes (SA, NA), and (5) the ca. 2723 Ma synvolcanic gabbroic rocks within the arc-type formations (SA). Although the absolute and relative ages of some of these intrusions are uncertain, a correlation between the BRS and the MI has been proposed by several workers. A new geochronological result from a xenolith of leucogabbro within heterolithic intrusive breccia zone of the MI yielded a U-Pb ID-TIMS age of 2742.8 ± 0.8 Ma, which is interpreted to be the age of crystallization. This new age for the MI is equivalent, within error, to the 2743.0 ± 0.5 Ma crystallization age interpreted for the BRS. The data strongly suggest that a single large mafic-ultramafic magmatic event generated both the BRS and the MI, and may have extended for over 75 km laterally and 20 km across the entire BRGB, on either side of the Maskwa Lake Batholith. However, the internal stratigraphies of the BRS and MI are quite different; the very well layered BRS consists of a lower ultramafic zone overlain by an upper mafic zone, whereas the less well stratified MI is composed essentially of a mafic zone overlain by a heterolithic intrusive breccia zone; a marginal mafic to ultramafic zone occurs sporadically along the basal contact of the MI. It has been proposed, in the case of the BRS, that the upper anorthositic part crystallized from residual magmas generated during the formation of the underlying ultramafic zone. This mechanism is problematic in the case of the MI because of the apparent absence of an ultramafic component in the intrusion. Another possibility is that an ultramafic component was detached from the main anorthositic part of the MI, and could exist at depth. The MI and BRS, although interpreted to be derived from the same magmatic source, apparently had separate emplacement mechanisms and magmatic evolutionary paths during their ascent through the crust. These differences may be the key to explain the different styles of mineralization that characterize each intrusion. (SS9; Wed. 10:20)

Solid solution in the (F, OH, Cl) apatite ternary system

Hughes, J.M., University of Vermont, Burlington, VT 05405 USA, jmhughes@uvm.edu, and Nekvasil, H., Department of Geosciences, Stony Brook University, Stony Brook, NY 11794 USA

Apatite is one of the most common minerals; solid solutions of the calcium phosphate apatite minerals (fluorapatite, chlorapatite, hydroxylapatite) are ubiquitous. Apatite is the foundation of the global phosphorus cycle; the phase also forms all hard tissue in humans except small portions of the inner ear, and is essential for life in numerous species. Apatite is the main source of phosphate for fertilizers, and the minerals are used increasingly in the capture and sequestration of nuclear and heavy metal contaminants through phosphate-induced metal stabilization. The phases are used in many geological measurements, such as apatite fission-track dating that provides rates and dates of geologic processes, and apatite is also fundamentally important in controlling rare-earth element variation in rocks. Recent studies in medicine have demonstrated the efficacy of the non-invasive determination of carbonate-content of apatite in the distinguishing benign and malignant tumors in breast tissue, and bioengineering of the



fluorapatite content of human teeth has long been utilized as a method to reduce dental caries and is listed by the U.S. Centers for Disease Control as one of the ten great public health achievements of the 20th century. Thus, apatite is the mineral with perhaps the widest applications in the fields of geology, medicine, dentistry, agriculture, environmental mineralogy and biology.

Despite its widespread occurrence and importance in disparate fields, the atomic arrangement of apatite is not well understood. Apatite is a compound wherein the atomic arrangements of the binary members of the (F, OH, Cl) ternary system are not predictable from the individual end-members. In the apatite atomic arrangements the anions exist in [0,0,z] anion columns, at positions contained within, or disordered about, mirror planes at $z = 1/4, 3/4$ in the P6₃/m unit cell. It has been shown that ternary solution of the column anions can be effected by creation of a second Cl site that enables acceptable distances between column anions, but the anion solution along the (F, OH, Cl) binary systems are not well-understood. We have recently elucidated the atomic arrangement of apatite along the F-Cl binary, and subsequently can report on the method of "anion-stuffing" in the apatite anion column along that binary, with our crystal structure results confirming previous predictions of column anion behavior along the binary. We will also present the constraints regarding solid solution along the F-OH and Cl-OH binary systems, and comment on previous and current work to resolve those atomic arrangements. (SY1; Thurs. 11:00)

Evaluating the degree of transport and time averaging among Burgess Shale fossil assemblages via taphonomic analysis of the trilobite *Elrathina cordillerae*

Hughes, N.C., nigel.hughes@ucr.edu, Balint, M.B., Dept. of Earth Sciences, University of California, Riverside, CA 92521 USA, and Caron, J-B., Department of Natural History, Royal Ontario Museum, 100 Queen's Park, Toronto, ON M5S 2C6

Evaluating the extent to which the Burgess Shale biota has been affected by transport, decay and time averaging is critical for estimating how this important fossil assemblage represents local community ecology during the Cambrian. The multi-component trilobite exoskeleton and associated soft parts can provide sensitive indicators of biostratigraphic history, and here we examine the taphonomy of the most common polymerid trilobite within several bedding assemblages from the "Greater Phyllopod Bed" (Walcott Quarry), the olenimorph *Elrathina cordillerae*. Soft part preservation, high degrees of articulation, and aspects of posture including encapsulated enrollment confirm that many individuals were probably alive at the time of their burial. Two distinct taphonomic modes occur among eight bedding assemblages bearing common *E. cordillerae*. One mode, characterized by the -420 assemblage, almost exclusively includes freshly killed mature individuals, which are found in a variety of attitudes to bedding in complex postures involving dorsal flexure. Many show soft part preservation, and specimen distribution is apparently patchy on an outcrop scale. Although their taphonomy is broadly consistent with transportation prior to burial, it does not require it, as similar patterns could have been achieved if the animals were trying to extract themselves following burial *in situ* by mud. The second mode contains some associations of disarticulated sclerites that cannot have been transported in their present disposition. Particular arrangements also suggest *in situ* congregation of living individuals immediately prior to burial, and overall specimen density is higher than in the -420 assemblage. Some specimens show soft part preservation or encapsulated enrollment indicating that they were alive as burial events began but only about 15% of the specimens are complete articulated dorsal exoskeletons. Individuals generally lie parallel to bedding, but many are inverted. This second taphonomic mode apparently contains live individuals mixed with sclerites that were biologically inert before the events leading to assemblage preservation began, and is thus more time averaged than the first mode. The second mode precludes transportation for at least some individuals of *E. cordillerae*, and thus

suggests that some of these trilobites were living in this environment. (SY3; Thurs. 9:00)

Magmatic layering in a peralkaline intrusion: An example from Layer 0, Ilímaussaq Complex, S. Greenland

Hunt, E.J., ejh9@st-andrews.ac.uk, Finch, A.A. and Donaldson, C.H., Department of Earth & Environmental Sciences, University of St Andrews, St Andrews, Fife, KY16 9AL

The Ilímaussaq Complex, S. Greenland, contains some of the most evolved igneous rocks in the world and is considered as a substantial deposit of rare-earth elements, Ta, Nb and Zr. These elements are concentrated within the Kakortokite Layered Series, on which our work focuses. This comprises 29 repetitive 3-unit layers, numbered -11 to +17 relative to a marker horizon Layer 0. The units of each layer are distinguished by modal mineralogy the lower unit is arfvedsonite-rich black kakortokite, the middle unit is eudialyte-rich red kakortokite and the upper unit is nepheline- and alkali feldspar-rich white kakortokite. Despite much work on the development of the Kakortokite Layered Series, no consensus on the physico-chemical processes that led to the formation of the rhythmic layering has been forthcoming, although most hypotheses suggest gravitational sorting and settling contributed to layer formation. We present a detailed petrographical, quantitative textural and mineral chemical study of Layer 0, with the aim of defining the magmatic processes involved in the development of the layer. Crystal size distribution (CSD) analysis was performed on hand-digitised photomicrographs to give insight into processes of crystal nucleation and growth. Layer 0 crystallised above a sharp boundary to Layer -1, which is traceable across the entire complex, suggesting that large-scale magma chamber processes formed Layer 0. The CSD for arfvedsonite in the Layer 0 black kakortokite indicates multiple modes of formation, with 95% of the arfvedsonite forming *in situ* with crystal sizes between 0.1 to 2.1 mm, while larger crystals up to 3.4 mm, accounting for 5% of the total arfvedsonite, formed through crystal settling. This was followed by *in situ* crystallization of eudialyte (0.4 to 2.3 mm) in the red kakortokite and alkali feldspar (0.4 to 10.0 mm) in the white kakortokite. Chemical variations in Fe_{TOT}/Mn of eudialyte were noted between the 3 units of Layer 0, indicating they formed from an evolving magma. The results suggest that processes of cumulate settling cannot account for all the petrographical and textural characteristics of Layer 0. Instead multiple processes contributing to magmatic layering must have operated during its formation. (SS8; Thurs. 2:40)

Multi-stage evolution of non-gem diamonds at the Diavik diamond mine, Canada

Hunt, L., lhunt@ualberta.ca, Stachel, T., Pearson, D.G., Stern, R., Muehlenbachs, K., University of Alberta, Edmonton, AB T6G 2E3, and McLean, H., Rio Tinto, Diavik Diamond Mines Inc., Yellowknife, NWT X1A 2P8

Diavik is located in the Cretaceous-Miocene Lac de Gras Kimberlite Field of the Central Slave Craton. Gem diamonds have traditionally been studied here, being the most economically valuable, however, a lack of impurities limits insight into their formation. Non-gem diamonds contain abundant impurities and as such may enable a much more detailed understanding of diamond formation. Evidence collected to date suggests that non-gem diamonds grow from multiple and compositionally diverse melts/fluids over a prolonged time period.

Whole diamond samples have been analysed by Fourier Transform Infrared spectroscopy; whilst it is difficult to obtain infrared spectra from zones of non-gem growth, initial results indicate that they grew from multiple diamond forming fluids. A number of peaks associated with carbonate inclusions are observed in a selection (6 to date) of non-gem diamond growth whilst a further subset (5 to date) display peaks associated with silicate inclusions.

Research on a 54 carat boart fragment indicates formation from a different melt/fluid. The $\delta^{13}C$ is typical of eclogitic diamonds (~23.6‰) however, intergrown silicate minerals are predominantly G9 garnets



and peridotitic clinopyroxene. This suggests interaction of a slab derived melt/fluid with a very negative $\delta^{13}\text{C}$ with mantle peridotite.

Cathodoluminescence of five sectioned non-gem diamonds (three coated and two hailstone boart) revealed fine scale complexities not observed in visible light, suggesting multiple growth stages. Secondary Ion Mass Spectrometry was used to determine nitrogen content and $\delta^{13}\text{C}$ along transects perpendicular to growth. Despite the visual complexities of the hailstone boart, little change is observed in either the nitrogen content (960-1100ppm) or $\delta^{13}\text{C}$ (-6.5 to -6.0‰) whilst the coated stones show more variation (coats: average nitrogen content ~1700ppm, $\delta^{13}\text{C}$ range from -8 to -5.5‰; cores: average nitrogen content ~1300ppm, $\delta^{13}\text{C}$ range from -4.5 to -5‰). The change from gem to non-gem growth appears visually sharp and may represent precipitation from two distinct fluids. However, a subtle shift in nitrogen content and $\delta^{13}\text{C}$ is already observed prior to the visual transition in two of the three coated stones, suggesting a more continuous evolution of the diamond precipitating medium. This may have occurred through mixing processes with non-gem growth commencing after a critical point of supersaturation was reached. The mantle-like $\delta^{13}\text{C}$ suggests a melt/fluid derived from the asthenosphere.

Mantle residence temperatures, determined from nitrogen content and aggregation state, indicate that the non-gem diamonds grew prior to, after, and alongside gem diamonds throughout the entire depth section of the lithospheric mantle. (SS4; Fri. 9:20)

Keynote (40 min): How difficult was subduction in the Archean?

Hynes, A., Earth & Planetary Sci., McGill University, 3450 University St., Montreal, QC H3A 0E8, andrew.hynes@mcgill.ca

As asthenospheric mantle rises at oceanic spreading centres, its upper part undergoes partial melting, producing oceanic crust and depleted mantle, both of which have lower intrinsic density than the asthenospheric mantle from which they were derived. It has been suggested that with higher mantle temperatures in the Archean, the greater degree and depth of partial melting might have reduced this intrinsic density sufficiently to prevent subduction from occurring. I investigate the density of the oceanic crust and underlying mantle for a mantle with temperatures 200° higher than today, using detailed models of the chemistry of melting and the mineralogy of the ensuing rocks. For the melting model used, crustal thicknesses are 21 km and the depth to which the mantle is partially melted is 114 km, compared with 7 km and 54 km for a comparable model of modern Earth. Two models similar to the 'plate' model for thermal evolution of modern oceanic lithosphere are examined. A first assumes twice the heat flow into the base of the plates, which severely restricts the depths to which the plates can cool with age. A second assumes the plates can cool to the depth to which the asthenosphere undergoes partial melting. The heat flow into the base of the plates with this model is only 1.3 times as large as today. With the first model, the relatively shallow depths to which cooling takes place in the mantle prevents the oceanic plates from becoming negatively buoyant. With the second model, however, oceanic plates become negatively buoyant after approximately 50 Ma of cooling. For both models, plates are negatively buoyant by ages of 30 Ma if the upper 15 km of the crust is detached. Given our present knowledge of Archean thermal conditions, there does not appear to be any compelling theoretical argument against efficient subduction at that time. (SS11; Fri. 10:40)

Micro-porosity distribution in the Tagish Lake C2 carbonaceous chondrite

Ibrahim, M., eibrah4@uwo.ca, McCausland, P.J.A., Brown, P.G., Umoh, J. and Holdsworth, D.W., Western University, London, ON N6A 5B7

The physical response of meteoritic rock to impact-related shock events or to crush-ing during atmospheric entry is governed to a large extent by the rock's porosity and its po-rosity distribution. Microporosity in meteorites is predominantly found to reside in small fractures and as intergranular voids. But are these meteorite physical properties truly representative of the objects which struck the Earth's atmosphere or of

their parent bodies? Amongst recovered meteorite classes, the Tagish Lake (hydrous C2) carbonaceous chondrite represents perhaps the most porous, primitive material available, with previous work showing a mean bulk density of $1.64 \pm 0.02 \text{ g/cm}^3$ and porosity of 40% for fragments ranging between 13.7 g to 77.2 g. Two separate collection phases in 2000 recovered ~11 kg of Tagish Lake material with two or more distinct lithologies present, including "inclusion rich" and "dark dusty" lithologies. A previous mass distribution investigation using conventional sieving methods showed that a significant "roll-off" occurs at sizes <2 mm, possibly caused by limited sampling at small sizes or a potential change in the mechanism of sample fragmentation from primary to secondary. In this study, the variation in porosity of the Tagish Lake meteorite with fragment mass (down to <1 g) is investigated along with the distribution of micro-cracks and voids in fragments using medical X-ray computed tomography (micro CT). Preliminary results suggest that bulk density is higher for small fragments than for the larger (>13 g) fragments that were previously reported. Cracks have a potentially important effect on the microporosity (and strength behaviour) for Tagish Lake fragments, but may have a lesser contribution to the microporosity of small fragments. (SS18; Thurs. 3:20)

Modal mineralogy of Howardite, Eucrite and Diogenite (HED) meteorites by Rietveld refinement of X-ray diffraction data

Izawa, M.R.M.¹, matthew.izawa@gmail.com, Cloutis, E.A.¹, Pompilio, L.², Reddy, V.^{3,4}, Hiesinger, H.⁵, Nathues, A.⁴, Mann, P.¹, Le Corre, L.⁴, Palomba, E.⁶, and Bell III, J.F.⁷, ¹Department of Geography, University of Winnipeg, 515 Portage Avenue, Winnipeg, MB R3B 2E9; ²Department of Human and Earth Sciences, D'Annunzio University, via Dei Vestini, 30-I, 66013, Chieti, Italy; ³Dept. of Space Studies, Box 9008, University of North Dakota, Grand Forks, ND, USA 58202; ⁴Max-Planck-Institute for Solar System Research, Katlenburg-Lindau, Germany; ⁵Institut für Planetologie, Westfälische Wilhelms-Universität, Wilhelm-Klemm-Str. 10, 48149 Münster, Germany; ⁶Istituto di Fisica dello Spazio Interplanetario, Via del Fosso del Cavaliere, INAF, 00133 Roma, Italia; ⁷School of Earth and Space Exploration, Box 871404, Arizona State University, Tempe, AZ, USA 85287-1404

Howardite, Eucrite and Diogenite (HED) meteorites are mafic silicate-dominated igneous or metaigneous rocks with very old crystallization ages, characteristics which point to an origin in a large differentiated asteroid. Asteroid 4 Vesta has been suggested as the most likely HED parent body based on numerous criteria.

Modal mineralogy is an important parameter for constraining rock paragenesis, and strongly affects the physicochemical behaviour of rocks during geological processes. Modal mineralogy is not as widely reported for meteorites as is bulk chemical composition or the mineral chemistry of constituent minerals. Rietveld refinement of power X-ray diffraction data provides a reliable means to quantify the modal mineralogy of bulk meteorite samples. Modal mineralogy for the HED samples JaH 626 (shocked polymict eucrite), Millbillillie (polymict eucrite), NWA 1836 (variably shocked cumulate monomict eucrite), NWA 1942 (howardite), NWA 1943 (howardite), NWA 5751 (howardite), NWA 6013 (olivine-rich diogenite), NWA 6477 (eucrite), Talampaya (cumulate eucrite), and Tatahouine (diogenite) have been determined by Rietveld refinement of XRD data. Shocked samples JaH 626 and NWA 1836 contain significantly lower amounts of plagioclase than similar unshocked meteorites, possibly due to the conversion of some plagioclase to maskelynite (diaplectic glass) or impact melt glass. Structural characterization of meteoritic minerals by diffractometry also provides important complementary information to chemical analysis, for instance, by determining whether 'low-Ca pyroxene' is pigeonite or orthopyroxene.



Modal mineralogy of HED meteorite samples, values in wt. %.

sample	plagioclase	pigeonite	augite	orthopyroxene	olivine	trace minerals	R _{wp}
JaH 626	40	59	n.d.	n.d.	n.d.	Ilm	5.95
Millbillillie	49	24	12	14	n.d.	Ilm, Tro, Chr	4.60
NWA 1836	28	55	n.d.	17	n.d.	Ilm, Ol	6.28
NWA 1942	35	34	n.d.	30	1		5.41
NWA 1943	43	27	15	15	n.d.	Ol	5.04
NWA 5751	28	13	7	50	1	Ol, Chr	5.64
NWA 6013	7	n.d.	n.d.	65	27	Chr	6.07
NWA 6477	54	33	13	n.d.	n.d.	Ilm, Tro, Chr	6.55
Talampaya	65	32	1	n.d.	n.d.	Ilm, Tro, Chr	9.32
Tatahouine	n.d.	n.d.	n.d.	97	Tr	Ol, Chr, Crs, Ant	8.83

n.d. = not detected. Trace phases (<~1-2%): Ilm = ilmenite, Tro = troilite, Chr = chromite, Ol = olivine, Crs = cristobalite, Ant = anatase. R_{wp} is the weighted profile residual of the Rietveld refinement, values less than 10% are considered acceptable by many authors. Mathematical fit errors in refined abundances (from the covariance matrix of the least-squares fit) are typically less than ~1%. (SS18; Thurs. 2:00)

Orogenic Ni-Cu-PGE deposits: Cu-PGE mineralization in the DJ/DB Zone of the Turnagain Alaskan-type intrusion, north-central British Columbia, Canada

Jackson-Brown, S.¹, sjackson@eos.ubc.ca, Scoates, J.S.¹, Nixon, G.T.² and Ames, D.E.³, ¹Dept. of Earth, Ocean and Atmospheric Sciences, 2207 Main Mall, University of British Columbia, Vancouver, BC V6T 1Z4; ²British Columbia Geological Survey, Ministry of Energy and Mines, PO Box 9333 Mtn Prov Govt, Victoria, BC V8W 9N3; ³Geological Survey of Canada, Central Canada Division, 750-601 Booth St., Ottawa, ON K1A 0E8

The ca. 190 Ma Turnagain intrusion is an Alaskan-type, subduction-related ("orogenic") ultramafic body that is host to a significant nickel-cobalt resource (865 Mt at 0.21% per tonne Ni and 0.013% per tonne Co). The intrusion is approximately 24 km² in size and comprises a suite of ultramafic rocks including dunite, wehrlite, olivine clinopyroxenite, hornblende clinopyroxenite, and hornblendite with minor late-stage dioritic intrusions and inclusions of hornfelsed country rocks. A recent geochemical soil survey and subsequent drilling by Hard Creek Nickel Corporation (2004-2007) has revealed an area of copper and platinum group element (PGE) enrichment in a previously under-explored area of the intrusion, the DJ/DB zone, located 2.5 km northwest of the current nickel resource. Within the DJ/DB zone, the Cu and Pt+Pd soil geochemical anomalies are spatially associated, but show a distinct separation between the regions of elevated Cu and Pt+Pd with high Cu values covering a much larger area (2.1 km²) to the south, east, and northwest of the PGE anomaly (1.2 km²). From assays on drill core that intersected rocks within the DJ/DB zone, maximum Cu values have been reported in excess of 0.3 wt.% over 7.3 m and combined Pt+Pd of greater than 500 ppb over 19.3 m. The anomalous Cu-PGE values are typically found within magnetite-bearing clinopyroxenite and are associated with areas of increased serpentinization. Sulfur isotope analyses for sulfides from the DJ/DB zone range from $\delta^{34}\text{S} = -11$ to +2.2 ‰, values that are similar to those reported for the rest of the Turnagain intrusion. Inclusions of graphite-

bearing pyritiferous phyllitic sedimentary rocks are characterized by values as low as $\delta^{34}\text{S} = -17.8$ ‰, indicating a significant role for assimilation of S-bearing crustal rocks during emplacement of the Turnagain intrusion. A reconnaissance SEM investigation has revealed an association between Cu-PGE abundances and the presence of accessory sulfide and arsenide minerals, including digenite (Cu₉S₅), millerite (NiS), nickeline (NiAs), cobaltite (CoAsS), gersdorffite (NiAsS), and ullmanite (NiSbS). Millerite and digenite, 25-250 µm in diameter, are typically intergrown with pentlandite and magnetite surrounding early chromite crystals. The arsenides and antimonides are found as inclusions (10-50 µm) within chalcopyrite, although nickeline is typically fully enclosed by gersdorffite or cobaltite. The relationship between areas of high PGE (>300 ppb) and the abundance of arsenides and arsenic-antimony sulfides will be further investigated to determine any potential links between arsenic and PGE in orogenic Ni-Cu-PGE mineralization and its potential use in exploration. (SS9; Wed. 3:40)

Research on the prediction of mine drainage and the colloidal transport of metals

Jamieson, H.E., Buckwalter-Davis, M.J., Dongas, J. and Fenwick, L., Queen's University, Kingston, ON K7L 3N6, jamieson@geol.queensu.ca

Mine permitting requires a clear understanding of whether drainage from tailings and waste rock is likely to be acidic and contain dissolved metals above regulatory limits. The application of advanced research tools to samples from an abandoned PbZn mine has provided new insights into prediction and risk assessment. The New Calumet Mine, located 90 km west of Ottawa, is a metamorphosed massive sulfide deposit mined between 1944 and 1968. Approximately 2.5 million tons of tailings remain, and produce pH-neutral drainage with elevated concentrations of zinc.

The first project involves the comparison of an indirect chemical method of predicting acid mine drainage (acid-base accounting, or ABA) with a direct mineralogical assessment using scanning electron microscopy and energy dispersive X-ray spectroscopy (SEM-EDS) with Mineral Liberation Analysis (MLA). Six samples of near-surface tailings were tested using ABA, a widely-used method that compares the amount of acid-generating sulfide to acid-neutralizing carbonate by laboratory tests of sulphur content and inorganic carbon. The results were compared with those obtained by MLA analysis of hundreds of thousands of particles on thin sections. The acid potential (AP) was calculated from the modal per cent of acid generating sulfides including pyrite, pyrrhotite, chalcopyrite, and high-iron sphalerite. The neutralization potential (NP) was based on the modal per cent of calcite and dolomite and was corrected for ankerite/ferroan dolomite content. The difference the neutralization potential ratio (NP/AP) between the two methods is less than 15% for five of the six samples tested, and 23% for the sixth sample. A further six samples with a wider range of tailings types, including some highly weathered tailings with field-measured paste pH as low as 2, have also been analysed by MLA. This mineralogical approach offers an alternative tool for prediction of acid rock drainage and metal leaching for materials with complex mineralogy.

The second project involves the determination of Zn and other metals that are present in mine drainage as colloidal particles. Water samples are typically filtered to <0.45 microns before acid is added as a preservative, and all metal concentrations measured in the filtered samples are considered dissolved. Drainage samples from the Calumet tailings have been processed using an ultrafiltration cell which captures particles <0.45 and >10 nm. SEM imaging of the filters has revealed sub-micron spheres of Zn oxides and/or carbonates and Fe-Zn. Understanding the fraction of metal carried in a colloidal form has important implications for bioavailability and mobility. (SS20; Fri. 2:40)



Characterization of cassiterite parageneses in metasomatic altered meta-mafic rocks of the “Felsitzzone”, Großschirma - Freiberg mining district, Erzgebirge, Germany

Járóka, T. and Seifert, T., thomas.seifert@mineral.tu-freiberg,
Division of Economic Geology and Petrology, Department of
Mineralogy, TU Bergakademie Freiberg, Brennhaussasse 14, D-
09596 Freiberg, Germany

The “Felsitzzone” is an arch-shaped Sn-polymetallic mineralization zone with a lateral extension of about 18 km. It is located within metamorphic units on the NW margin of the Freiburger anticline structure. Two-mica gneisses and mica schist are the main cover rocks of the Freiburger anticline towards the NW margin. Amphibolites, red gneisses and metacarbonates can also be found subordinately. Light microscopy and scanning electron microscopy of certain exploration drill cores samples from Großschirma show a close connection between the “Felsitzzone” mineralization and structurally controlled zones which are closely associated with mylonitization zones in this area. Most of the ore minerals occur in fine-grained metasomatites which can be derived from strong metasomatic altered meta-mafic rocks and gneisses. Higher Sn, Li, and F grades of all investigated samples display some metasomatic alteration processes (e.g., metasomatic overprinted meta-mafic dike rocks [Sn: average 1030 ppm (170-3090 ppm), Li: 170 ppm (50-250 ppm), F: 2010 (1000-3420 ppm), n=8]). Two ore types can be distinguished: a sulfide-rich and a low-sulfide one. The sulfide-rich ore type is marked by different hydrothermal mineralization events indicated by numerous thin veins. The most important event is mainly characterized by a pyrite-marcasite mineralization, while chalcocopyrite, galena, sphalerite as well as medium-grained cassiterite occur only subordinately. In comparison the low-sulfide ore type is only marginal influenced by the hydrothermal vein systems and features smaller amounts of sulfides, predominantly pyrite and chalcocopyrite. A few fine-grained cassiterite is also appearing in this ore type, usually in intergrowth with Ti-bearing minerals. (*GSI; Thurs. Poster*)

Deformation and partial melting as critical processes for the remobilization of uranium: Example of Mudjatik-Wollaston Transition Zone (Saskatchewan, Canada)

Jeanneret, P.¹, pauline.jeanneret@univ-fcomte.fr, Goncalves, P.¹,
Trap, P.¹, Marquer, D.¹, Durand, C.² and Quirt, D.³, ¹UMR
Chrono-Environnement, Université de Franche-Comté, Besançon,
France; ²UMR Géosystèmes, Université de Lille 1, France;
³AREVA Resources Canada, Saskatoon, SK

In the eastern part of the Athabasca basin, the great majority of U ore deposits and prospects are located along the Mudjatik-Wollaston Transition Zone (MWTZ), where the Athabasca Basin unconformably overlies highly-deformed anatectic metasedimentary rocks, locally U-mineralized pegmatites, and granitoids. This spatial distribution suggests that Archean (~2.5 Ga) and/or Trans-Hudsonian (~1.8 Ga) deformation and partial melting of metasedimentary rocks could constitute a major first stage of uranium remobilization and concentration that is necessary to obtain the world-class uranium ore deposits at 1.6-1.3 Ga.

To understand the role of these early tectonometamorphic events, we have conducted a multidisciplinary study of the basement rocks across the MWTZ, northeast of the Athabasca Basin margin. This approach consists on deciphering the P-T-t-D-M (M: Mineralization) evolution of the basement and supracrustal rocks. In most lithologies, and particularly in metasediments, the main Uranium carrier is monazite. Consequently a particular attention is paid to its behavior during deformation and metamorphism.

The finite strain pattern results from the superposition of two deformation events: a D₁ event associated with a N90-100° gently-dipping foliation and a D₂ event that is characterized by the development of vertical N40-50° high-strain zones that are locally affected by N05-15° shear bands. This D₂ event is consistent with a sinistral transpressive deformation. Paleoproterozoic metasediments are partially melted and contain garnet, cordierite, sillimanite, and

biotite. Preliminary thermobarometric data suggest peak metamorphic conditions of 5-6 kbar and 800-850°C, followed by an isobaric cooling. The development of D₂ high strain zones is characterized by a strong enrichment in sillimanite and biotite and the partial breakdown of garnet.

The effect of deformation and partial melting on monazite behaviour has been studied in samples showing a strong partitioning of the D₂ deformation. D₂ low-strain zones are characterized by the abundance of quartz-feldspathic leucosomes and peritectic garnet. In these domains, monazite is abundant and shows complex zoning interpreted as the effect of *in-situ* dissolution-precipitation during partial melting. In contrast, monazite is almost completely absent from the sillimanite-biotite-rich D₂ high-strain zones. This suggests that monazite was dissolved during the development of D₂ high-strain, probably under sub-solidus conditions as suggested by the metamorphic assemblage. These preliminary results suggest that although partial melting is widespread, its effect on monazite dissolution and therefore Uranium mobility remains weak. In contrast, the transpressive deformation and associated fluid flow may be major processes for the Uranium transfer. (*SS10; Thurs. 2:40*)

Biofacies constraints on the Ordovician equator in Laurentia: A test of Early Paleozoic geomagnetic field geometry

Jin, J.¹, Harper, D.A.T.², Cocks, L.R.M.³, McCausland, P.J.A.⁴,
Rasmussen, C.M.O.⁵ and Sheehan, P.M.⁶, ¹Western University,
London, ON N6A 5B7; ²Durham University, Durham DH1 3LH,
UK; ³The Natural History Museum, London SW7 5BD, UK;
⁴Western University, London, ON N6A 5B7; ⁵Natural History
Museum, University of Copenhagen, Copenhagen K-1350,
Denmark; ⁶Department of Geology, Milwaukee Public Museum,
Milwaukee, WI 53233 USA

The Late Ordovician equatorial zone, like today, had few hurricane-grade storms within 10 degrees of the equator, as witnessed by the preservation of massive-bedded Thalassinoides ichnofacies (Tyndall stone) in a trans-Laurentian belt more than 6,000 km long from southwestern USA through Manitoba to North Greenland. That belt also includes non-amalgamated shell beds dominated by the brachiopod Proconchidium, which would not have been preserved in life position after hurricane-grade storms. The belt lacks such storm-related sedimentary features as rip-up clasts, hummocky cross stratification or large channels. In contrast, other contemporaneous Laurentian Thalassinoides facies and shell beds lying on either side of the belt have been much disturbed by severe storms below fair-weather wave base. The position of the biofacies-constrained equatorial belt coincides with the Late Ordovician equator deduced from paleomagnetic data from Laurentia, thus providing both a high-precision equatorial location and an independent test of the Geocentric Axial Dipole (GAD) hypothesis for that time. (*SS11; Thurs. Poster*)

Using ³¹P NMR to probe the solution dynamics of a large uranyl-peroxo cluster

Johnson, R.L.¹, rljohnson@ucdavis.edu, Ohlin, C.A.², Pellegrini, K.³, Burns, P.C.³ and Casey, W.H.¹, ¹University of California,
Davis, Davis, CA 95616 USA; ²Monash University, Clayton
Victoria, 3168, Australia; ³University of Notre Dame, South
Bend, IN 46556 USA

A large and previously unsuspected class of uranyl-peroxide clusters was discovered only a decade ago as nanometer-size ions that form spontaneously in aqueous solutions. Little is known about the chemistry of these ions in spite of their obvious importance as soluble forms of actinide elements which are potentially present in the environment. Here we show reversible structural 2 nm in–changes in an example uranyl(VI) cluster of this class that is diameter. It contains 24 uranyl moieties, 12 pyrophosphate units that are detectable via ³¹P NMR and has a nominal stoichiometry of [(UO₂)₂₄(O₂)₂₄(P₂O₇)₁₂]⁴⁸⁻. NMR spectroscopy shows that the ion has two distinct forms that interconvert on the millisecond to second time scale depending upon temperature and the size of the charge-compensating counterions. This



dynamic interconversion may relate to the onset of dissociation of the cluster into smaller fragments. Extrapolated broadly, this result supports a model where nanometer-size features at the oxide-solution interface have sets of accessible low-energy metastable states that control isotope exchanges and dissociation. (SS5; Wed. 9:40)

Keynote (40 min): Assembling Pangea: Not a linear process

Johnston, S.T., University of Victoria, PO Box 1700 Station CSC, Victoria, BC V8W 2Y2, stj@uvic.ca

Pangea is commonly inferred to have formed in the Upper Carboniferous as a result of closure of the Rheic ocean and ensuing collision of Gondwana and Laurussia. The Appalachians in eastern North America, and the Variscan Orogen of western Europe are interpreted as having formed a single contiguous orogen that developed in response to, and provides a record of, the Gondwana - Laurussia continental collision. Palinspastic closure of the post-Pangea Atlantic Ocean should, therefore, restore continuity of the Appalachian and Variscan orogens. It does not, which begs the question, 'why?' The problem lies in the Variscan orogen of westernmost Europe, which has been depicted as a convex to the west arcuate feature referred to as the Ibero-Armorican Arc. The Ibero-Armorican arc geometry, which requires closure of the orogen to the west leaving no easy way to establish continuity with the Appalachians, is based on assumed continuity of geological belts of southern Great Britain and northern France, including the Rheic suture, around the Cantabrian orocline, a 180 degree bend that characterizes Variscan orogen of northern Iberia, into western and southern Iberia. We demonstrated that two coupled oroclines characterize the Variscan orogen in Iberia, the convex to the west Cantabrian and a more southerly, convex to the east Central Iberian Orocline. Together these coupled oroclines (1) define a continental scale S-shaped fold of the Variscan orogen; and (2) provide a way to establish former continuity of the Appalachian and Variscan orogens. They do, however, present us with two additional problems. Palinspastic restoration of the coupled oroclines yields a 2300 km long previously linear orogen. Paleomagnetic, structural and stratigraphic data constrain orocline formation to a 10 Ma interval starting at 300 Ma, involving 1100 km of relative translation at rates of translation of 10 cm/a. The magnitude and rate of translation indicate subduction was involved. However, the oroclines post-date the Carboniferous formation of Pangea and hence are inferred to have formed in the absence of oceanic lithosphere internal to the supercontinent. Secondly, the 2300 km long, pre-orocline orogen consisted of juvenile oceanic arc sequences obducted over the distal west edge of the Gondwana passive margin along east-verging thrust faults, implying that Variscan orogenesis consisted of the collision of a juvenile oceanic arc with a Gondwanan-affinity ribbon continent. There is, therefore, no indication of a Gondwana - Laurussia continental collision, and hence no support for the Carboniferous construction of Pangea. (SS11; Fri. 2:00)

Major and trace element geochemistry of the Elsie Mountain Formation volcanic rocks, Southern Province, Canada: Implications for contact metamorphism along the southern margin of the Sudbury Igneous Complex

Jørgensen, T.R.C., Leshner, C.M. and Tinkham, D.K., Mineral Exploration Research Centre, Department of Earth Sciences, Laurentian University, 935 Ramsey Lake Road, Sudbury, ON P3E 2C6, tx_joergensen@laurentian.ca

Two-pyroxene hornfels rocks in the 2450 Ma Elsie Mountain Formation (EMF) define a 500 m wide high-T contact aureole along the southern margin of the 1849 Ma Sudbury Igneous Complex (SIC). The EMF is a dominant footwall lithology in the southern footwall of the SIC and > 85% of the formation consists of metabasalts which dip vertically and face southward. Historically, EMF metabasalts have been interpreted as Fe-rich tholeiitic rocks originating from an E-MORB type mantle source related to rifting of the margin of the Superior craton. However, a paucity of high-quality geochemical data leaves the potential for unrecognized lithological and petrogenetic differences between EMF metabasalts, dissimilarities that could be

controlling factors on mineral assemblages and microtextures during contact metamorphism. Our studies show that EMF metabasalts exhibit a chemostratigraphy comprising a northern (older) unit with higher Mg-Ni-Cr and lower highly incompatible lithophile element (Cs-Rb-Ba-Th-U-K) contents, and a southern (younger) unit with lower Mg-Ni-Cr and higher HILE contents in combination with depletion in Ti, Nb and Ta, and that a two-pyroxene metamorphic zone crosscuts this stratigraphy. The most primitive and least HILE-enriched samples plot between N-MORB and E-MORB on a Th/Yb-Nb/Yb projection, with the remaining samples plotting along a crustal contamination trajectory towards Total Archean Crust (TAC). The above geochemical fingerprints are often used to argue for crustal contamination, an enriched mantle source or formation by arc processes. Assimilation-fractional crystallization modelling can reproduce the contamination trajectory, but requires crystallization to end at an unrealistically 99% to explain the most enriched samples. The lack of interlayering of the units could favor a difference in primary source, however the enriched younger unit does not have primary mantle melt geochemical characteristics (#Mg 0.27-0.42, low Ni and Cr) and therefore, the difference is unlikely explained by different source regions alone. Alternatively, the geochemical trends may be caused by mobilization of HILE during contact metamorphism. In this case, these data are consistent with field evidence for a partially preserved metamorphic aureole along the southern margin of the SIC, and the preservation of least contaminated metabasalts closest to the SIC contact suggest that redistribution of relatively mobile elements was either incorporated into the SIC melt or propelled outwards into the footwall during contact metamorphism. The northern geochemical unit has not previously been documented and represents a useful marker unit within the EMF that will provide information on variations in the levels of thermomechanical erosion and contact metamorphism. (GS2; Wed. 9:20)

Sulfur partitioning between silicate melts and volatile phases: A better way to understand the "sulfur solubility minimum"?

Jugo, P.J., Laurentian University, Department of Earth Sciences, Ramsey Lake Rd., Sudbury, ON P3E 2C6, pjugo@laurentian.ca

The notion of a "sulfur solubility minimum" as a function of fO_2 in silicate melts has been discussed for decades. The concept is based on experiments conducted at atmospheric pressures and with a S-bearing gas in equilibrium with a silicate melt. However, "sulfur solubility" is a term also commonly used to describe the S content at sulfide saturation (SCSS) in silicate melts. This terminology is a source of confusion because "sulfur solubility minimum" experiments are not saturated in sulfide or sulfate phases, and therefore, the documented "minimum" has no relevance to the SCSS of silicate melts. Sulfur is a trace element in the silicate melts and the coexisting gas phase, therefore, S behavior is better understood if expressed in terms of partitioning (ΔS) between the two coexisting phases: $\Delta S_{\text{gas/melt}} = [S]_{\text{gas}}/[S]_{\text{melt}}$ (where [S] refers to the concentration of S). When data is recast in this manner ($\Delta S_{\text{gas/melt}}$ instead of $[S]_{\text{melt}}$), the geometry of the curves are inverted (*i.e.* showing a maximum instead of a minimum) with an apex representing the S partitioning maximum at $fO_2\text{-DMax}$ (*i.e.* the fO_2 condition that is most favorable to transfer of S from a silicate melt into a coexisting gas). This $fO_2\text{-DMax}$ is caused by a combination of: (a) dominance of SO_2 (S^{4+}) species in the gas phase (relative to H_2S and SO_3), (b) the inability of S to dissolve in silicate melts as S^{4+} species (as shown by XANES studies). Linking the two types of data ($\Delta S_{\text{gas/melt}}$ and SCSS) is useful to better understand S transfer from silicate melts into volatile phases during magma ascent (decompression), resulting in volatile exsolution and degassing. Documented position (in fO_2 space) of the $\Delta S_{\text{gas/melt}}$ maxima and the exponential increase in SCSS vary with melt composition, however, the general scenario (for basaltic and andesitic melts) is that the $\Delta S_{\text{gas/melt}}$ maxima will occur roughly at the onset of the exponential increase in SCSS. Thus, two "regions" separated by $fO_2\text{-DMax}$ can be identified. At $fO_2 < fO_2\text{-DMax}$ there is little S in the melt but increase fO_2 maximizes S transfer to the gas phase. At $fO_2 > fO_2\text{-DMax}$ increase in fO_2 decreases $\Delta S_{\text{gas/melt}}$ but the gas phase can still



be sulfur rich because the silicate melt can contain more S. Refinement of the effect of melt composition on $\Delta S_{\text{gas/melt}}$ and SCSS, will allow more accurate modeling of the conditions most favorable to high-S degassing. (GS2; Wed. 8:40)

Relationships between pluton emplacement, mineralization and deformation at the Gander/Avalon boundary, Newfoundland from a geochronological and thermochronological perspective

Kellett, D.A.¹, dawn.kellett@nrcan.gc.ca, Rogers, N.¹, McNicoll, V.¹ and van Staal, C.², ¹Geological Survey of Canada, Natural Resources Canada, 601 Booth St., Ottawa, ON K1A 0E8, ²Geological Survey of Canada, Natural Resources Canada, 1500 - 605 Robson Street, Vancouver, BC V6B 5J3

Devonian plutonic suites in the Canadian Appalachians are locally associated with Sn, W, Mo and In mineralization. In central Newfoundland some of the most mineralogically-prospective plutons, for example the Ackley Granite, are spatially associated with the Gander/Avalon terrane boundary. This relationship suggests that there may be tectonic and/or structural controls on pluton emplacement and localization of mineralization.

Within the Geological Survey of Canada's Targeted Geoscience Initiatives IV Intrusion-Related Mineralization Project the tectonic controls on porphyry-style mineral systems are under examination to determine their potential as a vector towards zones of high mineral prospectivity. Identifying such relationships is especially significant in regions like the Canadian Appalachians where extensive glacial cover often masks direct observations of mineralisation. Here we present preliminary results from our SHRIMP U-Pb and ⁴⁰Ar/³⁹Ar single crystal and *in situ* geochronological and thermochronological data set. These data are used to constrain the timing of deformation along the Dover fault, which marks the Gander/Avalon terrane boundary, and the regional emplacement/cooling history of plutonism. Implications for tectonics and mineral potential of the region are considered. (GS3; Thurs. Poster)

Keynote (40 min): A tale of two triple junctions

Keppie, D.F., Dept. of Natural Resources, Halifax, NS B3J 2T9, keppiedf@gov.ns.ca

It was the best of plate tectonic models, it was the worst of plate tectonic models; it was the epoch of belief, it was the epoch of incredulity... Over the past fifty years, researchers have proposed widely different models for the tectonic evolution of the western Caribbean region; competing reconstructions can be grouped into three general categories: (1) Pacific models, (2) *In-Situ* models, or (3) Pirate models. These three categories of model differ in many respects, but perhaps most critically differ in their predictions for the time evolution of the western Caribbean Plate corners – which appear to host diffuse and unstable triple junction configurations at present. The models of rigid plate evolution proposed in Pacific and *In-Situ* reconstructions are incompatible with the present configurations of the western Caribbean corners. And, studies have generally failed to identify evidence supporting the stable configurations predicted in both Pacific and *In-Situ* models. If the classic methods of triple junction stability analysis are extended to consider the unstable configurations of the western Caribbean corners, a solution space for western Caribbean tectonics that includes lateral intrusion and microplate capture (*i.e.*, the Pirate category of models) can be identified. I argue that Pirate models – new though they may be – best reconcile the geological record of the western Caribbean. As the new analysis shows, lateral intrusion and microplate capture processes may be generally applicable elsewhere on Earth as well. (SS19; Wed. 3:20)

A new middle Cambrian Burgess Shale-type Lagerstätte from the Middle Cambrian of the Mackenzie Mountains, Northwest Territories, Canada

Kimmig, J., j.kimmig@usask.ca, and Pratt, B.R., Department of Geological Sciences, University of Saskatchewan, Saskatoon, SK S7N 5E2

Burgess Shale-type Lagerstätten are known from the Cambrian and Ordovician of most continents, and these snapshots of benthic marine communities are critical for the understanding of the early evolution and diversity of life. Here we present an overview of a new Lagerstätte from the Mackenzie Mountains of northwestern Canada. The fossils occur in a unit of greenish mudstone, ~1 m thick, that is part of a deeper water succession of shales and lime mudstones that onlaps a fault block of Lower Cambrian sandstone. The host bed consists of illite, quartz, clinocllore and dolomite. Trace element analysis shows an oxygenated water column but with some fluctuations. The fossiliferous mudstone is of similar age as the Burgess Shale itself (Elrathina Zone), and has a similar fossil community as the 'Thin Stephen' Formation in British Columbia. The biota includes sponges, the crustaceans Isoxys and Perspicaris, the priapulid Ottoia, and the macroalga Margaritella, along with hyolithids, agnostoid and pychoparioid trilobites, and round organic blobs that represent either microbial mats, coprolites, regurgitates or maybe anomalocarid parts. While a couple of the fossils represent new species, most are known from the early to middle Cambrian Lagerstätten in western Canada and the United States. Arthropods dominate this new assemblage with respect to diversity, whereas hyolithids are the most abundant macrofossil. (SY3; Thurs. 9:20)

NI43-101 mineral resource estimation and the role and responsibilities of the qualified person

Kirkham, G.D., Kirkham Geosystems Ltd., 6331 Palace Place, Burnaby, BC V5E 1Z6, gdkirkham@shaw.ca

Professional Geoscientists (P.Geo.) are "responsible" for the mineral resource and reserve estimation. This practice has changed significantly in the past 30 years from primarily manual techniques to where complex geostatistical techniques have become commonplace and continue to evolve. Computational horsepower has revolutionized all facets of data analysis, numerical modeling, graphical presentation and allowed for increasingly complex methods and techniques to be employed to solve geological and mining related problems. With the introduction of NI43-101 in the 1990's, a prescribed format and detailed set of rules guide the reporting of resources. In addition, the basic principles of "best practices" have been created and guide the practitioner in all aspects of mineral resource evaluation and estimation from data management, data analysis, geological modeling and domaining, geostatistical analysis, estimation and classification. (SS21; Fri. 10:20)

Details from a belt of magmatic Ni-Cu occurrences and deposits preserved in a granulite facies terrain, Dodge Domain eastern Rae craton margin

Knox, B., bernadette.knox@gov.sk.ca, and Ashton, K.E., Saskatchewan Geological Survey, 200-2101 Scarth Street, Regina, SK S4P 2H9

The eastern Dodge Domain, Rae Province is located ~50 km north-northwest of Stony Rapids, Saskatchewan and extends to the Northwest Territories (NWT) border. It is bounded by two crustal-scale features, the Grease River shear zone and the Snowbird tectonic zone (Stz), which separates it from the Tantan Domain, Rae Province to the south and the Mudjatik Domain, Hearne Province to the east respectively.

Regionally, Ni-Cu-bearing deposits are known in the Rae Province adjacent to the Stz at Axis and Currie lakes in the Tantan Domain and at Thye Lake (Nickel King) in the NWT. These deposits, along with Ni-Cu occurrences and bedrock geochemical anomalies from grab samples, create a 150 km zone of mineralization. In the Dodge Domain mafic and ultramafic dykes are emplaced up to 50 km from the Stz. Despite generally low sulphide percent in dykes grab samples up to 1.17% Ni and 0.40% Cu have been reported.

Recent bedrock mapping at 1:20 000 scale reveals the Dodge Domain to be a granulite-facies terrain dominated by orthogneiss (quartz diorite to monzodiorite, mixed tonalite to gabbro, and monzogranite to quartz monzogranite, and granite) that form the basement to unconformably overlying metasedimentary rocks



(psammopelitic gneiss, minor psammitic gneiss and quartzite) and derived garnet-bearing anatectic granite. Mafic and ultramafic dykes of the type hosting the Nickel King Ni-Cu deposit at Thye Lake, NWT intrude these units. Finally, undeformed muscovite leucogranite dykes intrude all other units. Five periods of ductile deformation affected the Dodge Domain, the three youngest of which affect the mafic and ultramafic dykes.

A SHRIMP geochronological study was undertaken on main units. The tonalitic end member of the tonalite to gabbro unit provided an upper and lower intercept age of 2603 ± 85 Ma and 1905 ± 12 Ma. Detrital zircons from the psammopelitic gneiss ranged from ca. 3.8 Ga to 2.2 Ga, the latter provides a maximum age of deposition. A metamorphic event produced zircon grains and overgrowths in this unit at ca. 1.90 Ga. A mafic dyke gave an upper intercept age of 2724 ± 89 Ma with a metamorphic age of 1890 ± 9 Ma. Although this apparent Archean crystallization age agrees with a ca. 2.7 Ga age obtained for a norite at Thye Lake, NWT age relationships constrain emplacement of the Saskatchewan norite to be during the Paleoproterozoic (post-2.2 Ga). A muscovite leucogranite dyke has a crystallization age of 1802 ± 5 Ma. (SS9; Wed. 11:00)

Deciphering the origin of red inclusions within trinitite using *in-situ* chemical and isotopic (Pb & U) evidences

Koeman, E.C., Simonetti, A., Bellucci, J., Wallace, C. and Burns, P.C., Dept. Civil & Environmental Engineering & Earth Sciences, University of Notre Dame, Notre Dame, IN 46556 USA

The study of post detonation material (PDM) plays a crucial role in nuclear forensics. PDMs incorporate chemical and isotopic (U, Pu, Pb) signatures from the nuclear device components, and are therefore critical for source attribution. However, deciphering the device components within PDMs is complicated by the incorporation of the background associated with the blast site; the nature of the latter can be extremely variable and complex, in particular if detonation occurs in an urban setting. By studying PDMs from historic nuclear tests, forensic protocols and methodologies can be developed, as the chemical and isotopic (U & Pu) signatures of device components are well-documented. The Trinity test was the world's first nuclear detonation and took place on July 16, 1945 at White Sands Missile Range, New Mexico. The heat from the fireball melted the arkosic sand at ground zero, and allowed for mixing with radioactive debris from the bomb. When the debris re-solidified, it formed the glassy material known as "trinitite".

Trinitite hosts multiple types of inclusions from the Trinity device ("Gadget") and test site-related components. Red inclusions within trinitite are interpreted to originate from the copper wiring used within the device and these are the focus of this study. Petrographic thin sections of two trinitite samples with red inclusions were investigated using a variety of imaging and microanalytical techniques, including: optical microscopy, scanning electron microscopy (SEM), back scattered electron imaging, and energy dispersive X-ray spectral (EDS) analysis. The distributions of the abundances of Cu, Pb and U within the "red areas" were investigated using laser ablation inductively coupled plasma mass spectrometry (LA-ICP-MS). The latter yield extremely high concentrations of Pb ($>25,000 \mu\text{g/g}$). Uranium is also present in the red areas and exhibits positive correlations with the abundances of Cu and Pb. The U present within trinitite originates from three sources: 1- the geological background at the test site, 2- the tamper used in the device, and 3- an unknown source characterized by a high U content; Pb and U isotopic characterization of these areas is ongoing. (SS5; Thurs. 10:40)

The Upper Beaver Au-Cu deposit, Kirkland Lake, Ontario, Canada: An Archean IOCG analogue or just an intrusion-related iron oxide copper gold deposit (?)

Kontak, D.J.¹, dkontak@laurentian.ca, Dubé, B.², McNicoll, V.³, Creaser, R.⁴ and Kyser, T.K.⁵, ¹Department of Earth Sciences, Laurentian University, Sudbury, ON P3E 2C6; ²Geological Survey of Canada, 490 rue de la Couronne, Quebec, QC G1K

9A9; ³Geological Survey of Canada, 601 Booth Street, Ottawa, ON K1A 0E8; ⁴Department of Earth and Atmospheric Sciences, University of Alberta, Edmonton, AB T6G 2E3; ⁵Department of Geological Sciences, Queen's University, Kingston, ON K7L 3N6

The Upper Beaver Au-Cu deposit of the world-class Kirkland Lake gold camp produced 136,650 oz Au from 0.5 Mt grading 7.9 g/t and 1% Cu (1912-1972), but new exploration (to November 2012) has delineated an indicated resource of 6.87 Mt @ 6.62 g/t Au and 0.37 % Cu. The abundance of iron oxide (Mt >> Hmt) associated with some of the Au-Cu mineralization suggests comparison to the IOCG deposit magnetite-subtype. The deposit area is underlain by mafic to felsic volcanic rocks intercalated with sedimentary rocks of the Tisdale and Blake River groups that are overlain by the Timiskaming Group sedimentary rocks; all units are cut by syenitic intrusions (<2680 Ma). At Upper Beaver, located on a splay off the main, regional E-W trending and metallogenetically significant Larder Lake-Cadillac break, mineralization is spatially related to a 2679 Ma (U-Pb Zr) multi-phase syenite complex cut by magmatic and hydrothermal breccias. The structurally controlled deposit is centered on the syenite, but also occurs in adjacent volcanic rocks, which show both enrichment and depletion in Fe related to hydrothermal processes. Compared to the syenite-hosted Au-Te quartz vein and breccia ore of the world-class Kirkland Lake deposit, the Upper Beaver system has the unusual association of mineralization with abundant hydrothermal Fe oxide (Mt >> Hmt) and variably pervasive epidote-albite±sericite±actinolite±tourmaline alteration; rare late-stage anhydrite also occurs. Our studies indicate: (1) fractionation of an early amphibole-bearing syenite to late quartz-feldspar dykes coincident with some ore zones; (2) the absence of a Eu anomaly in both syenite and late-stage vein calcite, which suggests the system remained oxidized throughout its evolution; (3) that apatite is F-enriched through the magmatic and hydrothermal stages; (4) an association of Au with potassic enrichment; (5) that although free Au dominates, silver, bismuth telluride phases (Bi-Hg-Te-Se-Pb-Ag) occur; and (6) that isotopic data indicate mineralization at 400°-450°C with $\delta^{34}\text{S}(\text{H}_2\text{S}) = 0 \text{‰}$ 2σ , $\delta^{18}\text{O}(\text{H}_2\text{O}) = +8 \text{ to } +10 \text{‰}$ 2σ for mineralized and barren stages, and $\delta^{13}\text{C}(\text{CO}_2) = 0\text{‰}$. The data are permissible with a model for the Upper Beaver deposit that involves focusing of mineralizing fluids, either magmatic and/or metamorphic derived, that coincided with syenite intrusion, as supported by a Re-Os age of 2685 Ma for molybdenite from a mineralized zone. The Fe-enrichment, from Hmt "Mt" characterizes the evolution of the system, a parallel with some IOCG systems. However, such an analogy is speculative as the definition of IOCG as a deposit type remains controversial. (SS23; Fri. 2:20)

The Archean Côté gold Au(-Cu) deposit, northern Ontario, Canada: A large tonnage, low-grade Au deposit centred on a 2740 Ma magmatic-hydrothermal diorite complex

Kontak, D.J.¹, Katz, L.¹, Creaser, R.A.² and Hamilton, M.³, ¹Department of Earth Sciences, Laurentian University, Sudbury, ON P3E 2C6; ²Department of Earth and Atmospheric Sciences, University of Alberta, Edmonton, AB T6G 2E3; ³Department of Geology, University of Toronto, 22 Russell Street, Toronto, ON M5S 3B1

The Côté Gold Au(-Cu) deposit, located in the Archean Shining Tree domain of northern Ontario, is a recently discovered (2010), large tonnage, low grade deposit (239 Mt at 0.9 g/t for 6.9 M oz; Feb. 2012) of unusual character. The deposit occurs in the 2740 Ma, Chester Intrusive Complex (CIC) located immediately south of the Swayze Greenstone Belt. Field relationships and supporting U-Pb TIMS zircon dating indicate that at the deposit site the CIC consists of an older leucocratic tonalite phase (2741.1 ± 0.9 Ma) that is intruded by a hornblende diorite-tonalite suite (2738.7 ± 0.8 Ma). Mineralization is centred on dioritic intrusive bodies, diorite breccias and biotite-rich hydrothermal breccias. The ore envelope defines a NE-SW oriented ellipse (1200 m by 300 m) within which the Au mineralization is dominated by long intervals (100s m) of disseminated and fracture



controlled sulphides (pyrite-chalcopyrite) that are coincident with biotite alteration within both magmatic and hydrothermal breccias and the enveloping, biotite altered earlier tonalite phase. High-grade Au mineralization also occurs in quartz-carbonate-sulphide (pyrite-chalcopyrite-molybdenite) veins and molybdenite from two such veins yielded Re-Os ages of 2739 ± 8 Ma. The biotite altered mineralized rocks are overprinted by later stage silica-sodic and phyllic alteration styles; rare, fracture controlled propylitic alteration also occurs. Emplacement of gold-bearing quartz-carbonate \pm sulphide \pm muscovite \pm tourmaline shear veins, part of a regional system of similar Au-Cu mineralized veins in the area, cross cut the mineralized zone and may relate to movement along the regional, E-W trending, steeply dipping Rideout deformation zone. Whole rock chemistry integrated with SEM-EDS indicates the biotite alteration in the early tonalite is characterized by both Ba and LREE enrichment, the latter due to hydrothermal allanite, epidote, bastnaesite and euxenite. Field relationships, the nature of mineralization and alteration types, and spatial and temporal relationship of the latter with a magmatic-hydrothermal centre suggests affinities to younger porphyry-style Au-Cu mineralization. Stable isotope data for the vein minerals (O, C, S) are consistent with a dominantly magmatic sourced hydrothermal system, possibly with some involvement of meteoric water. (**SS3; Fri. 8:40**)

Distribution of eclogites in the Slave mantle: The effect of subduction and metasomatism

Kopylova, M.G., mkopylov@eos.ubc.ca, and Beausoleil, Y.L., University of British Columbia, 2207 Main Mall, Vancouver, BC V6T 1Z4

Eclogite xenoliths with the varied mineral chemistry and petrography are common among mantle xenoliths of central and northern Slave kimberlites. Studies of 109 eclogite xenoliths from the Jericho and Muskox kimberlites combined with the analysis of the spatial, mineralogical and age relationships of xenoliths from Diavik, Ekati, Jericho and Muskox pipes produced a combined model of the eclogite distribution in the Slave mantle.

Eclogites of a crustal origin are interspersed with peridotites at 110-190 km below the Northern Slave and at greater depths, 130-210 km, below the Central Slave. Within these depths, the N. Slave eclogites concentrate mainly around 120-130 km indicating the site of the major slab localization. The lesser presence of crustal eclogites at greater depths may be ascribed to foundered, imbricated or sunk eclogite remnants below the original subducted plate. Its similar ~1.8 Ga ages reported for the Central and Northern Slave suggest the slab's lateral continuity and link to a subduction event that formed the Great Bear magmatic arc. The dip of the slab from the Northern to the Central Slave matches the more proximal position of the Northern Slave to the Great Bear magmatic zone. This easterly dip is also observed in the localization of diamondiferous eclogites of the crustal origin, which occur in a restricted depth interval in the deeper part of the eclogite-bearing mantle.

Superimposed onto the deep, subduction-related structure of the cratonic mantle are local heterogeneities produced by metasomatic and magmatic events. These are recorded in the Jericho eclogites and diamonds. At Jericho, Mg-rich eclogites of Group A all occur in a tight depth interval, rather than being evenly distributed at a larger depth range together with crustal eclogites, as observed below the Central Slave. The generally higher Mg content of Jericho eclogites explains the presence of accessory olivine, which is not found at Central Slave or Muskox situated 15 km west of Jericho. Diamonds are absent in crustal eclogites at Jericho, and are found only within a thin lens of Group A eclogites. Their spatial localization beneath the inferred subducted slab is explained by underplating of metasomatic fluids causing a longer and more effective recrystallization of crustal eclogites to Mg-rich compositions. These fluids and melts stalled beneath a rigid, impenetrable slab, extracted basic magmaphile elements, produced distinctly Mg-rich eclogites and formed diamonds. (**SS4; Fri. 3:00**)

Crystal structures of two novel compounds in the PbO–NiO–SeO₂ system

Kovrugin, V.^{1,2}, Colmont, M.¹, Olivier, M.¹ and Krivovichev, S.²,
¹Unité de Catalyse et de Chimie du Solide, UMR 8181, Université Lille 1, 59652 Villeneuve d'ASCQ Cédex, France;
²Crystallography department, St. Petersburg State University, University Emb. 7/9, 199034 St. Petersburg, Russia

Selenium-containing lead compounds are of special interest due to their geochemical and mineralogical abundance. During the last decade there has been a surge of research activity in the studies of the PbO–MO–SeO₂ ($M = \text{Cu}^{2+}, \text{Fe}^{3+}, \text{V}^{5+}, \text{Mo}^{6+}$) ternary systems. Specific attention was attracted to selenium-containing lead compounds as promising noncentrosymmetric polar materials with consequent interesting physical properties, such as second harmonic generation. The investigations of conformable ternary systems with nickel as transition metal have not yet been carried out by the present time. Here, we report on the structural characterization of two novel compounds in the PbO–NiO–SeO₂ ternary system.

Crystals of two novel inorganic compounds, PbNi(SeO₃)₂ (**I**) and PbNi₂(SeO₃)₂(SeO₂OH)₂ (**II**), have been prepared by hydrothermal methods from the mixtures of PbO, NiO, SeO₂, and distilled water. Their crystal structures have been studied by means of single crystal X-ray analysis.

The crystal structures have been solved by direct methods and refined using least-squares techniques: **I** is orthorhombic, space group *Pnma*, $a=12.7476(4)\text{\AA}$, $b=5.4562(2)\text{\AA}$, $c=7.8332(2)\text{\AA}$, $V=544.83(3)\text{\AA}^3$, $R_1=0.0139$ for 742 unique reflections with $|F_o| \geq 4\sigma_F$; **II** is monoclinic, space group *P2/c*, $a=13.6824(10)\text{\AA}$, $b=5.2962(5)\text{\AA}$, $c=19.3476(13)\text{\AA}$, $\beta=129.524(4)^\circ$, $V=1075.94(15)\text{\AA}^3$, $R_1=0.0387$ for 1132 unique reflections with $|F_o| \geq 4\sigma_F$.

The structures of **I** and **II** contain one and two symmetry independent Pb²⁺ cations, respectively. They are coordinated by eight O atoms each forming asymmetric PbO₈ polyhedra. Two and four symmetrically independent Ni²⁺ sites have been observed in the crystal structures of **I** and **II**, respectively. Each Ni²⁺ cation has an essentially regular octahedral coordination. There are two and four symmetrically independent Se⁴⁺ cations in **I** and **II**, respectively. Each atom is coordinated by three oxygen atoms, forming triangular pyramids [SeO₃]²⁻ with Se⁴⁺ located at its apical corner and a stereoactive lone pair as a complementary ligand. In the crystal structure of **II** the sum of the valence bonds for the oxygen atoms of two independent Se⁴⁺–O bonds are characteristic of hydroxyl groups (OH)⁻ within protonated selenite groups [SeO₂OH]⁻. In both crystal structures, coordination polyhedra of Pb, Ni, and Se are linked into a 3D heteropolyhedral frameworks.

This work was supported by the French Ministry of Foreign affairs with Campus France, and the Federal Targeted Program "Scientific and Scientific-Pedagogical Personnel of the Innovative Russia" (agreement no. 3818). (**GS1; Thurs. Poster**)

Application of the principle of dimensional reduction to uranyl oxysalts with monovalent cations

Kovrugin, V.M., kovrugin_vm@hotmail.com, Gurzhiy, V.V. and Krivovichev, S.V., Dept. of Crystallography, St.Petersburg State University, University Emb. 7/9, 199034, St.Petersburg, Russia

Uranyl oxysalts are remarkable by the large diversity of structures and chemical compositions. However, the relations between structural and chemical features in this class of compounds are poorly understood. In 1996 Long *et al.* proposed the principle of dimensional reduction for the description of decreasing dimensionality of chalcogenide structural units in Re sulphides and selenides. This principle was applied to various materials, including organic-inorganic composites, and certain inorganic oxysalts systems. The principle of dimensional reduction indicates that incorporation of an ionic reagent and H₂O into parent highly-condensed framework results in formation of derivative compounds with decreasing dimensionality of the structural unit.

In this work, we apply the principle of dimensional reduction to uranyl oxysalts with general formula $A_n(\text{UO}_2)_p(\text{TO}_4)_q(\text{H}_2\text{O})_r$, where $A^+ =$



monovalent cation, and $T^{6+} = \text{S, Se, Cr, Mo}$. The relationship between structure and composition for the compounds with general formula $A_n(\text{UO}_2)_p(\text{TO}_4)_q(\text{H}_2\text{O})_r$ may be visualized using the $\text{UO}_2\text{TO}_4\text{--}A_2\text{TO}_4\text{--}\text{H}_2\text{O}$ compositional diagram. The $\text{UO}_2\text{TO}_4\text{--}A_2\text{TO}_4\text{--}\text{H}_2\text{O}$ system includes 40 different phases. Here, we consider the UO_2TO_4 component as being responsible for the structural organization. The basis of the structures is a structural unit formed by linkage of U-centered polyhedra and TO_4 tetrahedra. $A_2\text{TO}_4$ is considered as an ionic component, whereas H_2O molecules are considered as modifiers of the structure dimensionality. The diagram demonstrates that incorporation of $A_2\text{TO}_4$ and H_2O molecules into the structure would result in the decreasing dimensionality of the UO_2TO_4 unit, and it is in agreement with the principle of dimensional reduction.

The analysis of the $A_n(\text{UO}_2)_p(\text{TO}_4)_q(\text{H}_2\text{O})_r$ compounds using the principle of dimensional reduction and composition-structure diagram allows to separate specific fields corresponding to the formation of structures with specific dimensionalities of their structural units [Struct. Chem. 2012, 23, 2003-2017].

This work was supported by RFBR (grant 12-05-31344), Saint-Petersburg State University through the internal grant 3.37.84.2011. XRD study was carried out in the X-ray Diffraction Centre of St. Petersburg State University. (SS5; Thurs. 9:20)

Dolní Bory pegmatite field - New evolution concept

Krejsek, S., Masaryk University, Faculty of science, 611 37 Brno, Czech Republic, krejsek.stepan@seznam.cz, and Kynický, J., Mendel University in Brno, 613 00 Brno, Czech Republic, jindrich.kynicky@mendelu.cz

Pegmatite deposit Dolní Bory is well known and associated with the so called "Dolní Bory – Olší nad Oslavou pegmatite field" spatially related to Bory granulite massif, Czech Republic.

Despite pegmatites are quite widespread in the area, from economical point of view only Dolní Bory has potential as source of quartz and K-feldspar. This is caused by their geological setting in Bory granulite massif, where veins of considerable sizes were found. Usually NW – SE orientated with 50-60° dip to NE, up to 750 m long and 30 m thick, they are considered among biggest in Czech Republic. During geological exploration, over 200 veins with thickness over 1 m were found in area of 5,9 km².

Pegmatite veins of the Dolní Bory district shows concentric zonality – from the borders to core granitic, graphic, blocky zone and rarely quartz core can be distinguished. Albite zone is emplaced irregularly through blocky zone. Mineralogically the most important are blocky and albitic zones and miarolitic cavities, which hosts accessory minerals (schorl, sekaninaite, garnet, monazite, löllingite, apatite and andalusite).

The first serious mineralogical research and industrial exploration started at the end of 19th century. Although several new minerals were described from the area – the main topics – like genesis and relationship of different veins is still unclear.

There is also serie of newly identified smaller scale granitic pegmatite dykes, which is under actual serious research. While all the previous researches say that there are 2 types or populations of pegmatite dykes (older hypothesis: large veins has different evolution than smaller spatially more widespread dykes), new hypothesis based on recent research (2007-2013) brings different interpretation. All dykes of the pegmatite field are not only spatially and temporally related, but also of the same or almost identical genesis and evolution. This interpretation is strongly supported by detailed mineralogical and petrological research based on both macro element and trace element data of pegmatites and their accessory minerals. The most valuable mineral for research is apatite, which is present in different populations in all representative dykes and their zones. (SY2; Thurs. 2:20)

Syn-deformational emplacement of the Bernic Lake pegmatite group, Bird River greenstone belt, southeastern Manitoba

Kremer, P.D.¹, paul.kremer@gov.mb.ca, Davis, D.W.², Lin, S.³ and Linnen, R.L.⁴, ¹Manitoba Geological Survey, 360-1395 Ellice Ave., Winnipeg, MB R3G 3P2; ²Jack Satterly Geochronology Laboratory at the University of Toronto, 22 Russell St., Toronto, ON M5S 3B1; ³Department of Earth and Environmental Sciences, University of Waterloo, 200 University Ave. W., Waterloo, ON N2L 3G1; ⁴Department of Earth Sciences, University of Western Ontario, London, ON N6A 5B7

Rare element bearing pegmatites in the Cat Lake – Winnipeg River pegmatite field of southeastern Manitoba are invariably localized around belt scale, formation-bounding D₂ shear zones. In the case of the Bernic Lake pegmatite group, of which the world famous Tanco pegmatite is most noteworthy, pegmatites are emplaced into structural traps in a variety of lithologies and around the north Bernic Lake shear zone. Two end member styles of pegmatite emplacement are evident in the Bernic Lake pegmatite group: 1) shear-hosted pegmatites, and 2) fracture-hosted pegmatites. East of Bernic Lake, pegmatites are hosted in highly-deformed metavolcanic rocks (shear-hosted pegmatites) and, although they show many features consistent with passive crystallization, they are folded and/or boudinaged. Conversely, the Tanco pegmatite is hosted in a medium- to coarse-grained sub-volcanic gabbro and occurs as a doubly-dipping, subhorizontal body intruded along a prominent brittle, conjugate fracture set (fracture-hosted pegmatites). Structural and geochronological analyses on both shear- and fracture-hosted pegmatites indicate that they were emplaced coevally during a belt-wide tectonomagmatic event associated with D₃ deformation. We present a syn- to late-deformational emplacement model for the Bernic Lake pegmatite group, where pegmatitic melt ascended from depth along the reactivated north Bernic Lake shear zone during D₃ deformation. The contrasting styles of emplacement are related to rheological heterogeneities in the various host rocks and their differing responses to D₃ strain. This data suggests that pegmatite intrusion occurred while the host rocks were at or near the brittle-ductile transition. (SY2; Thurs. 9:20)

Major- and trace-element composition of Fe-Ti oxides from the Lac de Gras kimberlites

Kressall, R.D. and Fedortchouk, Y., Department of Earth Sciences, Dalhousie University, Halifax, NS B3H 4R2, ryan.kressall@dal.ca

Rapidly evolving conditions during emplacement of kimberlites is indicated by the large compositional range observed in Fe-Ti oxides from kimberlites. We examine the variability observed in spinel group minerals and ilmenite from six kimberlites (Grizzly, Leslie, Beartooth, Panda, Koala and Misery) from the Ekati Mine, Northwest Territories. The kimberlites are of similar age but variable lithology, fluid regime and diamond grade. The objective of this study is to understand the relationship between compositional variability of Fe-Ti oxides and emplacement conditions.

Textural variations of spinel and ilmenite consist of macrocrysts, groundmass, olivine inclusions and replacement of other accessory minerals. Reaction rims and evidence of dissolution such as surficial features and atoll rims suggest disequilibrium between Fe-Ti phases and the evolving melt. All textural variations were analyzed for major-element chemistry by electron microprobe. Macrocrysts were also analyzed for trace-elements by laser ablation – inductively coupled plasma – mass spectrometer. Surficial dissolution features were studied using a scanning electron microscope.

Three trends are identified in the spinel compositions. 1) Spinel from Panda and Beartooth evolved from chromite [(Fe,Mg)Cr₂O₄], to magneiso-ulvöspinel–magnetite (Mg₂TiO₄ - Fe²⁺Fe³⁺₂O₄: MUM). 2) Spinel from Grizzly and Leslie evolved along a similar but more aluminous trend. Koala contains spinel compositions within the range defined by both trends 1 and 2. 3) Spinel from Misery evolved from chromite to pleonaste [(Fe,Mg)Al₂O₄]. At the trace element level, the chromite-rich phases are the most enriched in transitional elements (V,



Cr, Mn, Fe, Co, Ni, Cu, Zn and Ga) whereas MUM-enriched phases are enriched in both large-ion-lithophile-elements (Cs, Sr and Ba) and high-field-strength-elements (HFSE: Zr, Nb, Hf, REE, Th, Ta). Pleonaste-rich phases have the lowest concentrations of transitional and incompatible trace elements.

Two groups of ilmenite are identified in the Ekati kimberlites: 1) high-MgO (>8.0 wt.%); and 2) low-MgO (<3.5 wt.%). Group 1 is further separated from Group 2 by higher concentrations of Sc, V, Co, Ni, Cu, Zn and HFSE. Group 1 likely represents magmatic ilmenite whereas group 2 was likely assimilated from crustal rocks.

Spinel dissolution features consist predominately of octahedral protrusions. These features are found on macrocrysts from kimberlites belonging to trend 1 and trend 3. Macrocrysts belonging to trend 2 have rough surfaces free of protrusions. Dissolution features were not observed on ilmenite, instead a reaction rim composed of combinations of titanite, chromite or perovskite was present. Differences in composition and dissolution support variable fluid regimes and emplacement conditions between kimberlites. (SS4; Fri. 10:40)

Structural complexity and metastable crystallization

Krivovichev, S.V., Department of Crystallography, St. Petersburg State University, University Emb. 7/9, 199034 St. Petersburg, Russia, skrivovi@mail.ru

Metastable crystallization is a widespread natural process, when formation of crystalline phases is governed by kinetics rather than thermodynamics of chemical reactions. Crystallizations from supercooled melt or supersaturated solutions frequently result in formation of metastable phases with structural arrangements different from those of the stable phases. In order to estimate the 'ease of crystallization', J. Goldsmith in 1953 proposed a 'simplicity principle', which states that metastable phases that form according to the Ostwald rule of stages are structurally simpler than stable phases. One of the reasons for such a behaviour is that simpler structures have smaller diameter of their critical nuclei than more complex structures, which strongly favors their formation in non-equilibrium conditions. In this contribution, we shall use Shannon information measures to evaluate complexity of mineral structures and to provide quantitative comparison of complexities different polymorphs of the same chemical compound. Metastable appearances of mineral phases will be discussed. (SY1; Thurs. 3:20)

Amazonitic lead-rich orthoclase from Broken Hill, Australia

L. Sánchez-Muñoz, Institute for Ceramics and Glasses (CSIC), Kelsen 5, E-28049 Madrid, Spain, lsm@icv.csic.es; I. Sobrados and J. Sanz, Instituto de Ciencia de Materiales de Madrid (CSIC), E-28049 Madrid, Spain; G. Van Tendeloo and Xiaoxing Ke, EMAT, University of Antwerp, Groenenborgerlaan 171, B-2020 Antwerp, Belgium; A. Cremades, Dpt. Física de Materiales, Fac. Ciencias Físicas, Univ. Complutense de Madrid, E-28040, Spain; M.A. Rodríguez and A. del Campo, Institute for Ceramics and Glasses (CSIC), Kelsen 5, E-28049 Madrid, Spain; Z.H. Gan, NHMFL, Tallahassee, Florida State Univ., 32306 Florida, USA

Alkali feldspar-quartz pegmatites occurring in the Broken Hill Pb-Zn-Ag deposit (New South Wales, Australia) contain green amazonitic lead-rich orthoclase (amazonite) and galena as the more typical features. Amazonite specimens have been studied by polarized light optical microscopy (PLOM), X-ray diffraction (XRD), X-ray fluorescence (XRF), confocal Raman microscopy (CRM), cathodoluminescence imaging (CL) under scanning electron microscopy (SEM), high resolution transmission electron microscopy (TEM), high resolution magic angle spinning multi-nuclear magnetic resonance spectroscopy (NMR), including ^{29}Si , ^{27}Al , ^{23}Na and ^{207}Pb spectra at 9.4 as well as ^{27}Al , ^{39}K , ^{23}Na and ^{207}Pb spectra at 19.6 T. Amazonite with deep green color occurs in specimens which are uniform at the optical scale without exsolution microtextures, having an orthoclase XRD patterns, as well as twinned contrast in TEM images, homogeneous CL-SEM contrast using the blue and infrared light emissions, and the highest quantity of $\text{PbAl}_2\text{Si}_2\text{O}_8$ from XRF data

circa 3 % mol. The NMR spectra suggest that partial Si/Al order in framework sites is correlated with partial order for the alkali atoms in the cavity sites, implying a medium-range structure with molecular-like Al-O-X⁺ arrangements, in a triclinic-like structure at the local scale. The ^{207}Pb spectra in orthoclase and galena are different, and the orthoclase spectra are consistent with Pb atoms in the cavity sites of the feldspars structure. When some exsolution take place, orthoclase to microcline recrystallization units propagate in the typical orthogonal configuration from interfaces and stress centers at the macroscopic scale as seen by PLOM, forming crossovers involving positive and negative interference effects which were clearly recorded by CMR images, as well large scale microcline twins. The development of macroperthitic textures and later sericitic alteration (from retrogressive metamorphism) seen in other specimens is not related to total recrystallization into low microcline. It is suggested that the modulated structure of orthoclase is partly stabilized by Pb atoms in the cavity sites which act as chemical hinderers, similarly as it occurs with P atoms in the framework sites. Orthoclase is also preserved due to the lack of water fluids during both, the magmatic stage during pegmatite crystallization from melt at peak granulite metamorphism and also during the subsolidus stage on cooling. (SY2; Fri. 8:40)

Petrogenesis and mineral chemistry of the McFaulds Lake chromite deposits

Laarman, J.E.¹, jlaarman@uwo.ca, Barnett, R.L.², and Duke, N.A.¹ and Weston, R.J.³, ¹Western University, 1151 Richmond Street, London, ON N6A 5B7; ²R.L. Barnett Geoanalytical Consulting Ltd., 9684 Longwoods Road, London, ON N6P 1P2; ³Cliffs Chromite Ontario Inc., 1159 Alloy Drive, Suite 200, London, ON P7B 6M8

Cliffs Natural Resources Inc. is currently completing a definitive feasibility study for the development of the Black Thor and Black Label chromite deposits in the Ring of Fire District of the James Bay Lowlands. Cliffs also has an interest in the Big Daddy chromite deposit in the same locality. The chromitite is hosted by the the Black Thor/Black Label intrusion, which is part of the more regionally extensive 'Ring of Fire' ultramafic to mafic intrusive suite in the McFaulds Lake greenstone belt of Northwestern Ontario. Mineral analyses of chromite demonstrate a complex history of primary magma replenishment and fractionation in the origin of the chromitite layers. Over 4200 electron microprobe analyses and 142 laser ablation ICP-MS analyses performed to date record individual differentiation sequences of chromitite below the metre scale. In comparing trends, the dunite-hosted Black Thor chromites are higher grade with more primitive compositions of 53 to 49 wt% Cr_2O_3 than the Black Label chromites with lower 50 to 46 wt% Cr_2O_3 . Heterogeneous growth of orthopyroxene oikocrysts in harzburgite hosting the Black Label chromitite account for increased silicate content, thereby lowering the Cr_2O_3 content. Massive chromitite at Big Daddy has different mineral chemical profiles with remarkable homogeneity at 50 to 51 wt. % Cr_2O_3 . The homogeneity of the massive ores is attributed to development of chromitite layers by double diffusive convection. A strong linear regression of Cr_2O_3 with MgO from massive to disseminated chromite at all deposits is indicative of magmatic differentiation in forming chromitite layers. Other elemental variation in the chromites include increasing Fe, slightly decreasing Al and decreasing Mg due to magmatic differentiation. Near constant low-Al compositions are characteristic of komatiitic chromites.

Laser ablation results show trends of depletion in Ti, V, Zn, Mn and Co, but enrichment in Ni and Sc with fractionation of chromitite. These trace element signatures are similar to trends documented in chromitite in the Bushveld and the Great Dyke layered complexes. The Black Label chromitite is more fractionated, enriched in FeO_T , and markedly depleted in Ni compared to Black Thor and Big Daddy.

The Black Thor/Black Label intrusion has been pervasively hydrated, causing total serpentinization and unalutization of host dunite and pyroxenite. Secondary ferrichromite with higher wt. % FeO_T and Cr_2O_3 forms as rims on magmatic chromites, thereby enriching the Cr



content of the ore. The rims of original chromites are leached of Mg and Al leaving high Cr and Fe. The released Mg and Al forms magnesian clinocllore that contains 3 to 5 wt. % Cr_2O_3 . (SS9; Wed. 2:20)

Formation of regional-scale Neoproterozoic charnockitic plutonism in the Rae Province

LaFlamme, C., d6g44@unb.ca, McFarlane, C., Department of Earth Sciences, University of New Brunswick, Fredericton, NB E3B 5A3, and Corrigan, D., Geological Survey of Canada, 615 Booth Street, Ottawa, ON K1A 0E9

(Withdrawn)

Gold mineralisations in the Duquesne-Ottoman property, Abitibi greenstone belt, Quebec, Canada

Lafrance, S., lafrance.sacha@gmail.com, and Jébrak, M., jébrak.michel@uqam.ca, Université du Québec à Montréal, PO Box 8888, Président-Kennedy Avenue, Montréal, QC H3C 3P8

Gold mineralizations in Abitibi's Archean greenstone belts occur in a wide range of style and geological context. In the Duparquet district (Quebec), volcanogenic, intrusive-hosted felsic porphyry (Beattie Mine) and orogenic gold models coexist along the Porcupine-Destor fault. This area is therefore a key area where the relationship between these different models may be deciphered. The Duquesne-Ottoman Property (DOP) is being explored and developed by Xmet Inc. for its gold potential.

The area is located approximately 30 km northwest of the city of Rouyn-Noranda, and 10 km east of the town of Duparquet. The rocks of this area are mainly volcanic in origin and Archean in age (2722 to 2718 Ma). The property is located in the volcanic Kinjévis group, north of the Porcupine-Destor fault. This fault separates the Kinjévis group from the Blake River Group to the south. The Kinjévis group is interpreted as a volcanic arc and was subsequently deformed during continental collision. The studied sector is composed of mainly intermediate to mafic volcanic rock with the relative presence of ultramafic and felsic volcanic rock and quartz-feldspar porphyry. A large polymict breccia is also present on the property and demonstrates the existence of early hydrothermal processes associated with a high level of volcanism.

A shear zone cuts across the property's volcanic sequence. This fault zone is part of the Porcupine-Destor fault system. It has an average width of 5-10m and is generally oriented 070N to 090N with a 75° to 90° dip. Within this shear zone are slivers of feldspar-quartz porphyries who emphasize, by rheological contrast, the shearing of the intermediary to mafic volcanic sequence. This east-west fault displacement displays a dextral inverse movement.

The three principal auriferous zones on the DOP (Liz, Shaft and Fox), are located within this, east-west trending, fault zone. The Fox zone occurs mostly in altered mafic tuff near the south contact of a quartz-feldspar porphyry. The Shaft zone occurs in schistose mafic volcanic proximal to quartz-feldspar porphyries and syenites. The Liz zone is in a sheared and widely altered mafic volcanic. Mineralizations are discordant with the stratigraphy and are structurally controlled. Multiple quartz-carbonate veins are associated with an ankerite-sericite-pyrite alteration. Chloritisation is widely developed. The alteration intensity is maximal in the intermediate to mafic host rock, near quartz-feldspar porphyries contacts. (GS2; Wed. Poster)

Characterization of uranium and REE mobility downstream of a uranium tailings impoundment near Bancroft, Ontario

Laidlow, A.M.¹, a.laidlow@queensu.ca, Parsons, M.B.², Jamieson, H.E.¹ and Gault, A.G.¹, ¹Department of Geological Sciences and Geological Engineering, Queen's University, Kingston, ON K7L 3N6; ²Natural Resources Canada, Geological Survey of Canada (Atlantic), Dartmouth, NS

Attenuation of uranium (U) and rare earth elements (REEs) has been observed in stream and wetland sediments, but the processes involved

in sequestering these elements in natural systems are not well understood. The decommissioned Bicroft Uranium Mine near Bancroft, ON uses a modified stream and wetland system to reduce the concentrations of U and other metals in tailings pond effluent to levels below the Provincial Water Quality Objectives. The Bicroft Mine was operated from 1957 to 1963, and processed low-grade, disseminated U hosted by pegmatite dykes in amphibolite gneiss. In this study, we used tangential flow filtration (TFF), ICP-ES/MS, scanning electron microscopy, and synchrotron techniques (bulk and μ -XANES, μ -XRF, and μ -XRD) to characterize sediment, tailings and colloid samples.

In conducting TFF on waters downstream of the tailings impoundments, orange-brown staining of the filter membrane was observed, suggesting that dissolved Fe(II) was oxidized and precipitated during TFF processing. TFF reservoir mass balance calculations identified losses of Fe, Mn, and Al on the filter membrane, as well as similar losses of REEs (Ce and La). In contrast, U present at concentrations of 18-27 $\mu\text{g/L}$ (median = 21 $\mu\text{g/L}$; <0.45 μm fraction), showed little to no filter loss during TFF, which suggests that U is not primarily associated with colloidal Fe- and Mn-oxy-hydroxides in solution. These results indicate that reduced forms of Fe and Mn remain in solution at least 200 m downstream of the Bicroft tailings impoundments, and that the mobility of U and REEs may be governed by different processes. Analyses of colloids by SEM, μ -XRF, and μ -XRD confirm that REEs are strongly associated with Fe- and Mn-oxy-hydroxides, including goethite, lepidocrocite, 2-line ferrihydrite, and birnessite.

The lack of diffraction under the micro-focused synchrotron beam and poor element correlation between U and Fe- and Mn-oxy-hydroxides suggests that U is most likely present in coarser detrital crystals, such as the primary ore minerals uraninite [UO_2] and uranophane [$(\text{Th,U})\text{SiO}_4$]. Micro-XANES analyses show that U in the colloids from Bicroft is primarily (80%) U(IV), providing further evidence that U is mainly hosted in detrital minerals and has not been extensively oxidized and re-precipitated in the colloids. This observation is important, as U(IV) is relatively insoluble in neutral pH environments and less mobile than oxidized hexavalent U(VI) species. The results of this study will help to develop better monitoring strategies for U tailings sites and should reduce the impacts of future U mining operations. (SS5; Wed. 2:40)

The metallogeny of the Turgeon deposit: A middle Ordovician volcanogenic massive sulfide (VMS) deposit in Belledune, New Brunswick

Lalonde, E. and Beaudoin, G., Université Laval, 1065 Avenue de la Médecine, Québec, QC G1V 0A6, erik.lalonde.1@ulaval.ca

The Turgeon deposit is a mafic-type Cu-Zn volcanogenic massive sulfide (VMS) deposit hosted in the middle Ordovician volcano-sedimentary rocks of the Elmtree-Belledune Inlier (EBI), located 20 km northwest of Bathurst in northern New Brunswick. The deposit is hosted in the tholeiitic pillow basalts of the Devereaux Formation of the Fournier Group. The Fournier Group represents an incomplete ophiolitic suite comprised of the gabbros and sheeted dykes of the Devereaux Formation at its base, stratigraphically overlain by the pillow basalts and sedimentary rocks of the Pointe Verte Formation.

The Turgeon deposit consists of two lensed-shaped Cu-Zn massive sulfide mounds (100m Zinc zone, 48-49 zone) underlain by Cu-rich stringer zones. Mineralization is found at the contact between the sheeted dykes and pillow basalts of the Devereaux Formation. Trace element geochemistry indicates that the host rock is composed primarily of tholeiitic basalts with mid-ocean ridge basalt (MORB) signatures. Petrographic studies show that the host footwall basalts distal to mineralization have undergone pervasive spilitization and are composed of plagioclase microcrystals, with minor sericite, in a chloritized volcanic glass matrix \pm epidote. Alteration mineral assemblages of the footwall basalts proximal to mineralization are dominantly chlorite \pm quartz in the stockwork zone, and carbonate \pm pyrite \pm talc near the massive sulfide lenses. Geochemical alteration box plots show a hydrothermal alteration trend between that of chlorite



- pyrite – (sericite), and chlorite - carbonate. Footwall basalts are characterized by mass gains in Fe, Mg, and Mn, and mass losses in Na, Ca, and Si. In the extensively chloritized stockwork zone, mineralization is present in the form of late stage chalcopyrite – quartz veins overprinting early stage pyrite veins. Trace element geochemistry shows a linear relationship between Cu - In and Cu - Se. The 100m Zinc zone lens features a distinct sulfide breccia unit consisting of subrounded to subangular pyrite, chalcopyrite, and basalt fragments in a pyrite \pm quartz matrix. The 48-49 lens is zoned with a base characterized by chalcopyrite – pyrrhotite - quartz \pm magnetite, whereas towards the top, the lens is characterized by massive euhedral pyrite \pm magnetite in a carbonate and talc matrix. Similarly to other Phanerozoic VMS deposits, sulfides at Turgeon have an average $\delta^{34}\text{S}$ of 6.9 ‰, indicating that a portion of the sulfur in the ore forming fluids was derived from seawater sulfate. (SS7; Wed. 3:40)

Identification of metamorphic assemblages and textures associated with gold mineralization at the Lalor deposit, Snow Lake, MB

Lam, J., judylam9@gmail.com, Tinkham, D.K. and Gibson, H.L.,
Department of Earth Sciences, Laurentian University, 935
Ramsey Lake Rd., Sudbury, ON P3E 2C6

The Lalor Au-rich VMS deposit is located within the prolific Paleoproterozoic Snow Lake arc assemblage. A middle amphibolite facies regional metamorphic event *circa* 1.81 Ga resulted in a wide array of mineral assemblages within hydrothermally altered VMS host rocks. The extent to which metals were remobilized or introduced to the system during metamorphism is uncertain. The complex metamorphic fluid evolution as indicated by the diversity of mineral assemblages and the occurrence of arsenopyrite at peak metamorphic temperatures could both facilitate processes that could mobilize metals. To help decipher the role of metamorphism in the mineralization process and the mobility of metals, the initial phase of this research combined drill core and petrographic studies with existing assay data to identify the various environments of Au-enrichment, specifically focusing on relationships between Au and metamorphic assemblages, alteration styles, metamorphic fabric and textures, primary rock types, and sulfide associations. The next phase of research will use detailed litho-geochemistry, mineral chemistry, and phase equilibria modeling to further investigate the potential of metamorphic metal mobility, specifically concentrating on the fluids released during metamorphic decarbonation and dehydration reactions and the possibility of mixing of COHS fluids and fluid-rock interaction at various metamorphic temperatures.

Seven rock types with associated Au-enrichment have been identified at the Lalor deposit: massive sulfide, unaltered to weakly altered volcanics, Ca-altered rocks, Fe-Mg altered rocks, kyanite/sillimanite \pm muscovite/biotite schists, silica-rich rocks, and plagioclase pegmatite rocks. Sulfide mineralization with associated Au-enrichment is often Cu-rich, ranging from disseminated to massive in nature, and is either concordant or discordant to foliation. In the massive sulfide environment, the typical minerals are pyrite, sphalerite, pyrrhotite, chalcopyrite, and/or galena. In unaltered to weakly altered rock, gold is typically found with chalcopyrite, galena, and/or arsenopyrite mineralization. In Ca-altered assemblages, Au is primarily associated with chlorite-carbonate assemblages containing actinolite-tremolite, diopside, epidote, galena, and/or chalcopyrite. The Fe-Mg altered assemblages consist of garnet, staurolite, chlorite, anthophyllite, and/or cordierite, with disseminated to stringer chalcopyrite. In the kyanite/sillimanite \pm muscovite/biotite assemblages, disseminated pyrite mineralization typically occurs with disseminated to vein chalcopyrite. Silica-rich rocks contain chalcopyrite and/or galena. An anomalous gold-rich environment also occurs within a pegmatitic plagioclase rock containing coarse biotite and vein-like galena between the plagioclase crystals. (SS7; Wed. 1:40)

Global carbon capture and storage (CCS) to mitigate climate change: Is it worth the price?

Langenberg, C.W., University of Alberta, Edmonton, AB,
cwlanger@telus.net

Canada (together with the USA and Australia) has the largest emissions of CO₂ per capita in the world: about 21 tonnes of CO₂ per capita equivalent. Alberta exceeds that amount significantly with close to 70 tonnes per capita. Because Alberta considers the rapid development of the oil sands important for its economy, it is unlikely that these numbers will decrease significantly in the foreseeable future. If anything, Alberta's CO₂ output is likely to increase. It is estimated that CCS will cost somewhere in the range of \$70-\$150/tonne. This estimate is well above the current \$15/tonne Alberta carbon price, which the Alberta Government charges to large emitters.

To mitigate climate change, Alberta is planning to store yearly 139 Mt of CO₂ by 2050 at a cost of \$15 billion per year (at an average cost of \$110/tonne). Leakage of natural gas can be observed in most petroleum reservoirs and potential leakage of stored CO₂ needs to be taken into consideration. There are about four hundred thousand wells in Alberta. Several thousand of these wells leak through surface casing and about 25% of these gases are identified as coming from the deep production horizons. It is clear that these leaking wells could cause serious hazards for any CCS project in Alberta.

It is estimated that for mitigating global climate change by storing 3 GT of CO₂, \$330 billion per year is needed at an average cost of \$110/tonne of stored CO₂. It is possible that 8 GT needs to be stored, which would cost \$1 trillion per year. CCS is very expensive, would require large amounts of energy and is still untested at this scale. Thus, it is clearly more cost-effective to increase the contribution of energy conservation in obtaining reduced CO₂ emissions. (SS20; Fri. 11:00)

Paleogeographic differentiation of the Early Silurian Virgiana brachiopod fauna in Laurentia

Lapenskie, K., klapens@uwo.ca, and Jin, J., jjin@uwo.ca,
University of Western Ontario, 1151 Richmond Street, London,
ON N6A 5B7

After the terminal Ordovician mass extinction, the Virgiana brachiopod fauna was among the first shelly benthos to re-colonize the paleocontinent Laurentia. The precursor of Virgiana is considered to be Brevilamulella in the Late Ordovician (Hirnantian) extinction interval. Brevilamulella is characterized by a small, smooth shell. The intermediate form between Brevilamulella and Virgiana is the earliest Silurian Viridita. It is the ancestor of all Virgiana faunas which span several paleocontinents. Viridita is also relatively small with a low ventral umbo, but has Virgiana-type rounded costae.

A major invasion of the Virgiana fauna into epicontinental seas of Laurentia occurred during the mid-Rhuddannian Stage sea level rise and marine inundation of the Laurentian paleocontinent. Adaptations to environmental conditions across paleolatitudes and the utilization of different modes of life are reflected in morphological variations among Virgiana species. In subtropical environments at higher latitudes, shells are of moderate size, quasi-smooth to weakly ribbed, with a low to moderately high ventral umbo, and ventral-dorsal valve depth ratios of approximately 2:1. These forms are typical of the Virgiana fauna from the Beccie Formation of Anticosti Island. In paleoequatorial regions (e.g. Williston and Hudson Bay basins), the shells are larger, prominently elongated, with higher ventral umbones, numerous fine costae, and notably greater ventral-dorsal valve depth ratios. The enlarged and thickened ventral valve and the correspondingly reduced dorsal valve are interpreted as adaptations to living in the hurricane-free, shallow equatorial seas – the ventral valve became a sessile base anchored on the substrate, and the dorsal valve serving as a mobile lid. In severe storm-influenced environments in mid- to high-tropics, both valves would be in a vertical position to avoid smothering by frequent, storm-generated mud deposits.

The paleo-geographical extent of Virgiana was limited to tropical regions. The most southerly species, *V. mayvillensis*, occurs in the Michigan Basin at approximately 20° south. At higher latitudes,



Virgiana was replaced by the superficially similar Platymerella. Virgiana has a total range of 2 myrs, becoming extinct at the end of the Rhuddanian. (SY3; Thurs. 3:00)

Animating Mother Earth

Laramée, M. (Consultant) and Robinson Settee, H. (Director),
Aboriginal Education Directorate, 520 Selkirk Ave, Winnipeg,
MB R2W 2M7, myra.laramée@gov.mb.ca

The participants in this session will be provided with a cultural understanding of how the rock formations from the largest mountains to the smallest pebble are considered animate and have a life which contributes the betterment, health and well being of the Indigenous peoples of this land. The animation of the natural order is part of the philosophies, belief systems and ways of living for Indigenous people who inhabited this part of Mother and this animation has been understood since the beginning of time. Mother Earth was created as a living entity to be respected and understood as the first life giver in this part of the universe. The rocks and mineral life are an integral part of this belief system. (SS22; Thurs. 9:20)

GeoCapture – Geological and geochemical database management system for drill hole and surface data

Lee, S.K.Y., Sharon.Lee@gov.mb.ca, Lenton, M. and Keller, G.,
Manitoba Geological Survey, Winnipeg, MB R3G 3P2

GeoCapture is a free, soon-to-be released geological and geochemical database management system created by the Geoscience Information Services department of the Manitoba Geological Survey (GIS-MGS). GeoCapture is a Microsoft Access database that was initially designed for the collection and management of hundreds of HudBay diamond drill hole (DDH) logs and their thousands of geochemical samples located in the sub-Phanerozoic Precambrian basement of the Flin Flon Belt in Manitoba and Saskatchewan. To compliment the DDH data, the capability to enter surface geological data was later added into GeoCapture.

GeoCapture has now become a database management system that not only collects and organizes, but also standardizes data and allows for browsing and exporting of DDH and surface lithological and/or geochemical data. Data may be entered either manually (e.g. entering geological data from hardcopy DDH logs) or digitally imported (e.g. text files of geochemistry analyses). The Format Tool is an additional tool that was created at the GIS-MGS to assist with the import of geochemical data into GeoCapture. When geochemical analyses from laboratories such as X-Ray Assay Laboratories Ltd. (XRAL), AcmeLabs™ and Activation Laboratories Ltd. (Actlabs) are opened in the Format Tool, the data are reformatted into a standard text (.TXT) or comma space delimited (.CSV) file format. The geological and geochemical database may then be queried to export: 1- select DDHs, 2- DDHs based upon UTM coordinates within an area of interest; or, 3- based upon a lithology amongst all or some DDHs. The output file then opens in Microsoft® Office Excel® in which the user can reformat (if desired) the exported dataset for input into other software for mapping or modeling purposes such as ArcGIS®, Gocad® or IsoPlot®.

A demonstration of GeoCapture will be performed with the data from the sub-Phanerozoic Precambrian basement of the Flin Flon Belt. From GeoCapture, lithological and geochemical data will be extracted from the Spruce Point-McClarty region in Manitoba and then mapped using ArcGIS® and modeled in 3D using Gocad®. (GS7; Wed. 2:20)

Hydrothermal alteration and uranium mineralization at the Camie River prospect (Otish Basin, Québec)

Lesbros, M. and Beaudoin, G., Université Laval, 1065 Avenue de la Médecine, Québec, QC G1V 0A6, marion.lesbros-piat-desvial.1@ulaval.ca

The Camie River prospect is interpreted as an unconformity-related uranium deposit, located in the Paleoproterozoic Otish Basin, approximately 250 km NE of Chibougamau (Québec). The basin is situated along the southeastern margin of the Superior Province, close

to the Grenville tectonic front. Mineralization at Camie River consists of disseminated and vein pitchblende near the unconformity between sandstones and conglomerates of the Matoush Formation and the underlying metavolcanic and metasedimentary rocks of the Archean Tichegami Group.

This study involved the examination of fifteen drill holes selected along seven cross-sections, including one hole far outside of the mineralized zone to distinguish diagenetic processes from those associated with the mineralization. A petrographic study of 140 thin sections established a paragenetic sequence in which the basement units show early carbonate ± brick-red hematite ± chlorite veins cut by quartz ± pyrite veins. The uranium mineralization is associated with carbonate veins hosted in graphitic units in the basement. The overlying sedimentary rocks show an early pervasive, pinkish albite-hematite & K-feldspar alteration replaced by a pervasive, greenish muscovite-illite alteration. Fractured zones are characterized by brick-red hematite ± chlorite matrix replacement and veins. These are cut sporadically by quartz ± carbonates ± K-feldspars ± sulphides veins. Limonite overprints these veins and alteration types, both as pervasive replacement and in veins. The uranium mineralization is associated with chlorite matrix replacement and carbonates ± sulphides veins in sedimentary rocks. In the pervasive albite-hematite & K-feldspar alteration, albite is pure end-member Ab₉₈ whereas muscovite is phengitic in the pervasive muscovite-illite alteration. Replacement chlorite is ferro-clinocllore whereas vein chlorite is magnesian-rich clinocllore. A lithogeochemical study of the host rocks (50 sedimentary rocks samples and 28 basement samples) has been conducted: pervasive albite-hematite & K-feldspar and muscovite-illite alterations in sedimentary rocks have LREE fractionated patterns with a weak negative Ce anomaly, a negative Eu anomaly and flat HREE patterns. Some pervasive albite-hematite & K-feldspar alteration samples are characterized by an HREE enrichment. (SS5; Thurs. 1:40)

Keynote (40 min): The roles of local incorporation, *in-situ* segregation, and physical transport in the genesis of magmatic sulfide and oxide deposits

Leshner, C.M., Mineral Exploration Research Centre, Department of Earth Sciences, Laurentian University, Sudbury, ON P3E 2C6, mlesher@laurentian.ca

The solubilities of sulfide and oxide are both relatively low in mafic-ultramafic magmas, typically 50-100× less than associated silicates, so most magmatic sulfide and oxide ores form by i) incorporation of sulfide or oxide-rich country rocks, ii) *in situ* exsolution/crystallization and accumulation from much larger masses of magma, or iii) one or both of those processes followed by physical transport into their current locations. Geological, geochemical, and isotopic data indicate that massive and semi-massive ores commonly form by melting of sulfide-rich country rocks (e.g., Kambalda, Noril'sk, Raglan, Sudbury contact ores, Thompson), whereas oxide ores less commonly form by incorporation of oxide-rich country rocks (e.g., Duluth, possibly McFaulds Lake). Sulfides in laterally-restricted sills likely formed more-or-less *in situ* (e.g., Noril'sk, Thompson), whereas sulfides in long lava channels were likely transported some distance before being trapped (e.g., Kambalda, Raglan). Disseminated and net-textured sulfides or chromites hosted by cumulate rocks may have formed locally or been transported (accounting for the debate regarding Jinchuan and most chromite deposits), but massive or semi-massive sulfides hosted by non-cumulate rocks (e.g., dike-hosted ores at Sudbury and possibly Voisey's Bay) were likely transported. Once formed, sulfides and oxides segregate rapidly and are very difficult to engulf, entrain, and transport upward, accounting for the absence of significant amounts of chromite in lava flows and why sulfides present in lava flows appear to have formed at high levels. Vertical transport of dense molten sulfide melts or chromite from staging chambers requires a mechanism to extract previously-segregated dense cumulus phases in amounts low enough (<10%) that the bulk density of the magma does not exceed the bulk density of the crust through which the magma must be transported, a driving mechanism forceful enough over a time



interval short enough to transport very dense magmas (e.g., seismic pumping), or a very viscous enclosing medium (e.g., podiform chromitites). In case of a low-viscosity magma, it is critical that the dense phases not coalesce (immiscible sulfides) or agglomerate (fine chromite) during transport, which would increase the bulk density of that part of the system and lead to backflow. Semi-massive inclusion-rich dike-hosted ores at Sudbury and Voisey's Bay may therefore represent backflow, but may also represent seismic-driven vertical slug flow. More detailed geometrical studies will be required to distinguish between these possibilities. Inclusion-poor stratiform-stratabound sulfide and chromite mineralization exhibit none of these features and are more likely to have formed *in situ*. (SS9; Wed. 1:40)

Mining a till geochemical database for new mineral prospects in British Columbia

Lett, R.E., British Columbia Geological Survey Emeritus, 3956 Ashford Rd, Victoria, BC V8P 3S5, Raylett@shaw.ca

The British Columbia Geological Survey till geochemistry data compilation can be a valuable aid to mineral exploration given that glaciogenic sediments cover much of the province and that basal till geochemistry has a proven ability to detect buried mineralized bedrock. First published in 2008 this database now has information for over 8000 mainly basal till samples collected by the British Columbia Geological Survey, the Geological Survey of Canada and Geoscience BC. Sample attributes in the database include location coordinates, information about bedrock geology beneath the sample site and the surficial sediment type. Most of the till samples have geochemical data from the analysis of a 0.063 mm size fraction for major, minor and trace elements by a combination of instrumental neutron activation, aqua regia digestion – inductively coupled plasma emission or mass spectroscopy, lithium metaborate fusion - inductively coupled plasma emission spectroscopy and loss on ignition. A smaller number of the till samples also have gold grain abundances and gold grain shapes in a heavy mineral concentrate and the results of a clay size (0.002mm) fraction analysed for trace elements including gold.

Statistical analysis of the data and filtering different element combinations can reveal distinct till geochemical signatures that could reflect concealed mineralized or altered bedrock. For example, over one hundred till samples have anomalous gold-copper-arsenic-molybdenum values including several from near the Huckleberry and Mount Milligan porphyry copper-gold deposits. While major oxides alone do not seem to show evidence of bedrock contacts, a ratio of aqua regia extractable potassium oxide to total potassium oxide in till samples can highlight the potassium alteration associated with known porphyry deposits. Hence, a comparison of the geochemical data generated by different analytical methods can reveal much more than just element variations in till and increase the size of a detectable hydrothermal alteration envelope. (GS6; Wed. 9:00)

Preliminary 3D modelling and structural interpretation of the southeastern Athabasca basin

Li, Z., Bethune, K., Chi, G., Department of Geology, University of Regina, 3737 Wascana Parkway, Regina, SK S4S 0A2, lizenghua@gmail.com, Bosman, S. and Card, C., Saskatchewan Geological Survey, 2101 Scarth Street, Regina, SK S4P 2H9

The southeastern part of the Athabasca basin hosts some of the largest high-grade unconformity-related uranium deposits in the world, including McArthur River and Key Lake. As a first step of an effort to reconstruct and model the fluid flow related to uranium mineralization, a 3D model of the sub-Athabasca unconformity and basin stratigraphy has been constructed using drill-hole log data. Several cross-sections have been built and integrated into the 3D model to constrain the spatial configuration of Athabasca Group units. Faults have been identified using an iterative approach first identifying potential fault lineaments using the basement geophysical signature, and then checking if these linear features have any spatial relationship to offsets of the unconformity surface. Using this approach, two dominant sets of faults, inferred to be near vertical, have been identified in the area of study:

one trending approximately NE and the other NW. The unconformity surface in the 3D model shows an approximately NE-trending zone of elevated topography with elevations changing from about -100 m to 400 m. This topographic ridge of the unconformity is associated with the Wheeler River (Phoenix)/McArthur River deposits trend. A preliminary cross-section illustrates that this may be controlled by NE-trending reverse faults that have uplifted the basement. Regional clay anomalies in the Athabasca Group are broadly coincident with the topographic highs of the unconformity surface. Draping of the major uranium deposits, prospects and occurrences onto the unconformity surface indicates that the majority of deposits and prospects are located where these structures appear to have offset the unconformity. Future work will be focussed on increasing resolution of the model in this and other key areas to gain a better understanding of the geometry and kinematics of regional and local structures and their control on fluid flow and mineralization. (SS5; Fri. 9:00)

Recent research on indium from The Lagoa Salgada orebody, Iberian Pyrite Belt, Portugal

Lima, A.M.C., Rodrigues, B.C., Geology Centre of Porto, Porto, Portugal, allima@fc.up.pt, Oliveira, A. and Guimaraes, F., LNEG, S. Mamede de Infesta, Portugal

The Iberian Pyrite Belt is one of the most outstanding European ore province, hosting one of the largest concentrations of massive sulphides in the Earth's Crust. Lagoa Salgada orebody, the most northerly of the Iberian Pyrite Belt known so far, is a small massive sulphide deposit with an inferred mineral resource of 3.7 Mt. The orebody has been described as composed of a central stockwork zone – a thick Volcano Sedimentary Complex with more than 700m – and a massive sulphide lens in the northwest. It is covered by more than one hundred meters beneath sediments of the Sado Tertiary basin.

A Junior Exploration Company has implemented an exploration program with recent drilling holes in new areas of the northwest lens of the deposit. Different types of ores have been identified on preliminary metallographic study that have established five basic textural domains: (i) Massif pyrite; (ii) Banded texture with layers of sphalerite and, rarely, of sphalerite and galena; (iii) Secondary transformation of massif pyrite; (iv) Infilling veins texture; (v) Supergenic banded texture.

The ore mineralization assemblage is mainly composed of pyrite with minor sphalerite, tetrahedrite-tennantite, arsenopyrite, chalcopyrite, galena, stannite, cassiterite, and supergene minerals which are in different amounts represented throughout the basic textural domains.

Polished sections of massive sulphide ore samples were studied by Electron-probe microanalyses (EMPA). Most of the minerals phase are behind the detection limit of Indium values, however, related with banded basic textural domain (ii) it was identified one generation of sphalerite, with mean granular dimension of 20 micra included on recrystallized arsenopyrite, that have 23000 ppm of Indium. This value is four times more Indium content than the best average values of other studied sphalerite examples on the same orebody deposit, in recent published results. This discovery proves again the complexity of this deposit and highlights the needed of prospecting new areas inside the ore body with predominance of this generation of sphalerite.

Ongoing works will demonstrate the Lagoa Salgada orebody potential for this rare trace metal, that is used in high-tech applications and is critical for European Industry. (SS7; Wed. Poster)

Young-Davidson and Hemlo gold deposits in the Superior Province, Ontario: Contrasting styles of mineralization of common tectonic origin?

Lin, S.¹, Zhang, J.¹, Linnen, R.² and Martin, R.¹, ¹University of Waterloo, Waterloo, ON N2L 3G1; ²Western University, London, ON N6A 5B7

Young-Davidson and Hemlo gold deposits occur in the Abitibi-Wawa Subprovince of the Superior Province. The Young-Davidson deposit is an intrusion-related lode-gold deposit that at least in part is structurally



controlled. It is associated with the development of the Cadillac – Larder Lake deformation zone and hosted in a syenite of ~2679 Ma. Three main generations of veins are identified in the syenite. V_1 veins are characterized by folded and boudinaged quartz-ankerite veins, V_2 veins are represented by folded quartz-pyrite veinlets and disseminated sulfides, and V_3 veins are comprised of en echelon or planar quartz-carbonate veins with sulfide minerals. Petrological studies reveal that the major phase of gold mineralization is associated with V_2 veins, and partially with V_1 and V_3 veins. Gold mineralization and emplacement of the associated veins appear to have occurred during shearing and the syenite acted as a mechanical trap due to competency contrast.

The Hemlo deposit appears quite different from a typical Archean lode-gold deposit in the Superior Province. It is a disseminated and replacement style gold deposit that is spatially associated with the stratigraphically lower contact of a volcanic quartz-feldspar porphyry. The protolith is mainly a fragmental rock and a barite horizon occurring at the contact. The contact and the fragmental rock at the contact probably served as mechanical traps and the barite horizon as a chemical trap. The deposit is located in the Hemlo shear zone and mineralization occurred during shearing, before mid-amphibolite-facies peak metamorphism. Mineralization was occurring at ~2677 Ma and most likely had started earlier. Mineralizing fluids probably had a magmatic source, interpreted to be related to the 2682–2677 Ma granodioritic (sanukitoid) plutons abundant in the vicinity.

In spite of the obvious differences, the two deposits share many similarities. Both are genetically related to shear zones and late mantle-derived intrusions that are of similar ages, and the associated shear zones have similar kinematic history and probably have similar ages. The two deposits appear to share a common tectonic origin and their different characteristics may be due to variation in local geological settings. In particular, we suggest that the gold deposits, the intrusions and the hosting shear zones all developed within a regime characterized by synchronous vertical and horizontal tectonism. They were all possibly linked to a range of processes associated with the accretionary growth and stabilization of the craton, in particular slab break-off and the associated extensional orogenic collapse following terrane accretion. (SS3; Fri. 10:20)

Keynote (40 min): Long-term biogeochemistry of mine tailings amended with organic carbon for managing water quality

Lindsay, M.B.J., Department of Geological Sciences, University of Saskatchewan, Saskatoon, SK S7N 5E2, matt.lindsay@usask.ca

Water quality degradation is a pervasive environmental issue and substantial financial liability for the mining industry worldwide. Unmitigated drainage from mine waste deposits can have widespread impacts on water quality, ecosystem function and human health. The long-term environmental sustainability of the mining industry therefore depends on the development of innovative strategies for managing mine wastes and associated water quality. These strategies must be pragmatic and cost effective, and provide sustained improvements in water quality. Proactive strategies that enhance or augment intrinsic biogeochemical processes present considerable potential for reducing contaminant fluxes and lessening environmental impacts associated with mining activities. Long-term field experiments were conducted to assess the use of organic matter amendments to induce sulfate reduction and metal attenuation in the vadose zone of an active tailings deposit. Six experimental cells were constructed in sulfide- and carbonate-rich tailings characterized by neutral drainage. Varied mixtures of peat, spent brewing grain (SBG) and municipal biosolids (MB) were incorporated into fresh mill tailings. Sulfate-reducing conditions developed within three years in cells amended with multiple OC sources. Removal of sulfate generally corresponded to alkalinity production, growth of sulfate-reducing bacteria, H_2S production, ^{34}S - SO_4 enrichment, and Zn, Mn, Sb and Tl removal. The addition of OC initially induced Fe and As mobilization; however, this process was most pronounced for cells that contained MB. Large increases in pore-water SO_4 concentrations below the tailings surface in all cells resulted

from sulfide-mineral oxidation over time. Sustained sulfate removal was observed below the oxidation zone in tailings amended with peat + SBG. Increased SO_4 concentrations observed with other amendments were attributed to declining rates of sulfate reduction with time. Terminal restriction fragment length polymorphism profiling of 16S rRNA genes revealed substantial metabolic diversity, and complementary cellulase assays suggested that long-term rates of sulfate reduction are controlled by cellulose degradation. (SS15; Wed. 1:40)

Keynote (40 min): The importance of fluorine in pegmatite melts

Linnen, R.L.¹, rlinnen@uwo.ca, Aseri, A.¹, Che, X.², Botcharnikov, R.³, Holtz, F.³, and Thibault, Y.⁴, ¹Department of Earth Sciences, University of Western Ontario, London, ON; ²Nanjing University, Nanjing, China; ³Leibniz University, Hannover, Germany; ⁴CANMET-MMSL, Ottawa, ON

There is conflicting data in the literature as to whether fluorine directly (by forming complexes) or indirectly (creating non-bridging oxygens) increases high field strength element solubility in silicate melts or conversely has no effect, or even decreases solubility. To resolve this problem, experiments were conducted using a synthetic melt composition, representative of a highly evolved pegmatite: 1.1 wt% Li_2O , 1.7 wt% P_2O_5 and 2.0 wt% B_2O_3 , with up to 8 wt% F, with a major element composition that corresponds to the projection of the 200 MPa granite minimum to the Ab-Or tie line. The ASI (molar $Al/(Na+K)$) is one, but if Li is included as alkali element, the melt is peralkaline. Experiments were at or near fluid saturation, at 650 to 1000°C and 200 MPa.

At constant pressure and temperature, manganocolumbite ($MnNb_2O_6$) and manganotantalite ($MnTa_2O_6$) solubilities are nearly independent of the F content of the melt. A similar result was observed for hubnerite ($MnWO_4$) and ferberite ($FeWO_4$), although in the case of tungstate solubility a weak positive and negative F-dependence was noted for hubnerite and ferberite, respectively, which may indicate Mn-F and Fe-F interactions in the melt. The solubilities of each of these HFSE minerals is much higher than in a subaluminous melt (ASI=1) at the same temperature and pressure. However, if Li is considered to be an alkali and alkali phosphate interactions are taken into account, then the increase in HFSE mineral solubility can largely be explained by a decrease in the effective ASI of the melt.

The effect of fluorine on the solubilities of zircon ($ZrSiO_4$) and hafnon ($HfSiO_4$) is different. Their solubilities increase with an increasing fluorine content of the melt, suggesting that fluorine complexes of Zr and Hf in the melt may exist. One common feature of the solubility of all of the HFSE minerals is that they are strongly temperature dependent. Consequently, the most important role of fluorine may be to lower liquidus temperatures, thereby decreasing the amount of HFSE required for mineral saturation, rather than have a direct influence on HFSE mineral solubility in the melt. (SY2; Thurs. 1:40)

Sequestration of uranium in mesoporous silica SBA-15 as uranyl clusters

Liu, Y., Jouffret, L., Szymanowski, J.E.S. and Burns, P.C., University of Notre Dame, South Bend, IN 46656 USA, yliu10@nd.edu

Immobilizing radionuclides, such as uranium, during processing of used nuclear fuel is important for the safe and sustained application of nuclear energy. Sequestration of uranium by mesoporous silica has been investigated because of the high loading capacities of the mesoporous materials resulting from their high surface area and large pore volume. Traditionally, high loading amounts of uranium in the mesoporous silica was achieved by functionalization of the inner surface of the mesoporous silica with organic ligands. The organic ligands can bind with uranium ions to sequester the uranium, which, however, limits the loading amount of uranium to one-molecular layer on the inner surface of the pore. To increase the loading of uranium, we propose to increase the dimension of the sequestered uranium from



a two-dimensional surface layer to a three-dimensional cluster by growing uranium clusters *in situ* in the pores of mesoporous silica, SBA-15. Previous work in our group showed that uranyl clusters can be formed in aqueous conditions, and the size of the uranyl clusters, taking U60 as an example, is smaller than the average pore size of the SBA-15. In this work, the results indicate that the U60 is formed in the pores of the SBA-15 based on the analyses by Raman spectra, N₂ adsorption and desorption, small angle X-ray scattering, and transmission electron microscopy. The loading capacity of the SBA-15 for the uranium by this method will be tested. (SS5; Wed. Poster)

Assessment of soil erosion and sedimentation in South Tobacco Creek using radiochemistry and geochemistry as tracers

Lobb, D.A.¹, david.Lobb@AD.UManitoba.CA, Koiter, A.J.², Owens, P.N.², Tiessen, K.H.D.³ and Li, S.⁴, ¹Watershed Systems Research Program and Department of Soil Science, University of Manitoba, Winnipeg, MB R3T 2N2; ²Environmental Science, University of Northern British Columbia, Prince George, BC; ³International Development Research Centre, Ottawa, ON; ⁴Agriculture and Agri-Food Canada, Fredericton, NB

Soil erosion and sedimentation is a significant environmental issue in Canada, adversely affecting the quality of our soil, water and air resources. In South Tobacco Creek watershed, and across the country, sediment contamination of waterways has been given great attention. This water quality concern has contributed to the widespread implementation of soil conservation practices, conservation tillage in particular. The intensity of tillage has reduced and the residue cover has increased over the past few decades, however, sediment delivered from the watershed remains a concern, as it does in other watersheds. The South Tobacco Creek watershed is a predominantly agricultural watershed, which extends across the Manitoba Escarpment; its upper reaches lay in undulating glacial tills and its lower reaches lay in the lacustrine sediments of glacial Lake Agassiz. The watershed is situated in a semi-arid region in which the hydrology is dominated by snowmelt runoff when soils are frozen and the vegetation is dormant. The current and historical rates of in-field soil erosion and relative contributions of wind, water and tillage erosion have been assessed using ¹³⁷Cs. This research found that water and tillage erosion have both resulted in considerable soil erosion within cultivated fields, but that most of the eroded soil does not make it into the streams. In 2009, a comprehensive study of the sources of sediments in the streams was initiated using sediment fingerprinting techniques. Suspended sediments were sampled using paired time-integrated samplers fixed to the stream bed. Samples were collected periodically over the course of three years at several locations along the main stem of the creek. Sediment samples were analyzed for ¹³⁷Cs as well as other radiochemical and geochemical elements and the values were compared to those measured within the surface soil of agricultural fields and riparian areas, and streambank profiles. The suspended sediments in the upper reaches are dominated by field and riparian area sources while the majority of suspended sediments moving through the lower reaches and being exported from the watershed appears to be coming from streambank sources. This may be due to low upland erosion rates, sediment storage within the watershed, high sediment input from steep cut-banks, streambank failure and the highly erodible shale bedrock common to this region. As this research continues we are expanding the number of sampling sites and developing a composite fingerprint (multiple tracers) to improve sediment source discrimination. (SS14; Thurs. 3:20)

Lithochemistry and sulfur isotopic composition of hydrothermal mudstones associated with the Lemarchant volcanogenic massive sulfide (VMS) deposit, Tally Pond belt, central Newfoundland

Lode, S.¹, slode@mun.ca, Piercey, S.J.¹, Devine, C.A.², Layne, G.D.¹ and Piercey, G.³, ¹Memorial University, 300 Prince Philip Drive, St. John's, NL A1B 3X5; ²Canadian Zinc Corporation, PO Box 11644, Vancouver, BC V6B 4N9; ³MAF-IIC MicroAnalysis Facility, Memorial University, St. John's, NL

The Cambrian precious metal-bearing bimodal felsic Lemarchant Zn-Pb-Cu volcanogenic massive sulfide deposit has a close association of hydrothermal sedimentary rocks to mineralization. Metalliferous mudstones occur immediately above and distal to mineralization - either stratigraphically on top of the massive sulfide deposit, or as interflow mudstones within hanging wall basaltic units. The mudstones range from samples that have hydrothermal signatures (high Fe/Al and base-metal values), to those with minor detrital input (lower Fe/Al and base metal values). When normalized to upper crustal shales, redox-sensitive positive Ce- and Eu-anomalies (Ce/Ce* and Eu/Eu* ≥ 1) and the redox-independent Y/Ho-ratio ~27 of the Lemarchant mudstones, suggest that they precipitated from reduced, high-T hydrothermal fluids with a short residence time in the hydrothermal plume and thus, a vent proximal setting. A second group of Lemarchant mudstones have negative Ce-anomalies, which may represent stronger mixing with seawater and REE-scavenging onto iron-oxyhydroxide particles, implying a more vent distal deposition. *In-situ* analyses by secondary ion mass spectroscopy (SIMS) of various sulfides from the mudstones (euhedral and framboidal pyrite, anhedral chalcopyrite and pyrrhotite, and euhedral arsenopyrite) yielded δ³⁴S values from -38 to -8‰ indicating a predominantly diagenetic-biogenic sulfur source and precipitation of the secondary sulfides under open system conditions. The absence of hydrothermal sulfur signatures suggests the potential for reduced vent fluid sulfur having been removed immediately after mixing with the seawater at or below the seafloor as the massive sulfides were formed. The predominance of biotic signatures in the sulfides suggests that most of the sulfides in the mudstones formed during diagenesis and are not primary, hydrothermal sulfides. It is proposed that the hydrothermal mudstones formed via deposition as black smoker plume fall-out - after mixing of hot, reduced and metal-rich vent fluids with cold, oxidized, sulfate-rich ambient seawater; initially as amorphous iron-oxyhydroxide particles and silicagels, which were subsequently altered during diagenetic and hydrothermal alteration. Based on our study, lithochemical and sulfur isotope data show potential as an indicator of the proximity to massive sulfide mineralization within a mudstone-bearing host sequence. (SS7; Wed. 3:00)

Rapid development and subsidence of a Neoproterozoic volcanic arc hosting the Winston Lake VMS ore bodies, Wawa subprovince, Superior Craton

Lodge, R.W.D.¹, rx_lodge@laurentian.ca, Gibson, H.L.¹, Stott, G.M.² and Franklin, J.M.³, ¹Laurentian University, 935 Ramsey Lake Road, Sudbury, ON P3E 2C6; ²Ontario Geological Survey (Retired), Stott Geoconsulting Ltd., 92 Crater Crescent, Sudbury, ON P3E 5Y6; ³Franklin Geosciences Ltd. 24 Commanche Drive, Ottawa, ON K2E 6H7

The 2720 Ma Winston Lake greenstone belt of the Wawa subprovince, Superior Craton, hosts the Winston Lake, Pick Lake, and Zenith volcanogenic massive sulphide (VMS) deposits but has not received a significant amount of research since the closure of the mines in the 1990's. The belt is subdivided into two main lithotectonic assemblages: (1) the Winston Lake assemblage (WLA) composed of tholeiitic to calc-alkalic bimodal volcanic lithofacies, which is overlain by (2) the Big Duck Lake assemblage (BDLA) composed of transitional to tholeiitic mafic flows and sills. These assemblages were interpreted to be conformable and are separated by the differentiated Zenith gabbro, which intrudes the Winston Lake VMS ore body and is host to the Zenith ore body.

Hydrothermal alteration during the formation of the VMS deposits was followed by lower amphibolite grade metamorphism that resulted in a complex range of mineral assemblages and trace element mobility. Despite these complications, distinct geochemical patterns and trends are recognizable in both the mafic and felsic strata. The felsic volcanic flows and volcanoclastic rocks in the WLA are FII- to FIII-type rhyolite indicating a high crustal level of formation. Mafic lithofacies that are intercalated with these felsic lithofacies are typically calc-alkalic in composition and have negative Nb and Ti anomalies and are enriched in



LREE, consistent with an island arc geochemical signature. Mafic flows from the overlying BDLA are tholeiitic and have flatter REE patterns and primitive mantle normalized Nb/Th ratios greater than 1.0 suggestive of an ocean plateau affinity.

Magmatic zircons from the felsic volcanics of the WLA and the Zenith gabbro both have ages *ca.* 2720 Ma. Epsilon-Nd values from mafic and felsic lithofacies in both assemblages are very similar and indicate a juvenile source. Th/Nb ratios greater than 0.2 and enriched LREE in mafic flows in the WLA suggest contamination from juvenile crust that was the same age in order to preserve the juvenile Nd-isotopic signature. Similar REE patterns and primitive-mantle normalized trace element patterns between phases of the Zenith gabbro and the overlying flows of the BDLA suggest they are genetically related. The felsic lithofacies of the WLA represent an early juvenile arc that experienced rapid subsidence and rifting, that was accompanied by mafic volcanism (the BDLA) and sill injection (the Zenith gabbro). The Winston VMS deposit formed during the early rifting and subsidence of the volcanic arc prior to the intrusion of the Zenith gabbro. (SS3; Thurs. 2:20)

Geochronology and geochemistry of Neoproterozoic Timiskaming-type assemblages in the Shebandowan and Vermilion greenstone belts, Wawa subprovince, Superior Craton

Lodge, R.W.D.¹, rx_lodge@laurentian.ca, Gibson, H.L.¹, Stott, G.M.², Hudak, G.J.³ and Jirsa, M.A.⁴, ¹Laurentian University, 935 Ramsey Lake Road, Sudbury, ON P3E 2C6; ²Ontario Geological Survey (Retired), Stott Geoconsulting Ltd., 92 Crater Crescent, Sudbury, ON P3E 5Y6; ³Precambrian Research Center, Natural Resources Research Institute, University of Minnesota Duluth, 5013 Miller Trunk Highway, Duluth, MN, USA 55804; ⁴Minnesota Geological Survey, 2642 University Avenue W., St. Paul, MN, USA 55114-1032

The Neoproterozoic Shebandowan and Vermilion greenstone belts (SGB, VGB) in the Wawa subprovince, Ontario and Minnesota, are tectonostratigraphically complex belts that contain pre- and syn-orogenic volcanic and sedimentary assemblages. The younger, syn-orogenic basins, known as Timiskaming-type assemblages, comprise mainly locally-derived sedimentary assemblages that were deposited in transpressional, pull-apart basins developed during the final stages of terrane accretion. In addition, they are commonly associated with calc-alkalic to alkalic magmatism that was emplaced along crustal-scale deformation zones. Timiskaming-type assemblages are important because of their association with world-class orogenic gold mineralization, especially in the Kirkland Lake area of the Abitibi subprovince of Ontario. However, the Timiskaming-type assemblages of the Wawa subprovince have significantly less economic precious metal mineralization than geodynamically-equivalent greenstone belt assemblages of the Abitibi subprovince and the timing of deformation and magmatism in the SGB and VGB is less well constrained.

This study presents new detrital and magmatic zircon U-Pb geochronology from the SGB and VGB. Thermal ionization mass spectrometric analyses of magmatic zircons in a dacitic tuff breccia from the Gafvert Lake sequence, the volcanic member of the Lake Vermilion Formation in the VGB, indicates that the volcanism is co-depositional with the *circa* 2690 Ma Timiskaming-type Shebandowan assemblage of the SGB. LA-ICPMS analysis of the sedimentary rocks of the Lake Vermilion Formation indicate that the detritus was locally derived from the Gafvert Lake metavolcanic lithofacies, and show a similar temporal pattern as the Timiskaming-type sedimentary rocks in the SGB. However, one sample from the SGB had a temporal distribution of detrital zircon ages that are significantly older and are more akin to magmatic ages in the Wabigoon Subprovince. This suggests trans-terran transport of detritus in a foreland-type basin.

A geochemical comparison of Timiskaming-type volcanic rocks in the VGB and SGB to those found in the Kirkland Lake area of the Abitibi subprovince may provide an explanation for their different gold-endowment. Volcanic rocks of the VGB and SGB are less enriched in incompatible elements and are more calc-alkalic when compared to the alkalic volcanic rocks in the Timiskaming assemblage of Kirkland

Lake. This may have resulted in significantly different magmatic fluid compositions, which are partially responsible for mobilizing and depositing gold in these systems. This difference in composition may also indicate that the structures that formed the basins within the SGB and VGB in the Wawa were not as deeply penetrating as those in the Abitibi. (SS2; Wed. 9:20)

Keynote (40 min): Petrologic assessment of zonation within granitic pegmatites

London, D., University of Oklahoma, Norman, OK 73019 USA, dlondon@ou.edu

The internal zonation of granitic pegmatites is deceptively simple. From the margins inward, the recognized units are the border zone, wall zone, intermediate zones, and core. The border and wall zones, which are commonly treated as one on the basis of composition, normally surround pegmatite bodies completely, whereas the intermediate zones and cores are less regular or persistent. Aplite, texturally distinct from any other units, may be present. Modal and chemical analysis of pegmatites by zones is rarely feasible, and very few accurate zonal or bulk compositions are available. From this limited database, these observations emerge: (1) in a zoned pegmatite, no single zone possesses the bulk composition of the entire pegmatite. However, the bulk compositions of zoned pegmatites are remarkably close to those of granitic liquids. (2) Border/wall zones are chilled margins that do not capture the bulk compositions of their pegmatite. In dikes at Ramona, California (USA), the wall zones along the footwall and hanging wall are different in composition in texture. Together in their proportion, however, they add up to the bulk composition of the pegmatite. (3) Aplites are always internal to pegmatites. A wall zone of sodic or potassic pegmatite underlies them. (4) In concentric pegmatites, intermediate zones evolve from plagioclase- to K-feldspar-rich toward the center. In layered pegmatites, the zonation of feldspars (Na- versus K-dominant) is oscillatory between complementary hanging-wall and footwall zones. Plagioclase and K-feldspar manifest normal and continuous igneous fractionation trends from margins to center. (6) Modal Qtz lies below the bulk average in the wall zone, aplites, and intermediate zones; the cores are correspondingly Qtz-rich. (7) Quartz-poor albite-lepidolite bodies are the last primary zones of pegmatites. (8) The sequence of zones in thin (20-40 cm) layered pegmatites from San Diego County, California (USA) mirror the texture and sequence of the same zones at Tanco, Manitoba (Canada), which is an order of magnitude greater in scale. (9) The textures and oscillations in composition among zones are attributable to the effects of pronounced undercooling of granitic melt prior to the onset of crystallization, and to the consequent oscillations in composition that ensue. (10) Field diffusion can account for much of the spatial heterogeneity of pegmatites. (SY2; Thurs. 8:20)

Stable isotopic compositions of kerolite from microbial deposits in basaltic caves, Kauai, Hawaii

Longstaffe, F.J., The University of Western Ontario, Department of Earth Sciences, London, ON N6A 5B7, flongsta@uwo.ca, and Léveillé, R.J., Canadian Space Agency 6767, route de l'Aéroport, Saint-Hubert, QC J3Y 8Y9

Stable isotopic compositions have been determined for unusual deposits of kerolite formed in association with secondary Ca-Mg carbonates in speleothems from the photic zone of open basaltic sea caves on the island of Kauai, Hawaii. In these caves, kerolite is commonly the only inorganic phase associated with poorly mineralized, actively-growing microbial mats, as well as being abundant in completely calcified (mostly aragonite and/or calcite) microbialite deposits. Previous work has indicated possible microbial influences on neoformation of such Mg-clays in extreme environments. Hence determination of the isotopic signatures of such clays is of special interest.

Ten samples of cave water from pools and drips analyzed over a five-year period had average oxygen and hydrogen isotopic compositions of -2.9 ± 0.6 permil and -7.5 ± 2.9 permil, respectively, and the average cave temperature was $21 \pm 1^\circ\text{C}$. TG-DTA results for the



kerolite samples were characterized by variable weight loss patterns with an inflection point at 160-180°C followed by either more rapid or slower rates of weight loss up to about 850°C, thus making choice of a degassing temperature for loosely-bound water problematic. Stepwise *in vacuo* heating of nine previously dried (90°C) samples, however, yielded similar hydrogen isotopic compositions: -84 ± 15 permil (25-90°C), -76 ± 6 permil (90-250°C), -86 ± 9 permil (250-1000°C), with a weighed average of -84 ± 7 permil. A proportionally larger range of oxygen isotopic compositions for these samples ($+16.3$ to $+23.5$ permil) may indicate some role for cave solution evaporation in kerolite formation, though it typically precipitated first in the microbialite paragenetic sequence, well before magnesite, hydromagnesite and gypsum. Microbial activity is considered a main driver of kerolite formation in this system, and intimate microbial involvement is supported by the isotopic composition (-27.0 ± 2.6 permil) of carbon retained in the $< 2 \mu\text{m}$ fraction following conventional oxidation of organic matter. The isotopic data suggest a kerolite-water permil fractionation of $+22.7$ for oxygen, similar to that obtained using a Savin and Lee-style bond-type empirical calculation. The kerolite-water permil separation of -80 for hydrogen observed here is larger than predicted based on limited high-temperature data for talc, but consistent with values known for serpentine and ferric iron-rich smectite formed at low temperatures. Hydrogen released from occluded organic matter may also have contributed to the kerolite hydrogen isotopic compositions measured here. (SYI; Wed. 9:00)

Interactions between uranyl peroxo nanoclusters and solid surfaces in aqueous environments

Lussier, A.J., aaron.j.lussier@gmail.com, McGrail, B.T., Dzik, E.A., Na, C., and Burns, P.C., Department of Civil & Environmental Engineering & Earth Sciences, University of Notre Dame, Notre Dame, IN, USA 46556

Uranyl peroxo nanoclusters are caged polyoxometalates (POMs) that can adopt a wide range of stoichiometries, sizes and topologies. Their contrasting chemical behaviours and high solubilities make them potentially important for: (1) developing safer, more efficient, nuclear fuel cycles; and (2) modeling uranium mobility in groundwater following the failure of engineered barriers in spent fuel repositories. In the laboratory, U-nanoclusters form spontaneously where U^{6+} , H_2O_2 and certain cations are present in aqueous solution, and they may remain stable for years. Were spent nuclear fuel to contact groundwater, the production of H_2O_2 by radiolysis may result in U-nanocluster formation, and subsequent transport could depend on interactions with mineral surfaces. In general, interactions between POMs and surfaces are poorly understood; however, our preliminary investigations, using atomic force (AFM) and scanning electron microscopies (SEM), demonstrate the self-assembly of aqueous U-nanoclusters (e.g., U60 and U24) into arrays of well-faceted, micron-to-sub-millimeter-scale geometrical forms (hexagons, triangles, rectangles) on flat mineral surfaces. Here, we investigate the mechanisms by which U-nanoclusters interact with surfaces of geologic interest (phyllosilicates, calcite, zeolites, etc.) using: (1) AFM imaging in open air and liquid-cell modes; and (2) batch-type adsorption / desorption experiments. The AFM images show evidence that suggest the exact mechanism of self-assembly is dependent upon evaporation rate, solution chemistry and substrate surface topology, e.g., certain forms show evidence of layer-by-layer assembly, whereas others show evidence of more complex assembly mechanisms. The batch-type experiments conducted over longer periods of time (days-to-weeks) indicate different minerals adsorb U-nanoclusters at significantly different rates, e.g., kaolinite – slow (weeks), apophyllite – very fast (minutes-to-hours). To date, these results show that the nature of nanocluster/surface interactions is complex, and developing a comprehensive model requires simultaneous consideration of nanocluster chemistry/topology, solution chemistry and substrate surface chemistry/structure. (SS5; Wed. 10:20)

Structural isomerism in minerals based on octahedral $[\text{M}^{\text{VI}}\text{MO}_4]$ chains

Lussier, A.J., University of Notre Dame, Department of Civil & Environmental Engineering & Earth Sciences, Notre Dame, IN, USA 46556, aaron.j.lussier@gmail.com, and Hawthorne, F.C., Department of Geological Sciences, University of Manitoba, Winnipeg, MB R3T 2N2

A common fundamental building block (FBB) in oxysalt minerals is the chain of edge-sharing octahedra $[\text{M}^{\text{VI}}\text{MO}_4]_{\infty}$ (where $\text{O} = \text{O}^{2-}$, $(\text{OH})^-$, (H_2O) , Cl^- , or F^-). This chain may be decorated with TO_4 tetrahedra and DO_3 triangles such that the complete stoichiometry of the corresponding mineral may be expressed as $\text{A}_x[\text{M}(\text{T}\text{O}_4)_x(\text{D}\text{O}_3)_y\text{O}_z]$ where A = a low-charge interstitial cation, commonly an alkali or alkaline earth, M = a cation in octahedral coordination, T = a cation in tetrahedral coordination, and D = a cation in triangular coordination. In minerals, there are three basic types of $[\text{M}^{\text{VI}}\text{MO}_4]_{\infty}$ chain: (1) straight trans chains, in which octahedra share directly opposing edges; (2) cis chains, in which octahedra share non-opposing edges, and (3) trans-cis chains, in which octahedra link through both cis and trans edges. Trans and cis chains have typical repeat lengths of ~ 6 and $\sim 5.3 \text{ \AA}$ (or a multiple thereof), respectively; mixed trans-cis chains have more diverse repeat lengths. Although a large number of topologically distinct chains is possible, only a small number occur in minerals: Nature uses a few distinct chains to construct many structure types by varying how they connect. For instance, the relatively simple geometry of the trans chain, $[\text{M}(\text{T}\text{O}_4)\text{O}_2]$, allows certain stereoisomers to link directly, forming progressively more dense structures. The $[\text{M}(\text{T}\text{O}_4)\text{O}_2]$ chain consists of (TO_4) groups linking the apical oxygens of every second pair of adjacent octahedra. In the brackebuschite-group minerals, $[\text{M}(\text{T}\text{O}_4)\text{O}_2]$ chains are isolated; in tsumcorite-group minerals, $[\text{M}(\text{T}\text{O}_4)\text{O}_2]$ chains are linked along edges to form sheets; in adelite-descloizite group minerals, $[\text{M}(\text{T}\text{O}_4)\text{O}_2]$ chains stack and cross-link to form 3-dimensional frameworks. There is a large family of chemically and structurally diverse oxysalts based on topological isomerism, geometrical isomerism and condensation of $[\text{M}^{\text{VI}}\text{MO}_4]$ chains. (SYI; Wed. Poster)

Anisotropy of magnetic susceptibility (AMS) studies in two impact structures in Parana basin basalts, Brazil

MacDonald, W.D., Dept. Geological Sciences, State University of New York, Binghamton, NY, USA 13902, wdmacdon@binghamton.edu, and Crosta, A., Depto. Geociencias, Universidade Estadual de Sao Paulo, Campinas, S.P., Brazil

Study of anisotropy of magnetic susceptibility (AMS) of two impact structures in basalts of the Parana Basin in Santa Catarina state, SE Brazil is underway. 154 oriented cores, from 17 sites in the 12 km diameter Vista Alegre impact of Parana state and from 16 sites in the 10 km diameter Vargeao impact of Santa Catarina state, were measured. The structures are thought to be late Cretaceous in age, the host formation, Serra Geral basalt, is approx. 132 Ma. old. Samples at the Vargeao structure were taken along a diametral profile of N25W trend. K_{max} axes, the maximum axes of susceptibility, are approximately horizontal and orthogonal to that profile, with considerable scatter. K_{min} axes trend nearly vertical, with a steep northward inclination bias. At the Vista Alegre structure, sampling sites are widely distributed across the structure. K_{max} axes there are also mainly subhorizontal, but more scattered in azimuth than at Vargeao. K_{min} axes are somewhat more tightly clustered than at Vargeao, and are predominantly steep with a SE inclination bias. No steep K_{max} axial directions were found at either structure. The degree of anisotropy P is low at both structures, with maxima of 1.055 at Vargeao and 1.03 at Vista Alegre; average P values are near 1.01. T values, representing the shape parameter, are quite variable at both structures and mainly oblate; about 25% of the samples have prolate signatures. At both structures there is a slight increase of anisotropy with increasing susceptibility. The observed susceptibility range of Vargeao samples is 7.0×10^{-3} to 1.7×10^{-1} SI, and for Vista



Alegre samples is 1.4×10^{-2} to 9.2×10^{-2} SI. Observed anisotropy patterns will be compared with published experimental shock anisotropy results and implications for the impact conditions will be discussed. (*SS16; Wed. 9:20*)

Fluorine-rich tourmalines from a classical topaz locality Schneckenstein, Vogtland, Germany

Macek, I., Department of Mineralogy and Petrology, National Museum, Prague, Czech Republic, ivo_macek@nm.cz

Black tourmaline (fluor-schorl~fluor-dravite > oxy-schorl~oxy-dravite > foitite/magnesio-foitite) is a minor phase at the greisen-like vein deposit of topaz Schneckenstein situated 500 m W of the contact of the Cambrian phyllites with the Permian intrusive complex of Eibenstocker granite. Tourmaline in the form of radial aggregates and elongated grains, up to 2 mm long, occurs in banded, porous, quartz-dominant rock. Its brecciated fragments form a matrix of quartz veins with common crystals of yellow topaz and accessory wolframite, cassiterite, minerals of the crandallite group, Nb-rutile, fluorite, sulphides, numerous secondary phases and late dickite. The tourmaline contains common euhedral grains ($\leq 200 \mu\text{m}$) of complexly zoned, Cr,V,Fe-enriched TiO_2 phase and rare monazite-(Ce). In the center of some tourmaline needles very rare porous cores of foitite/magnesio-foitite overgrown by fine oscillatory zones of fluor-schorl~fluor-dravite > oxy-schorl~oxy-dravite were found. Oscillatory zoning in BSE in controlled mainly by Mg/Fe ratio. Minor concentrations of $\text{Cr} \leq 0.11 \text{ apfu}$, $\text{V} \leq 0.08 \text{ apfu}$, $\text{Ca} \leq 0.07 \text{ apfu}$ and $\text{Ti} \leq 0.06 \text{ apfu}$, are typical. The oscillatory-zoned tourmaline exhibits very good negative correlations Al/R^{2+} and Al/F^{+} and positive correlation R^{2+}/F all close to 1 but no apparent relations of F to X-site occupancy (vacancy or charge). Consequently, the Y-site along with W-site and Z-site played a dominant role and the substitution $2\text{YR}^{2+} + \text{ZAl}^{3+} \text{F} = 2\text{YAl}^{3+} + \text{ZR}^{2+} \text{O}^{2-}$ controls incorporation of F into the tourmaline structure. The role of X-site is rather negligible and variations in Na are controlled by non-specified distinct mechanisms. No relations of F and Mg/Fe imply absence of Fe-F avoidance in tourmaline known in micas or humite-group minerals. The chemical system in this greisen-like deposit characterized by very high activity of F (abundant topaz) and rather low activities of Ca, Li and Na (tourmaline is the only Na-bearing mineral) is suitable for study of behavior of F in tourmalines. It exhibits that X-site is not necessarily the principal site controlling the content of F in tourmaline.

This work was supported by internal grant of the National museum, Prague 2011/05/IG-PM to IM and research project GAP210/10/0743 to MN. (*GS1; Thurs. Poster*)

Unraveling the nature and origin of the Grey Gabbro unit, host to the Podolsky Cu-Ni-PGE deposit, Sudbury, Ontario

MacInnis, L.M., lmacinnis@laurentian.ca, Kontak, D.J., Department of Earth Sciences, Laurentian University, Sudbury, ON P3E 2C6, Ames, D.E. and Rayner, N.M., Geological Survey of Canada, 750-601 Booth St, Ottawa, ON K1A 0E8

The 1850 Ma Sudbury impact produced a melt sheet and both radial and concentric offset dykes, the latter of which commonly includes a homogeneous quartz diorite marginal phase and a variably mineralized interior zone. The Podolsky Cu-Ni-PGE deposit, located within the radial Whistle-Parkin offset dyke in the North Range of the Sudbury Structure, is a hybrid-type Cu-Ni-PGE system that includes both sharp-walled and breccia-type veins and low-sulphide disseminated mineralization. A unique phase in the offset structure is a large body of gabbroic rock informally named the "grey gabbro" (GG). Understanding the nature and origin of the GG is important, as it hosts sharp-walled chalcopyrite veins unique to offset deposits, this one having produced ~20 M lbs Cu, 1 M lbs Ni, and ~23,000 oz total precious metals (TPMs). In order to address the origin of the GG, part of a broader study of the Podolsky deposit, a petrological investigation was undertaken. Remapping the GG unit integrated core logging and a photo library to define lithology, structure, and alteration indices. The typically homogeneous, medium- to coarse-grained GG displays an

ophitic texture with Cpx-Plg and has rare pegmatite clots; it exhibits pervasive alteration (saussuritization, sericite) where sulphide veins are abundant in the unit. A chilled margin ($\leq 1 \text{ m}$) observed in drill core suggests the GG is intrusive rather than a fragment of a larger body. Importantly, primary plagioclase (An_{50}) of the GG is pseudomorphed by a granoblastic-textured plagioclase of An_{20} composition. This texture is interpreted to be a feature of contact metamorphism related to the superheated melt sheet. A preliminary, concordant U-Pb zircon TIMS age of ca. 1850 Ma is interpreted as the crystallization age of the GG. This suggests that the intrusion of the GG overlapped the generation and cooling of the 1850 Ma melt sheet, thus consistent with the inferred origin of the granoblastic-textured plagioclase. Bulk-rock geochemistry for the GG indicates that it: (1) equates to an alkali basalt based on both TAS and $\text{SiO}_2\text{-Zr/TiO}_2$ plots; (2) is in part of cumulate origin; and (3) is characterized by LREE enrichment ($\text{La}_N = 250\text{-}400$), lacks any Eu anomaly, and is strongly fractionated [$(\text{La}/\text{Lu})_N = 25\text{-}40$]. The chemistry of the GG contrasts markedly with the crystallized products of the melt sheet (e.g., quartz diorite, norites), which are strongly depleted in LREE compared to the GG, and indicates derivation of the GG melt from a metasomatised mantle source region. (*SS9; Wed. Poster*)

Developing a competencies profile for the profession of geoscience

MacLachlan, K.¹, KateM@apegs.sk.ca, Bonham, O.², Broster, B.³ and Johnson, K.⁴, ¹Association of Professional Engineers and Geoscientists of Saskatchewan, Regina, SK; ²Geoscientists Canada, Burnaby, BC; ³Department of Earth Sciences, University of New Brunswick, Fredericton, NB; ⁴Consultant, Toronto, ON

In September 2012, Geoscientists Canada received funding from Human Resources and Skills Development Canada's Foreign Credentials Recognition Program for a 30 month project to carry out four interrelated initiatives in the area of admissions support for the provincial/territorial professional bodies. The central and largest initiative involves the development of a competency profile for the geoscience profession. Competencies are defined by the Canadian Information Centre for International Credentials as "a set of knowledge, skills and abilities obtained through formal or non-formal education, work experience or other means, required to perform an occupation at the point of entry to a profession". In addition to describing competencies, the profile document will include specific indicators of proficiency related to each competency that an individual is expected to demonstrate in order to become a P.Geo. Subsequent work will determine appropriate methodologies to assess competencies.

A key rationale is the move by professions both in Canada and around the world, away from credentials-based admissions assessments towards a system that is based on a combination of academic outcomes and practice attributes. Other reasons and project objectives include, to:

- give prospective applicants for registration an indication of their likelihood of becoming a P.Geo;
- allow assessors to recommend remediation options to applicants, when appropriate;
- provide clarity for applicants, employers, assessors, validators, referees, Fairness Commissioners and the public;
- ensure a transparent, rigorous and objective process, this is defensible;
- establish common requirements leading to consistency in assessments and admission decisions, and to;
- facilitate development of a comprehensive body of knowledge, which appropriately describes the profession.

The resulting profile must address academic competencies derived from each of Canada's three principle Earth educational foundations – geology, environmental geoscience and geophysics – as well as attributes necessary to undertake geoscientific work, independent of direct supervision. Development of the profile will follow an iterative process that includes input from Subject Matter Experts (practising geoscientists – representing a diverse sampling of the profession across the country), extensive consultation and validation procedures. The



Canadian Geosciences Standard Board (CGSB) is playing a key role. CGSB, Geoscientists Canada's principle advisory panel, is made up, almost exclusively, of members of faculty from Earth Science departments, from across Canada. In addition to describing this important new national initiative, this contribution will provide an opportunity for those geoscientists considering serving as Subject Matter Experts to learn how they may be able to assist. (*SS21; Fri. 10:40*)

Mineralogical studies of a low-temperature hydrothermal barium-rich skarn deposit, Gunn Claim, Yukon Territory

MacNeil, L.A.¹, 8lam5@queensu.ca, Peterson, R.C.¹, Färber, G.², Groat, L.³ and Witzke, T.⁴, ¹Department of Geological Sciences, Queen's University, Kingston, ON K7L 3N6; ²Gunnar Färber Minerals, Bornsche Str. 9, 39326 Samswegen, Germany; ³Department of Earth, Ocean and Atmospheric Sciences, University of British Columbia, Vancouver, BC V6T 1Z4; ⁴PANalytical Laboratory, Lelyweg 1, 7602 Almelo EA, Netherlands

A barium-rich skarn deposit associated with a quartz monzonite porphyry located on what is known as the Gunn Claim, Yukon Territory (130°0'51"W, 62°50'50"N) was investigated in order to understand the complexity of a suite of barium silicates, barium carbonates, barium sulfates and barium phosphates. The deposit was first described by J.H. Montgomery in 1960 who observed many different barium-containing minerals such as sanbornite, gillespite, pellyite, taramellite, witherite, and barite. The mineralogical associations and textures of this deposit have been studied using newly collected material with a variety of instrumental techniques including X-ray diffraction, scanning electron microscopy, and an electron microprobe. Several unknown minerals have been identified and are currently being investigated. Additional minerals not described by Montgomery (1960) from this deposit have been found in low-temperature, late-stage veins and include alforsite, cerchiarite (Fe) and cerchiarite (Al). These low-temperature veins exhibit cryptocrystalline quartz coating a mixture of barium silicates, barium carbonates, and barium sulfates that exhibit alteration textures indicative of disequilibrium. The Gunn Claim deposit is similar to the barium silicate deposits located in Fresno and Mariposa Counties, California, which are also barium-rich skarn deposits. The mineralogical associations and geological settings of these deposits will be compared and contrasted. (*GSI; Fri. 2:40*)

Lithium isotopes in giant pegmatite bodies – implications for their sources and evolution

Magna, T.¹, tomas.magna@geology.cz, Novák, M.², and Janoušek, V.¹, ¹Czech Geological Survey, Klárov 3, CZ-11821 Prague, Czech Republic; ²Department of Geological Sciences, Masaryk University, Kotlářská 2, CZ-61137 Brno, Czech Republic

New Li isotope data are presented for important temporally distinguished economic pegmatite deposits of Li (Ta, ...). Major Li-bearing phases (spodumene, amblygonite, lepidolite, petalite) as well as other Li-rich minerals (beryl, muscovite, schorl, elbaite) were analyzed in order to deconvolve source Li signature and constrain crystallization histories of the respective localities. The data shows significant spread in $\delta^7\text{Li}$ (–0.5 to +32‰) that by far exceeds Li isotope variations intrinsic to continental crustal lithologies. Considering muscovite, schorl and beryl formed in early stages of pegmatite solidification, these phases always cover the whole span of $\delta^7\text{Li}$ values for each locality indicative of high mobility of Li in pegmatitic liquids and isotope fractionation that cannot be related to crystallization sequence. This is further stressed by subsequent evolution of $\delta^7\text{Li}$ in the residual liquid that does not follow uni-directional trend from low to high $\delta^7\text{Li}$ (or vice versa) during progressive crystallization of pegmatite (petalite ~ amblygonite → spodumene → elbaite ~ lepidolite). Instead, $\delta^7\text{Li}$ values tightly correlate with mean Li–O bond length for individual suites indicating that Li–O bonding is the determining factor in Li

isotope fractionation process irrespective of the absolute magnitude of $\delta^7\text{Li}$ variations. This observation must thus reflect crystallographic preference for ^6Li or ^7Li within the crystal lattice of individual phases and is further supported by preferential incorporation of ^7Li into crystallographic sites with lower coordination number, i.e., energetically favored configuration (beryl and petalite are the heaviest phases). Interestingly, the slope of the anti-correlation in $\delta^7\text{Li}$ vs. Li–O length space is identical within error for individual localities and is clearly reminiscent of global rule of such isotope fractionations. The variations among individual deposits are not related to their corresponding magmatic ages although some older pegmatite bodies [Tanco (2.7 Gyr); Black Hills (1.8 Gyr)] show overall high $\delta^7\text{Li}$ values in individual mineral phases compared to Bikita (2.7 Gyr) and Nová Ves (0.3 Gyr). Although the source must be identified in the continental crust, its exact nature remains unclear. It could, however, hinge on Li isotope signature of muscovite, one of major mineral phases in the continental crust. Cumulatively, the results indicate (i) different sources, perhaps formed at distinctive p–T conditions and likely reflecting different activities of fluids/melts, and (ii) unique Li isotope signatures in mineral phases that could potentially be used to fingerprint the origin of gem-quality stones. (*SY2; Thurs. 10:40*)

Keynote (40 min): Petrogenesis of the Bushveld Complex and its PGE-Cr-V deposits

Maier, W.D., Dept. of Geosciences, University of Oulu, Finland, Barnes, S.-J., Sciences de la Terre, Université du Québec à Chicoutimi, Canada, and Groves, D.I., Centre for Exploration Targeting, University of Western Australia, Perth

Large layered intrusions are emplaced in stable cratonic or intracratonic settings, under locally extensional, but far-field compressive regimes that allow the formation of thick composite sills. The parental magmas to many of the PGE-bearing intrusions are siliceous magnesian basalts (Bushveld, Great Dyke, Stillwater, Penikat) derived from both asthenospheric and lithospheric mantle sources, and variably modified by contamination with crust during magma ascent. The existence of mineralised intrusions of tholeiitic lineage (e.g., Skaergaard) highlights that specific mantle sources or contamination are non-essential for PGE reef formation. The layering, including in the PGE reefs and oxide seams, is proposed to have formed when the large, incompletely solidified, magma chambers subsided due to crustal loading, resulting in slumping of semi-consolidated cumulate slurries and hydrodynamic sorting of the slurries to form dense layers enriched in sulfides, oxides, olivine and pyroxene, and less-dense layers enriched in plagioclase. The most economic PGE, Cr and V reefs formed in large, multiply replenished intrusions because these cool relatively slowly and subside prior to termination of magmatism and complete cumulate solidification. In smaller intrusions, cooling rates are faster, subsidence is less pronounced and, where it occurs, the cumulates may already have largely solidified, resulting in insignificant mush mobility and mineral sorting. Layering is thus less pronounced and less regular and continuous and the grades of the reefs are lower. (*SS8; Thurs. 10:20*)

PGE mineralization in the Highbank Lake layered intrusion, northern Ontario, Canada

Maier, W.D., Dept. of Geosciences, University of Oulu, Oulu, Finland, wolfgang.maier@oulu.fi, and Vaillancourt, C., Northern Shield Resources, Canada

The ca. 600 km², 2.8 Ga Highbank Lake layered intrusion is located on the Superior craton, 350 km N of Hearst, near the boundary between the Oxford-Stull Terrane to the north and the North Caribou Terrane to the south. Outcrop is mainly confined to gabbro-norite and anorthosite exposed on islands within the Atawapiskat river. The bulk of the intrusion is covered by glacial deposits, but its approximate outlines are delineated by airborne magnetic data. In order to locate possible PGE reefs Northern Shield drilled 13 DC boreholes in 2006, up to 375 m in depth, into the eastern portion of the intrusion. The boreholes intersected weakly PGE mineralised (up to 100 ppb Pt+Pd) layered gabbro-norites, (mottled) anorthosites, minor pyroxenites, magnetite



gabronorites, and magnetites. Due to alteration and deformation, layer contacts are usually diffuse, and no good indicators of stratigraphic orientation were found. Geochemistry was used to constrain the stratigraphic orientation, the approximate stratigraphic level of the exposed portion of the intrusion compared to other PGE reefs in layered intrusions, and thus the postulated depth below surface of any undiscovered reef horizons. Comparison to the Bushveld Complex indicates that the exposed portions of Highbank Lake represent the equivalent of the upper Critical to upper Main Zone and the lower to central Upper Zone of the Bushveld Complex. The magnetite-bearing rocks in the upper portions of the Highbank Lake intrusion are highly PGE depleted, implying that PGE have been extracted from the magma by sulfides segregating in the unexposed lower portion of intrusion. Based on the results and interpretations of the initial drilling programme, a continuation drill programme was conducted in 2007. It intersected sulfides (up to ca 1-3%) and PGE (up to ca 500 ppb) in dm-wide melanocratic layers, reminiscent of PGE reef-style mineralization in other layered intrusions. Further drilling targets have been delineated and are presently prepared for drilling. (SS3; Thurs. 2:40)

Developing indicator mineral methods; Application of iron oxides in discovery of VMS deposits

Makvandi, S.¹, sheida.makvandi.1@ulaval.ca, Beaudoin, G.¹, Ghasemzadeh-Barvarz, M.¹ and McClenaghan, B.², ¹Université Laval, Département de géologie et de génie géologique, 1065, avenue de la Médecine, Québec, QC G1V 0A6; ²Geological Survey of Canada, 601 Booth St., Ottawa, ON K1A 0E8

Magnetite is a useful indicator mineral for provenance discrimination studies because it can incorporate a large number of minor or trace cations in its crystalline structure, and it is resistant to both chemical and physical weathering. Magnetite is known to be present at the base of a massive sulphide (MS) lens and the top of the alteration pipes where it replaces sulfide minerals such as pyrite, pyrrhotite, and/or chalcopyrite. Magnetite from two VMS deposits, the Izok Lake Zn-Cu-Pb-Ag (Nunavut) and Halfmile Lake Zn-Pb-Cu (Bathurst Camp) have been examined. The MS mineralization, related alteration zones, host rocks, and till, both up- and down-ice flow, were sampled in each area. Major, minor and trace element concentrations in magnetite were determined by Electron Probe Micro-Analysis (EPMA) and Laser Ablation-Inductively Coupled Plasma-Mass Spectrometry (LA-ICP-MS). The results show high concentrations of P, Ge, W, Sn, Mn, Mg, Cu, Co and Zn in the Izok Lake MS Magnetite (ILMSM) and elevated contents of P, Pb, Sn, Ge, Ga, Mn, Mo, Ti and Zn in the Halfmile Lake MS Magnetite (HLMSM). Multivariate Principal Component Analysis (PCA) was used to discriminate different lithologies based on the chemistry of magnetite. The results show that the ILMSM and the HLMSM form different clusters because of their different contents of Mg, Cu, Al and Ti. These variations in composition relate to different geological settings and grades of metamorphism that have affected these deposits. In the Izok Lake area, the statistical results demonstrate that detrital magnetite grains are mainly clustered with the ILMSM or magnetite from the gahnite-rich dacite because of their Mg, Cu and Mn contents. The gahnite-rich zone is located at the margins of, or within the sulphide stringer zone. Magnetite from host rock dacite has high Ge, Sn, Ga, Mn, Zn and Ni contents. In the Halfmile Lake area, the chemical signature of the HLMSM is found in detrital magnetite more than 2 km far away from the ore zone, though, a high proportion of magnetite grains show signatures similar to those derived from local andesitic rocks. In conclusion, applying magnetite chemistry to trace VMS deposits is a reliable exploration technique because 1) magnetite carries the chemical signature of its host lithology, 2) magnetite persists for a long distance of glacial transport, and 3) it is relatively abundant in till samples. These characteristics provide the ability to track a VMS deposit eroded by glaciers for a distance of several kilometers. (SS12; Thurs. 8:40)

Entry into the end-Cryogenian glaciation of South Australia

Maloof, A.C., Department of Geosciences, Princeton University, Princeton, NJ 08544 USA, and Rose, C.V., Department of Earth and Planetary Sciences, Washington University, St. Louis, MO 63130 USA

The Cryogenian Period is defined by at least two glaciations, 'Sturtian' (~716 million years ago) and 'Marinoan' (~635 million years ago), where ice may have extended to low-latitudes near the equator. We present a combination of field observations and chemostratigraphy that record the arrival of the younger Marinoan ice-sheet near the paleo-equator in South Australia.

Carbonates preceding the Marinoan glacial succession record an ~18 per mil negative shift in the $\delta^{13}\text{C}$ of carbonate around the world. This 'Trezona' isotopic anomaly is the largest $\delta^{13}\text{C}$ shift in Earth history and its origin and timing with respect to the glaciation remain controversial. The $\delta^{13}\text{C}$ anomaly could record a dramatic reorganization of Earth's carbon cycle and be linked causally to the initiation of Marinoan ice-house conditions. Alternatively, the $\delta^{13}\text{C}$ anomaly might record secondary fluid alteration following carbonate deposition. Here we document dropstones within the carbonate platform sediments immediately below the Marinoan glacial diamictite in South Australia. The partly contemporaneous Yaltipena Fm records the pro-glacial influx of sediment from encroaching land-based ice sheets. These advancing ice sheets caused soft-sediment deformation of beds below the glacial diamictite, as well as up to 130 m of subglacial erosion into the carbonates containing the recovery from the Trezona negative $\delta^{13}\text{C}$ anomaly. Together, these paired sedimentological observations and chemostratigraphic data show that the Trezona isotope anomaly was recorded prior to the local glacier advance and late-stage burial diagenesis, and that $\delta^{13}\text{C}$ recovery toward 0 per mil was synchronous with the appearance of icebergs in the tropics. (SY4; Fri. 10:40)

Developing pegmatitic textures in a Li-rich granitic system - an experimental perspective

Maneta, V. and Baker, D.R., McGill University, Earth and Planetary Sciences, 3450 University St., Montreal, QC H3A 2A7, viktoria.maneta@mail.mcgill.ca, don.baker@mcgill.ca

The effect of Li on the development of pegmatitic textures was evaluated experimentally in H₂O-saturated and H₂O-undersaturated conditions at 500 MPa pressure and temperatures ranging from 400°C to 800°C. The addition of ~3700 ppm Li in a starting material of common granitic composition that originally contains no other fluxing agents (Lake County obsidian) substantially enhances crystallization from originally 2% in "Li-free" up to 80% in "Li-rich" samples and promotes the formation of pegmatitic textures between quartz and feldspar. The addition of Li lowers the position of the liquidus and the solidus in the granitic system by 200-300 °C, leading to 40-60 °C undercooling for the development of quartz-feldspar graphic and granophyric intergrowths. The feldspar crystals developed in the "Li-rich" samples incorporate 150-250 ppm Li and assume skeletal and spherulitic morphologies. Growth rates measured for feldspar crystals in the "Li-rich" samples exhibit one order of magnitude faster growth rates (maximum of 10^{-8.2} m/s) than feldspars formed in the "Li-free" samples (maximum of 10^{-9.2} m/s). The results of this study attest to the effectiveness of Li as a fluxing agent and highlight the crucial role it plays in the development of pegmatitic textures, leading to important implications for the conditions of formation of Li-bearing granitic pegmatites. (SY2; Thurs. 9:00)

Isotopic signatures of the Ordovician radiation

Mángano, M.G.¹, gabriela.mangano@usask.ca, Buatois, L.A.¹, Wilson, M.A.² and Droser, M.L.³, ¹University of Saskatchewan, 114 Science Place, Saskatoon, SK S7N 5E2; ²The College of Wooster, Wooster, Ohio 44691, USA; ³University of California, Riverside, CA 92521, USA



The Ordovician radiation was undoubtedly one of the most significant evolutionary events in the history of the marine biosphere. A continuous increase in ichnodiversity occurs through the Ordovician in both shallow- and deep-marine environments. In the case of shallow-marine settings, the number of ichnogenera doubled from the Tremadocian to the Hirnantian. The ichnodiversity increase in the deep sea seems to be less pronounced. The earlier view that early Paleozoic deep-marine ichnofaunas are of low alpha diversity has been challenged by discoveries of moderately diverse associations. Interestingly, however, the increase in global ichnodiversity through the Ordovician is not paralleled by an increase in ichnodiversity of bioturbation structures. In fact, while global ichnodiversity in the Ordovician doubled Cambrian levels, Ordovician ichnodiversity of bioturbation structures is roughly similar to that resulting from the Cambrian explosion. Macroboring organisms also display significant evolutionary innovation and diversification in shallow-water hardgrounds and other carbonate substrates, resulting in the Ordovician Bioerosion Revolution. Along with this macroboring ichnodiversity and ichnodiversity increase is a significant rise in the rate of bioerosion in carbonate substrates. Ichnofaunal changes in lower-shelf and offshore siliciclastic deposits through the Ordovician reveal faunal turnovers resulting from the evolutionary radiation. Lower Ordovician deposits tend to be dominated by abundant trilobite-produced trace fossils. Middle to Upper Ordovician shallow-marine ichnofaunas tend to show more varied behavioral patterns and trilobite trace fossils are rarely the dominant components. During the early Paleozoic, the tiering structure of ichnofaunas become more complex, as a result of both the addition of deeper tiers and of a wider variety of biogenic structures in previously occupied tiers. Infaunalization by deposit feeders in offshore siliciclastic environments was most likely diachronic, with the establishment of a mid-tier infauna first in Laurentia and Baltica, and only subsequently in Gondwana. (SY3; Thurs. 2:00)

Ultramafic intrusions in orogenic terrains: Late Cretaceous Ni-Cu-(PGE) mineralization at the Giant Mascot sulfide deposit, Hope, B.C.

Manor, M.J.¹, mmanor@eos.ubc.ca, Scoates, J.S.¹, Nixon, G.T.² and Ames, D.E.³, ¹Pacific Centre for Isotopic and Geochemical Research, 2020 - 2207 Main Mall, University of British Columbia, Vancouver, BC V6T 1Z4; ²BC Geological Survey, Ministry of Energy & Mines, PO Box 9333 Stn Prov Govt, Victoria, BC V8W 9N3; ³Geological Survey of Canada, Central Canada Division, 750-601 Booth St., Ottawa, ON K1A 0E8

The Giant Mascot Ni-Cu-(PGE) deposit remains British Columbia's only past-producing nickel mine (1958-1974), having produced ~4.2 Mt of ore with 0.77% Ni, 0.34% Cu, minor Co, Ag, and Au, and unreported platinum group elements (PGE). The intrusive ultramafic suite host to Ni-Cu sulfide mineralization is ovoid (~2.5 km in diameter) and comprises mainly cumulates of olivine-orthopyroxene (±hornblende±clinopyroxene) emplaced within a supra-subduction zone environment. Orogenic Ni+Cu±PGE sulfide deposits have been increasingly recognized as important economic resources (e.g., Aguablanca, Spain; Americano do Brasil, Brazil; Portneuf-Mauricie Domain, Québec), however, the origin of the ores, modes of emplacement, and their relationship to regional tectonic activity remains poorly known. Preliminary high-precision CA-ID-TIMS U-Pb and ⁴⁰Ar/³⁹Ar geochronology results for a pyroxenite and feldspathic hornblende from Giant Mascot are 93.04 ± 0.06 Ma (U-Pb zircon; n=5) and 93.0 ± 1.3 Ma (⁴⁰Ar/³⁹Ar plateau, hornblende), respectively. These dates establish an early Late Cretaceous age for the Giant Mascot intrusive suite and indicate that emplacement was apparently followed by relatively rapid uplift and cooling. The Ni-Cu sulfide ores at Giant Mascot were extracted from 28 north-plunging, sub-vertical pipes and north-dipping, tabular sheets at structural footwall contacts. The ores (pyrrhotite+pentlandite+chalcopyrite) display four distinct textures: 1) disseminated irregular and rounded coarse blebs (<1.5 cm); 2) net-textured; 3) semi-massive; and 4) fracture-filled. The relative modal

abundances of pentlandite are highest in net-textured and lowest in disseminated ores, but overall there appears to be no correlation between ore textures and mineralogical composition of the host rock. Sulfur isotope analyses (n=22) show a limited range of δ³⁴S values from -3.7 to 0.1‰, typical of mantle-derived magmas. Chalcophile elements and PGE variations reveal two distinct groups in sulfide ore samples (n=45): 1) net-textured to semi-massive Ni-rich (Ni/Cu = 8.4) ores that contain average Ni, Cu, Pd, and Pt abundances of 3.7 wt%, 2.0 wt%, 983 ppb, and 637 ppb, respectively; and 2) variably-textured ores (Ni/Cu = 5) characterized by significantly lower average Ni, Cu, Pd, and Pt values of 1.3 wt%, 0.46 wt%, 57 ppb, and 7.6 ppb, respectively. Geochemical trends in Giant Mascot Ni-rich ores share similar characteristics to those from other orogenic Ni deposits, most notably Aguablanca in Spain, indicating possible similar mechanisms of formation and concentration of magmatic sulfides related to arc-derived parental magmas. (SS9; Wed. 3:20)

Fluid-precipitated jadeitites and jadeite-lawsonite-quartz rocks from the Dominican Republic: Novel records of aqueous fluids in an intra-oceanic subduction zone

Maresch, W.V., Schertl, H-P. and Hertwig, A., Institute of Geology, Mineralogy und Geophysics, Ruhr-University Bochum, 44780 Bochum, Germany, walter.maresch@rub.de

The Rio San Juan Complex (RSJC) of the northern Dominican Republic contains serpentinite mélanges that host different types of metamorphic blocks such as jadeite±lawsonite blueschist, garnet±omphacite blueschist, eclogite, marble, granitic orthogneiss. The mélanges originated within the subduction channel of an intra-oceanic arc system that spanned the Caribbean and was active from at least 120 Ma to ca. 55 Ma. Jadeite-rich rocks occur as blocks in lag deposits covering the mélanges and as boulders in river beds. In contrast to most other occurrences in the world, they also form concordant layers and discordant veins in blocks of blueschist. Two suites of jadeite-rich rocks are found: the first (JLQ-suite) comprises quartz-bearing jadeite s. str. (i.e., >90 vol% jadeite), jadeite quartzite, jadeite-lawsonite quartzite and transitional rock types. Examples occur as discrete blocks/boulders and as layers/veins in blueschist. The second suite (J-suite) consists of quartz-free and albite-bearing jadeite s. str., exclusively found as discrete blocks/boulders and so far never in direct contact with a country rock. Additional minerals can be omphacite, phengite, glaucophane, albite, calcite, epidote as well as rare garnet and paragonite. Titanite, apatite, rutile and zircon are important accessories. Presently available age data (U-Pb on zircon) for a J-suite example indicate crystallization early in subduction-zone history at ~115 Ma and P-T conditions >500°C and >11 kbar. Layers/veins of the JLQ-suite hosted in dated blueschist must have crystallized at 80-62 Ma and P-T conditions 350-500°C, >15 kbar. The formation of jadeite-rich rocks was thus possible over a time span of at least 50 Myr in a thermally evolving and maturing subduction zone. Most jadeite-rich rocks exhibit features (e.g., oscillatory zoning in jadeite, apatite, calcite, zircon, etc.) typical of open-system crystallization conditions, in keeping with current ideas that they formed from fluid-rock interactions within the subduction-channel environment. Many are homogeneous and massive; in others crystals grew outward from systems of hairline fractures, suggesting crack-seal processes in zones of weakness, and leading to heterogeneous examples. In order to use such rocks as monitors of mass-transfer processes in subduction zones, a number of intriguing questions remain to be answered. Accepting present thought that temperatures of at least 600°C are necessary to achieve necessary solute concentrations in aqueous solutions, we must first of all clarify where these fluids can form in a subduction zone, and how, as evidenced in the RSJC, they can intrude at T below 400°C in the necessary supersaturated condition. (SY1; Wed. 10:20)



Hydrothermal mineralization at the Prince Albert impact structure, Victoria Island, Canada

Marion, C.L., cmarion3@uwo.ca, Osinski, G.R., gosinski@uwo.ca, and Linnen, R.L., rlinnen@uwo.ca, Western University, Dept. of Earth Sciences, London, ON N6A 5B7

Evidence for meteorite impact-generated hydrothermal alteration has been identified at over 70 impact structures worldwide. The goal of this study is to characterize the hydrothermal alteration products observed at the newly-discovered 28-km Prince Albert impact structure, NWT, Canada. Mineralization occurs primarily in the form of vugs and veins in the preserved shocked and uplifted target rocks. Carbonate vugs are abundant along displacement planes of thrust-faulted blocks in the central uplift, particularly as long (>1 m) narrow (< 25 cm) vugs. A network of quartz-carbonate-sulfide veins occurs in the southern periphery of the central uplift as well as marcasite vugs. The veins cross-cut a fine-grained dolostone host rock at an angle to bedding, as well as shatter cones, providing excellent timing constraints. Vein mineralogy, as confirmed by Raman spectroscopy and scanning electron microscopy – energy dispersive X-ray spectrometry (SEM-EDX), consists of dolomite, quartz and marcasite with accessory amounts of sphalerite, pyrite and an iron oxide or hydroxide. Framboidal pyrite occurs in quartz. Preliminary fluid inclusion petrography has identified primary and secondary fluid inclusion assemblages (FIA) in the quartz. Primary inclusions are aqueous liquid-vapour with <10% vapour and liquid-only inclusions. Secondary FIAs consist of vapour-only, liquid-only and liquid-vapour inclusions. To date, freezing and ice melting of single-phase inclusions have not been observed and on cooling these inclusions do not nucleate vapour bubbles. To date only two homogenization temperatures (Th) have been observed. The first homogenizes at 83.6 ± 0.3 , but freezing and melting were not observed. The second inclusion had a Th of $95^\circ\text{C} \pm 10$, a freezing temperature of $-34.1^\circ\text{C} \pm 0.2$, and final melting temperature (Tm) of $-4.1^\circ\text{C} \pm 0.1$. These values are representative of aqueous inclusions containing primarily H_2O and NaCl. The salinity of the above mentioned inclusion is $6.5 \text{ wt}\% \text{ NaCl} \pm 0.2$. The moderate salinity indicates that the circulating fluids were not pure meteoric waters. Further analyses are planned. (SS16; Wed. 10:20)

The fall and rise of calcium in a granitic pegmatite, and the explanation of mixed NYF–LCT assemblages at Anjanabonoina, Madagascar

Martin, R.F., Earth & Planetary Sciences, McGill University, Montréal, QC H3A 2A7, robert.martin@mcgill.ca, and De Vito, C., La Sapienza, Università di Roma 1, I-00185 Roma, Italia

A batch of pegmatite-forming magma can be expected to start to crystallize quickly at the wall zone. There, fluorapatite likely attains supersaturation in the melt; the prisms adopt an acicular habit, oriented more or less perpendicular to the contact. Oligoclase or andesine also appears early. In the border zone, graphic intergrowths of sodic plagioclase + quartz and K-feldspar + quartz both are possible. The sodic plagioclase shows a progressive enrichment in Na toward the interior. The feldspars reveal a steady buildup in incompatible elements like Rb and Cs, and a comparably steady drop in Ca. In an LCT pegmatite, fluorapatite becomes progressively scarcer inward. The intermediate zone contains a feldspar assemblage virtually free of Ca, but yet enriched in phosphorus. Apatite is even lacking in any nodules of triphylite that may form as the core zone is approached. An A-type granitic magma follows the same pattern, except that initial levels of phosphorus are inconsequential. Magmas of both LCT and NYF affiliations are likely to contain fluorine; this allows the melt to accommodate a small amount of Ca in its structure. The trend toward ever smaller amounts of Ca in the melt follows what is well documented in phase-equilibrium studies in the quinary system Qtz–Ab–Or–An– H_2O . But after a steady drop, calcium starts to build up at the end of the pegmatite's evolution. This reversal in the trend is best seen in miarolitic pegmatites. In the well-studied Anjanabonoina NYF granitic pegmatite, which is initially mildly alkaline, the pocket environment becomes more aluminous, distinctly subalkaline, and

calcium-bearing. Boron also is introduced, and strikingly zoned tourmaline prisms become an important constituent of the pockets. The assemblage indicates a mixed NYF–LCT signature. These important changes are attributed to plagioclase in the wallrocks. Any plagioclase is kinetically stranded in a partly disordered, partly unexsolved state. The phase diagram for the system Ab–An predicts that below 400°C , any plagioclase between An₂ and An₉₆ is unstable. In comes a dilute solution of hydrofluoric acid that leaks out from the cooling pegmatite. It immediately dissolves the plagioclase, deposits pure albite and K-bearing phases in the exocontact area, picks up Ca, Al, B, as well as some Fe and Mg, and makes its way back into the solidified but still hot pegmatite. There it dissolves K-feldspar and precipitates Ab + Ms ± gem-quality topaz and tourmaline (liddicoatitic and fluordravitic) in the cavities that it has created, giving rise to a baffling NYF–LCT signal. (SY1; Wed. 3:40)

Phanerozoic diagenesis and associated economic potential of Proterozoic and Paleozoic dolostones on Victoria Island (NWT and NU)

Mathieu, J., jy_mathieu@laurentian.ca, Kontak, D.J. and Turner, E.C., Laurentian University, Ramsey Lake Road, Sudbury, ON P3E 2C6

Despite the presence of known economic resources in Canada's Arctic archipelago, Victoria Island remains relatively unexplored and understudied. This study addresses the economic potential of two major carbonate units on Victoria Island using fluid inclusion microthermometry coupled with SEM-EDS analysis of evaporate mounds. Three cements (saddle dolomite, brown dolomite, and calcite) are hosted in the Neoproterozoic Wynniatt Formation and contain abundant fluid inclusion assemblages (FIA). The dolomite cements have similar average homogenisation temperatures (Th) of 105°C . Calcite-hosted FIAs are too small to obtain Th values, but have salinities that range from 1.7 to 0.4 wt. % NaCl equiv. Mixing of two end-member fluids, one Na-rich and the other K-rich, in changing proportions through time, resulted in a systematic change in evaporate mound composition: a K-rich fluid (saddle dolomite), a K+Na fluid (brown dolomite), and a Na-rich fluid (calcite). Map-unit 10b, a lower Paleozoic dolostone, hosts two cements: quartz and calcite. The FIAs in quartz have an average Th of 125°C , and salinity of 23.2 wt. % NaCl equiv., whereas the FIAs in calcite have Th values that range from 109° to 124°C ; metastability precluded obtaining salinity data. Evaporate mounds from map-unit 10b cements indicate fluid evolution from a Na-rich fluid to a Na+K fluid through interaction with reservoir rocks. Fluorescence data from secondary petroleum inclusions hosted in the quartz cement limit the total burial depth of these strata to <5–6 km thickness of overlying strata now lost to erosion. Both a reduced fluid and a metal-saturated fluid were present during quartz precipitation, as inferred from the presence of pyrite framboids along growth zones and nanoparticles of barite and sulphides (Zn, Cu, and Pb) in evacuated inclusions, suggests that this area may have potential to host base-metal mineralisation. An important part of this study was the integration of evaporate mound SEM-EDS analysis with standard thermometric data. Distinguishing the different fluid compositions documented here would not have been possible without evaporate mound analysis; the results emphasise the utility of integrating this technique into diagenetic studies. (SS1; Thurs. Poster)

Coupling garnet growth modeling and *in situ* LA-ICP-MS monazite geochronology: Unraveling the Grenvillian orogeny in the Mazinaw Domain of southeastern Ontario

McCarron, T., travismccarron@email.carleton.ca, and Gaidies, F., fgaidies@earthsci.carleton.ca, Carleton University, 1125 Colonel By Drive, Ottawa, ON K1S 5B6

The Flinton Group, a SW-NE trending succession of metasediments deposited after 1157 ± 10 Ma, was deformed and metamorphosed during the Grenvillian orogeny. Previous studies have provided estimates for peak metamorphic conditions along the Flinton Group, indicating that metamorphic grade increases from the southwest to the northeast from



greenschist to upper amphibolite facies, respectively. However, detailed information on the pressure-temperature evolution and the rates of metamorphic processes experienced by the Flinton Group are not known.

In this study, high-resolution X-ray micro-computed tomography was used to determine the crystal size distribution of garnet in mica schists of the Flinton Group. Electron microprobe traverses performed on the centrally cut garnet porphyroblasts that range in diameter between 4000 and 200 μm reveal a prograde growth zoning and minor diffusional zoning developed in the outermost $\sim 40 \mu\text{m}$ of the garnet rims. Garnet isopleth thermobarometry applied to the core of the largest garnet porphyroblasts indicates conditions of ca. 500°C/3800 bar for initial garnet crystallization. This corresponds to a geothermal gradient of ca. 40°C/km. Results from garnet-growth modeling with the THERIA_G software suggest that the largest garnet porphyroblasts grew along a clockwise P-T path over the pressure-temperature range of ca. 3800 to 5800 bar and 500 to 600°C. Modeling of diffusional relaxation of growth zoning developed in smaller garnet crystals indicates an average rate of metamorphism of approximately 5–7°C/Ma.

In situ LA-ICP-MS geochronology, applied to monazite grains ranging in diameter from 15–35 μm , reveal a single monazite age population at 974 \pm 5 Ma. In order to guide the 6- μm ablation pits produced by LA-ICP-MS, electron microprobe X-ray maps of ca. 60 monazite grains were prepared. Monazite grains occur as individual grains in the rock matrix and as inclusions in the garnet rims. The spatial distribution of yttrium in garnet and the textural relationships between allanite, monazite and garnet suggest allanite as a precursor to monazite, and monazite growth late in garnet's crystallization history at conditions of ca. 600°C/5800 bar. (GS2; Wed. 1:40)

Palynological proxies of anthropogenic impact in North American lakes

McCarthy, F.M.G.¹, fmcCarthy@brocku.ca, Krueger, A.M.¹, Danesh, D.², Volik, O.¹, Drljepan, M.¹, Roy, H.¹ and Hubeny, J.B.³, ¹Brock University, St. Catharines, ON L2S 3A1; ²Queens's University, Kingston, ON; ³Salem State College, Salem, MA, USA

Palynomorphs include a wide variety of acid-resistant microfossils in addition to the pollen that is usually studied from freshwater environments. These non-pollen palynomorphs (NPP) make up the bulk of the palynodebris in samples from processed from lake sediments, and they provide insights into the entire lacustrine ecosystem. Recent studies of small lakes from eastern North America illustrate the impact of human settlement on all trophic levels within the lakes. The fossilizable cysts of algae, particularly dinoflagellates (Peridinium, Parvodinium), zygnetaceans (desmids) and chlorophytes (e.g. Pediatrum) record a rapid increase in primary productivity response to the increased flux of nutrients accompanying human settlement. The acid-resistant remains of protozoans (e.g. ciliates and testate amoebae) and animals (e.g. rotifers) record the response of grazers to the increased availability of algae, and changes in vegetation can be interpreted from the pollen record. The palynological assemblages also reflect fluxed of heavy metals and other contaminants associated with economic and recreational activities in the watersheds. Pollen analysts and paleolimnologists are urged to pay more attention to these generally ignored microfossils. (GS6; Wed. 9:40)

Rare earth elements in volcanogenic massive sulfides: Evidence for their origin from hydrothermal gangue minerals

McClenaghan, S.H., New Brunswick Department of Energy and Mines, Geological Surveys Branch, Bathurst, NB E2A 3Z1, Sean.McClenaghan@gnb.ca

Rare earth element (REE) mobility in hydrothermal systems has been the focus of numerous studies, with the most direct evidence coming from active hydrothermal vents, displaying prominent enrichments in Eu and LREE. Exhalative sedimentary rocks generally contain small quantities of REE when compared to volcanic and clastic sedimentary lithotypes; e.g., massive sulfides of the Bathurst Mining Camp have

ΣREE contents that average 36.8 ppm, and range from 0.93 to 249 ppm. Nevertheless, REE in massive sulfides of these exhalative horizons can exhibit considerable fractionation, with chondrite-normalized REE profiles displaying prominent Eu anomalies. Values of Eu_N/Eu^* calculated for massive sulfides are consistently positive with values as high as 36.7 (ave., 6.26). A positive Eu_N/Eu^* correlation ($n=286$) with Sn ($r^2=0.55$) and In ($r^2=0.40$) suggests enrichment in primary hydrothermal fluids associated with base-metal sulfide precipitation.

Petrography and micro-analytical data for massive sulfides have shown that exhalative gangue and accessory minerals, in particular phosphates control REE contents; this is supported by a strong correlation (bulk) between ΣREE and P_2O_5 ($r^2=0.53$). Fluorapatite is the most abundant phosphate in exhalites of the BMC, occurring as nodular to colloform masses and intimate mixtures with carbonate and sulfide minerals. Imaging of fluorapatite reveals a distinct cathodoluminescence consistent with the substitution of Mn^{2+} and Eu^{2+} in the fluorapatite mineral structure and suggests formation under reducing hydrothermal conditions.

In situ laser-ablation ICP-MS analyses ($n=169$) reveal elevated ΣREE contents in fluorapatite, averaging 1,548 ppm, and ranging from 250 to 24,038 ppm. Europium accounts for approximately 1/4 of all REE substitution in apatite, with Eu contents as high as 1,554 ppm (ave., 295 ppm). Chondrite-normalized REE profiles display prominent enrichment in Eu, with Eu_N/Eu^* values as high as 222 (ave., 19.0). To date, these anomalies represent the largest reported fractionation of Eu in the solar system, exceeding values for mesosiderites, and both terrestrial and lunar anorthosites. This extreme fractionation of Eu suggests protracted growth of apatite or some precursor phase (i.e., francolite) under reducing (low $f\text{O}_2$) and high temperature hydrothermal ($>250^\circ\text{C}$) conditions, further corroborated by the prevailing pyrrhotite-pyrite-chalcocopyrite stockwork assemblage. Apatite associated with lower temperature assemblages exhibits diminished Eu signatures, reflecting a more-distal hydrothermal environment and defining a vector for mineralization. (SS7; Wed. 3:20)

Conodont biostratigraphy of the Hudson Bay and Moose River basins, Ontario and Manitoba

McCracken, A.D.¹, samccrac@nrcan.gc.ca, Armstrong, D.K.², Lavoie, D.³, Brunton, F.R.² and Nicolas, M.⁴, ¹Geological Survey of Canada – Calgary, 3303-33 Street NW, Calgary, AB T2L 2A7; ²Ontario Geological Survey, 933 Ramsey Lake Road, Sudbury, ON P3E 6B5; ³Geological Survey of Canada – Quebec, 490 rue de la Couronne, Quebec, QC G1K 9A9; ⁴Manitoba Geological Survey, 360-1395 Ellice Avenue, Winnipeg, MB R2G 3P2

The results reported here are part of Hudson Bay and Foxe Basins GEM (Geoscience Mapping for Energy and Minerals) Project of the Geological Survey of Canada. Within this GEM project archival petroleum and mineral exploration cores and new mineral exploration cores were sampled for conodonts. A few critical outcrop collections were also made.

This is the first attempt to bring together these new GEM samples with other samples from the Hudson Bay and James Bay lowlands submitted over the last two decades for conodont analyses. These other samples were reported by the senior author in GSC Paleontological Reports that predate the GEM program, but the data have not been published elsewhere.

The one petroleum exploration well drilled in the Hudson Bay Lowlands of Ontario is the 1969 Aquitaine Sogepet *et al.* Pen No. 1. The Bad Cache Rapids Group and Churchill River Formation yielded abundant conodonts. Faunas from the Bad Cache contain Late Ordovician species of Amorphognathus, Belodina, Drepanoistodus, Panderodus, Oulodus?, Paroistodus, Periodon, Phragmodus, Plectodina, and Pseudobelodina. Churchill River conodonts include Late Ordovician species of Amorphognathus, Belodina, Drepanoistodus, Panderodus, Paroistodus, Plectodina, Plegagnathus and Pseudobelodina. Severn River Formation samples are generally sparse



of conodonts, but do include Silurian species of the following genera: Apsidognathus, Aspelundia, Aulacognathus, Carniodus, Distomodus, Oulodus, Ozarkodina and Panderodus. Samples from the Late Ordovician Red Head Rapids and the youngest two Silurian formations, the Ekwan River and Attawapiskat, yielded few conodonts.

Recently discovered outcrop of organic-rich Boas River Formation on the Asheweig River yielded abundant Phragmodus and Drepanoistodus, as well as Plectodina, Pseudooneotodus, and rare Rhipidognathus symmetricus and Amorphognathus duftonus. Overall the fauna is comparable to those from the Boas River Formation in two mineral exploration cores to the north in the Winisk River area.

In Manitoba, samples from the Merland *et al.* Whitebear Creek STH #1 well yielded a sparse Silurian conodont fauna. These collections represent the Severn River, Ekwan River and Attawapiskat formations (samples from the Red Head Rapids, and Kenogami River were barren of conodonts).

Samples collected from the Moose River Basin mineral exploration cores include collections of Late Ordovician through Silurian conodonts. (*SS13; Thurs. Poster*)

On the crystal structure of UK77, a potentially new mineral from Mont Saint-Hilaire, QC: Pushing the limits of 'routine' Single-crystal X-ray Diffraction (SXRD) analyses

McDonald, A.M., Department of Earth Sciences, Laurentian University, 935 Ramsey Lake Road, Sudbury, ON P3E 2C6

The mineral informally known as UK77 was first discovered in 1985 as white to yellowish 'spiky' balls up to several mm across, in vugs in nepheline syenite at Mont Saint-Hilaire, QC. Individual crystals occur as colorless, transparent blades with sharp terminations; while chemistry indicate it to be a Na-Ca-fluorosilicate and a preliminary unit cell had been obtained, a formal description of the mineral was hampered by variability in both chemistry and obtained PXRD patterns. As traditional SXRD techniques were unsuccessful in resolving its crystal structure, it remained undefined. Recently, a new attempt to collect SXRD data was made using a Bruker D8 three-circle diffractometer equipped with a rotating-anode generator, a multi-layer optics incident beam path and an APEX-II CCD detector. Analysis was of a microcrystal of dimensions $1 \times 1 \times 20 \mu\text{m}$; results indicated it to be a poor diffractor (data observable only to $40^\circ 2\theta$) and of low symmetry (triclinic), but the crystal structure of UK77 was successfully solved and refined to $R = 8.2\%$ for 2956 unique reflections. Results indicate the mineral is triclinic, P1, with a 9.609(2), b 9.630(2), c 15.739(3) Å, α 75.21(3), β 85.22(3), γ 60.12(3)°, V 1212.3(1) Å³, and the ideal formula, $\text{Na}_2\text{Ca}_2\text{Si}_8\text{O}_{18}(\text{OH})\text{F}\cdot 7\text{H}_2\text{O}$. The mineral has a strongly layered crystal structure, with sheets of tetrahedra (T), octahedra (O) and interlayer cations. The T layers consist of six-membered rings of SiO_4 tetrahedra linked by SiO_4 whose vertices are opposite to those in the rings. The O-sheets are composed of edge-sharing $\text{M}\phi_6$ octahedra (M: Na,Ca; ϕ : unspecified ligand) arranged in a closest-packed arrangement, interspersed with H_2O groups. They are positioned between two symmetrically equivalent T layers, producing a strongly bonded T–O–T unit. The interlayer component (X) houses disordered Na polyhedra and H_2O groups. Stacking of these components perpendicular to [001] results in a OTXTO module, characteristic of minerals belonging to the reyerite-gyrolite group. Thus, UK77 represents a potentially new member of this group, emphasizing the great diversity that is possible on this theme. Preliminary studies of minerals similar to UK77 from Aris, Namibia and Poços de Caldas, Brazil, suggest it may be more widespread than originally thought. This study highlights the important role that modern-day SXRD analyses can play in resolving questions relating to complex, weakly-diffracting minerals: in some cases, new instrumental approaches supercede the necessity of exhaustive searches for crystals of higher quality. (*SY1; Wed. 3:20*)

Anatexis of phosphatic metalliferous shales as an ingredient in unusual pegmatite-hosted monazite-apatite-ilmenite occurrences

McFarlane, C.R.M. and McKeough, M., University of New Brunswick, Department of Earth Sciences, 2 Bailey Drive, Fredericton, NB E3B 5A3, crmm@unb

The exposed mid-crustal levels of orogenic belts such as the Trans-Hudson Orogen (THO) in northern Saskatchewan, locally host abundant granitic pegmatite dykes that intruded syn- to post-tectonically with respect to exhumation-related deformation. These granitic pegmatites are locally host to U and REE mineralization envisioned to reflect enrichment mechanisms controlled by assimilation and fractional crystallization processes affecting peraluminous melts generated during anatexis of metasedimentary protoliths. Experimental data for P and REE saturation in granitic liquids is well constrained and predicts variable dissolution of accessory apatite and REE-phosphates (monazite, xenotime) depending on the bulk chemistry of the melt (*i.e.*, ASI, alkali-alumina ratios, water content, F content). Because of the relatively low phosphorus and REE content of typical metapelitic protoliths and high saturation levels in peraluminous granitic melt, it is generally held that significant fractional crystallization of incipient anatectic melts is required to achieve P- and REE-saturation.

There are other metasedimentary protoliths, however, that can contain abundant P and REE in addition to other heavy metals. For example, metalliferous black shales formed in euxinic sub-basins in continental margin settings are typically enriched in LREE/HREE and can contain elevated As, Mo, V, Ba, and U, sometimes at toxic levels (*e.g.*, Pennsylvanian black shales). Authigenic alteration of greywacke can also locally lead to the growth of nodular monazite. Partial melting of these P- and LREE-enriched protoliths during subsequent orogenesis and high-temperature metamorphism is likely to generate incipient melts that are rapidly saturated in P and REE such that a large volume fraction of inherited apatite and REE-phosphates can be preserved.

A LA-ICP-MS case study of a sinuous monazite-apatite-ilmenite zone hosted by (and coeval with) granitic aplite and pegmatite dykes at Kulyk Lake, Wollaston Domain, northern Saskatchewan has revealed evidence for the entrainment of abundant detrital or authigenic monazite enriched in V, As, and Mo. The measured U-Pb ages of these metal-enriched monazite domains matches the provenance of the middle Wollaston-group sedimentary succession based on previous detrital zircon studies. This dataset provides direct evidence for the involvement of monazite-rich metalliferous protoliths in the source region to the pegmatite dyke. A number of scenarios have been envisioned to account for the field relationships, modal mineralogy, texture, U-Pb ages, and trace-element chemistry of the monazite-apatite-ilmenite zone. In addition entrainment and possible boundary-layer mechanisms, the Fe-P-rich composition of the zone may also be consistent with silicate-phosphate liquid immiscibility. (*SS10; Thurs. 2:20*)

Spectroscopy and supramolecular assembly of uranyl peroxide cage clusters

McGrail, B.T., bmcgrail@nd.edu, Joffret, L.J., Lussier, A.J. and Burns, P.C., University of Notre Dame, Notre Dame, IN, USA 46556

Uranyl peroxide cage clusters represent the largest group of actinide-bearing polyoxometalates (POMs) and have been shown to aggregate into large, supramolecular assemblies similar but not identical to the "blackberry" type assemblies known for transition metal POMs. Whether these assembly processes are driven primarily by electrostatics, similar to the aggregation of charged lyophobic colloids as described by DLVO theory, or are better described by a coordination model (*i.e.*, supramolecular POM assembly as a reaction between dissolved molecules or ions) remains an open question. We address this question through a combination of spectroscopic, light scattering, and microscopic methods. Preliminary results suggest inner-sphere interactions between uranyl peroxide POMs and coordinating cations or hydrogen bond donors (*e.g.*, K^+ , mannitol) result in the strengthening of the bonds between uranium and the "yl" oxygen atoms at the



expense of strength of the equatorial U-peroxo and peroxo O-O bonding through distortion of the U-peroxide bond angles. Conversely, interactions between uranyl peroxide POMs and non-coordinating cations (e.g., tetrapropylammonium, Pr₄N⁺) results in neither aggregation of the POMs nor alteration of bond strengths or angles. (SS5; Wed. 9:00)

Petrogenetic model for U-Th-REE mineralized granitic pegmatites in the high-grade metamorphic rocks of the Wollaston Domain, Saskatchewan: Evidence from Fraser Lakes Zone B

McKechnie, C.L.¹, Annesley, I.R.² and Ansdell, K.M.¹,

¹University of Saskatchewan, 114 Science Place, Saskatoon, SK S7N 5E2; ²JNR Resources Inc., Saskatoon, SK S7K 0G6

At Fraser Lakes Zone B (Wollaston Domain, Saskatchewan), numerous U-Th-REE-mineralized granitic pegmatites/leucogranites intrude the deformed contact between Paleoproterozoic metasedimentary gneisses of the Wollaston Group and Archean orthogneisses. The mineralization is mixed in origin; some of the U-Th-REE minerals are magmatic, and others are xenocrystic. The peraluminous pegmatitic melts are interpreted to have formed at depth, based on a lack of connection to migmatitic leucosomes in the host pelitic gneisses, with the source postulated to be U-Th-REE-enriched peraluminous pelitic gneisses similar to the Wollaston Group metasediments exposed at surface. The melt was generated by different degrees of batch melting via biotite-dehydration reactions during peak thermal metamorphism of the Trans-Hudson Orogeny (THO), at 6–9 kbar and 800–850°C, at ca. 1815 Ma.

During transport, the amount of U, Th, and REE in the melt would have increased due to fractionation; however, the amount of fractionation at Fraser Lakes Zone B is interpreted to be relatively low. Thus, the U-Th-REE contents of the pegmatites were controlled mainly by their sources, with their mineralogical and chemical heterogeneity indicative of multiple melt source compositions and/or varying degrees of partial melting in the lower to middle crust.

The concordant to subcordant nature of the pegmatites relative to the regional foliation, plus their location within a NE-plunging antiformal fold nose, is indicative of a strong structural control on their emplacement. The pegmatitic melts were emplaced at ~750° to 625°C, in the middle of a ~20 km thick, crustal melt-transfer zone. Melt transfer from the lower crustal source to its emplacement level was aided by deformation during the THO; the melt mostly moved along/within major structural zones to where it was emplaced preferentially in dilational structures (*i.e.* like the antiformal fold nose at Fraser Lakes Zone B).

The composition, lack of connection to large intrusions, and concordant nature of the pegmatites suggests they are not related to fractionation of a hypothetical granitoid at depth, unlike many known upper crustal pegmatites. This adds credence to our model for the origin of these pegmatites via partial melting of enriched source rocks at depth.

This petrogenetic model reinforces and adds to models developed for the formation of U-enriched pegmatites and leucogranites in the Pan-African Orogen of Namibia, the Svecofennian Orogen of Sweden and Finland, and the Grenville Province of Canada. Furthermore, it can be applied to other pegmatite-hosted U-Th-REE deposits in northern Saskatchewan, Canada, and has implications for uranium exploration. (SS5; Wed. 1:40)

Stratigraphy and U-Pb zircon-titanite geochronology of the Aley carbonatite complex, Northeast British Columbia: Evidence for Antler-aged orogenesis in the Foreland Belt of the Canadian Cordillera

McLeish, D.F.¹, mcleish@uvic.ca, Johnston, S.T.¹, Friedman, R.M.² and Mortensen, J.K.², ¹School of Earth and Ocean Sciences, University of Victoria, Victoria, BC V8W 3V6;

²Department of Earth and Ocean Sciences, University of British Columbia, Vancouver, BC V6T 1Z4

The tectonic significance and age of carbonatite intrusions in the central Foreland Belt of the Canadian Cordillera are poorly constrained.

Recent 1:5,000 scale field mapping of one of these carbonatite intrusions, the Aley carbonatite (NTS 94 B/5), has demonstrated that it was emplaced as a syn-kinematic sill, coeval with a major nappe-forming tectonic event. Determining the age of the Aley carbonatite therefore provides a means of directly dating tectonism related to carbonatite magmatism. Attempts at dating carbonatite units failed due to low U-Pb content in sampled zircons; however, a U-Pb titanite age of 365.9 ± 2.1 Ma was obtained from the Ospika pipe, an ultramafic diatreme spatially and genetically related to the carbonatite. We interpret the Late Devonian age of the Ospika pipe to be the minimum possible age of the carbonatite and syn-magmatic nappe-forming tectonic event. The maximum possible age of the carbonatite is constrained by the Early Devonian age of the Road River Group, the youngest strata intruded by carbonatite dykes and involved in the nappe forming event. Our dating results for the Aley carbonatite closely correlate with U-Pb zircon and perovskite ages obtained for the Ice River carbonatite complex in the central Foreland Belt of the southern Canadian Cordillera, and support the interpretation of carbonatite intrusions of the western Foreland Belt as genetically linked components of an alkaline-carbonatitic magmatic province. Structural, stratigraphic, and geochronological data from the Aley area indicate that deformation was similar in style to and coeval with structures attributable to the Antler Orogeny, and are consistent with the Antler orogen having extended the length of Cordilleran margin from the southern United States to Alaska. (SS2; Wed. 3:20)

Assessment of the electrical resistivity structure of the northwest Superior craton and adjacent Trans Hudson Orogen using the magnetotelluric method

McLeod, J.¹, ummcleo6@cc.umanitoba.ca, Ferguson, I.J.¹, Craven, J.² and Jones, A.G.³, ¹University of Manitoba, Winnipeg, MB R3T 2N2; ²Geological Survey of Canada, 615 Booth St, Ottawa, ON K1A 0E9; ³Dublin Institute for Advanced Studies, Dublin, Ireland

Magnetotelluric (MT) data from two projects in northeastern Manitoba, the Lithoprobe Western Superior transect and the Geological Survey of Canada Knee Lake profile, were compiled to investigate the geoelectric structure of the Archean Superior Province and Paleoproterozoic Trans-Hudson Orogen. Analysis and modelling was completed with the objectives of (1) imaging the subsurface resistivity structure of the northwestern Superior craton and adjacent Trans-Hudson Orogen, and (2) investigation of North American tectonic processes. The MT method is a passive-source geophysical method that uses time-varying electromagnetic fields measured at the Earth's surface to image the deep subsurface electrical resistivity. The resistivity of the crust and lithospheric mantle is sensitive to constituents including water and graphite, the presence of which can indicate processes such as subduction or plume interaction, and the absence of which can indicate significant thermal events.

The geoelectric structure of the study area was defined in terms of its dimensionality and strike and using 2-D inversion of the MT responses. The results indicate that some parts of the study area have regional 2-D structure but 3-D elements occur at large depth and also at more shallow depth near the margin of the Northern Superior superterrane and Pikwitonei Granulite belt. Strong three-dimensional galvanic distortion of the MT responses occurs throughout the study area. Extended Groom-Bailey tensor decomposition, implemented in the STRIKE program was used to further define distortion and geoelectric strike. This method enables determination of the regional MT response as a function of specified frequency range or depth range. At crustal depths the geoelectric strike azimuth throughout the study area has a dominantly northwest-southeast direction. At lithospheric mantle depths the azimuth has a bimodal distribution with both a northwest-southeast component and an east-west component that is particularly prominent close to east-west terrane boundaries at the northern margin of the Superior craton. Two-dimensional inversion of the data was done using an overall geoelectric strike azimuth of 127°. The results show a generally-resistive heterogeneous crust overlying a



more conductive mantle throughout the study region. The 2-D resistivity model includes a conductive body in the lower crust beneath the Fox River belt and Kiseeynew domain. Mantle conductors include a well resolved conductor dipping to the northwest beneath the Island Lake and Munro lake subprovinces, and a less well resolved conductor beneath the Northern Superior superterrane. The results suggest significant refertilization of the mantle lithosphere of the northern Superior craton. (SS3; Thurs. Poster)

The Musselwhite gold deposit, North Caribou greenstone belt, Ontario: New high-precision U-Pb ages and their impact on the geological and structural setting of the deposit

McNicoll, V.¹, vmnicoll@nrcan.gc.ca, Dubé, B.², Biczok, J.³, Castonguay, S.², Oswald, W.⁴, Mercier-Langevin, P.², Skulski, T.¹ and Malo, M.⁴, ¹Geological Survey of Canada, 601 Booth Street, Ottawa, ON K1A 0E8; ²Geological Survey of Canada, 490 rue de la Couronne, Québec, QC G1K 9A9; ³Goldcorp Canada Ltd., Musselwhite Mine, PO Box 7500, Thunder Bay, ON P7B 6S8; ⁴INRS Institut national de la recherche scientifique, centre Eau Terre Environnement, 490 rue de la Couronne, Québec, QC G1K 9A9

The Musselwhite mine is a world-class, banded iron formation (BIF)-hosted gold deposit, located in the southern part of the North Caribou greenstone belt in the ~3.0-2.8 Ga North Caribou terrane of the Superior Province. It has been in production for over 15 years with a total gold endowment of ≥ 5.6 million oz. New high-precision U-Pb ages are presented that constrain the geological setting of the deposit, with major implications for regional geological, structural, and exploration models in the North Caribou greenstone belt.

U-Pb samples were collected from drill holes from the folded stratigraphic sequence in the mine area which includes greenschist to amphibolite facies metavolcanic rocks of the South Rim assemblage, metavolcanic and metasedimentary rocks of the Opapimiskan-Markop assemblage, and metasedimentary rocks of the Zeemel-Heaton assemblage (Eyapamikama assemblage). At least three regional deformation events are recognized in the North Caribou greenstone belt, including major D² folding and high-strain zones in the mine area.

The deposit consists of structurally controlled pyrrhotite-rich ore zones mainly hosted by a folded garnet-grunerite-chert silicate facies (mine unit 4EA) of the Northern BIF, part of the Opapimiskan-Markop assemblage. Samples from a volcanoclastic sediment (unit 6) and a garnet-biotite-staurolite schist (unit 4F) both indicate that the Northern BIF is <2967 Ma. A felsic tuff (unit Avol) from the South Rim assemblage that structurally overlies basalts and ore-bearing Northern BIF yielded an age of ca. 2978 Ma. These data indicate that the Opapimiskan-Markop assemblage in the mine area may be overturned, perhaps due to early megascopic F₁ folding, which is documented at outcrop-scale in areas of lower D₂ strain. Felsic ash tuff and a fine grained siliciclastic metasediment from the "Lower Sediments" unit (Zeezel-Heaton assemblage), have much younger ages of <2850 Ma and <2846 Ma, respectively. The ~100 Ma time gap between the Opapimiskan-Markop and the structurally underlying Zeemel-Heaton assemblage is interpreted to be marked by a high-strain zone located within iron-carbonatized ultramafic rocks.

The new data provide important constraints on the mine stratigraphy and help to better understand the structural evolution and geometry of the main host units and ore-bearing horizons. These results will be integrated with an ongoing deposit-scale study that aims at defining the geological and hydrothermal footprint(s) of the deposit and better understanding the parameters and processes that led to the formation of this multi-million ounce BIF-hosted gold deposit. (SS3; Fri. 9:40)

Determination of the bedrock stratigraphy of the South Tobacco Creek area in the Pembina Hills portion of the Manitoba Escarpment using field investigation, LIDAR and photo imagery

McWhirter, B.R., Red River College, Winnipeg, MB R3H 0J9, brittmcw@mts.net

South Tobacco Creek cuts through the Manitoba Escarpment exposing bedrock of the Cretaceous Period present in Southwestern Manitoba. During the summer of 2012, all Cretaceous bedrock outcrops were mapped using photos, GPS coordinates and tracking. This was done to create a visual stratigraphic picture of the Cretaceous formations present in this region. This information is now being combined with LIDAR (Light Detection and Ranging Data) to create a 3D model of the creek. Analyzing the LIDAR data using ArcGIS 10.1 we will be able to create an elevation model of the watershed. This will assist us in indicating where slumping of bedrock has occurred. This information combined with the ground truthing data has the potential to indicate the nature of minerals and geochemical composition within the bedrock units, which may assist us in ultimately determining the age of suspended sediments moving downstream. A stratigraphic model of the watershed may be interpreted for the surrounding region and facilitate the detection of possible alluvial mineralization patterns downstream from South Tobacco Creek and other portions of the Escarpment. (SS13; Thurs. Poster)

Archean sulfur records the arrested development of a Proterozoic igneous complex

Mealin, C.A.¹, caroline.memail@ontario.ca, Leshner, C.M.¹, Bedard, J.², Hryciuk, M.³ and Wing, B.³, ¹Mineral Exploration Research Centre, Department of Earth Sciences, Laurentian University, Sudbury, ON P3E 2C6; ²Geological Survey of Canada, Quebec City, QC G1K 9A9; ³GEOTOP, Department of Earth and Planetary Sciences, McGill University, Montreal, QC H3A 2A7

Crustal contamination and incorporation of external sulfur are considered to be important processes in the petrogenesis and mineralization of large mafic intrusions, but despite numerous studies, remain poorly understood. This study has utilized multiple sulfur isotope data to identify crustal contamination, to constrain the nature of the sulfur source, and to provide further insights into the petrogenesis of the 2025 Ma Booth River intrusive complex (BRIC) in the Slave Craton, Nunavut.

The BRIC is exposed along the northwestern and southeastern flanks of the Burnside River Synclinorium and is interpreted on the basis of geological and geophysical data to represent outcroppings of a single ~80 km × ~40 km intrusion. It is remarkably undifferentiated, comprising pyroxene-plagioclase-olivine gabbroanorites. The basal contact is highly irregular with km-wide convex cusps of the intrusion separated by m- to km-wide zones of partially melted metasedimentary Archean Yellowknife Supergroup (YSG) footwall rocks, which by analogy with similar features in the Bushveld Complex have been interpreted as the root zones of remnant country-rock diapirs. The BRIC provides an excellent opportunity to further investigate this potential contamination mechanism, as the BRIC is smaller, less differentiated, and appears to have crystallized from a single magmatic pulse.

Twelve samples across the exposed part of the northern limb of the BRIC and adjacent footwall rocks were analysed for multiple sulfur isotopes. Most Archean sedimentary sulfides show δ³⁴S values near that of the mantle but record nonzero Δ³³S and Δ³⁶S values due to mass-independent sulfur isotope fractionation. Δ³³S and Δ³⁶S values form a linear mixing line between YSG contaminants (+0.70 to +0.81 per mil Δ³³S and -1.1 to -1.3 per mil Δ³⁶S) and mantle values (0 per mil for both Δ³³S and Δ³⁶S), indicating a major contribution of external sedimentary sulfur to the BRIC. However, the degree of contamination is non-systematic through the stratigraphy, with least contaminated signatures occurring both near (~35 m) and distant (~1260 m) from the basal contact and most contaminated signatures occurring at an intermediate distance (~725 m).

The non-systematic degree of contamination requires a mechanism – like the proposed diapirs – to enable partially molten country rock to reach upper levels of the magma chamber. Diapirism would promote locally enhanced mixing within the magma chamber and more rapid cooling of the intrusion. These effects would, in turn,



contribute to the poorly differentiated nature of the intrusion and ultimately aid in the preservation of the remnant country-rock diapires. (SS8; Thurs. 2:00)

Bird River Intrusive Complex in the western Superior Province, Manitoba: Evidence for a conduit model and controls on Ni-Cu-PGE and Cr mineralization

Meal, C.A.¹, caroline.meal@ontario.ca, Linnen, R.L.², Lin, S.¹, Theyer, P.³, and Corkery, M.T.⁴, ¹Department of Earth and Environmental Sciences, University of Waterloo, Waterloo, ON N2L 3G1; ²Department of Earth Sciences, University of Western Ontario, London, ON N6A 5B7; ³Wildcat Exploration Ltd., Winnipeg, MB R3H 1B3; ⁴Manitoba Geological Survey, Manitoba Innovation, Energy and Mines, Winnipeg, MB R3G 3P2

The Archean Bird River greenstone belt is a significant district for ore deposits hosting the Tantalum Mining Corporation of Canada (TANCO) rare-element (lithium, cesium, and tantalum) pegmatite deposits, the Maskwa West Ni-Cu-Co-PGE deposit, the Dumbarton Ni-Cu deposit and stratiform Ni-Cu-PGE and Cr mineralization. Of these, the Bird River Intrusive Complex (BRIC), historically known as the Bird River Sill and the focus of the current investigation, hosts the now closed Maskwa West mine and stratiform Ni-Cu-PGE and Cr mineralization. The BRIC as currently exposed consists of eight layered mafic-ultramafic intrusive bodies which intruded the northern portion of the Bird River greenstone belt. Field relationships and geochemistry of the western half of the BRIC indicate that the mafic-ultramafic bodies are spatially separated and were emplaced as separate intrusions through multiple-magmatic injections as opposed to a previous interpretation that they were displaced blocks of a single large intrusion. It is proposed that the three central intrusions (Chrome, Peterson Block and Page) are connected and represent a part of a single conduit system. Trace element and Nd isotope signatures indicate that these bodies share a common depleted magma source which is geochemically akin to modern back-arc basin basalts. There was little to no evidence of crustal contamination, with exception of the most westerly National-Ledin intrusion.

An implication of the separate intrusion model is that the separate bodies may contain different styles of mineralization and that conduits are favourable exploration targets. It is evident that all significant concentrations of Ni-Cu-PGE and Cr in the study area are contained in the ultramafic series of the separate intrusions. Massive sulphide mineralization is present at the base of the Page intrusion whereas the Chrome intrusion contains multiple disseminated sulphide horizons with enriched PGE. Both contain massive chromite mineralization near the mafic-ultramafic transition which coincides with the upper PGE-rich horizon. The character of PGE mineralization varies from intrusion to intrusion. Mineralization is magmatic in origin and stratigraphically correlates with interpreted magmatic recharge events indicating that magma mixing may have been the trigger for sulphide immiscibility. Significant remobilization of Ni-Cu-PGE is associated with late felsic magmatism. (SS9; Wed. Poster)

Evidence of the Laurentia-Australia connection? Detrital zircons from Mesoproterozoic strata in Yukon, Canada

Medig, K.P.R.¹, kmedig@gmail.com, Thorkelson, D.J.¹, Davis, W.J.², Rainbird, R.H.², Gibson, H.D.¹, Turner, E.C.³ and Marshall, D.D.¹, ¹Simon Fraser University, 8888 University Drive, Burnaby, BC V5A 1S6; ²Geological Survey of Canada, 601 Booth St., Ottawa, ON K1A 0E8; ³Department of Earth Sciences, Laurentian University, 935 Ramsey Lake Road, Sudbury, ON P3E 2C6

In North America, igneous sources for detrital zircon grains with U-Pb ages between 1490 and 1610 Ma are rare, and hence are referred to represent the "North American magmatic gap" (NAMG). Where grains of this age are preserved, an exotic (non-Laurentian) source is implied. Mesoproterozoic strata in the western Ogilvie Mountains in Yukon, Canada, yielded detrital zircon grains with U-Pb ages that reflect a

single source that lies in the middle of the NAMG. The grains were selected from three samples collected from fine- to coarse-grained sandstone beds from unit PR1, the basal unit of the Fifteenmile Group. Each sample yielded a unimodal population of grains with an age of approximately 1500 Ma. Two of the samples also contain a few grains with Paleoproterozoic to Archean ages. The turbiditic sandstone beds are texturally and compositionally immature and appear to be entirely epiclastic and devoid of contemporaneous tuffaceous input. The sediment was likely eroded from a single-aged plutonic highland that flanked this part of the Fifteenmile basin.

The apparent absence of such a source in northwestern Laurentia is best resolved by the presence of a suitable landmass fully connected to Laurentia that permitted a drainage system to carry sediment from nearby uplands to the margins of the newly formed Fifteenmile basin where it was subsequently deposited deeper in the basin. A short distance and a restricted river network are preferred to transport sediment from the highlands to the basin margins because of the paucity of grains with ages other than 1500 Ma. A suitable landmass is Australia, in a SWEAT-like configuration, as it contains igneous complexes of the required age such as the Mavis Granodiorite, part of the Naraku Batholith, in the Mt. Isa inlier. A plausible sequence of events is the docking of Australia and Laurentia during the 1.67-1.60 Racklan and Forward orogenies, followed by erosion and transport of sediment into the Fifteenmile basin in Yukon. The Belt-Purcell basin, 2400 km to the south, also received NAMG detritus from an exotic source, likely Australia. The presence of two, widely spaced Mesoproterozoic basins containing NAMG-rich sediment strongly suggests that Australia was the immediate conjugate to northwestern Laurentia in the Mesoproterozoic iteration of the supercontinent Columbia. (SS2; Wed. 2:40)

The character and distribution of Cu-PGE mineralization at the Geordie Lake deposit within the Coldwell Complex, Ontario

Meghji, I.¹, imeghji@uwo.ca, Linnen, R.L.¹, Samson, I.M.², Ames, D.E.³ and Good, D.J.⁴, ¹Western University, 1151 Richmond St., London, ON N6A 5B7; ²University of Windsor, 401 Sunset Ave., Windsor, ON N9B 3P4; ³Geological Survey of Canada, 750-601 Booth St., Ottawa, ON K1A 0E8; ⁴Stillwater Canada, 11 Sydenham St., Dundas, ON L9H 2T5

Preliminary investigations indicate that Cu-PGE mineralization at the Geordie Lake deposit (GLD) is spatially associated with variably weak to intense actinolite alteration within a heterogeneous-textured gabbro. The mineralized gabbro is unusual in that it contains pink albite alteration (termed Unit 3a) that is variable in intensity, but common throughout the host gabbro, and the presence of abundant skeletal olivine (termed Unit 3b). Four drill holes along a north-south section of the Geordie Lake Deposit have been logged in detail with particular emphasis placed on the lithology, alteration type, alteration intensity, texture, and sulfide mineralogy. The platinum-group element (PGE) mineralization in the GLD is stratiform, and occurs above the basal contact with syenite. This mineralization has been previously interpreted to be either the result of magmatic processes, due to the overall distribution of sulphides, or the result of magmatic-hydrothermal processes, based on the spatial association of platinum group minerals (PGM) with secondary albite pods. Scanning electron microscopy of the mineralized units show that PGM are hosted by disseminated to blebby chalcopyrite and bornite. In addition, chalcopyrite and bornite mineralization is strongly associated with actinolite alteration, predominantly in Unit 3a, but is not associated with pink albite alteration. Whole rock geochemistry coupled with core logging of the mineralized intersections show that the degree of Cu-PGE enrichment correlates with the intensity of actinolite alteration in Unit 3a, but that mineralization is not associated with actinolite alteration in Unit 3b. There is a progressive enrichment of rare-earth elements between Units 3a and 3b which suggests that these lithologies are genetically linked, but that Unit 3b is less evolved. Pearce element ratios suggest that magma evolution is controlled by olivine and plagioclase crystallization. Future work will determine the relationship



between the actinolite alteration and albite alteration, and how these alteration types affect mineralization at the GLD. Unmineralized gabbros will also be examined in order to quantify metasomatism. (SS9; Wed. Poster)

Mineral geochemistry of granites and pegmatites from Seixoso-Vieiros pegmatite field, northern Portugal

Mendes, L.U.D.S., Lima, A.M.C. and Noronha, F., Geology Centre of Porto, FCUP, DGAOT, Porto, Portugal, allima@fc.up.pt

The Seixoso-Vieiros pegmatite field is located in northern Portugal and contains numerous granitic pegmatite-aplite veins (Seixoso and Vieiros pegmatites). The studied area is included in "Galicia Trás os Montes geotectonic zone". The area is surrounded by Variscan granitoids: at NW by late-tectonic Celorico de Basto granite massif, and at SE by the syntectonic Felgueiras granodiorite. The pegmatites are hosted by schists of Silurian age within the cordierite-andalusite isograd. The field is known for old mining cassiterite and columbite-tantalite in last century.

In Seixoso area also outcrops two granite specialized cupolas at Seixoso and Outeiro and also numerous small apices or dike-like bodies. The cupolas exhibit a muscovite tourmaline facies on the apex roofs. These facies evolved from a biotite bearing facies at depth. This is shown by Outeiro open pit, a very heterogeneous unit, characterized by a subhorizontal layering accentuated by pervasive albitization and greisenization process.

The Outeiro granitic body contains typical granitic mineral assemblage and lithium-bearing minerals, such as amblygonite-montebrazite, petalite, cookeite, although most of them in accessory quantity together with beryl, chrysoberyl, tourmaline, sekaninaite, among others. In the surrounding pegmatitic segregations we found Li-bearing minerals.

Muscovites and K-feldspars of Outeiro granite and surrounding Seixoso pegmatites were studied by Electron-probe microanalyses (EMPA). The results for muscovite from Outeiro, reveal 1203 ppm of Rb (K/Rb = 72) and 4980 ppm of Rb (K/Rb ratio is 15) for the Seixoso pegmatites. In K-feldspar the values at Outeiro are 968 ppm of Rb (K/Rb ratio is 138) and 5762 ppm of Rb (K/Rb = 23) to Seixoso pegmatites.

As was suggested in the past from bulk rock analysis, these results show a granitic system evolution from Outeiro Granitic body to surrounding Seixoso pegmatites. (SY2; Thurs. Poster)

Definition of structural controls on formation of lode deposits of associated to mayor OTU shear zone fault system at El Limon Au vein, Zaragoza - Antioquia, Colombia

Mendoza, F., Universidad Nacional de Colombia, Medellín, famendozav@gmail.com.co

The Zaragoza area is characterized by the occurrence of a sequence of metamorphosed Paleozoic rocks of the Cajamarca complex, which were intruded by Jurassic quartz-diorites and granodiorites associated to the Segovia batholith. All these units are covered by latest Tertiary and Quaternary alluvial deposits. In this geological context emplace a series of Au - Ag veins composed of pyrite, Pb-sulfides (galena) and sphalerite with quartz. These veins mainly define NS trends and dip with varying inclinations to W.

El Limon deposit has been predicted stressing a direct relationship with the dynamics of the OTU fault and its associated secondary structures [1],[2]. This approach has been corroborated by detailed survey geological mapping during field work, showing that the structures in which the veins are located with varied width and mineralization (N05-10W/15-20W and N05-15W/30-45SW) but very well defined trends (fluid flow in cracks system associated with shear Zone - Riedel) correspond to two overprinted Riedel shear systems and apparent shear zones with two temporal occurrences consistent with a very expressed change in the system of regional stress. That can be very important for wing cracks and schelones development, represented

by veins and veinlets. On the planes of the El Limon vein and other secondary veins, as well as faults that cut the vein, could be found gouge development, which has abundant sulfides and calcite.

To the East of the area can be found phyllonites and mylonites marking the trace of the OTU fault, with an obvious shear zone trend N10-30W and about 50m wide. There can be observed kinematic indicators showing a dextral movement, in the top of this shear zone may be found a folded and faulted fine sandstone alluvial formation (not known the age of this formation, thus to be able to know the age of the last movement) with about 60m of difference with the current Juan Vara creek level, gauge development on the veins and local faults, shows a clear recent tectonic activity in the area, the structures show that this last movement of the its fault was a OTU fault reversed displacement. All the collected evidence of structural, lithological and mineralogical nature associated with El Limon Deposit gives insights that this corresponds to a Shear Zone Hosted Orogenic Gold Deposit [3],[4]. (GS4; Fri. 9:00)

References:

- [1] Lopez D. (2004), Univ. Nacional de Colombia.
- [2] Monterroza A (2005), Univ. Nacional de Colombia.
- [3] Goldfarb, R.J., Hart, C.J.R., and Marsh, E.E., (2008).
- [4] Goldfarb, R.J. *et al.* (2005) Econ Geol., 100th Anniversary Volume, pp. 407-450.

Geodynamic influences on the genesis of Archean world-class gold-rich VMS deposits: Examples from the Blake River Group, Abitibi greenstone belt, Canada

Mercier-Langevin, P.¹, pmercier@nrcan.gc.ca, Hannington, M.², Dubé, B.¹, McNicoll, V.³, Goutier, J.⁴, Monecke, T.⁵, ¹Geological Survey of Canada, 490 rue de la Couronne, Québec, QC G1K 9A9; ²Department of Earth Sciences, University of Ottawa, Ottawa, ON K1N 6N5; ³Geological Survey of Canada, 601 Booth St., Ottawa, ON K1A 0E8; ⁴Ministère des Ressources naturelles et de la Faune, 70 Avenue Québec, Rouyn-Noranda, QC J9X 6R1; ⁵Department of Geology and Geological Engineering, Colorado School of Mines, 1516 Illinois St., Golden, CO 80401 USA

Six of the world's richest and largest gold-rich volcanogenic massive sulphide (VMS) deposits are located in the 2704-2695 Ma Blake River Group (BRG) of the Abitibi greenstone belt, including the two largest ever found (Horne: 54 Mt, 328 t Au, and LaRonde Penna: 80 Mt, 290 t Au), suggesting district and deposit-scale primary geological control(s) on the gold enrichment in VMS deposits.

The gold-rich VMS deposits of the BRG are found in distinctly different volcanic and structural settings from other "conventional" VMS deposits in the district. The ~2701 Ma Horne gold-rich deposit is separated in time and space from the ~2698 Ma Noranda Mine Sequence Cu-Zn VMS; it is located in the southern part of the Noranda camp in fault-bounded structural blocks separated from the slightly younger Cu-Zn deposits. The Bousquet Formation, which hosts the ~2698 Ma LaRonde Penna deposit, was coeval with the volcanic rocks that host the Cu-Zn VMS of the Noranda Mine Sequence but is distinguished by its transitional to calc-alkaline affinity and dominantly felsic composition. The Bousquet Formation is thought to have been formed in a volcanic complex at the periphery of the central part of the BRG, possibly in an area characterized by a thicker crust undergoing early extension and closer to an inferred arc (immature or early arc-rift stage). Recent dating in the BRG indicates that Horne also formed during an episode of early extension-subsidence and transitional felsic volcanism at Noranda (2702-2701 Ma). Extension, VMS-related hydrothermal activity and transitional to calc-alkaline volcanism moved away from the central part of the BRG, and by 2698-2697 Ma, at which time Horne had already formed, the Cu-Zn deposits of the Noranda Mine Sequence were being deposited in the more mature, tholeiitic to transitional, mafic-dominated extensional setting.

Despite obvious limitations of reconstructions of Archean volcanic complexes, analogies can be made with the architecture and evolution of modern volcanic arcs such as those formed along the



western Pacific. The BRG gold-rich VMS deposits were formed during incipient extension episodes at different times and places in a setting that is thought to have been transitional between arc and back-arc regions. Specific time-stratigraphic intervals related to arc extension are viewed as an important guide to exploration for gold-rich VMS in ancient volcanic belts. The concentration of gold-rich VMS deposits in the eastern BRG highlights a region with favourable gold “heritage”, where gold deposits of multiple ages and styles are formed throughout the evolution of the belt. (SS7; Wed. Poster)

Geology, alteration and mineralization of the Lemoine auriferous VMS deposit, Chibougamau camp, Abitibi greenstone belt, Québec, Canada: Geologic evidence for a magmatic input

Mercier-Langevin, P.¹, pmercier@nrcan.gc.ca, Lafrance, B.², Bécu, V.¹, Dubé, B.¹, Kjarsgaard, I.³, Guha, J.⁴, Ross, P.-S.⁵,
¹Geological Survey of Canada, 490 rue de la Couronne, Québec, QC G1K 9A9; ²Focus Graphite Inc., 138 rue Price Ouest, Chicoutimi, QC G7J 1G8; ³Consulting Mineralogist, 15 Scotia Place, Ottawa, ON K1S 0W2; ⁴Université du Québec à Chicoutimi, 555 blvd. de l'Université, Chicoutimi, QC G7H 2B1; ⁵Institut national de la Recherche scientifique – Centre Eau, Terre et Environnement, 490 rue de la Couronne, Québec, QC G1K 9A9

The Abitibi greenstone belt hosts many of the world's best examples of Au-rich deposits and a few auriferous volcanogenic massive sulphide (VMS) deposits, including the ~2728 Ma Lemoine deposit (0.76 Mt at 4.6 g/t Au, 4.2 wt % Cu, and 9.5 wt % Zn) located in the Chibougamau camp. The deposit is hosted by a steeply dipping, south-facing homoclinal volcanic succession (~2729-2726 Ma Waconichi Formation, Lemoine Member) composed of effusive and intrusive tholeiitic rhyolites and andesites cut by comagmatic diorite and gabbro dikes and overlain by transitional to mildly calc-alkaline basalts, andesites, and rhyolites.

Seven synvolcanic alteration assemblages, now intensely deformed and metamorphosed to upper greenschist facies, were defined based on their mineralogy and position relative to ore. Albite-quartz, sericite-carbonate, sericite-chlorite, sericite-chlorite-(sphalerite), and chlorite-sericite-epidote-carbonate assemblages define semiconcordant zones that are stacked from the paleosea-floor to the deep footwall. In contrast, chlorite and chlorite-sericite-chloritoid assemblages overprint the other alteration zones and form subconcordant to now transposed discordant zones in the deposit footwall. Whole-rock oxygen isotopes indicate that the temperatures of alteration ranged from ~100-150°C (sericite-carbonate assemblage) to ~350°C (sericite-chlorite, chlorite-sericite-chloritoid and chlorite assemblages). The chlorite-sericite-chloritoid assemblage, and to some extent the sericite-chlorite assemblage, are associated with strong to near total depletion of light rare earth elements.

Although speculative, the high-temperature (~300-400°C) and strongly light REE-depleted alteration zones present at depth in the Lemoine footwall are consistent with alteration by reaction with acidic, possibly CO₂-rich and Cl-bearing solutions. Both CO₂ and HCl are considered likely to be added to hydrothermal systems through magmatic degassing. It is proposed that hydrothermal alteration at Lemoine was controlled by both HCl and CO₂ in a steep thermal gradient developed above the synvolcanic Doré Lake Complex.

The massive sulphides at Lemoine are particularly rich in Bi, which most probably came from a magmatic source. Even if all evidences indicate that Au is synvolcanic (e.g., metals distribution), it is not clear if Au was sourced in a magmatic chamber and provided through devolatilization. Moreover, the presence of Bi in the system may have helped optimize Au transport and precipitation within the ore zone by acting as a sink for Au, preventing it from being lost to the water column.

The Au-rich nature of the Lemoine auriferous VMS deposit can be explained by a possible magmatic contribution to the hydrothermal system and by the combination of very efficient metal transport and

highly effective capture of metals at or near the sea floor. (SS7; Wed. 8:20)

Trace element and PGE content of chromites from komatiites in the Alexo area (Abitibi, Ontario) and implication for exploration: A LA-ICP-MS study

Méric, J., julien_meric@voila.fr, Pagé, P., Barnes, S.-J., Canada research chair in magmatic metallogeny, Université du Québec à Chicoutimi, 555 bd. Université, Chicoutimi, QC G7H 2B1, and Houllé, M.G., Geological Survey of Canada, GSC-Québec, 490 Couronne Street, Québec, QC G1K 9A9

Komatiite-associated Ni-Cu-(PGE) sulphide deposits exhibit a relatively small footprint and are becoming more and more difficult to find especially within poorly exposed and extensively covered Archean and Proterozoic greenstone belts. This is why the development of lithogeochemical tools is important for discovering new deposits. Chromite which is a common accessory mineral in ultramafic rocks can be used to discriminate between rocks from mineralized and barren environments. Recent studies have demonstrated that in absence of sulphide melt, PGE and particularly Ru are preferentially incorporated into chromite and into sulphide when sulphide melt droplets are present. Therefore, it has been suggested that a better understanding of the behaviour of Ru in komatiitic systems might lead to the development of new exploration strategies for magmatic Ni-Cu-PGE deposits. Chromites from various facies (olivine cumulate, spinifex zone, disseminated and massive sulphides) from two komatiite-associated deposits in the Abitibi greenstone belt (Alexo and Hart deposits) have been characterized with EMP (majors) and LA-ICP-MS (traces and PGE). The Alexo komatiite has been selected for their excellent degree of preservation (prehnite-pumpellyite facies) but pervasively serpentinized samples from the Hart deposit have also been included to investigate the effect of alteration on chromite composition. Results show that chromite from Alexo komatiites have Cr# [Cr/(Cr+Al)] and Fe²⁺# [Fe²⁺/(Fe²⁺+Mg)] values typical of fresh komatiite. Chromites found within massive sulphide show higher Cr# and Fe²⁺# values, they are depleted in Al, Ni and Mg and enriched in Ti, Zn, Mn, Fe and V compared with chromites from unmineralized samples. Chromite from altered samples are depleted in Mg and enriched in Zn, Co, Mn and Fe. Unmineralized, mineralized and altered samples can all be distinguished when chromite compositions are projected on graph of Ni/Mn or Ni/Zn to Ni/Cr. Most chromites show Ru content above detection limits (~60 ppb) and up to 450 ppb, surprisingly chromites from disseminated sulphides cover the full range of values in Ru. Chromites from massive sulphides are strongly depleted in Ru, this combined with high Cr# can be used as an indication of massive sulphide mineralization. These results imply that either chromite started to crystallize before sulphide saturation (Ru-rich chromite) and continued during sulphide saturation (Ru-poor chromite), or the dynamism of komatiitic systems could also have transported and mixed chromite populations. (SS9; Thurs. 9:00)

Geological investigations in the McFaulds Lake greenstone belt (“Ring of Fire”), Oxford-Stull domain, Superior Province

Metsaranta, R.T., Ontario Geological Survey, 933 Ramsey Lake Rd, Sudbury ON P3E 6B5, riku.metsaranta@ontario.ca, and Houllé, M.G., Geological Survey of Canada, GSC-Québec, 490 Couronne Street, Québec, QC G1K 9A9, michel.houle@nrcan.gc.ca

The McFaulds Lake greenstone belt (MGB) is an extensive (>200km long), arcuate-shaped, dominantly Neoarchean, greenstone belt occurring in the central part of the Oxford-Stull domain in Northern Ontario. New field, geochemical, geophysical, and geochronological constraints allow us to subdivide the supracrustal rocks of the MGB into a provisional tectonostratigraphy including: (1) the Kitchie assemblage (KA), a west striking package comprised of mafic metavolcanic and clastic metasedimentary rocks; (2) the Butler assemblage (BA), dominated by felsic to intermediate metavolcanic rocks with lesser mafic and ultramafic metavolcanic rocks; (3) the



2785-2737 Ma Muketei assemblage (MA), a northeast striking lithologically diverse package that consists dominantly of mafic to felsic metavolcanic rocks with lesser clastic and chemical metasedimentary rocks; (4) the <2714 Ma Winiskis assemblage (WA), an east-striking package, dominated by mafic metavolcanic rocks with lesser felsic to intermediate metavolcanic and clastic metasedimentary rocks, and (5) the Attawapiskat assemblage (AA), a generally northwest-striking package comprised of a western felsic to mafic metavolcanic panel, a <2702 Ma central metasedimentary panel, and an eastern mafic-dominated metavolcanic panel. Mafic and ultramafic intrusions, are a ubiquitous feature of all of these assemblages but remain poorly constrained. Felsic to intermediate intrusive rocks in the region span from synvolcanic to post tectonic with known ages ranging from ca. 2773 to 2690 Ma.

The unusual abundance of mafic to ultramafic intrusive rocks is one of the most prominent features of the MGB, particularly as they host world-class chromite deposits, a significant Ni-Cu-PGE magmatic sulfide deposit, and numerous Fe-Ti-V-P occurrences. At least two generations of mafic-ultramafic intrusive rocks are recognized based on previous geochronology, but it is likely that multiple distinct generations of mafic to ultramafic rocks are present in the area. Known Cr and Ni-Cu-PGE mineralization occurs essentially within ultramafic-dominated intrusions in the MA whereas Fe-Ti-V-P mineralization occurs within mafic-dominated intrusions in several of the provisionally outlined assemblages (KA, BA, MA, AA). Further, field relationships suggest that magnetite-bearing, Fe-Ti-V-P mineralized gabbroic sills may cross cut the mineralized ultramafic units. Noteworthy, in addition to the high fertility of these mafic-ultramafic intrusions to host orthomagmatic Cr-PGE/Ni-Cu-PGE/Fe-Ti-V-P mineralization, is the spatial association between the magnetite-bearing mafic-dominated intrusions and VMS occurrences in all assemblages within the MBG. This suggests that these intrusions might represent the heat engines responsible for the formation of large-scale hydrothermal circulation and the genesis of Cu-Zn VMS deposits/occurrences throughout the MGB. (SS3; Thurs. 3:20)

Building bridges and positive results: The Manitoba Mineral Resources Training Program - An example of industry and First Nation collaboration

Mihychuk, M., President, CR Services, 406 Albert Street, Suite 406, Winnipeg, MB R3B 1G4

The Mineral Resources Training Program (MRTP) known as 'Resource Rangers' conducted its fourth annual program in 2012. Administered by Manitoba Keewatinowik Okimakanak Inc. (MKO) and with the support and collaboration of over 125 industry partners, program sponsors, and community participants, the program exposes northern and aboriginal youth to the many types of careers in the mineral sector. Through classroom activities and site visits students learn such things as prospecting, exploration, mining, milling, refining and smelting, reclamation and environmental aspects of the mineral business. Students also enjoyed meaningful cultural and cooperative components of program. With results of over 80% graduation rate and 50% of trainees were looking at a career in the mineral sector, the program builds bridges and produces positive results. (SS22; Thurs. 2:00)

The arsenopyrite stockpile at Snow Lake Manitoba: An example of university research leading to remediation by industry

Mihychuk, M., Vice President, BacTech Manitoba, 406-63 Albert Street, Winnipeg, MB R3B 1G4, and Sherriff, B.L., Department of Geological Sciences, University of Manitoba, Winnipeg, MB R3T 2N2

The Arsenopyrite Residue Stockpile (ARS) in Snow Lake, Manitoba was deposited between 1950 and 1959 in an open waste rock impoundment. It remained exposed until 2000, when the pile was capped with waste rock and clay. The pile contains approximately 250 000 tons of cyanide treated, refractory arsenopyrite ore concentrate with an average grade of approximately 9.7 grams per tonne of gold. Research at the University of Manitoba determined the mineralogy and

geochemistry of the residue and the progress of arsenic contamination from the stockpile. In December 2011, BacTech Environmental signed a contract with the Mines Branch of the Manitoba Department of Innovation, Energy and Mines, to remediate a stockpile of arsenopyrite concentrate located in the community of Snow Lake in Northern Manitoba. BacTech proposed a "no cost to the taxpayer" approach to the clean up. The Company will recover payable metals for its own account from the stockpile, while stabilizing the contained arsenic. The Company's bio-oxidation technology has been used successfully in the gold industry for many years to aid the extraction of gold from arsenical concentrates, while stabilizing arsenic values into a benign form. (SS20; Fri. 3:00)

Constraining magma compositions for the ultramafic cumulate rocks of the Ungava Craton's Q-suite (2.7 Ga) ~ using the program MELTS

Milidragovic, D. and Francis, D., Dept. of Earth and Planetary Sciences, McGill University, Montreal, QC H3A 2A7, dejan.milidragovic@mail.mcgill.ca

The plutonic Qullinaaraaluk suite (Q-suite) of northern Ungava comprises small, cumulate ultramafic to mafic cumulate bodies that are scattered across the width of the Ungava Craton. The ca. 2.72 Ga emplacement ages, and the ubiquitous and wide spread occurrence of the Q-suite plutons, suggest that Neoproterozoic crustal reworking of the Ungava craton at ca. 2.74-2.72 Ga may have been driven by underplating by the mantle-derived parental magmas of the Q suite. Fine-grained rocks approximating Q-suite magma compositions have not been found in the field, making the geochemical characterization of the Q-suite magma(s) an elusive challenge. We estimate the major element composition of the Q-suite parental magma by performing equilibrium melting calculations on dunites from of the north-central Ungava's Lac Couture region. The thermodynamic-based program MELTS (Ghiorso and Sack, 1995) was used to estimate the liquid composition at which the last non-cumulus phase (clinopyroxene) is melted out of each dunitic sample. The calculations were then extended until the Mg-number ($Mg/(Mg+Fe^{2+})$) of the model liquids reached the value in equilibrium with the earliest crystallized olivines (Fo84), assuming a KD value of 0.3. This approach assumes a "closed system" in which the interstitial minerals represent the composition of the trapped interstitial liquid. Our results suggest the Q-suite parental magmas were Fe-rich picritic olivine tholeiites ($MgO > 14.0$ wt.), with Mg-numbers ($Mg/(Mg+Fe) < 0.63$). The calculated parental magmas are enriched in Fe compared to most modern-day mantle-derived magmas, and the estimated parental magmas of most of the world's ultramafic plutonic rocks. The trace-element contents of the Q-suite parental magma's were calculated using the method of Bédard (1994), assuming a 5 % trapped liquid component. The unfractionated character of the HREE profile of the calculated parental magmas ($Yb_{MORB} = 0.5-0.9$; $Dy/Yb_{MORB} = 1.2-1.5$), suggests that they were derived at relatively shallow mantle depths, in the absence of garnet. The inferred shallow melting depths of the Q-suite magmas may reflect rapid thinning of the Ungava crust at ~ 2.74 Ga. (SS8; Thurs. 2:20)

Li and B isotopic composition of basement rocks from multiple sites of the Eastern Athabasca Basin, Saskatchewan, implications as a possible vectoring tool?

Millar, R.^{1,2}, Annesley, I.R.^{1,3}, Rudnick, R.L.⁴, Liu, X.⁴ and Ansdell, K.¹, ¹University of Saskatchewan; ²Saskatchewan Research Council; ³JNR Resources; ⁴University of Maryland

The Proterozoic Athabasca Basin in northern Saskatchewan contains the largest and richest unconformity-type (U/C-type) uranium deposits in the world. Uranium mineralization occurs at or near the unconformity, between the sedimentary rocks of the basin and the metamorphosed Archean to Paleoproterozoic basement rocks. The faults cutting these rocks, which provided focal points for fluid flow and mixing, initially formed during the Paleoproterozoic Talston Magmatic Zone and Trans Hudson Orogen and were subsequently episodically reactivated.



Current literature suggests Li isotopic fractionation of minerals can occur during weathering, hydrothermal alteration, and igneous/metamorphic processes, while the B isotopic signature preserved in refractory minerals, such as tourmaline, can record the source of fluids and P-T conditions during crystallization. Many researchers agree that oxidized basinal brines flowed through the basement lithologies but the source of uranium remains controversial. If hot, saline fluids transporting U interact with the basement rocks, both the B and Li isotopic systems should fractionate and thus generate significant $\delta^7\text{Li}$ and $\delta^{11}\text{B}$ variations. This study is documenting the $\delta^7\text{Li}$ and $\delta^{11}\text{B}$ of fresh to significantly altered basement lithologies and determining the potential of the Li and B isotopic systems to provide insight into the fluids interacting with the basement and as a possible vectoring tool.

Fresh and altered graphitic pelitic gneisses and granitic pegmatites in proximity to known U/C-type uranium mineralization, including the Dawn Lake and McArthur River deposits, were selected. Li and B concentrations of whole rocks range from 24 to 591 ppm and from 62 to 915 ppm, respectively, with a considerable range of concentrations occurring within/between multiple sites in the eastern Athabasca Basin. These concentrations of Li and B provided suitable material for isotopic analysis, $\delta^7\text{Li}$ measured by MC-ICP-MS display values between +4‰ and +13‰ for pelitic and graphitic pelitic gneisses and -0.40‰ to +18.6‰ for granitic pegmatites. The $\delta^{11}\text{B}$ measured by HR-ICP-MS for granitic pegmatites range from -5.3‰ to +1.6‰, whereas the $\delta^{11}\text{B}$ for metasediments range from -0.8‰ to +3.5‰. The significant range in isotopic values for both $\delta^7\text{Li}$ and $\delta^{11}\text{B}$ in the bulk samples is interpreted to result from the interaction of hydrothermal fluids with primary magmatic/metamorphic minerals in the basement, as it potentially leached and transported uranium for deposition at the unconformity. (SS5; Thurs. 2:40)

The Layered Series at Duluth – Evidence for magmatic venting from a shallow mafic layered intrusion

Miller, J.D., Dept. of Geological Sciences, University of Minnesota Duluth, Duluth, MN 55812 USA

Most mafic intrusive systems show chemical and phase evidence of being open to multiple magmatic recharge events. Evidence of magmatic venting is less obvious because it leaves little to no chemical signature. Decompression attending magma venting can cause phase changes and, under volatile-saturated conditions, a change in texture, though these changes are most pronounced under shallow crustal pressures. The Layered Series at Duluth (DLS) demonstrates litho- and chemostratigraphic variations that record not only the effects of fractional crystallization and magma recharge, but also magma venting from a large, volatile-saturated, shallow mafic intrusion.

The Layered Series at Duluth (DLS) is one of the best exposed intrusions composing the 1.1 Ga Duluth Complex of northeastern Minnesota. The Duluth Complex is a composite of multiple mafic to felsic intrusions that were emplaced into the basal section of a comagmatic edifice of volcanics during the 1.1 Ga Midcontinent Rift. The DLS is a 4-5-km-thick intrusion that is capped by anorthositic rocks that were emplaced earlier. The lithostratigraphy and chemostratigraphy of the DLS are consistent with the differentiation of a tholeiitic magma due to bottom-up fractional crystallization. However, in detail, phase and mineral chemical variations indicate that the DLS was open to multiple magmatic recharge and venting events.

Evidence of magmatic venting from the DLS include:

- 1) A cyclical transition between troctolitic (PO) and gabbroic (PCFO) cumulates over a 1-km-thick medial interval (Cyclic Zone). It is composed of five macrocycles, each defined by a gradational change from PO to PCFO cumulates followed by an abrupt regression back to PO. This phase layering does not correlate with cryptic mineral variation as would be expected if related to recharge, but is consistent with decompression.
- 2) Fine-grained biotitic ferrodiorite that underlies and dikes into an overlying cap of hydrothermally altered anorthositic rocks. The evolved composition of the “DLS chill” precludes it being a

thermal quench of DLS parent magma, but is consistent with it being a decompression quench of a hydrous magma that was comagmatic with cyclic zone cumulates.

- 3) Further evidence of a comagmatic link between the “DLS chill” and the Cyclic Zone is the presence of anorthositic inclusions and microgabbro cumulates that occur near the tops of macrocyclic zones.
- 4) A volcanic sequence about 4-5 km above the DLS, compositionally matches the “DLS chill” which is consistent with the “chill” being created by decompression quenching of hydrous magma attending venting to a volcanic eruption. (SS8; Thurs. 1:40)

The epithermal Engineer Mine gold deposit, British Columbia

Millonig, L.J.¹, lmillonig@eos.ubc.ca, Groat, L.A.¹, Linnen, R.² and O'Brien, D.³, ¹Department of Earth, Ocean and Atmospheric Sciences, University of British Columbia, 2020 - 2207 Main Mall, Vancouver, BC V6T 1Z4; ²Department of Earth Sciences, University of Western Ontario, London, ON N6A 5B7; ³BCGold Corp., Suite 520 – 800 Pender Street, Vancouver, BC V6C 2V6

The Engineer Mine in northern British Columbia belongs to the relatively rare group of epithermal gold deposits where gold, in the form of electrum, occurs intimately associated with roscoelite (vanadium-bearing mica). This paragenesis is commonly interpreted to be indicative for epithermal gold deposits related to alkaline magmatism. However, unlike other deposits, such as, Cripple Creek, Colorado and Porgera, Papua New Guinea, where the roscoelite is interpreted to be a replacement product, textural evidence suggests that at the Engineer Mine it precipitated together with the electrum. In addition, and also in contrast to other deposits with a comparable paragenesis, tellurides are absent from the electrum-bearing quartz-carbonate veins at the Engineer Mine. These peculiarities indicate that the genesis of this bonanza-style deposit differs in important aspects from deposits with broadly similar characteristics.

Gold-bearing veins at the Engineer Mine are characterized by multiple stages of vein development, replacement textures, and frequently, but not always, textures indicative of boiling. Commonly, and in a simplified way, the following stages can be distinguished: (1) sulfidation (pyrite, pyrrhotite) and/or silification of the host rocks, coeval with, or followed by (2) brecciation; (3) repetitive precipitation of fine grained quartz, sulfides (e.g., pyrite, arsenopyrite, stibnite) and carbonates; (4) crystallization of cockscomb quartz and coarse grained carbonate; and (5) infill of Fe-carbonates in vugs. Textural evidence suggests that the deposition of electrum and roscoelite occurred during stage (3). This interpretation is supported by the fact that vein intervals with elevated Au content are commonly also enriched in As and Sb. However, based on petrographic evidence, electrum occurs with pyrite and arsenopyrite, and as free electrum, in addition to the association with roscoelite. (SS23; Thurs. Poster)

Rare earth element-bearing perovskites in slags formed by the aluminothermic reduction of pyrochlore

Mitchell, R.H., Lakehead University, Thunder Bay, ON P7B 5E1, rmitchel@lakeheadu.ca, and Mariano, A.N., 48 Page Brook Rd, Carlisle, MA 01741 USA

Slags from Araxa (Brazil), Oka (Québec) and Fen (Norway) resulting from the production of ferro-niobium by the aluminothermic reduction of pyrochlore were investigated by back-scattered electron petrography and quantitative energy dispersive X-ray spectrometry. Slag “mineralogy” is a function of composition of the pyrochlore feed and the diverse additives (FeO, CaO, CaF₂) to the aluminium used in the reduction process. All slags are modally-dominated by diverse prismatic crystals of beta-alumina (Ba and/or Ca-Ti varieties), with other compounds and glass occurring in the interstices between these crystals. Slag from Araxa contains: a magnetoplumbite-like Ca-Ba-Na aluminate; a Ba-hibonite-like phase; [Ba,Ca](Al,Si)₂O₄; Ba₃Nb₂O₈; and compositionally zoned Ca-Ti-REE-Al rich perovskites with high Th and Nb contents; Na and Nb rich perovskites. The REE rich



perovskites contain up to 25 wt.% Ce_2O_3 , 4 wt.% La_2O_3 ; 12.5 wt.% Al_2O_3 ; 8 wt.% Nb_2O_5 and 13.5 wt.% ThO_2 . They are essentially members of the quaternary solid solution $\text{ThTi}_2\text{O}_6\text{-Ca}_2\text{AlNbO}_6\text{-CaTiO}_3\text{-REEAlO}_3$. Compositional evolution is towards Th-poor (< 1 wt.% ThO_2) NaNbO_3 -perovskites (up to 9 wt.% Na_2O and 56 wt.% Nb_2O_5) associated with Th- (7-9 wt.% ThO_2) and U- rich (14-15 wt.% UO_3) pyrochlore. Similar REE-rich, but Th-poor, perovskites are found slag from Oka in association with: REE-bearing hibonite (~8 wt.% Ce_2O_3 ; 1-2 wt.% La_2O_3); anorthite; calzirtite, $(\text{Zr,Ti})\text{O}_2$ solid solutions; rutile; Al-Zr-titanate; MgAl_2O_4 ; relict corundum; and REE-bearing calc-silicate glass. In contrast, slag from Fen contains Th-bearing REE-poor perovskites in association with celsian, Na-Ba-“feldspathic” glass: Th-U-zirconolite; and diverse Ti-Ba-Nb-oxides and Ti-Al-Nb oxides. Absent from all slags investigated are Fe-bearing compounds, including those from Oka which contain spherules consisting of diverse Fe-Nb and Fe-Nb-Si alloys. These data demonstrate that during ferro-niobium production that REE, Zr, Th, U and significant amounts of Nb are sequestered in the oxide phases in accord with their lithophile geochemical character. None of these elements are present as compounds in ferro-niobium alloys. These data demonstrate that the aluminothermic reduction process results in the loss of significant amounts of Nb to the slag. The REE content of the slags is considered to be greater than that of many carbonatite-related mineral occurrences currently being evaluated for their REE potential. Slags originating from ferro-niobium production if enriched in Th and U could be considered either as an environmental hazard or a useful proxy for radwaste synthetic containment strategies. (SS6; Wed. 9:20)

Volcanological setting of the Archean world-class gold-rich Horne and Quemont VMS deposits, Blake River Group, Abitibi Greenstone Belt, Canada

Moncke, T.¹, tmoncke@mines.edu, Gibson, H.², McNicoll, V.³, Dubé, B.⁴ and Hannington, M.⁵, ¹Colorado School of Mines, Golden, CO 80401 USA; ²Laurentian University, Sudbury, ON P3E 2C6; ³Geological Survey of Canada, Ottawa, ON K1A 0E8; ⁴Geological Survey of Canada, Quebec, QC G1K 9A9; ⁵University of Ottawa, Ottawa, ON K1N 6N5

The 2704-2695 Ma Blake River Group (BRG) of the Abitibi greenstone belt hosts some of the world's richest and largest volcanic-hosted massive sulphide (VMS) deposits, including the Horne (53.7 Mt at 2.2% Cu and 6.07 g/t Au) and Quemont (13.8 Mt at 1.32% Cu, 2.44% Zn, and 5.49 g/t Au) deposits in the Noranda camp.

Detailed volcanic facies mapping has shown that the 2702 Ma volcanic successions that host the Horne and Quemont deposits share many similarities. Both deposits are hosted by successions of dominantly felsic volcanic rocks deposited in an extensional setting. The location of both deposits was strongly controlled by syn-volcanic faulting, creating graben subsidence. Ore formation at Horne coincided with a major shift in volcanism. The felsic rocks hosting the Horne deposit are overlain by a thick succession of mafic rocks that are interpreted to record the upwelling of mantle-derived melts into shallow crustal levels during peak extension. The felsic host rock succession of the Quemont deposit is crosscut by a mafic dyke swarm. Individual dykes range from several centimetres to several metres in thickness and dyke-in-dyke intrusions are common. Composite dykes that formed by contemporaneous intrusion and mingling of rhyolitic and basaltic magmas are hallmarks of bimodal volcanism associated with crustal extension.

Volcanic lithofacies are particularly important in the host rock successions of both deposits. A wide variety of volcanoclastic lithofacies occur, ranging from proximal facies associated with coherent rhyolite domes and sills to mass-flow-derived volcanic debris containing pyroclasts generated by explosive eruptions from a felsic volcanic source. A high proportion of the volcanoclastic debris was originally glassy in nature. Processes of subsea-floor infiltration and replacement within the volcanoclastic strata are responsible for the formation of a significant proportion of the sulphide mineralization at Horne and Quemont. Due to the high permeability of the clastic strata,

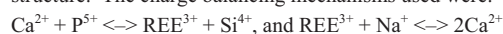
hydrothermal fluid flow was diffuse resulting in the formation of large, alteration zones (sericite and chlorite) around the massive sulphide lenses.

The volcanic setting of the Horne and Quemont deposits is distinct from the Cu-Zn-rich VMS deposits of the main Noranda camp. The latter deposits are slightly younger (2702-2697 Ma) and hosted by flow-dominated, mostly mafic volcanic successions that contain $< 5\%$ volcanoclastic rocks. Subseafloor infiltration and replacement was only of minor importance during massive sulphide formation in the main Noranda camp. In contrast to Horne and Quemont, the deposits are underlain by well-defined discordant alteration zones. (SS7; Wed. 8:40)

Rare earth element substitution and charge balancing in synthetic apatite

Moore, B.T., Hanchar, J.M., Chafe, A., Department of Earth Sciences, Memorial University of Newfoundland, St John's, NL A1B 3X5, and Fournelle, J., Department of Geoscience, University of Wisconsin, Madison, WI 53706 USA

The widespread occurrence of fluorapatite ($\text{Ca}_5[\text{PO}_4]_3\text{F}$), and its ability to concentrate rare earth elements (REE), makes it an ideal mineral to study substitution and charge balancing in natural systems. In order to assess the amount of chemical substitution of REEs that can occur in apatite, and possible charge balancing mechanisms, six syntheses of REE-doped fluorapatite were done. Three apatite syntheses with increasing amounts of REEs equal to $1\times$, $10\times$, and $100\times$ natural concentrations were charge-balanced with Si. An additional three syntheses were with also doped at the same concentration of REEs and charge balanced with Na in order to determine which element allowed for a higher amount of REEs to become incorporated in the apatite structure. The charge balancing mechanisms used were:



The $100\times$ Si+REE doped apatite crystals resulted in a higher concentration of REEs in the apatite than the equivalent Na+REE doped crystals. The apatite crystals showed a general decrease in REEs from the crystal centers to the edges. In some crystals, however, it was difficult to determine if the crystal centers were perfectly exposed in the polished epoxy mounts thereby making it difficult to confidently observe the center to rim trend. None of the synthetic apatite crystals were highly depleted in REEs at the crystal edges which suggests that the “reservoir” in which the crystals grew did not become depleted in REEs during the syntheses and that any concentration gradient across the crystals was due to other factors. The significant increase in REEs with increasing doping levels suggests that the apatite crystals did not become saturated with REEs. In the lower doping levels ($1\times$ and $10\times$) the Si and REE-doped crystals resulted in a higher concentration of REEs than the REE and Na-doped crystals. It was subsequently determined that the REE and Na-doped crystals did not contain REEs charged balanced with Na, but instead with Si in its place which was likely an impurity from one of the starting synthesis reagents. The Na may have been lost in the synthesis due to volatilization or it was not preferentially incorporated into the apatite structure. The dominance of Si as a preferential charge-balancing element over Na cannot be confirmed, however, by the results in this study. Further experiments are currently being done, under vacuum, to establish the efficacy of Na and Na and Si to charge balance the REEs in apatite. (SS6; Wed. 8:40)

Rare-earth mineralization in the Bear Lodge alkaline complex, Wyoming: Mineralogical and isotopic characteristics

Moore, M.A., Chakhmouradian, A.R., Sidhu, R., Yang, P., Department of Geological Sciences, University of Manitoba, Winnipeg, MB R3T 2N2, mamarsters@gmail.com, Mariano, A.N., 48 Page Book Road, Carlisle, MA USA, and Spencer, E.A., Carleton Geoscience Centre, Department of Earth Sciences, 1126 Herzberg Laboratories, Carleton University, Ottawa, ON K1S 5B6



The Bear Lodge alkaline complex, part of the northern Black Hills intrusive suite of alkaline to sub-alkaline rocks, hosts complex rare earth element (REE) mineralization in carbonatite veins, dikes, and stockwork in the Bull Hill area. The deposit is zoned; near-surface samples are pervasively oxidized, whereas unoxidized carbonatite veins are present at depth. A transitional zone occurs between the unoxidized and oxide zones. Burbankite is a primary REE mineral in the carbonatites, but is rarely preserved. We identified complexly zoned burbankite crystals showing Ce- and Nd-dominated REE patterns in two different parageneses. Postmagmatic processes caused replacement of this burbankite by ancyllite-Ce and barite (\pm strontianite). Other samples from the unoxidized zone contain four different types of polycrystalline pseudomorphs after a hexagonal mineral, most likely burbankite. The dominant rare-earth mineral(s) in these parageneses are, respectively, ancyllite, REE fluorocarbonate, REE fluorocarbonate + fluorite, and REE fluorocarbonate + ancyllite. Polyphase mineralization events in the unoxidized zone, followed by carbo-hydrothermal reworking in the transitional and oxide zones are manifested by variations in texture, mineralogy and mineral chemistry (notably La/Ce_{m} vs. La/Nd_{m}). Chondrite-normalized REE profiles are sub-horizontal in the La-Pr region, and often profiles from the same mineral have distinct pairs that pivot around Ce.

Preliminary interpretations of stable-isotope C-O data indicate that only the REE fluorocarbonate paragenesis from the unoxidized zone plots in the primary igneous carbonate field. Other parageneses from the unoxidized zone, including calcite from one burbankite sample, are relatively homogeneous and indicate a light-carbon-enriched mantle source ($\delta^{13}\text{C}_{\text{V-PDB}} = -10.2$ to -7.3‰ ; $\delta^{18}\text{O}_{\text{V-SMOW}} = 8.7$ to 12.5‰). Samples from the transitional and oxide zones do not show consistent correlations, but could reflect low-temperature alteration ($\delta^{13}\text{C}_{\text{V-PDB}}$ up to -2.7‰ and $\delta^{18}\text{O}_{\text{V-SMOW}} = 9.6$ to 18.0‰). Radiogenic isotopic data from unoxidized parageneses are generally homogeneous and fall in the following range: $^{87}\text{Sr}/^{86}\text{Sr} = 0.704584$ – 0.704639 , $^{143}\text{Nd}/^{144}\text{Nd} = 0.512594$ – 0.512635 . The calculated Nd ages reflect prolonged REE enrichment in the mantle source. (SS6; Wed. 2:40)

Olivine grain growth in a Fe-S matrix. A tool to interpret formation of Pallasite meteorites

Muir, S.L. and Solferino, G.F.D., Mount Royal University, 4825 Mount Royal Gate SW, Calgary, AB T3E 6K6, muir.sarah@gmail.com

Pallasite meteorites are thought to represent samples of early-formed planetary bodies that have been successively disrupted by large impacts before the separation of the metal from the silicates. Pallasites can be divided into two groups, one with angular olivines and the other one with rounded crystals. These crystals range from 1 mm to 2–3 cm in size (e.g., Eagle Station, Brenham) within a metal matrix. This dualism is evident again when considering the composition of the metal phase, which could be almost pure Fe-Ni alloy (e.g., Esquel, Imilac) or high-S rich (e.g., Phillips County). For more than three decades studies on Pallasite mineralogy, texture, major and trace element compositions have been carried out to better understand their origin and formation conditions (this includes temperature, depth, and time of formation). Pallasite-like material was synthesized in a number of experimental studies. In this study, a series of annealing experiments was performed on aggregates of San Carlo's olivine and Fe-S powder with a starting grain size of about 2 micrometers, similar to the supposed particle size of silicates in the solar nebula. Experiments were performed in an end-loaded piston cylinder press at 1 GPa and 1100 to 1430 °C for 8 to 300 h. Digital analyses of BSE images from samples cut-sections enabled the derivation of a grain growth law for olivine in a molten metal matrix for the first time. By using the newly calculated growth curve we computed the amount of time required for olivine grains to reach a grain size of 1–20 mm, as observed in Pallasite meteorites, for a range of temperatures within the accepted limits for terrestrial proto-planet interiors, i.e. 1000–1400 °C. Annealing at 1000 °C yields 20 mm olivine grains in 10 million years, whereas at 1400 °C, the time is reduced to 50,000 years. The growth rate of olivine in Fe-S can also be

used to estimate the rounding time of olivine fragments, and therefore estimate maximum cooling time and/or original temperature of Pallasites with angular olivine. Comparison with literature may indicate two possible distinct origins for Fe-Ni- and Fe-Ni-S-bearing Pallasite meteorites. (SS18; Thurs. Poster)

Petrological and chemical characterization of high-purity quartz deposits with examples from Norway

Müller, A., axel.muller@ngu.no, Wanvik, J.E. and Ihlen, P.M., Geological Survey of Norway, N-7491 Trondheim, Norway

Demand for high-purity quartz (HPQ) is strongly increasing worldwide owing to growing consumption and an increasing range of high-technology applications. Ensuring security of supply requires the identification and characterization of new HPQ deposits and possibly of a different kind to those currently in production. Prerequisites for developing exploration tools for such deposits are the application of state-of-the-art micro-analytical methods for appropriate petrological and chemical characterization of potential deposits and to gain a better understanding of the geological environment and conditions of HPQ formation.

HPQ is generally defined as quartz containing less than $50 \mu\text{g g}^{-1}$ of contaminating elements. However, the industry requires concentrations limits for a number of detrimental elements controlling the quality of the quartz product. A refined HPQ definition is suggested proposing concentration limits $\text{Al} < 30 \mu\text{g g}^{-1}$, $\text{Ti} < 10 \mu\text{g g}^{-1}$, $\text{Na} < 8 \mu\text{g g}^{-1}$, $\text{K} < 8 \mu\text{g g}^{-1}$, $\text{Li} < 5 \mu\text{g g}^{-1}$, $\text{Ca} < 5 \mu\text{g g}^{-1}$, $\text{Fe} < 3 \mu\text{g g}^{-1}$, $\text{P} < 2 \mu\text{g g}^{-1}$ and $\text{B} < 1 \mu\text{g g}^{-1}$ while the sum of all elements should not exceed $50 \mu\text{g g}^{-1}$. The content of these elements is controlled by intracrystalline impurities including (i) lattice-bound trace elements, (ii) submicron inclusions $< 1 \mu\text{m}$, and (iii) mineral and fluid micro-inclusions ($> 1 \mu\text{m}$) in quartz. These impurities cannot be removed by conventional processing and examples of them are discussed on the hand of potential and economic Norwegian HPQ deposit. The deposits include the Melkfjell quartzite, Solor kyanite quartzites, Nedre Øyvollen pegmatite and the Kvalvik, Nesodden and Svanvik hydrothermal quartz veins. They represent a wide range of formation environments including hydrothermal, igneous and metamorphic settings. Impurities in quartz of these deposits were identified and analyzed by backscattered electron (BSE) and cathodoluminescence (SEM-CL) imaging and laser ablation inductively coupled plasma mass spectrometry (LA-ICP-MS).

The processes leading to HPQ formation differ for the various deposits and include (i) crystallization of quartz from primitive niobium-yttrium-fluorine (NYF)-type pegmatite melts (Nedre Øyvollen), (ii) crystallization of hydrothermal quartz at greenschist-facies conditions and subsequent quartz refinement due to post-crystallisation re-crystallization at greenschist- to lower-amphibolite-facies conditions (Nesodden, Kvalvik, Svanvik), and (iii) solid-state crystallization of quartz-rich rocks at amphibolite-facies conditions and subsequent quartz refinement due to post-crystallisation re-crystallization at greenschist- to lower-amphibolite-facies conditions (Melfkjell, Solor). (SS12; Thurs. 9:00)

Evolution of magmatic-hydrothermal ore systems in response to secular changes in sulphur, oxygen, biospheric processes, and geothermal gradients from the Archean to the present

Mumin, A.H., Department of Geology, Brandon University, 279-18th Street, Brandon, MB R7A 6A9, mumin@brandonu.ca, and Richards, J.P., Earth and Atmospheric Sciences, University of Alberta, Edmonton, AB T6G 2E3

Magmatic-hydrothermal ore systems evolved from the Archean to present day in response to secular changes in atmospheric oxygen levels, seawater sulphur concentration and oxidation state, biospheric processes and decreasing geothermal gradient. These changes are manifested in a continuum of porphyry copper (PC) and iron oxide-copper-gold (IOCG) systems generated from subduction modified subcontinental lithosphere.

IOCG and PC deposits share many characteristics, but remain distinct. Both deposit types originate with the introduction of volatiles



(H₂O, CO₂, S, Cl) to sub-continental lithospheric mantle during slab dehydration, and subsequent generation of Cu±Au rich calc-alkaline to mildly alkaline, oxidized and H₂O rich magmas. Emplacement of these magmas in high-level batholiths followed by post-emplacement system evolution within a variety of orogenic and post-orogenic settings results the observed variety of porphyry copper and IOCG deposit types. However, IOCG deposits dominated in the Archean and Proterozoic while PC deposits dominate in the Phanerozoic.

IOCG systems also differ in the greater extent of their high-temperature (>3500C) alterations (Na, Na-K-Fe-Ca, K-Fe), which can reach 1 to >7 kilometres in width. In contrast, high temperature K-Fe alteration in PC systems is typically 1-2 km in extent. While magmatic-hydrothermal fluids start out neutral for both deposit types, abundant SO₂ in PC fluids disproportionates during cooling to generate strongly acid conditions and great extents of phyllic ± advanced argillic alteration. IOCGs are low sulphur systems and therefore do not generate acid fluids on cooling; associated alteration is equilibrated with neutral to only mildly acidic fluids, and is typically characterized by hematite-chlorite-sericite-carbonate±quartz assemblages. The more extensive high-temperature alteration associated with IOCG deposits is believed to result primarily from their formation in "hot" rock. We attribute the higher ambient host-rock temperatures to higher paleo-geothermal gradients, and/or formation within the metamorphic aureoles of their associated batholiths.

Secular changes in seawater and seafloor sulphate concentration caused by changing biospheric oxygen levels, the onset of oxidative weathering, ocean ventilation, and oxidative bioturbation directly affected sulfate fixing in the seafloor and consequently sulfate available for slab dehydration and formation of fertile oxidized magmas. A paucity of seawater sulphate in the Archean and earliest Proterozoic (~0.2 mM) led to sulphate-poor magmas that favoured generation of IOCG over PC deposits in the Precambrian. A gradual increase in seawater sulphate during the Proterozoic followed by a dramatic increase in the Phanerozoic to present levels of ~28.4 mM facilitated formation of sulphate-rich magmas that favoured PC generation in the Phanerozoic. (SS23; Fri. 9:00)

An eastern Mediterranean analogue for the Late Palaeozoic evolution of the Pangaea suture zone in SW Iberia

Murphy, J.B., bmurphy@stfx.ca, Braid, J.A., Dahn, D., Gladney, E., Dupuis, N., Department of Earth Sciences, St. Francis Xavier University, PO Box 5000, Antigonish, NS B2G 2W5, and Quesada, C., Instituto Geológico y Minero de España (IGME, c/ Ríos Rosas 23, 28003 Madrid, España

It has long been recognized that the Late Paleozoic evolution of SW Iberia preserves a record of collision and suturing between Laurussia (South Portuguese Zone) and Gondwana (Ossa Morena Zone), which is one of the key events in the development of the Variscan orogen and the amalgamation of Pangea. The suture zone (Pulo de Lobo Zone) is an accretionary complex characterized by greenschist facies polydeformed and imbricated assemblage meta-sedimentary rocks, mélanges, mafic complexes and recent work has shown that it also contains clastic sequences derived from exotic crustal fragments. Mafic complexes have NMORB compositions, highly depleted Sm-Nd isotopic signatures and geochronological data imply that their protoliths probably formed between ca. 350 and 340 Ma. The accretionary complex was intruded by ca. 340-310 Ma composite plutons and related dykes ranging from gabbro to granite in composition. The oldest phases of these intrusions are syn- to late-tectonic with respect to the deformation. Much of the tectonic evolution of the Pulo de Lobo suture zone post-dates the onset of collisional tectonics elsewhere in the Variscan orogen, and is broadly analogous to the Cenozoic evolution of the eastern Mediterranean oceanic tracts relative to the ongoing collision between the African, Eurasian and Arabian plates. (SS11; Fri. 10:20)

Keynote (40 min): Grandmother teaching Earth Science

Murphy, L.A., Manitoba Geological Survey, 360-1395 Ellice Ave., Winnipeg, MB, Linda.Murphy@gov.mb.ca, and Sinclair, K., Anishinabe Grandmother, Winnipeg, MB

Grandmothers and Grandfathers are the ancestral teachers of Anishinabe. Elders of each community are experts in their fields of study in much the same way that mainstream educators are in schools today. Members of each community learned to live well in harmony with the land, to understand Earth processes, and to prosper in a respectful way. These ancestral world views came from Circle teachings conducted and delivered by Elder experts in each community. The focus of this teaching will be on Anishinabe connection to our Mother Aki and the teaching Circle will focus on key principles from Anishinabe's Creation Story and how this connects all peoples to Earth. (SS22; Thurs. 8:40)

Bismuth dispersion in the supergene zone

Murphy, T.M., timothy.murphy@uws.edu.au, Leverett, P. and Williams, P.A., University of Western Sydney, Locked Bag 1797, Penrith, NSW

Proper understanding of the dispersion of Bi in the regolith will depend on an appreciation of its low temperature aqueous chemistry and knowledge of the important secondary Bi minerals that serve to buffer the element between the solid and solution states. The behaviour of Bi in terms of its solution speciation as a function of pH is well-established and provides a first-order, but over-simplified, assessment of its mobility in pore solution in the regolith. However, very little is known of the chemistry of formation of secondary Bi species in the supergene zone or of their stabilities. This is a serious deficiency for the interpretation of Bi anomalies in the regolith formed as a result of the oxidation of primary, Bi-bearing mineralisation.

The mineralogy of Bi is surprisingly diverse for an element which is rare. Some 200 plus separate species that contain essential Bi are currently recognised by the IMA and of these 61 are secondary phases. Primary phases vary from the comparatively "simple", in terms of stoichiometry, to the exceedingly complex. Native bismuth and bismuthinite, Bi₂S₃, are both common, but many complex Bi-bearing sulfosalts are known. However, a survey of the literature reveals that the majority of the Bi minerals, whether of primary or secondary origin, are extremely rare and that only a few are found repeatedly in Nature.

Chemical modelling of the solubility of the common secondary species bismutite, Bi₂O₂CO₃, and bismoclite, BiOCl, under various conditions suggests that their solubilities are quite limited, even under relatively acid conditions. This work has now been extended to include studies of bismite, Bi₂O₃, koechlinite, Bi₂MoO₆, Russellite, Bi₂WO₆, cannonite, Bi₂(SO₄)O(OH)₂, and a series of secondary Bi arsenates. This has led to a understanding of Bi dispersion in the supergene environment. The model has widespread applications in exploration geochemistry where Bi is used as a pathfinder element and suggests that bismuth may be an extremely useful pathfinder element when used in combination with other geochemical indicators. Applications involving a number of deposits, focussed on the New England region of New South Wales, Australia are presented. (GS1; Fri. 2:00)

Did komatiites contribute to TTG formation in the Archean?

Nair, R.¹, rnair@ucalgary.ca, Chacko, T.², Verwimp, J.¹ and McDowell, K.¹, ¹University of Calgary, 2500 University Drive NW, Calgary, AB T2N 1N4; ²University of Alberta, 1-26 Earth Sciences Building, Edmonton, AB T6G 2E3

Archean TTGs are considered by some to be equivalent to Phanerozoic adakites; direct partial melts of the basaltic portion of the down-going slab, leaving behind an eclogitic residue. Adakites and some late-Archean TTGs have higher Mg# (Mg/(Mg+Fe))(Mg#>51) than melts generated from basaltic source rocks (average Mg# ~40). Some (e.g. Martin and Moyen, 2002) have attributed the higher Mg#'s of TTGs to interaction of TTG melts with mantle peridotite during ascent. However, it is also plausible that Mg-rich lithologies like komatiites



and komatiitic-basalts may have been important constituents of Archean mafic crust and may have melted to produce Mg-rich melts.

To investigate this possibility, we conducted dehydration-melting experiments on a metamorphosed komatiite (SiO_2 -48.26; Al_2O_3 - 7.19; MgO -18.66, TiO_2 -0.5, CaO -8.49, Na_2O -0.5, K_2O -0.05, hydrous totals in wt.%) from the Isua greenstone belt (Furness *et al.*, 2007). The experiments were conducted in a piston cylinder apparatus at 900 and 1000°C from 7-20 kbar. Preliminary results show that tonalitic-trondhjemite melts can be generated from the partial melting of hydrated komatiites. Melts produced have 56-65 wt.% SiO_2 and Mg\# 's ranging from 0.22 to 0.71 (calculated on an anhydrous basis and after correcting for Na loss). The higher end of the range of Mg\# is much higher than the most magnesian melts produced from basaltic source rocks. Unlike the granulite or eclogite residue produced by partial melting of basaltic compositions, melts generated from komatiite coexist with a residual assemblage that changes from olivine websterites or garnet-free pyroxenites at low pressure (<12.5 kbar at 900°C and <15 kbar at 1000°C) to garnet-bearing pyroxenites at higher pressures. Garnet formation occurs at relatively lower pressure (10 kbar) in basaltic compositions than in the komatiite composition investigated in this study.

Partial melts need to equilibrate with a garnet-rich residue to explain the strong heavy rare earth element (HREE) depletion observed in natural TTG's. The present results indicate that for komatiitic bulk compositions melting must occur at depths >40 km to produce the requisite HREE depletion. Alternatively, TTGs could form by crystallization from hybrid melts produced by mixing of melt from basaltic and komatiitic source rocks at similar depths. Contribution of melts from a high-Mg source rock like komatiite may also explain (as an alternative to TTG melt-peridotite interaction) the formation of TTGs with high Mg\# 's. Generating large volumes of typical TTGs through burial of hydrated source rocks to depths >40km requires either substantial thickening of oceanic crust or could more reasonably be explained by subduction type processes that produce Phanerozoic adakites. (GS2; Wed. 3:00)

From uraninite to clusters to uranyl minerals - Thermochemical studies

Navrotsky, A., University of California Davis, One Shields Ave, Davis, CA 95616 USA, anavrotsky@ucdavis.edu

The oxidation of uraninite (nominally UO_2 , which has low solubility in water) to soluble U^{6+} species can occur by a variety of pathways. Here we consider the thermodynamic stability of peroxide-containing uranyl minerals, ranging from the mineral studtite to U28 and U60 clusters, which may persist in solution or precipitate as solid phases. New thermochemical data, obtained by high temperature oxide melt solution calorimetry, are presented. Stabilized by alkali cations, these uranyl peroxide clusters offer a thermodynamically viable pathway for uranium oxidation and transport in aqueous environments including seawater. They are intermediate in energy between dissolved U^{6+} species and the final solid products: uranyl hydroxide, carbonate, phosphate, and silicate minerals. (SS5; Wed. 8:20)

Hydrothermal synthesis, crystal structure, and characterization of three silver uranium diphosphonate and a 3D thorium carboxylate

Nelson, A-G.D., nelsona@umich.edu, Ewing, R.C., University of Michigan, North University Avenue, Ann Arbor, MI 48109 USA, and Albrecht-Schmitt, T., Florida State University, Tallahassee, FL 32306 USA

The applications of diphosphonate ligands to nuclear waste remediation and actinide separation have been well developed. A series of actinide phosphonates have been synthesized and structurally characterized, allowing structural comparisons to be made. In an expansion, three heterobimetallic $\text{UO}_2^{2+}/\text{Ag}^+$ methylenediphosphonates have been prepared from mild hydrothermal treatment of uranium trioxide, methylenediphosphonic acid (C1P2) with silver nitrate, and small aliquots of HF at 200°C. The three compounds are layered but differ in the coordination around the metal center and successive binding by the

ligands to the silver center. The three-dimensional thorium carboxylate compound possesses a thorium trimer that is bonded through the CO_3^{2-} moiety of the carboxylate ligand, and further connects to produce small channels filled with occluded water molecules. Here, we will compare and contrast the phosphonate and carboxylate ligand, and look at the effects of counter ions on structure formation. High pressure Raman studies will also be discussed for these samples. (SS5; Wed. Poster)

Quaternary glaciation and stratigraphy of the Ridge River area, northern Ontario

Nguyen, M.K., mnguye48@uwo.ca, Hicock, S.R., Western University, Biological & Geological Sciences Building, Room 1026, London, ON N6A 5B7, and Barnett, P.J., Ontario Geological Survey, 933 Ramsey Lake Rd., Sudbury, ON P3E 6B5

A comprehensive study of the Quaternary sediments in the Ridge River area in northeastern Ontario provides valuable insight into the glacial past of a region which until now has been studied only in reconnaissance. An information gap exists in this area which lies near the southern margin of the James Bay Lowland and relatively close to the geographic centre of what was once the Laurentide Ice Sheet. A stratigraphic study of riverbank exposures not only provides details regarding the behaviour of the Laurentide Ice Sheet in this area but also advances our understanding of the distribution of materials and their related depositional environments in this sparsely studied region.

Conducted during the summer of 2012, fieldwork consisted of helicopter supported exploration of exposed riverbanks in the Ridge River area located approximately 85 km northwest of the town of Hearst, Ontario (with the entire study area covering nearly 6000 km²). Stratigraphic units at every exposed section examined were carefully measured and described. Till matrix samples collected were subsequently analyzed for particle size distribution and carbonate content (including calcite and dolomite proportions). Supplementary data include heavy mineral content, pebble counts (pebble lithology identification), till fabrics and various structural measurements (e.g. orientation of shear planes, extension fractures, striations, etc.) within and below the till units.

The information garnered from field observations and subsequent analyses should reflect the number of distinct till units and their associated ice-flow directions. Such information should provide a better understanding of local glacial history including ice-flow patterns and past glacial and non-glacial episodes. Furthermore, the location of the Ridge River study area is of particular importance since it may reveal links between the distribution of Quaternary sediments in the Hudson Bay Lowland and the Canadian Shield to the south. (GS6; Wed. Poster)

Diamond sources beneath the Hall Peninsula, Nunavut: A preliminary assessment based on micro-diamonds

Nichols, K.¹, Stachel, T.¹, Stern, R.A.¹, hogberg@ualberta.ca, Pell, J.² and Mate, D.³, ¹University of Alberta, Edmonton, AB T6G 2E3; ²Peregrine Diamonds, Vancouver, BC V6B 1C6; ³Canada-Nunavut Geoscience Office, Iqaluit, NU X0A 0H0

The Chidliak kimberlites, 120km northeast of Iqaluit on the Hall Peninsula, Southern Baffin Island, Nunavut, tap diamond sources in the lithospheric mantle of unknown paragenesis, age and history. Many of the recently discovered kimberlites have proven to be diamondiferous. Micro-diamonds (here defined as $\leq 600 \mu\text{m}$) and macro-diamonds ($>600 \mu\text{m}$) were recovered during the initial kimberlite sampling: 46 of 64 kimberlites were tested for diamonds, and commercial sized diamonds were recovered from 41% of the kimberlites. Approximately 740 micro-diamonds have been provided by Peregrine Diamonds Ltd., of which 210 (size range of 210 to 600 μm) are utilized for geochemical analyses. Morphological characteristics, carbon isotopic compositions, and nitrogen characteristics of Chidliak micro-diamonds are used to constrain diamond sources in the cratonic root, mantle residence times, and conditions of diamond formation and preservation beneath the Hall Peninsula.



Cathodoluminescence imaging of polished micro-diamonds shows octahedral, cuboid, and aggregate growth, although extremely complex internal growth structures are also observed. Carbon stable isotope compositions and nitrogen contents were measured *in situ* (MC-SIMS) for 92 micro-diamonds. The $\delta^{13}\text{C}$ (defined as: $\delta^{13}\text{C}(\text{sample}) = [(((^{13}\text{C}/^{12}\text{C})_{\text{sample}}/(^{13}\text{C}/^{12}\text{C})_{\text{std}}) - 1) \times 1000]$) values range from -1.3 to -28.6‰, with a mode around the mantle value (-5‰), and another minor mode about -15‰. Nitrogen was subsequently measured on the same spot locations as the carbon isotopes. Chidliak micro-diamonds have nitrogen contents ranging from 0.2 to 3833 atomic ppm (at.ppm), with a median of 1170 at.ppm. Using FTIR spectroscopy, it is observed that Chidliak micro-diamonds have nitrogen contents ranging from below the limit of detection (~10 at.ppm) to 3356 at.ppm, with an average nitrogen concentration of 1237 at.ppm. Combining the presence of ^{13}C depleted diamonds with such overall high nitrogen contents suggests that Chidliak diamonds derive, at least partially, from eclogitic mantle sources.

Assuming a mantle residence time (*e.g.*, 3 Ga or 1 Ga), it is possible to use the measured nitrogen abundance and aggregation to calculate time averaged mantle residence temperatures. Only high quality infrared spectra are used in determining temperature; the Chidliak micro-diamonds show a range from ~960 to 1260°C, when projected onto the local paleo-geotherm of Pell *et al.* 2012, this corresponds to a depth range of ~150-190km. (SS4; Fri. 9:00)

Mineralogy, geochemistry and facies variations of a potential shallow shale gas play within the Cretaceous Carlile and Favel formations, southwestern Manitoba

Nicolas, M.P.B., michelle.nicolas@gov.mb.ca, Bamburak, J.D., Manitoba Geological Survey, 360-1395 Ellice Avenue, Winnipeg, MB R3G 3P2, Hosseinienejad, S. and Pedersen, P.K., Department of Geoscience, University of Calgary, Calgary, AB T2N 1N4

The potential for shallow shale gas within the Upper Cretaceous strata in southwestern Manitoba has been the centre focus of the Shallow Unconventional Shale Gas Project. Geochemical, mineralogical and facies mapping has indicated that the Cretaceous Carlile and Favel formations are two of the most prospective gas-bearing formations in southwestern Manitoba. With limited core data, most of the work was first conducted by detailed mapping and sampling of all the Upper Cretaceous formations along the Manitoba Escarpment. Recently, core sampling, analysis and detailed core logging has assisted in understanding the variations and similarities between the outcrops and the subsurface.

The biggest difference between outcrop and subsurface mineralogy is the abundance of secondary minerals in the shale units exposed at surface, versus the relatively simple carbonate and siliciclastic-dominated mineralogy in the subsurface. In contrast, Rock-Eval geochemistry, particularly total organic content (TOC) and organic maturation levels, are relatively unaffected by weathering, thus the abundant outcrop data can serve as a guide to understand the subsurface. Classified as a biogenic gas play, the organic shale units have TOC values up to as high as 11% but are thermally immature, having never been subjected to enough burial and heat for the organic shale to enter the oil window.

Detailed facies descriptions from core have identified ten major lithofacies within the Morden Member of the Carlile Formation and the Favel Formation. These facies range from noncalcareous organic mudstone to highly calcareous, bioturbated very fine-grained sandstone. These represent a change from offshore shale deposits to shallow water carbonate-rich sediments. The bioturbation intensity varies from rare to moderate representing more distal environmental settings from relatively anoxic to oxic interfaces. (SS13; Thurs. Poster)

Oil shale and reservoir rocks of the Hudson Bay Lowland, northeastern Manitoba

Nicolas, M.P.B.¹, michelle.nicolas@gov.mb.ca, Lavoie, D.² and Armstrong, D.K.³, ¹Manitoba Geological Survey, 360-1395 Ellice Avenue, Winnipeg, MB R3G 3P2; ²Geological Survey of

Canada, 490 de la Couronne, Québec, QC G1K 9A9; ³Ontario Geological Survey, 933 Ramsey Lake Road, Sudbury, ON P3E 9B5

The Hudson Bay and Foxe Basins Project is part of the Geological Survey of Canada Geo-mapping for Energy and Minerals (GEM) program. In Manitoba, the Hudson Bay Basin is represented by the Ordovician to Devonian carbonate succession of the Hudson Bay Lowland (HBL) in the northeastern corner of the province, and measures up to more than 900 m thick in the most northeasterly point near the Ontario boundary.

Only three onshore hydrocarbon exploration wells have been drilled and cored in Manitoba. Several mineral exploration boreholes and geotechnical holes have also provided core and stratigraphic data. Core samples for biostratigraphical analysis were collected, and conodont and chitinozoan analyses were used to assist in formational assignments. RockEval™ 6 analyses were conducted on 37 samples from Silurian and Ordovician formations to identify potential source rocks in the succession preserved in the HBL of Manitoba.

Overall, the RockEval™ 6 analyses resulted in the recognition of a fair number of samples having moderate to good source rock potential, but most of them are thermally immature. One sample from the Red Head Rapids Formation yielded a total organic carbon content of 8.44 wt. %, thus it is considered a true oil shale, and two other samples of this formation are considered thermally mature with excellent oil-generation potential. The new discovery of oil shale in Manitoba, combined with previous discoveries onshore in Nunavut and Ontario and offshore in Hudson Bay, indicates potential source rocks occur at a number of different stratigraphic levels across the Hudson Bay Basin. These results are supported by core evidence for oil generation and subsequent long-distance migration.

Previously, the presence of hydrothermal dolomite (HTD) in core in the Hudson Bay Lowland was confirmed petrographically and with stable isotopes geochemistry. Two more occurrences of potential HTD in core indicate that this type of feature may be common in the Hudson Bay Lowland, which can serve as oil reservoirs. A magnetotelluric survey near the confirmed HTD occurrence indicated potential fault-controlled porous zones in the subsurface, which is common in HTD. Another potential reservoir target is the large reefal mounds within the Attawapiskat Formation which are pervasive throughout the Hudson Bay Lowland in Manitoba and Ontario.

Overall, this project has demonstrated that the Hudson Bay Basin has all the right elements and conditions for hydrocarbon systems to exist, including mature and diverse source rocks, attractive reservoirs and efficient traps and seals. (SS13; Fri. 8:20)

Compositional variations in Cs,Li,Mg-rich beryl from exocontact of the complex Manjaka pegmatite, Sahatany Valley, Madagascar

Novák, M.¹, mnovak@sci.muni.cz, Gadas, P.¹, Galiová Vašinová, M.² and Pezzotta, F.³, ¹Department of Geological Sciences, Masaryk University, Brno, Czech Republic; ²Department of Chemistry, Masaryk University, Brno, Czech Republic; ³Museo di Storia Naturale, Milano, Italy

Beryl shows compositional evolution from common beryl locally Na,Mg,Fe-enriched in outer zones to Cs,Li-rich beryl or pezzotite in the most evolved parts of some granitic pegmatites; however, beryl was also found in exo-/endocontacts. The complex Manjaka pegmatite (spodumene>Li-tourmalines+pollucite+rhodizite/londonite), ~5 m thick, cuts concordantly and discordantly banded Fe-poor calc-silicate rock. The pegmatite exhibits heterogeneous internal structure; the individual textural-paragenetic units including alplitic unit, spodumene-bearing units and elbaite-bearing units are rather randomly distributed. On direct endocontact with the host rocks, black tourmaline associated with blue fluorapatite is locally developed. Exocontacts do not show any visible changes; however, in the distance of several mm from the contact noteworthy and very complex mineral assemblages are developed forming bands arranged subparallel to the contact and distinct in their mineral composition. The bands contain the assemblage Di+Tr+Tur±Kfs±Qz±Cs-rich phlogopite in variable



proportions along with accessory Ta-rich titanite, scapolite, danburite, microcline, Mn-rich apatite, Nb-rutile and zircon. Subhedral to anhedral grains of highly heterogeneous beryl ($\leq 200 \mu\text{m}$) show oscillatory to patchy zoning apparent in BSE images controlled by high contents of Cs (0.24–0.50 *apfu*) and Mg (0.37–1.88 *apfu*). Beryl is also enriched in K (≤ 0.1 *apfu*; 0.8 wt.% K_2O), Na (≤ 0.09 *apfu*; 0.45 wt.% Na_2O), and Rb (≤ 0.04 *apfu*; 0.53 wt.% Rb_2O). Highly heterogeneous Cs, Mg-rich beryl from exocontact shows features of high fractionation (Cs, Li, Be) and *in-situ* contamination (Mg). The substitutions include (1) $\text{CH}_3\text{OAl}^{3+} = \text{CHR} + \text{OR}^{2+}$, where $\text{R}^+ = \text{Cs}, \text{Na}, \text{K}, \text{Rb}$; and $\text{R}^{2+} = \text{Mg} > \text{Fe}^{2+}$ leading to the theoretical formula $\text{CsBe}_3\text{AlMgSi}_6\text{O}_{18}$. Some analyses with very high Mg content and higher totals of oxides point to the substitution (2) $\text{T}_2\text{BeOAl} = \text{T}_2\text{AlOMg}$ leading to the theoretical formula $\text{CsBe}_2\text{AlMg}_2\text{Si}_6\text{O}_{18}$. Both formulas indicate potentially new species in the beryl group. Preliminary LA-ICP-MS data (≤ 2400 ppm Li) suggest minor participation of the substitution (3) $\text{CH}_3\text{OTBe} = \text{CHR} + \text{TLi}$ in both types of beryl. Beryl appears a good geochemical indicator of exo-/endocontact processes. It demonstrates high mobility of Cs, Be and Li, and high activity of Mg. High ability of beryl to incorporate some elements in contrast to the associated tourmaline (Li-poor dravite to uvite) is evident. This work was supported by the research project GAP210/10/0743 to MN and PG. (**SY2; Thurs. Poster**)

The Late Ordovician conodont extinction event in the context of carbon isotopic data and interpretation of the Ordovician - Silurian boundary in the Hudson Bay and Williston basins

Nowlan, G.S.¹, gnowlan@NRCan.gc.ca, Elias, R.J.², Young, G.A.³, Demski, M.W.², Stewart, L.A.², Wheadon, B.J.² and Dobrzanski, E.P.³, ¹Geological Survey of Canada, 3303 33rd Street NW, Calgary, AB T2L 2A7; ²Department of Geological Sciences, University of Manitoba, Winnipeg, MB R3T 2N2; ³The Manitoba Museum, 190 Rupert Avenue, Winnipeg, MB R3B 0N2

The formal placement of the Ordovician-Silurian boundary based on graptolites is not coincident with the major extinction event experienced by conodonts, but rather slightly above it. This has caused considerable difficulty in interpreting the location of the Ordovician-Silurian boundary precisely in the carbonate sequences of intracratonic basins in North America, where graptolites are essentially absent. Recent work on exposures and cores of the Stonewall and Fisher Branch formations in the Williston Basin of west-central Manitoba (Grand Rapids Uplands and Cormorant Hill) and on cored intervals and outcrops of the Port Nelson and Severn River formations in the vicinity of Churchill, Manitoba in the Hudson Bay Basin has provided new options for the interpretation of the boundary interval.

The Late Ordovician conodont extinction event represents a massive reduction of conodont diversity in which abundant and diverse Late Ordovician conodonts were replaced by an impoverished fauna, dominated by a few (pelagic?) simple cone taxa that made it through the extinction event and by representatives of the genus *Ozarkodina* which has a complex denticulate apparatus. The direct ancestor of *Ozarkodina* is not known but it was one of only two lineages of conodonts with complex denticulate apparatuses to survive the extinction. In shallow water deposits of intracratonic basins and in the basins marginal to Laurentia the key elements of the post-extinction fauna are typically *O. hassi* and *O. oldhamensis*. The equivalent strata in deeper water marginal basins are typically devoid of conodonts and other fossils until much later in the Llandovery, probably due to low oxygen levels in the deeper ocean. In a few sections in northern Canada, it is possible to demonstrate that post Late Ordovician extinction faunas occur with latest Ordovician graptolites. In other places the *Ozarkodina* fauna appears within strata interpreted as recording the Late Ordovician Hirnantian Isotopic Carbon Excursion (HICE). The demonstration of a positive $\delta^{13}\text{C}_{\text{carb}}$ excursion in sections in the Williston and Hudson Bay basins, albeit of smaller magnitude than typical HICE values, may point to an alternative placement of the Ordovician-Silurian boundary slightly above the Late Ordovician extinction event of conodonts. (**SS13; Fri. 9:20**)

Towards a model for HT behaviour of (orthorhombic and monoclinic) amphiboles

Oberti, R.¹, oberti@crystal.unipv.it, Boiocchi, M.², Welch, M.D.³ and Zema, M.⁴, ¹CNR-Istituto di Geoscienze e Georisorse, UOS Pavia, Italy; ²CGS, University of Pavia, Italy; ³Dept. Earth Sciences, The Natural History Museum, London, UK; ⁴Dept. Earth and Environmental Sciences, University of Pavia, Italy

Research over the last 30 years has significantly changed our knowledge of the amphibole supergroup, most particularly in recognizing new compositional spaces, including Li- and oxo-amphiboles. Systematic studies and the use of databases have provided detailed crystal-chemical models that have helped in deciphering the relations between cation ordering and structure. From this analysis it has been possible to evaluate the petrological significance of homovalent and heterovalent cation ordering. This detailed knowledge has also enabled a more accurate, comprehensive and robust scheme for amphibole classification and nomenclature to be constructed (Hawthorne *et al.* 2012), which takes into account all the chemical variability. In contrast, up to 2007 few data were available on the high-temperature behaviour of amphiboles, and especially of more geologically relevant compositions. These studies were hampered by the fact that thermal annealing generally induces in amphiboles three simultaneous processes: thermal expansion, cation disordering, and deprotonation. In order to unravel this complex behaviour, we have undertaken a program of systematic work that is still in progress. Thermal expansion was studied first in the simplest compositions, for which cation disordering and deprotonation processes are excluded. The study was extended to more complex compositions, which are of major relevance to petrology. Measurement of unit-cell parameters was combined with single-crystal structure refinement done at temperatures chosen to follow the irreversible deprotonation process, which occurs via ordering of Fe^{2+} at the *M*(1) and *M*(3) sites and its oxidation to Fe^{3+} , followed by data collection on cooling to investigate the deprotonated phase. All the available crystal-chemical knowledge was used to interpret changes (site-scattering, site and chain geometry, displacement parameters). Based upon these recent studies we present our first conclusions on the main chemical parameters and structural constraints affecting the complex HT behaviour of orthorhombic (anthophyllite, gedrite, ferro-holmquistite) and monoclinic (pargasite, potassic-pargasite, kaersutite, richterite, ferro-richterite) amphiboles and their partially deprotonated or oxo counterparts. The importance of symmetry, the nature of the B cations, the amounts of $^{\text{A}}(\text{K}, \text{Na})$, $^{\text{T}}\text{Al}$, $^{\text{C}}\text{Fe}$ and $^{\text{W}}\text{O}^{2-}$, and the consequent constraints in the relative expansion of the ribbon of octahedra and the double-chains of tetrahedral are discussed. (**SY1; Thurs. 9:20**)

Chemistry of the uranyl – sulfide systems

Oh, G.N. and Burns, P.C., University of Notre Dame, 301 Stinson-Remick Hall, South Bend, IN, USA, oh.15@nd.edu
[K(18-crown-8)]₂[UO₂(SH)₄], was synthesized from the reaction of 18-crown-6, K₂S, S, UO₂Cl₂, N(CH₂CH₃)₃, and PtCl₂ in DMF. The single-crystal structure shows that this compound contains typical U–S distances of 2.673(1) angstroms in a square planar coordination environment, and has the familiar uranyl moiety. The reaction mixture contains large species that are visible using ESI-MS and DLS. Attempts to synthesize the compound rationally from the reactions of KHS and UO₂(CF₃SO₃)₂ or UO₂Cl₂ in DMSO result in the formation of different large species, as determined by ESI-MS and DLS. (**SS5; Wed. Poster**)

Variations in shear-wave splitting across the Mid-Centroid Rift

Ola, O., Frederiksen, A., Deniset, I., Toni, D., Department of Geological Sciences, University of Manitoba, Winnipeg, MB R3T 2N2, ola@cc.umanitoba.ca, and the SPREE project team
The Mid-Centroid Rift (MCR) is a major feature of the North American continent: a 1.1 Ga rift that failed to develop into an ocean basin. Though the crustal expression of the rift is preserved, it is



impossible to determine from crustal evidence the nature of the lithospheric contribution to the rifting process. The installation of teleseismic instrumentation through the Superior Province Rifting Earthscope Experiment (SPREE) is allowing investigation of the lithosphere beneath the MCR, which will help in addressing questions about the initiation, propagation, and failure of the rift structure. We focus on observing the strength and orientation of lithospheric fabric through measurements of the splitting of teleseismic SK(KS) waves at instruments in and near the rift axis, using the method of Silver and Chan (1991) to find the set of parameters that optimally restores linear particle motion. Preliminary results show that the strong fabric observed in the Superior Province is interrupted by the MCR, suggesting that the rifting process affected the full thickness of the lithosphere. The direction of fabric is close to that of absolute plate motion, implying that an asthenospheric contribution is also present. (SS3; Thurs. Poster)

Hydrothermal remobilization of rare earth elements in a carbonatite-hosted rare earth element deposit, Bear Lodge Mountains, Wyoming

Olinger, D.A., Texas Tech University, Lubbock, TX 79409, USA, danielle.olinger@ttu.edu

The Bear Lodge Mountains of northeast Wyoming is the locality of a carbonatite-hosted rare earth element (REE) deposit. The carbonatite is emplaced as subvertical, northwest trending dikes primarily situated within three diatreme structures. The carbonatite dikes are primarily composed of calcite and < 20 percent hexagonal REE-mineralized-pseudomorphs after burbankite. The secondary REE-mineralization present in pseudomorphs progresses from ancylite [$\text{SrCe}(\text{CO}_3)_2\text{OH}\cdot\text{H}_2\text{O}$] at depth to bastnaesite group minerals [e.g. bastnaesite $(\text{Ce},\text{La})\text{CO}_3\text{F}$] nearer the surface. Up to three calcite textures are observed in samples: coarse-grained calcite with well-defined cleavage; fine-grained, anhedral to consertal, inclusion free calcite; and coarse-grained, consertal calcite with abundant inclusions of fluorite and calcite.

Calcite from several carbonatite samples were analyzed using laser ablation inductively-coupled mass spectrometry. The coarse-grained calcite with well defined cleavage have steep, negatively sloped, log-linear chondrite normalized REE patterns which parallel bulk rock patterns. The coarse-grained, consertal calcite with abundant inclusions have convex up, "humped" patterns whereas the fine-grained, anhedral, inclusion-free calcite have relatively flat patterns; neither of these patterns are typical of magmatic calcite and are more likely related to sub-solidus processes. The "humped" and relatively flat patterns are interpreted as the products of calcite recrystallization in the presence of a hydrothermal fluid. A hydrothermal fluid with hard ligands such as F^- and CO_3^{2-} would preferentially complex with and subsequently mobilize the light rare earth elements (LREE) producing the observed non-magmatic calcite REE patterns. The progression in REE mineralization from primary burbankite to bastnaesite group minerals is characterized by an increase rare earth oxide content which suggests that the mobilized LREE are being sequestered into the secondary REE-minerals throughout the dikes. (SS6; Wed. Poster)

Keynote (40 min): Metallogenic evolution of the Mackenzie and eastern Selwyn mountains of Canada's northern Cordillera, Northwest Territories: A compilation and review

Ootes, L.¹, Gleeson, S.², Turner, E.³, Rasmussen, K.⁴, Gordey, S.⁵, Falck, H.¹, Martel, E.¹ and Pierce, K.¹, ¹Northwest Territories Geoscience Office, Yellowknife, NT X1A 2R3; ²Earth and Atmospheric Sciences, University of Alberta, Edmonton, AB; ³Department of Earth Sciences, Laurentian University, Sudbury, ON; ⁴Department of Earth and Ocean Sciences, University of British Columbia, Vancouver, BC; ⁵Geological Survey of Canada, Vancouver, BC

The Mackenzie and eastern Selwyn mountains, Northwest Territories, Canada, are the northeast expression of the Cordilleran orogen and have a geologic history that spans the last one billion years. The region has

undergone a diverse tectonic evolution, which is reflected in an equally diverse collection of mineral deposits and prospects. More than 300 of these deposits and prospects have been documented in this area of the Northwest Territories and here they are categorized into mineral deposit types and their mode of formation evaluated and highlighted. The assignment of deposits and prospects to mineral deposit types in this study, highlights their characteristics and regional and temporal distribution. This study will be a useful guide for future mineral deposit research in the region, allow comparison with southern equivalents (southern Canada, United States, and Mexico), and assist the mineral explorationist in searching for and classifying new discoveries.

Stratiform/stratabound Cu-Ag occurrences are hosted in the Neoproterozoic Coates Lake Group, generally preserved in the hanging wall of the Cretaceous Plateau fault, and define a belt through the central part of the Mackenzie Mountains. Low-grade phosphatic stratiform iron (47.5% Fe) is preserved as iron formation in the Neoproterozoic Rapitan Group in the very northwest of the Mackenzie Mountains. Sedimentary exhalative Zn-Pb (\pm Ba) deposits are preserved in Cambrian through Devonian Selwyn Basin strata in the eastern Selwyn Mountains. Numerous carbonate-hosted Zn-Pb (\pm base-metals) occurrences are within the Paleozoic Mackenzie Platform strata of the Mackenzie Mountains. Cretaceous felsic-intermediate plutons that are present throughout the eastern Selwyn Mountains, are associated with Tungsten-skarn (proximal to intrusions), base-metal skarn (distal from intrusions), rare-metals and semi-precious tourmaline related to pegmatites, and vein-hosted emeralds. Other types of potential interest include coal deposits, placer gold, and possible Carlin-type gold deposits that have recently been identified to the west in the Yukon. (SS19; Wed. 2:00)

Keynote (40 min): Whence came Hottah Terrane?

Ootes, L.¹, luke_ootes@gov.nt.ca, Davis, W.J.² and Jackson, V.A.¹, ¹NWT Geoscience Office, Box 1500, Yellowknife, NT X1A 2R3; ²Geological Survey of Canada, 601 Booth Street, Ottawa, ON K1A 0E8

The Hottah Terrane is the westernmost exposed bedrock of the Canadian Shield. It has been interpreted as an exotic micro-continent with an overriding arc that collided with the western Slave Craton at 1882 Ma. The oldest bedrock preserved in the Hottah Terrane is the Holly Lake metamorphic complex (HLMC), which is dominated by ca. 1.97 Ga detrital zircon, with older zircons at 2.1, 2.3-2.45, and 2.63 Ga. The Hottah plutonic complex was emplaced between ca. 1931 and 1913 Ma, and the younger phase may represent an arc root. These units were rapidly unroofed by 1906 Ma. They are unconformably overlain by volcanogenic conglomerate and sandstone that give way to overlying subareal high-temperature rhyolite with less voluminous basalt and andesite. These volcanic rocks were derived from a subduction-modified mantle in a pull-apart setting. This sequence is topped by quartzite, which is in turn overlain by 1895 Ma marginal basin basalt with minor interbedded rhyolite. This stratigraphy on the HLMC and Hottah plutonic complex is consistent with an extensional or transtensional environment from ca. 1910 to 1890 Ma. The younger Treasure Lake Group and <1873 Ma Great Bear magmatic zone were constructed on this composite basement.

The pre-2.0 Ga temporal evolution of the Hottah Terrane is similar to other terranes of the western Canadian Shield (WCS), such as the Queen Maud block, Buffalo Head Terrane, or western Rae Craton. The timing of 2.0 to 1.93 Ga events are identical to that of the Thelon and Taltson magmatic zones and other more cryptic WCS terranes. These, including the source region to the ca. 1.97 Ga Coronation passive margin and Goulburn Supergroup, were all exposed to the same tectonic processes. However, the post 1.9 Ga Hottah history is not similar to these other terranes. To account for this, it is interpreted that the >1.91 Ga Hottah Terrane evolved in an active margin adjacent to other WCS terranes to the south of the Slave craton. Between 1.91 and 1.89 Ga, Hottah was rifted off this margin and translated northward along the proto-Wopmay fault, where it arrived alongside the western Slave craton at 1.88 Ga. Orogenesis continued through to the end of the



Great Bear magmatism at 1850 Ma. A comparable example of this terrane translation may be the evolving Baja California. This pericratonic model for Hottah Terrane accounts for its temporal affinity with other WCS terranes, yet its exotic position to the west of the Slave Craton. (SS2; Wed. 8:20)

Canada's newest confirmed meteorite impact structure: The Prince Albert impact structure, NWT, Canada

Osiniski, G.R., gosinski@uwo.ca, Abou-Aly, S., Francis, R., Marion, C.L., Pickersgill, A.E., Tornabene, L.L., Dept. of Earth Sciences/Physics & Astronomy, Centre for Planetary Science and Exploration, Western University, London, ON N6A 5B7, and Hansen, J., Canadian Space Agency, St. Hubert, QC J3Y 8Y9

Meteorite impact craters are one of the most common geological landforms throughout the Solar System. On Earth, however, the impact record is being continually lost due to active erosion, plate tectonics, and volcanic resurfacing. Despite this, ~185 impact structures have been confirmed to date based on the report of shock metamorphic effects. Here, we report on the confirmation of a new complex impact structure – the Prince Albert impact structure – located on Victoria Island in the Canadian High Arctic. This structure was discovered by K. Dewing and B. R. Pratt during reconnaissance mapping in 2010. These authors reported the presence of shatter cones, a diagnostic feature unique to impact craters and nuclear test sites. The Prince Albert structure is situated adjacent to the Collinson Inlet on the Prince Albert peninsula on northwestern Victoria Island. The target rocks consist of flat lying sedimentary rocks from Neoproterozoic to Ordovician–Silurian in age. Younger Devonian-age rocks may have been present at the time of impact but no preserved evidence was found.

We carried out fieldwork over a 2 week period in July 2012.

Mapping was carried out at both the outcrop and regional scale. We mapped evidence for inward-dipping listric faults out to a radius of ~14 km in several quadrants of the crater, which defines the apparent crater diameter at 28 km – making this one of the largest structures to be documented in recent years. We are able to confirm the impact origin for the Prince Albert impact structure, through the confirmation of shatter cones and the first report of planar deformation features (PDFs) in quartz. Two main types of allochthonous impactites we documented in the field. The first consists of monomict breccias with a pale yellow groundmass, occurring as dyke-like bodies in target rocks up to ~1 m across and traceable for >50 m in length. The second type are polymict in nature with a pale grey groundmass, present as cm- to dm-scale dykes and sills in target rocks. Evidence for impact-generated hydrothermal activity was also documented at several locations within the central uplift (see Marion *et al.* this conf.).

Acknowledgements: We thank the Polar Continental Shelf Project (PCSP) for logistical support, and NSERC, Canadian Space Agency (CSA), MDA, and INAC for funding. Edward Tabarah and Jean-Marc Comtois from the CSA are thanked for supporting J. Hansen's participation in this project as part of an ongoing field geology program for Canadian astronauts. (SS16; Wed. 8:40)

Trace-element analysis and U-Pb geochronology of perovskite and its importance for tracking unexposed rare-metal and diamond deposits

Osovetskii, B.M.¹, Reguir, E.P.², umreguir@cc.umanitoba.ca, Chakhmouradian, A.R.³, Veksler, I.V.³, Yang, P.², Kamenetsky, V.S.⁴ and Camacho, A.², ¹Perm State University, 15 Bukireva St., Perm, Russia, 614990; ²University of Manitoba, Winnipeg, MB R3T 2N2; ³GFZ German Research Centre for Geosciences, Potsdam, Germany; ⁴School of Earth Sciences and Centre for Ore Deposit Research, University of Tasmania, Hobart, Australia

Perovskite-group minerals are resistant to weathering in a temperate climate and can be used in exploration for kimberlites, carbonatites and apaitic syenites that contain appreciable concentrations of these minerals. The present work is a pilot study aiming to establish some criteria for the use of perovskite in tracking unexposed intrusions of kimberlites and other industrially important rocks. We examined

perovskite from the heavy mineral concentrate extracted from Jurassic terrigenous clastic sediments collected in the basin of the Veslyana River (tributary of the Kama River) in the eastern part of the East European Platform. Other minerals found in the same concentrate include loparite, calzirtite, baddeleyite and alkali amphiboles. To date, there have been no reports of kimberlite or carbonatite magmatism in this part of the Platform.

In this work, the trace-element composition and U-Pb age of perovskite grains were determined using LA-ICP-MS. The examined perovskite is characterized by high levels of rare-earth elements (30000–60000 ppm ΣREE), Nb (5000–12000 ppm), Sr (2600–7800 ppm) and Ta (400–800 ppm). The Th, U and Pb contents are variable (500–1600 ppm, 65–170 ppm and 25–80 ppm, respectively), with a strong positive correlation between Th+U and Pb. Chondrite-normalized REE profiles are dominated by light rare-earths and show a prominent Y anomaly. These trace element characteristics are comparable with those of perovskite from carbonatites, kimberlite and alkali-ultramafic rocks. However, trace-element ratios, particularly Nb/Ta, Nb/Zr and Hf/Sr are most consistent with a carbonatitic origin, and differ significantly from those in perovskite from kimberlites. The U-Pb geochronological study was carried out using the well-calibrated zircon standard GJ-1 (608.5±0.4 Ma). Correction for common Pb was done using two alternative methods: the Cumming and Richards' (1975) growth model and Tera-Wasserburg diagram (1972). The first method yielded a ²⁰⁷Pb/²³⁸U age of 366.8±2.7. On a Tera-Wasserburg diagram, the regression line constructed through the uncorrected ²⁰⁷Pb/²⁰⁶Pb and ²⁰⁶Pb/²³⁸U ratios gave an age of 363.7±7.5 Ma.

To summarise, our data suggest the existence of an undetected carbonatite intrusion of Upper-Devonian age. These findings complement the previous reports of Devonian rifting and associated magmatism along the entire margin of the Platform. (SS4; Fri. 10:20)

Uranium-bearing phases in mill tailings from Gunnar, Canada

Othmane, G.^{1,2}, guillaumeothmane@gmail.com, Allard, T.¹, Morin, G.¹, Sélo, M.³, Llorens, L.⁴, Chen, N.⁵, Brest, J.¹, Fayek, M.² and Calas, G.¹, ¹Institut de Minéralogie et de Physique des Milieux Condensés (IMPMC), UMR 7590 CNRS-UPMC/Paris VI-IRD, Case 115, 4 place Jussieu, 75252 Paris Cedex 05, France; ²Dept. of Geological Sciences, University of Manitoba, Winnipeg, MB R3T 2N2; ³Laboratoire de Minéralogie & Cosmochimie du Muséum (LMCM), UMR 7202 CNRS, CP 52, 61, rue Buffon, 75005 Paris, France; ⁴Synchrotron SOLEIL – Ligne MARS – L'Orme des Merisiers, Saint-Aubin, BP 48, F-91192 Gif-sur-Yvette Cedex, France; ⁵Canadian Light Source Inc., University of Saskatchewan, Saskatoon, SK S7N 0X4

Understanding the processes of uranium migration and sequestration in near surface environments is important to predict its mobility in mine tailings. Uranium speciation, including its oxidation state and the type(s) of phases under which uranium occurs, controls its fate and transport in the environment. The Gunnar uranium mine, located on the north shore of lake Athabasca, Saskatchewan, Canada, operated as both an underground and open-pit mine from 1955 to 1963. More than 5 million tons of ore were processed, leading to the disposal of 4.4 million tons of mill tailings at three near-surface sites in the vicinity of the mine. At the Gunnar site, the tailings consist of residual fractions from the sulfuric acid ore extraction and subsequent magnesium-diuranate precipitation process. The speciation, concentration and distribution of uranium within these tailings were investigated using geochemical and mineralogical analyses, fission track mapping and electron microscopy. The oxidation state of uranium was characterized using X-ray absorption near edge structure (XANES) spectroscopy and its molecular scale speciation was determined using Extended X-ray Absorption Fine Structure spectroscopy (EXAFS). Although uraninite inherited from the ore was observed, uranium is mostly associated with iron-bearing minerals in all tailing sites. Microscopic observation and EXAFS analysis of samples with the highest uranium concentrations (~400 to 700 ppm) indicated that uranium primarily occurs as uranyl complexes sorbed onto ferrihydrite and to a lesser extent chlorite.



Thus, the stability and mobility of uranium at the Gunnar site are likely to be mainly influenced by pH changes as well as the presence of U(VI)- and/or Fe(III)-complexing agents. (*SS5; Wed. 3:40*)

Merging Indigenous and Western Science

Ouellette, R-F., Program Director, Aboriginal Focus Programs, 166 Extended Education Complex, Extended Education, University of Manitoba, MB R3T 2N2, robert_ouellette@umanitoba.ca, www.attheedgeofcanada.com indigenous research, www.robertfalcon.com

In 2011 the Aboriginal Focus Programs at the University of Manitoba developed a course in Native Studies with the objective of exploring Indigenous Science and Western Science together. The objective was not only look at philosophical aspects of each science, but how these sciences are applied in real life to inform our understanding of the world. The goal of this presentation is to enable the participants to consider how to build relationship between Indigenous Knowledge and Western science within education. Too often traditional Western sciences and traditional Indigenous sciences are seen as existing separately. There will be a brief introduction to the foundational philosophies of Indigenous and Western science followed by a demonstration of how Indigenous science may form the basis of an exploration of traditional Western topics such as chemistry, physics, mathematics and biology. The subjects of physics, chemistry, mathematics, and biology are often seen as being apart from Indigenous Knowledge and are often seen to exist separately. It is my feeling that this does not need to be so and that these "traditional" Western science subjects can be reviewed in conjunction with the Indigenous perspectives.

Participants will learn about the applied experiences at the University of Manitoba and gain an understanding of how to take ideas within the Indigenous world-view and create a relationship with Western science. Many educators are asking about Indigenous Knowledge and how they can use it in their classroom and field in a manner which is respectful, but also enables deeper learning for students. How does one take the philosophy behind Indigenous Knowledge and present that information at the secondary and post-secondary level, helping to prepare students for western science related careers while still showing the seriousness and ingenuity of IK and being respectful of that knowledge? I hope to offer some interesting, creative and practical techniques based on my experiences at the University level to answer questions such as these and enable participants to gain an understanding of how to include foundational components of Western Science and IK in their courses. The objective is to allow individuals the opportunity to pursue further western based sciences and be successful while being respectful and cogitate of Indigenous Science as knowledge. (*SS22; Thurs. 1:20*)

Chromite composition by LA-ICP-MS: Upgraded petrogenetic and provenance tools, the new generation

Pagé, P. and Barnes, S-J., Chaire de Recherche du Canada en Métallogénie Magmatique, Sciences de la Terre, Université du Québec à Chicoutimi, QC, Philippe_Page@uqac.ca

Chromite constitutes a persistent phase in the mantle even after high degree of partial melting and is one of the first phases to crystallize in ultramafic and mafic silicate melts due to the low solubility of chromium in silicate melts. The study of chromite allows the investigation of magmatic systems at early stages and its composition should be link to that of its parental melt, which in its turn is linked to the geological setting. Chromite is a ubiquitous accessory phase of mafic and ultramafic rocks from both volcanic (MORB, boninite, Hawaiian tholeiite, flood basalt, komatiite) and plutonic (mantle and crustal peridotites) settings. Disseminated chromites are locally observed within magmatic sulphides. Chromite can also form massive accumulations in ophiolitic complexes and large layered intrusions, which constitute the only source of primary chromium. Laser ablation ICP-MS analysis allows us to determine a whole suite of elements (Al, Si, S, Ca, Sc, Ti, V, Cr, Mn, Fe, Co, Ni, Cu, Zn, Ga, Ge, As, Sr, Y, Mo,

Ru, Rh, In, Sn, Sb, Hf, Ta, W, Os, Ir) that can be used in binary plots, elemental ratios and multi-element diagrams to improve the discrimination between rocks of various origin, and to identify early magmatic processes (*i.e.*, evolution in a staging magma chamber, fractional crystallization, magma mixing, segregation of immiscible sulphide liquid), and late alteration. The segregation of a sulphide liquid has a particularly dramatic on the concentration of the chalcophile elements (Ru, Ir and Os) which preferentially partition into the sulphide melt. The use of chromite chemistry as a diagnostic provenance tool is of great interest to determine geological settings and the sulphide mineralization potential of ultramafic - mafic rock assemblages of uncertain origin, and of detrital chromites from covered terrains. (*SS9; Thurs. 8:40*)

Allanites, melt and fluid inclusions in the Hoidas Lake REE deposit, Saskatchewan, Canada: Constraints on a complex magmatic-hydrothermal system

Pandur, K.¹, lewendula@gmail.com, Ansdell, K.¹, Kontak, D.², Creighton, S.³, Harper, C.⁴, Pearson, J.⁵ and Halpin, K.⁵, ¹Department of Geological Sciences, University of Saskatchewan, Saskatoon, SK S7N 5E2; ²Department of Earth Sciences, Laurentian University, Sudbury, ON P3E 2C6; ³Saskatchewan Research Council, Saskatoon, SK S7N 2X8; ⁴Harper Geological Consulting & Exploration, Regina, SK S4S 4C8; ⁵Great Western Minerals Group Ltd., Saskatoon, SK S7L 6M8

The Hoidas Lake deposit consists of LREE-enriched veins spatially associated with regional structures in the southern Rae Province, northern Saskatchewan, Canada. The vein paragenesis is complex and commences with hyalophane-bearing granitic pegmatite dikes that are cut by diopside-allanite-(Ce)-hyalophane veins and fluorapatite breccia veins. Hematite-monazite-REE-carbonate alteration and quartz-carbonate-hematite veinlets constitute the latest stage of hydrothermal activity. Mineralogy and chemistry of the vein-filling phases, and incorporated data on fluid and melt inclusions, acquired through a combination of petrography, EMPA, microthermometry and decrepitate mound analyses, suggest a transition from an early melt-dominated system to a more volatile-rich system which might have been derived from a carbonatitic or alkalic magma source at depth.

The early hyalophane-bearing pegmatite dikes show evidence of an intense Ba-Ca alteration related to the introduction of REE mineralization. The allanite-(Ce) crystals in the early mineralized veins are strongly zoned in REE and vary from up to 24 wt.% TREO (total rare earth oxides) in crystal cores to as low as 7 wt.% TREO in the intermediate zones. The margins of these allanites also have high TREO (up to 23 wt.%), elevated Sr, Ti and Cr contents. Later euhedral allanite crystals associated with quartz-carbonate veins exhibit oscillatory zonation and are characterized by variable TREO (7-40 wt.%) and La/Nd ratios below 1. All allanite generations were affected by secondary alteration resulting in irregular REE-depleted areas, and the formation of REE-carbonates.

Apatite in the younger veins contains melt inclusions with a graphic-like texture. Preliminary SEM study of the melt inclusions suggests the coexistence of two compositionally distinct melts during apatite crystallization: (1) a carbonate melt enriched in S (3-8 wt.%) and LREE, but Ce-poor (La+Pr+Nd=48-71 wt.%, Ce= 0-5 wt.%), and (2) a silicate melt enriched in Th (2-5 wt.%) and all LREE (La+Pr+Nd=16-35 wt.%, Ce=15-34 wt.%). The apatite veins likely formed due to immiscibility between a silicate magma and carbonatitic melt, possibly linked to a sudden pressure decrease related to the brecciation. The variability of fluid inclusion assemblages and large range in Th(CO₂-L) values (6.5 to 31.0°C) in secondary inclusions also suggest transient pressure. Overall, two fluids are observed throughout the paragenesis: (1) a carbonic fluid and (2) a mixed Na-Ca-K(Mn-Fe-Ba-Sr), saline (<40 wt.%) aqueous fluid. The late hematite-monazite-REE-carbonate alteration of the allanite- and apatite-rich veins is likely coeval with the presence of the aqueous fluids and formation of quartz-carbonate veinlets, which emphasizes the continual mobility of REE in the system. (*SS6; Wed. 10:40*)

**Variation in REE-enrichment of A-type granites in complex shear zones, Cobequid Highlands, Nova Scotia**

Papoutsas, A.¹, angeliki_papoutsas@hotmail.com, Pe-Piper, G.², and Piper, D.³, ¹Dalhousie University, Halifax, NS B3H 4R2; ²Saint Mary's University, Halifax, NS B3H 3C3; ³Geological Survey of Canada (Atlantic), Dartmouth, NS B2Y 4A2

Several synchronous A-type granitic plutons, with varying amounts of gabbro, were emplaced along the active Cobequid Shear Zone in the late Paleozoic. The mineralogy and geochemistry from five of these plutons has been studied, revealing a large variation in the distribution and types of REE-minerals present, as well as in emplacement and crystallization history. Field observations suggest that the northern part in each of the plutons of the shear zone was emplaced in higher structural levels than the southern part. Furthermore, the western plutons seem to have emplaced at a relatively shallower crustal level, compared to the eastern plutons. In the west, the Cape Chignecto pluton, with 20% gabbro, shows well-defined hydrothermal alteration and contains allanite-(Ce), bastnäsite-(Ce), thorite, pyrochlore, and a mineral resembling hingganite-(Y) in vugs. The West Moose River pluton, with 5% gabbro, is a strongly fractured intrusion containing very rare relics of chevkinite-(Ce), together with thorite, xenotime, niobo-aeschynite, samarkite-(Y), hingganite-(Y), tantal-euxenite-(Y), cerianite, bastnäsite-(Ce) and synchysite-(Ce) in late fractures. The North River pluton is a simple homogenous granite pluton in the central part of the shear zone, with less than 5% gabbro. The eastern plutons of the shear zone are the composite Pleasant Hills pluton with 10% gabbro and the Wentworth plutonic complex which has the largest gabbroic body in the region. Evidence of late-stage alteration in the North River and Pleasant Hills plutons is sparse and the REE-minerals present are allanite-(Ce) in the former and chevkinite-(Ce), allanite-(Ce), monazite and thorite in the latter. The Wentworth pluton is the most alkaline intrusion in the Cobequid Shear Zone and contains allanite-(Ce), chevkinite-(Ce), hingganite-(Y), samarskite-(Y), fersmite, aeschynite-(Y), hydroxylbastnäsite-(Ce) and thorite. The emplacement of the Wentworth gabbro after the main granite led to a major remobilisation of REE, as described in the literature. Comparison between the various plutons shows that the primary REE-minerals are associated with plutons of a relatively deeper level of emplacement and with significant amounts of gabbro, whereas secondary REE-minerals are concentrated mostly in the shallow intrusions of the shear zone. The importance of late magmatic and resulting hydrothermal systems in concentrating REE-minerals is explored, as well as the relationship between secondary REE-minerals and the style of hydrothermal alteration.

(GS2; Wed. 2:40)

Computational study of plutonium (VI) and uranium (VI) complex reduction on quartz surface (100)

Park, S., University of Michigan, Ann Arbor, MI 48109, USA, sulgiye@umich.edu

Density functional theory calculations are used to investigate the interaction between quartz surface (100) with a plutonium (VI) complex. The study aims to determine the energetics of various hydrogen and oxygen-containing species adsorbed on top of the plutonium (VI) complex using the program Dmol3. The reaction energies and charge redistribution are investigated for vacuum and dielectric fluid conditions. Exothermic reactions are observed when reactants, (H, O, OH, H₂O₂, and H₂O – of which H₂O₂, OH, H, and O are radiolysis products of plutonium) are adsorbed on top of the plutonium (VI) complex. For the given stoichiometric surface, the most stable configuration for plutonium (VI) complex is when it is adsorbed to the quartz (100) surface, with OH at the top of the plutonium (VI) complex. When H₂O₂ is adsorbed on top of the plutonium (VI) complex, the reaction energy is less negative relative than for the other reactants, indicating the least probability for the redox reaction to occur. Charge redistribution analysis shows that there is transfer of electrons, but electron transfer is different depending on the type of charge-distribution calculation (Mulliken or Hirshfeld). The surfaced-mediated

reactions of plutonium are being compared with the redox reactions of uranium (VI) to further understand the thermodynamics and potential for electron transfer. The kinetic and thermodynamic investigations will be discussed to constrain how the reactions of the two actinides differ. (SS5; Wed. Poster)

Keynote (40 min): Turning geoscience research into environmental outcomes at the Geological Survey of Canada

Parsons, M.B., Geological Survey of Canada (Atlantic), Natural Resources Canada, Dartmouth, NS B2Y 4A2, Michael.Parsons@NRCan.gc.ca

The successful uptake and application of environmental geoscience research requires deliberate planning during the design and execution of the study, as well as strategic follow-up with key stakeholders throughout the publication process. Geoscientists in both academia and government organizations are increasingly being asked to demonstrate how their research results have had an impact on policy development and how their achievements translate into benefits for Canadians. An essential element of project planning is to understand how environmental decisions are made, and what type of information is of most use to risk assessors, environmental managers, and government regulators. Engaging the most likely end-users early in the design of a new study helps to ensure consensus on research priorities, and provides an opportunity for both researchers and decision-makers to define what a successful outcome would look like to them. This interaction should continue throughout the course of a study to encourage feedback from key project partners, and to allow decision-makers sufficient lead time to respond to important new research results. Strategic communication of research findings is a crucial element to the success of all environmental geoscience studies. Material prepared for specific audiences, appropriate venues, timeliness, and informed and media-savvy presenters are key factors. Publishing research results in high-quality, peer-reviewed scientific journals is an essential part of sharing information with the global scientific community; but, in many cases, it is not an effective means of directly influencing environmental decisions. Different groups will have different priorities and objectives. These groups will be most interested in information that matches their mandates and is in a form that can readily be understood by non-specialists. To nurture the most effective environmental outcomes, researchers in the earth sciences should seek out opportunities to engage end-users directly to explain why their results are important and how the information can be used. This presentation will describe the key steps involved in planning environmental geoscience projects at the Geological Survey of Canada, and will review some lessons learned from recent studies of the environmental and human health risks associated with historical gold mines in Nova Scotia. (SS20; Fri. 10:20)

Transport and fate of uranium, rare earth elements, and radionuclides from decommissioned tailings at the historical Bicroft Uranium Mine, Ontario

Parsons, M.B.¹, Michael.Parsons@NRCan.gc.ca, Friske, P.W.G.², Ford, K.L.² and LeBlanc, K.W.G.¹, ¹Geological Survey of Canada (Atlantic), Natural Resources Canada, Dartmouth, NS B2Y 4A2; ²Geological Survey of Canada, Natural Resources Canada, Ottawa, ON K1A 0E8

Uranium (U) tailings pose complex environmental risks because of their: large volumes; long-lived radioactivity; and their potential to release radionuclides, metal(loid)s, radon gas, and milling reagents into the surrounding environment. The primary objective of this study was to characterize the processes controlling the release, transport, and fate of U, its daughter products (²²⁶Ra, ²¹⁰Pb), and rare earth elements (REEs) in a stream and retention pond system downstream from two decommissioned tailings impoundments at the Bicroft Uranium Mine near Bancroft, Ontario. The Bicroft Mine operated from 1957 to 1963, and milled approximately 2,470,000 tonnes of U ore from granitic pegmatite dykes. This type of U deposit is relatively widespread throughout the Grenville Province in Ontario, Québec, and Labrador,



and has recently been the focus of renewed exploration as a source of REEs and other strategic metals.

Samples of tailings, sediments, and surface waters were collected from the Bicroft Mine between 2010 and 2012. Regional-scale sampling of sediments, waters and soil gas radon, as well as reanalysis of archived stream and lake sediments were undertaken to determine natural background variation. The concentration of U in the Bicroft tailings samples varies from 3.1 to 210 mg/kg (median 14 mg/kg). However, much higher concentrations were found in stream and pond sediments below the tailings impoundments (31 to 730 mg/kg; median 150 mg/kg). Uranium concentrations in regional lake sediments range from 0.4 to 140 mg/kg (median 4.2 mg/kg), and regional stream sediments range from 1.2 to 110 mg/kg (median 4.6 mg/kg). Soil gas radon measurements show regional values from 3.2 to 48 kBq/m³ (mean 17 kBq/m³), with higher values in soils near U-REE mineralization (up to 770 kBq/m³) and in tailings from the Bicroft Mine (1800-12,000 kBq/m³). Seasonal sampling of effluent from the tailings impoundments in 2011 shows that the concentrations of U and ²²⁶Ra are generally lower in the summer than in the fall. The filtered (<0.45 µm) concentration of U in stream water draining the Bicroft site was 7.6 µg/L in June compared to 25 µg/L in October. Similarly, the concentrations of ²²⁶Ra were 0.40 Bq/L and 0.72 in June and October, respectively. These observations provide improved understanding of the long-term stability of U tailings, and have implications for the design of environmental monitoring plans. The results of this study are being used to develop improved guidelines to reduce the environmental risks associated with any future development of U-REE granitic pegmatite-hosted deposits. (SS5; Wed. 2:20)

Examining the apparent 2.45 to 2.2 Ga magmatic gap using the record of U-Pb, Hf, and O isotopes in magmatic and detrital zircon from the Canadian Shield

Partin, C.A.¹, umpartin@cc.umanitoba.ca, Bekker, A.¹, Sylvester, P.J.², Wodicka, N.³, Stern, R.A.⁴, Chacko, T.⁵ and Heaman, L.⁵, ¹University of Manitoba, Winnipeg, MB R3T 2N2; ²Department of Earth Sciences, Memorial University, St. John's, NL A1B 3X5; ³Geological Survey of Canada, 601 Booth Street, Ottawa, ON K1A 0E8; ⁴Canadian Centre for Isotopic Microanalysis, University of Alberta, Edmonton, AB T6G 2E3; ⁵Department of Earth and Atmospheric Sciences, University of Alberta, Edmonton, AB T6G 2E3

Despite several decades of research on secular variations in the growth of the continental crust, it remains unclear whether the production and addition of juvenile continental crust was continuous or episodic in the early Precambrian, specifically after the Archean Eon. Hypotheses of episodic crustal growth have recently gained traction through compilations of global U-Pb zircon age abundance spectra, which are interpreted to delineate peaks and lulls in crustal growth through geologic time. One such apparent trough in zircon age abundance spectra between ~2.45 and 2.22 Ga is thought to represent a pause in continental crustal addition, resulting from a global shutdown of magmatic and tectonic processes. The ~2.45 - 2.22 Ga magmatic shutdown model of Condie *et al.* (2009) envisions a causal relationship between the cessation of plate tectonics and accumulation of atmospheric oxygen over the same period via reduced flux of reductants associated with magmatic and metamorphic processes. Here, we present new coupled U-Pb, Hf, and O isotope data for detrital and magmatic zircon from the western Churchill Province and the Trans-Hudson internides of Canada that demonstrate significant juvenile crustal production during the ~230 million-year interval, contradicting the magmatic shutdown hypothesis. Active plate tectonics between ~2.45 and 2.22 Ga would have contributed to efficient burial of pyrite and organic matter and the consequent rise in atmospheric oxygen documented for this time interval. Geochronologic and isotopic zircon data from three siliciclastic successions, the Penrhyn and Piling groups (Nunavut) and the Pukatawakan Assemblage (Manitoba) as well as from granitoid rocks of the North Shore plutons (Saskatchewan), the

Queen Maud Block (Nunavut), and the Meta Incognita microcontinent (Nunavut), will be discussed. (SS2; Wed. 10:00)

Low field AMS and rock magnetic studies on the lava flows from Mandla lobe of the eastern Deccan volcanic province, India

Pathak, V.¹, Patil, S.K.² and Shrivastava, J.P.¹, ¹Department of Geology, University of Delhi, Delhi-110 007; ²Dr. K.S. Krishnan Geomagnetic Research Laboratory, Jhansi, Allahabad-221505

The 900 m thick lava pile in Mandla lobe (developed around Mandla town) forms an outlier in the eastern periphery of the Deccan volcanic province extends 344 km E-W and 156 km N-S, (covering an area of 29,351 km²) that comprises of thirty seven distinct basaltic lava flows (Pattanayak and Shrivastava, 1999; Shrivastava and Pattanayak, 2002) and based on the physical and mineralogical properties of lava flows, 3-5 oriented block samples were collected from each lava flow, the Block samples were re-oriented (in the laboratory), cored and cut into standard sized (2.2 cm length and 2.5 cm diameter) cylindrical specimens. Low field anisotropy of magnetic susceptibility (AMS) was studied to understand the lava flow directions. AMS data-sets show that the maximum susceptibility axes (K1) of lava flows grouped well with the steep inclinations (>75°), whereas, the intermediate (K2) and minimum (K3) susceptibility axes are spreading along the peripherals of the stereogram. When shape parameters (T) plotted against degree of anisotropy (Pj), indicate equal distribution of 'prolate' and 'oblate' shaped magnetic fabrics in the rock samples. Rock magnetic investigations based on IRM curves, LF test and high temperature versus magnetic susceptibility measurements revealed titanomagnetite as the major contribution for magnetic remanence. (GS2; Wed. 2:20)

Metamorphic minerals as vectors to mineralization

Pattison, D.R.M., Dept. Geoscience, U. Calgary, Calgary, AB T2N 1N4, pattison@ucalgary.ca

Metamorphism of chemically altered (metasomatized) rocks associated with hydrothermal mineralization leads to the development of unusual metamorphic mineral assemblages compared to those contained in the unaltered host rocks. Such mineral assemblages therefore have the potential to be used as indicators, or "vectors", to hydrothermal alteration and perhaps mineralization. An advantage of this technique as an exploration tool is that it is visual and can therefore be applied in the field cheaply. A distinction is made between unusual rock compositions and metamorphic mineral assemblages that develop during contemporaneous metamorphism and metasomatism at elevated temperatures and pressures (*e.g.*, skarn), and those that develop where metamorphism occurs later than metasomatism (*i.e.*, metamorphosed alteration zones). This paper emphasizes the latter. The effectiveness of the technique depends on a combination of the metamorphic grade, and how different the composition of the altered rock compositions is compared to that of the unaltered host rocks. In the Purcell Mountains of southeastern British Columbia, most hydrothermal mineral deposits and occurrences (SEDEX, veins) contain garnet, whereas garnet is largely absent in the unaltered, biotite-zone regional metasediments. In this case, garnet alone is effective as a "vector" because the metamorphic grade is high enough grade that garnet will develop in the altered rock compositions, yet low enough that garnet is not widespread as a metamorphic mineral in the normal (unaltered) rock compositions. In settings of higher metamorphic grade where metamorphic porphyroblasts are widespread even in unaltered rock compositions, such as in the Flin Flon-Snow Lake belt of Manitoba, metamorphic "vectors" to hydrothermally altered rock compositions associated with VMS mineralization consist of unusual aluminous, sometimes magnesian (*e.g.*, kyanite or cordierite-bearing) mineral assemblages not seen in the unaltered host rocks, or unusually high modal abundances of porphyroblasts (*e.g.*, garnet, staurolite) compared to the unaltered regional rocks. (SS10; Thurs. 9:00)

**Ice-flow history and glacial dispersal from the Izok Lake Zn-Cu-Pb-Ag volcanogenic massive sulphide deposit, Nunavut**

Paulen, R.C.¹, ropaulen@nrcan.gc.ca, McClenaghan, M.B.¹, Hicken, A.K.², Layton-Matthews, D.², Duso, G.³ and Sader, J.³,
¹Geological Survey of Canada, 601 Booth Street, Ottawa, ON K1A 0E8; ²Department of Geological Sciences and Geological Engineering, Queen's University, Kingston, ON K7L 3N6; ³MinMetals Resources Limited (MMR), Vancouver, BC V6C 3E1

Reconstruction of past ice-flow trajectories is fundamental for successful drift prospecting mineral exploration, as it provides knowledge of former flow directions and dispersal characteristics of former Pleistocene glaciers. Ice-flow directions are indicated by a variety of erosional and depositional landforms and features. Several glacial history and paleo-flow models for northern Canada have been published at various continental and regional scales. However, applications of these continental and regional-scale ice sheet models to property-scale mineral exploration in any given prospective region are often not realistic. Indeed there are many documented examples of how localized glacial flow at a given location can be highly complex with multiple trajectories and ages, which can vary considerably from regional-scale ice-flow models.

Ice directional indicators were compiled from detailed field mapping at the Izok Lake Volcanogenic Massive Sulphide deposit, in the Point Lake region of western Nunavut and eastern Northwest Territories. Cross-cutting erosional relationships and depositional landforms indicate that the Izok Lake area was affected by four ice-flow phases throughout the Wisconsin glaciation. The resultant indicator mineral dispersal train down-ice of the Izok Lake deposit is the net effect of all ice flow phases, but its fan-shaped morphology is a function of the duration and intensity of two dominant glacial trajectories. Palimpsest dispersal patterns are easily detected in the finer (0.25-0.50 mm) indicator mineral fraction. This dispersal fan serves as a model for future exploration in the glaciated terrain of the north-central part of the Slave Structural Province. (*GS6; Wed. 8:20*)

Cobalt and silver mineralization of Central Asia

Pavlova, G.G., Borisenko, A.S., Tretiakova, I.G., Prokopiev, I.R., Institute of Geology and Mineralogy SB RAS, Pr. Koptyuga, 3, Novosibirsk, 630090, Russia, galinapavl@gmail.com, and Lebedev, V.I., Tuvanian Institute of natural resources SB RAS, 117a International st., Kyzyl, 667007, Russia

Several types of cobalt deposits are recognized: (Ni)Co-As, Ni-Co-As, Ag-Ni-Co-As, and Cu-Co-As. The (Cu)Ni-Co-As mineralization is represented by Q-vein zones in hornfels or zones of metasomatic apokarn mineralization with chalcopyrite, pyrite, cobaltite, pyrrhotite and pentlandite. Chalcopyrite-cobaltite-pyrrhotite mineral association occurs in black shale in reduce environment, but molybdenum (magnetite, hematite)-bearing association occurs in red beds, mottled and carbonate rocks or in metamorphic green schist in oxidizing conditions. The Ni-Co-As deposits are represented by carbonate veins with Co,Ni,Fe-sulfoarsenides and arsenides. The Ag-Ni-Co-As veins are characterized by high Ag contents in the ore up to several kg/ton. The Cu-Co-As deposits are composed by carbonate veins with predominant tennantite and gersdorffite, which sometimes are cut by siderite veins with tetrahedrite.

Increased PGE contents (Pt, Pd, Rh) are determined in all cobalt deposits. Platinum and palladium occur in native form, compounds with Hg, Te, Sb, and as Pt,Pd-rich phases in pyrrhotite. The highest Au content is characteristic for the high temperature (Cu)Co-As mineralization. Gold occurs as ultrafine native Au with Hg impurity, rarely as tellurides. Geochemical association of Au with Pt and Pd is established for Co-bearing skarn at the exocontact of intrusions with Cu-Ni mineralization (Maksut, Kazakhstan), in Ni-Co-As ores superimposed on Au-bearing Co-As mineralization (Khovu-Aksy, Tuva) or on the skarn with molybdosheelite, hematite, Au, U and Th at the exocontact of granosyenite (Askhatin-gol, Tuva), or on the molybdenite mineralization with Au, Pd and tellurides linked with

granodiorite (Bou-Azzer, Bleida, Morocco). Association of Au with Pd, Cu and Mo we explain by genetic link of (Cu)Co-As ore with gabbro-granite magmatic complexes.

The highest silver content in Ag-Ni-Co-As mineralization appears due to specific composition and PTX-parameters of ore-forming fluids and superimposition of Ag-(Hg)-Sb mineralization.

The age of cobalt mineralization in Central Asia is determined using Ar-Ar and U-Pb dating and several time spans of Co ores formation are established: Early Devonian (416-400 Ma) and Late Devonian (380-355 Ma), Permian (286-280 Ma) and Permo-Triassic (255-240 Ma). Existing during that time magmatic sources (mafic, alkaline-mafic, syenite, granosyenite/alkaline granite) correlate in time and space with formation of cobalt ores of different types. Ore-forming Devonian events correspond to basalt-rhyolite volcanism and intrusive gabbro-granite/syenite magmatism. Permian and Triassic cobalt mineralization is linked genetically to the Permian dolerite, Early Triassic lamprophyre, syenite, and granosyenite. Approximation of these events to the earlier geological age leads to the assumption that probably cobalt deposits in Canada are linked with the similar events. (*SS2; Wed. Poster*)

Keynote (40 min): Mafic and ultramafic magmatic provinces: Deposit types, mineral endowment, prospectivity and exploration approaches

Peck, D.C., Peck Geoscience & Exploration Corporation, 738 23rd Street, Brandon, MB R7B 1W3, dcpnickel@yahoo.com

Mafic and ultramafic igneous provinces are documented on all continents and span Earth's history. Currently, they are estimated to account for three of the world's top ten mineral belts in terms of total metal endowment and economic value. The "super-giant" Bushveld, Sudbury and Noril'sk-Talnakh mining camps remain highly productive despite decades of resource extraction. The Bushveld Complex is resplendent with world-class PGE, Cu-Ni, V-Fe and chromite resources. The Sudbury and Noril'sk-Talnakh camps remain at or near the top of the ladder in terms of established and potential Ni-Cu-PGE sulfide resources. Emerging or expanding camps such as the Mid Continent Rift system and the Nain Plutonic Suite in North America, and the Karelian craton in northern Finland, Norway and the Kola Peninsula in Russia retain excellent prospectivity for major new discoveries.

Over a century of prospecting and exploration of mafic-ultramafic igneous provinces has led to hundreds of significant discoveries. Despite this fact, opportunities for new discoveries remain extremely high. Advances in 2D and 3D data integration and analysis and in geochemical and geophysical exploration methods has paved the way for innovation in deposit and process modeling and exploration strategies that will support major new discoveries in both greenfields and brownfields environments.

Current research into the relationship between plate tectonic processes and the location and prospectivity of large igneous provinces is highlighting an increasing number of overlooked or disregarded exploration targets and concepts. This extends to both oxide and sulfide deposits and to a wide range of highly-valued commodities. As with most precious and base metal deposit types, those associated with geographically extensive mafic-ultramafic magmatic provinces tend to occur in clusters of high-value deposits located along or adjacent to major crustal-scale structures. Improvements in age determinations and tectonic reconstructions have made prioritization of exploration opportunities much easier. Within a given magmatic province, specific periods of ultramafic and mafic magmatism appear to control ore localization and thereby provide an immediate exploration focus. (*SS9; Wed. 8:20*)



Extent and metallogenic significance of the Racklan-Forward orogen in Canada

Pehrsson, S.¹, pehrsson@nrcan.gc.ca, Ramaekers, P.², Fayek, M.³, Eglington, B.E.⁴, Rainbird, R.¹ and

e, M.¹, ¹Geological Survey of Canada, 601 Booth St., Ottawa, ON K1A 0E8; ²Calgary, MF Resources, Calgary, AB; ³University of Manitoba, Winnipeg, MB; ⁴Saskatchewan Isotope Laboratory, University of Saskatchewan, Saskatoon, SK

Mesoproterozoic orogenesis is well established on the western and southern flanks of Laurentia in the well-known Racklan-Forward and Mazatzal orogens, but its significance within the previously assembled interior of Laurentia has not been established. We examine regional isotopic and structural evidence for Mesoproterozoic reactivation of Paleoproterozoic structures in Wopmay and Trans-Hudson orogens and highlight that related east-vergent thrusting is plausibly temporally coincident with Racklan-Forward orogenesis. The metallogenic importance of this reactivation and regional crustal shortening to orogenic-related and influenced mineral deposits is beginning to be assessed.

The influence of Mesoproterozoic orogenesis on unconformity uranium mineralization is threefold. First it provides a geodynamic driver for abrupt reorganization of Mesoproterozoic Athabasca basin sedimentation, which effectively became a foreland basin with westward-derived input. Secondly, related gentle contraction of the basin and inversion of its growth faults contributed to movement of basinal brines and unconformity uranium mineralization. Thirdly, paleogeography and changes in basin fill in the foreland can explain evaporative conditions which are thought to have played a role in mineralizing fluids.

The oldest accepted and significant carbonate-hosted Mississippi Valley-Type (MVT) Pb-Zn deposits in the world are the Esker and related deposits in ca. 1.9 Ga platform carbonates of Wopmay Orogen. The ore occurs as sulfide matrix breccias that may be related to evaporate host facies and is interpreted to be late-syn- or post-depositional, conceptually allowing mineralization to be related to foreland fold-thrust belt driven fluid movement, as is proposed for many MVT deposits worldwide. Transcurrent and associated reverse faults were active in Wopmay orogen ca. 1.6 Ga in some cases of are equivocal geometry (are they younger reverse or normal faults?). This raises the intriguing question of whether the Esker ore system is part of a younger 1.6 Ga MVT belt related to Racklan-Forward contractional orogeny as opposed to older 1.8 Ga Wopmay. Recent paleogeographic reconstruction places western Laurentia near the well known ca. 1.6 Ga Kamarga MVT district of McArthur basin in North Australia, which also hosts the world's oldest hydrocarbon play. This highlights the potential for a spectrum of Mesoproterozoic Racklan-Forward fold-thrust-related mineralizing systems in northern Canada. (SS2; Wed. 2:20)

Did plate tectonics shutdown in the Paleoproterozoic? A global-spatial assessment

Pehrsson, S.J.¹, pehrsson@nrcan.gc.ca; Buchan, K.L.¹, Eglington, B.E.², Berman, R.L.¹ and Whalen, J.¹, ¹Geological Survey of Canada, 601 Booth Street, Ottawa, ON K1A 0E8;

²Saskatchewan Isotope Laboratory, University of Saskatchewan, Saskatoon, SK

The early Proterozoic Era is an intriguing time period in Earth Evolution owing to the large number of fundamental changes in Earth Systems processes occurring between 2.45-2.22 Ga and distinct minima in the juvenile magmatic and detrital zircon records. A recent hypothesis seeks to explain this 'quiet interval' as the result of a shutdown of plate tectonics, one in which extended tectonic quiescence is due to widespread lithospheric stagnation characteristic of an episodic mantle overturn regime. The model suggests this represents a 'pre-modern' geodynamic style before 'modern' vigorous, continuous plate tectonics and has profound implications for many geodynamic processes and, importantly, mineral deposit systems.

We use spatially-linked chronostratigraphic and paleomagnetic databases as a starting point from which to assess the major predictions of the shutdown model and find five of its key predictions are not supported by current data. Specifically:

- 1) A lack of active orogenesis and preponderance of LP-HT metamorphism related to higher upper mantle temperatures from decreased upper mantle cooling is not evident in the global record for this time. Peak conditions include eclogite, high pressure granulite and commonly moderate pressure granulite.
- 2) Glacial conditions during this Era should be global in scope and related to cooling from decreased CO₂ input. Coincidence of the onset of magmatic shutdown with the end of mass-independent sulphur isotope fractionation and oxygenation of the atmosphere is not clear, as glacial deposits are present on only 6 of the 24 known cratons of this period, representing less than 25% of the possible record.
- 3) A proposed gap in Large-Igneous-Province (LIP) formation between 2.45 and 2.22 Ga, proposed to be related to decreased mantle vigour, is not apparent.
- 4) The proposal that the quiet interval magmatism includes no arc-type or TTG magmatism and no Nd or Hf isotopic evidence for significant crustal additions, is not supported by global data showing distinct clusters of such magmatism on specific cratons, a pattern resembling that of many younger peripheral margins.
- 5) The prediction of negligible plate velocities during shutdown is not borne out by an assessment of the well-constrained Superior Province paleomagnetic record, showing that it moved significantly during this period.

We suggest plate tectonics did not shut down but that the Early Paleoproterozoic quiet interval is one of peripheral orogenesis and locally diminished tectonic activity, as is known for other relatively quiet periods following supercontinent or supercraton amalgamation. (SS11; Fri. 8:40)

Dissolution studies of autunite minerals

Pellegrini, K.L., kpellegr@nd.edu, Martinez, M., Jouffret, L.J., Fein, J.B. and Burns, P.C., University of Notre Dame, Notre Dame, IN, USA 46556

Meta-autunite (Ca(UO₂)₂(PO₄)₂•2-6 H₂O), meta-torbernite Cu(UO₂)₂(PO₄)₂•8 H₂O, meta-ankoleite (K₂(UO₂)₂(PO₄)₂•6 H₂O), and saleeite (Mg(UO₂)₂(PO₄)₂•10 H₂O) are uranyl phosphate minerals that contain the autunite-type sheet structure. Synthetic mineral phases of these four minerals were crystallized using adapted slow mixing by diffusion, and have been verified as structurally identical to that of natural samples. Uranyl phosphate minerals are of particular interest in mitigation and remediation of areas with uranium contamination. Mitigation of uranium transport by uranyl phosphate mineral precipitation is a technique that has been explored and is strongly dependent on thorough solubility measurements of predicted mineral species, such as the autunite group minerals. In this project we use *in situ* Raman spectroscopy, coupled with *ex situ* inductively coupled plasma-optical emission spectroscopy and ICP-mass spectrometry, for dissolution studies. Based on the dissolution behaviors, we examine the relative stabilities of these mineral groups based on interlayer cation and slight structural differences. (SS5; Wed. Poster)

Keynote (40 min): Superior Province: The orogenic context

Percival, J.A., Geological Survey of Canada, 601 Booth St., Ottawa, ON K1A 0E8, joperciv@nrcan.gc.ca

Analysis of major Canadian orogens of Precambrian to Phanerozoic age based on parameters including lithospheric structure and evolution reveals common characteristics and significant variability throughout geological time. Evidence for the operation of plate tectonics extends back at least to 3.0 Ga in the Superior Province, consistent with global observations suggesting that widespread subduction began around 3.2 Ga. Superior Province exhibits as many as 8 basement terranes with distinct pre-2.7 Ga history, separated by fault-bounded domains of



geochemically juvenile rocks thought to represent oceanic crust. In well-preserved parts of the North Caribou and La Grande terranes, volcanic-dominated sequences built on older basement appear to mark rift initiation, followed 150–250 m.y. later by oceanic and continental arc-like magmatism, polyphase deformation and syn-orogenic deposition of turbiditic greywacke over strike lengths exceeding 1000 km. This period of oblique convergence from 2.75 to 2.68 Ga imposed many of the Superior Province's first-order features, including major magmatic arcs and a series of 5 discrete orogenies, each characterized by polyphase deformation, between 2.72 and 2.68 Ga. In the western Superior, accretion took place progressively from north to south and is responsible for the imbricate stacking and Moho-penetrating faults observed on Lithoprobe seismic profiles. In duration, these Wilson cycles fall well within the 100 to >1000 m.y. range for Phanerozoic orogens. Subduction remnants (ophiolites, UHP rocks) are not observed in the Superior Province and are rare elsewhere in Canadian orogens outside of the Appalachians. The eastern Superior exhibits a broad oroclinal bend to northerly strikes, possibly a reflection of the original geometry of the ancient Hudson Bay terrane and its *ca.* 2.74 Ga suture with the Rivière Arnaud terrane.

Comparative orogenic analysis shows that the size of continental plates grew by orders of magnitude during the mid-Precambrian, from terranes like the North Caribou at *ca.* 100,000 km² in the Mesoarchean, to the first stable cratons like the *ca.* 1,400,000 km² Superior Province by 2.6 Ga, to the >5,000,000 km² Laurentia by 1.8 Ga. (SS3; Thurs. 10:20)

Geo-mapping Frontiers: A new look at some underexplored parts of mainland Nunavut and Northwest Territories

Percival, J.A.¹, joperciv@nrcan.gc.ca, Pehrsson, S.¹, Berman, R.G.¹, Wodicka, N.¹, Harris, J.R.¹, Kellett, D.¹, Davis, W.J.¹, Nadeau, L.² and Bethune, K.³, ¹Geological Survey of Canada, 601 Booth St., Ottawa, ON K1A 0E8; ²Geological Survey of Canada, 490 De la Couronne, Quebec, QC G1K 9A9; ³Dept. of Geology, University of Regina, Regina, SK S4S 0A2

The Geo-mapping Frontiers project is acquiring knowledge on areas lacking modern mapping through remote predictive mapping, analysis of archival materials including SHRIMP geochronology, new high-resolution aeromagnetic surveys and field checking. The Chantry transect extends (west to east) across the 2.0–1.9 Ga Thelon magmatic zone, the Queen Maud block, and the adjacent Rae Province. The Rae consists of variably metamorphosed supracrustal and granitoid rocks, transected by the Amer mylonite zone and overlain by the Paleoproterozoic Montresor metasedimentary belt. It is separated by the Chantry fault zone from a belt of 2.6–2.7 Ga granitoid rocks, 2.45–2.40 Ga migmatitic metasedimentary rocks of the Sherman basin and highly magnetic, *ca.* 2.5–2.45 Ga, commonly orthopyroxene-bearing granitoid rocks. New geochronological results for archival samples confirm the wide extent of the Mesoarchean Queen Maud block which is dominated by granitoid gneisses, some of supracrustal parentage. Reworking at *ca.* 2.5–2.3 and 1.91 Ga is evident west of the Chantry fault zone.

To the south across the Thelon basin, the South Rae is subdivided into 9 domains, from west to east: 1) Porter domain, including basement granitoids and the Paleoproterozoic Nonacho basin; 2) the west-dipping Howard Lake shear zone; 3) Penylan domain comprising *ca.* 2.04 Ga gabbro-diorite-anorthosite complexes and granite with 1.85 Ga metamorphism; 4) McCann domain, consisting of diatexite, charnockite and metatexite, with pervasive 2.47–2.3 Ga Arrowsmith metamorphism; 5) the east-vergent Black Bay ductile thrust fault; 6) Rennie-Abitau domain of intensely folded amphibolite- to granulite-facies ortho- and paragneisses; 7) Firedrake domain of shallow-dipping, variably deformed diorite-quartz-diorite-tonalite complexes; 8) Boyd domain of 2.6 Ga granodiorite-tonalite and related mafic to intermediate supracrustal rocks; and 9) Snowbird tectonic zone, a ductile thrust intruded by *ca.* 1.74 Ga Nuelin granite.

The Tehery area north of Chesterfield Inlet consists mainly of amphibolite or higher-grade Archean granitic gneiss and plutonic rocks,

several supracrustal assemblages of uncertain age, and local Paleoproterozoic intrusions. Within the central portion of the map area, new mapping confirmed the presence of a folded supracrustal assemblage, previously remotely predicted, consisting of quartzite, iron formation, mafic gneiss possibly derived from metavolcanic rocks, and dismembered ultramafic sills or flows. Two ages of supracrustal rocks may be present. Further northwest, supracrustal rocks along strike of the Paleoproterozoic Ketyet River Group are dominated by thick white quartzite and psammite to pelite.

New geochronology is testing long-range correlations and orogenic history, and analyses of gossans, till and stream sediment samples are helping to evaluate economic potential. (SS1; Fri. 10:20)

Terrestrial analogues of the Martian surface: Comparison of three distinctive sites in the Canadian Arctic

Peterson, R., Department of Geological Sciences and Geological Engineering, Queen's University, Kingston, ON K7L 3N6, peterson@geol.queensu.ca, and Tait, K., Department of Natural History, Royal Ontario Museum, Toronto, ON M5S 2C6

The Canadian Arctic contains numerous sites that are terrestrial analogues of the Martian surface. Temperatures fluctuate from -40°C to 20°C on an annual basis, often with precipitation levels and relative humidities that create polar desert conditions. Three such locations are compared and contrasted in terms of the geological setting, mineralogy and observed mineral equilibria. East Fiord on Axel Heiberg Island is an area where active gypsum diapirs bring mineral laden groundwater to the surface to create springs with waters rich in calcium sulfate. Gossan Hill on Victoria Island is a deposit that could be the surficial expression of an underlying diapiric structure. Unlike East Fiord, at Gossan Hill there is a high concentration of sulfide, native sulfur, and ferric sulfate frozen in permafrost. This arrested hot spring system contains permafrost ice that yields solutions with pH of 2. Mineral deposits in the Big Fish River Area, Yukon contain magnesium sulfates (epsomite) and hydrous magnesium carbonates (dypingite and hydromagnesite) as surface coatings and vein fillings. These three different locations represent three very different geochemical systems and are excellent analogues of conditions that probably exist or existed somewhere on the Martian surface. At the time of writing this abstract, the NASA rover Curiosity is about to drill into vein fillings at "Yellowknife Bay". These veins fillings are thought to be gypsum, a common mineral at all of the Arctic analogue sites that will be described. The three Canadian Arctic localities will be compared and contrasted with respect to their relevance to the observations coming back from the Martian surface. (SS17; Thurs. 9:00)

Crystal chemistry of hydrous magnesium sulfates and hydrous magnesium carbonates: Implications for the Martian surface

Peterson, R.C., Department of Geological Sciences and Geological Engineering, Queen's University, Kingston, ON K7L 3N6, peterson@geol.queensu.ca

Hydrous magnesium sulfate minerals are widely distributed on the Earth's surface and have been used for medicinal and industrial purposes throughout historic times. The atomic structures of magnesium sulfate minerals consist of Mg(O,H₂O)₆ octahedra that are linked directly to each other, linked by sulfate tetrahedra and, or linked by hydrogen bonding. The relative stabilities of all these minerals are controlled by temperature and relative humidity but disequilibria are commonly observed in nature and in experimental studies. Field observations of mineral associations and experimental studies of mineral stabilities are reviewed in relation to the crystal chemical details of the mineral group. The NASA Mars Exploration Rover Spirit disturbed soils in the Columbia Hills that are rich in magnesium and sulfur but the rover did not have the capability to study the material with X-ray diffraction. The details of recent mineralogical information obtained by the surface rover Curiosity and spectroscopic data from orbiting satellites will be compared with observations made in the field on Earth and in laboratory experiments. Hydrous magnesium carbonates are also likely to exist just below the Martian surface. The



NASA lander Phoenix observed water ice to exist a few cm below the surface. The combination of the high carbon dioxide content of the Martian atmosphere, water ice and carbon dioxide ice in polar regions, and in the subsurface in temperate zones, create conditions where hydrous magnesium carbonates can occur on Mars. (SY1; Wed. 9:40)

Channel morphology of the Tobacco Creek watershed in southern Manitoba

Petzold, H.¹, petzoldha@cc.umanitoba.ca, McWhirter, B.R.¹, Lobb, D.A.¹, Ali, G.², Owens, P.N.³, Brancourt, J.¹ and Liu, C.¹,

¹Department of Soil Science, University of Manitoba, 13

Freedman Crescent, Winnipeg, MB R3T 2N2; ²Department of

Geological Science, University of Manitoba, 125 Dysart Road,

Winnipeg, MB R3T 2N2; ³University of Northern British

Columbia, 3333 University Way, Prince George, BC V2N 4Z9

Southern Manitoba's Tobacco Creek watershed and its sub-basins have been the subject of research for decades. However, to date the hydrology of the watershed has been examined only on a cursory level. This project begins a more detailed investigation of Tobacco Creek's channel form characteristics, specifically at locations currently used as sampling points for sediment fingerprinting under the Watershed Evaluation of Beneficial Management Practices (WEBs) study. In the summer of 2012 topographic survey of channel cross sections was undertaken throughout the drainage basin for computation and comparison of geomorphic variables including channel area, widths and depths. Sinuosity of select reaches was determined using GPS and air photos. In total, channel characteristics were examined at thirteen locations between the headwaters of South Tobacco Creek above the Manitoba Escarpment, and the mouth of Tobacco Creek near Rosentort. The impact of the Escarpment on stream morphology can be seen in the differences between channel characteristics measured above versus below the escarpment. (SS14; Thurs. Poster)

Shock metamorphism in plagioclase from the Mistastin Lake impact structure, Canada

Pickersgill, A.E., apickers@uwo.ca, Flemming, R.L. and Osinski, G.R., Western University, 1151 Richmond Street, London, ON N6A 5B7

The extreme temperatures and pressures generated by hypervelocity impact events result in a variety of unique microscopic shock metamorphic effects in minerals. These effects are indicative of the pressure to which material was exposed during impact, information which is important for understanding the impact process. Studies of shock effects in feldspar group minerals have been limited due to the complexity of the crystal structure and the rapid rate at which feldspars weather. As a result, feldspar is often ignored in favour of quartz for use as a shock barometer. This has resulted in a purely qualitative shock scale for feldspar, despite some studies which have suggested that feldspar can be as useful as quartz for shock barometry.

Samples in this study were obtained from throughout the ~36 Ma, ~28 km diameter, Mistastin Lake impact structure, known locally as Kamestastin, located in central Labrador, Canada (55°53'N; 63°18'W). The presence of anorthosite in the target rock makes the Mistastin Lake structure an excellent scientific lunar analogue, given that anorthosite is the main constituent of the lunar highlands. Thin sections were studied by optical microscopy, which revealed microtextural variation within minerals and various shock metamorphic effects. Samples were then examined using micro X-ray diffraction (μ XRD) to identify high-pressure stages, and correlate optically-derived shock stage to streak length along the Debye rings (χ) in two-dimensional GADDS (General Area Detector Diffraction System) images.

Samples are dominated by large, well-formed plagioclase crystals. They exhibit well developed poly-synthetic twinning and are heavily fractured throughout. All grains exhibit undulose extinction. Approximately 10% of the plagioclase exhibits an odd mosaic/pseudo-fibrous patchy extinction pattern. Pristine (*i.e.*, undecorated) planar deformation features (PDFs) were observed in over half of the quartz grains observed.

In situ μ XRD of various locations within the thin sections revealed crystalline, polycrystalline, and strained textures (appearing as spots, rings, and "streaks", respectively, on the GADDS images). The majority of images show streaks rather than individual spots. The presence of PDFs in quartz, coupled with the lack of diaplectic feldspar (maskelynite) and quartz glass, suggests that the shock pressure to which these rocks were exposed is between 10-35 GPa. The high degree of streaking on GADDS images confirms that virtually all minerals in these samples have undergone inhomogeneous strain. The lack of post-impact tectonic deformation at Mistastin Lake suggests that this strain must be the result of shock metamorphism that occurred during impact. (SS16; Wed. 9:40)

Perseverance Mine, a deformed Archean volcanogenic massive sulphide deposit, Matagami mining camp, Quebec, Canada

Pierre, S.¹, samuel.pierre54@gmail.com, Jebrak, M.¹, Faure, S.² and Roy, G.³, ¹Université du Québec à Montréal, CP 8888 Centre Ville, Montréal, QC H3C 3P8; ²CONSOREM-Université du Québec à Montréal, CP 8888 Centre Ville, Montréal, QC H3C 3P8; ³Xstrata Zinc Canada, Bureau d'exploration Mine Matagami, Matagami, QC JOY 2A0

Located in northern Abitibi, the Matagami mining Camp is a historical base metal producer. For almost 50 years, the district has produced about 4.5 Mt of Zn and 0.4 Mt of Cu from 11 Archean volcanic-hosted massive sulphide (VHMS) deposits. Perseverance is the current operating mine, displaying 5.1 Mt at 15.82%Zn, 1.24%Cu, 29.37g/t Ag and 0.38g/t Au. Exploration models in the Camp are essentially based on detailed descriptions of the mines. The last study of this kind was made by Lavallière (1995) at the Isle-Dieu deposit, where mineralization was described as being mainly controlled by volcanic and hydrothermal processes. Even if significant singularities were observed and recorded over the years, the classic VHMS sea floor depositional model is currently used without any consideration for structural components.

Detailed descriptions made on the four mineralized lenses of Perseverance reveal a high structural complexity in relation with at least two deformation phases. Extensional faults and pre-lithification folds have been recorded in the host rocks, suggesting a synvolcanic hydrothermal dynamic setting. In addition, the deposit shows many evidences of a post-volcanic event related to the regional ductile deformation. Outcrops of the low dipping rhyolitic sequence in the vicinity of the mine shows that a well-developed vertical pressure solution schistosity is present. The massive sulphide lenses in Perseverance are characterized by an atypical vertical banding of sphalerite-pyrite which is perpendicular to the stratification. This banding, clearly formed by recrystallized sulphides, has the same direction than the observed schistosity and can be interpreted as reflecting the post-volcanic deformation. At macroscopic scale, synvolcanic gabbroic dykes crosscutting the mineralization display evidences of ductile deformation including strong boudinage, folding and faulting. Also, at the scale of the deposit, the homogeneity of copper distribution suggests a late remobilization of this element, which is consistent with a structural overprint.

These observations, made at various scales, help us understand which processes controlled the mineralization at Perseverance. Post-volcanic deformations have played a significant role both in grade and geometry of the deposit, and bring new elements to the exploration model, at least for the prospecting area in the vicinity of Perseverance. (GS4; Fri. 9:20)

Sedimentological analysis and reservoir potential of the Lower Silurian Ekwan River Formation, Hudson Bay Basin, northeastern Manitoba

Pietrus, E.C., Chow, N., Dept. of Geological Sciences, University of Manitoba, Winnipeg, MB R3T 2N2, pietrus.erik@gmail.com, and Nicolas, M.P.B., Manitoba Geological Survey, 360-1395 Ellice Avenue, Winnipeg, MB R3G 3P2



The Lower Silurian Ekwon River Formation occurs in the Hudson Bay and Moose River basins, comprising part of the Hudson Platform. The formation consists primarily of fossiliferous limestone and, to a lesser extent, dolomitic limestone and dolostone. The succession represents the most extensive marine transgression in the Hudson Bay Basin during the Silurian Period. The under-explored Hudson Bay Basin is considered a frontier petroleum prospect, due in part to its geological similarities with the major oil-producing Michigan and Williston basins to the south. The Ekwon River Formation has many lithological similarities with the overlying Attawapiskat Formation, which is a potential reservoir rock.

Three petroleum exploration wells were drilled and fully cored in the Hudson Bay Lowland in northeastern Manitoba: Merland *et al.* Whitebear Creek STH No. 1, Sogepet-Aquit Kaskattama Province No. 1, and Houston *et al.* Comeault STH No. 1. During this study, Ekwon River Formation cores from all three wells were examined. Seven lithofacies are recognized and grouped into three lithofacies associations based on core examination and thin-section petrography. The subtidal lithofacies association consists of five lithofacies: (A) nodular to mottled skeletal floatstone; (B) nodular to mottled skeletal wackestone; (C) intraclast floatstone; and (D) peloidal wackestone. The intertidal lithofacies association consists of two lithofacies: (E) laminated dolostone and (F) laminated lime mudstone. The supratidal lithofacies association consists of nodular anhydrite (G). These three lithofacies associations are interpreted to represent the platform interior of a rimmed-shelf setting.

The Ekwon River Formation is considered to have reservoir potential on the basis of the good porosity observed in this study. Most lithofacies have pinpoint and vuggy porosity, ranging from 1-10%. However, lithofacies D and E show particularly good reservoir potential. Lithofacies D (peloidal wackestone) is 0.05 to 1.54 m thick and locally has excellent moldic porosity ranging between 30 to 35%, which is related to neomorphism of the micrite matrix and peloid dissolution during burial diagenesis. Lithofacies E (laminated dolostone) is 0.94 to 10.52 m thick and is comprised of very fine to fine crystalline, idiopathic dolomite, which has excellent intercrystalline, moldic and vuggy porosity ranging between 25 to 35%. Burial cements of coarse crystalline, equant calcite partially occlude vugs and fractures. No oil staining was observed in any of the lithofacies. (SS13; *Fri. 8:40*)

Sulfur generations, formation of sulfide deposits and their association with platinum group elements

Pilchin, A., arkadypilchin@yahoo.ca, and Pilchin, M., Universal Geoscience & Environmental Consulting, 205 Hilda Ave., #1402, Toronto, ON M2M 4B1, mpilchin@gmail.com

The early atmosphere contained significant amounts of oxygen, CO₂ and water in upper layers preventing solar UV radiation with wavelengths ≤ 220 nm from forming mass-independent fractionation (MIF) of sulfur. Such UV radiation was provided by the magma-ocean, which with surface temperatures of 1300, 1500 or 2000 K had an intensity ~ 0.5 , 5-50, or >5000 times greater than solar radiation at 1 AU (distance of Earth from Sun), respectively, and could easily form MIF of first generation sulfur, which at that time was completely in the atmosphere. Sulfur of first generation was completely redistributed through interaction of the sulfur-layer with the surface, mostly forming sulfides during Hadean-Early Archean by ~ 3.2 Ga, marked by formation of huge amounts of barites and absence of significant MIF between 3.2-2.8 Ga. During atmospheric cooling the sulfur-layer was represented correspondingly by mostly: SO₂ (>1000 K), SO₃ (900-600 K) and H₂SO₄ (<600 K) interacting with the surface. The interaction of surface rocks with SO₃ and H₂SO₄ is evidenced by cherty layer formations in Pilbara Craton, Australia and Barberton Greenstone Belt, Africa, and their depletion of active metals and enrichment in metals resistant to H₂SO₄. Precious metals and Ni-Cu, Ni-Mo-Cr-Fe, Ni-Cr-Fe-Cu, Ni-Cr, Cu-Ni alloys are most resistant to H₂SO₄. The presence of platinum group elements (PGEs) in alloys of transitional metals always significantly increases their resistance to H₂SO₄. This led to the

collection and enrichment of resistant transitional metals mostly as alloys with presence of PGE. This is the reason why PGEs are usually associated with sulfide deposits of transitional metals. Formation of second generation sulfur is related to the maximum of komatiite magmatism ~ 2.8 -2.6 Ga. Having a melting point ~ 2000 K, it decomposed most sulfides formed during the Early Archean, mainly releasing elemental sulfur into anoxic conditions (no access of oxygen to surface ≥ 2.45 -2.3 Ga), which reacted with alloys of transitional elements forming Volcanogenic Massive Sulfide Deposits. Simultaneously komatiites formed MIF of sulfur, known during 2.8-2.45 Ga, by UV radiation (≤ 220 nm), since the radiative component of heat conductivity within a layer appears at about 1273-1473 K and higher. Third generation sulfur, liberated from decomposition of sulfides and sulfates during peak of komatiites and other high-Mg magmas (2.0-1.9 Ga) was under conditions with oxygen having contact with the surface and present within the crust, and so sulfur was released as SO₂ and H₂S, making the process of sulfides formation different from that of Early and Late Archean. (SS7; *Wed. Poster*)

Volcano-stratigraphic relationships, lithogeochemistry, and structural analysis of the 1807 zone, Ming Mine, Baie Verte Peninsula, Newfoundland

Pilote, J-L., jpilote@mun.ca, Piercey, S.J., Memorial University of Newfoundland, 300 Philip Drive, St. John's, NL A1B 3X5, Pilgrim, L. and Legrow, P., Rambler Metals & Mining Canada Limited, PO Box 291, Baie Verte, NL A0K 1B0

The Ming Cu-Zn-Au-Ag Ming volcanogenic massive sulfide deposit (10.6 Mt) is part of the Rambler mining camp, located in the upper ophiolitic sequence of the Baie Verte Oceanic Tract, northern Notre Dame subzone. The deposit is hosted by intermediate to felsic volcanic and volcanoclastic rocks of the early Ordovician (*ca.* 487 Ma) Pacquet Harbour Group, which is part of a regional mafic-dominated rock assemblage of boninitic to tholeiitic affinity. By means of systematic detailed underground mapping and diamond drill-hole description, the purpose of this study is to characterize the stratigraphy, primary and secondary lithogeochemistry, and structure of the Ming Mine.

The 1807 zone consists of a Cu-Zn-Au-rich massive sulfide horizon hosted by a sequence of dacitic to rhyolitic quartz-phyric tuff, lapilli tuff, and tuff breccia. It is structurally to disconformably overlain by a mafic-dominated subaqueous volcanic sequence, including minor magnetite-rich horizons and mafic to intermediate epiclastic rocks. Immediate footwall alteration includes chlorite + quartz + sericite \pm biotite \pm calcite \pm epidote, with zones of quartz + sericite \pm fuchsite, whereas the deeper (~ 100 m below the massive sulfide) footwall contains only chlorite + quartz alteration. The massive sulfide horizon in the 1807 zone shows evidence of remobilization during compressional deformation and contain a NE-SW trending axial plane with a shallow plunging 030°N trending mineral lineation. These folds transpose an early predominant E-W discrete shear fabric with crenulation lineation steeply to shallowly plunging WNW. Overall, the deposit consists of parallel elongated shallow plunging lenses trending NE, named (from NW to SE) the 1807 zone, 1806 zone, Ming South, and Ming North. In addition, at least two generations of mafic to intermediate dykes are present; 1) a syn-kinematic (high Zr/TiO₂) suite deformed within the massive sulfide; and 2) texturally and compositionally different (low Zr/TiO₂) mafic dykes, interpreted as pre-sulfide deformation with magmatic contact relationships. The latter dykes may have played a significant role during deformation of the massive sulfide by thickening and controlling sulfide distribution due to differences in rock competency. Ongoing research will increase confidence and resolution on the stratigraphy and test the hypothesis of a close structural relationship between the dykes and remobilization of the massive sulfide. Hence, studying the 1807 zone will provide a better understanding on the evolution of the Ming deposit and also has implications on the tectonic evolution of the Baie Verte Peninsula. (SS7; *Wed. 2:40*)



Regional zoning and topology for the chrysoberyl and alexandrite mineralizations at the Oriental Pegmatite province of Minas Gerais, Brazil

Pires, F.R., frmpires@yahoo.com, UERJ, Rua Gilberto Cardoso, 230 apt 902, Leblon, Rio de Janeiro, RJ, 22430-070, Fonseca, M.A., CPRM, and Silva, L.F., INE

The area is worldwide known since the first half of the twenty century by the presence of beautiful aquamarine, tourmaline and chrysoberyl gems and by muscovite deposits intensely mined since the 2nd World War. Chrysoberyl specimens as large as 22 × 15cm, a yellowish green gem weighing 43 ct from Aracuai lies in the British Museum, a 114 ct cushion is at Smithsonian Institution, a 10 × 9mm dark yellow gem in possession of Duke of Dree in Paris, a 400 ct, world's largest "cimophane" found at Aracuai (Calhau), a green-lettuce, 70 ct-gem after lapidated from Itambacuri are some gems found. It was noticed that the chrysoberyl deposits are mostly in recent and ancient placers, which may correspond to, in some way, the proximity of source rock. The main deposits are distributed in the Oriental Pegmatite Province at Americaninhas, Santana river valley, where the gems and cat's-eye variety are exploited in "garimpos" and mines in Corrego do Gil, Barro Preto, Faisca and Ciliandro and at Lambusa, Pavao and Crisolita region, all at Mucuri River headwaters. Additional chrysoberyl occurrences in the OPP are Itambacuri, Corrego do Cascalho, Santa Cruz brook, nearby Catuji, and Corrego Comprido. Critical questions are: Do the chrysoberyl occurrences constitute a belt? What is the genetic and spatial relation between the chrysoberyl and regional/ contact metamorphism? Some facts are unquestionable, such as the ubiquitous presence of K-feldspar, mainly orthoclase, biotite and topaz and almost complete absence of albite, tourmaline, Li- and phosphate-minerals. Muscovite may occur, but is not frequent, forming during late stages. Actually the Pavao-Americaninhas form a discontinuous belt parallel to a high-grade metamorphic rock sequence whereas charnockites predominate. The belt is connected to Jequitinhonha and southward to Itambacuri, through a complex shear zone to Corrego do Fogo and Soturno. Jacinto-Alho belt represents another belt. Charnockite-granulite belts continue along NS-trend to Malacacheta area to allow chrysoberyl formation. Later the charnockites underwent K-metasomatism. Minas Novas represents little stone spread by wind winnoing from source areas. The western boundary of the belt consists of surface separating the belt from the tourmaline-Li-mineral zone which follows northward to Itambe Li-bearing pegmatite fields. Occasional beryl and phenakite association with chrysoberyl suggest metasomatic transformation. Additional chrysoberyl belt may be defined by Itaguacu, Colatina, Santa Tereza, Cachoeira do Itapemirim localities. Alexandrite deposits are confined to Hematita and Nova Era. Construction of μH^+ - $\mu\text{H}_2\text{O}$ diagrams allowed the study of the equilibrium conditions. (SY2; Fri. 9:00)

New approach in the phosphate mineral study, topology, equilibrium conditions and pegmatite emplacement in the Galileia fields, Minas Gerais, Brazil

Pires, F.R.M., Rio de Janeiro State University, Rua Sao Francisco Xavier, Rio de Janeiro, frmpires@yahoo.com, and Silva, L.F., Environmental State Intitute of Rio de Janeiro, Rua Sacadura Cabral, Rio de Janeiro, ferrerl2004@yahoo.com.br

In the decades of 40' and 50' several new phosphate minerals have been discovered and described from the Galileia and Corrego Frio fields by investigators from DNPM, USGS and Brazilian Universities. Brazilianite, scorzalite, souzalite, barbosolite, faheyte, moraesite, tavorite, frondelite, Mn-lipscombite the new phosphate minerals discovered in addition to messelite, whiteite, childrenite-eosphorite, ludlamite, wolfeite, triphylite, bermanite, montebrasite, roscherite, cyrilovite, gordonite, heterosite, hureaulite, leucophosphite, lipscombite, metastrengite, strengite, variscite, vivianite, ferrisicklerite, gormanite, lazulite, lithiophyllite, roeddingite, purpurite, herderite, saleeite, augelite, arrojadite, berlinite, cacoenite, duffenite, laueite, phosphosiderite, lindbergite, zanazzite, roscherite and greifensteinite besides several generations of apatite, murion and rose quartz. The

complete reference list is found (Pires *et al.*, 2007). The distribution of the pegmatites may be visualized in the map, where a district zoning can be depicted: The northern, Corrego Frio fields. In addition sabugalite, rutherfordine, autunite, siderite and sulfide minerals have been recognized. The existence and distribution of at least fifty phosphate minerals at the Galileia fields could have some mineralogical significance. An additional field aspect is the emplacement of the pegmatites, displayed in two main types: 1. Intrusive pegmatites in granite, tabular, subhorizontal, "sheet-like" partly zoned with gigantic hyaline, well-formed quartz crystals in the core surrounded by cleavelandite-muscovite. 2. Intrusive pegmatites biotite schists, sub-vertical, boudinaged, pinch-and-swell structure, "canoe-shaped", discreet and obscure zoning without hyaline quartz. Type "2" in schist is regionally zoned, Li-poor, Be-rich minerals and brazilianite-herderite association defined as Corrego Frio field, separated from the Sapucaia field, whereas pegmatites are Be-poor, Li-rich characterized by relatively frequent triphylite, spodumene and rubellite. Understanding the phosphate behavior in the Galileia District it must be build μH^+ - $\mu\text{H}_2\text{O}$ -diagrams for the Corrego Frio and Sapucaia fields. Granitic and pegmatitic systems are very viscous consequently the element diffusion is restricted or actually inoperative. However, granite and pegmatites from the Oriental Province experienced a brittle deformation succeeding ductile deformation, which propitiated inter-crystalline fluid percolation where most of primary phosphate minerals deposited. Pockets result from dissolution along the fissures and inter-crystalline spaces. According to this process phosphate mineral crystallization proceeded as either isolated or semi-open systems. Small veins in fissured triphylite, found at Sapucaia, previously described show a particular zoning with hureaulite+vivianite in the selvages, barbosolite+tavorite in the intermediate zone and heterosite+ferrisicklerite in the core allowing the construction of μH^+ - $\mu\text{H}_2\text{O}$ diagram to explain the evolution. Most of the phosphate mineral previously identified by chemical, optical and XRD methods have been confirmed during a sabbatical stay at Universite de Liege. (SY2; Fri. 8:20)

Gormanite distribution and equilibrium conditions in pegmatite from Corrego Frio fields, Galileia, Minas Gerais, Brazil

Pires, F.R.M.¹, frmpires@yahoo.com, Amorim, H.S.², hsalim@uol.com.br, and Silva, L.F.³, ferrerl2004@yahoo.com.br, ¹Rio de Janeiro State University, Rua Sao Francisco Xavier, Rio de Janeiro, 398; ²Federal University of Rio de Janeiro, Ilha do Fundao, Rio de Janeiro, s/n; ³Environmental Institute of Rio de Janeiro, Rua Sacadura Cabral, Rio de Janeiro, 121

The phosphate-rich Corrego Frio pegmatites at the Oriental Province of Minas Gerais, Galileia district are Li-poor and rich in brazilianite-herderite in contrast with the Li-rich Sapucaia pegmatites characterized by triphylite (Fig. 1). Joao Teodoro (JT) pegmatite (Corrego Frio) consists of gormanite ($\text{Fe}^{2+}_3\text{Al}_4(\text{PO}_4)_4(\text{OH})_6 \cdot 2\text{H}_2\text{O}$) recognized by optical, EMP and XRD analyses. It was formed by low-T, late stage hydrothermal-pegmatite together with barbosolite, scorzalite, strengite, vivianite, kingsmountite, heterosite, hureaulite and brazilianite. The pegmatites intrude Proterozoic granite plutons and north-south trending, Archean Sao Tome biotite-sillimanite-schists. The JT pegmatite is 15m thick, subvertical, boudinaged and partly altered. Gormanite is a bluish green, triclinic phosphate mineral, occurring in pockets with partly kaolinized albite, barbosolite, scorzalite and brazilianite. Isolated pockets of strengite-vivianite-hureaulite, scorzalite-gormanite-variscite and gormanite-kingsmountite-barbosolite confirm the isolated pocket nature. Gormanite was previously described from a pegmatite at the type locality Big Fish River, Yukon, Canada, but also in the south of Karibib, Tsaobismund pegmatite, Namibia, at Newport, Sullivan Co. and at Charles Davis pegmatite, Groton, Grafton Co. The JT gormanite averages 35.61% SiO_2 , 23.06% Al_2O_3 , 6.36% MgO , 21.69% FeO , 0.61% MnO (six UnB/EMP-analyses), occurring as blue needles perched on scorzalite, barbosolite and brazilianite. Small pockets of fine-grained with gormanite-variscite-vivianite-barbosolite are frequent. Similarly to the H-metasomatism it is possible to build in μH^+ - $\mu\text{H}_2\text{O}$



diagrams, displaying separated sub-systems, respecting that at equilibrium, the chemical potential of any component must be the same in all phases in a system. The graphical representation of the stability fields implies that gormanite is destabilized at any increase of μH^+ in favor of vivianite or kinsmountite. Significant increases in $\mu\text{H}_2\text{O}$ result in augmenting the vivianite stability in any condition. It also shows the large barbosolite divariant field, coexisting with all phases. The univariant reactions plot reveal slight decrease in f_{O_2} and the phase stability and Mg, Fe^{3+} , Fe^{2+} , Al^{3+} and Ca^{2+} and Mn^{2+} were not considered in stoichiometric balance. The result of scorzalite consumption is the allocation of Al^{3+} in gormanite and variscite. Apparently barbosolite abundance is governed by scorzalite breakdown in a reaction to produce gormanite under increasing μH^+ condition: $3\text{Scorzalite} + 20\text{H}^+ = \text{Barbosolite} + \text{Gormanite} + 6\text{H}_2\text{O}$, or by the partial barbosolite succumb: $2\text{Fe}^{2+}\text{Fe}^{3+}_2(\text{PO}_4)_2(\text{OH})_2 + 4\text{H}_2\text{O} + 4\text{Al}^{3+} = \text{Fe}^{2+}_3\text{Al}_4(\text{PO}_4)_4(\text{OH})_6 \cdot 2\text{H}_2\text{O} + 2\text{H}^+ + 3\text{Fe}^{2+}$. Studying the stability of the Al-rich phases for JT pegmatite three univariant reactions can be plotted in space, showing that gormanite succumbs in μH^+ systems, mostly to variscite. (SY2; Thurs. Poster)

Broadening the knowledge of the crystal chemistry of zippeite-group minerals

Plášil, J., Institute of Physics ASCR, v.v.i., Na Slovance 2, CZ-18221 Praha 8, Czech Republic, plasil@fzu.cz

So-called "zippeites", in general, hydrated uranyl sulfates containing monovalent (K, Na, NH_4), divalent (Mg, Zn, Co, Ni, Cu, Ca) or trivalent (Y, REE) cations, form the group of the minerals, which are paragenetically, chemically and structurally closely related. They have a variable ratio of OH/O^{2-} within the structure sheets and differ in the overall symmetries of the structures, from triclinic to orthorhombic space-groups. The resulting symmetry of the structure depends namely on the interlayer complex, held primarily due to the weak bonding interactions (e.g. hydrogen bonds). All structures of zippeite-group minerals pose topologically identical sheets, giving rise of the zippeite-topology, which is characteristic by the U:T ratio equal to 2:1. Recently, the complex crystallographical characterization of several natural minerals of the zippeite-group has been undertaken. This contributed a lot to the knowledge of the crystal chemistry of the whole group, which was previously thought to be well characterized based on the studies of the synthetic analogues. Besides the single-crystal X-ray diffraction, synchrotron powder diffraction or electron-microprobe analysis, the bond-valence approach allowed to describe in detail such complex mineral group, at least more complex than was previously thought to be. (SS5; Thurs. 8:40)

A crystal-chemical investigation of the suitability of scheelite as a discriminator for different ore-forming settings: Initial results from cathodoluminescence studies

Poulin, R.S.¹, RY_Poulin@laurentian.ca, McDonald, A.M.¹, Kontak, D.J.¹ and McClenaghan, M.B.², ¹Department of Earth Sciences, Laurentian University, 935 Ramsey Lake Road, Sudbury, ON P3E 2C6; ²Geological Survey of Canada, 601 Booth Street, Ottawa, ON K1A 0E8

Scheelite (CaWO_4) is a relatively common primary or accessory mineral in a large number of geologically diverse ore-deposit settings that span a broad range of physico-chemical (PTX) conditions: vein/stockwork, skarn, porphyry and disseminated deposits.

In an effort to assess criteria that may be useful in discriminating scheelite from these diverse environments, a suite of grains from a range of environments and regions has been studied using cathodoluminescence (CL). The results represent the first in a series of analytical methods that will be used to fully document the crystal-chemical features of these samples.

Alteration- and inclusion-free, subhedral scheelite grains, ranging in size from 0.5-5 mm, were selected for detailed study characterization. The initial backscattered secondary electron images of the grains indicate a lack of a pronounced zonation with regards to major and minor element chemistry. Whereas scheelite is known to

exhibit a strong fluorescence under short wave UV radiation (254 nm), its fluorescence character under CL is significantly weaker.

This work indicates that extremely low beam currents (0.007-0.002 nA) are required to detect a CL-response; higher beam currents do not generate any CL-response as a result of quenching. It is also noteworthy that in cases where a CL response is evident, the beam current employed varies from grain to grain and that several beam currents must be tested in order to evaluate which is effective. These results show that scheelite grains obtained from disseminated epithermal quartz veins exhibit a long wavelength (blue-yellow) response, with grains typically showing complex oscillatory zoning patterns (on the scale of 5-100 μm). A preliminary interpretation attributes the zonation to be a likely product of chemical changes during crystal growth. Conversely, scheelite grains from vein/stockwork and skarn deposits show almost no CL-response. In a few cases where there is a CL-response is minor and not oscillatory, the areas showing the greatest activation are located near fractures, suggesting late-stage, fluid-mediated alteration may be responsible. Previous studies investigating the CL-response of scheelite have suggested that it is directly related to REE³⁺ concentrations. Investigations are proceeding to study this relationship further.

The initial results of differing CL-responses of scheelite from different deposit types may be useful for screening scheelite from surficial sediment samples as a tool in determining ore genesis and drift prospecting. (SS12; Thurs. 9:20)

A depositional model for hydromagnesite-magnesite playas

Power, I.M.¹, ipower@eos.ubc.ca, Harrison, A.L.¹, Dipple, G.M.¹, Kenward, P.A.¹, Wilson, S.A.², McCutcheon, J.³ and Southam, G.⁴, ¹Department of Earth, Ocean and Atmospheric Sciences, The University of British Columbia, Vancouver, BC V6T 1Z4; ²School of Geosciences, Monash University, Clayton, Australia VIC 3800; ³Department of Earth Sciences, The University of Western Ontario, London, ON N6A 5B7; ⁴School of Earth Sciences, The University of Queensland, St Lucia, Brisbane, Australia QLD 4072

Hydromagnesite-magnesite playas presently occupy what were once glacial lakes near the town of Atlin, British Columbia, Canada. Mineralogical and hydrogeochemical data are coupled with microscopy and field observations to formulate a comprehensive depositional model that describes hydromagnesite-magnesite playa genesis at this site. Four surface environments exist: wetlands, grasslands, localized mounds, and amalgamated mounds composed primarily of hydromagnesite. Rietveld refinement of X-ray diffraction data was used to quantify the mineralogical composition of surface samples and seven sediment profiles of up to 4 m depth. The sedimentary sequence consists of Mg-carbonate sediments (hydromagnesite + magnesite) overlying Ca-Mg-carbonate sediments (magnesite + aragonite + dolomite + ankerite) that in turn overlie glaciolacustrine clays. The sedimentary sequence records two major changes in the depositional environment. The transition from glaciolacustrine sediments to Ca-Mg-carbonate sediments corresponds to a shift from siliciclastic to chemical carbonate deposition as the supply of fresh glacier meltwater was replaced by alkaline groundwater. In the region, weathering of ultramafic bedrock produces Mg-HCO_3 groundwater that feeds the playas and concentrates by evaporation in the closed basins. Wetlands in the playas have a Mg:Ca molar ratio of >100:1, yet deposition of aragonite is more common than Mg-carbonate precipitation. The second change in the depositional environment occurred once sediments emerged from the water surface, shifting from subaqueous to subaerial, and resulting in another mineralogical shift. A subaerial environment favours supersaturation with respect to hydrated magnesium carbonate minerals. Capillary action and evaporation draws Mg-HCO_3 water towards the ground surface from the water table where a hardpan consisting of up to 39% lansfordite is present. Radiocarbon dating of buried vegetation indicated there has been ~8000 years of continuous magnesium carbonate deposition. Estimates of carbonate accumulation rate ranged from 0.3 to 1.3 mm/year. The depositional



model accounts for the many sedimentological, mineralogical and geochemical processes that occur in the four surface environments, thereby elucidating past and present carbonate deposition. (*GS3; Thurs. 2:40*)

Microbially and biochemically facilitated carbon sequestration

Power, I.M.¹, ipower@eos.ubc.ca, Harrison, A.L.¹, Dipple, G.M.¹, Wilson, S.A.² and Southam, G.³, ¹Mineral Deposit Research Unit, Department of Earth, Ocean and Atmospheric Sciences, The University of British Columbia, Vancouver, BC V6T 1Z4;

²School of Geosciences, Monash University, Clayton, Australia VIC 3800; ³School of Earth Sciences, The University of Queensland, St Lucia, Brisbane, Australia QLD 4072

Strategies for sequestering carbon dioxide are likely required to achieve the desired reduction in atmospheric carbon dioxide concentration and prevent irreversible damage to Earth's climate. Carbon sequestration via mineral carbonation involves silicate dissolution and carbonate precipitation, both of which are natural processes that microorganisms are able to mediate in near-surface environments. Ultramafic rock such as serpentinite is an advantageous feedstock for mineral carbonation because of its abundance and high MgO content (~40 wt.%).

Weathering of ultramafic rock may lead to Mg-carbonate formation, and therefore storage of carbon dioxide in a solid, benign form. Carbonate precipitation generally depends on pH and the concentration of cations (e.g., Mg and Ca ions) and dissolved inorganic carbon; all of which may be controlled through biological processes. Experimental evidence demonstrates that the release of cations from mine wastes can be accelerated by at least one order of magnitude through bioleaching using *Acidithiobacillus* spp. This increases the availability of cations for carbonate precipitation. Similarly, phototrophic microbes (algae and cyanobacteria) have cell surface characteristics and metabolic processes that can promote carbonate precipitation, such as through alkalization of their microenvironment. Field-based studies and corroborating laboratory experiments demonstrate the ability of a microbial consortium to precipitate hydrated magnesium carbonate minerals. The use of phototrophic microbes has the added advantage that biofuel and other value added products could be produced concurrently with carbonate minerals. Uptake of carbon dioxide is often rate-limiting for the precipitation of hydrated magnesium carbonate minerals, and hence carbon sequestration in surface environments. This limitation may be circumvented by the use of the carbonic anhydrase (CA) enzyme, that catalyses the hydration of aqueous carbon dioxide. In experiments using free CA, rates of carbon dioxide uptake into solution were accelerated by up to 710%, while carbonate precipitation was enhanced by up to 420%. Sequestration methods could be engineered to utilize microbial and biochemical processes; likely in a two-stage method that separates silicate dissolution and carbonate precipitation. As a potential application of this biogeochemical approach, mining environments that contain vast quantities of pulverized ultramafic rock may represent a valuable carbon sink that could be an economically efficient alternative to other technologies currently under development for carbon sequestration. (*SS15; Wed. 2:40*)

Surface media expressions above buried uranium: The Phoenix & Millennium deposits, Athabasca Basin

Power, M.J.¹, mpowel02@uottawa.ca, Hattori, K.H.¹, Sorba, C.², Kotzer, T.³, Pinti, D.L.⁴ and Potter, E.G.⁵, ¹Department of Earth Sciences, University of Ottawa, 140 Louis Pasteur Ottawa, ON K1N 6N5; ²Denison Mines Corp., 200-230 22nd St East, Saskatoon, SK S7K 0E9; ³Cameco Corp., 2121-11th St West, Saskatoon, SK S7M 1J3; ⁴GEOTOP, Université du Québec à Montréal, CP 8888, succ. Centre-Ville, Montréal, QC H3C 3P8; ⁵Geological Survey of Canada, 601 Booth St., Ottawa, ON K1A 0E9

In order to evaluate surficial geochemical anomalies over deeply-buried unconformity-related uranium deposits, we selected two deposits with no apparent surface expression of mineralization: The Phoenix and

Millennium deposits. The Phoenix deposit, owned by Denison Mines Corporation, has currently defined indicated resources of 52.3 million lbs U₃O₈ situated ~400 m below the surface, whereas Cameco Corporation's basement-hosted Millennium deposit has indicated resources of 46.8 million lbs U₃O₈, at a depth of ~750 m. Both are located in the southeastern margin of the Athabasca Basin in northern Saskatchewan. The area is covered by 25-100 m thick glacial tills comprised of moraine plains, streamlined moraines and subordinate eskers. Whole rock compositions of till samples from both properties suggest that the glacial sediments were sourced from a mixture of granitic basement rocks and Athabasca sandstones.

2011 field sampling above the Phoenix deposit yielded anomalous concentrations of U, Ni, Cu, Mo, Ag and W in humus, B-horizon soil and C-horizon glacial till in the areas directly above the A and B deposits and the WS Shear zone. 2012 sampling reproduced similar geochemical anomalies in soil samples (2-17 ppm U, 10-27 ppm Cu, 4-7 ppm Ni, 1000-1500 ppb As). Furthermore, leaching of humus samples in H₂O, HBr, HNO₃ and HF-HBr solutions show that these metals are not simply adsorbed on the surface; instead, they are tightly held in organics. Finally, analyses of the uppermost Manitou Falls "D" Formation sandstones with partial HF-HNO₃-HCl digestion above the ore zones contain anomalous U (up to 2 ppm).

Following the successes at Phoenix, soil sampling was carried out along the transects over the Millennium deposit in the summer of 2012, and yielded anomalies in U (0.4-0.6 ppm), Pb (15-35 ppm) and Cu (5-15 ppm) in aqua regia digestion of humus as well as anomalies in ammonium acetate leach of B horizon soils again above the ore zones and surface traces of B1 and Marker faults. Broad surficial geochemical anomalies in the property likely reflect abundant faults and fault-bound mineralization. Gas samples placed in water-filled drill holes at depths of several m yielded anomalously high radiogenic ⁴He as indicated by ⁴He/³⁶Ar ratios up to 700 times the atmospheric one, confirming the upward migration of ⁴He from the Millennium deposit. The combined results suggest upward migration of both mobile metal ions and uranium decay products from the ore zones to the surface. (*SS12; Thurs. 9:40*)

The Ediacaran Doushantuo microbiota: Animal, mineral or vegetable?

Pratt, B.R., Department of Geological Sciences, University of Saskatchewan, Saskatoon, SK S7N 5E2, brian.pratt@usask.ca, and Zhang, X-g., Key Laboratory for Palaeobiology, Yunnan University, Kunming, Yunnan 650091, China

Because of its paleontological riches, the Ediacaran (~580 Ma) Doushantuo Formation of Guizhou, southern China, has achieved iconic status enjoyed by precious few stratigraphic units. Phosphatic dolomites and cherts have yielded a spectacular diversity of fossil remains—indeed, shallow-water, cross-laminated grainstones at the famous Weng'an locality are entirely composed of sand-sized microfossils. These were initially studied petrographically, then with scanning electron microscopy, and recently, synchrotron tomography has been employed to reveal cryptic internal features. Early interpretations hypothesized algal and acritarch affinities. However, after the discovery of apatite-replaced invertebrate embryos which we announced in 1994, attention was pulled in that direction. Despite the absence of phosphatized juveniles and adults or any fragments of definitive animal tissues, the copious and quite varied particles consisting of clusters of two or more spheroids were interpreted as invertebrate embryos, an improbable but seductive conclusion that was widely embraced. Other speculations have since entered the literature including, particularly wishfully, the identification of convoluted laminae inside some objects as bilaterian animal guts. We reject the embryo hypothesis for all the Doushantuo microfossils hitherto described plus observed in our collection of many thousands of specimens. Various 'algal' affinities are still the most reasonable, on first pass, especially given the shallow-water depositional environment. For example, spheres and clusters of spheroids with a unique helical feature—the first example of fixed asymmetry in the fossil record—



may be separate stages of the life cycle of an algal taxon, likely representing a stem group with no direct younger or extant analogues. Abandoning the embryo interpretation does not reduce the importance of the Doushantuo biota. As well as the most reasonable affinities of the microfossil flora, the unique paleoenvironmental setting and diagenetic processes that led to the preservation of this biota are yet to be understood. (SY3; Thurs. 8:40)

New bedrock geology map of Alberta

Prior, G.J.¹, Glen.Prior@ercb.ca, Hathway, B.¹, Glombick, P.¹, Pana, D.I.¹, Banks, C.J.¹, Hay, D.C.², Schneider, C.L.³, Grobe, M.¹, Elgr, R.¹ and Weiss, J.A.¹, ¹Alberta Geological Survey, #402, 4999 - 98 Ave, Edmonton, AB T6B 2X3; ²Neftex Petroleum Consultants, 97 Milton Park, Abingdon, Oxfordshire, England, UK; ³University of Alberta, Edmonton, AB

Map 600 shows the bedrock geology of Alberta at a scale of 1:1 000 000. It has been prepared by staff of the Alberta Geological Survey (AGS) based upon a combination new mapping and compilation. This map supersedes Map 236 (Hamilton *et al.*, 1999) and Map 27 (Green, 1972).

Map 600 represents the compilation of existing geological maps and new geological mapping by staff of the Alberta Geological Survey (AGS). The representation of the Canadian Shield and Athabasca Basin is based on compilation. The geology of the Rocky Mountains and the Rocky Mountain Foothills is also the product of compilation with rare instances of new geological interpretation (*e.g.* the interpretation of bedrock geology beneath drift-filled valleys). The Devonian geology of northeast Alberta is also largely a product of compilation with some reinterpretation based, in part, on field observations. The Cretaceous geology of the Plains throughout most of northern and east-central Alberta is based on new geological mapping of the Fort St. John Group, the Dunvegan Formation, the Smoky Group, the Mannville Group, the Colorado Group and the Belly River Group. In addition, the Battle Formation (Cretaceous) and the Scollard Formation (Cretaceous - Paleogene) are based on new mapping north of Township 17 and east of Range 4 west of the 6th Meridian.

Mapping undertaken in support of Map 600 included field observations and the creation of three-dimensional models of subsurface stratigraphy based on the interpretation of geophysical logs from oil and gas wells. Each three-dimensional formation surface was projected to a model of the bedrock surface and the intersection formed the first approximation of the position of the geological contact at the base of drift. These preliminary contacts were then adjusted to honour outcrop data and the interpretation of the bedrock unit immediately below drift in individual wells. (SS13; Thurs. Poster)

First Nations, Metis and Inuit perspectives

Pruden, G.P., Manitoba Education, 1567 Dublin Avenue, Winnipeg, MB, greg.pruden@gov.mb.ca

"First Nations, Métis and Inuit Perspectives" offer participants an overview of Indigenous nations in Manitoba, with a focus on First Nations. The presentation includes a succinct history of First Nations on Turtle Island (North America) and in the territory that became Manitoba: nations that have called these territories home since time immemorial. The presentation includes an account of Indigenous worldviews. Although First Nations are diverse, their worldviews include elements common to most, including belief in a supreme spirit, the Creator, an intimate relationship to the land which is considered to be sacred, a communal focus that emphasizes harmony with others, and balance among the emotional, mental, spiritual and physical aspects of an individual. Successful partnerships with First Nations depend on establishing meaningful relationships with First Nations, whose traditional territories are often where mineral exploration or mining occur. In order to develop a respectful, sustainable and productive relationship with First Nations, geoscientists need to become knowledgeable about First Nations' histories, the evolving relationship with non-Indigenous Canada, the worldviews that shape and guide First

Nations' communities and individuals, the effects of colonialism, and the vision of First Nations for a sustainable future.

(SS22; Thurs. 9:40)

Rare earth elements in tailings leachate from Nechalacho, Northwest Territories: Are they truly dissolved?

Purdy, C.J.K. and Jamieson, H.E., Queen's University, 36 Union St., Kingston, ON K7L 3N6, colin.purdy@queensu.ca

Increased demand for rare earth elements (REEs) for applications in modern technologies has led to an increase in REE exploration. Several deposits are expected to begin mining within a decade, but few studies have examined the possible environmental effects created by these mines. Metal toxicity is thought to be greater in aqueous environments when metals occur as free ions rather than complexes, and the speciation can also impact the treatment technologies utilized to reduce metal concentrations. This research investigates the mechanism of REE mobility in low-temperature waters that have interacted with pilot plant tailings from the Nechalacho deposit, Northwest Territories. Nechalacho deposit is owned by Avalon Rare Metals Inc. and located approximately 100 km east of Yellowknife. The deposit is hosted within a hydrothermally altered layered nepheline-sodalite syenite in the peralkaline Blatchford Lake complex. The main REE ore minerals are zircon, fergusonite, allanite, monazite, bastnaesite, and synchysite/parasite. In low-temperature aqueous environments, REEs are known to be transported by complexation to inorganic and organic ligands, as colloids, and through sorption to colloids or suspended particles. PHREEQ-C modelling of tailings leachate suggests that carbonate ligands will form the dominant complexes with the REEs. However, elevated levels of typically immobile elements under these conditions (*e.g.* Al, Zr) indicate another mechanism may be involved. Shake flask experiments were designed to simulate the interaction of tailings with leach water to identify soluble phases and mobile elements. Nechalacho pilot plant tailings were mixed 3 to 1 by weight with distilled deionized water and lake water then gently agitated on an orbital shaker for 24 h at 25°C. Decants from these experiments were processed using tangential flow filtration, separating water into a permeate (containing only particles less than 1 nm), and a retentate (including all particles between 1 nm and .45 microns). The initial water, permeate and retentate were analyzed to determine whether the REEs are truly dissolved or are a part of colloidal material. The colloidal material was captured by centrifuging the retentate and analysed by scanning electron microscopy to determine whether the REEs are hosted in a colloidal rare earth mineral (*e.g.* zircon) or are sorbed to another mineral (*e.g.* biotite, iron oxyhydroxide). (SS6; Wed. 1:40)

Other commodities of interest in unconformity-type uranium deposits

Quirt, D.H., AREVA Resources Canada Inc., PO Box 9204, Saskatoon, SK S7K 3X5, david.quirt@areva.ca

Trace element enrichment signatures are characteristic of unconformity-type uranium mineralization processes. Boron enrichment and LREE+Sr enrichment indicate the diagenetic-hydrothermal environment. The ore element suite includes U, Ni, Co, As, and Pb, with lesser S, Cu, Zn, Mo, V, REEs, and Au. Mineralization-related reactions include desilicification, destruction of graphite, and variable precipitation of a variety of arsenide, sulpharsenide, sulphide, and phosphate minerals.

The trace element/mineralization signatures for some deposits are:

- Collins Bay B, Caribou - U+Ni+As (±Pb, B)
- Sue C/D/E - U+V+B+Pb (±Mo, Be, ±Ni, As)
- Eagle Point - U, Pb, Cu, Bi
- Dawn Lake - U+Ni+Co (±As, B?) to U+Cu
- Shea Creek - U, Pb (Au, REE, ±Ni, As)

Basement-hosted deposits tend to lack Ni, Co, and As, and have locally significant V, Cu, or Au contents.

Trace element residence sites are:



- U - pitchblende and coffinite (with Si, P, Bi, Al, Te, and Pb; with pyrite, rutile, arsenides/sulpharsenides, sulphides, phosphates). Pitchblende contains Y+HREE enrichment, with REE ranging up to 2 wt% and Y up to 0.3 wt%.
- Ni, As, Co, S - niccolite, rammelsbergite, gersdorffite, skutterudite, cloanthite (in pyritic material Co also resides in cobaltite inclusions in pyrite and Ni is often present in the pyrite lattice)
- Pb - galena
- Cu - native Cu in pitchblende, chalcopryite, chalcocite, covellite (with pyrite,)
- Mo - molybdenite (with pitchblende, pyrite)
- V - carnotite (with U, K) (often with rutile)
- P - phosphates
P, LREE, Sr - APS (florensite, goyazite/svanbergite), apatite. Enrichments of LREE occur in host-rock alteration minerals, with the LREE-Sr correlation suggesting an APS host.
- P, Y, HREE - xenotime, pitchblende (often with rutile, zircon)
- LREE (without P) - illite, dravite
- Ti - rutile (often U-enriched)
- Au - in pitchblende and/or hematitic clay
- B - dravite

Possibilities for by-product extraction from unconformity-type deposits include Au (Australia: Coronation Hill, Jabiluka, Westmoreland; Canada: Rabbit Lake, Cluff Lake, Shea Creek, Kiggavik) and the (H)REE. Ni extraction has also been historically considered. (*SS5; Fri. 8:40*)

Remote predictive geological mapping utilizing high resolution satellite imagery, western Minto Inlier, Victoria Island, NWT

Rainbird, R.¹, rrainbir@nrcan.gc.ca, Behnia, P.² and Harris, J.R.¹, harris@nrcan.gc.ca, ¹Geological Survey of Canada, 601 Booth Street, Ottawa, ON K1A 0E8; ²Geofirma, 1 Raymond St., Ottawa, ON

The very high spatial resolution and stereo capability of GeoEye-1 images were utilized to map the geology of a part of the western Neoproterozoic Minto Inlier on Victoria Island. To optimize the results of predictive mapping, a LANDSAT-7 image together with a SPOT-5 image were also used in concert with the GeoEye-1 images. The predictive bedrock geology map, interpreted based on 3D stereo visualization, presents much more detailed geological information compared to the existing 1:500,000 scale geological map of the area. The high spatial and moderate spectral resolution of GeoEye images allowed us to distinguish a black shale unit (black shale member), and resolve subtle spectral and textural differences between massive stromatolitic dolostone and dolostone containing fine-grained interlayers in an upper carbonate member. As well, an important distinction could be made between Proterozoic sedimentary strata and unconformably overlying interlayered sandstone and carbonate rocks of Cambro-Ordovician age. The SWIR bands in the LANDSAT and SPOT images proved to be very useful in identifying gabbro sills. A geological map, based on field work, was used to evaluate the remote predictive map. Comparison of the predictive map with the field map shows that the two maps look similar in terms of the regional distribution of the lithological units; however there are discrepancies between the two maps especially in areas in which the bedrock is covered by glacial sediments and/or other overburden materials. The spectral similarity between different stratigraphic units comprising similar rock types, also contributed to differences between the predictive map and the field map. (*SS19; Wed. 1:40*)

The Amundsen Cratonic Basin of northwestern Canada: Remnant of supercontinent Rodinia's interior

Rainbird, R.H.¹, rrainbir@nrcan.gc.ca, Thomson, D.², Prince, J.² and Krapež, B.³, ¹Geological Survey of Canada, Ottawa, ON K1A 0E8; ²Carleton University, Ottawa, ON K1S 5B6; ³Curtin University of Technology, Perth, WA, Australia

Early Neoproterozoic sedimentary rocks of the Shaler Supergroup are well exposed in a series of structural inliers along Canada's northern mainland and western Arctic Islands (e.g. Minto Inlier on northwestern Victoria Island, N.T.). These inliers have an arcuate distribution and their interpreted zero edge defines what has been termed the Amundsen Embayment or Amundsen Basin. Together with correlative strata in the northern Canadian Cordillera, these exposures are considered to be remnants of one side of a large cratonic sedimentary basin that lay within the Neoproterozoic supercontinent Rodinia. Overlying strata in the Cordillera record rifting of the supercontinent and separation of the cratonic cover successions. Possible conjugate basins are preserved in Australia and eastern Asia. Sedimentary strata within the basin include fluvial sandstone and deltaic siltstone, shallow marine carbonate and basinal shale, and both basinal and supratidal sulphate evaporite. Facies analysis and sequence stratigraphy suggest deposition within a relatively shallow epicontinental basin or epeiric sea that was periodically connected to an exterior ocean. The sedimentary succession in Minto Inlier is capped by flood basalts, which are part of a regional mafic magmatic event that signifies rifting and break-up of Rodinia. The stratigraphic evolution of the basin can be understood in terms of five regional-scale transgressive-regressive sequences (T-R cycles). These are of similar scale, character, and inferred duration as the classic, second-order, supersequences documented for intracratonic, lower Paleozoic strata in North America (Sloss sequences). The base of each sequence is a flooding surface, above which the sequence shoals upward. Some sequence boundaries are conformable; others show evidence of weathering and erosion. Features of the Amundsen Basin that fit the cratonic basin model include: 1) broad arcuate shape of the basin margin; 2) layer-cake stratigraphy with shallow marine and terrestrial fill forming large-scale (second-order?) sequences or T-R cycles; 3) lack of significant syn-tectonic faulting (i.e. lack of well-developed initial rift deposits, marked by arrays of extensional faults and associated graben and half-graben); 4) sedimentation kept pace with prolonged thermal subsidence (>200 million years). (*SS13; Fri. 11:00*)

Geophysical applications for non-invasive forensic searches

Raisuddin, I., Wolf, R. and Bank, C., Department of Earth Sciences, University of Toronto, 22 Russell Street, Toronto, ON M5S 3B1, intesar.raisuddin@mail.utoronto.ca

Geophysical methods can have broad applications in subsurface forensic investigations, but limited research from both a field and computer aided perspective has rendered these methods to be underutilized by forensic teams. The Ontario Provincial Police's USAR CBRNE Response Team (U.C.R.T.), with the assistance of three universities and one manufacturer, is engaged in a multi-year study at a test site near Bolton, Ontario. In summer 2012 the OPP buried weapons, drums and pigs (naked, clothed, and tarped) to simulate clandestine graves and caches in a rural setting, and to monitor changes the objects will undergo (for example gradual decomposition of pigs), and to examine strengths and weaknesses of various detection methods. Our team from the University of Toronto has been involved with this project since its inception. Thus far our surveys have focused on multi-electrode resistivity measurements using an IRIS Syscal Junior with 48 electrode switching system resistivity-meter, a GSSI SIR-300 ground penetrating radar unit with 400MHz antenna, and a GEM Systems Overhauser magnetometer. We have been conducting repeat surveys, with the aim of monitoring and quantifying changes in the geophysical data. Preliminary findings have returned promising results including noticeable magnetic anomalies as well as prominent resistivity changes and radar reflections coinciding with the location of fresh graves. (*GS7; Wed. Poster*)

Deccan Traps associated Obsidian and its suitability for radioactive waste disposal in geological repository

Rani, N., Shrivastava, J.P., Department of Geology, University of Delhi, Delhi - 110007, India, and Bajpai, R.K., BETDD, Nuclear Recycle Group, BARC, Mumbai - 400008, India



Glass is considered as a suitable matrix for immobilization of high-level nuclear waste. Acid volcanic glass dissolution studies were aimed at their potential utility as nuclear waste hosts. Hydrothermal leach tests performed on rhyolite glass for a limited period, show much lower leach rates than the borosilicate glass and survives several years in the natural environment, thus considered as a natural analogue.

Alteration studies on acid volcanic glasses are rare and framework of micro-textures and microchemistry of altered obsidian glass of this area show reliable evolutionary changes - (a) partial to complete leaching of all the ions, profusely of Si and Na ions and (b) growth of secondary phases such as palagonite, smectite, illite and montmorillonite, calcite and zeolite. Glassy material is devitrified. Yellow to yellowish brown and dark brown stains on the rock commonly seen indicate intense glass alteration. Fresh obsidian over which less, moderately and intensely weathered residual profile developed when compared with the experimentally altered specimens show that pH, ionic release and glass-water interface operative at hydrothermal-like conditions, played significant role for micro textural and mineralogical changes that occurred in the experimentally altered as well as naturally weathered obsidian. Petrography revealed yellow to yellowish brown palagonite, chlorite, calcite, zeolite and smectite from less to intensely weathered profile. Short-term alteration studies at low temperature shows presence of palagonite. Less weathered obsidian contains initial product of volcanic glass alteration, formed by glass dissolution with the concomitant precipitation of insoluble residue at glass - water boundary. Ionic mobility is enhanced in the alteration experiments causing depletion of $\text{Na} > \text{Si} > \text{K} > \text{Ca}$ and enrichment of $\text{Al} > \text{Mg} > \text{Fe} > \text{Mn} > \text{Ti}$ ions from the glass, resulted formation of palagonite. Experiments in hydrothermal conditions when continued for a longer period, degeneration of glass network are accompanied by the formation of smectite. The process and extent of palagonitization and at later stage formation of smectite is comparable with the experimentally altered as well as naturally weathered obsidian. The mode of glass dissolution and the properties of the secondary phases played significant role in the rates of ionic release, thus, critical in establishing the long-term alteration process that affects obsidian glass, suggest its suitability for radioactive waste disposal in geological repository. (*GSI; Fri. 3:20*)

Ethical responsibilities of geoscientists in environmental geology

Reichelt, R.A.S., Manitoba Conservation and Water Stewardship,
25 Tupper St. N, Portage la Prairie, MB R1N 3K1,
Raymond.Reichelt@gov.mb.ca

Professional Geoscientists have definite and definable ethical responsibilities. These responsibilities include those to society, to their profession and to their own conscience. The responsibilities of geoscientists engaged in environmental geology are of particular concern because of the consequences of their findings to their client's financial concerns of in particular and to public health in general. Investors use environmental assessments to determine the liabilities associated with a property and hence its net monetary value. Environmental assessments can also reveal potential threats to public health. These conditions mandate a high standard of ethical responsibility for geoscientists engaged in environmental geology. (*SS21; Fri. 9:00*)

Preliminary investigation of fluids associated with Mackenzie dykes in the Centennial deposit area, south-central Athabasca Basin, Saskatchewan

Reid, K.R., kdr197@mail.usask.ca, Ansdell, K., University of Saskatchewan, 114 Science Place, Saskatoon, SK S7N 5E2, and Guoxiang, C., University of Regina, College West Building 230, 3737 Wascana Parkway, Regina, SK S4S 0A2

The 1270 Ma Mackenzie dykes are the only known igneous event to affect the whole of the Athabasca Basin. In the south-central Athabasca Basin, Mackenzie diabase dykes and sills are observed in drillcore intruding Athabasca Group sandstones and basement rocks along the trend of the Snowbird Tectonic zone/Dufferin Fault zone. Intrusions in

the Centennial unconformity-related uranium deposit area provide an excellent time marker in the overall paragenesis of the deposit. Primary uranium mineralization and associated hematite, illite, sudoite and APS minerals, followed by quartz-dravite veins pre-date the intrusions. The intrusions themselves are altered and cut by: 1) adularia rhombs; 2) quartz-biotite-muscovite-uraninite-coffinite veins; 3) pervasive clinocllore and vein quartz-clinocllore-apatite; and 4) quartz (sometimes plumose)-carbonate-pyrite-galenite-chalcocopyrite veins. The earliest carbonate is comb-textured, whereas the later are rhombohedral. The compositions of chlorites suggest that primary mineralization occurred at temperatures of less than 195°C, whereas the earliest post-diabase chlorite formed at about 285°C. Post-diabase vein and alteration stages are interpreted to have resulted from interaction with fluids heated by the intrusion of the Mackenzie dykes into this area, with the later stages forming as this hydrothermal system waned. This study reports preliminary data on the composition and temperature of the fluids that might have formed the post-diabase veins and alteration.

Preliminary analysis of primary and pseudo-secondary aqueous two-phase fluid inclusions in quartz from several samples of quartz-clinocllore veins cutting the diabase and wall rock yield homogenization temperatures to liquid that vary from 112°C to 258°C, although the range is much smaller in each sample. First melting typically occurs from -55°C to -79°C while last ice melting occurs from -25.5 to -29.0°C, which emphasizes that solutes other than NaCl, such as CaCl_2 or MgCl_2 , are present. The $\delta^{18}\text{O}$ values of the early 'comb'-textured calcite and dolomite have values ranging from 13.6‰ to 15.8‰, whereas rhomboid carbonates range from 5.2‰ to 7.9‰ relative to SMOW. Chlorite, assumed to be coeval with carbonate formation, suggests temperatures ca. 280°C, which yields $\delta^{18}\text{O}$ values of the fluids from 6.9‰ to 9.5‰ for 'comb' and -1.0‰ to 1.6‰ for rhomboid carbonates. $\delta^{13}\text{C}$ values of 'comb'-textured and rhomboid carbonates in veins cutting the diabase are -10.6‰ and -7.6‰, respectively, whereas the $\delta^{13}\text{C}$ values of carbonate in veins that cut the mineralized zones vary from -4.3‰ to -62.0‰. Values of $\delta^{13}\text{C}$ lower than -40‰ suggest that oxidation of methane may have been involved in the production of carbonate in the mineralized zone. (*SS5; Thurs. 2:20*)

Aluminum hydroxide molecular clusters to minerals - Comparison of the thermochemistry of solid ϵ -GaAl12 and flat-Al13 to ϵ -Al13 Keggin compounds

Reusser, D., Casey W.H., Navrotsky, A., University of California Davis, 4415 Chemistry Annex, One Shields Avenue, Davis, CA 95616, USA, dlreusser@ucdavis.edu, and Elliott, W.S., University of Oregon, 1253 University of Oregon, Eugene, OR 97403, USA

Nanoscale species often play critical roles as intermediate species in environmental systems. Understanding the reaction pathways and processes that act on these intermediates, allows researchers to better predict various system descriptors, ranging from likely formation products to contaminant transport. Key to modeling fate and transport are mineral dissolution and precipitation processes which rely heavily on accurate thermodynamic data. Nanometer-size molecular clusters provide researchers with tunable experimental models for many of these mineral surfaces. These molecular clusters provide a necessary bridge between structural theory and experiment, yet systematic thermodynamic information on the molecular cluster formation and coarsening pathways is lacking. Here we report thermodynamic results for a class of aluminum molecular clusters measured with isothermal acid solution calorimetry. We compare the thermochemistry of the ϵ -Al13-Keggin, $\text{Na}(\text{AlO}_4)\text{Al}_{12}(\text{OH})_{24}(\text{H}_2\text{O})_{12}(\text{SeO}_4)_4 \cdot x\text{H}_2\text{O}$, to the corresponding selenate salt of the gallium-centered Keggin, ϵ -GaAl12: $\text{Na}(\text{GaO}_4)\text{Al}_{12}(\text{OH})_{24}(\text{H}_2\text{O})_{12}(\text{SeO}_4)_4 \cdot x\text{H}_2\text{O}$. Additionally, we report thermodynamic data for flat-Al13 solids, and similarly compare their thermochemistry to that of the ϵ -Al13-Keggin solids. These thermochemical measurements show that these clusters are energetic intermediates in the pathway from dissolved ionic species to stable mineral phases. This work contributes to the chemistry that governs the



structure, bonding, reactivity, and stability of molecular clusters and the geochemistry of mineral formation processes. (*SY1; Wed. Poster*)

Keynote (40 min): Subduction-zone magmatism as a source for lithospheric metallogeny

Richards, J.P., Dept. Earth and Atmospheric Sciences, University of Alberta, Edmonton, AB T6G 2E3

A wide spectrum of mineral deposit types occurs in tectonomagmatic settings related to subduction, either directly as in the case of many porphyry and epithermal deposits, or indirectly, as in spatially distant or temporally delayed systems. The latter include: calc-alkaline to mildly alkaline Cu±Mo- and Au-rich porphyry deposits; felsic Mo-/Sn-W-rich porphyry deposits; and low-sulfidation to alkalic-type epithermal Au deposits.

A common link for these various deposit types is the remobilization of previously subduction-modified lithosphere, which represents a hydrous, and therefore potentially fusible, source of metals residual from prior arc magmatism. Phanerozoic arcs are typically S-rich and moderately oxidized, such that, although the bulk of sulfur is present as dissolved sulfate in the melt, sulfide saturation is still likely. Small amounts of early fractionating sulfide will strongly partition highly siderophile elements such as Au and PGE, depleting the magma in these components and leaving them within amphibolitic cumulates. (Note, however, that it is not clear that PGEs are efficiently extracted from the mantle wedge during subduction zone magmatism: they may be preferentially left behind as restite alloy phases.) Because of the higher magmatic concentrations and lower sulfide/silicate melt partition coefficients for Cu and Mo, derivative fractionated magmas may not be significantly depleted in these elements, and therefore have the potential to form typical Au-poor arc porphyry Cu±Mo deposits.

Later tectonomagmatic events, such as crustal thickening and or mantle-delamination in response to collision, extensional orogenic collapse, or arc rifting, may cause remelting of the roots of former arc systems. Low-degree partial melting of amphibolitic cumulates in the deep crust or lithospheric mantle will generate intermediate-to-felsic, mildly alkaline magmas that are S-undersaturated. Residual cumulate sulfide phases will readily dissolve in these magmas, transferring their enrichments of Au and other metals to the upper crust via magma ascent, and then into magmatic-hydrothermal ore deposits upon shallow-crustal volatile exsolution. In the mineralogy and alteration styles of these relatively S-poor Cu-Au systems there is an analogy to iron oxide-copper-gold deposit formation, and this link is explored in a separate presentation at this meeting. (*SS23; Fri. 8:20*)

New insights into Serrinha Nucleus evolution: The Quijingue Archean megacryst anorthosite

Rios, D.C.¹, debora.rios@utoronto.ca, Davis, D.W.¹, Conceicao, H.², Santos, I.P.L.⁴ and Rosa, M.L.S.², ¹University of Toronto, ON; ²University of Sergipe, Brazil; ³Geological Survey of Brazil

Anorthosites are rocks mainly (>90%) composed of Ca-plagioclase which have distinctive ages, textures and tectonic environments. Examples are known in all continents except that there was an apparent lack of the typical Archean megacrystic type in South America. The Quijingue Archean Megacrystic Anorthosite (QAMA) in the Itapicuru River Greenstone Belt, Northeastern region of the Sao Francisco Craton, Brazil, is the first Archean Megacrystic Anorthositic cumulate to be described on the continent.

QAMA rocks were initially recognized as belonging to the Archean group of anorthosites by the presence of Ca-plagioclase (An > 80%) mega to gigacrysts (10-60 cm; ~30cm). This texture and compositional range is rare and entirely restricted to the Archean anorthosites. QAMA consists of ~80% Bitwonite gigacrysts in a coarse noritic matrix containing Al-augite (hornblende) and Ca-plagioclase. Tiny zircon crystals recovered from the mafic matrix, give an age of 2.08 Ga, coincident with the Palaeoproterozoic thermal metamorphic event that affected SerN terranes. However, Pb model ages for the plagioclase megacrysts give an average of 2.75 Ga. The zircon may be a product of baddeleyite decomposition during metamorphism.

The similarity between the tectonic environments and rocks of Pipestone Lake Anorthosite (Canada) and QAMA argues for a detailed metallogenetic and petrogenetic investigation at SerN involving QAMA. Furthermore, the new data, coupled with the petrological and geochemical information available from the Quijingue TTG Pluton (2.15 Ga with reported 3.6Ga zircon xenocrysts); the Archean ophiolitic complex at Pedras Pretas (~150km South); and the Archean Lagoa da Vaca Anorthosite Complex (3.16 Ga, ~100 km North), provide strong evidence for an Archean subduction system at Serrinha Nucleus.

The discovery and characterization of QAMA has many implications for the understanding of Serrinha Nucleus evolution as they are evidence for the existence of an oceanic crust, probably related to the development of an Archean granite-greenstone terrane, and also suggest the presence of komatiitic magmas, still not described at SerN, to which Archean anorthosites are believed to be linked, reinforcing the evidences for remains of an Early Earth crust preserved in this area. Also, the uniqueness and rarity of this educational and scientific geosite adds value to the geoheritage in Serrinha Nucleus supporting a Geopark proposal. (*GS3; Thurs. 10:40*)

Characterization of fluids associated with uranium mineralization in the Beaverlodge area, northern Saskatchewan

Rong, L., liang23r@uregina.ca, Guoxiang, C., University of Regina, 3737 Wascana Parkway, Regina, SK S4S 0A2, Ashton, K. and Normand, C., Saskatchewan Geological Survey, 2101 Scarth St., Regina, SK S4P 2H9

The Beaverlodge area north of Lake Athabasca in northern Saskatchewan was a premier uranium producing district until the discovery of high-grade uranium deposits related to the Athabasca Group unconformity moved the focus of exploration in the early 1980's. It is generally agreed that the majority of the uranium deposits in the Beaverlodge district were formed before the Athabasca basin and represent products of pre-Athabasca uranium mineralization events. Most of the Beaverlodge deposits are hosted by ca. 1.93 Ga leucogranite (and albite derived from it by Na metasomatism) and by ca. 2.3 Ga Murmac Bay group amphibolite, both of which are unconformably overlain by ca. 1.8 Ga redbeds of the Martin Group, and by the ca. 1.75-1.5 Ga Athabasca Group. In contrast to the unconformity-related uranium deposits in the Athabasca basin, for which mineralizing fluids have been well characterized and linked to brines derived from the basin, little is known about the character and origins of mineralizing fluids associated with the vein-type uranium deposits in the Beaverlodge district.

Fluids derived from regional metamorphism, the Martin basin, meteoric water and those associated with alteration of the leucogranites have been proposed or implied to have been responsible for mineralization in previous work. Fluid inclusion and stable isotope studies will be carried out to better constrain the sources of the mineralizing fluids. Preliminary studies indicate that workable fluid inclusions are present in the quartz and carbonates in the ore veins, quartz in alaskite, quartz veins and carbonates in the albite, and in some quartz overgrowth in the Martin Group sandstones. Abundant methane inclusions are observed in ore veins and in some quartz veins from albite, suggesting that methane may have been an important reducing agent responsible for precipitation of uraninite. This interpretation is partly supported by low ¹³C values (-8‰ to -17‰ PDB) of carbonates from ore veins as reported in previous studies. It is proposed here that the vein-type uranium mineralization in the Beaverlodge district resulted from mixing of a uranium-bearing oxidizing fluid with a CH₄-rich reducing fluid. The origins of these fluids are being investigated in our on-going studies. (*SS5; Wed. Poster*)

Towards a comprehensive geochemical model for antimony in the oxidized environment

Roper, A.J., a.roper@uws.edu.au, Leverett, P. and Williams, P.A., University of Western Sydney, Locked Bag 1797, Penrith, NSW



Several hundred primary Sb minerals are known and all are essentially insoluble in water under ambient conditions. When these are oxidized however, the resulting secondary phases are much more soluble, acting as metal ion buffers and controlling the dispersion of Sb in surface and soil waters. However, little is known of the solid-state control of the extent of Sb solubility in oxidised environments. Hence, dispersion of Sb and the nature and development of Sb anomalies formed as a result of the oxidation of primary Sb-bearing mineralisation is not completely understood. Conflicting solubility and thermochemical data in the literature for some Sb minerals have hampered an understanding of the chemical fate of Sb in oxidising Sb ore deposits. This has led to problems concerning the use of Pourbaix diagrams with respect to just which species are of importance. The need for reliable solubility and thermochemical data is significant if the supergene geochemistry of Sb is to be adequately modelled. This has implications for other applications, including suggestions that Sb may be used as a mobile pathfinder element in geochemical exploration for Au and other ore bodies. Recent studies developed a geochemical model for the element in oxidized settings with respect to common Fe-bearing secondary Sb phases tripuyhite, FeSbO_4 , and schafarikite, FeSb_2O_4 , in relation to the common species s  narmontite and valentinite, Sb_2O_3 , and cervantite, Sb_2O_3 . However, a considerable amount of work concerning the geochemistry of many of the somewhat rarer secondary Sb minerals is required in order to generate a comprehensive model for the supergene behaviour of the element. For most of these, the development of new syntheses is required. Such work also needs to be undertaken against a detailed study of the thermodynamic behaviour of the members of the rom  ite group, taking into account associated ion exchange phenomena.

New thermochemical data for bystr  mite MgSb_2O_6 , ordo  ezite, ZnSb_2O_6 , rosiaite, PbSb_2O_6 and nadorite, PbSbO_2Cl will be presented and an assessment of their roles in controlling the dispersion of Sb made. The solubility model that has been developed will be reviewed in terms of a number of settings including the Mineral Hill group of mines, New South Wales, Australia, and the D  brava Sb deposits of Slovakia. The overarching aim is to generate a reliable model for Sb geochemistry that will be applicable in the exploration context. (**GS1; Fri. 1:40**)

Exit from the end-Cryogenian glaciation of South Australia

Rose, C.V., Dept. of Earth and Planetary Sciences, Washington University in St. Louis, 1 Brookings Dr., St. Louis, MO 63130 USA, crose@eps.wustl.edu, and Maloof, A.C., Dept. of Geosciences, Princeton University, Guyot Hall, Princeton, NJ 08544 USA

Between 1000 and 542 million years ago, the geologic record shows evidence for the progressive rise in atmospheric oxygen, large changes in the carbon cycle, and extreme climatic states. This era was punctuated by the ‘Sturtian’ (~716 million years ago) and ‘Marinoan’ (~635 million years ago) glaciations, where ice may have extended to low-latitudes near the equator. We present a combination of field observations and chemostratigraphic data to study the sedimentary rocks in South Australia that document the exit from the younger Marinoan ice-sheet near the paleo-equator.

The syn-glacial Elatina Fm records an array of facies at different water depths across the Adelaide Rift Complex and provides a unique opportunity to study the peak glaciation and subsequent retreat of this low-latitude ice sheet. We quantify the degree of erosion, identify the provenance of sediment and clasts, and determine temporal variability in chemical weathering to test predictions of the snowball Earth model. The advancing ice sheets caused soft-sediment deformation of the beds below the glacial diamictite and sub-glacial push structures, which document the peak of the glaciation, as well as sub-glacial erosion of the carbonates beneath. $\delta^{13}\text{C}$ measurements of carbonate clasts within the glacial diamictites were used to assess provenance and relative timing of $\delta^{13}\text{C}$ acquisition, and suggest that, based on the pre-glacial chemostratigraphy, at least 500 m of erosion occurred. Detrital zircon provenance data from the Elatina Fm suggest that glacial sediment was at least partially sourced from the cratons of Western Australia and that

the Whyalla Sandstone, even if stratigraphically correlative, was not a sediment source. Together, paired sedimentological and chemostratigraphic observations reveal a heavily glaciated terrain that was incised down to at least the base of the pre-glacial Trezona Fm.

Sedimentologically and geochemically distinctive carbonate sequences consistently drape the glacial deposits associated with the Marinoan ice age record the deglaciation. An isochronous model proposes that cap dolostones were deposited synchronously as a blanket around the world regardless of water depth, whilst a diachronous model proposes that deposition tracked glacioeustatic flooding during deglaciation. We present a comprehensive carbon isotope dataset that supports neither a uniquely isochronous or diachronous model, and given the high frequency spatial variability of $\delta^{13}\text{C}$ values, temperature cannot be the dominant control on the isotopic variability of the cap dolostone. (**SY4; Fri. 11:00**)

Multi-sensor logging of exploration drill cores – Why? How? Any case studies?

Ross, P.-S., rossps@ete.inrs.ca, Bourke, A. and Fresia, B., Institut national de la recherche scientifique, centre Eau Terre Environnement, 490 rue de la Couronne, Qu  bec, QC G1K 9A9

WHY? Diamond drilling typically constitutes a major part of costs in advanced mineral exploration programs. This generates thousands of meters of rock cores during major exploration campaigns, but the cores are not currently utilized to their full potential. They could supply three-dimensional information on physical properties, geochemistry and mineralogy; such data could be used to model or improve models of geology or physical properties in 3D, characterize hydrothermal alteration, or provide chemo-stratigraphic constraints, for example. But measuring all the parameters one by one at high spatial resolution by traditional methods would be impractical due to cost and time considerations. Also, for some parameters, it would destroy the core (e.g. geochemistry).

HOW? We describe a multi-sensor core logger and its use on rock cores from exploration diamond drill holes. The logger is not meant to replace the geologist but instead is utilized to acquire rock properties measurements useful for geological and geophysical interpretations. Our semi-automated system, contained in a mobile laboratory, can measure near-simultaneously, non-destructively and at high spatial resolution, the following parameters: (1) volumetric magnetic susceptibility; (2) density using gamma-ray attenuation; (3) several chemical elements through energy-dispersive X-ray fluorescence spectrometry; and (4) visible light/near infrared spectrometry, which allows numerous hydrothermal alteration minerals to be detected and characterized. The logger also acquires a continuous image of the core using a line-scan camera, which allows the user to compare other properties with the visual aspect of the core and creates a complete virtual archive.

ANY CASE STUDIES? We present preliminary results from the Matagami mining camp (Abitibi Subprovince, Qu  bec, Canada), which contains numerous Zn-Cu-Ag-Au volcanogenic massive sulphide deposits and has good potential for additional discoveries. We have collected more than 30 000 multi-parameter measurements distributed over about 7000 metres of drill core in the main mineralized trends of the camp. One of the applications illustrated here is the improvement of down-hole lithological discrimination within non-mineralized units when such rocks are fine-grained and/or hydrothermally altered. Improved lithological discrimination can aid better understanding the geology of an area, which can lead to better targeting for future drilling. (**SS12; Thurs. 10:20**)

Intrusive rocks associated with the Neoproterozoic Troilus Au-Cu deposit, Frot  t-Evans greenstone belt, Qu  bec

Rowins, S.M.^{1,2}, stephen.rowins@gov.bc.ca, and Howarth, L.², ¹British Columbia Geological Survey, 1810 Blanshard Street, Victoria, BC V8W 9N3; ²The University of Victoria, PO Box 1700 STN CSC, Victoria, BC V8W 2Y2



The Neoproterozoic Troilus Au-Cu deposit is a low grade, high-tonnage resource hosted in calc-alkaline intrusive rocks in the Frotet-Evans greenstone belt of northern Quebec. In 2009, its last year of production, Troilus produced 135,200 oz Au and 5,900 t Cu from 6 Mt milled @ 0.83 g/t Au & 0.11% Cu. Although deformed and metamorphosed, the deposit has geological features that are consistent with a porphyry Au-Cu system, albeit of the reduced variety (*i.e.*, abundant hypogene pyrrhotite and a lack of primary hematite and sulphate minerals). Porphyry-style features include the large amount of Cu, the absence of a regional shear zone associated with the mineralization, abundant felsic intrusions, and the disseminated nature of the sulfide mineralization. Five intrusive phases are recognized in the immediate vicinity of the deposit, although field relationships and geochronological data preclude several of these as potential sources of mineralization. These phases include the “Troilus” diorite (2791 Ma) and altered granite dykes (~2782 Ma) that host the main orebody and pre-date mineralization. A suite of ~2698 Ma biotite granites (the “Parker” granites) are undeformed and post-date mineralization. One possible magmatic fluid source may be the weakly deformed granite to alkali granite dykes that intrude mineralized diorite pseudobreccia, but are also cut by quartz-sulphide veins and sulfide “stringer” veins. These cross-cutting relationships suggest alkali granites are syn-mineralization, however, it is also possible that the vein sulfides were remobilized from pre-existing mineralization. Alkali granites have phenocrysts of plagioclase, biotite and garnet. Ilmenite, not magnetite, is the main primary Fe oxide. Alkali granites are weakly peraluminous (ASI < 1.1) with low P₂O₅ (< 0.02 wt%), La/Yb < 17, Sr/Y < 14 and negative Eu, Ti, and Nb anomalies on extended trace element diagrams. On petrochemical discrimination diagrams, alkali granites plot as volcanic arc granites. These mineralogical and geochemical features classify alkali granites as slightly contaminated (ilmenite-series) I-type arc magmas and not continental S-type magmas. The reduced nature of the alkali granite as inferred from the predominance of ilmenite over magnetite is consistent with the pyrrhotite-rich and anhydrite-absent nature of the Troilus ores and its classification as a reduced porphyry Au-Cu deposit. The exact role of the alkali granites, however, remains uncertain and attempts are underway to date the alkali-granite using U-Pb methods on individual mineral grains. The precise age of the Au-Cu mineralization is unknown because Re contents in hydrothermal pyrite are too low for application of the Re-Os technique. (SS23; Fri. 3:20)

Structural geology of the McLeod Road-Birch Lake thrust panel with emphasis on the importance of structures relating to gold mineralisation, Snow Lake, Manitoba

Rubingh, K.E., Lafrance, B. and Gibson, H.L., Department of Earth Sciences, Laurentian University, Sudbury, ON P3E 2C6

The McLeod Road-Birch Lake thrust panel (MB panel) is located within the Flin Flon – Snow Lake greenstone belt, in the internides of the Trans-Hudson Orogen. The MB panel is a north-dipping homoclinal sequence of mafic and felsic volcanic and volcanoclastic rocks, which is bounded to the south by the McLeod Road Thrust (MRT) and to the north by the Birch Lake Fault. The New Britannia mine is a structurally controlled gold deposit whose mineralisation is spatially associated with the hanging wall of the MRT. The deposits are located at stratigraphic contacts between units of contrasting competency at the intersection of a fault and a secondary structure, typically a fold hinge. However, the sequence of deformational events and the structural and lithological controls on mineralisation are uncertain.

Refinement of the volcanic stratigraphy and structural history of the MB panel has identified early structural repetition within the panel along bedding-parallel thrusts, which precede the Nor-Acme anticline and the MRT. The Nor-Acme anticline has an axial planar cleavage defined by the flattening of volcanic clasts, which parallels the MRT and is the main foliation observed in the MB panel. The MRT cuts across the Nor-Acme anticline; however they share the same foliation and lineation, suggesting that they formed during the same progressive deformation event. Reactivation of the MRT resulted in the formation

of a north-trending cleavage that overprints both the thrust and the Nor-Acme anticline. All structures were subsequently folded around the open Threehouse synform.

Gold mineralisation is hosted by both quartz–albite–iron carbonate veins and quartz veins and is associated with acicular arsenopyrite within the wall rocks and wall rock fragments. Observations suggest that there are at least two separate structural and mineralisation events within the deposits of the MB panel. Mineralisation at the New Britannia mine is associated with the hanging wall of the Howe Sound fault. The style of mineralisation changes along the Howe Sound fault and it is associated with different generations and styles of quartz veins, such as; i) brecciated wall rock fragments with a pre existing foliation, ii) veins which are deformed parallel to the main flattening foliation, and iii) veins which cut the main flattening foliation but are also further intensified and folded during the development of the foliation suggest late syn-foliation. These observations indicate that gold was emplaced during the main flattening foliation. (GS4; Fri. 8:40)

The green book – A Ludvigsen legacy

Rudkin, D.M., Royal Ontario Museum, Department of Natural History (Palaeobiology), Toronto, ON M5S 2C6, davidru@rom.on.ca

In January 1979, the Royal Ontario Museum published the inaugural contribution to a brand new series entitled Fossils of Ontario. Part 1: The Trilobites, was authored by an enthusiastic young Assistant Professor in the Department of Geology at the University of Toronto (and ROM Research Associate) – one Rolf Ludvigsen. The series foreword, by P.H. von Bitter, declared: “The authors of each contribution are experts in the particular taxonomic group or topics being considered and their synthesis is directed to the student, the collector, the professional palaeontologist, as well as to the interested person who wishes to be informed.” Part 1 certainly lived up to that statement and, in the 34 years following its publication, Rolf’s initial foray into the popularization of palaeontology has intrigued and inspired amateurs and academics alike. The slim hardcover volume, usually known simply as the “green book”, now graces the shelves of a whole generation of trilobitophiles, not only in Ontario, but scattered around the world. In addition to documenting the main characters and distributions of just over 60 genera of Ordovician, Silurian, and Devonian trilobites then known within provincial boundaries, the book featured a concise summary of Ontario Palaeozoic geology, and an elegant introduction to trilobites in general. The main attraction for most, however, lay in the crisp, clear black and white photographs, an enduring hallmark of all of Rolf’s published work. This was the first time that illustrations of all major Ontario trilobite taxa had been brought together in a single comprehensive and accessible volume.

After more than three decades, and despite new discoveries and significant advances in our understanding of their palaeobiology and systematics, the “green book” remains the principal starting point for anyone seeking Ontario’s increasingly elusive trilobites. (SY3; Thurs. 10:20)

Preliminary magnetic study of the newly discovered Prince Albert impact structure

saboual2@uwo.ca, Salma.aboualy@gmail.com

It has become generally accepted that impact cratering is an important geological process throughout Earth’s history. Geological studies of impact craters on Earth abound but fewer have been studied by geophysical techniques. Compared to gravity signatures, magnetic anomalies have greater disparity in terms of the rock’s magnetic properties. Although low magnetic anomalies can also be found in complex craters, they tend to represent a smaller sampled region across the crater center. There is a significant correlation between the size of the crater and its magnetic anomaly. There are also several different mechanisms that alter the target rocks, which ultimately affect the magnetic anomaly post-impact. Here we report on the results of a



preliminary magnetic study at the newly-discovered Prince Albert impact structure, NWT.

Fieldwork was conducted over a 2-week period in July 2012. The initial phase of the expedition required gathering magnetic data around the region of the central crater with the use of walking magnetometer. Base station measurements were also taken at a set up base station in the beginning and end of each day in order to correct for duration and magnetic drift throughout the day. Once the data was collected it was brought into Oasis monaj to create the maps for each day. Then an overall map was made that combined the data from every working day into it. After the creation of these maps, the magnetometer data was uploaded on to ARC GIS with a TOPO DEM and the geological map of the area.

Several inconsistencies were observed due to the amount of coverage that were surveyed by the walking magnetometer. This was highly dependent on the fact that area of the impact crater was exponentially large and did not allow the ability to cover the center of it with a walking magnetometer. There was an area with very high magnetic susceptibility that was observed in different section within the same region, which was a result of diabase dykes. These outcrops have been sampled and thin sectioned to be later compared.

Certain areas of study needed further examination in order to attain best results. New and more efficient processing techniques are constantly implemented in order to get a better idea regarding the overall type of anomaly at this impact structure. Additionally, more emphasis on magnetization of the dykes is needed to assist in concluding whether the dykes came from the same origin. Lastly, comparison between the Prince Albert and Houghton impact structures would prove to be beneficial due to their similar attributes in terms of the target rock and overall size of the craters. (*SS16; Wed. Poster*)

Diagenetic pyrite, a source of gold in sediment-hosted gold deposits? Examples from the Selwyn basin, Yukon

Sack, P.J., Yukon Geological Survey, 102-300 Main Street, Whitehorse, YK Y1A 2C6, patrick.sack@gov.yk.ca, Danyushevsky, L.V., Gilbert, S., Large, R.R. and Gregory, D., CODES, ARC Centre of Excellence in Ore Deposits, University of Tasmania, Private Bag 79, Hobart, TAS, 7001, Australia

Diagenetic and hydrothermal pyrites from three locations in the Selwyn basin of Yukon, Canada have been characterized using laser ablation-inductively coupled plasma mass spectrometry (LA-ICPMS). The three locations are: 1) an unmineralized 'control' site from the Fox property in north Yukon, with Devonian shales of the Canol Formation and Road River Group; 2) the Carlin-type Conrad gold occurrence in Neoproterozoic shales of the Windermere Supergroup, east-central Yukon; and 3) the orogenic gold 3Ace occurrence in Neoproterozoic sediments of the Hyland Group, south-east Yukon.

Diagenetic pyrites from all locations occur as microcrystalline nodules, fine-grained sooty clusters, and thin stratiform beds of very fine-grained framboids or euhedra. Hydrothermal pyrites, from the Conrad occurrence, occur as disseminated spongy aggregates of anhedral grains generally $\leq 10 \mu\text{m}$ in diameter, as thin rims ($\leq 20 \mu\text{m}$ thick) on sooty diagenetic cores, and as coarse-grained euhedra, commonly with sooty diagenetic cores; only the coarse-grained euhedra were found at the 3Ace occurrence. We analyzed 29 samples from 5 diamond drill holes and conducted 188 spot analyses and 8 maps on diagenetic pyrite and 108 spots and 7 maps on hydrothermal pyrite; the analytical suite contains 42 major and trace elements.

Diagenetic pyrites from the Fox property, compared with those collected from the two gold occurrences, are depleted in Au, Co, and weakly depleted in Te, while being enriched in Ag, Mo, and Se. Diagenetic pyrites from both gold occurrences, compared with their respective hydrothermal pyrites, are enriched in trace elements, typically Au, Ag, Ba, Cr, Pb, Mo, Ti, V, Zn, and Mn. From our preliminary data, three observations related to gold ore genesis can be made: 1) Co/Ni values in both diagenetic and hydrothermal pyrite from Fox and Conrad and diagenetic pyrite from 3Ace are generally ≤ 1 , suggesting a sedimentary metal source. Hydrothermal pyrite from

3Ace has Co/Ni values ranging from below 1 to a maximum of 30, indicating a hydrothermal component to the metal source; 2) Thallium in the Fox and Conrad pyrites varies from 1 to 100 ppm, suggesting a halo relationship to gold or base metal mineralization; and 3) Au values in diagenetic pyrite from the 3Ace and Conrad occurrences are weakly anomalous ($\geq 200 \text{ ppb}$), with values ranging from below detection ($< 5 \text{ ppb}$) to 10 ppm. These observations are consistent with those from other Carlin-type and orogenic gold deposits and suggest that diagenetic pyrite may be a contributing source of gold for these two occurrences. (*SS1; Fri. 3:20*)

Relationships between the twin patterns of perthitic K-feldspars from granitic pegmatites and their geotectonic setting during the subsolidus stage

Sánchez-Muñoz, L.¹, lsm@icv.csic.es, Modreski, P.J.², Zagorsky, V.³, Frost, B.R.⁴ and De Moura, O.J.M.⁵, ¹Institute for Ceramics and Glasses (CSIC), Kelsen 5, E-28049 Madrid, Spain; ²U.S. Geological Survey, Federal Center Denver, CO, USA; ³Vinogradov Institute of Geochemistry, Siberian Branch of Russian Academy of Science, Irkutsk, Russia; ⁴Department of Geology and Geophysics, University of Wyoming, USA; ⁵Joaquim Neves Ferreira 238, 35030-391 Gov. Valadares, Brazil

Granitic pegmatites are singular rocks because in most cases their origin can be framed in the context of thickened continental crust, during orogenic collisions in the aggregation stage of supercontinents (syn-collisional), immediately after during their late/post-orogenic extension (post-collisional), and sometimes during their anorogenic breakup. Syn-collisional pegmatites have a typical LCT geochemistry and are associated with S-type peraluminous granites, post-collisional pegmatites are rare element and/or rare-earth elements-rich rocks, whereas anorogenic pegmatites shows a distinctive NYF signature, as the inherited features from the source lithologies of the original melts. However, the coupling between tectonic setting and geochemistry can be problematic and it is not always evident. In this work, it is shown that twin patterns of perthitic K-feldspars from granitic pegmatites can be used as additional criterion to recognize geotectonic settings.

K-feldspars have twin patterns formed during the subsolidus stage from the order-disorder transformation of an orthoclase precursor (formed after magmatic sanidine), and also from microcline to microcline recrystallizations related to changes in the orientations of the twin variants without modification in the local order. Here, these minerals are considered as complex systems having certain adaptation capability to the geological environments related to the cooling rate and directed tectonic stresses, and involving self-organization capacity.

Twin patterns have been studied in (001) sections by a combination of optical microscopy and a confocal Raman microscopy-based imaging system. This experimental procedure allows distinguishing the distribution of the alkali feldspar phases, the order-disorder states and the structural strains in the K-feldspars through the patterns. Samples were obtained in selected outcrops from twenty-nine granitic pegmatite districts around the world of Phanerozoic, Proterozoic and Archean age. Mirolitic pegmatites were not studied because in most cases the feldspar mineralogy is mostly controlled by interactions with residual aqueous fluids. The twin patterns can be described by three twin-generations (I-, II-, and III-tg) which different developments imply particular and distinguishable evolutionary trends, toward single twin orientation (low) microcline perthite as the ending stage. The evolutionary trends can be correlated with the characteristic geotectonic setting in which the K-feldspars were formed and resided on cooling. The studied anorogenic pegmatites have orthoclase-microcline mixtures, or microcline twin-patterns formed mainly by the I-tg. The analyzed syn-collisional pegmatites have microcline twin patterns formed mostly by the II- and III-tg. The considered post-collisional pegmatites can have microcline mostly formed by a single-twin orientation as a distinctive character, which has not been seen in the other two cases. (*SY2; Thurs. Poster*)

**Mafic and ultramafic intrusions in the eastern Uchi Domain of the Superior Province, Northern Ontario: New insights from mineralogical and geochemical analysis**

Sappin, A.-A.¹, asappin@nrcan.gc.ca, Houlé, M.G.¹, Vaillancourt, C.², Leshner, C.M.³ and McNicoll, V.J.⁴, ¹Geological Survey of Canada, 490 Couronne Street, Québec, QC G1K 9A9; ²Northern Shield Resources, 440 - 55 Metcalfe St., Ottawa, ON K1P 6L5; ³Department of Earth Sciences, Laurentian University, 935 Ramsey Lake Road, Sudbury, ON P3E 2C6; ⁴Geological Survey of Canada, Ottawa, 601 Booth St., Ottawa, ON K1A 0E8

Several mafic and ultramafic intrusions occur within the eastern Uchi Domain (2.8-2.9 Ga) of the North Caribou Terrane (Superior Province). The geological context of these intrusions is poorly constrained, but they are interpreted to have been emplaced mainly within a volcanic-dominated supracrustal succession representing the eastward extension of the Miminiska-Fort Hope greenstone belt. Despite the limited geological knowledge on many of these intrusions, they can be subdivided into mafic-dominated (more abundant) and ultramafic-dominated (less abundant) bodies. The most significant intrusions in the area are the spatially close ultramafic-dominated Max intrusion (4 km²), mafic-dominated Wabassi North intrusion (12 km²), and mafic-ultramafic Wabassi Main intrusion (42 km²). The Max intrusion is composed mainly of well-preserved peridotite, containing cumulus olivine (Fo₆₇₋₈₀) and intercumulus pyroxene, that is slightly enriched in HILE relative to MILE but less enriched in Nb and, locally, Ta relative to other HILE. Wabassi North is composed of more metamorphosed gabbroic rocks, dominated by an assemblage of plagioclase-hornblende, that are enriched in HILE relative to MILE but less enriched in Nb-Ta relative to other HILE and less enriched in Zr-Hf relative to other MILE. The Wabassi Main intrusion exhibits more complex geochemical signatures and appears to be a composite intrusion characterized by two major components. The first component consists of feldspathic peridotite, olivine-bearing gabbroic rocks, and olivine-free gabbroic rocks with well-preserved cumulate textures. The peridotites are composed of olivine (Fo₇₃₋₇₄) as cumulus phase with interstitial pyroxenes and plagioclase, whereas the gabbroic rocks (\pm olivine) are composed of plagioclase as the dominant cumulus phase surrounded by intercumulus pyroxenes and olivine (Fo₃₅₋₇₈). The second component is composed of hornblende-bearing gabbroic rocks with, locally, similar textures to those of the Wabassi North intrusion. The rocks in this intrusion are unenriched to enriched in HILE relative to MILE but commonly less enriched in Nb relative to other HILE but enriched to depleted in Ta relative to Nb and Hf-Zr-Ti relative to other MILE. The uniformly low Fo contents indicate that the parental magmas were basaltic rather than komatiitic. The variable amount of olivine cumulate rocks in the intrusions indicates that some systems were more open (dynamic) and that some were less open (less dynamic). The trace element signatures suggest variable degrees of upper crustal contamination. If the contaminants contained sulfides, then these intrusions may be prospective magmatic Ni-Cu-(PGE) or PGE mineralization. (*SS3; Thurs. 3:00*)

Rock coatings: Forensic tools for atmospheric compositions

Schindler, M., Department of Earth Sciences, Laurentian University, Sudbury, ON P3E 2C6, mschindler@laurentian.ca
Rock coatings provide a record of atmospheric processes and emitted particulate matter. For example, black rock coatings in the Greater Sudbury area are remarkable geological records of atmospheric conditions, including mixing, scavenging, and oxidation processes, deposition rates, and the nature and source of anthropogenic releases to the atmosphere by the local smelters. The coatings are composed of an amorphous silica matrix that has trapped atmosphere-borne nanoparticles and has preserved their chemical and isotopic signature. These coatings are the product of high emissions of SO₂ and subsequent non-stoichiometric dissolution of exposed siliceous rocks. The coatings contain spherical smelter-derived Cu-Ni-oxide particulate matter (micrometer and nanometer-sized) and metal-sulfate-rich layers composed of nanometer aggregates of Fe-Cu sulfates. Lead, As, and

Se-bearing nanoparticles emitted from smelters are incorporated in metal-sulfate-rich layers along the atmosphere-coating interface, presumably during coating formation. On a regional scale, ratios between different metal(loid)s in the coatings indicate that small diameter primary Pb, As and Se-bearing sulfate aerosols have been deposited at higher rates compared to larger, Ni-bearing particulate matter. High sulfur isotope values in coatings closer to smelting centers and their decrease with distance from the smelters is attributed to an increase in mixing of primary and secondary sulfates. (*SY1; Thurs. 10:20*)

HRTEM investigation of the mineral assemblages associated with cryptoendolithic communities in Beacon Sandstone, University Valley, Antarctica

Schumann, D.¹, dirk.schumann@mail.mcgill.ca, Andersen, D.T.², Sears, S.K.³, Vali, H.^{1,3}, ¹Department of Earth & Planetary Sciences, McGill University, 3450 University Street, Montréal, QC H3A 0E8; ²Carl Sagan Center for the Study of Life in the Universe, SETI Institute, 189 Bernardo Avenue, Mountain View, CA 94043, USA; ³Facility for Electron Microscopy Research, McGill University, 3640 University Street, Montréal, QC H3A 0C7

Understanding processes of bioalteration and biomineralization in modern and ancient terrestrial environments, particularly in cold and permafrost conditions, is critical to recognizing biosignatures and how they may be used in the search for extinct and extant life in both terrestrial and extraterrestrial rocks. The University Valley of Antarctica is an excellent terrestrial analogue for the cold and dry conditions on much of the surface of Mars. The orange colored Beacon Sandstone of University Valley is colonized by cryptoendolithic communities creating distinct black, white and green banding beneath the rock surface. The upper black zone and the lower green bands are formed by dark brown or green masses of fungal hyphae and algal cells. Colorless fungal filaments form a network around the sandstone grains in the white zone in which reddish-orange iron oxide grain coatings and other minerals in the pore spaces were dissolved. After the death of the microorganisms, the leached zone as well as darker orange bands where iron oxides re-precipitated, give the sandstone a distinctive pattern. Such patterns may serve as a biosignature for extinct life on Mars as cryptoendolithic communities may also have developed in Martian rocks. Processes of mineral dissolution and precipitation associated with microbial activity would have likely created similar zones as those found in Beacon Sandstone.

The objective of this study is to apply a combination of high-resolution transmission electron microscopy (HRTEM), high-angle annular dark-field (HAADF) imaging, and energy dispersive spectrometry (EDS) analyses in order to characterize the mineralogy in the different coloured zones of the Beacon Sandstone and determine whether they formed *in situ* owing to the presence of microorganisms or whether they have an allochthonous origin. Preliminary results of HRTEM imaging and EDS analysis of the minerals from the black zone reveal the presence of muscovite and newly precipitated crystallites (<100 nm in length) of illite and smectite-group minerals attached to extracellular polymeric substances (EPS) that surround the microorganisms. Lattice-fringe images also reveal the presence of aggregates (50 to 200 nm in size) of nano-crystallites of titanium oxide (anatase) and titanium-bearing iron oxides that occur together with the clay minerals around the EPS. While the muscovite is likely allochthonous in origin, the TEM data suggest that the illite and smectite-group minerals, as well as the anatase and the iron oxide phases, precipitated *in situ* as the result of microbiological activity. (*SS17; Thurs. 10:20*)

Arsenic mobility and attenuation in a natural wetland at Terra Mine, Silver Bear, Northwest Territories

Sealey, H.N., Gault, A.G. and Jamieson, H.E., Department of Geological Sciences and Geological Engineering, Queen's University, Kingston, ON K7M 4G6, jamieson@geol.queensu.ca



The mobility of arsenic (As) is sensitive to both pH and redox, and thus remediation of As-bearing mine drainage requires careful design. Here, we describe a case where the original remediation design involving a constructed wetland has been reconsidered after a detailed study of seasonal variation in As attenuation at an existing natural wetland.

At Terra Mine, an abandoned silver and copper mine in the Northwest Territories, the tailings lake contains dissolved As concentrations of 50-80 µg/L, exceeding the 5 µg/L maximum guideline for aquatic life. A natural wetland located downstream appears to be attenuating As from surface water. The objective of this study was to understand the sources of As to the wetland, the effectiveness of the wetland to sequester As, the form and stability of As in the sediments, and the processes controlling As mobility including any seasonal changes. Surface and pore waters were analyzed to identify how As moved through the wetland in the dissolved phase. Arsenic speciation and element associations were identified using synchrotron-based As K-edge XANES and scanning electron microscopy.

Most of the As enters the wetland by surface flow from the tailings lake. In spring, dissolved As concentrations in surface water increased downstream. However, in late summer, As concentrations in the upstream portion of the wetland decreased, but in the downstream wetland, surface water As concentrations were comparable to those of the lake water. Scanning electron microscope and XANES indicate that As in the sediments was associated with both iron (oxy)hydroxides and secondary sulphides. We hypothesize that during the higher water levels from spring snow melt, iron (oxy)hydroxides formed and captured As, while oxidation of As sulphides in the sediments led to the release of As into surface water. Over the summer, the onset of reducing conditions from higher levels of microbiological activity drove the formation of As-bearing sulphides and reductive dissolution of (oxy)hydroxides.

While As was precipitating in the sediments at most sites in the wetland over the summer, these results suggest that the wetland may not effectively sequestering As from the surface water permanently, and that sediment-water cycling of As in the wetland is a result of seasonal redox variations and were contributing As to the surface water. The results of this study indicated that using the natural wetland would not be a viable remediation method without controlling redox conditions. (SS20; Fri. 3:20)

Late- and post-Variscan vein-type silver mineralization in the Erzgebirge-Krušné hory, Germany and Czech Republic

Seifert, T., thomas.seifert@mineral.tu-freiberg, Division of Economic Geology and Petrology, Department of Mineralogy, TU Bergakademie Freiberg, Brennhaugasse 14, D-09596 Freiberg, Germany

Because of the occurrence of thousands of old Sn, Ag, Cu, Zn, Pb, As, Co, and Fe mines and some large Sn(-W-Mo-Li), W(-Mo), Sn-Zn-In, Ag-Pb-Zn-In, U(-Ag), Sb, fluorite, and barite deposits which were exploited or only explored in the 20th century, the Erzgebirge-Krušné hory area in Saxony and Bohemia is one of the key localities to study hydrothermal Ag mineralization. Three groups of Ag vein-type mineralization can be distinguished in the Erzgebirge-Krušné hory metallogenic province which is located at the NW rim of the Bohemian Massif.

- (1) The late-Variscan (310-290 Ma) Ag-polymetallic sulfide mineralization stage ("kb" ore-type) is characterized by three mineral successions: "Fe-As(-Au-Ag)" with pyrite, arsenopyrite, pyrrhotite, "Zn-Sn-Cu(-In)-Ag" with sphalerite (Ag- and/or In-rich), stannite, freibergite/tetrahedrite/tennantite (Ag-rich), chalcocite/bornite (Ag-rich), cassiterite, "Pb-Ag" with galena (Ag-rich); examples: Freiberg, Marienberg, Annaberg, and Hora Sváté Kateřiny ore districts. Average Ag contents of mined ore veins: 60 - 500 g/t.
- (2) The late-Variscan (310-290 Ma) Ag-Sb(-Au) polymetallic mineralization stage ("eb" and "eq" ore-type) with two successions: "Sulfide" with sulfides like "kb" ore-type (but Fe-poor sphalerite with low In contents) and "Ag-Sb" with

freibergite, jamesonite, miargyrite, stephanite, polybasite, argentite native silver) partly located in Ag-polymetallic districts with "kb" ore-type veins; examples: Freiberg-South ("eb"), Freiberg-North ("eq"), Drebach ("eb"). Average Ag contents of mined ore veins: 0.05 - 2 wt.%.

- (3) The post-Variscan (150-90 Ma) Ag-sulfide succession of the Bi-Co-Ni-As-U-Ag mineralization stage with proustite, argentite, native Ag; examples: Schneeberg-Oberschlema, Jachymov, Johanngeorgstadt, Pöhl-Tellerhäuser, Annaberg-Buchholz, Marienberg-Poberschau. Average Ag content of mined ore veins: 0.05 - 2 wt.% (and high grade ore shoots with more than 5 wt.% Ag, after historical records).

(1)+(2): The late-Variscan Ag-polymetallic mineralization show spatial and temporal relationships to post-collisional (calc-)alkaline lamprophyric intrusions and partly to post-collisional Li-Rb-Cs-F granites and Sn-polymetallic mineralization: lamprophyre II (LD2: 315-295 Ma) → post-collisional "small intrusions" Li-Rb-Cs-F granite and associated rhyolitic dikes (315-290 Ma) → Sn(-W-Mo-Li-Rb-Cs) mineralization (317-310 Ma) → lamprophyre III (LD3: 310-290 Ma) → 'kb' ore-type / 'eb' and 'eq' ore-type → U-mineralization ('uqk' ore-type: 290-270 Ma). The ore deposit characterization, mineralogical composition, and trace element and isotopic signatures of the Ag-polymetallic mineralization in the Erzgebirge indicate a genetic link to the late-Variscan Sn(-W-Mo) mineralization and both to mantle-derived (lamprophyric) magmatic events. (3): The post-Variscan Bi-Co-Ni-As-U-Ag parageneses occur in different metamorphic host rocks (ortho- and paragneisses, micaschists, phyllites, granites). Their relationship to hidden basic or ultrabasic intrusions is postulated from different authors. (GSI; Thurs. Poster)

The giant Beaver Brook antimony deposit, central Newfoundland, Canada

Seifert, T., thomas.seifert@mineral.tu-freiberg, Sandmann, D., Division of Economic Geology and Petrology, Department of Mineralogy, TU Bergakademie Freiberg, Brennhaugasse 14, D-09596 Freiberg, Germany

The Beaver Brook deposit, located in central Newfoundland, Canada, is one of the largest antimony deposits outside of Asia. An underground mine was recommissioned at the deposit in 2008 by Beaver Brook Antimony Mine Inc. (BBAM). The concentrate produced (grading about 63% Sb) was trucked to Halifax, Nova Scotia for shipping to the P.R. of China. In 2009, Hunan Nonferrous Metals Corporation Limited (HNC), the largest antimony company in the world, acquired 100% equity of BBAM for 29.5 million US\$. In November 2012, HNC had announced that production of antimony at Beaver Brook mine will be suspended. The suspension of production will be due to the expected insufficient reserves of mineral resources, a lower-than-expected cut-off grade and high production costs that resulted in losses to BBAM. The mine was shut indefinitely in January 2013, with most of the approximately 100 year-round workers and 15 seasonal employees to be laid off. The current established resources of the Beaver Brook deposit are about 1.94 Mt @ 4.32% Sb, resulting in 84 kt Sb metal.

The monomineralic hydrothermal mineralisation consists predominantly of stibnite ore. Only subordinate amounts of pyrite can be found in certain parts of the deposit. The stibnite mineralisation is structurally controlled and occurs as aggregates that display stringer, bleb, clot, patch, seam, and disseminated aggregate textures. The ore bodies are hosted by Palaeozoic meta-sedimentary rocks of the Newfoundland Appalachians which were intersected by faults and breccia zones. Quartz and carbonates, as gangue minerals, occur in multiple stage generations, but mineral paragenesis is in general marked by an older stage of quartz-pyrite mineralisation, followed by a younger stage of stibnite-carbonate mineralisation. Stibnite partially encloses irregular remnants of partly replaced pyrite.

Geochemical data confirm the monomineralic composition of the stibnite ore, the absence of base metals as well as very low concentrations of gold. Host and hanging wall rocks show no



remarkable metal content. Sulphur isotope studies of stibnites suggest stable physico-chemical conditions with a uniform sulphur source.

The genesis of the antimony mineralisation at Beaver Brook is unambiguously associated with a structurally-controlled syn-deformational hydrothermal fluid flow. It may tentatively be suggested that the antimony was provided by leaching of underlying meta-sedimentary rocks by hydrothermal fluids. However, metamorphic or magmatic sources are further options for the metal-bearing fluids. More detailed studies will be required to improve the understanding of the origin of antimony mineralisation. (*SS2; Wed. Poster*)

Unusual supergene U^{4+} minerals from the Geschieber vein, Jáchymov, Czech Republic

Sejkora, J.¹, Plášil, J.², plasil@fzu.cz, Hloušek, J.³ and Škoda, R.⁴,
¹National Museum, Cirkusová 1740, CZ-19300, Praha 9, Czech Republic; ²Institute of Physics ASCR, v.v.i., Na Slovance 2, CZ-18221 Praha 8, Czech Republic; ³U Roháčových kasáren 24, CZ-100 00, Praha 10, Czech Republic; ⁴Faculty of Science, Masaryk University, Kotlářská 2, CZ-611 37, Brno, Czech Republic

The three novel supergene minerals were recently approved by CNMNC of IMA. All three new minerals contain U^{4+} in their crystal structures as dominant constituents, which is quite unusual under the oxidizing conditions. However, at the occurrence they were found (Geschieber vein, Svornost mine, Jáchymov) the formation of these minerals is bounded onto extremely acid (pH=0) As-rich (up to 13% As in the solution) AMD derived from weathering of native arsenic, which allowed U to be found in tetravalent state. Short-prismatic or tabular green crystals of běhounekite (IMA 2010-046) are orthorhombic (Pnma) $U(SO_4)_2(H_2O)_4$, with $a = 14.6464(3)$, $b = 11.0786(3)$, $c = 5.6910(14)$ Å, $V = 923.43(4)$ Å³, $Z = 4$, $D_{calc} = 3.62$ g·cm⁻³. The structure consists of 2-D layers containing 4-connected U-polyhedra ([8]-coordinated tetragonal antiprismatic) and 2-connected S polyhedra. Each U^{4+} is coordinated by four O atoms from the SO_4 tetrahedra and four H_2O molecules. The adjacent layers are bonded by hydrogen bonds. Emerald green tabular crystals of štěpíte (IMA 2012-006) are tetragonal (I41/acd) $U(AsO_3OH)_2(H_2O)_4$, with $a = 10.9894(1)$, $c = 32.9109(6)$ Å, and $V = 3974.5(1)$ Å³, $Z = 16$, $D_{calc} = 3.90$ g·cm⁻³. Its structure is based upon the sheets of tetragonal antiprismatic coordinated U atoms and AsO_3OH groups. Each U atom is linked to six As-tetrahedra by sharing vertices, while two remaining O atoms belong to H_2O groups. Adjacent sheets are linked by hydrogen bonds only. Greenish white long prismatic fibrous crystals of vysokýkite (IMA 2012-067) are triclinic (P-1) $U[AsO_2(OH)_2]_4(H_2O)_4$, with $a = 10.749(2)$, $b = 5.044(3)$, $c = 19.1778(7)$ Å, $\alpha = 89.872(15)^\circ$, $\beta = 121.534(15)^\circ$, $\gamma = 76.508(15)^\circ$, $V = 852.1(6)$ Å³, $Z = 2$, $D_{calc} = 3.38$ g·cm⁻³. Uranium coordination polyhedra are antiprisms, sharing all vertices As-tetrahedral units, forming infinite chains along [010]. The H_2O molecules are located within the channels between the adjacent chains and are held in the structure by hydrogen bonds involving also the H-atoms within the four independent As-tetrahedra of the structure units. (*SS5; Wed. Poster*)

Petrography and uranium mineralogy of the BaiYangHe volcanic-hosted uranium deposit, Xinjiang Autonomous Region, China

Shabaga, B.M.¹, brandishabaga@gmail.com, Fayek, M.¹, Guo, W.² and Zhanjiu, W.², ¹University of Manitoba, Dept. Geological Sciences, Winnipeg, MB R3T 2N2; ²Geology Party No. 216, No.467 BeiJinNan Road, WuLuMuQi City, Xinjiang Prov, China, 830011

The BaiYangHe uranium deposit is located in the Xuemistan volcanic zone, NW China. Although this region is actively being explored and exploited for its gas and mineral resources, very little is known about the BaiYangHe deposit. In 1956, the host rocks were identified as Lower Permian pyroclastic units, which overly Carboniferous rocks. An Upper Permian sill of micro-granitic porphyry was reported to control uranium mineralization. However, the association between the volcanic and porphyritic units is poorly understood. The objectives of

this study are to characterize the host rock associated with uranium mineralization and develop a genetic model.

Three drill-holes and numerous outcrops were sampled to characterize the mineral paragenesis and uranium mineralization. Outcrop samples are relatively unaltered and devoid of uranium mineralization, whereas samples from drill core were obtained from altered and mineralized zones. Samples from the ore zone contain up to 10,000 ppm U. Based on whole rock geochemistry and petrography, the suite of rocks associated with the BaiYangHe deposit range from alkali basalt to rhyolite. However, uranium mineralization is predominantly hosted by a strongly peraluminous rhyolite.

Uranium mineralization occurs along fractures. Based on powder XRD, SEM-EDS analysis and preliminary EMPA data, the dominant U mineralization is uranophane ($Ca(UO_2)_2[HSiO_4]_2 \cdot 5H_2O$). Uranophane is intergrown with Mn and Pb oxides, which can only be identified using BSE imaging. Our results contrast with previous reports, which identified uraninite (UO_2) as the dominant uranium mineral. However, the fine intergrowths of uranophane and Mn-Pb oxides can be mistaken for uraninite because of their similar appearance (in hand specimen) and high reflectance.

Multiple generations of fluorite (CaF_2) occur along the same fractures that host pyrite (FeS_2), uranophane and hematite (Fe_2O_3). The fluorite and pyrite predate the uranophane and hematite. Mineral textures suggest that fluids (meteoric water) interacted with the fluorite, oxidized the pyrite to hematite, and leached uranium from the host rhyolite. Uranium was most likely transported as a uranyl-fluoride complex (e.g., UO_2F^+). Fluoride complexes predominate in low pH fluids (<4) at 25°C. The oxidation of pyrite could lower the pH of meteoric water and produce an acidic fluid (e.g., $FeS_2 + H_2O = Fe_2O_3 + H + H_2SO_4$) favorable for the remobilization of F^- and U^{6+} .

While the genesis of this deposit remains controversial, results from our study suggest that the BaiYangHe deposit is a volcanic-hosted uranium deposit. Supergene enrichment and evaporation are the most likely mechanisms for concentrating uranium and precipitating uranophane along fractures. (*SS5; Wed. Poster*)

Textural character and chemistry of plagioclase and apatite in the Marathon Cu-PGE deposit, Ontario: Implications for mineralizing processes

Shahabi Far, M.¹, shahabim@uwindsor.ca, Samson, I.¹, Linnen, R.² and Good, D.³, Gagnon, J.¹, ¹University of Windsor, Windsor, ON N9B 3P4; ²University of Western Ontario, London, ON N6A 5B7; ³Stillwater Canada Inc., Thunder Bay, ON P7B 4A3

The Marathon deposit mineralization is hosted within the Two Duck Lake gabbro (TDLG) of the Mesoproterozoic Coldwell alkaline complex, in three zones (Footwall Zone, Main Zone, and W Horizon), which have different textural, mineralogical and geochemical characteristics. Plagioclase and apatite have complex textures, including evidence of dissolution and replacement, normal or reverse zoning, oscillatory zoning, patchy zoning in plagioclase, and growth (oscillatory) and replacement zoning in apatite.

Magmatic plagioclase is characterized by a strong positive Eu anomaly, and ΣREE increases from core to rim. Plagioclase with replacement rims containing high Cu and Pb concentrations occurs adjacent to granophyric patches in the vicinity of the footwall, suggesting alteration by fluids exsolved from the granophyric melts.

Apatite both predated and postdated plagioclase. Apatite crystals from the Main and Footwall zones, which lie closest to the country rocks, generally have high Cl contents, whereas apatite from the W Horizon, which is higher in the intrusion, has low Cl content. Rocks with higher grades of mineralization in the Main and Footwall zones generally contain apatite with higher Cl contents, whereas, in the W Horizon, higher grades correlate with lower Cl in apatite. In addition, zoning, recrystallization textures, and the presence of primary fluid inclusions are more common in apatite from the Main and Footwall zones. Apatite has a strong negative Eu anomaly, the magnitude of which increases from core to rim, as does ΣREE . Late apatite has a ΣREE abundance between that of the core and rim of early apatite,



suggesting that late apatite probably crystallized from a new influx of magma rather than from continued crystallization of a resident magma.

The spatial variations in apatite Cl/F could be explained if compositionally distinct magma pulses were responsible for each mineralized zone, as most early apatite crystals are euhedral to subhedral, and magmatic. Intracrustal basaltic melts are, however, reported to be poor in Cl. Chalcopyrite in the Main Zone commonly replaces pyrrhotite and is intergrown with hydrous silicate minerals, suggesting Cu (re-) mobilization. Therefore, a zone-refining process in which volatiles, derived from footwall country-rock dehydration, migrated through the crystallizing gabbros and transported Cu to the Main Zone is an attractive model by which Cl could also be added to the system. The low Cl contents of apatite in the W Horizon can be explained if these fluids did not reach the W Horizon, or the W Horizon represents late-stage magma infiltration. (GS1; Fri. 2:20)

Ichnology of the Ediacaran-Cambrian Soltanieh Formation of northern Iran: Reconstructing animal-substrate interactions during the Cambrian explosion

Shahkarami, S., Mangano, M.G., Buatois, A.L., Department of Geological Sciences, University of Saskatchewan, 114 Science Place, Saskatoon, SK S7N 5E2, ses830@mail.usask.ca, and Siab Ghodsi, A.A., Geology department, University of Urmia, Urmia, Iran

Strata in the Central Alborz Mountains, northern Iran, show continuous sedimentation from Ediacaran through Cambrian time. The Meidanak section, 65 km north of Tehran, includes two major units: the Kahar and Soltanieh formations. The Soltanieh Formation consists of five members: Lower Dolomite, Lower Shale, Middle Dolomite, Upper Shale and Upper Dolomite. The Ediacaran-Cambrian transition is coincident with the boundary between the Lower Shale Member and the Middle Dolomite Member.

The Soltanieh Formation is interpreted as having been accumulated in a shallow-marine carbonate ramp. This formation experienced two transgressive episodes. The first of these transgressions occurs in the late Ediacaran, and is represented by the passage of tidal-flat deposits of the Lower Dolomite Member to the open-marine dark grey, silty micaceous shale of the Lower Shale Member. Some problematic fossils (e.g. *Chuarina circularis*, *Vendotaenia* sp., *Tawuia fosiformis*) are present in this unit.

The second transgression took place in the early Cambrian, and is represented by the transition from the Middle Dolomite Member to the Upper Shale Member. This unit consists of black to gray, silty micaceous shale alternating with very fine-grained sandstone. These deposits contain an ichnofauna representative of the *Cruziana* Ichnofacies, characterized by the dominance of shallow horizontal trails and burrows produced by deposit feeder and the absence of vertical domiciles of suspension-feeders. Elements of the Soltanieh ichnofauna include presumed bivalve trace fossils (*Protovirgularia* and *Lockeia*), presumed trilobite trace fossils (*Cruziana*), shallow burrows and trails of vermiform organisms (*Phycodes*, *Torrowangea Planolites*, *Palaeophycus*, *Treptichmus*) and trails of mollusk-like animals (*Archaeonassa*).

The sedimentological and ichnological evidence suggests that both the Lower and Upper Shale members of the Soltanieh Formation have been deposited under very similar environmental condition, most likely during the transgression that led to the establishment of an open-marine setting. The rich ichnologic content of the Cambrian Upper Shale Member contrasts with the absence of trace fossils in similar deposits of the Ediacaran Lower Shale Member, pointing to the rapid appearance of new body plans and novel forms of animal-substrate interactions during the Cambrian explosion. (GS5; Thurs. Poster)

The GRYPHON multi-parameter airborne platform: The future of regional exploration

Shales, A., Fugro Airborne Surveys, 1500-701 West Georgia St., Vancouver, BC V7Y 1C6, ashaless@fugroairborne.com

Airborne geophysical methods are extremely useful tools in exploration and mapping programs. There are many different types of airborne geophysical systems and each type measures a different physical parameter which in turn provides different information about the subsurface of an area of interest. Regardless of the type of target or targets being sought, in order for a given target to be detected by geophysical methods, a contrast in a given physical parameter must exist between the target and the surrounding host rock. Some targets may have a contrast in one or more parameters but not in another. Therefore it is been important to select the most appropriate geophysical method that captures the parameter exhibiting the most contrast. In areas where limited previous information exists, this can pose a problem as often one may not know what target types are present and therefore which survey method is most appropriate.

However this dilemma is solved with the introduction of the GRYPHON Multi-Parameter Platform which is the only system to combine the full suite of airborne geophysical measurements onto a single platform. The simultaneous collection of: electromagnetic, magnetic, gravity, radiometric, LiDAR and digital video data by the GRYPHON system provides a cost-effective and time-efficient way to obtain unparalleled information on an area's geophysical signature. Integrating this information together provides a fuller understanding of an area's geology and ensures information on all possible parameters is measured thereby reducing the chance of missing a target. Details on this exciting new technology along with examples will be discussed. (SS12; Thurs. 11:00)

Keynote (40 min): Empirical electronic polarizabilities in oxides, hydroxides, oxyfluorides and oxychlorides

Shannon, R.D., Geological Sciences, CIRES, University of Colorado, Boulder, CO 80309, USA, and Fischer, R.X., Universität Bremen, FB 5 Geowissenschaften, Klagenfurter Str., D-28359 Bremen, Germany

An extensive set of refractive indices determined at $\lambda = 589.3$ nm (n_D) from ~1570 measurements on 850 oxides, 215 oxyfluorides, 40 oxychlorides, 500 non-hydrogen-bonded hydroxyl-containing compounds, and 47 hydrogen-bonded hydroxyl-containing compounds was used to obtain mean total polarizabilities for approximately 1080 minerals and synthetic compounds. These data, using the Lorenz-Lorentz relation:

$$\alpha_{De} = \frac{1}{b} \quad V_m \cdot \frac{n_D^2 - 1}{n_D^2 + 2}$$

where n_D = the refractive index at $\lambda = 589.3$ nm, V_m = molar volume in \AA^3 , and $b = 4\pi/3$, in conjunction with the polarizability additivity rule and a least-squares procedure, were used to obtain electronic polarizabilities for 89 cations in various coordinations, H_2O , 4 H_2O_y species $[(\text{H}_3\text{O})^+, (\text{H}_3\text{O}_2)^-, (\text{H}_4\text{O}_4)^+, (\text{H}_7\text{O}_4)^-]$ and 4 anions (F^- , Cl^- , OH^- , O^{2-}). As in a previous publication, we modified a light-scattering (LS) model by Jemmer *et al.* to provide for a smooth decrease in polarizability at low CN's to the free-cation value at infinite CN's (infinite distance) and to allow fitting polarizability values for Mg, Ca, Sr, Ba, Pb, Y, and La. This refinement process excluded hydrates and zeolites and compounds with (1) structures containing lone-pair and uranyl ions (2) sterically-strained structures, (3) corner-shared octahedral network and chain structures such as perovskites, tungsten bronzes and titanite-related structures, (4) edge-shared Fe^{3+} and Mn^{3+} structures such as piemontite and pumpellyite and (5) compounds exhibiting fast-ion conductivity. The refinement for 1570 polarizability values using 89 cation polarizabilities with values for Li, Na, K, Rb, Cs, Ag, Tl, Mg, Ca, Sr, Ba, Pb, Mn, Fe^{2+} , Co, Cu, Zn, B, Al, Ga, Fe^{3+} , Sc, Y, Lu \rightarrow La, Si, Ge, Ti, Th and V^{5+} in varying CN's, yields a standard deviation of the least squares fit of 0.19 (corresponding to an R^2 value of 0.9997) and no discrepancies, Δ , between observed and calculated polarizabilities $> 3\%$. Systematic discrepancies are associated with sterically-strained compounds ($\Delta = 2-10\%$) and structures that support fast-ion conductivity ($\Delta = 2-10\%$). Values of Δ , up to 10%, are found in perovskite compounds such as SrTiO_3 . (SY1; Wed. 8:20)

**A genetic model for the Bong uranium deposit, Thelon Basin, Nunavut, Canada**

Sharpe, R.W.¹, umsharpr@cc.umanitoba.ca, Fayek, M.¹, Quirt, D.² and Jefferson, C.W.³, ¹Department of Geological Sciences, The University of Manitoba, 125 Dysart Road, Winnipeg, MB R3T 2N2; ²AREVA Resources Canada Inc., PO Box 9204, 817 - 45th Street W., Saskatoon, SK S7K 3X5; ³Geological Survey of Canada, Rm 659 - 601 Booth, Ottawa, ON K1A 0E8

The Thelon Basin, Nunavut is geologically similar to the uranium-producing Athabasca Basin, Saskatchewan; however, the uranium deposits associated with the Thelon Basin are relatively poorly understood. The Kiggavik project area (AREVA Resources Canada) is located near the northeastern terminus of the Thelon basin and comprises multiple uranium deposits. In the Kiggavik area, the Thelon Formation has been eroded and the uranium deposits are hosted exclusively in basement rocks: highly deformed metagreywacke, metavolcanic and volcanoclastic strata of the Neoproterozoic Woodburn Lake Group, ~2.6 Ga mylonitized rhyolite (quartz-eye rhyolite), and undeformed 1.83 Ga to 1.75 Ga Lone Gull granite. The Bong deposit, southwest of the Kiggavik deposits, is located at the intersection of two camp-scale faults.

The Bong deposit is hosted by Woodburn Lake Group metasediments, composed predominately of quartz and feldspar, with biotite and muscovite. Rare graphite layers comprise nodules and blebs, many of which are mineralized. Bitumen is observed within the illitic alteration zone along pre-existing fractures. Two stages of uraninite mineralization have been identified. Stage A uraninite forms veinlets parallel to foliation; it also coats and fills fractures in graphite. The uraninite is highly fractured and locally altered to uranophane. Stage A uraninite is intergrown with paragenetically contemporaneous illite that records ~225°C fluids ($\delta^{18}\text{O}$: -7.9‰, δD : -100.9‰). The temperature of these fluids is similar to those associated with the basement-hosted deposits in the Athabasca basin however the isotopic composition of the fluids differs significantly. Stage B uraninite forms "mini-roll-fronts" at redox boundaries between an oxidized zone rich in hematite and an illitic reduced zone. U-Pb ages obtained from uraninite are 1117 ± 15 Ma (Stage A) and 1040 ± 39 Ma (Stage B). Graphite occurs with Stage A uraninite and bitumen with Stage B uraninite. The $\delta^{13}\text{C}$ value for unmineralized bitumen (-44.3 \pm 5.7‰) is significantly lower than that for mineralized bitumen (-24.2 \pm 3.1‰); apparently the result of hydrothermal alteration by mineralizing fluids.

A four-stage metallogenetic model is proposed for the Bong deposit. Stage 1 is characterized by host-rock silicification, while Stage 2 is characterized by pervasive host-rock argillization and formation of Stage A uraninite in veins and coating graphite (~1120 Ma). During Stage 3, bitumen formed, along faults and permeable clay-rich alteration zones. At ~1040 Ma, an oxidizing fluid event (Stage 4) reconcentrated uraninite into redox fronts (Stage B uraninite) and altered Stage A uraninite to uranophane. (*SS5; Wed. 3:20*)

Natural attenuation of metals from the No Cash 500 mine adit discharge, Keno Hills Mining District, Yukon Territory, Canada

Sherriff, B.L.¹, BLSherriff@gmail.com, Johnson, B.², Eary, L.E.², Harrington, J.³, Davidson, S.⁴, Jamieson, H.E.⁵, Gault, A.⁵ and Londry, K.⁶, ¹Sherriff Environmental Inc., Powell River, BC V8A 3P4; ²Interralogic, Inc., 4715 Innovation Drive, Suite 110, Fort Collins, CO, USA; ³Alexco Environmental Group, 88 Inverness Circle East, Suite 102, Englewood, CO, USA; ⁴Access Consulting Group, #3 Calcite Business Centre, 151 Industrial Road, Whitehorse, YK Y1A 2V3; ⁵Department of Geological Sciences and Geological Engineering, Queen's University, Kingston, ON K7L 3N6; ⁶Edmonton Waste Management Centre of Excellence, Edmonton, AB

Alexco Resources Canada (Alexco) is developing a District Closure Plan for historical mining operations in the Keno Hills Silver District, Yukon Territory in a unique joint-funding partnership with the federal government. Historic mining activities resulted in a number of mine adits that discharge water to surface streams, including the No Cash 500

adit. Metal concentrations at the portal are: Mn (10 to 12 mg/L), Zn (13 to 19 mg/L), Cd (0.2-0.5 mg/L). Solutions are circumneutral with alkalinity from 150 to 200 mg/L and sulphate from 300 to 500 mg/L. After leaving the adit, the discharge plunges over a steep hillside aerating the water, then is captured in a poorly-drained peat bog. Metal concentrations rapidly decrease along the stream course; Zn decreases by 100 \times , Cd by 100 \times to 1000 \times , and Mn by 20 \times to 10,000 \times .

Alexco has assembled a team of consultants, university-based researchers and mining company representatives to explore the potential for using natural attenuation as a closure option as sites such as the No Cash system. Mineralogical data from the University of Manitoba and Queens indicate that zinc phases are related to multiple Zn-Mn coatings with heterolite (ZnMn_2O_4) identified as the dominant crystalline mineral. Characterization of mineral precipitates included scanning electron microscopy, electron microprobe, LA-ICP-MS and synchrotron-based micro-XRF, micro-XANES and micro-XRD. Further research is presently underway to determine the long-term stability of this natural attenuation system, including laboratory-based simulation of the interaction of the Zn-Mn precipitates with adit water under variable conditions of temperature, pH, alkalinity and redox. Discussions are being held with federal, territorial and First Nation governments about the feasibility of natural attenuation as an innovative closure option for the elevated Zn in No Cash mine discharge. The collaboration of consultants, university-based researchers, government and mining company representatives provided an opportunity to apply advanced research techniques to test a novel solution for a problem frequently found at abandoned mine sites. (*SS20; Fri. 2:20*)

Compositional variation and paragenesis of Li tourmaline from Nagatare, Fukuoka Prefecture, Japan

Shirose, Y., shirose@kyudai, and Seiichiro, U., University of Kyushu, 6-10-1 Hakozaki, Higashi-ku, Fukuoka City, Japan
Nagatare pegmatite, Fukuoka Prefecture, Japan, is a complex type granitic pegmatite, LCT families. Tourmaline from Nagatare pegmatite was classified into 5 types, black, indigo, light blue-pink, pink and pink-light blue, on the basis of localities, associated minerals, color and texture. A total of 30 samples were analyzed by EPMA and XRD.

A substitution of (Li + Al) for Fe at the Y site was significant, showing the chemical development of the melt. The minor cations at the Y site, such as Mg, Mn, Zn and Ti, were also characteristic on each type. For the X and W site, indigo type tourmaline had large amounts of Na and F, however, pink type was abundant with vacancies and (OH), respectively. The mineral species of the tourmaline from Nagatare pegmatite were composed of elbaite, fluor-elbaite, rossmanite, schorl and fluor-schorl. The unit cell parameters were in the range between rossmanite, elbaite and schorl.

Compared to other LCT pegmatites, the chemical trends of tourmaline from Nagatare pegmatite were similar on major chemical components, but different on minor elements such as Zn and Mn. The intermediate fractionated tourmaline, indigo type, had Zn (0.20 apfu/ 1.60 Wt%) and Mn (0.28 apfu/ 1.98 Wt%), which indicates that the pegmatite forming melt contained less Fe and more Zn and Mn than other localities.

In pink-light blue type, the rim had greater Fe and Mn than the core, which shows that it crystallized in a hydrothermal environment. Vacancy, Al and OH rich Li tourmaline (pink type and pink part of pink-light blue type) were selectively replaced by muscovite. In addition, metasomatic replacement of associated montebrasite was confirmed. These features indicate that several stages of alterations, including a sericitization, occurred in the late stage of the pegmatite forming process. (*SY2; Thurs. Poster*)

Solid solutions between silicate and phosphate minerals of the olivine structure type: Example from Poibyslavice metagranite, Czech Republic

Škoda, R.¹, rskoda@sci.muni.cz, Novák, M.¹, Havránek, V.² and Lens, C.³, ¹Department of Geological Sciences, Masaryk University, Brno, Czech Republic; ²Nuclear Physics Institute of



the ASCR, Oež, Czech Republic; ³Institut für Mineralogie und Kristallographie, University of Vienna, Vienna, Austria

Natural olivine structure-type phases (Pbnm) include olivine-group (Mg,Fe,Mn)₂SiO₄ and triphylite-group Li(Fe,Mn,Mg)PO₄ minerals. Solid solution between olivine and triphylite is limited mainly due to distinct geochemistry of their host rocks, although X ppm Li enters olivine from ultrabasic rocks. Phosphoran olivine (X wt.% P₂O₅) is known from meteorites and ultrabasic rocks; triphylite, solely occurring in pegmatites, contains <1 wt.% SiO₂. The Li,P-enriched, peraluminous Poibyslavice metagranite contains cm- to dm-sized phosphate veins and nodules with dominance of graptolite or triphylite. Besides major graptolite, triphylite and sarcopside typical minor to accessory minerals include:

quartz-muscovite>gahnite>graphite-wolfeite-fluorapatite >pyrrhotite>fayalite>harrisonite; textural relations of major phosphates are complex. Triphylite contains numerous lamellas of sarcopside and euhedral to subhedral domains brighter in BSE relative to triphylite (BD). They usually do not host sarcopside lamellas and have elevated contents of FeO and SiO₂ (≤17 wt.%; mostly 2-11 wt.% SiO₂). The SiO₂ content is <1 wt.% in associated sarcopside and graptolite. The size of the BD decreases with increasing SiO₂ content: from X00 to X μm. Increasing content of SiO₂ (<7 wt.%) in triphylite (Tph) is accompanied by increasing of fayalite (Fa) as well as the Fe_{1.5}PO₄ (FeP) phase in the following trend: Tph100 → Fa₂₀Tph₃₀FeP₅₀, leading to theoretical Fe₅(PO₄)₂SiO₄. Additional increase of the SiO₂ (<17 wt.%) is running along the trend Fa₂₀Tph₃₀FeP₅₀ → Fa₅₀Tph₂₀FeP₃₀ towards fayalite. PIGE measurements confirmed the depletion of Li in BD and measured Li is in good agreement with the calculated one. Raman spectroscopy of the BD's (3.5, 5, 10 wt.% SiO₂, respectively) revealed continuous broadening of most intensive triphylite P-O stretching band in the region 940-950 cm⁻¹ with increasing SiO₂ content. Increasing content of SiO₂ in BD is also accompanied by increasing intensity of the broad vibration bands in region around 840 and 966 cm⁻¹. Low contents of Si in triphylite nodules commonly enclosed in massive quartz from pegmatites indicate only negligible solid solution. It may be explained by lower pT-conditions of their crystallization (~2-3 kbar; 400-500 °C) relative to the Poibyslavice metagranite (~5-6 kbar; 650-700 °C). (SY1; Wed. Poster)

A fresh look at Eu anomalies: The effect of Cl-rich fluids

Smith, E.M., esmith@eos.ubc.ca, and Kopylova, M.G.,
Department of Earth, Ocean and Atmospheric Sciences,
University of British Columbia, 2207 Main Mall, Vancouver, BC
V6T 1Z4

Europium anomalies are conventionally interpreted as indicators of plagioclase involvement in rock formation. The present paradigm assigns Eu anomalies to the presence of plagioclase in the magma source, or its accumulation or fractionation in the melt. Many petrogenetic models critically depend on these interpretations, including our understanding of certain mantle processes. Eu anomalies in mantle rocks are commonly interpreted as a reflection of plagioclase accumulation or removal in the crust or shallow mantle, and a subduction origin is inferred. However, other processes can also produce Eu anomalies. We show that the Cl content in a hydrothermal or metasomatic fluid can control Eu fractionation, independently from plagioclase. We analyzed REE's within mantle fluid captured as inclusions in "fibrous" diamonds from the 2.701–2.697 Ga Wawa metaconglomerate, Ontario, Canada, and found positive Eu anomalies (Cl chondrite normalized Eu/Eu* = 7–14). A subduction origin for this anomaly, however, would disagree with the consistent, convecting mantle-like carbon and nitrogen stable isotopes characteristic of fibrous diamonds. These are K-, Na-, and Cl-rich carbonate-bearing saline fluid inclusions, which bear a strong resemblance to other saline fluids reported from fibrous diamonds. A review of published fibrous diamond trace element data reveals that Eu anomalies also occur in other examples of Cl-rich saline fibrous diamond fluid, but not in more silicic or carbonatitic fluid varieties. This restriction suggests that Cl-rich fluid can fractionate Eu from other REE's in the mantle. A similar

tie between Eu and Cl-rich fluid is observed at seafloor vents, where hydrothermal fluids have positive Eu anomalies that correlate with fluid ligand concentrations more so than with rock composition. The Cl-rich fluids present in our samples could have preferentially scavenged Eu as it percolated through the mantle, giving the fluid a positive Eu anomaly. Interaction with Cl-rich fluid may therefore lead to Eu anomalies in mantle rocks. A subduction origin for Eu anomalies in mantle rocks should not be inferred without considering the potential involvement of Cl-rich fluids in the petrogenetic history. The same principle applies to crustal rocks that were in contact with hydrothermal Cl-rich fluids and may have reacted with them. (SS6; Wed. 8:20)

Nitrogen bubbles in the mantle: Evidence from diamond inclusions

Smith, E.M.¹, esmith@eos.ubc.ca, Kopylova, M.G.¹, Frezzotti, M.L.² and Afanasiev, V.P.³, ¹Department of Earth, Ocean and Atmospheric Sciences, University of British Columbia, 2207 Main Mall, Vancouver, BC V6T 1Z4; ²Department of Geological Sciences and Geotechnologies, University of Milano-Bicocca, Piazza della Scienza 4, 20126 Milano, Italy; ³Sobolev Institute of Geology and Mineralogy, Siberian Branch of the Russian Academy of Sciences, pr. Akademika Koptyuga 3, Novosibirsk, 630090, Russia

Mantle volatiles sampled at mid-ocean ridge settings or preserved as fluid inclusions in mantle xenoliths are dominated by CO₂, with only small amounts of nitrogen. Nitrogen generally appears as a trace component in the Earth's mantle. However, diamonds from three different localities, the Kaapvaal, Congo, and Siberian cratons, have been found to contain nitrogen-rich fluid inclusions and melt inclusions. Nitrogen in the inclusions was analyzed using confocal laser-Raman spectroscopy. Melt inclusions in the diamonds from the Kaapvaal and Congo cratons contain exsolved bubbles of volatiles that are >90 mol% N₂. At the time of trapping, before bubble nucleation, the silicate melt would have contained ~1 wt% dissolved N₂. The fluid inclusions in diamonds from the Siberian craton are CO₂-N₂ mixtures with 40±4 mol% N₂. These melt and fluid inclusions suggest nitrogen's presence in the mantle has been underestimated. Such nitrogen-rich fluids/melts designate the existence of hidden, concentrated nitrogen fluxes escaping the convecting mantle, which are not accounted for in current fluid models that suggest two thirds of subducted nitrogen is not returned to surface. Concentrated fluxes of nitrogen entering the base of the continents raise the possibility that continental lithosphere could trap significant amounts of nitrogen. The occurrence of this nitrogen in the studied diamond samples demonstrates a tie between N₂ and oxidized diamond-forming carbon species percolating up from the asthenosphere. In turn, this tie suggests redox conditions pose an important control over mantle nitrogen behaviour, both in terms of its storage and geodynamic cycling. We propose that the observed N₂ in our samples was liberated by the oxidation of NH₄⁺-bearing silicates, roughly concurrent with a parallel oxidation process releasing carbonate melt from the asthenosphere. The oxidation and nitrogen liberation from the mantle should change the N isotopic signature and help explain the ¹⁵N/¹⁴N mismatch between influxed and effluxed mantle nitrogen without invoking a unique, isolated upper mantle nitrogen reservoir. This isotopic fractionation explains the isotopic mismatch between isotopically heavy subducted carbon and the isotopically light N in diamonds and mid-ocean ridge basalts. (SS4; Fri. 8:40)

Analysis of fluid inclusions from the Marathon Cu-Pd deposit: The role of hydrothermal fluids in mineralization

Smoke, R.¹, renatasmoke@yahoo.ca, Linnen, R.¹, Samson, I.², Good, D.³ and Shahabifar, M.², ¹University of Western Ontario, London, ON N6A 1K7; ²University of Windsor, Windsor, ON N9B 3P4; ³Thunder Bay, ON P7B 4A3

The Marathon Cu-Pd deposit is hosted by the Two Duck Lake Gabbro, which intruded the Eastern Gabbro of the Proterozoic Coldwell Complex. There is definitive evidence for water-rock interaction in the deposit, but the importance of hydrothermal fluids to mineralization is unclear. The solubility of PGE in hydrothermal fluids has been



demonstrated experimentally and observations from some ore systems also suggest the participation of fluids in their formation. We are studying fluid inclusions in the Marathon Cu-Pd deposit to characterize the nature of the hydrothermal fluids associated with this deposit and evaluate their importance to mineralization.

The deposit consists of three zones based on sulfide content, the degree of hydrothermal alteration, and ore metal ratios. These are the W-horizon, which has low sulfide and Cu content, a high PGE content and minimal hydrothermal alteration; the Main Zone which has higher sulfide and Cu content, and a higher degree of hydrothermal alteration; and the Footwall Zone which is poorly mineralized, in part comprises semi-massive sulfides, and has the highest degree of hydrothermal alteration.

Petrography of fluid inclusions in apatite shows that late-stage chalcopyrite deposition is related to vapour-rich carbonic, and liquid-vapour aqueous fluid inclusions. Inclusions containing variable proportions of vapour, liquid, and solid phases and are also present. In some of these liquid-vapour-solid inclusions from the Main Zone, the solids include chalcopyrite, and there are high vapour to liquid ratios. Fluid inclusions vary in character and abundance between the three zones. Inclusions in the W-horizon are mostly vapour-rich, whereas in the Main Zone they comprise vapour-rich, liquid-vapour, and solid-liquid-vapour. The Footwall Zone contains all inclusion types, but has the greatest abundance of solid-rich fluid inclusions of the three zones. Microthermometric analysis of vapour-rich inclusions coeval with chalcopyrite from the W-Horizon and Footwall Zone yielded melting temperatures of -56.6 °C (indicating the vapour consisted of CO₂), and liquid-vapour inclusions coeval with late chalcopyrite from the Basal Zone have homogenization temperatures of 315-318 °C. It remains to be established whether these fluids simply locally remobilized Cu-Pd or played a more important role in forming the mineralization at the Marathon deposit. (SS9; Wed. 9:40)

Towards exploration tools for high purity quartz in the Bamble-Evje pegmatite belt, south Norway

Snook, B.R.¹, bs225@ex.ac.uk, Müller, A.², Williamson, B.J.¹ and Wall, F.¹, ¹Cambridge School of Mines, University of Exeter in Cornwall, Penryn, Cornwall, TR10 9EZ; ²Norges Geologiske Undersøkelse (NGU), Postboks 6315 Sluppen, 7491 Trondheim

High Purity Quartz (HPQ; quartz containing less than 50 ppm trace elements) is of increasing economic significance due to its use in certain high-tech components (computer chip/semiconductor manufacture) and in green technologies (silicon wafer production). Current HPQ deposits (hydrothermal veins/leuco-granites/alaskites) are rare and volumetrically small. Unless significant new deposits are found, increasing demand will raise its prices, elevating the strategic nature of this limited commodity. The large volumes and simple mineralogy of pegmatites and the high chemical purity of their constituents make them an attractive target for HPQ. PhD studies are being carried out on quartz from the Evje-Iveland pegmatite field of the Bamble-Evje pegmatite cluster, southern Norway. The area was targeted due to its well constrained geological setting and previously identified potential for HPQ. The aim of the investigation is to develop exploration tools for HPQ by determining the genetic history of the pegmatites and mode of HPQ formation.

The study is focussing on 7 pegmatites and their country rocks. Each shows typical pegmatite zonation, with quartz/feldspar intergrowths at the margins, a massive quartz core and a variety of accessory (including REE-bearing) phases. The proximal Høvringsvatnet granite was previously suggested to have supplied late-stage, highly fractionated melts to form the pegmatites. However, from their trace element systematics (no relationship was observed between trace element content and degree of fractionation in each pegmatite body), and a difference in U/Pb age of approximately 70 Ma, the pegmatites cannot be related to the granites. From field evidence (corroborated by geochemical modelling) the pegmatites formed by 'in situ' anatexis of country rocks; some locally, some from distal sources.

Some pegmatites contain brecciated feldspar and replacement quartz. From LA-ICP-MS analyses, hydrothermal quartz, compared with magmatic quartz, typically contains lower quantities of trace elements. Hydrothermal material shows relatively elevated levels of Al and Li, low Ge and a complete absence of Ti, indicating relatively low temperature hydrothermal formation. Different quartz domains (from SEM-CL imaging) show distinct $\delta^{18}\text{O}$ values; late stage low trace element zones show values consistent with meteorically derived fluids. *In situ* LA-ICP-MS and fluid inclusion studies will provide further information about the characteristics of the fluids which have replaced/refined magmatic quartz to form HPQ. This beneficiation process is a potential mechanism for the generation of economically significant HPQ deposits. (SY2; Thurs. 2:40)

Computational study of energetics and defect-ordering tendencies for Y and La in UO₂

Solomon, J.M.¹, jsolom@berkeley.edu, Alexandrov, V.^{1,2}, Shvarevac, T.Y.³, Sadigh, B.⁴, Navrotsky, A.^{3,2} and Asta, M.^{1,2}, ¹Department of Materials Science and Engineering, University of California, Berkeley, CA 94720, USA; ²Department of Chemical Engineering and Materials Science and NEAT ORU, University of California, Davis, CA 95616, USA; ³Peter A. Rock Thermochemistry Laboratory and NEAT ORU, University of California, Davis, CA 95616, USA; ⁴Physical and Life Science Directorate, Lawrence Livermore National Laboratory, Livermore, CA 94550, USA

The formation enthalpies and defect ordering tendencies of trivalent fission products (Y and La) in UO₂ are calculated using atomic-scale simulations. Low-energy defect structures are first screened with calculations based on core-shell ionic-potential models. The most stable structures are then studied by density functional theory with Hubbard-U corrections (DFT+U), and by hybrid DFT methods. The calculations consider compositions of the form (U_{1-x}M_x)O_{2- δ} and (U_{1-x}M_x)O₂, where the trivalent cations (M) are charge-compensated by oxygen vacancies and U⁵⁺ ions, respectively. Calculated formation enthalpies and cation-ordering tendencies are compared with recent calculations for Y and La doped ThO₂, as well as calorimetry measurements. (SS5; Wed. Poster)

Application of portable XRF in ore exploration and mining: Examples from Mexico, Colombia and South Africa

Somarin, A.K., 2 Radcliff Road, Tewksbury, MA, 01876 USA, alireza.somarin@thermofisher.com

Field-portable X-ray fluorescence (FPXRF) is a technique that is gaining momentum and acceptance in addressing applications in various fields in geology and mining. Thousands of these instruments are currently used in exploration and mining projects around the world. Light weight (1.5 kg) and capability to analyze elements from Mg to U in real time (*in-situ*) make this instrument an invaluable tool in exploration and mining of wide range of ore deposits. XRF is a surface analysis technique which can be used on any types of geological samples and can report elemental composition as ppm or percentage. This paper summarizes application of Thermo Scientific Niton FPXRF in three projects in Mexico (Pb-Zn-Ag), Colombia (Au) and South Africa (PGEs).

The Francisco I. Madero Zn-Cu-Pb-(Ag) deposit is operated as an underground mine in Zacatecas, central Mexico. There are two types of sulfide ore assemblages in the ore body: Pb-Zn and Cu-Ag sulfide assemblages. The ore minerals include sphalerite, galena, chalcopyrite, cubanite, enargite, and tetrahedrite accompanied by quartz, clay, pyrite, chlorite and epidote. This comparative study shows high correlation between data from FPXRF and lab methods. Also it shows that sample preparation has a significant effect on the accuracy of XRF data.

The FPXRF was used in two gold exploration projects in Colombia (Mina El Cairo and San Fernando) on the eastern flanks of the Cordillera Oriental of the Colombian Andes. The host for gold-bearing veins is the Cajamarca metamorphic complex composed of



greenschist to amphibolite grade metamorphic rocks ranging from chlorite-albite-epidote to chlorite-albite-actinolite and quartz-sericite-graphite schists. This complex is intruded by the El Bosque quartz monzonite to biotite granite batholith. The FPXRF was used on whole rock, vein and heavy concentrate stream sediment samples and the assay data were compared with the lab-based ICP (MS and ES) analyses. The XRF geochemical maps indicate that portable XRF can be successfully used in delineating anomalous zones of gold and/or pathfinder elements.

The target area for the third investigation is the Merensky Reef in the Bushveld Complex, South Africa. This reef is a layer of igneous rock, which, together with an underlying layer, the Upper Group 2 Reef (UG2), contains most of the world's known reserves of PGEs. In the studied area, the stratigraphy includes pyroxenite, anorthosite, and harzburgite (pseudo/altered) with local strings of chromite. The PGEs are hosted in disseminated sulfides with typical grades ranging from 3 to 10 g/t (ppm). To investigate the application of FPXRF in PGE exploration, 63 samples were collected along a stratigraphic section. The samples then were analyzed by commercial lab using ICP. Two types of portable XRF analyses (direct shot on the sample and pulverized sample-pulp) were carried out on these samples. Using lab assays, pathfinder elements were selected based on their correlation with the target elements (Pt, Pd and Au). The investigation shows that Ni and Cu from FPXRF can be used as pathfinder elements not only for Pt, but also for both Pd and Au. (*SS12; Thurs. 8:20*)

Thermometric studies of the Mag Hill IOCG system, Contact Lake belt, Northwest Territories, Canada

Somarin, A.K., somarina@brandonu.ca, and Mumin, A.H.,
Brandon University, Brandon, MB R7A 6A9

Intrusion of synvolcanic diorite-monzodioritic plutons into andesitic host rocks produced several characteristic hydrothermal assemblages in the Echo Bay stratovolcano complex and Contact Lake Belt of the Great Bear Magmatic Zone, Northwest Territories.

These hydrothermal assemblages include early and proximal albite, magnetite-actinolite-apatite and potassic (K-feldspar) alteration, followed by more distal hematite, phyllic (quartz-sericite-pyrite), and propylitic (chlorite-epidote-carbonate±sericite±albite±quartz) alteration, and finally by late stage polymetallic epithermal veins. The highest temperature (~560 °C) is recorded in the magnetite-actinolite-apatite alteration with an average 12.83 wt% NaCl equivalent salinity. This was followed by a high-temperature phase of propylitic and phyllic alterations with intermediate formation temperatures and a wide range of salinities. Then a Cu-Ag-U-Zn-Co-Pb sulfarsenide mineralization occurred in late stage epithermal veins at shallow depths and temperatures from 270 °C to as low as 105 °C. Fluid mixing and boiling were the main mechanisms of evolution of hydrothermal solution in this deposit. (*SS23; Fri. 2:00*)

HREE and Y anomalies in U-mineralized granites of the São José de Espinharas deposit, northeastern Brazil: Evidence of the composition of ore-forming metasomatic fluids

Souza Neto, J.A., Department of Geology and Graduate Program in Geosciences, Federal University of Pernambuco, Avenida Acadêmico Hélio Ramos s/n, Cidade Universitária, CEP: 50.740-530, Recife, Pernambuco, Brazil, адаuto@ufpe.br, and Santos, E.J., Brazilian Geological Survey, CPRM, edilton.santos@cprm.gov.br

The São José de Espinharas Deposit (SJED) is located in the state of Paraíba state, in the Borborema province, Northeastern Brazil. This deposit is a U-REE-P hosted in Neoproterozoic granitic rocks affected by Na metasomatism (albitization). The SJED is the fifth Brazilian U deposit in terms of reserves, and contain about 10,000 tons of U₃O₈. In the area of the SJED there was a lack of detailed geological mapping, being only recorded maps of geophysical anomalies (gamma spectrometry for U-Th-K, and magnetometry). Thus a detailed geological mapping (scale 1:40,000) was carried out in an area of approximately 150 km² around the SJED, and revealed that the main

mineralized body corresponds to a dyke of a fine- to medium-grained equigranular syenogranite with about 2 km long and 100 m wide, disposed to along the NE-SW direction. The mineralized rock is characterized by a pervasive albitization of alkali feldspar with iron oxides (e.g. hematite) associated. This alteration imposes a deep reddish color to the mineralized rock that makes easy to recognize it. Another important finding reveals that the augen gneisses occurring as country rocks also show the typical deep reddish color, and are also U-REE-P mineralized, preferably in a halo around the mineralized albitites. The geochemical analyses (whole rock) of the mineralized rocks revealed relatively high Na₂O (10-11 wt.%) and P₂O₅ (up to 4.9 wt.%) amounts, indicating that the mineralizing fluids were Na- and P-rich, besides U and REE. The maximum U amount found was 808 ppm, which also had anomalous contents of Th (up to 710 ETR up to 863 ppm) associated. The oreΣppm, Y (up to 1,040 ppm), and REE (samples showed a particular HREE enrichment in relation to the LREE as evidenced by the (La/Lu)_N = 0.5. Dy, Er, and Yb show the higher concentrations among the HREE, while the Ce and Nd are highlighted among the LREE. The FRX data in the ore samples show a significative strong correlation between Sr-Ba-Te-Cs, and Pd amounts (in ppm) can be considered anomalous. The MEV-WDS data revealed that the U-hosted mineral phases are mainly uraninite and coffinite, and semi-quantitative analyses showed that the former mineral contain U > Th > Y > Ce > P. The data reveal that the geochemical association of this mineralization is U-ETR-Th-Y-Na-P, which reveals the compositional signature of the ore-forming metasomatic fluids involved in the genesis of this deposit. (*SS6; Wed. Poster*)

Keynote (40 min): The chemistry of gahnite and garnet in lode horizon rocks as exploration guides to Broken Hill-type mineralization, Broken Hill area, Australia

Spry, P.G.¹, pgspry@iastate.edu, O'Brien, J.J.¹, Heimann, A.², Teale, G.S.³, Jackson, S.E.⁴ and Rogers, D.⁵, ¹Iowa State University, 253 Science I, Ames, IA 50011-3212, USA; ²East Carolina University, 101 Graham Building, Greenville, NC 27858, USA; ³Teale & Associates, PO Box 740, North Adelaide, South Australia 5006, Australia; ⁴Natural Resources Canada, Geological Survey of Canada, 601 Booth Street, Ottawa, ON K1A 0E8; ⁵Perilya Limited, PO Box 5001, Broken Hill, NSW 2880, Australia

Quartz garnetite, blue quartz gahnite lode, garnetite, and lode pegmatite comprise an important group of rocks known as "lode horizon", which constitutes an empirical field guide to Broken Hill-type (BHT) mineralization in the Proterozoic southern Curnamona Province (SCP), Australia. Of these rock types, the first two, which are exhalites, inhalites, and highly altered metasedimentary rocks, are volumetrically most abundant (> 95%) and are spatially associated with the supergiant, 300 Mt Broken Hill Pb-Zn-Ag deposit, and over 400 minor BHT occurrences. Despite this spatial association, distinguishing sulfide-bearing from sulfide-free occurrences has been a difficult task. To this end, major and trace element studies have been done on both garnet and gahnite to determine whether or not geochemical fingerprints can be identified for exploration purposes.

Major and trace element data (LA-ICP-MS and electron microprobe) of gahnite from BHT deposits were discriminated using a principal component analysis to distinguish gahnite associated with the main ore lode from that associated with unmineralized lode pegmatite and sillimanite gneiss. Gahnite from the Broken Hill deposit has a restricted compositional range that, based on a series of bivariate plots, partially overlaps gahnite compositions from minor BHT occurrences. Based on contour maps of ore grade associated with each gahnite locality, gahnite associated with the highest Pb-Zn grades from minor BHT deposits have compositions that plot within the field for gahnite from the main Broken Hill deposit.

Chondrite-normalized REE patterns of garnet in garnet-bearing rocks in minor BHT deposits are generally light REE depleted, heavy REE enriched and have negative Eu anomalies, whereas garnet in Mn-rich garnetite and Fe-rich quartz garnetite from the Broken Hill deposit



exhibit similar REE patterns and positive and negative Eu anomalies, respectively. For garnet in Mn-Fe garnet-rich rocks, a positive Eu anomaly is favored by Mn-rich compositions of garnet and the host rock. Garnet in quartz garnetite exhibit negative Eu anomalies and lower concentrations of Mn and total Eu contents than that in garnetite.

Garnet from the Broken Hill deposit has a characteristic REE pattern and is enriched in Mn, Zn and Cr and depleted in Co, Ti, and Y compared to garnet in other garnet-rich rocks in the SCP, whereas gahnite associated with ore contains Zn/Fe = 2-4, Co = 20-90 ppm, and Ga = 15-390 ppm. This study suggests that the major and trace element content of gahnite and garnet can be used as exploration guides to BHT mineralization. (*SS10; Thurs. 8:20*)

Diamonds from the Argyle lamproite (Western Australia): Different from any other mine?

Stachel, T.¹, tstachel@ualberta.ca, Harris, J.W.², Hunt, L.¹ and Muehlenbachs, K.^{1,3}, ¹University of Alberta, Edmonton, AB T6G 2E3; ²University of Glasgow, G12 8QQ, UK; ³EIMF, University of Edinburgh, Edinburgh, EH9 3JW, UK

The Argyle diamond mine is located in the Proterozoic (~1.85 Ga) Halls Creek Orogen at the SE edge of the Kimberley Craton, Western Australia. In terms of diamond quantity, it is the largest deposit known and has produced over 670 million carats to date. That Argyle is the first olivine-lamproite hosted diamond deposit mined and located on a Paleoproterozoic orogenic belt rather than an Archean craton, further distinguishes this diamond mine from other deposits worldwide. The diamonds also have unique characteristics: (1.) They contain a suite of primarily eclogitic inclusions (not an unusual feature in itself), but with abundant coesite (3% of our sample set) and overall unusually high concentrations of P, Na and K in both garnet and clinopyroxene; (2.) Carbon isotopic compositions ($\delta^{13}\text{C}$) of the eclogitic diamonds show a mode in class -12 to -11‰ (with mean value of -11‰) without a prominent (and typical) second mode about the mantle value of -5‰; (3.) The eclogitic diamonds originated at unusually high temperatures (mean T_{Krogh} of 1250°C versus 1170°C for eclogitic diamonds worldwide).

To further investigate whether or not these distinctive features are indicative of a unique origin for Argyle diamonds we studied a suite of 155 inclusion-bearing diamonds. Our new data on nitrogen concentration-aggregation state relationships confirm a high temperature origin of the diamonds. Assuming a mantle residence of 0.5 Ga, the nitrogen data show that the average residence temperature is about 160°C higher than for lithospheric diamonds worldwide. As the paleogeotherm for Argyle (1.18 Ga emplacement) is similar to other diamond producing areas (e.g., the Cretaceous paleogeotherm for the Kaapvaal Craton), a thermal pulse could only explain such elevated residence temperatures if it had dissipated by 1.18 Ga. Alternatively, the unusually high time averaged residence temperatures reflect diamond formation and storage at depth generally >180km.

Both the eclogitic paragenesis of Argyle diamonds and the ^{13}C depleted diamond compositions suggest a possible relationship with Paleoproterozoic subduction along the Kimberley Craton rim. Bulk rock trace element patterns derived from eclogitic garnet and clinopyroxene inclusions indicate that a section of oceanic crust reaching from lavas and sheeted dikes (flat and high MREE-HREE) to shallow gabbros (lower HREE, positive Sr and Eu anomalies) acted as diamond substrates. The usually high-temperature origin aside, the predominantly eclogitic diamonds from Argyle, therefore, compare well with productions from several other mines worldwide for which the mantle source can also be linked to oceanic protoliths. (*SS4; Fri. 9:40*)

Chemical weathering of Miocene sediments from the Dry Valleys, Antarctica

Steffen, A.L., ashley.steffen.3@my.ndsu.edu, Lewis, A.R., Zamora, F. and Saini-Eidukat, B., Department of Geosciences, North Dakota State University, PO Box 6050, Fargo, ND 58108 USA

We are testing the use of the chemical index of alteration (CIA) on sediment samples from the Dry Valleys in Eastern Antarctica. The goal is to better understand past weathering environments. During the austral summer of 2011 samples were taken near Mount Jason and Mount Aeolus (n=10) in McKelvey Valley, and near Mount Cerberus in Bull Pass (n=4). Samples FZE-11-01, FZE-11-16, and FZE-11-18 are from debris flows in McKelvey Valley, while samples from site FZE-11-48 are taken from a debris flow in Bull Pass, all of which have water sources originating from cirque glaciers. Three additional till samples were taken adjacent to debris flows. Samples FZE-11-01A-B, FZE-11-16A-C and FZE-11-18A-E, have all been dated to approximately 14 Ma. Three additional samples taken from the Friis Hills in the summer of 2010, were also analyzed. Samples ASS-10-07 and ASS-10-09A-B have been age dated at about 19 Ma. All samples were collected in the field by dry sieving sediments to remove clasts greater than 16 mm, and were sieved in the laboratory using a 2mm mesh. Samples were pulverized to 250 micrometers and fused into glass beads. Analysis of major elements was done by XRF. Results show that McKelvey Valley samples FZE-11-16 and FZE-11-18 have CIA values ranging from 40 - 43, with an average of 42 (n = 8). However, samples FZE-11-01A (CIA = 36) and B (CIA = 50), from a pit in a valley approximately 2 km to the E, fall well outside this range. Among the McKelvey debris flow sediments, site FZE-11-01B has the highest CIA. CIA values for the 19 Ma group from Friis Hills average 52 (n = 3) and are distinct from most of the 14 Ma samples. Site FZE-11-48 near Mount Cerberus in Bull Pass is as yet undated, and shows CIA values ranging from 36 - 41 (ave. = 39). The overall CIA trend for the samples is approximately parallel to the A-CN trend line on an A-CN-K plot, consistent with increased weathering in the older samples. Samples from the Friis Hills show slight variation from the expected trend toward K. Bivariate element comparisons show distinct groupings, potentially allowing sediments to be chemically fingerprinted. (*GS3; Thurs. Poster*)

Use of a GIS/stratigraphic model to predict zones of elevated trace element concentrations in soils derived from Cretaceous Pierre Shale on the Pembina Escarpment, Cavalier County, North Dakota

Steffen, A.L.¹, ashley.steffen.3@my.ndsu.edu, Hopkins, D.G.², Saini-Eidukat, B.¹ and Breker, J.S.², ¹Department of Geosciences, North Dakota State University, Dept. 2745, PO Box 6050, Fargo, ND 58108 USA; ²Department of Soil Science, North Dakota State University, Dept. 2745, PO Box 6050, Fargo, ND 58108 USA

Trace metal concentrations can be elevated in certain sedimentary rocks, notably shales. Soils derived from these rocks contain disproportionate levels of metals. One such unit, the Upper Cretaceous Pierre Formation, consisting of mud- and siltstones, is exposed along the Pembina (Manitoba) Escarpment. The Escarpment is a significant geomorphic feature extending from south central Manitoba to mid-central eastern ND. This work is part of a larger study of trace element distributions, micronutrients as well as potentially toxic metals, on the Pembina Escarpment. Here, we test the integrity of a GIS model based on stratigraphic position of organic shales, or associated bentonite lenses. Well logs in the Cavalier and Pembina County area were used to project elevations of the highest priority shale facies to the surface of the eastward sloping Pembina Escarpment. Because of uncertainty of dip, target sampling zones were designed at 1, 5 and 10 m variance around the projection. We hypothesized that trace element concentrations would be elevated within the projected zones. Samples from 10 sites along a 1.5 km transect were collected to depths of about 2 m. Four satellite samples at 20 m distance from each core were taken at 0-15 and 30-50 centimeters. Samples were ground to a grain size of 250 micrometers, digested according to EPA Method 3050B, and analyzed by ICP-OES. Grand mean values over the entire transect are elevated relative to prairie top soils of north central North Dakota by 2.6× (Cu), 2.3× (Ni) and 3.0× (Zn). Maximum enrichments for zinc, for example, are 10× the regional background. Barium, beryllium, manganese, nickel, thallium, and zinc are more concentrated in the 0-15 cm depths relative to the 30-50 cm depths. Elements that correlate well



to the model are arsenic, copper, nickel, and zinc, all of which appear to have their highest values located within the 1 meter lateral zone of the projected shale outcropping. Interestingly, aluminum and iron both show a strong decrease in concentrations in the 30 to 50 cm depth within this zone. Vanadium shows a gradual increase throughout the center of the transect, with its highest values just east of the “hot spot.” The resultant data corroborate the model and show that it is possible to predict element variation within the landscape.

This project was supported by grants from the National Center for Research Resources (P20 RR016471) and the National Institute of General Medical Sciences (P20 GM103442) from the National Institutes of Health. (*GS3; Thurs. Poster*)

Petrography and fluid inclusions reflect a history of pervasive fluid-mediated metasomatism in the Granophyre Unit of the 1.85 Ga Sudbury Igneous Complex, Ontario

Stewart, R.C., rx1_stewart@laurentian.ca, Kontak, D.J., Department of Earth Sciences, Laurentian University, 935 Ramsey Lake Road, Sudbury, ON P3E 2C6, and Ames, D.E., Geological Survey of Canada, 601 Booth Street, Ottawa, ON K1A 0E8

The 1.85 Ga Sudbury Igneous Complex (SIC) is a differentiated impact melt sheet that hosts one of the largest Ni-Cu-PGE mineralized districts globally. The complex contains four major units which, from bottom to top, are the sublayer, norite, quartz gabbro, and granophyre (GRPHY). This complex is overlain by the Onaping Formation, a crater fill breccia containing hydrothermal massive sulfide (Zn-Cu-Pb-Ag) deposits generated at ca. 1848 Ma. The GRPHY accounts for 50 vol. % of the SIC, is 1.5 km thick, is interpreted to have cooled separately from the norite, and is dominated (80-98%) by quartz, K-feldspar, and plagioclase with abundant ($\leq 60\%$) granophyric texture; the rest consists of biotite, amphibole (fe=0.4), apatite, titanite, and ilmenite with secondary biotite, amphibole (fe=0.8), chlorite, and epidote. The feldspars are uniform in composition (An_{0-5} , Or_{95-100}), perthitic textures are rare to absent, and there are abundant pits lined with rare secondary phases (e.g. zircon, baddeleyite, uraninite) and filled with aqueous fluid inclusions. The feldspar compositions and textures reflect a subsolidus, fluid-mediated dissolution-precipitation process at $<350-300^\circ\text{C}$, which is also recorded by the textures of the Fe-rich amphiboles. Magmatic quartz in the GRPHY hosts three fluid inclusion assemblages (FIAs), all of which are of secondary origin: (1) L-V with 20-30% V; a (2) L-V with 10% V; and (3) L-V-H±solids; types 2 and 3 are the most abundant. Thermometric data for the FIAs indicate: (1) type 1 have $T_h = 320^\circ\text{C}$ and salinities of 23 wt. % eq. NaCl; (2) type 2 have $T_h = 100-112^\circ\text{C}$ and salinities of 20-25 wt. % eq. NaCl; and (3) type 3 have $T_h = 131-140^\circ\text{C}$ and salinities of 28 wt. % eq. NaCl. SEM-EDS analysis of evaporate mounds indicate these fluids are Na dominant with lesser Ca and K in a proportion of 70:20:10; enrichment in Fe, Mn and F is also indicated. The data suggest that the GRPHY interacted with two thermally distinct, but chemically similar fluids, both of which require extensive fluid:rock exchange. These two fluids may record different stages in the progressive collapse of hydrothermal fluid circulation fuelled by the cooling SIC that gave rise to Zn-Cu-Pb-Ag massive sulphide mineralization at the top of the Onaping Formation. Whereas the earlier, high T fluid may be in part orthomagmatic and responsible for the pervasive metasomatism, the lower T fluid is considered to relate to the dominance of a more regional fluid as the hydrothermal cell collapsed. (*GS2; Wed. 9:00*)

From glacial lake Coppermine rhythmites to the olistostrome of the Sleigh Creek Formation

St-Onge, D.A., Geological Survey of Canada, 601 Booth Street, Ottawa, ON K1A 0E8

A series of Late Wisconsinan sedimentary sequences occupy parts of the Coppermine River valley, and are grouped into five morphosedimentary zones representing four environments at the time of last ice retreat: glacial, paraglacial, lacustrine and marine. The sequences commonly interfinger, and document episodic deposition in

time-transgressive environments related to ice frontal positions. Glacial and paraglacial sediments are, in part, reworked in a glaciolacustrine environment extending from delta topsets of bouldery gravel to bottomset rhythmites of silt-clay. The glacial-lake rhythmites formed the matrix of a later sequence of debris-flow events, which emplaced a wedge of massive diamictos in the postglacial marine sediments. This sedimentary sequence, composed of a chaotic mass of heterogeneous material that is intimately mixed, and is accumulated in the form of a semi-fluid body in a marine environment, is possibly the best exposed Quaternary olistostrome. (*SY4; Fri. 9:00*)

Characterization of the ~2.7 Ga ankerite at the Dome Mine, Timmins, Ontario: Implications for understanding Martian paleoenvironments and biomarker preservation

Stromberg, J.M.¹, jstromb@uwo.ca, Banerjee, N.R.¹, Flemming, R.¹, Harris, R.¹, Barr, E.², Slater, G.³ and Cloutis, E.A.⁴,
¹Department of Earth Science, Western University, 1151 Richmond St. London, ON N6A 3K7; ²Goldcorp Porcupine Gold Mines, 4315 Gold Mine Road, South Porcupine, ON P0N 1H0; ³McMaster University School of Geography and Environmental Science, 1280 Main St. West, Hamilton, ON L8S 2G4; ⁴University of Winnipeg, Department of Geography, 515 Portage Avenue, Winnipeg, MB R3B 2E9

In order to make interpretations of past habitability, geologic processes and paleoenvironments on other planets, we must first understand how Earth's geologic record can inform us on depositional contexts, diagenetic histories and biomarker preservation. The part of Earth's history that is most analogous to the “warm and wet”, early Noachian Mars in which carbonates and sulphates were aqueously deposited, is the Archean Eon from 3.5-2.5 Ga.

The Abitibi Greenstone belt in Northern Ontario and Quebec, Canada, is the world's largest and best preserved Archean greenstone terrain. We are undertaking a multi-technique, “mine-to-micron” scale study to characterize a unique set of 2,690-2,679 Ma crustiform banded ankerite veins within the Tisdale volcanics at the Dome Mine in Timmins, Ontario. The Tisdale volcanics are overlain by the Porcupine metasediments, in which endogenous biomarkers of a Late Archean sub-seafloor hydrothermal biosphere have been identified. The ankerite is part of a world-class greenstone-hosted quartz-carbonate vein gold deposit. Previous work interpreted this horizon as a chemical exhalative; however, this is inconsistent with cross cutting relationships observed in the mine workings.

Preliminary samples representative of the system (500m strike, 900m vertical, up to 2m width) have been collected and characterized for their mineralogy and selected samples for organic content. Mineralogical analysis (XRD, SEM, EDS, UV/VIS/NIR spectroscopy) indicate large scale variations in fluid composition throughout the system. We observe alteration products representative of low-temperature, low-salinity, CO_2 -rich fluids interacting with mafic volcanics, with possible fluid inputs from a magmatic source. This data is being used to identify fluid composition and flow, as well as regions of fluid mixing, which are integral to providing redox gradients relevant to habitability and gold mineralization. In characterizing the organic content of the system, a novel sample preparation and extraction method for remnant organics preserved within Archean carbonate has been developed and tested. Preliminary results indicate that there are very low abundances of extractable organics, primarily n-alkanes, as expected if these are endogenous to the system.

With this data and subsequent higher resolution analysis (ToF-SIMS, XAFS), evidence for pencontemporaneous organic preservation in the system and hydrothermal fluid composition, flow and source are being characterized to provide a better depositional context. By studying Archean deposits on Earth, we gain valuable insights into the habitability of early Earth systems, and mineralogical data can be correlated to what is observed on Mars to make more informed interpretations of depositional paleoenvironments and diagenetic histories. (*SS17; Thurs. 9:20*)



Keynote (40 min): Tectonic evolution of the Paleoproterozoic Flin Flon Belt and regional setting of volcanogenic massive sulphide deposits

Syme, E.C., Manitoba Geological Survey, 360-1395 Ellice Ave., Winnipeg, MB R3G 3P2, syme@mts.net

Regional mapping by the Manitoba Geological Survey prior to and during federal-provincial NATMAP (1991–96) and Targeted Geoscience Initiative (2000–03 and 2005–10) programs has resulted in a robust understanding of the setting of volcanogenic massive sulphide (VMS) deposits in the Flin Flon granite-greenstone belt (FFB). While most work in the last decade has focused on detailing the stratigraphic setting of the deposits at Flin Flon, the geochronologic, geochemical and isotopic results from all of these investigations now allow a re-evaluation of the tectonic evolution of the FFB, in light of detailed mapping of 1000 km² within the central and western FFB.

The 1.90–1.88 Ga ‘early arc and ocean-floor’ tectonostratigraphic assemblages that dominate the FFB include 1) 1.90 Ga, isotopically juvenile basalts with chemical affinity to N- and E-type MORB and BABB, and kilometre-scale tectonic fragments of mafic-ultramafic complexes similar to cumulate complexes preserved in ophiolite sequences, and 2) 1.89–1.88 Ga juvenile and isotopically contaminated arc volcanic and associated plutonic rocks. These assemblages were dissected and juxtaposed along early shear zones (D₁) and subsequently isoclinally folded (D₂) to form the accretionary ‘Amisk’ collage at approximately 1.87 Ga.

This collage was basement for 1.87–1.86 Ga ‘early successor arc’ tholeiitic and calcalkalic magmatism, accompanied by the development of intra-arc sedimentary basins. The 1.86–1.84 Ga ‘middle successor arc’ calcalkalic plutons, rarely preserved coeval volcanoclastic rocks, and siliciclastic fluvial-alluvial basins record multiphase deformation (D₃–D₅), associated with development of a microcontinent (‘Flin Flon-Glennie Complex’) by 1.85–1.84 Ga. Crustal-scale shear zones separating ca. 1.9 Ga arc and ocean-floor assemblages presumably initiated during D₁, but were long-lived and generally contain panels of 1.86–1.85 Ga sedimentary rocks. Subsequent collision of the Flin Flon-Glennie Complex with the Archean Sask craton and late deformation associated with terminal collision with the Superior craton resulted in the present configuration of the FFB.

Stratigraphic and geochemical evidence suggests that VMS deposits in the western FFB are related to extension and rifting of the early arc assemblages; the MORB- and BABB-like basalt successions are apparently barren. Syn-volcanic extension and faulting provides volcanoclastic-filled depositional basins and conduits for hydrothermal fluids, is associated with upwelling asthenosphere and resulting high heat flow, and may result in the production of observed geochemically unique rift basalts. Isotopic evidence further suggests that juvenile arc assemblages, and not those that have been contaminated by older crust, are the main hosts to VMS deposits. (SS2; Wed. 1:40)

Garyansellite and kryzhanovskite from Rapid Creek, Yukon, Canada

Tait, K.T.¹, ktait@rom.on.ca, Chu, K.² and Abdu, Y.³,

¹Department of Natural History, Mineralogy, Royal Ontario Museum 100 Queens Park, Toronto, ON M5S 2C6; ²Department of Earth Sciences, University of Toronto, 22 Russell Toronto, ON M5S 3B1; ³Department of Geological Sciences 125 Dysart Road, University of Manitoba, Winnipeg, MB R3T 2N2

The Rapid Creek area in northeastern Yukon is an incredibly important mineral locality, especially for phosphate minerals. The geological environment that allowed these assemblages of rare phosphates to form is unique; the sedimentary rocks host several mineral species previously known only from igneous and hydrothermal environments. There have been fifteen new minerals discovered in this region; some that have never been found anywhere else in the world. Many of these discoveries were in the 1970s–1980s; recently, with new analytical techniques we have started analyzing these samples again and new minerals are once again being discovered, such as bobdownsite.

In the Phosphoferrite Group there are three ideal end-members, reddingite (Mn), phosphoferrite (Fe²⁺) and kryzhanovskite (Fe³⁺); with garyansellite (Mg, Fe³⁺) and landesite (Mn, Fe³⁺) being intermediate members. Garyansellite (Mg, Fe³⁺)₃(PO₄)₂(OH, H₂O)₃ from Rapid Creek, Yukon, Canada was first described to honor H. Gary Ansell, former Associate Curator at the Geological Survey of Canada. Kryzhanovskite (Fe³⁺, Mn²⁺)₃(PO₄)₂(OH, H₂O)₃ although not first described from the Yukon, forms in the cliffs in this region with garyansellite. The garyansellite-kryzhanovskite mineral series is poorly understood.

A common problem that arises during the identification of hydrated iron and manganese phosphates, such as phosphoferrite-kryzhanovskite is when the Fe²⁺ and Mn²⁺ oxidize without significant change in crystal structure. As a result, it is extremely difficult to identify whether the mineral is in the reduced or oxidized form. Samples of this group were analyzed by Mössbauer spectroscopy, in combination with Raman spectroscopy, Fourier-transform infrared (FTIR) spectroscopy, single-crystal diffraction and electron microprobe to study the chemical variation and textural relationship of these two minerals.

Veins of garyansellite and kryzhanovskite are found high above Rapid Creek (68° 34'N and 136° 46'W) about 1 km north of the junction of Lake Creek. Many samples were found loose in the talus slope leading up to the outcrop. On most specimens garyansellite-kryzhanovskite occurs as plates, 1–3 mm, associated with ludlamite, arrojadite-group minerals, quartz, vivianite, metavivianite and souzalite. They range from chocolate to clove to reddish brown and typically exist as subhedral to euhedral crystals, with a characteristic bronze lustre. A field program was conducted in this region summer 2012, to collect mineral specimens and map the area to put these discoveries in a wider geological context. (SYI; Wed. Poster)

Ni-Cu-(PGE) mineralization associated with the Tamarack intrusion, Midcontinent Rift system; Geochemical and isotopic constraints on sulfide genesis

Taranovic, V.¹, vtaranov@indiana.edu, Ripley, E.M.¹, Li, C.¹, Rossell, D.² and Shirey, S.B.³, ¹Department of Geological Sciences, Indiana University, Bloomington, IN 47405 USA; ²Rio Tinto Exploration (Kennecott Exploration), Salt Lake City, UT 84116 USA; ³Department of Terrestrial Magnetism, Carnegie Institution of Washington, Washington, DC 20015 USA

(Withdrawn)

Public Lecture: The drowning and draining of Manitoba: From Lake Agassiz to today

Teller, J.T., Department of Geological Sciences, University of Manitoba, Winnipeg, MB

The Red River Lowlands have been repeatedly flooded since retreat of the Laurentide Ice Sheet about 12,000 years ago. Initially that ice sheet formed a dam that prevented drainage of the Canadian Prairies and Northern Great Plains of the U.S. from reaching Hudson Bay. The largest lake in the world, Lake Agassiz, was ponded in front of the glacier for nearly 5000 years, inundating most of southern Manitoba and parts of northwestern Ontario, Saskatchewan, North Dakota, and Minnesota. Sandy beaches formed around the shorelines of the lake when it was at different levels, and clay was deposited in the deeper waters of the basin. Overflow from Lake Agassiz during its life was through several different routes: (1) south into the Mississippi River and Gulf of Mexico, (2) east into the Great Lakes to the St. Lawrence Valley and North Atlantic Ocean, and (3) northwest into the Mackenzie River and the Arctic Ocean. The lake finally drained away into Hudson Bay about 8400 years ago, after which modern drainage patterns were established across central Canada. Each change in routing of Lake Agassiz overflow was accompanied by a catastrophic burst of water; when that burst reached the oceans it changed the way they circulated and, in turn, caused global cooling.

After Lake Agassiz drained away, the modern Red River was established on the floor of the old lake bed. Because of the low



gradient of the river and low relief of the lake plain, flooding has repeatedly occurred along the river, inundating large areas during spring runoff; major floods in the 19th century were recorded in 1826, 1852, and 1861. Saturated ground conditions in the fall, early freezing of the ground, high precipitation, and rapid and late snow melt in the spring commonly have led to spring flooding. In recent years, such as 1979, 1996, 1997, 1999, 2006, and 2009, large floods have occurred. Only construction of the 48-km-long Red River Floodway in 1968 around the city of Winnipeg has prevented flood disasters in the city of Winnipeg like the one in 1950; the Floodway prevented an estimated \$10 billion in flood damage in 2009. (*SS24; Wed. 7:00*)

Mineralogical and geochemical assessment of possible iron formations at the Red Lake gold mine

Therrien, S.J., Red Lake Gold Miners, 17 Mine Road, Bag 2000, Balmertown, ON P0V 1C0, Conly, A.G., andrew.conly@lakeheadu.ca, and Moore, L.C., Department of Geology, Lakehead University, 955 Oliver Rd, Thunder Bay, ON P7B 5E1

The Red Lake Mine contains three possible iron formation units that are hosted in the metamorphosed, Archean tholeiitic volcano-sedimentary Balmer assemblage. Mineralogical and geochemistry attributes of these three suspect units were evaluated to assess their potential to be categorized as the sulphide-facies, of an Algoma-type iron formation. Samples were collected from the 16, 21 and 46 levels of the Red Lake Mine's Balmer Complex. All samples consist of macroscopic to microscopic sulphide-rich and sulphide-poor bands. Sulphide-rich bands are comprised mainly of pyrite and pyrrhotite, in contrast to sulphide-poor (<5 modal% sulphide) bands that consist mainly of quartz, muscovite and chlorite. Samples from the 46 level are mineralogically distinct due to the presence of carbonate (up to 20 modal%). All units display slightly positive Eu anomalies and fractionated LREE<HREE profiles that are indicative of hydrothermal input and characteristic of Archean iron formation. However, The majority of samples from the 16 and 21 levels do not meet the required 14 wt% Fe₂O₃ contents to be classified as iron formation, with approximately half the 46 level samples having sufficiently high iron contents. To better evaluate the nature of these units, a Fe/Ti versus Al/(Al+Fe+Mn) diagram was used to assess the relative proportion of detrital to hydrothermal inputs. Samples from the 16 and 21 levels are best described as weakly mineralized, terrigenous sediment, as these units generally contain less than 20 modal% metalliferous sediment. The mineralogy and geochemistry of the 16 level also reflects variations in the degree of aluminous alteration, which occurs throughout the mine. Samples displaying the effects of aluminous alteration have greater abundances of muscovite (over chlorite) and are relatively enriched in Ba and K. Samples from the 46 level typically contain between 30 modal% and 60 modal% metalliferous sediment and, thus, correspond to a diluted sulphide-facies Algoma-type iron formation. The detrital sediment component was likely derived from weathering of calcalkaline volcanic rocks, and not tholeiitic volcanic rocks that dominate the Balmer assemblage. However, less fractionated LREE profiles and elevated Zr, Th and U contents of the 46 level samples (relative to the 16 and 21 levels) suggest more than one detrital source. The geochemical characteristics of 46 level samples may be explained by the mixing of calc-alkaline-derived sediment with an unidentified alternative source lithology characterized by high zircon abundances. (*SS3; Thurs. Poster*)

Paired organic carbon and carbonate carbon isotope records from the Tonian-Cryogenian Shaler Supergroup, Victoria Island, NWT

Thomson, D.¹, dthomso2@connect.carleton.ca, Rainbird, R.², Bekker, A.³ and Prince, J.¹, ¹Carleton University, 1125 Colonel By Drive, Ottawa, ON K1S 5B6; ²Geological Survey of Canada, 601 Booth Street, Ottawa, ON K1A 0E8; ³University of Manitoba, 66 Chancellors Cir, Winnipeg, MB R3T 2N2

Global carbon isotope data show covariant $\delta^{13}\text{C}_{\text{carb}}$ and $\delta^{13}\text{C}_{\text{org}}$ records from approximately 820 - 720 Ma, after which, and following the

Sturtian glaciation, they become completely decoupled. The Bitter Springs Stage is a negative shift in the global carbon isotope record that has been reported from Australia, Africa, Svalbard, Scotland, and North America, and is dated at approximately 811 Ma. The Bitter Springs Stage is unrelated to a glaciation, in contrast to typical negative excursions in the Neoproterozoic that herald the post-glacial cap carbonates; but does represent a major global perturbation to the carbon cycle.

We present a new, paired $\delta^{13}\text{C}_{\text{carb}}$ and $\delta^{13}\text{C}_{\text{org}}$ data set from the upper Shaler Supergroup, Minto Inlier, Victoria Island, Northwest Territories. The Tonian-Cryogenian Shaler Supergroup is a thick (>4 km) succession of sedimentary rocks that comprises predominantly marine carbonates, with intervals of fluvial-to-deltaic sandstones and siltstones, and sulphate evaporites. Both core and outcrop were sampled through approximately 2 km of the upper Shaler Supergroup, including (in stratigraphic order) the Boot Inlet, Jago Bay, Minto Inlet, Wynniatt, and Kilian formations. $\delta^{13}\text{C}$ analyses returned modal values of ~5‰ for carbonate carbon, and ~23‰ for organic carbon, which are typical for Neoproterozoic carbonates. However, the sampled interval displays dramatic variations in both $\delta^{13}\text{C}_{\text{carb}}$ and $\delta^{13}\text{C}_{\text{org}}$ values associated with the Bitter Springs Stage. $\delta^{13}\text{C}_{\text{carb}}$ data records a 22.0‰ shift (from 7.7‰ to -14.3‰), and $\delta^{13}\text{C}_{\text{org}}$ values show a 19.8‰ shift (from -14.4‰ to -34.2‰). Such extreme negative values have not been reported so far from other localities.

The Bitter Springs Stage occurs within a transgressive sequence in the Upper Carbonate member of the Wynniatt Formation, which directly overlies an erosional (ravinement) sequence boundary. We correlate this sequence to a similar sequence in the Fifteenmile Group (S7), Ogilvie Mountains, Yukon Territory. Therefore, the Bitter Springs Stage corresponds with a regional sea-level rise in northwestern Laurentia, preceding break-up of the Rodinia supercontinent. We propose that the Bitter Springs Stage might be genetically linked with the progressive oxidation of the atmosphere-ocean system related to enhanced burial of organic carbon, which preceded the break-up of the Rodinia supercontinent and ushered Cryogenian glaciations. (*GS3; Thurs. Poster*)

Testing the relationship between LIPs, BIF, and VMS deposits in the Abitibi greenstone belt

Thurston, P.C., Laurentian University, Sudbury, ON P3E 2C6, pthurston@laurentian.ca, and Kamber, B.S., Trinity College, Dublin, Dublin Ireland

Archean greenstone belts consist of multiple ultramafic/mafic to felsic volcanic cycles. LIPs produce the tholeiite-komatiite base of the cycles and most of the felsic volcanic units are a product of melting of mafic precursors. We have tested the LIP-BIF-VMS relationships by examining the 2734-2724 Ma Deloro assemblage in the Abitibi greenstone belt which is overlain by the 2710 Ma Tisdale assemblage south of Timmins. This represents a depositional gap of ca. 14 m.y. The Deloro assemblage consists of 90% tholeiites with minor komatiites surmounted by <10% rhyolitic units with 3 intercalated iron formations. We modeled the rates of volcanic processes constrained by dating of rhyolites above and below a Deloro assemblage iron formation. Magma production rates for silicic ash-flow zoned magma chambers, modern arcs or LIP systems yields rates of 0.01-1 km³/yr, 5 km³/year/km of arc, and 0.15-8.2 km³/yr respectively. Applying these rates to the 750,000 km³ 2734-2724 Ma Deloro assemblage in the Abitibi greenstone belt yields accumulation times of 7500-75,000 yr for ash-flow systems, and ~100,000-5 m.y. for plume systems. Using the above magma production rates and dates on the middle of 3 iron formations indicates that the iron formation accumulated in 4-10 m.y. The 14 m.y. depositional gap is not taken up by volcanism, plume activity occurs relatively rapidly whereas up to 90% of the duration of volcanic assemblages is occupied by chemical sedimentation and/or VMS hydrothermal systems.

These concepts are reinforced by BIF geochemistry. REE+Y patterns indicate that Deloro BIFs originated as seawater precipitates or hydrothermal precipitates for the most part. In fact some of the highest



Eu/Eu* values (*ca.* 30) ever recorded for BIF are interpreted to represent the existence of a regional scale hydrothermal system at the time of deposition of Deloro BIF. This Deloro assemblage hydrothermal activity produced at least 7 VMS deposits. BIF geochemistry also reveals very low contamination rates as measured by Th/U. Given the general lack of clastic detritus in Archean greenstone belts and the lack of contaminants in BIFs, these systems likely represent deposition in an oceanic plateau setting. (*SS3; Thurs. 1:40*)

Geochemistry and geochronology of Tertiary magmatism from the north-central Great Basin, Nevada, to the Ancestral Cascade Arc, California

Timmermans, A.C., Cousens, B.L., Dept. of Earth Sciences, Carleton University, 1125 Colonel By Drive, Ottawa, ON K1S 5B6, atimmerm@connect.carleton.ca, and Henry, C.D., Nevada Bureau of Mines and Geology, Mackay School of Earth Sciences and Engineering, University of Nevada, Reno, NV 89557-0178, USA

Between 40 and 5 Ma, a complex mix of mafic, intermediate to felsic magmatism swept southwestward across the Great Basin (GB), Nevada, towards the Ancestral Cascade Arc (ARC), Sierra Nevada, California, concurrent with rollback of the subducting Farallon plate beneath the North American plate. The fundamental questions plaguing this Tertiary magmatic event are: 1) the role of the asthenospheric mantle wedge, lithospheric mantle and potential crustal influences, and 2) the influence of extension (prevalent in central GB by 15 Ma), on the chemistry of the magma.

We have collected and compiled geochemical and isotopic data on subalkaline basalts, basaltic andesites and basaltic trachyandesites ($Mg\# = 0.75 - 0.55$) along an east-west transect through the west-central GB (>15 Ma) to the ARC (<15 Ma). High K- basaltic trachyandesites, abundant in plagioclase, pyroxene and olivine, dominate the GB. Basalts and basaltic andesites east of and into the ARC are mildly phryc with phenocrysts of olivine, pyroxene and less abundant plagioclase. The entire domain is characterized by a calc-alkaline geochemical signature with negative Ta and Nb anomalies and depletion in Ti, and most rocks have elevated LILEs. The GB mafics are consistent with an older lithospheric mantle source with high REEs, Zr, P, Ti, and K; lower La/Ta and Th/Ta values; and $^{87}Sr/^{86}Sr = 0.7045 - 0.7053$ and $^{143}Nd/^{144}Nd = 0.5126$ to 0.5129 . The chemistry shifts for lavas to the west (ARC) indicative of contributions from both the lithospheric and asthenospheric mantle ($^{87}Sr/^{86}Sr = 0.7035 - 0.7065$ and $^{143}Nd/^{144}Nd = 0.5123 - 0.5129$).

We propose that at ~40 Ma the flat-slab subduction of the Farallon plate slowed and rolled back causing metasomatism of the mantle wedge by the dehydrating slab. The initial magmas were probably mafic and pooled at the base of the lithosphere causing melting of the lithosphere via mafic underplating. The magmas evolved chemically and isotopically by interaction with the lithospheric mantle, then migrated through the crust and high-K alkaline magmatism began in the GB. Magmatism continued west as the Farallon plate continued to roll back. By 15 Ma, extension thinned and faulted the lithosphere in the GB and mafic magmatism increased in the ARC as well as the transition zones surrounding the GB. The steepened slab equilibrates in the east underneath the Sierra Nevada (<10 Ma) and magmatism peaks in the ARC, due to enhanced melting of the asthenospheric mantle wedge. (*GS2; Wed. 2:00*)

Niobium and tantalum mineralization in the Nechalacho REE deposit, NWT, Canada

Timofeev, A., alexander.timofeev@mail.mcgill.ca, and Williams-Jones, A.E., Dept. of Earth and Planetary Sciences, McGill University, Montreal, QC H3A 0E8

The Nechalacho Layered Nepheline-Aegirine Syenite suite at Thor Lake, North West Territories, which forms part of the alkaline to peralkaline Blachford Lake Complex, contains significant reserves of both niobium and tantalum. It also contains large reserves of Rare Earth Elements (REE), Zr and Ga in two ore zones (Upper and Basal

zones). Intense hydrothermal alteration involving replacement of primary magmatic mineral assemblages by a potassic assemblage comprising K-feldspar, biotite, zircon and magnetite, affected the upper 300 m of the layered suite including both ore zones. This was followed by albization.

Previous studies of niobium and tantalum mineralization have focused on columbite group minerals and the systematic compositional trends they display within pegmatites during crystal fractionation. The distribution of niobium and tantalum at Thor Lake is of an entirely different character. Niobium and tantalum are hosted by fergusonite-(Y) and columbite group minerals, and occur as minor components in zircon. In the Basal ore zone, yttrium-rich zircon is closely associated with fergusonite-(Y). By contrast, in the Upper ore zone, zircon depleted in yttrium is associated with columbite group minerals. Moreover, bulk niobium and zirconium abundances in core correlate closely over tens to hundreds of meters within individual drill holes. It therefore follows that niobium must initially have been concentrated within a zirconium-silicate and remained relatively immobile during later pervasive hydrothermal alteration.

We propose a model in which niobium and tantalum were concentrated at the magmatic stage in a zirconium-silicate, such as eudialyte. Subsequent decomposition of the eudialyte by hydrothermal fluids resulted in the formation of zircon with yttrium- and niobium-rich cores. Fergusonite-(Y) subsequently crystallized during hydrothermal alteration of these zircon cores in the heavy REE-enriched Basal ore zone. Concurrent alteration of yttrium-poor zircon in the heavy REE-depleted Upper ore zone resulted in the development of fine-grained columbite group minerals. Outside the main rare metal-bearing ore zones, niobium and tantalum were initially concentrated in a uranium-bearing mineral, likely of the pyrochlore group, which was subsequently altered to columbite group minerals enriched in uranium relative to the columbite group minerals observed in the ore zones. Unlike other niobium and tantalum-bearing intrusions, the Nechalacho Layered Suite hosts these two metals in minerals that are predominantly of secondary origin. (*SS6; Wed. 2:20*)

A model for metamorphic devolatilization in the Lalor deposit alteration system, Snow Lake, MB

Tinkham, D.K., Dept. of Earth Sciences, Mineral Exploration Research Centre, Laurentian University, 935 Ramsey Lake Rd., Sudbury, ON P3E 2C6, dtinkham@laurentian.ca

Metamorphic assemblages and macroscopic reaction textures within the Paleoproterozoic Lalor deposit alteration system illustrate a partially coupled dehydration and decarbonation evolution that produced variable COH \pm S fluid compositions. Metamorphic assemblages consisting of cordierite \pm chlorite \pm garnet \pm staurolite \pm biotite \pm anthophyllite show the variable and progressive nature of dehydration via chlorite breakdown during prograde metamorphism. The temperatures of initiation and completion of chlorite breakdown is a function of effective whole rock composition and is reflected by a complete spectrum of assemblages ranging from chlorite-absent cordierite + anthophyllite \pm garnet \pm biotite \pm staurolite \pm kyanite/sillimanite assemblages to chlorite-rich schists containing only minor amounts of other Fe-Mg and Al-silicates. These assemblages constitute a significant proportion of the deeper sections of the footwall alteration system and indicate a significant amount of H₂O-rich fluid was produced via dehydration below the Lalor deposit during prograde metamorphism. Metamorphic assemblages more proximal to massive sulfide bodies are variable and locally consist of calcite-rich, carbonate-silicate, calc-silicate, chlorite-rich + Ca-amphibole, talc-bearing, and muscovite-rich assemblages with lesser amounts of the Fe-Mg-silicate dominant assemblages seen at deeper levels. Local occurrences of rocks with remnant granoblastic dolomite directly below massive sulfide produced tremolite via the generalized reaction $5 \text{ Dol} + 8 \text{ Qtz} + \text{H}_2\text{O} = \text{Tr} + 3 \text{ Cc} + 7 \text{ CO}_2$, and it is proposed that significant zones of dolomite locally existed below massive sulfide lenses.

Tremolite-bearing rocks immediately below massive sulfide locally grade into chlorite-rich rocks with post-foliation actinolitic



amphibole \pm epidote before reaching the deeper and extensive Fe+Mg+Al-silicate rich assemblages. The intervening Ca-amphibole + chlorite-rich schists are interpreted to represent either 1) original chlorite-rich VMS alteration that experienced carbonate alteration prior to or during the early stages of metamorphism, but that subsequently experienced decarbonation due to the influx of H₂O-rich fluids produced via chlorite dehydration at depth, or 2) the addition of Ca to an already chlorite-altered rock during post-foliation metamorphism, perhaps driven by fluid flux along localized shear zones.

The tremolite forming reaction and presence of peak-metamorphic granoblastic diopside \pm tremolite rocks indicate the production and/or presence of a CO₂-rich metamorphic fluid proximal to massive sulfides. The abundance of calcite and calc-silicate assemblages, evidence for CO₂-rich fluid production in the deposit-proximal environment, and the production of H₂O-rich fluids via chlorite dehydration in underlying rocks indicate the Lalor deposit footwall alteration system experienced a significant amount of H₂O-CO₂ \pm S fluid mixing during prograde metamorphism. (SS10; Thurs. 9:40)

Stabilities of actinyl ion complexes in aqueous phase

Tiwari, S.P., stiwari@nd.edu, and Maginn, E.J., Department of Chemical and Biomolecular Engineering, University of Notre Dame, Notre Dame, IN, USA 46556

Actinyl ions, the form in which actinides are mainly found in solutions, are important species in nuclear fuel cycle. These actinyl ions form complexes with ions/ligands such as hydroxide, nitrate, chloride, peroxide, phosphate *etc.* and also sometimes with cations such as sodium ion or other actinyl ions in aqueous phase. A quantitative treatment of the stability of these actinyl ion complexes will be helpful in fundamental understanding of the formation of such complexes in separation processes used in recycling and also in the formation of actinyl nanoclusters. The hazardous nature of actinides and also sometimes inability of available experimental techniques to probe into these molecular level properties make simulation an attractive proposition.

In the present work, molecular dynamics (MD) simulations along with umbrella sampling technique have been used to calculate the potential of mean force (PMF) between actinyl ions (of U, Np, Pu, and Am in their mono- and di-cation states) and various ligands (hydroxide, nitrate, chloride, peroxide, sodium ion, other actinyl ions *etc.*) in aqueous solution modeled by explicit waters. The PMF is the free energy change as a function of distance between actinyl ion and ligand in the aqueous solution. Furthermore, equilibrium association constants, calculated from PMFs, have been compared for the equilibration between these actinyl ions and ligands in the aqueous solution. Di-cation actinyls show stronger affinity for anions compared to mono-cation actinyls; whereas the opposite is true for cation-cation interactions between actinyls. (SS5; Wed. Poster)

Phosphate nodules from Big Fish River, Yukon, Canada

Tomes, H., University of Toronto, 22 Russell Street, Toronto, ON M5S 3B1, tomes@es.utoronto.ca, Tait, K.T. and Nicklin, I., Royal Ontario Museum, 100 Queen's Park, Toronto, ON M5S 2C6

The Cretaceous Rapid Creek Formation, exposed at Rapid Creek and Big Fish River (68° 28' N, 136° 30' W), in the Richardson Mountains, Yukon, contain unusual phosphate nodules that host a variety of rare phosphate minerals. This formation is a phosphorite-rich ironstone facies composed of alternating beds of phosphate and siderite-rich mudstones and shale. The phosphate nodules occur in the lower part of the Rapid Creek Formation in alteration zones where vivianite-baričite is interlayered and parallel to the bedding of the shale and mudstone layers. Previous studies have suggested that the phosphate nodules appear to be recrystallized replacement of ammonites and pelecypods, although there are examples that bear little to no resemblance at all to these organisms. Phosphate nodules from Big Fish River were thought to be dominantly composed of satterlyite, wolfeite, maričite, ludlamite, pyrite, and vivianite-baričite. In the summer of 2012, a field program was carried out in the region. Extensive collecting of the nodules has

yielded the identification of a number of other minerals such as arrojadite-group minerals, wicksite, quartz, and siderite in much higher abundances than previously found. In nodules these minerals are often found radiating from the centre at the base of the nodule. Nodules were identified both *in situ* and on talus slopes at all exposures along Big Fish River, although the type of nodules varied with position in the section. The lowest portion of the Rapid Creek Formation was dominated by microcrystalline pyritic nodules. As you move up-section at Big Fish River, the pyrite nodules disappear and phosphate nodules are abundant. The Rapid Creek exposures are higher in the formation and neither pyrite nor phosphate nodules were identified there. Not all nodules are disc or ammonite shaped some examples of 'cigar'-shaped nodules and massive sprays of satterlyite will be discussed. Satterlyite was identified as radiating masses in crosscutting veins located in close proximity to fault zones. Cross-sections through nodules within the surrounding host rock show that the discernable bedding planes appear to drape around the nodule which is evidence for soft sediment deformation. Depositional and replacement relationships between the nodules and their surrounding host rocks will be presented. (GS1; Thurs. Poster)

Keynote (40 min): The critical role of deformation in metamorphic sulfide melting

Tomkins, A.G., School of Geosciences, Monash University, Clayton, VIC, 3800, Australia, andy.tomkins@monash.edu

In most disseminated gold or massive zinc-lead \pm copper deposits, there is a range of minor sulfosalt, telluride and native metal minerals that will melt if metamorphosed at greenschist or amphibolite facies conditions. However, the most important ore minerals, in terms of target commodities, including gold, sphalerite, galena and chalcopyrite, have much higher melting temperatures (T_m). Although the minor low melting point minerals can lower the melting points of these refractory phases, ore minerals often exist in chemical isolation from each other, particularly in disseminated deposits. Consequently, initial melting, particularly in disseminated gold deposits, largely involves isolated melting of minor sulfosalts and tellurides, which in most deposits would produce 0.1 vol.% melt or less. The chemical composition of these initial isolated melts is consequently relatively simple, involving only a small number of elements. Even in massive Zn-Pb \pm Cu deposits, minerals do not ubiquitously coexist in ideal configurations that most favour generation of melt. In these deposits, arsenopyrite is likely to be the first mineral to melt, provided that high f_{S_2} conditions are generated during mid-amphibolite facies metamorphism. The resulting As-Smelt can melt a significant proportion of galena, but only if they are in contact. Again, the initial melt volume is small and chemically simple. The only way these minor quantities of melt can migrate is through deformation-induced mobilisation. Deformation of heterogeneous media (*i.e.*, rocks) produces localised domains of compression and dilation, and thus pressure gradients that drive migration of mobile phases. Because polymetallic melts have viscosities similar to water, they are highly responsive to such pressure gradients. Deformation of the solid phases, particularly massive sulfides, typically proceeds via ductile flow in the upper greenschist facies, involving grain boundary migration as individual grains become stretched. This continued gradual changing of solid grain interfaces allows progressive migration of any melt present along the grain boundaries towards dilatational domains. In this way deformation-induced mobilisation improves the chemical communication between melt and unmelted ore minerals, and therefore drives additional melting. As a simple example: a migrating globule of native Bi melt ($T_m = 271^\circ\text{C}$) might encounter an isolated Au grain ($T_m = 1064^\circ\text{C}$), and since their combined melting temperature is very low (241°C), Au is incorporated into the melt. In addition, some elements preferentially partition from solid solution in residual phases (such as Ag, Sb, Bi in galena) into the migrating polymetallic melts. Deformation-driven mobilisation thus allows the melt becomes both more voluminous and more chemically diverse. (SS10; Thurs. 1:40)



Application of hydrogeology and glacial geology to native orchid conservation in Manitoba

Toop, D.C., Manitoba Conservation and Water Stewardship, 200 Saulteaux Cres., Winnipeg, MB R3J 3W3, david.toop@gov.mb.ca

Native cypripedium orchids, commonly known as lady's slippers are highly specialized flora, with selective growth and habitat requirements. While their range is quite wide, the actual distribution generally consists of scattered, localized colonies. Orchid seeds carry no food of their own and are entirely dependent on the presence of certain types of mycorrhizal fungi in the soil as a food source to survive. Plants may take 7 to 12 years to reach blooming size and may live for over a century. The plants are threatened primarily through habitat destruction and by plant collectors in populated areas.

Two species *Cypripedium parviflorum* (yellow lady's slipper) and *Cypripedium reginae* (showy lady's slipper) may be found growing in relative abundance in roadside ditches over wide areas of south-eastern Manitoba. Plant surveys were undertaken by Native Orchid Conservation Inc. (NOCI) over several years and by Manitoba Conservation and Water Stewardship in spring 2011 and 2012, noting gps locations, orchid species, associated plant species and hydrogeological and topographic settings.

Cypripedium orchids were found to be restricted primarily to the glacial Sandilands complex, a collection of elevated coarse-grained moraines and related terraces, having limestone source areas. Within the Sandilands, orchids colonized low lying sites influenced by groundwater discharge.

The coarse glacial deposits and elevated terrain of the Sandilands region favour high infiltration and groundwater movement, while discouraging surface runoff. Reliable precipitation and terrain contrasts have resulted in the development of active flow systems. Moisture stress occurs in upland areas, with water-logged fens at the base. Stony soils and moisture stress have limited agricultural cultivation and disturbance.

Groundwater discharge maintains consistent moisture levels needed to sustain the mycorrhizal fungi and orchid growth. Groundwater flow mobilizes needed calcium to the root zone by dissolving it at higher elevation and re-depositing it in discharge areas. Nesting of flow systems at varying scales, including some highly localized flow helps to fine-tune the required moisture and geochemical balance into the optimum habitat.

In sites favoured by *Cypripediums*, groundwater discharge occasionally takes the form of seeps or springs, but was often released through evapotranspiration. The plants were most commonly found in seasonally damp or wet ditches or hollows, fens, wet forests and occasionally near slow moving streams. It is likely that actively flowing water lowers the water table in the adjacent banks, while flushing away calcium and nutrients.

Geological and hydrogeological studies may form an important contribution to orchid conservation. (SS14; Thurs. 3:00)

Unconventional origins of the Spiritwood Buried Valley aquifer in Manitoba

Toop, D.C., Manitoba Water Stewardship, Winnipeg, MB

The standard geological construct of buried valleys in western Canada has largely been determined by their western extents. They were carved into mostly Cretaceous bedrock by Tertiary aged rivers draining the eastern slopes of the Rocky Mountains. Their v-shaped bottoms are lined with resistant quartzite and chert laid down in the Tertiary. The rivers flowed east from the Rockies in a pattern not unlike the current Hudson Bay drainage area.

While buried valleys have been extensively mapped in the west, less is known of buried valleys in Manitoba where drill data are sparse. Previous work on buried valleys in Manitoba pointed to a different type of geology. Buried Valleys like the Pierson and the Medora-Waskada and Hatfield had variable fill and often lacked coarse fill to make viable aquifers, while gravels had mixed pre-glacial and glacial provenance.

Recent studies of the Spiritwood Buried Valley and the nearby Brandon Channel Aquifer indicate they are unlike buried valleys found further west. The Spiritwood Valley in Manitoba is 6 to 10 km and up to 100 m deep and may reach 16 km wide in North Dakota. The valley has steep sides and a flat bottom. A narrower deeper channel about 1.5 km wide is incised into the floor of the valley. Gradients indicate that the Spiritwood flowed south from Manitoba toward the Gulf of Mexico crossing past and present divides between the Hudson Bay and Mississippi basins. The orientation, valley shape and gradient are characteristic of glacial spillways found in the region. Exposures of the Spiritwood Valley reveal massive clay and silt diamict fill, with less extensive exposures of bedded sands and gravels. Some exposures indicate rapidly deposited sediments.

Manitoba is close to the spreading centre of continental glaciation. A continental ice front in the province would have blocked the northeast flow of existing rivers. Water pooled against the ice had nowhere to go but south. Large releases of meltwater could have carved the major channel we see in the Spiritwood Valley. A retreat of the ice front would have allowed western rivers and local streams to occupy the valley, only to be buried in later ice advances.

An unusual origin of the Spiritwood Valley has implications for groundwater exploration and development. The deeper incised channel has the highest and most dependable yields. Within the broader valley, aquifer zones are poorly developed and scattered. (SS14; Thurs. 2:00)

A revised global depth-diameter scaling relationship for Mars based on pitted impact melt-bearing craters

Tornabene, L.L.^{1,2}, Itornabe@uwo.ca, Ling, V.³, Osinski, G.R.^{1,4}, Boyce, J.M.⁵, Harrison, T.N.¹ and McEwen, A.S.⁶, ¹Dept. of Earth Sciences & Centre for Planetary Science and Exploration, Western University, London, ON N6A 5B7; ²The SETI Institute, Mountain View, CA 94043, USA; ³Central Secondary School, London, ON N6B 2P8; ⁴Dept. Physics & Astronomy, Western University, London, ON N6A 5B7; ⁵Hawaii Institute of Geophysics and Planetology, University of Hawaii, Honolulu, HI 96822, USA; ⁶Lunar and Planetary Laboratory, University of Arizona, Tucson, AZ 85721, USA

Crater-related pitted materials, thought to be impact melt-rich deposits formed from volatile-rich substrates, have been observed in high-resolution images of both the youngest and best-preserved craters on both Mars and Vesta. To date, 205 such craters have been identified on Mars ranging from 1–150 km in diameter, and are randomly distributed between ± 60°N latitudes.

Because pitted materials may represent primary crater-fill deposits, we explore their use to reassess a general depth-to-Diameter (d/D) scaling relationship using Mars Orbiter Laser Altimeter (MOLA) data. Constraining this relationship for the youngest and best-preserved craters on Mars is useful as a tool in planetary studies. Crater d/D can be used to specifically address the effect of target properties on crater morphology and the extent of erosion, degradation and deposition in various regions, or within specific craters on Mars.

Here we seek to measure the d/D ratio of as many pitted material-bearing craters as possible to further test the assertion of Tornabene *et al.* (2012) that pitted material-bearing craters are amongst the freshest and best-preserved craters on Mars. We will also compare the d/D relationship with previously published relationships. If pitted material-bearing craters are indeed amongst the freshest craters on Mars, then their depths should be comparable or deeper than the estimated depth values derived from these previous relationships.

For simple craters, our initial results indicate that the PEDR d/D data provides a better fit over the MEDGR data, with a best-fit power law:

$$dr = 0.276D^{0.68} \quad (r^2 = 0.87) \quad n = 31$$

The power-law relationship for pitted material-bearing complex craters is:

$$dr = 0.357D^{0.52} \quad (r^2 = 0.90) \quad n = 137$$



Boyce and Garbiel (2007) used the very deepest craters per diameter from their sample population to derive their d/D scaling relationship. As such, we also include the deepest most consistent craters from our sample population, and that do not originate from the high target strength regions, to compare with theirs (Fig. 2). These craters yield a best-fit equation of:

$$dr = 0.361D^{0.56} \quad (r^2 = 0.99) \quad n=20$$

When compared to previous general d/D scaling relationships, the pitted material bearing crater d/D relationships provides a consistently deeper estimate for both simple and complex craters. The greater depth of PM-bearing craters cannot be easily explained by target properties, as they are widespread over Mars. The consistently higher d/Ds provide additional corroborative evidence that pitted materials are primary crater deposits. **(SS16; Wed. Poster)**

Soft-sediment deformation as indicators of paleoseismic activity in lacustrine deposits (Green River Formation, Eocene, USA)

Törö, B., bat205@mail.usask.ca, Pratt, B.R., Renaut, R.W.,
Department of Geological Sciences, University of Saskatchewan,
114 Science Place, Saskatoon, SK S7N 5E2

Lacustrine sediments are regarded as particularly suitable deposits for the analysis of soft-sedimentary deformation features induced by shaking during ancient earthquakes. Their heterolithic nature gives them a high susceptibility to deformation owing to their variable rheological properties, and deposition in an overall quiet-water environment eliminates other trigger agents.

The Eocene Green River Formation (53 – 43 Ma), one of the largest and best known lacustrine deposits in the world, was laid down in an interconnected lake system in ponded basins during the Laramide orogeny in Wyoming, Utah and Colorado. Despite the known syndepositional tectonic activity and the large number of geological studies, which provide a detailed chronological background, horizons of soft-sediment deformation in the Green River Formation have not previously been studied and linked to tectonic movements.

Synsedimentary deformation features in various lacustrine deposits (paludal coal and sands to profundal oil shales) are described, classified and interpreted according to their composition and geometric characteristics. They have a wide range of morphology and size as a result of various driving forces (inverse density gradient, uneven loading, horizontal or vertical stresses) that arose during liquefaction and fluidization of the sediments, coupled with the areal extent and thickness of the original deposits. Deformation style ranges from brittle (fragmented laminites and faulted beds), to sedimentary injection into cracks, to plastic (convolution, folding). Deformed horizons are separated by undeformed sediments, which imply short-lived events that effected only near-surface sediments with a susceptible rheological state at the time.

In most cases other proposed trigger mechanisms such as overloading, oversteepening of depositional slopes, wave-induced cyclical stresses, sudden changes in groundwater level or bioturbation, which are thought to be capable of producing such deformation structures, can be excluded due to the absence of direct evidence in each case. The deformation structures identified in the Green River Formation are interpreted as having developed as a result of increased pore pressure and vertical or horizontal stresses induced by seismic activity, based on the tectonic setting of the basin, the detailed characteristics of the deformed features, the presence of undeformed layers adjacent to deformed horizons, and similarities with structures interpreted as being seismically induced in other areas as well as those reproduced experimentally. Seismites are pervasive in these rocks, but their concentration in some areas and within certain stratigraphic intervals indicate episodic tectonic activity along nearby fault systems and uplifts. This distribution helps refine the overall tectonic history of the lake basin. **(SS13; Thurs. Poster)**

Stratigraphy and physical volcanology associated with the Paleoproterozoic Back Forty VMS deposit, Menominee County, Michigan

Totenhagen, C.F.¹, Hudak, G.J.², Morton, R.L.¹ and Quigley, T.O.³, ¹Department of Geological Sciences, University of Minnesota Duluth, Heller Hall 229, 1114 Kirby Drive, Duluth, MN 55812-3036 USA; ²Precambrian Research Center, NRRI, University of Minnesota Duluth, 5013 Miller Trunk Highway, Duluth, MN 55811-1442 USA; ³Aquila Resources Inc., 414 10th Avenue, Suite 1, Menominee, MI 49858-3066 USA

The most recently discovered volcanogenic massive sulfide (VMS) deposit within the Paleoproterozoic Wisconsin Magmatic Terrane is Aquila Resources' Back Forty Deposit, located approximately 35 km north of Menominee, Michigan. The deposit contains open pit and underground measured and indicated resources of 17.9 million tonnes grading 1.57 g/t Au, 19.6 g/t Ag, 2.44% Zn and 0.19% Cu. The deposit occurs within a structurally deformed hydrothermally altered sequence of felsic volcanic breccias, tuff-breccias, lapilli-tuffs and tuffs. Stratigraphic correlation to this point has been based largely on lithogeochemical characteristics, which have determined three chemically distinct units. Detailed field mapping, diamond drill hole logging of exploration diamond drill core, and petrographic and lithogeochemical studies have been utilized to evaluate the detailed volcanic stratigraphy, volcanic facies, and volcanic environment associated with the mineralization. Four main felsic volcanic units have been defined based on: 1) lithofacies characteristics; 2) crystal composition, size, shape, abundance and distribution; 3) fragment composition, size, shape, abundance and distribution; and 4) grain size. These felsic units appear to originally have been deposited from high- and low-concentration, eruption-fed, subaqueous mass flows. Similar stratigraphic sequences have been documented in felsic-dominated caldera complexes; however, more regional mapping will be needed to evaluate whether the Back Forty stratigraphy and mineralization formed in this type of volcanic edifice. Petrographic and geochemical analyses indicate that the multiple massive sulfide horizons comprising the deposit are associated with a widespread, semiconformable sericite ± chlorite alteration assemblage. Textures associated with semi-massive and massive sulfide intersections are consistent with subsea-floor replacement style mineralization in a shallow subaqueous, low sulfidation epithermal mineralizing environment. More detailed regional studies are needed to better understand the full extent of the sulfide mineralization and hydrothermal alteration mineral assemblages, which may help further constrain the hydrothermal alteration model. **(SS7; Wed. 2:20)**

A spatial mosaic of overprinting and inheritance within the till sheet of northeastern Manitoba

Trommelen, M.S.¹, michelle.trommelen@gmail.com, Ross, M.² and Campbell, J.³, ¹Manitoba Geological Survey, Winnipeg, MB R3G 3P2; ²University of Waterloo, Waterloo, ON N2L 3G1; ³Geological Survey of Canada, Ottawa, ON K1A 0E8

The net effect of ice-flow shifts resulting in dilution or reworking of clasts on a single preserved till sheet is often unknown yet has major implications for paleoglaciology and mineral exploration. Herein, we analyze variations in till clast lithology and geochemistry from a single till sheet, within palimpsest-type Glacial Terrain Zones in northeast Manitoba, Canada, to better understand sediment-landform relationships in this area of high landform inheritance. We show that a seemingly homogenous 'Keewatin' till sheet is comprised of local (>15 km) and continental-scale (~100 km long carbonate train and 350-600 km long Dubawnt red erratic train) fan, amoeboid and irregular or lobate palimpsest dispersal patterns. Local dispersal is more complex than the preserved local landform flowset(s) record, but appears consistent with the overall glacial history reconstructed from regional flowset and striation analyses. The resultant surface till is a spatial mosaic interpreted to reflect variable intensities in modification (overprinting) and preservation (inheritance) of a predominately pre-existing till sheet. **(GS6; Wed. 8:40)**

**Experimental investigation of Pt and Rh solubility in basalt-rhyolite mixtures**

Turchiaro, F., turchiaro@es.utoronto.ca, and Brenan, J.M.,
University of Toronto, 22 Russell St., Toronto, ON M5S 3B1

Past work on platinum-group element (PGE) solubility in mafic magmas has largely focussed on the role of oxygen fugacity and temperature, with little attention to melt composition effects. However, the latter may be important to PGE saturation behaviour during the interaction of mafic magmas with felsic crustal contaminants. This study presents the results of experiments to measure the solubility of Pt and Rh in basalt-rhyolite mixtures at 1400°C, 1 bar, and FMQ + 3.8. Mixtures of calcined natural basalt and rhyolite were equilibrated for 5-100 hours on loops of Pt10%Rh then quenched in water. The resultant glass was analyzed for Pt and Rh by LA-ICP-MS. Both the solubility of Pt and Rh dropped from ~1 ppm in basalt to <0.06 ppm in rhyolite, indicating a strong melt composition control. The change in solubility correlates with a drop in the proportion of non-bridging oxygens, consistent with the likely high coordination state of dissolved Pt and Rh species. The solubility of Pt and Rh decreases exponentially with rhyolite content, such that the concentration of Pt or Rh in a mixture of saturated basalt with PGE-free rhyolite will exceed the solubility. Simple models of diffusive exchange between basalt and rhyolite have shown that cation concentration gradients parallel that for silica. If this is true for Pt and Rh, then our results predict that PGE oversaturation can occur within the zone of diffusive exchange. If the degree of oversaturation is sufficient to overcome the surface energy term for metal nucleation, or if pre-existing nuclei are available, then metal grains will form in the zone of contamination. This process may be significant in systems for which chromite precipitation is triggered by contamination, providing a mechanism for the simultaneous growth of chromite and PGE alloys. (SS9; Wed. Poster)

Spatial and temporal constraints on base-metal distribution in the Mesoproterozoic Borden Basin (Nanisivik District), NU

Turner E.C.¹, eturner@laurentian.ca, Kamber, B.S.², Kontak, D.J.¹, Long, D.G.F.¹, Hnatyshin, D.³, Creaser, R.³, Morden, R.¹ and Hahn, K.¹, ¹Department of Earth Sciences, Laurentian University, Sudbury ON P3E 2C6; ²School of Natural Sciences, Trinity College Dublin, Dublin, Ireland; ³Department of Earth and Atmospheric Sciences, University of Alberta, Edmonton, AB

Recent results from five field and analytical projects aimed at understanding the evolution and economic potential the Borden Basin Zn district (Nanisivik mine; 1976-2002) redefine the nature of host rocks, identify the stratigraphic and structural controls on the district's main showings, establish a depositional age for the critical stratigraphic units, produce a depositional age for the Nanisivik Zn deposit, and illuminate the region's untapped economic potential. (1) A mapping study of the district's known Zn-Pb±Cu showings identified the structural and stratigraphic controls on the spatial distribution of three showing types. The most important areas of known mineralisation (including the Nanisivik ore body) are primarily controlled by the shape of a hitherto unrecognised, aquiclude-capped, undulatory unconformity surface beneath which metal-reducing gas was trapped. A second major showing type is controlled by carbonate stratigraphic patterns adjacent to a lengthy fault that bounded one of the district's depositional grabens. (2) A field-based and analytical study of a thick (>100 m) and unexplored black shale unit showed that geochemical and geologic conditions in the basin during shale accumulation would have been appropriate for the deposition of SEDEX-type sulphides if local vent sources had been present (currently unknown). This work also yielded the first direct date for the depositional age of the Bylot Supergroup (~1092±59 Ma; U-Th-Pb whole-rock on black shale), which is considerably younger than the previously assumed depositional age, and coincides with assembly of Rodinia. (3) A fluid inclusion study of the Nanisivik ore body showed that ore-forming fluids were Na-rich and comparatively low-temperature (<100°C; in striking contrast to <200-250°C results of earlier studies), with increasing temperature towards the "mine dyke", a Franklin-aged (~720

Ma) intrusion that cross-cut the ore-body and locally reset the fluid inclusions to higher homogenisation temperatures). (4) Re-Os dating of pyrite from the Nanisivik ore-body provides for the first time a direct date for the mineralising event: ~1100 Ma. This date refutes recent work suggesting a Phanerozoic age for the mineralising event and refocuses the economic potential of the area to Proterozoic host rocks only. The results also suggest that fluid movement post-dated deposition of the Bylot Supergroup by only a brief time, and may have been driven by tectonic events associated with the amalgamation of Rodinia. (5) Study of the clastic basal rocks of the Mesoproterozoic succession showed that the potential for unconformity-type U deposits in this basin is low. (SS1; Fri. 2:00)

High pressure structural response of U60

Turner, K.M., katlynmt@umich.edu, Zhang, F. and Ewing, R.C.,
University of Michigan Earth and Environmental Sciences, Ann Arbor, MI, USA

Single crystals of the uranyl peroxide nanocluster U60 were analyzed by *in situ* Raman spectroscopy and X-ray diffraction in diamond anvil cells. The U60 cluster, $[\text{UO}_2(\text{O}_2)(\text{OH})]_{60}^{60-}$, is composed of 60 identical edge-sharing uranyl hexagonal bipyramids with peroxide and hydroxide as equatorial coordinating ligands. The U60 nanocluster is topologically identical to C60 buckminsterfullerene. At pH~9, clusters of U60 form crystals with the approximate chemical formula $\text{Li}_{68}\text{K}_{12}(\text{OH})_{20}[\text{UO}_2(\text{O}_2)(\text{OH})]_{60}(\text{H}_2\text{O})_{310}$. At ambient pressures, U60 has an isometric crystal structure with fm-3 symmetry and $a=37.884(2)$ Å. U60 single crystals are transparent yellow, cubic and can grow up to 1 mm in diameter. Single crystals of U60 less than 200 microns in diameter were used in these studies. Pressures ranged from ambient to 20 GPa. Two symmetric stretch modes of the uranyl ion are evident in the Raman spectra with wavenumber of ~850 cm^{-1} ; they are clearly observed at pressures up to 8-10 GPa. From 10-15 GPa, the uranyl ion vibrational modes broaden significantly and shift slightly toward higher wavenumbers, indicating stress in the crystal. At pressures higher than 15 GPa and following pressure quenching, the vibrational modes are not present in the spectra. This indicates an irreversible change in the U60 crystalline structure. High pressure X-ray diffraction measurements were completed at Brookhaven National Lab to quantify structural unit cell changes over the pressure ranges indicated previously. This study represents the first examination of the high pressure response of uranyl peroxide nanoscale cage clusters. (SS5; Wed. Poster)

Evaporate mound analysis of quartz-hosted fluid inclusions by SEM/EDS: Evaluation and application of method to assess granitoid metal fertility

Tweedale, F.M., Saint Mary's University, Halifax, NS B3H 3C3, fergus.tweedale@smu.ca, Daniel Kontak, Department of Earth Sciences, Laurentian University, Sudbury, ON, Jacob Hanley, Department of Geology, Saint Mary's University, Halifax, NS, Neil Rogers, Geological Survey of Canada, Ottawa, ON

A cost-effective, simple, and time-efficient method to determine the bulk composition of fluid inclusions is evaporate mound analysis. This method is semi-quantitative and determines inclusion composition by integrating SEM imaging with energy-dispersive analysis of precipitates, or mounds, produced by thermal decrepitation of fluid-inclusions. The method is applicable to magmatic-hydrothermal systems where fluid inclusions contain solute ions (e.g., Na, K, Ca, Cl, F). In order to assess the application of this method for evaluating hydrothermal evolution and metal fertility with regards to intrusion-related mineralisation, a test study is being conducted on the large (7800 km^2) and variably mineralized (e.g., Sn, W, Cu, U, Mo, Ta) South Mountain Batholith (SMB) of Nova Scotia.

Decrepitate mounds were analyzed using a LEO 1450VP (SEM) imaging system linked to an Oxford X-Max 80 mm^2 SDD detector energy-dispersive detector. Based on decrepitating over a range of temperatures, from 325° to 500°C, it appears that $T = 500^\circ\text{C}$ is optimal to produce large, well-shaped, and readily identifiable mounds. To



optimize analysis time and, hence, increase research efficiency while maintaining result accuracy, data were collected with 5-, 10-, and 30-second acquisition times. A comparison of results is discussed herein. The number of analyses required to produce a representative result is also discussed by comparison of results for 4, 8, 16, 32, and 64 analyses of mounds for individual samples. Multiple ($N = 12$) point-mode analyses on individual decrepitate mounds substantiate mound heterogeneity. Results that accurately reflect in-situ fractionation are shown to be achievable with single, 10-second raster-mode analysis.

The results of the aforementioned analytical conditions are utilised to define optimal operational protocols for efficient (*i.e.*, cost effective) analysis for a regional study of the SMB. This test case is the first of its kind conducted on a batholithic scale, with the resulting methodological protocols being readily exportable for the mineral fertility assessment of other regions. In addition to presenting the method protocol, the initial results of this work will be shown. The latter integrates a petrographic alteration index designed for granitic samples, fluid inclusion types and density, and evaporate mound chemistry for 100 samples. Samples are chosen such that the entire batholith may be assessed, and all mapped lithologies represented. Fluid compositions determined thus far include brines with 5- 15 % fluorine, which are quantitatively indeterminable using other methods. (*SY1; Wed. Poster*)

Measurements of fusion enthalpies of rare earth oxides, perovskites and pyrochlores

Ushakov, S.V. and Navrotsky, A., Peter A Rock Thermochemistry Laboratory and NEAT ORU, University of California at Davis, Davis, CA USA, svushakov@ucdavis.edu

Data on fusion enthalpies are essential for the thermodynamic modelling of phase equilibria. However, melting temperatures of rare earth oxides, aluminates, hafnates and zirconates are higher than 2000 °C and measurements of fusion enthalpies are scarce. We used high temperature thermal analysis to measure fusion enthalpy of LaAlO_3 perovskite for the first time. The values of 124 ± 10 kJ/mol at 2134 ± 10 °C were obtained from 11 experiments on melting LaAlO_3 samples in sealed tungsten crucibles. Fusion enthalpy of Al_2O_3 was used for temperature and sensitivity calibration. The sources of uncertainties in the measurements above 2000 °C will be discussed and new data on melting of Y_2O_3 and $\text{RE}_2\text{Zr}_2\text{O}_7$ pyrochlores ($\text{RE} = \text{La}, \text{Nd}$) will be presented. Thermal analysis above 2000 °C and classic drop calorimetry methods of fusion enthalpies measurements are limited to reducing conditions imposed by using of tungsten, molybdenum or tantalum capsules. New instrumentation for drop calorimetry in variable atmosphere using laser heating and aerodynamic levitator with splittable nozzle is under development and the progress will be reported. (*SS6; Wed. 9:40*)

Applications of gas adsorption calorimetry for surface characterization: Water on UO_2 and other examples

Ushakov, S.V., Shvareva, T.Y. and Navrotsky, A., svushakov@ucdavis.edu, Peter A. Rock Thermochemistry Laboratory and NEAT ORU, University of California at Davis, Davis, CA USA

Data on energetics of hydration of oxide surfaces are important for understanding of phase equilibrium in high surface area materials. During last eight years the measurements of enthalpies of water adsorption were performed on a number of oxide compounds using Micromeritics ASAP 2020 analyzer for dosing the gases in Setaram Calvet calorimeters cells. In this method, enthalpy of adsorption per dose of gas is measured as a function of coverage. Surface coverage ($\text{H}_2\text{O}/\text{nm}^2$) at which differential adsorption enthalpy reaches the condensation enthalpy of water (-44 kJ/mol) allows quantitative distinction between chemisorbed and physisorbed water on the surface and indicates if dissociative or molecular chemisorption prevails. Integral enthalpy of chemisorption allows calculating surface energies for anhydrous surfaces from high temperature oxide melt solution calorimetry measurements of drop solution enthalpies as a function of

surface area. Water vapor adsorption calorimetry experiments were performed on bulk and nanophase UO_2 degassed in vacuum at 200-800 °C. Enthalpies of adsorption at low coverage were found not to exceed -140 kJ/mol and reached condensation enthalpy at coverage 4.5-5.5 $\text{H}_2\text{O}/\text{nm}^2$. Integral enthalpy of chemisorption of water on UO_2 was in the range from -65 to -80 kJ/mol. Differential adsorption enthalpy at low coverage and integral chemisorption enthalpies of water vapor are similar for UO_2 and ThO_2 , however, higher degree of water dissociation on UO_2 can be inferred from our data on coverage. More exotic applications of gas adsorption calorimetry will be discussed on example of measurements of Xe and Kr adsorption on HKUST-1 metal-organic frameworks. (*SS5; Wed. 8:40*)

Applied mineralogy using short-wave infrared reflectance spectroscopy to define temperatures of clay alteration around ore deposits

Uvarova, Y., CSIRO Earth Science and Resource Engineering, 26 Dick Perry Avenue, Kensington, WA 6151, USA, Yulia.Uvarova@csiro.au, and Kyser, T.K., Department of Geological Sciences and Geological Engineering, Queen's University, Kingston ON K7L 3N6, kysyer@geol.queensu.ca

Fluids that produce ore deposits also produce significant alteration zones around the mineralization. Clay minerals are ubiquitous up to hundreds of meters from many deposits, and often there is zoning in the type of alteration minerals involved. Clay mineralogy can be used as an exploration technique in the field with the use of a portable short-wave infrared reflectance (SWIR) spectrometer. The SWIR technique is a rapid, non-destructive and cost-effective method allowing accurately and consistently identify groups and species of clay minerals, such as kaolin-group varieties, smectites, white micas and chlorites. Moreover, SWIR is not only capable of identifying mineral species, but it can also provide information on crystallinity of clay minerals, and crystallinity in turn can provide information on the crystallization temperature of a particular clay species.

As an example of applied mineralogy using SWIR, clay minerals from the Paleoproterozoic Athabasca and Thelon basins were separated from sandstones and analyzed by X-ray diffraction and EMP for phase identification and chemical analysis. Temperatures of crystallization were estimated from XRD patterns using the Kübler index (for illite) or using the EMPA data and cation exchange geothermometer (for chlorite). Samples of sandstones from the basins were then analyzed with a FieldSpec 3 portable SWIR instrument at wavelengths from 350 to 2500 nm and a spectral sampling interval of 2 nm. TSG Pro software package was used to identify clay minerals, estimate their percentages and quantify diagnostic spectral features and then correlated with the temperature of crystallization of a particular clay mineral. For illite, there is a positive correlation between the temperature of crystallization and illite crystallinity, which is estimated based on the ratio of reflectance value of deepest absorption feature between 2180 and 2230nm and the reflectance value of the deepest H_2O peak between 1860 and 1960nm. For chlorite-group minerals there is a positive correlation between the temperature of crystallization and a depth of the Fe-OH feature, which is the reflectance value of deepest absorption feature in the range 2238-2262 nm. Using these correlations for well-characterized sandstones, equations for temperature calculations were obtained. This allows rapid SWIR spectroscopy analysis of sandstone samples and temperature estimation using specific spectral features of clay minerals. (*SY1; Thurs. 9:00*)

Pretulite ScPO_4 from the Dolní Bory pegmatite, Czech Republic and its miscibility with zircon and xenotime

Výravský, J.¹, Novák, M.¹, Škoda, R.¹, 357118@mail.muni.cz, Johan, Z.² and Šrein, V.³, ¹Department of Geological Sciences, Masaryk University, Brno, Czech Republic; ²CRSMC, GIS BRGM-CNRS, Orléans, France; ³Czech Geological Survey, 165 00 Praha, Czech Republic

Miscibilities in tetragonal ABO_4 minerals of the zircon-type (zircon, hafnon, thorite, xenotime, coffinite, pretulite) are variable; complete in



the zircon-hafnon series but more or less limited in the zircon-xenotime, zircon-thorite and zircon-pretulite series. Two paragenetic types of pretulite were recognized at the pegmatite No. 3, Dolní Bory pegmatites (LCT family, Li-poor, peraluminous with common biotite, muscovite, schorl, sekaninaite, andalusite). (i) Irregular inclusions of rather homogeneous pretulite I ($\leq 10 \mu\text{m}$) associated with prevailing inclusions of xenotime-(Y) in host altered zircon ($\leq 3.72 \text{ wt.}\% \text{ Sc}_2\text{O}_3$) or overgrowths of homogeneous pretulite I ($\leq 20 \mu\text{m}$) around this altered zircon were found. Both textural types of pretulite I occur in the primary assemblage zircon+xenotime-(Y)+monazite-(Ce) enclosed in ilmenite. (ii) Irregular inclusions of heterogeneous pretulite II ($\leq 20 \mu\text{m}$) are randomly distributed within fine-grained mixture of secondary Nb-wolframite, W-columbite, Nb-rutile, and scheelite forming by a subsolidus breakdown of crystals of primary Sc-enriched wolframioxiolite to ferberite ($\leq 4.36 \text{ wt.}\% \text{ Sc}_2\text{O}_3$, $\leq 2.84 \text{ wt.}\% \text{ ZrO}_2$). Both pretulite mineral assemblages occur in the same sample of diaspore+andalusite aggregate from the quartz core. Pretulite I shows much lower compositional variations than pretulite II with 0.89-0.92/0.61-0.99 Sc *apfu*, 0.04-0.07/0.00-0.30 Zr *apfu*, 0.03/0.00 Y *apfu*, and 0.03-0.04/0.02-0.28 Si *apfu*, respectively; A/B ratio is close to 1 in both types. The substitution $\text{ZrSi}(\text{ScP})^{-1} \leq 30 \text{ mol.}\%$ of zircon component is prevailing, whereas YSc^{-1} substitution $\leq 3 \text{ mol.}\%$ of xenotime component is negligible. The mineral assemblages of diaspore+andalusite aggregate suggest $T \leq 410^\circ\text{C}$ and $P \leq 2 \text{ kbars}$ (presence of nearly end-member sekaninaite in the pegmatites) for the primary crystallization of host zircon, ilmenite and wolframioxiolite, respectively. Close association of pretulite with secondary pyrophyllite and ilite indicates subsolidus conditions at $T < \sim 350^\circ\text{C}$. It implies quite high miscibility in the zircon-pretulite series in pretulite dominant compositions even in rather low T but negligible miscibility of pretulite-xenotime. Distinct compositions of pretulite I and II, which underwent very similar evolution of PTX-conditions, are controlled by the associated minerals and composition of the system: pretulite I contains low Y and Zr (xenotime, zircon), pretulite II contains no Y but highly variable Zr (Nb-wolframite, W-columbite, Nb-rutile, scheelite), respectively. (SY2; Thurs. Poster)

Communicating Earth Science with the public: Part of our professional responsibility

Van der Flier-Keller, E., University of Victoria, Victoria, BC
V8W 3V6

Earth scientists contribute much to society. In our quest to understand the Earth and its processes, we pursue knowledge about how our Earth system works, evolves, and changes. We are the experts at finding and managing many of the resources our society relies on, including energy, minerals, metals, water, soil, and building resources. Geologists understand and help increase resiliency to natural hazards, and we are well placed in the areas of environmental management and quality.

In spite of this, the public is often unaware of what we do and how we contribute. We are sometimes reluctant to communicate outside of our professions.

Geoscience professionalism, which espouses duty to the public, service to society, and leadership, must surely encourage geoscientists to communicate with the public what we know, what we do and why, and how this can contribute to decisions we as a global society make about our planet.

Outreach and communication with the public is both personally and professionally rewarding, and can also be fun and creative. There are many ways that professional geoscientists can communicate better with the rest of society. Consider a show and tell or presentation in your local school, a café scientifique, writing a newspaper editorial, resolve to always agree to be interviewed by the media, accept requests to advise different levels of government, make presentations to the public where you live or in communities where you work during field seasons. Connecting with the public goes beyond knowledge mobilisation, it also helps form public opinion of geoscience and geoscientists, and clarifies our role in, and contribution to, society. Reaching out beyond our own profession may impact whether a school

district decides to offer an Earth science course in their curriculum, whether a young person decides to pursue geoscience as a career, or a local municipal council makes a sound decision based on geoscience. We hope that communicating better with the public will contribute to a more geoscientificalliterate society.

The presentation will include an introduction to the many excellent outreach and education resources (e.g. Media tools and training, websites, Geoscape posters, activity ideas, and peer groups such as CGEN (Canadian Geoscience Education Network), which will help you kick-start (or build on and strengthen) the Earth science outreach and communication aspects of your career as a geoscientist. (SS21; Fri. 9:40)

Polymict eucrite Northwest Africa 5232: The compositional and textural diversity of clasts and a previously undescribed Na-rich eucrite lithology

van Dronghelen, K.D., Department of Earth Sciences, University of Toronto, Toronto, ON M5S 3B1,
k.vandronghelen@es.utoronto.ca, and Tait, K.T., Department of Natural History, Mineralogy, Royal Ontario Museum, Toronto, ON M5S 2C6, ktait@rom.on.ca

The focus of this study was to examine the diversity of clasts within Northwest Africa (NWA) 5232, an 18.5 kg polymict eucrite. Polymict eucrites are impact breccias that likely formed near the surface of a large differentiated asteroid, possibly 4 Vesta, and belong to the Howardite, Eucrite, and Diogenite (HED) meteorite group. Studying HED surface breccias, such as NWA 5232, has important implications for understanding asteroid surface processes as well as applications for future sample return missions. Six polished thin sections from the Royal Ontario Museum (ROM) were examined with a petrographic microscope, electron microprobe (compositions), SEM (BSE textures and semi-quantitative EDS), and Raman spectrometer (silica polymorph identification).

Polymict breccia NWA 5232 is composed of eucrite, impact melt, and foreign carbonaceous chondrite clasts set in a fine- to medium-grained matrix. The eucrite clasts show a diversity of pyroxene compositions and igneous textures, primarily subophitic and granoblastic, from fine- to coarse-grained. The pyroxene exhibit pronounced exsolution lamellae, no zoning, and homogenous pyroxene compositions within clasts, with clast low-Ca pyroxene averages ranging from En_{29} to En_{47} . The QUILF two-pyroxene geothermometer of Andersen *et al.* (1993) was used to estimate the equilibration temperatures of eucrite clasts, ranging from $636^\circ\text{C} \pm 19$ to $924^\circ\text{C} \pm 78$ with an average of 731°C , and do not show a strong correlation between texture and equilibration temperature. Plagioclase compositions are more restricted, with clast averages from An_{86} to An_{89} . Clasts have either quartz or tridymite as a minor phase, as well as troilite, chromite, and ilmenite.

The most unusual subophitic eucrite clast observed in NWA 5232 contains pockets of very Na-rich plagioclase (Average $\text{An}_{25}\text{Ab}_{71}\text{Or}_4$) that exhibit a compositionally zoned mosaic texture. With the exception of these Na-rich pockets, the composition and texture of this clast is similar to other subophitic clasts in this polymict breccia. The pockets are up to $300 \mu\text{m}$ in size and contain anhedral Na-rich plagioclase concentrations up to $40 \mu\text{m}$. Immediately adjacent to the Na-rich plagioclase, the pyroxene is weakly enriched in Na, suggesting that this Na-enrichment might be a secondary metasomatic alteration product along fractures caused by impact-induced shock. Other shock features within this clast include fractures, bent pyroxene exsolution lamellae, and minor melt veins. Na-rich plagioclase within HED meteorites has not been reported in the literature and is an unexpected discovery, considering the extensive volatile loss suggested for the HED parent asteroid by the compositions of HED meteorites. (SS18; Thurs. 2:20)



Phosphorus-bearing Fe,Ni-sulphide in Murchison and carbonaceous chondrite clasts in polymict eucrite NWA 5232

van Drongelen, K.D.¹, k.vandrongelen@es.utoronto.ca, Tait, K.T.² and Dera, P.³, ¹Department of Earth Sciences, University of Toronto, Toronto, ON M5S 3B1; ²Department of Natural History, Mineralogy, Royal Ontario Museum, Toronto, ON M5S 2C6; ³Center for Advanced Radiation Sources, Argonne National Laboratory, University of Chicago, Argonne, IL, USA

An intriguing diagnostic accessory phase in CM carbonaceous chondrites was characterized for the first time by synchrotron single-crystal X-ray diffraction. For this study, grains of this phosphorian Fe,Ni sulphide (P-sulphide) within Murchison (CM meteorite) and eight carbonaceous chondrite clasts in polymict eucrite (breccia) NWA 5232 were examined. Several grains were reviewed, spanning a range of compositions, by semi-quantitative EDS (SEM) in preparation for synchrotron work. Diffraction data was collected at beamline 13-BM-D at the Advanced Photon Source, Argonne National Laboratory. Preliminary results show that this sulphide is likely a P-rich pentlandite. P-sulphide formed early in the Solar System and is likely tied to extra-solar contribution and may provide insight into the processes of condensation and alteration in the solar nebula.

P-sulphide grains within Murchison and NWA 5232 exhibit a diversity of forms and are most commonly associated with amoeboid olivine aggregates (AOA). The grains are either only located along the periphery of the AOA or restricted to the interior and were frequently present as multiple grains or strings of grains interstitial to olivine crystals. In rare cases, P-sulphide grains were observed within round voids in compact textured AOA, which may be related to secondary thermal annealing of the AOA. P-sulphide grains are anhedral and are variably uniform in composition. Larger grains may consist of multiple finer grains surrounded by a P-poor phase (Fe,Ni-sulphide or Fe-oxide). Some grains consist of two distinct phases, the P-sulphide host and submicron P-rich Fe,Ni metal within the P-sulphide (exact composition difficult to resolve due to size). No clear relationship between P-sulphide grain texture and minor element content was observed.

On a plot of S/P vs. Fe/Ni (at%), the composition of the P-sulphide in Murchison fits well with compositions observed by other workers' data for other samples of this meteorite. In NWA 5232, the compositions of the P-sulphide grains plot in clusters, each constituting a different carbonaceous chondrite clast. Some clusters overlap in composition, but at least three different compositional clusters can be resolved. This suggests that more than a single carbonaceous chondrite impactor was mixed into this eucrite breccia. This was an unexpected discovery, considering the small area over which the samples were taken and the friable nature of this material, which would limit the degree of mechanical mixing of these angular coherent clasts. (**SS18; Thurs. Poster**)

Evolution and deformation of the Mesoproterozoic Seal Lake Group in central Labrador

van Nostrand, T.S., Geological Survey, NL Department of Natural Resources, PO Box 8700, St. John's, NL A1B 4J6, timvannostrand@gov.nl.ca

The Middle Mesoproterozoic Seal Lake Group is a supracrustal sequence interpreted to have formed in an intracratonic rift environment on the Laurentia craton between 1270 and 1225 Ma. The stratigraphy consists of a fining-upward, subaerial to shallow-marine sedimentary succession, intercalated with amygdaloidal basalt flows and intruded by extensive gabbro sills. The upper stratigraphic formations are host to native copper and copper sulphide mineralization and local anomalous radioactivity is associated with some unconformities.

The rocks are disposed in a partially overturned, doubly-plunging syncline which was formed during north-directed thrusting of older igneous rocks along shear zones which transect the southern margin of the group. The structures associated with the southern unconformities are complex, and recumbent and north-verging folds, south-dipping mylonitic fabrics and other kinematic indicators affect both the basement and multi-phase deformed cover rocks.

Metamorphic grade attained a maximum of greenschist facies associated with shear zones on the southern limb of the syncline. Zeolite facies alteration and weakly deformed rocks on the northern limb of the structure reflect the decreasing effects of the Grenvillian Orogeny, from south to north, within the sequence.

Geochemistry of igneous rocks indicates a tholeiitic to calc-alkaline trend from lower to upper levels of the sequence. An alkali-rich basalt unit is anomalous with respect to this trend and may be related to a feeder dyke system for overlying sills and flows. Some alkali elements exhibit an increasing degree of variability with stratigraphic level, related to the effects of regional alteration. Basalt flows and gabbro sills have similar, LREE-enriched and flat HREE profiles, typical of continental basalt flows and suggests derivation of the igneous rocks from a common magmatic source. (**SS2; Wed. 3:00**)

Keynote (40 min): Evidence for hyper-extension during Late Ediacaran-Early Cambrian opening of the Iapetus Ocean in the northern Appalachians and British Caledonides

van Staal, C.R.¹, cvanstaal@nrcan.gc.ca, Chew, D.M.², Zagorevski, A.³, McNicoll, V.³, Skulski, T.³, Castonguay, S.⁴, Escayola, M.⁵ and Sylvester, P.J.⁶, ¹Geological Survey of Canada, 1500-605 Robson St., Vancouver, BC V6B 5J3; ²Department of Geology, Trinity College, Dublin, Ireland; ³Geological Survey of Canada, Ottawa, ON; ⁴Geological Survey of Canada, Québec, QC; ⁵University of Buenos Aires, Argentina; ⁶Department of Earth Sciences, Memorial University, St. John's, NL

Assemblages comprising highly deformed and metamorphosed ultramafic, mafic and clastic sedimentary rocks are commonly in tectonic slices below the ophiolite massifs and arc-related rocks that were emplaced on the Laurentian margin during the Taconic-Grampian orogeny. These slices commonly have preserved evidence of Early to Middle Ordovician high pressure-low temperature metamorphism typical of subduction-related settings. One of these assemblages we studied in detail is the Birchy Complex in Newfoundland, which is structurally sandwiched between overlying ca. 490 Ma ophiolite massifs of the Baie Verte oceanic tract and underlying metasedimentary rocks of the Fleur de Lys Supergroup of the Appalachian Humber margin. Birchy Complex gabbro yielded a Late Ediacaran U-Pb zircon ID-TIMS age of 558 ± 1 Ma, whereas LA-ICPMS concordia zircon ages of gabbro - and an intermediate tuffaceous schist gave ages of 564 ± 7.5 Ma and 556 ± 4 Ma respectively. These ages overlap the last phase of rift-related magmatism observed along the Humber margin of the northern Appalachians (565-550 Ma), yet the mafic rocks have MORB-like characteristics. The associated ultramafic rocks shed detritus into the interleaved sedimentary rocks and hence were exhumed by Late Ediacaran. Overlying psammite yielded a detrital zircon population typical of the Laurentian Humber margin. Age relationships and characteristics of the Birchy Complex and adjacent Rattling Brook Group suggest that the ultramafic rocks represent slices of continental lithospheric mantle exhumed onto the seafloor shortly before or coeval with magmatic accretion of MORB-like mafic rocks. Hence, they represent the remnants of an ocean-continent transition (OCT) zone formed during hyper-extension of the Humber margin prior to establishment of a mid-ocean ridge further outboard in the Iapetus Ocean. We propose that ribbon-shaped microcontinents such as Dashwoods and the Rattling Brook block formed as extensional crustal allochthons riding on a convex (concave-downwards) lithosphere-scale detachment. OCT's commonly show significant retardation of thermal subsidence due to structural emplacement of hot mantle beneath the thinning crust. The termination of rift-related magmatism (~550 Ma) is therefore the best proxy for the opening of Iapetus in the Northern Appalachians. (**SY4; Fri. 8:20**)



Size and source matter: New information on the giant, Proterozoic, Suwar/Wadi Qutaba layered mafic intrusion in Yemen

Venturi, C. and Greenough, J.D., EESc, Unit 7, SCI 216, 3333 University Way, Kelowna, BC V1V 1V7

Large, layered, generally-Proterozoic, mafic intrusions associated with melting of Archean subcontinental lithosphere host most of the world's Ni, Cr, Co and Pt-deposits. They formed during major rifting events. Previously published, high precision, identical (within precision), U-Pb zircon dates (638.6 ± 0.8 and 638.7 ± 0.7 Ma) from Ni and Pt-bearing noritic rocks at Suwar and Wadi Qutabah (30 km apart) support formation of a single, large, layered mafic intrusion in Yemen (Arabian Peninsula) at the end of the Proterozoic. Whole-rock geochemical similarities, geophysical data, and available mapping information also support a single intrusive complex $> \sim 250$ km² in area. Large, layered, noritic, and economically important intrusions are also associated with Archean lithosphere cut by Proterozoic rifting events. Using source composition-sensitive trace element ratios from previously-published whole rock data, it appears that melting of Archean, subcontinental lithosphere was involved in formation of the intrusion. Logging of 14 drill holes representing ~ 1.6 km of core drilled in the Wadi Qutabah area reveal a 0.5 km sequence of rocks that is apparently much more evolved (lower Mg/Fe) than rocks at Suwar. Mafic intrusions have changes in mineral solid-solution composition-versus-height that reflect thickness of the intrusion. Although crude, the low rate of change in orthopyroxene, augite and plagioclase composition over the 0.5 km of stratigraphy at Wadi Qutabah suggest an intrusion that is perhaps 5 km thick. This would make Suwar/Wadi Qutabah the second-thickest intrusion on Earth and provides further support for the idea that the intrusion is representative of a large igneous province. (SS8; Thurs. Poster)

Molecular dynamics simulations of uranyl-peroxide nanocapsules in aqueous solution

Vlaisavljevich, B.¹, vlai0001@umn.edu, Miro, P.¹, Hu, S.¹, Dzubak, A.¹, Spezia, R.², Cramer, C.J.¹ and Gagliardi, L.¹, ¹University of Minnesota, 207 Pleasant St SE, Minneapolis, MN 55455 USA; ²Laboratoire Analyse et Modélisation pour la Biologie et l'Environnement UMR 8587 CNRS, Université d'Evry Val d'Essonne Bd. F. Mitterrand, 91025 Evry Cedex, France

The self-assembly of uranium polyhedra into a wide variety of nanoclusters containing up to 60 uranyl moieties bridged through peroxide and hydroxyl ligands has been described by Prof. Burns (University of Notre Dame). The self-assembly of these species in aqueous solution is unique in uranium chemistry and has potential applications in the fabrication and reprocessing of actinide-based materials. We present the first study of these species in aqueous solution by means of molecular dynamics simulations. We developed a uranyl peroxide force field from *ab initio* calculation. Interaction energies were computed using second order Møller-Plesset perturbation theory (MP2) and fit to a Born-Huggins-Meyer (BHM) potential. Bonded parameters were fit from density functional (PBE/TZ2P) calculations. Water coordination for the uranyl ion and uranyl-peroxide species with two or five uranyl polyhedra has been explored. The U20 nanocluster, $[(\text{UO}_2)_{20}(\text{O}_2)_{30}]^{20-}$, and the ordering of water and sodium inside and outside the cluster was also analyzed. (SS5; Wed. 9:20)

Depositional environments, petrography and provenance of the mid-Cretaceous Dina and Cummings formations, Alberta

Wach, G.D.¹, grant.wach@dal.ca, Kidston, J.², Pelkey, R.³, Pothier, H.⁴ and Watson, N.⁵, ¹Department of Earth Sciences, Dalhousie University, Halifax, NS B3H 4R2; ²Stornoway Diamond Corporation, Vancouver, BC; ³Vale Base Metals, Sudbury, ON; ⁴Department of Earth and Atmospheric Sciences, University of Alberta, Edmonton, AB; ⁵Atlantic Petrophysics Ltd., Halifax, NS

The Dina Formation, late Barremian to late Aptian, is the basal unit of the Mannville Group in east-central Alberta, and the primary oil-

producing unit of the Provost field, discovered in 1956. The Dina Formation was deposited in a series of paleo-valleys cut into much older carbonate platformal rocks. This contact marks the sub-Cretaceous regional unconformity, present throughout much of the Western Canada Sedimentary Basin (WCSB). The Dina Formation is overlain by the Ostracode zone and the Cummings Formation.

Physical and biogenic sedimentary structures preserved in cores indicate the upper Dina Formation was deposited in an estuarine environment, and lithofacies show an upwards increase in marine influence, grading upwards from marine-influenced channel deposits on the bottom (of the cored interval) to moderately burrowed tidal flat and channel deposits on top. Oil-stained sandstone beds in the two cores indicate oil-distribution in the Dina Formation is lithofacies dependent, and concentrated within channel sands of the upper lithofacies. The presence of accessory zircon, muscovite, and feldspar grains suggest Canadian Shield provenance for the Dina Formation.

The Cummings Formation (late Aptian to early Albian) is a transgressive estuary deposit. Basal channel incision was followed by valley-fill deposits that exhibit progressive marine influences. Organic matter analyses suggest a terrestrial source of potential gas producing Type II kerogen. Vitrinite reflectance and rock evaluation suggest the Cummings Formation is thermally immature. Poor total organic percentages indicate the formation would be inadequate as a secondary source rock for the field. Abundant detrital chert, volcanic and lithic fragments suggest a Cordilleran provenance. (SS13; Fri. 2:20)

Geodynamics of Iapetus Ocean closure in the Appalachian-Caledonide orogen

Waldron, J.W.F.¹, john.waldron@ualberta.ca, Schofield, D.I.² and Murphy, J.B.³, ¹Department of Earth and Atmospheric Sciences, University of Alberta, Edmonton, AB T6G 2E3; ²British Geological Survey, Columbus House, Greenmeadow Springs, Cardiff, Wales, UK, CF15 7NE; ³Department of Earth Sciences, St. Francis Xavier University, PO Box 5000, Antigonish, NS B2G 2W5

The Appalachian-Caledonide orogen formed as a result of the Cambrian to Silurian closing of the Iapetus Ocean. In most reconstructions, the continental blocks which separated to form the Iapetus Ocean (Laurentia, Baltica, and Amazonia – West Africa) are the same three continents that subsequently collided during its closure, raising questions as to how and why its divergent margins became convergent.

During the opening of the Iapetus Ocean, the margin of Laurentia underwent protracted rifting from ~ 615 Ma to at least 550 Ma, and perhaps later. A Neoproterozoic 'early' Iapetan rift probably developed east of Dashwoods and other peri-Laurentian microcontinents; this was superseded by a western rift between these microcontinents and the Laurentian margin. Analogies with modern oceans suggests that this rift-drift history would have substantially separated Dashwoods from the Laurentian margin. Similar processes are inferred to have occurred between Baltica and Amazonia – West Africa, resulting in the generation of a number of peri-Gondwanan microcontinents that found their way into the Appalachian-Caledonide system.

Subduction of the Paleozoic Iapetus Ocean began relatively soon after its opening at ~ 515 -505 Ma. The earliest collisional events are recorded almost simultaneously in Laurentian and peri-Gondwanan elements during the Early Ordovician, 490-480 Ma. This suggests that subduction initiation did not occur at a mature passive margin, a commonly assumed, but non-actualistic part of the 'Wilson cycle'. Closure of the ocean between Avalonia and Laurentia was complete by ~ 425 Ma.

It is more likely that Iapetus Ocean closure was initiated at a subduction zone migrating from the adjacent external 'Paleopacific' in a manner analogous to the Mesozoic-Cenozoic capture of the Caribbean plate in the Atlantic realm. This hypothesis may help to explain: the initiation of subduction and the early closing of the Iapetus; the timing of the earliest collisional events; the isotopic character of Iapetan ophiolites; and the distribution of peri-Gondwanan terranes in the orogen. (SS11; Fri. 1:40)



A first-principles study of uranyl and neptunyl incorporation into sulfate minerals

Walker, S.M. and Becker, U., University of Michigan, Dept. of Earth and Environmental Sciences, 2534 CC Little, Ann Arbor, MI 48109, USA

Using a combination of periodic and cluster density functional theory calculations, the energies of incorporation of uranyl (UO_2^{2+}) into anhydrous sulfate minerals, anglesite (PbSO_4), barite (BaSO_4), and celestine (SrSO_4) are calculated. For each mineral, source and sink reference phases are chosen to facilitate the substitution of the uranyl ion with a cation from the host mineral as described by the general equation:

host mineral + uranium source	\longleftrightarrow	uranyl mineral phase + sink
solid UO_3		solid $(\text{Pb}, \text{Ba}, \text{Sr})\text{O}$
UO_2^{2+} (aqueous complex)		$(\text{Pb}, \text{Ba}, \text{Sr})^{2+}$ (aqueous complex)

Of the three sulfate minerals, the energy of uranyl incorporation into anglesite was the lowest for solid state oxide reference phases ($\Delta E_{\text{rxn}} = 1.57$ eV). Of the three host minerals, anglesite was also the lowest for incorporation of an aqueous species.

Since these static incorporation energies are most closely representation the enthalpy of incorporation, the free energy was estimated using vibrational entropy values from empirical force field calculations in order to keep computational expense within a reasonable range. Including these vibrational entropy data tends to make incorporation energy values less energetically uphill.

Incorporation of uranyl was then compared with incorporation of $\text{Np}(\text{VO})_2^{2+}$ and $\text{Np}(\text{V})\text{O}_2^+$ aqueous neptunyl complexes. For the latter, charge compensation was achieved by adding an H^+ to a sulfate group adjacent to the incorporation site. (SS5; Thurs. 10:20)

Identifying unconformities, unconformities, and “rockbergs” within the Stillwater Complex using high-precision U-Pb zircon geochronology

Wall, C.J.¹, cwall@eos.ubc.ca, Scoates, J.S.¹, jscoates@eos.ubc.ca, Friedman, R.M.¹, rfriedman@eos.ubc.ca, and Meurer, W.P.², william.p.meurer@exxonmobil.com, ¹Pacific Centre for Isotopic and Geochemical Research, Department of Earth, Ocean & Atmospheric Sciences, University of British Columbia, 2020-2207 Main Mall, Vancouver, BC V6T 1Z4; ²ExxonMobil Upstream Research, Houston, TX, USA

We present U-Pb CA-ID-TIMS results for zircon from the Stillwater Complex (Montana, USA) for samples from the exposed 8 km-thick intrusion that reveal the presence of distinct time gaps throughout its magmatic stratigraphy. The ~100 m-thick Basal Series, dominated by contaminated orthopyroxene cumulates, records the initial magmatic activity in the intrusion at ca. 2712 Ma (sulphide-bearing norite, 2712.26±0.54 Ma, Benbow). The majority of the 2 km-thick Ultramafic Series is younger at ca. 2711 Ma, with ages of 2711.39±0.29 Ma (mafic pegmatite above Chromitite J, top of Peridotite Zone, Benbow), 2711.35±0.39 Ma (feldspathic pegmatitic orthopyroxenite, base of Bronzite Zone, Iron Mountain), and 2711.07±0.85 Ma (orthopyroxenite, top of Bronzite Zone, Chrome Mountain), indicating a time gap or unconformity of at least several 100 ka between crystallization of the Basal and Ultramafic Series. In contrast, both the base of the Ultramafic Series (peridotite from Chromitite B, 2710.22±0.21 Ma, Benbow) and the Banded Series (noritic pegmatite in Norite-I Zone, 2710±0.56 Ma, Mountain View) record a distinct magmatic event at ca. 2710 Ma, suggesting that the lowermost Ultramafic Series was emplaced as separate magma batch into previously crystallized ultramafic rocks and that the Ultramafic/Banded Series contact may also be a unconformity. The majority of the overlying Banded Series, dominated by plagioclase-rich rocks and including the world-class J-M Reef platinum group element deposit,

crystallized at ca. 2709 Ma based on ages for the J-M Reef (2709.11±0.56 Ma, Frog Pond Adit; 2709.00±0.45 Ma, West Fork), an olivine gabbro in Olivine-bearing-III Zone (2709.01±0.53 Ma, Picket Pin), and an anorthosite horizon near the top of Gabbro-norite-III Zone (2709.10±0.45 Ma, Picket Pin). The age and locally discordant nature of the J-M Reef indicate that it represents a major magmatic unconformity and marks the onset of renewed magmatism in the Stillwater magma reservoir. The age for a sample of Anorthosite-II Zone in the upper part of the Middle Banded Series (2710.56±0.32 Ma, Picket Pin) is distinctly older than the rest of the Banded Series by 1.5 million years and is consistent with an origin for the enigmatic anorthosites as flotation cumulates (“rockbergs”) related to fractional crystallization of mafic rocks now preserved in the lower part of the Lower Banded Series. Based on these results for the Stillwater Complex, distinct time gaps and non-stratigraphic ages may well be typical of major mafic layered intrusions formed under open-system processes. (SS8; Thurs. 3:00)

Increased magmatic water content — the key to late-collisional porphyry Cu ± Mo ± Au formation in the Oligo-Miocene Gangdese belt, Tibet

Wang, R., rw5@ualberta.ca, Richards, J., Department of Earth and Atmospheric Sciences, University of Alberta, Edmonton, AB T6G 2E3, Hou, Z. and Zhiming, Y., Institute of Geology, Chinese Academy of Geological Sciences, Beijing 100037, PR China

The Himalaya–Tibet continent–continent collisional orogen provides a unique opportunity to study the relationship between collisional tectonism, magmatism, and metallogenesis. Neo-Tethyan subduction under the southern Lhasa terrane began in the Late Triassic–Early Jurassic, and developed with voluminous magmatism in the Cretaceous through Paleocene–Eocene. These magmatic rocks constitute the Gangdese magmatic belt, where a series of Cenozoic collision-related igneous rocks intruded or erupted since the start of the India–Asia collision at ~55 Ma. Porphyry copper deposits in the Gangdese magmatic belt are unevenly distributed over time in the mid- to late Cenozoic. Such deposits are rare in association with Eocene intrusive rocks, but are abundant in the Oligo-Miocene. The Eocene granitoids have intermediate $[\text{La}/\text{Yb}]_N$ ratios (average = 9.9 ± 8.1 , $n = 50$, range = 1.15–34.3), intermediate-to-low Sr/Y ratios (mostly <40), and negative Eu anomalies (average $\text{Eu}_N/\text{Eu}^* = 0.78 \pm 0.25$, $n = 50$, range = 0.24–1.33). These granitoids are mainly composed of pyroxene, plagioclase, and quartz, with minor interstitial amphibole and biotite. In contrast, Oligo-Miocene granitoids have high $[\text{La}/\text{Yb}]_N$ ratios (Oligocene: average $[\text{La}/\text{Yb}]_N = 42.5 \pm 13.5$, $n = 30$, range = 27.0–93.2; Miocene: average $[\text{La}/\text{Yb}]_N = 27.8 \pm 6.8$, $n = 73$, range = 11.6–44.9), high Sr/Y ratios (7gt;40), weak or absent Eu anomalies (Oligocene: average $\text{Eu}_N/\text{Eu}^* = 0.93 \pm 0.19$, $n = 30$, range = 0.52–1.58; Miocene: average $\text{Eu}_N/\text{Eu}^* = 0.93 \pm 0.16$, $n = 73$, range = 0.19–1.46), and their mineralogy consists of plagioclase, quartz, and amphibole. These geochemical and mineralogical characteristics suggest that the Eocene magmas were relatively dry and evolved primarily by fractionation of pyroxene and plagioclase, whereas the Oligo-Miocene magmas were more hydrous and fractionated significant amounts of hornblende and lesser plagioclase prior to upper crustal emplacement.

The Eocene magmas were generated during the onset of collision between India and Asia, and record the final stages of subduction of oceanic lithosphere beneath Asia; their low water contents may reflect final dehydration of the remnant Neo-Tethyan slab. After slab break-off at ca. 40–38 Ma, the Indian lithosphere began to subduct beneath the Lhasa terrane. We suggest that prograde metamorphic dehydration of subducted continental lithosphere and/or partial melting of Indian crustal rocks released water and/or melt, which react with previously subduction-modified Tibetan lithosphere to generate fertile, hydrous melts. Such melts would have had greater potential to form porphyry-type magmatic-hydrothermal ore deposits than the drier Eocene magmas. (SS23; Thurs. Poster)

**Physical volcanology and hydrothermal alteration at the Rainy River gold project, NW Ontario**

Wartman, J.¹, Jakob.Wartman@CliffsNR.com, Morton, R.² and Hudak, G.J.³, ¹Cliffs Natural Resources, PO Box 180, Eveleth, MN 55734 USA; ²Department of Geosciences, University of Minnesota Duluth, 229 Heller Hall, 1114 Kirby Drive, Duluth, MN 55812 USA; ³Precambrian Research Center, Natural Resource Research Institute, University of Minnesota Duluth, 5013 Miller Trunk Highway, Duluth, MN 55811, USA

The Rainy River Gold Project (RRGP) is located 75km northwest of Fort Francis, Ontario within the Neoproterozoic Rainy River Greenstone Belt. This advanced stage exploration project has an NI 43-101 compliant gold resources of 1.18 Moz grading 1.33 g/t in the Measured category, 4.98 Moz grading 1.18 g/t in the Indicated category, and 2.28 Moz grading 0.76 g/t in the Inferred category. Detailed field mapping and diamond drill core logging, supplemented with petrographic and lithogeochemical studies, have enabled the stratigraphy, volcanic facies, and hydrothermal alteration mineral assemblages to be identified, and processes associated with the gold mineralization to be better understood. The volcanic facies in the deposit include coherent dacitic flows and associated synvolcanic intrusions with autoclastic breccias, hyaloclastites, peperites, and syn- to postdepositional resedimented volcanoclastic deposits. The coherent dacitic flows are massive, range in thickness up to 150 m, and in lateral extent for 2500 meters. Coherent dacite flows grade into a heterogeneous facies, characterized by pods and lobes of coherent dacite, enveloped by autoclastic breccia and hyaloclastite. Flows are interspersed with strongly altered volcanoclastic sediments that are locally punctuated by peperites. Volcanic facies reconstruction indicates the presence of lobe-hyaloclastite dome/flow complex fed, and locally intruded by, synvolcanic dacite hypabyssal intrusions. An apparent feeding fissure is centered to the west of the main area of mineralization. Hydrothermal alteration is widespread throughout the deposit and is marked by silicification, chloritization, sericitization, and carbonitization (as well as minor epidote and local biotite alteration). Quartz, sericite and chlorite are ubiquitous in the deposit. Alteration assemblages are dominantly stratabound, and their distribution is related to original rock permeability, with flow tops, autoclastic breccias, and volcanoclastic sediments being most strongly altered. Shear zones also preserve stronger alteration intensities. Gold mineralization appears to have initially occurred within a synvolcanic, low sulfidation epithermal system. Elevated gold values are strongly correlated with highly permeable units and increased alteration intensity, suggesting enhanced mineralization in areas that experienced higher water: rock ratios. Post-volcanic remobilization of the gold appears to have occurred, as the highest gold values in the deposit are spatially related to shear-zones and associated quartz-carbonate-epidote veins. (SS7; Wed. 9:40)

Polyphase deformation and metamorphism in the southern Kootenay Arc and Purcell Anticlinorium, southeastern British Columbia

Webster, E.R. and Pattison, D.R.M., Department of Geoscience, University of Calgary, 2500 University Drive, NW Calgary, AB T2N 1N4, erwebste@ucalgary.ca

A fork shaped domain of Barrovian amphibolite facies rocks is located at the interface between three primary tectonic domains in southeastern British Columbia: the Kootenay arc, Purcell Anticlinorium and the northernmost extension of the Priest River Complex. The metamorphic belt is partly bound by two large Eocene normal faults that crosscut the study area: the Purcell Trench Fault and the Midge Creek fault, across which there are marked differences in structural style and metamorphic grade.

The rocks in the study area underwent three folding episodes, spanning the time interval from mid-Mesozoic to Eocene. Broadly, there is an increase in structural complexity and intensity of deformation from the southwest to the east and north, corresponding to progressively deeper structural levels and younger structures.

Therefore, the structural features were divided into a western, northern and eastern domain. The latest penetrative deformation in each of the three domains is Middle Jurassic in the west, becoming progressively younger to the north and east. The penetrative structures in all three domains are similar, with both the strike of foliation and the trend of the fold axes being north-northeast, suggesting that earlier structures were overprinted and tightened by later structures in the northern and eastern domains.

The two elongate domains of regional middle amphibolite facies rocks merge in the northern part of the study area, forming a southward facing forked isograd pattern. The western branch is parallel to strike of lithological units and is truncated by the Midge Creek fault. The eastern branch is broadly parallel to the Purcell Trench fault and transects strike. This branch continues south in to the United States and merges with amphibolite facies metamorphism in the Priest River Complex. The fork is separated by a large area of greenschist facies metamorphism. The age of the metamorphism is broadly similar to the age of the penetrative structures in each of the three structural domains. The oldest metamorphism is Middle Jurassic and primarily comprises the area of greenschist facies metamorphism. The metamorphism becomes progressively younger to the east as lower structural levels are exposed in the footwall of the Purcell Trench fault. Therefore, despite the apparent continuity of the isograd pattern it is actually an interplay of multiple periods of metamorphism from the Middle Jurassic to Late Cretaceous. (GS2; Wed. 10:20)

Investigating the development of biogeochemical redox gradients in Alberta oil sands tailings ponds

Weisener, C.G., University of Windsor, 401 Sunset Ave, ON N9B 3P4, weisener@uwindsor.ca

The oil sands deposits of north-eastern Alberta are one of the largest oil reserves in the world, containing an estimated 2.5 trillion barrels of recoverable bitumen held in a mineral matrix consisting of sand, clay and water. After bitumen extraction, tailings are pumped into retention ponds, where the sand fraction settles, and most of the aqueous slurry (i.e. fines consisting of silts, clays and residual hydrocarbons) slowly consolidates termed fluid fine tailings (FFT). The chemistry and the microbial drivers in these tailings can be very complex. There is a need for detailed systematic studies bridging the physico-chemical components with the microbial ecology for developing predictive models for future end pit lake remediation strategies. Establishing the biotic and abiotic controls influencing redox gradients is imperative in assessing and developing current end pit lake remediation prediction models. Here we investigate the effects of the established microbiology on the REDOX chemistry associated with the FFT/water interface. Laboratory microcosm experiments are used to investigate the flux of sulfur and oxygen during the onset of deposition. The ongoing investigations will be discussed providing links from laboratory scale to field scale systems currently being used to contain the waste material. (SS15; Wed. 3:00)

Topological possibilities for carpholite-like structures: A new double-chain silicate $\text{K Ba Fe}^{3+} \text{Mg}_7 \text{Si}_8 \text{O}_{22} (\text{OH})_2 (\text{OH}, \text{F})_6$

Welch, M.D., The Natural History Museum, London, SW7 5BD, UK, mdw@nhm.ac.uk, and Mitchell, R.H., Dept. of Geology, Lakehead University, Thunder Bay, ON

Carpholite-group minerals occur in diverse rock types that include metapelitic and metabasic schists, quartzites and pelitic enclaves in eclogites. Magnesiocarpholite is an index mineral of blueschist-facies metapelites. Recently, a new mineral related structurally to carpholite was discovered by one of us (RHM) in a dolomite carbonatite in the Ashram Zone of the Eldor carbonatite complex, Quebec, Canada, where it occurs as aggregates of matted fibrous and prismatic crystals in association with dolomite, monazite, fluorite and an unidentified Mg- and F-rich mica-like phase. Whilst sharing close topological similarities with carpholite, the new mineral is a double-chain silicate and has a distinctive Al-free composition $\text{KBaFe}^{3+} \text{Mg}_7 \text{Si}_8 \text{O}_{22} (\text{OH})_2 (\text{OH}, \text{F})_6$. It is orthorhombic with space group



Cmma (Cmma) and unit-cell parameters a 18.9506(3) Å, b 22.5045(3) Å, c 5.2780(1) Å, V 2250.93(6) Å³. The structure has been solved and refined to final agreement indices $R1 = 0.026$, $wR2 = 0.052$, $GoF = 1.116$. An amphibole-like 1-beam extending $\parallel c$ is composed of a ribbon $\parallel (100)$ of edge-sharing octahedrally-coordinated Mg-rich $M(1,2,3)$ sites, that is sandwiched between double-chains of SiO_4 tetrahedra $T(1)$ and $T(2)$. $M(1,2,3)$ cations are bonded to fluorine and oxygen. The double-chain $O-O-O = 178.4^\circ$ and unbowed. As such it is almost \angle is almost fully extended (undistorted). 1-beams are connected via narrower ribbons $\parallel (010)$ of edge-sharing $(Mg, Fe^{2+})O_4(OH, F)_2$ and $Fe^{3+}O_4(OH)_2$ octahedra to form a trellis-like tunnel structure that is similar to that of carpholite, for which the 1-beams are pyroxene-like. K occupies a channel site analogous to the A-site of amphibole. Ba occupies a cavity site at the corner where the two types of ribbon meet, corresponding to the A-site of carpholite, as in balipholite, and is coordinated to eight O and four (OH, F). Despite the topological similarities between the new mineral and the carpholite group, there are key aspects of the two structures that differ significantly and would seem to preclude polysomatic relationships between them. (SY1; Wed. 9:20)

Foreland basin formation, environmental change and trilobite paleoecology, Late Ordovician of eastern Laurentia

Westrop, S.R.¹, swestrop@ou.edu, Amati, L.M.², Carlucci, J.R.³ and Brett, C.E.⁴, ¹Oklahoma Museum of Natural History and School of Geology & Geophysics, University of Oklahoma, Norman, OK 73072 USA; ²Department of Geology, SUNY Potsdam, Potsdam, NY 13676 USA; ³Department of Geosciences, Midwestern State University, Wichita Falls, TX 76308 USA; ⁴Department of Geology, University of Cincinnati, Cincinnati, OH 45221 USA

Trilobite distribution, abundance and diversity in the Late Ordovician of Laurentia must be understood in the context of environmental changes associated with the Taconic Orogeny. Establishment and infilling of the Taconic Foreland basin led to profound changes in the distribution of lithofacies and biofacies across the eastern half of the continent. Here we report on trilobite faunas of the late Sandbian to Katian interval. In the late Sandbian, mid-continent regions such as Oklahoma, and foreland basin regions share similar deep-water faunas, dominated by raphiophorid and isoteline trilobites. Later, in the Katian, regions in the mid-continent, such as central Oklahoma, have a relatively continuous record of carbonate deposition, and diverse platform biofacies that pass down-ramp into deeper subtidal, low-diversity cryptolithine faunas. In the foreland basin, cryptolithine biofacies became widespread in the Katian, and expanded geographically as the clastic wedge prograded westward. Sedimentary evidence indicates that cryptolithines have a broader bathymetric range in the foreland basin and emerged at least locally into shallow subtidal, storm-influenced settings. Up-ramp, around the margins of the basin in such regions as southern Ontario, more diverse biofacies lack cryptolithines and share taxa with mid-continent faunas. Preliminary data also indicate that the distribution of trilobite biofacies reflects patterns in the carbonate isotope stratigraphy, suggesting a relationship with various water masses recorded by aquafacies. The emerging patterns of biofacies distribution demonstrate the influence of regional processes on trends in diversity, faunal turnover and replacement over a broad area of Laurentia. (SY3; Thurs. 11:00)

Au mineralization at 3Ace, south-east Yukon

Whelan, S.C.¹, shaunaug@ualberta.ca, Gleeson, S.A.¹, Stern, R.A.² and Buchanan, C.³, ¹University of Alberta, 1-26 Earth Sciences Building, Edmonton, AB T6G 2E3; ²Canadian Centre for Isotopic Microanalysis, University of Alberta, Edmonton, AB T6G 2E3; ³Northern Tiger Resources Ltd., Suite 220, 17010 - 103 Ave, Edmonton, AB T5S 1K7

The Tombstone Gold Belt (TGB), a subdivision of the Tintina Gold Province, is an economically important area of Au endowment that spans central Yukon and into Alaska. Due to the spatial and temporal

relationship of these deposits with Mid- to Late Cretaceous plutonism, much of the recent exploration for Au has been focused on or around intrusions. There are, however, Au showings at the distal end of the TGB, in south-east Yukon, that have no obvious association with intrusions and thus, have been interpreted to be orogenic Au systems, such as Northern Tiger Resources' 3Ace showing.

At 3 Ace, native Au occurs in quartz veins hosted by quartz pebble conglomerate (QPC) and lithic arenite of the Neoproterozoic to lowest Cambrian Yusezyu Formation. The Main Zone is a Au bearing, 1m by 6.5m quartz vein which dips moderately to the east, and is cut off on either side by steeply dipping E-W trending faults. Drill holes through the Main Zone have yielded Au grades as high of 4.6g over 35.0m, including 106.2g over 1.0m.

A petrographic study has shown that there are 5 separate generations of quartz growth. The oldest generation, quartz 1 (Q₁), is deformed, and there are two other generations of quartz, Q₂ and Q₃, which predate the Au mineralization. Q₄ is a clear, grey quartz that occurs in low abundance relative to Q₂ and Q₃ and is associated with Au. Au is occasionally coeval with arsenopyrite. Pyrite, galena, and sphalerite are also spatially associated with Q₄, but do not occur with the Au and are believed to postdate it.

A $\delta^{18}O$ study using Secondary Ion Mass Spectrometry (SIMS) guided by scanning electron microscope - cathodoluminescence (SEM-CL) shows that Q₂, Q₃, and Q₄ have $\delta^{18}O_{SMOW}$ values that range from +16.22 to +18.23‰. A previous fluid inclusion study yielded fluid temperatures of 250-310°C. Together with $\delta^{18}O$ values, this yields calculated $\delta^{18}O$ values in water between +7.33 and +11.82‰, which fall within the values for both metamorphic and magmatic fluids. $\delta^{34}S$ values from the base metals, C and O analyses of carbonate phases and fluid inclusion microthermometric data will also be presented. It is hoped that these techniques will constrain the nature of the fluid source, and therefore the origin of the 3Ace deposit. (SSI; Fri. 3:00)

The eastern Cobequid Highlands, northern mainland Nova Scotia, Canada: An enigmatic piece of the Avalonian puzzle

White, C.E., whitece@gov.ns.ca, and MacHattie, T.G., Nova Scotia Department of Natural Resources, Box 698, Halifax, NS B3J 2T9

The Cobequid Highlands of northern mainland Nova Scotia form part of the southern margin of Avalonia, a fault-bounded composite terrane positioned inboard of Meguma and outboard of Ganderia in the northern Appalachian orogen. Recent mapping in the eastern Cobequid Highlands is consistent with previous division of the area into two blocks, Bass River and Jeffers, but has resulted in better understanding of their components. The oldest unit in the Bass River block is the Bass River Complex, which includes the $<ca.$ 990 Ma and $>ca.$ 625 Ma Gamble Brook and Folly River formations, reinterpreted to be laterally equivalent. The Gamble Brook Formation consists of metasedimentary rocks previously interpreted on the basis of lithochemical characteristics to have been deposited in a rifted-arc environment. The Folly River Formation consists of back-arc mafic metavolcanic rocks and abundant ironstone. Both formations were metamorphosed to greenschist facies and intruded by a suite of $ca.$ 625-605 Ma calc-alkaline plutons and Devonian-Carboniferous within-plate bimodal plutons.

The oldest unit in the Jeffers block is the Mount Thom Complex, composed of $ca.$ 840 Ma paragneissic and orthogneissic rocks intruded by the $ca.$ 755-735 Ma calc-alkaline dioritic Mount Ephraim plutonic suite, and also by Ordovician within-plate syenitic and gabbroic rocks (Eight Mile Brook pluton). In faulted contact with the older units is the Late Neoproterozoic Dalhousie Mountain Formation which consists of volcanic and sedimentary rocks intruded by related dioritic to granitic plutons. Fossiliferous Silurian sedimentary rocks of the Wilson Brook Formation are in faulted contact with all of the older units. Devonian and Carboniferous sedimentary and volcanic rocks of the Byers Brook, Diamond Brook, and Nuttby formations and related within-plate Hart Lake-Byers Lake plutons are in faulted contact with



older units in both blocks and are host to REE and epithermal Au-style mineralization.

The Bass River and Mount Thom complexes and the *ca.* 755-735 Ma arc plutons have not been recognized in other parts of Avalonia. They may have originated on the margins of a rift basin formed during the breakup of Rodinia and subsequent subduction. By *ca.* 626-605 Ma subduction was widespread throughout Avalonia. The presence of Ordovician plutonic rocks and extensive Silurian sequences in both the Cobequid and Antigonish highlands, not typical of other areas of Avalonia, may have been because these areas were located in the outboard part of Avalonia during opening and closure of the Rheic Ocean. (*GS4; Thurs. Poster*)

The role of fault-related fluids and nano-precipitates in establishing architecturally suitable mineralization zones, Kiggavik region, Nunavut

White, J.C., University of New Brunswick, Fredericton, NB E3B 5A3

The Thelon basin, central Nunavut, is a major uranium district centred on the Kiggavik area deposits and several other significant prospects. Basement to the area comprises Neoproterozoic metagreywackes and extrusive volcanics (Woodburn Gp.) that are overlain by Paleoproterozoic strata characterized by a distinctive basal orthoquartzite (*e.g.* Ketyet River Gp.) and intruded by the 1.83 Ga Lone Gull granite. Thrusting, ductile deformation and transposition of Archean and Paleoproterozoic units has created a sub-horizontal regional fabric on which the current Thelon basin architecture is imposed. Crustal-scale dextral transcurrent faults (*e.g.* Thelon, Judge Sissons faults) that define the 'basin' were significantly active from 1.75-1.5 Ga. Periodic reactivation of faults continued throughout mineralization episodes.

Mesosopic structure of the major fault zones demonstrates extensive multiple fluid events, most commonly seen as quartz veining, or more notably, intense silicification and/or hematization of the host rock. U-mineralization occurs along brittle cross-structures associated with intense, sequential alteration. To date, two stages of uraninite have been recognized with alteration to coffinite. Each of the stages is associated with formation of distinctive illite at ~235°C and ~160°C, and have respective formation ages of 1192-838 Ma (least altered stage 1), 688-575 Ma (altered stage 1) and 113-10 Ma (stage 2). These thermometric and geochronology data determined by other workers supports the longevity of fault activity, and constrains the deformation environment of the faults.

Silicification and hematization of the large fault zones is concomitant with brecciation and microcataclasis of the host units with repeated cannibalization of fault clasts. In many cases, the end product is a micrometre or smaller grain size aggregate of quartz with nanometer-scale hematite distributed throughout the silica zones. The combination of deformation and precipitation textures opens the possibility for gel-like silica-rich fluids moving through dilatant zones. Given the absence of mineralization within the large movement zones, their role seems that of establishing zones of low permeability that restrict hydrothermal fluids associated with mineralizing alteration. Likewise, subhorizontal low permeability zones formed of quartzite layers and/or shallow silicified brecciation zones contribute to three-dimensional structuration of the basement to establish rock volumes in which fluids can be re-circulated over long time periods. (*GS4; Fri. 10:40*)

Structure and deformation history of the Appalachian thrust front in western Newfoundland

White, S.E. and Waldron, J.W.F., Department of Earth and Atmospheric Sciences, University of Alberta, Edmonton, AB T6G 2E3

The Humber Arm Allochthon is a significant component of the Humber Zone in the western Newfoundland Appalachians. It is a stack of structurally imbricated deep-water continental margin successions that have been assembled and emplaced over adjacent platform rocks during

the mid-Ordovician Taconian orogeny. Later Paleozoic deformation generated a zone of deep-seated, west-vergent thrusts which, unlike Taconian thrusts, extend into Grenvillian basement. On the Port au Port Peninsula, these faults are interpreted to have a protracted history, starting during Proterozoic rifting, continuing during Taconian flexure, and undergoing later reactivation and inversion during Acadian deformation. On the Port au Port Peninsula, fault scarp deposits constrain timing of Ordovician activity while later inversion is constrained by unconformable relationships.

Along the Northern Peninsula the Acadian thrust front has traditionally been viewed as a narrow, weakly emergent zone dominated by the Long Range thrust. The Long Range Inlier is interpreted to have been thrust over platform rocks and rocks of the Humber Arm Allochthon along this main fault. The absence of younger, flat-lying stratigraphic units in the region disallows direct age control on these faults, but an Acadian age is inferred.

A combination of surface mapping, aeromagnetic data, and 2D seismic reflection data demonstrates, however, that the deep-seated thrust faults on the Northern Peninsula are structurally analogous to faults on the Port au Port Peninsula and may share a similar protracted history. The Parsons Pond thrust structurally juxtaposes rocks of highly contrasting tectonic environments. Deep-water carbonates and siliciclastics of the Shallow Bay Formation and Lower Head Formation, respectively, are structurally overlain by correlative platform rocks and, at Portland Creek, by siliciclastics of the mid-Ordovician Goose Tickle Group. Limestone conglomerates within the Goose Tickle Group reside in the hanging wall of the Parsons Pond thrust and may represent fault-scarp deposits, formed during Taconian flexure.

These new observations may provide a genetic linkage between deep-seated thrust faults in the southern and northern parts of the Newfoundland Appalachians, suggesting an extensive basement-involved Acadian thrust front along the length of the Humber Zone in western Newfoundland. (*GS4; Fri. 10:20*)

The supergene geochemistry of antimony and bismuth (40 min)

Williams, P.A., School of Science and Health, University of Western Sydney, Locked Bag 1797, Penrith 2750 NSW, Australia

The recognition that secondary minerals act as buffers with respect to the dispersion of elements in the supergene zone is a key to understanding processes that have applications in areas ranging from pollution studies to geochemical exploration methods. The roles that secondary minerals play in this respect can be effectively modelled if their thermochemical properties are known and two examples are examined here. Conflicting views of the geochemical behaviour of antimony in the oxidised zone have recently been resolved by the discovery that the comparatively simple species tripuhyite, FeSbO₄, and schafarzskite, FeSb₂O₄, exert important controls on the solubility of Sb in near-surface environments. Tripuhyite is now recognised to be a particularly common mineral in the oxidised zones of Sb deposits and it is extraordinarily insoluble under ambient conditions. It may thus be concluded that the chemical dispersion of Sb is quite limited. Its congener, bismuth, has a secondary mineralogy dominated by Aurivillius-type phases, but certain other simple oxide species exert similar solubility controls. Two of these, koechlinite, Bi₂MoO₆, and russellite, Bi₂WO₆, are very common secondary minerals in the oxidised zones of many Bi deposits, notably in the granite-hosted ore bodies of eastern Australia. Both phases serve to effectively restrict the chemical dispersion of Bi in soils and waters in such settings. Coupled with studies of the wider secondary mineralogy of the elements, these observations have prompted a complete reassessment of the use of Sb and Bi as pathfinder elements in geochemical exploration, and point to methods to remediate Sb-contaminated anthropogenic wastes. (*SYI; Thurs. 8:20*)



Sources of diamond formation revealed by nano-inclusions in diamond

Wirth, R., GFZ Potsdam, 3.3, Telegrafenberg, Potsdam, Germany, wirth@gfz-potsdam.de, and Yang, J., Key Laboratory for Continental Dynamics, MLR, Institute of Geology, Academy of Geological Sciences, 26 Baiwanzhuang Road, Beijing, 100037, PRC, yangjingsui@yahoo.com.cn

Investigation of submicrometre-sized inclusions in diamond from different locations with focused ion beam (FIB) sample preparation and transmission electron microscopy (TEM) revealed new data on the origin of diamond. Preparation of electron transparent TEM foils applying FIB technique has no impact on the nature of nano-inclusions in diamond. Therefore, this technique allows identifying nanocrystalline phases in submicrometre-sized inclusions in diamond. In the last 10 years we studied nano-inclusions in diamond from kimberlites in Siberia, South Africa, Northern Canada as well as alluvial diamonds from Ukraine, Siberia, Brazil, metamorphic diamonds from Kazakhstan and diamonds in chromitites from ophiolites in Tibet and Ural Mountains (Russia). The results suggest three different types of diamond formation. Most of the kimberlitic diamonds showed a characteristic suite of nano-inclusions consisting of carbonates (Ca, Mg, Fe, Ba, Sr), silicates (phlogopite, high-silica mica), halides (NaCl, KCl), phosphate (F-apatite), Ti-phases (rutile, ilmenite), sulphides (Fe-Cu-Ni), quench phase Si, Ba, Sr, F) and fluid. These nano-inclusions have precipitated from trapped high-density fluids (HDF) enriched in Cl, K, P, Ba, Si, Sr + water. HDF is the medium diamond has grown from (1, 2). Olivine, pyroxene, garnet and sulfides are well known as micrometre-sized inclusions and are indicative for peridotitic or eclogitic mantle environment. Nano-inclusions in deep-seated diamond from Juina (Brazil) are completely different in phase composition. They are composed of Ca-carbonate, silicates (olivine that has been originally Ringwoodite, Ca-garnet, Wo-II), halides (NaCl, KCl), Mg-wüstite, ferro-periclase, Fe-carbide and Nyerereite a N-K-Ca-carbonate. Their common feature is a strong enrichment in Ca or Ca-carbonate phases. This suite suggests growth of diamond from carbonatitic melt (3,4,5). Diamonds from chromitites in ophiolites from the Ural Mountains (Russia) and from Tibet show totally different assemblages of nano-inclusions such as Ni-Mn-Co alloys associated with Mn-rich silicates such as olivine and garnet. It is suggested that these inclusions indicate formation of diamond in a similar way synthetic diamonds are produced. Carbon is dissolved in a metal alloy under high-pressure and -temperature. Under appropriate P-T conditions dissolved carbon exolves as diamond. (SS4; Fri. 8:20)

References

- (1) Klein BenDavid, O. *et al.*, (2006) *American Mineralogist*, **91**, 353 – 365.
- (2) Logvinova, A. *et al.*, (2008) *European Journal of Mineralogy*, **20**, 317 – 331.
- (3) Kaminsky, F. & Wirth, R. (2011) *Canadian Mineralogist*, **49**, 555 – 572.
- (4) Kaminsky, F. *et al.*, (2009) *Mineralogical Magazine*, **73**, 797 – 816.
- (5) Wirth, R. *et al.* (2009) *Earth and Planetary Science Letters*, **286**, 292 – 303.

Crystallization conditions of epidote in granitic pegmatites

Wise, M.A., Department of Mineral Sciences, Smithsonian Institution, PO Box 37012, Washington, DC, USA 20013-7012, wisem@si.edu

Epidote occurs sparingly in muscovite – rare-element and miarolitic classes of granitic pegmatites and has been recognized in three distinct parageneses: i) as euhedral crystals occurring in miarolitic cavities, ii) as euhedral crystals that formed in fractures and iii) as anhedral grains replacing microcline. Electron microprobe analyses show variable pistacite component [$Ps = 100 * (Fe^{3+} / (Fe^{3+} + Al))$] ranging from Ps13 to Ps32, with considerable overlap between paragenetic types. Backscattered electron imaging revealed oscillatory to patchy zoning patterns which are mainly caused by differences in Fe^{3+} , Al and REE

content. Some crystals have cores of REE-enriched epidote or allanite with total REE_2O_3 content that range from 13.2 to 25.7 wt%.

Textural, chemical and paragenetic data suggest limited P-T-X conditions for the crystallization of epidote in granitic pegmatites. The following conditions appear necessary for epidote crystallization in granitic pegmatites: (i) a high Ca content; (ii) a relatively low phosphorus and fluorine concentration such that apatite or fluorite is not stable; (iii) limited enrichment in REE and (iv) high f_{O_2} conditions. High pressure conditions do not appear to be necessary for the crystallization of epidote in granitic pegmatites, unlike pressures of greater than 5 kb which are generally required for epidote formation in granulites of intermediate compositions.

These chemical conditions are not conducive, in general, to epidote crystallization in pegmatites of the LCT (Li-Cs-Ta enriched) family, but are favorable for epidote growth in pegmatites with NYF (Nb-Y-F enriched) geochemical signatures. Epidote is only expected to occur in granitic pegmatites of the muscovite – rare-element class at estimated crystallization pressures in excess of 5 kbar and at temperatures between 450 and 600°C. Epidote in miarolitic pegmatites, on the other hand, may form at considerably lower temperatures (110–450°C) and pressures (<2 kbar). All things considered, epidote may be more common in NYF-family pegmatites than is currently recognized and therefore may serve as an “index” mineral for this type of granite-pegmatite suite. (SY2; Thurs. 3:20)

Did a proto-ocean basin form along the southeast Rae margin during the Paleoproterozoic? Evidence from U-Pb geochronology, Nd isotope data, geochemistry, and tectonostratigraphy

Wodicka, N., nwodicka@nrcan.gc.ca, Corrigan, D., Whalen, J.B., Sanborn-Barrie, M. and St-Onge, M.R., Geological Survey of Canada, 601 Booth, Ottawa, ON K1A 0E8

Paleoproterozoic cover sequences in the northeastern Rae craton are characterized by thick, deep-marine turbidite deposits and sulphide-enriched strata not observed in time-equivalent, intracratonic basin units further southwest. Various models proposed to explain some or all of these features include development of a proto-ocean basin along the southeast Rae margin. We present U-Pb geochronological, Nd isotope, geochemical, and tectonostratigraphic evidence from central Baffin Island and Melville Peninsula that support this model. The earliest rifting stages were manifested by *ca.* 2145 Ma dioritic and *ca.* 2018 Ma bimodal magmatism and post-*ca.* 2160 Ma deposition of craton-derived, shallow marine siliciclastic sediments (Dewar Lakes Fm, Piling Group). Marine transgression ensued, resulting in deposition of south-facing carbonate deposits (Flint Lake Fm), which, based on stratigraphic relationships, was broadly coeval with mafic-ultramafic magmatism farther outboard. We infer that this rifting stage was associated with lower Bravo Lake Fm tholeiitic to picritic volcanism and voluminous volcanoclastic sedimentation at *ca.* 1985–1970 Ma, based on compositional differences and detrital and inherited zircon ages. Nd isotopic and geochemical data, combined with U-Pb data from a late dyke, suggest that dominantly alkaline, upper Bravo Lake basaltic volcanism and sill emplacement occurred later, by *ca.* 1923 Ma, within highly extended crust. Bravo Lake rocks exhibit OIB-like signatures similar to basaltic rocks within young proto-oceanic rift troughs (*e.g.*, Red Sea), but lack depleted, MORB-type compositions characteristic of spreading axial troughs. Thus, our tentative interpretation is that by *ca.* 1923 Ma or shortly thereafter, the thinned Rae continental lithosphere fragmented into small continental block(s) and narrow zone(s) of incipient oceanic crust farther outboard of the Bravo Lake basin. This rifting stage may be responsible for rapid subsidence of the southeast Rae margin leading to deposition of euxinic (Astarte River Fm) and overlying post-*ca.* 1915 Ma turbidite deposits (Longstaff Bluff Fm). Mantle upwelling associated with incipient ocean formation may have triggered melting of highly thinned and fragmented crust resulting in emplacement of late-stage, *ca.* 1897 and 1883 Ma rapakivi granite and highly differentiated sills. Subsequent basin closure led to development of a north-verging fold-and-thrust belt after *ca.* 1880 Ma.



Consistent with this model is the identification of a potential rifted crustal fragment of Rae affinity on Cumberland Peninsula. Current comparison of the overall tectonostratigraphy and detrital zircon age signatures of the cover sequence (Hoare Bay Group) together with those documented for the Piling Group will provide critical tests of this hypothesis. (*SS2; Wed. 10:20*)

Thermal history of the Flinton Group, Mazinaw Domain, Grenville Province, Ontario

Wolczanski, H.E.¹, wolczanski@geoladm.geol.queensu.ca, Lee, J.K.W.¹ and Camacho, A.², ¹Department of Geological Sciences and Geological Engineering, Queen's University, Kingston, ON K7L 3N6; ²Geological Sciences, University of Manitoba, Winnipeg, MB R3T 2N2

The eastern section of the Flinton Group, from Cloyne to Lavant, is a long, narrow NE-SW trending belt of metasedimentary rocks belonging to the Mazinaw Domain of the Grenville Province. Rocks from various members of the Bishop's Corner, Meyer Cave and Fernleigh Formations within the Flinton Group contain abundant biotite and muscovite and very little evidence of alteration. Metamorphic grade increases southwest to northeast across the Flinton Group from greenschist to amphibolite facies, with metamorphic isograds perpendicular to the strike of bedding.

Detailed petrography, electron-microprobe analysis and ⁴⁰Ar/³⁹Ar dating were used to investigate the thermal history of the Flinton Group. In these rocks, biotite is observed to uniformly predate muscovite growth.

⁴⁰Ar/³⁹Ar ages were obtained on ten muscovite/biotite pairs and two muscovites from pelitic schists and a muscovite/biotite pair from a pegmatite. Biotite ages show a broad variation across the Flinton Group. Biotite ages in the western half of the study area range from 978 ± 9 Ma to 940 ± 8 Ma with an average pooled age of ~950 Ma, while the ages from the eastern half are much younger, from 908 ± 7 Ma to 888 ± 7 Ma with an average pooled age of ~902 Ma – reflecting a ~45 Ma age difference. Muscovite ages across the Flinton Group range from 936 ± 8 Ma to 893 ± 7 Ma (±2σ) with an average pooled age of ~902 Ma. All but the oldest muscovite age are uniform and close to the 902 Ma pooled age. The change between the two age groupings is abrupt, i.e. the age does not gradually decrease eastwards as would be expected if correlated with increasing metamorphic grade.

The marked change in biotite ages is spatially correlated with the Plevna Fault. The fact that muscovite ages are “uniform” and much younger indicates that significant vertical movement along Plevna fault can be constrained to have happened prior to muscovite growth at ~902 Ma. This result is surprising as movement along the Plevna fault has previously been dated at 599±16 Ma (Easton, 2006), and suggests that the fault was active much earlier. Biotites from the western half of the Flinton Group do not lie on the previously established cooling curve for the Mazinaw Domain (Busch, 1996) and suggest that the regional cooling history could be considerably more complex. (*GS3; Thurs. 2:00*)

Journey to the centre of Santoy: Structural study of the auriferous Santoy shear zone, northeastern Glennie domain, Saskatchewan

Wood, C.¹, Bethune, K.M.¹, McEwan, B.², Carlson, A.², McLintock, K.², Skanderbeg, B.², ¹Department of Geology, University of Regina, Regina, SK S4S 0A2; ²Claude Resources Inc., Saskatoon, SK S7K 5M5

The study area lies in the northeastern corner of the Glennie domain approximately 125 km north of LaRonge, SK. The Glennie Domain is characterized by variably deformed arcuate greenstone belts of volcanogenic and sedimentary rocks, intruded by granitoids. This region contains the Seabee gold mine, hosted within the 1.89 Ga Laonli Lake intrusive complex. Driven by the success of the Seabee mine, exploration in the past 15 years has identified several deposits that are situated east of the main mine. They include Santoy 7, 8 and the recently discovered ‘Santoy Gap’. Previous work indicates that these deposits have strong structural controls, but that these controls vary

significantly in detail and are extremely subtle and difficult to recognize. This talk presents the preliminary results of a structural study of the Santoy shear zone undertaken as a M.Sc. thesis and providing the first real test of the structural model put forth by for these deposits. Fieldwork this past summer indicates that the Santoy shear zone is characterized by a NNW-striking, E-dipping foliation with stretching, mineral and crenulation lineations, as well as minor fold axes, all sub-parallel and plunging 45 degrees to the N. This attitude corresponds closely to the regional L₃ lineation indicating that the shear zone formed during D₃. The shear zone, is situated along the contact between mafic volcanic rocks and a granodiorite pluton and gold mineralization is closely associated with abundant cm-scale foliation parallel quartz veins and calc-silicate altered wall rock. A diagnostic green alteration assemblage comprises quartz- diopside- K-feldspar-titanite- pyrrhotite- pyrite and chalcopyrite. The more competent calc-silicate alteration layers are boudinaged in two directions, both parallel and perpendicular to the stretching lineation, demonstrating a previously unrecognized co-axial component of strain. Preliminary observations suggest that sulphide minerals migrated into boudin necks during deformation of the calc-silicate alteration, which may have played a key role in localizing auriferous sulphides. Foliation-parallel ‘felsic’ dykes are also common within the shear zone and may be co-genetic with the adjacent granodiorite intrusion. Ongoing work will focus on further defining the geometry, kinematics, and controls on ore-hosting structures of the Santoy deposits, as well as determining the mechanisms and timing of gold mineralization with respect to the local and regional tectonic evolution of the Glennie domain. (*GS4; Fri. 8:20*)

New filtration methods for the aqueous separation of uranyl peroxoclusters from simulated used nuclear fuel

Wylie, E.M.¹, ewylie@nd.edu, Phillip, W.A.², and Burns, P.C.¹, ¹University of Notre Dame, 156 Fitzpatrick Hall, Notre Dame, IN, 46556 USA; ²University of Notre Dame, 182 Fitzpatrick Hall, Notre Dame, IN, 46556 USA

In an effort to develop new separation processes to isolate uranium from used nuclear fuel that are both proliferation resistant and environmentally friendly, we are utilizing the formation of uranyl peroxo cage clusters that result from the treatment of a uranium material with hydrogen peroxide and a templating agent when specific pH conditions are attained. Following a preliminary filtration to remove undissolved solids, these clusters can then be separated from other aqueous species using mass-based filtration. Previous experiments employed centrifugation of the peroxocluster solution through commercially available cellulose acetate membranes as the mass-based separation step. However, due to polarization of the membrane surface caused by the formation of a negatively charged cake-layer, the process proved inefficient at transporting several cations across the membrane. Here, we describe a new filtration method that utilizes a stirred-cell to reduce the effects of membrane surface polarization. In addition, several different membrane surface chemistries are explored to further enhance the efficiency of the separation process. (*SS5; Wed. Poster*)

The Neoproterozoic Mayville mafic-ultramafic intrusion in the Bird River greenstone belt, southeastern Manitoba: Geological setting, geochemical variation and the implications for Cu-Ni-PGE-Cr mineral exploration

Yang, X.-M.¹, eric.yang@gov.mb.ca, Gilbert, H.P.¹, Houli, M.G.², Bécu, V.², McNicoll, V.J.³ and Corkery, M.T.¹, ¹Manitoba Geological Survey, 360-1395 Ellice Avenue, Winnipeg, MB R3G 3P2; ²Geological Survey of Canada, 490 rue de la Couronne, Québec, QC G1K 9A9; ³Geological Survey of Canada, 601 Booth Street, Ottawa, ON K1A 0E8

The Mayville mafic-ultramafic intrusion located in the northern arm of the Bird River greenstone belt hosts significant Cu-Ni-PGE-Cr mineralization. It is an east-trending intrusion, approximately 10.5 km in length and up to 1.5 km in width, which is emplaced within various



supracrustal rocks including MORB-type basalt and related gabbro, epiclastic and minor volcanoclastic rocks. The Mayville intrusion consists of melagabbro and pyroxenite at the base, followed by a heterolithic breccia zone overlain by a suite of anorthositic gabbro, gabbroic anorthosite and anorthosite capped by strongly magnetic gabbro. This intrusion, which has undergone greenschist to amphibolite facies metamorphism, is similar to Archean anorthosite complexes elsewhere in the Superior Province.

Bedrock mapping and lithogeochemical data suggest that the Mayville intrusion may have been formed by the injection of successive batches of magma originating from a single magma chamber, in which assimilation and fractional crystallization (AFC) processes were probably the main controlling factors. The parental magma is interpreted to have been a high-alumina tholeiite, possibly derived from a subcontinental lithospheric mantle source characterized by a high degree of partial melting. The Mayville intrusion, together with the contiguous MORB-type basalt and related gabbro that are thought to be co-magmatic, may have been emplaced in an extensional environment (possibly back-arc setting), close to a continental margin characterized by a relatively thin crust.

An early sulphide saturation event triggered by AFC processes and/or introduced external sulphur is thought to have generated magmatic sulphide Ni-Cu-PGE mineralization at the base of the intrusion. Subsequent injections of mafic-ultramafic melts may have resulted in PGE and chromite mineralization at transitional zones between separate phases within the intrusion. An external sulphur source appears necessary in order to achieve sulphide saturation in the magma and the associated base-metal-sulphide (+ PGE) mineralization. Metasedimentary rocks in the supracrustal rock assemblage may represent such an external source of sulphur. Redox conditions during the evolution of the magma(s) may have varied from reduced to slightly oxidized, and thus facilitated the crystallization and accumulation of chromite, which is locally concentrated in chromitiferous bands or zones within the intrusion. Based on this study, the most likely sites for Cu-Ni-PGE-Cr mineralization in the Mayville intrusion appear to be 1) the basal contact along the footwall rocks, and 2) transitional zones between different intrusive phases. (SS9; Wed. 10:40)

Synvolcanic Au-Cu ± Ag-Zn-Pb massive sulphides, veins and disseminations of the Westwood deposit, Abitibi greenstone belt, Québec

Yergeau, D.¹, david.yergeau@ete.inrs.ca, Mercier-Langevin, P.², Dubé, B.², Malo, M.¹, Bernier, C.³, Savoie, A.³ and Simard, P.³, ¹INRS-ETE, 490 rue de la Couronne, Québec City, QC G1K 9A9; ²GSC-Québec, 490 rue de la Couronne, Québec City, QC G1K 9A9; ³Iamgold Corporation - Westwood Project, 1 chemin Arthur-Doyon, Preissac, QC J0Y 2E0

The Westwood deposit (3.715 Moz of gold) includes three distinctive mineralized corridors stacked from north to south: 1) Zone 2 Extension, 2) North Corridor and 3) Westwood Corridor. The Zone 2 Extension consists of cm- to dm-wide pyrite- and chalcopyrite-rich quartz veins and dissemination zones whereas the North Corridor consists of cm- to dm-wide quartz-pyrite-chalcopyrite ± sphalerite veins and disseminations as well as thin, semi-massive to massive sulphide veins. The envelopes of these two corridors are slightly discordant to the stratigraphy and main foliation. Finally, the Westwood Corridor consists of discontinuous stratabound polymetallic semi-massive to massive sulphide lenses, veins and disseminations.

The Westwood mineralized corridors are part of the Doyon-Bousquet-LaRonde mining camp and are hosted in metavolcanic rocks of the Bousquet Formation (2699-2696 My), which forms a steeply south-dipping, east-trending homoclinal sequence facing south. The study area is metamorphosed to greenschist-amphibolite facies transition and deformation is heterogeneous with high strain corridors localized typically at lithological contacts and within synvolcanic alteration zones.

The Warrenmac massive sulphide lens (Westwood Corridor) is characterized by pyrite-sphalerite-chalcopyrite ± galena-pyrrhotite and

is overlain by a highly transposed stringer zone, which are both anomalous in Sn, Hg, As and Sb. Sericite, quartz, biotite, chlorite and Mn-garnet define the metamorphosed proximal alteration assemblage whereas an aluminous alteration assemblage (staurolite, andalusite, kyanite) is preferentially developed at depth (> 1.5 km). Mapping of the Warrenmac discovery outcrop revealed that volcanoclastic felsic rocks hosting the massive sulphide lens are intruded by low-permeability mafic sills which acted as cap rocks for ascending hydrothermal fluids. Moreover, synvolcanic alterations discordant and strongly transposed into the main foliation combined with the presence of abundant sulphide fragments within felsic volcanoclastic breccias confirm the synvolcanic origin of mineralization.

Zone 2 Extension and Doyon mine mineralization (~1.5 km west of Westwood) are interpreted to be genetically related to the synvolcanic Mooshla pluton whereas Westwood and North corridors have a VMS-type origin and are located on the same stratigraphic horizon as LaRonde Penna mine 20 North lens to the east. U/Pb dating suggest that the three mineralized corridors might have been formed in less than 2 My. The Westwood deposit therefore represents a unique opportunity to test the hypothesis of a continuum between vein-type mineralization associated with a synvolcanic intrusion and auriferous massive sulphide lenses, and thereby contribute to a better understanding of Archean auriferous magmatic-hydrothermal systems. Metallogenic continuums are well documented in younger geological environments such as telescoped porphyry-epithermal systems. (SS7; Wed. 9:20)

The edge of a warm sea: Harmonious progression of facies and biotas at the Ordovician William Lake Lagerstätte, Manitoba

Young, G.A.¹, gyoung@manitobamuseum.ca, Rudkin, D.M.², Dobrzanski, E.P.¹, Cuggy, M.B.³, Robson, S.P.¹, Demski, M.W.⁴, Thompson, D.P.¹ and Stewart, L.A.⁴, ¹The Manitoba Museum, 190 Rupert Ave., Winnipeg, MB R3B 0N2; ²Royal Ontario Museum, Toronto, ON M5S 2C6; ³University of Saskatchewan, Saskatoon, SK S7N 5E2; ⁴University of Manitoba, Winnipeg, MB R3T 2N2

The William Lake Lagerstätte of central Manitoba preserves remarkable remains of soft-bodied and lightly sclerotized animals: eurypterids, xiphosurids (horseshoe crabs), pycnogonids (sea spiders), cnidarian medusae (jellyfish), and others. These lived along the margin of the tropical Williston Basin during the Late Ordovician (Katian), near the peak of the Great Ordovician Biodiversification Event. Detailed collecting for more than a decade, with bed-by-bed extraction each year since 2007, demonstrates an intimate tracking of organisms and facies during a regressive interval. Well over 1000 fossiliferous slabs have been collected and prepared, from just over 2.5 metres of strata. Samples document a transition from muddy, subtidal shallow marine facies, through various intertidal conditions, to restricted hypersaline intertidal to supratidal mud flat.

The lowest 40 cm of strata, assigned to the Gunton Member of the Stony Mountain Formation, consist of burrow-mottled and clotted dolomudstones. The sparse biota includes rhynchonelliformean brachiopods, bivalves, problematic phosphatic tubes, eurypterids, and the xiphosurid *Lunataspis aurora*, associated with abundant trace fossils: Chondrites and Arthropycus grading toward Thalassinoides.

In the lower 80 cm of the overlying Williams Member, dolomudstones show channels, ripples, trough cross-lamination, horizontal lamination, and dewatering structures. These indicate shallow subtidal to intertidal conditions. Fossils are generally rare but common in places. Lingulid brachiopods, gastropods, and arthropod sclerites are concentrated in particular horizons. Cnidarian medusae, articulated chelicerate arthropods, and large problematic tubes occur within homogeneous mud bodies or layers. In a few places, lingulids or cnidarian medusae are abundant in channel fills or in windrows beside ripple crests. Certain taxa, such as pycnogonids, occur in one or two horizons, while others such as eurypterids are found throughout this interval.



The overlying 50 cm interval consists of monotonous dolomudstones representing a less variable paleoenvironment. Strata are laminated or homogeneous, broadly rippled, and contain large salt crystal moulds. They apparently represent restricted intertidal or lagoonal conditions. Fossils are extremely rare, but some, such as xiphosurids and ctenophores (comb jellies), can be remarkably preserved.

The upper 90 cm of strata, still within the Williams Member, represent varying conditions in restricted intertidal to possibly supratidal environments. In parts, laminated dolomudstones, possibly deposited in lagoonal conditions, contain ostracodes, eurypterids, algal fronds, and tiny juveniles of *Lunataspis aurora*. Unfossiliferous microbial laminites are punctuated by vertical faulting and collapse breccias, and a depositional breccia is composed of subangular clasts of microbial laminite. Salt crystal moulds and lattices are common in this upper interval, indicating pervasive hypersalinity. (SY3; Thurs. 9:40)

Electromagnetic imaging of the Spiritwood Valley buried aquifer near Cartwright, Manitoba, Canada

Zaporozan, T., terryzap@gmail.com, and Ferguson, I.J.,
University of Manitoba, Winnipeg, MB R3T 2N2

In this study, ground time-domain electromagnetic (TEM) soundings are made to complement results from a helicopter EM (HEM) survey of the Spiritwood Valley, Manitoba, Canada. This feature is a diamicton-filled valley extending 500 km from Manitoba to South Dakota. In the study area, it is 10 km wide, its base is ~100 m below the surface, and it cuts into Cretaceous shale bedrock. The valley contains narrow (1-2 km wide) incised channels with gravel deposits that form an important aquifer. In 2010 the Geological Survey of Canada acquired an HEM survey over the valley and conducted seismic reflection imaging of the incised channels. The HEM data delineate the channels as resistive features within more conductive diamicton and shale bedrock but provide low resolution of their base. The ground TEM survey was completed to see whether higher resolution of the subsurface features could be obtained.

The ground TEM survey was conducted along a seismic line at the margin of the Spiritwood Valley. Measurements were made at seven sites, above the broader valley, two incised channels, and bedrock. GEONICS Protem 47 and 57 transmitters were used with an 80×80 m loop and Protem receiver to measure the response at five pulse frequencies. The responses show significant differences between the seven sites but their similarity at varying offset at individual sites indicates locally 1-D resistivity structures. 1-D inversion was used to determine best-fitting models and uncertainty in model parameters. The results delineate 2- to 30 m thick surficial sediments with resistivity 80-180 ohm.m. Within the Spiritwood Valley these sediments are underlain by conductive diamicton (8 to 11 ohm.m). The two incised channels contain more resistive (20 ohm.m) sediments. Both the top and base of the channels are resolved in the TEM models: the western channel extends from 29 to 140 m and the eastern channel from 40 to 152 m. The lower part of the channels is incised into conductive (3-4 ohm.m) shale bedrock. Assuming realistic values for the amount and resistivity of clay in the gravel, a groundwater salinity of 340-830 ppm is estimated. The results of the study demonstrate the ability of focused ground TEM surveys to contribute to large-scale aquifer studies. (SS14; Thurs. 2:40)

Sedimentary facies, depositional environment and sequence stratigraphy of the Upper Devonian-Lower Carboniferous Bakken Formation in the southeastern corner of Saskatchewan

Zhang, L., liz697@mail.usask.ca, and Buatois, L.A., Department of Geological Sciences, University of Saskatchewan, 114 Science Place, Saskatoon, SK S7N 5E2

The Upper Devonian-Lower Carboniferous Bakken Formation is one of the most important oil-producing units in Saskatchewan. In the southeastern corner of Saskatchewan, the Bakken Formation unconformably overlies either the Upper Devonian Big Valley Formation or the Torquay Formation, and is conformably overlain by

the Lower Carboniferous Souris Valley Formation. The research area includes Townships 1 through 17, Ranges 30 of the First Meridian to Ranges 1 of the Second Meridian, which is just west of the border between Saskatchewan and Manitoba. The lower black shale member is essentially absent in this area. The Bakken succession typically consists of the middle sandy to silty member and the upper black shale member. According to our detailed core analysis, the Bakken Formation is divided into eight facies: facies 1 (black shale); facies 2 (greyish green, highly bioturbated siltstone); facies 3 (interbedded dark grey, highly bioturbated siltstone and light grey, laminated sandy siltstone to silty very fine-grained sandstone); facies 4 (dark yellowish green pebble conglomerate); facies 5 (dark grey, very thinly interlaminated very fine-grained sandstone and muddy siltstone); facies 6 (light grey and beige, wavy-bedded very fine-grained sandstone); facies 7 (interlaminated light grey, very fine-grained sandstone and dark grey mudstone); and facies 8 (beige and light grey, very fine-grained sandstone with mudstone drapes and climbing ripples). Our integrated sedimentological, ichnological, and sequence-stratigraphic study suggests that the deposition of Bakken occurred in two different paleoenvironmental settings: open marine (facies 1 to 4) and brackish-water marginal marine (facies 5 to 8). The base of the marginal-marine interval is represented by a sequence boundary (coplanar surface or amalgamated sequence boundary and transgressive surface). This surface has been identified in previous studies west of our study area, therefore assisting in high-resolution correlation of Bakken strata. (SS13; Fri. Poster)

Conodonts from carbonate xenoliths in Chidliak kimberlites confirm the previous existence of Lower Paleozoic cover on Hall Peninsula, Nunavut and provide temperature estimates

Zhang, S., Canada-Nunavut Geoscience Office, PO Box 2319, Iqaluit, NU X0A 0H0, shzhang@NRCan.gc.ca, and Pell, J., Peregrine Diamonds Limited, 201-1250 Homer Street Vancouver, BC V6B 1C6

Hall Peninsula, located on southeastern Baffin Island, Nunavut, hosts 64 kimberlites discovered in the Chidliak and Qilaq project area, which collectively comprise the newly discovered Chidliak kimberlite province. At present, the Chidliak kimberlite area lacks Phanerozoic sedimentary cover, except for unconsolidated glacial deposits. However, the well-preserved Early Paleozoic microfossil conodonts in the carbonate xenoliths recovered from the kimberlites prove that this part of the Hall Peninsula was overlain by Lower Palaeozoic sedimentary rocks before and during the Late Jurassic and Early Cretaceous (*i.e.*, the time of kimberlite emplacement).

In total, 110 carbonate-xenolith samples were collected from 19 drillholes in the Chidliak kimberlites. Of the 110 samples, 76 were productive, with a total of over 1100 identifiable conodont specimens and numerous fragments being recovered.

The conodonts recovered from the sedimentary xenoliths within the kimberlites, such as *Appalachignathus delicatulus*, *Belodina* confluens, *Oulodus velicuspis* and many other species, are also known from the Upper Frobisher Bay, Amadjuak and lower Akpatok formations on the nearby southwestern Baffin Island. In turn, this suggests that these formations must also have been present in the Chidliak area prior to kimberlite emplacement but were erosionally removed from the study area sometime between the Early Cretaceous and the present. Other conodont species, such as the Late Ordovician *Rhipidognathus symmetricus* and Early Silurian *Ozarkodina elibata* and many others of the same age, have not been reported from southwestern Baffin Island, but occur in the Upper Ordovician Red Head Rapids Formation and Lower Silurian Severn River Formation in Hudson Bay and on Southampton Island. All these data allow estimating that a total of about 165–300 m of Upper Ordovician and Lower Silurian strata has been lost to erosion in the Chidliak area.

The conodont elements from the sedimentary xenoliths within the volcanoclastic and possible effusive kimberlites from the Chidliak kimberlite area have a wide Colour Alteration Index (CAI) range, from 1.5 to 8. The CAI data can be used to determine the temperatures to



which the sedimentary xenoliths were heated, which provides an independent estimate for the minimum temperature of emplacement of the various types of pipe infill found within the Chidliak kimberlites. The temperatures recorded within these xenoliths range from 50°C to more than 600°C. (*SY3; Thurs. 2:40*)

Pressure effect on diamond resorption morphology

Zhang, Z., zhang.zhihai@dal.ca, Fedortchouk, Y., Dalhousie University, 1459 Oxford Street, Halifax, NS B3H 4R2, and Hanley, J.J., Saint Mary's University, 923 Robie Street, Halifax, NS B3H 3C3

Mantle xenoliths and diamond inclusions show evidence of complex metasomatic processes during diamond growth and resorption in the subcratonic lithospheric mantle. However, our ability to define exact compositions and conditions of mantle fluids is still very limited. The footprints of mantle metasomatism in the morphology and surface features of resorbed diamonds capture the latest diamond-destructive event, and is perhaps less ambiguous than interpretation the chemical composition of mantle minerals such as garnet with combined signal from several events. Previous experiments investigated the effects of fluid composition, temperature, and oxygen fugacity on diamond resorption and provided constraints on fluid compositions during kimberlite ascent. To be able to examine mantle fluids through diamond resorption morphology, we conducted experiments in pressure range 1.0 – 3.0 GPa to investigate pressure effect on interaction of H₂O and CO₂ fluids with diamond, and applied our results to the natural diamond samples to probe fluid compositions in the mantle.

Experiments were conducted in piston-cylinder apparatus using natural octahedral diamonds and H₂O- MgO± SiO₂ and CO₂- CaO-SiO₂ synthetic systems at 1.0 - 3.0 GPa and 1150 - 1400 °C. The products were examined using Field-Emission Scanning Electron Microscopy and Atomic Force Microscopy. Fluid compositions were monitored by synthesizing fluid inclusions in olivines, and fluid inclusion isochores pass through the P-T conditions of the runs, confirming that inclusions were trapped at run conditions. In the H₂O-bearing system, pressure impacts on morphology are the presence of circular pits and rounding of diamond. Circular pits broadly forming at 1.0 GPa disappeared at 2.0 and 3.0 GPa. A cross at the bottom characterizes circular pits, and one stick is parallel to diamond edges and the other apparently points to the center of {111} face. At 1350 °C, increasing pressures result in faster transformation of diamonds from octahedron into rounded tetrahedron with smaller weight losses than those at 1.0 GPa and suppress diamond oxidation rates, decreasing approximately exponentially with increasing pressure.

Comparison of our experimental results with natural diamonds (total 603 stones) from Ekati kimberlites, Canada, shows that most of the mantle-derived resorption morphologies of diamond could not be products of dissolution in H₂O fluid. High degree of diamond rounding accompanied by high grade of Misery kimberlite might be a result of formation of aqueous fluid at greater depths rather than profound resorption. Presence of circular pits only on fragmented diamond faces indicates a late H₂O-rich fluid in kimberlites. (*SS4; Fri. 2:00*)

Lithology, alteration and structure of the Ogama-Rockland gold deposit in the southeast margin of the Ross River pluton, Rice Lake greenstone belt, Superior Province, Manitoba

Zhou, X., xzhou0718@gmail.com, Lin, S., University of Waterloo, 200 University Avenue West, Waterloo, ON N2L 3G1, and Anderson, S.D., Manitoba Geological Survey, 360-1395 Ellice Avenue, Winnipeg, MB R3G 3P2

The most productive lode gold district in Manitoba is situated in the Archean Rice Lake greenstone belt, in the western portion of the Uchi Subprovince of the Superior Province. In contrast to most other gold deposits in the Rice Lake belt, which are hosted by layered gabbro sills, basalt lavas or volcanoclastic rocks, auriferous quartz (-carbonate) veins of the Ogama-Rockland deposit are hosted by granitoid intrusive rocks of the Ross River pluton. In order to better understand structural setting and lithological control of the intrusion-hosted, shear-related, Ogama-

Rockland deposit, camp-scale (1:1000) bedrock geological mapping and selected outcrop-scale (1:50) mapping was carried out in the area around the deposit in the 2012 field season, aided by microscopic analysis of thin sections.

The Ogama-Rockland deposit is located in the southeast margin of the Ross River Pluton, which is constituted mostly of tonalite and granodiorite, with minor quartz diorite, monzogranite and alkali feldspar granite. Most of the contacts between these various intrusive phases are gradational. Numerous quartz-feldspar porphyry dikes, aplite dikes and a complex network of quartz veins crosscut the different phases of plutonic rocks. Laboratory observations show that carbonate, sericite, and chlorite alterations are relatively common within the host rocks adjacent to the quartz veins.

Gold-bearing quartz (-carbonate) veins in the Ogama-Rockland deposit have a close spatial relationship with west-northwest to northwest-striking, subvertical, dominantly dextral brittle-ductile to ductile shear zones. Minor north-trending, subvertical, sinistral brittle-ductile shear zones also contain quartz veins. The shear-zone rocks are mostly granitoid mylonite, mica-quartz schist or K-feldspar-porphyroblast-bearing chlorite schist. Based on the vein geometry and its relationship with shear zones, the auriferous veins are mainly classified into shear, extensional, and stockwork veins. These veins are mostly massive, but locally exhibit laminated or banded internal textures and asymmetric fabrics that indicate the same sense of shear as the hosting shear zones. They were most likely emplaced late during shearing. The ongoing detailed structural analysis of these veins will provide important new information to constrain exploration models, and will help draw attention to the potential for intrusion-hosted, shear-related, vein-type gold mineralization in the Rice Lake belt. (*SS3; Fri. 9:00*)

Geophysical modeling of pre-Carboniferous "basement" rocks in the Cabot Strait area: Implications for geological correlations and terrane accretion in the northern Appalachian orogen

Zsámboki, L.¹, Dehler, S.A.² and Barr, S.M.¹, sandra.barr@acadiau.ca, ¹Department of Earth and Environmental Science, Acadia University, Wolfville, NS B4P 2R6; ²Geological Survey of Canada (Atlantic), Dartmouth, NS B2Y 4A2

Magnetic and gravity data from northeastern Cape Breton Island, southwestern Newfoundland, and the intervening Cabot Strait area have been compiled and used to reassess pre-Carboniferous rocks underlying the Cabot Strait and their connections with rocks in adjacent onshore areas. Maps displaying magnetic (*e.g.*, filtered total field, first and second derivative, and downward continuation) and gravity (*e.g.*, Bouguer anomaly onshore, free-air anomaly offshore, and horizontal gradient) information were generated from the compiled data using UNIX-based GMT software. With further constraints from previously published seismic reflection interpretations, detailed maps of onshore geology, and measured and compiled magnetic susceptibility and density data from onshore units, five 2D subsurface models were generated with GM-SYS 4.2 2D modeling software. Based on geophysical signatures, anomalies in the offshore can be matched to onshore faults, rock units, and pre-Carboniferous blocks and terranes. The models confirm that the Cabot Fault separates Grenvillian basement to the northwest from peri-Gondwanan Aspy/Port-aux-Basques/Exploits (Ganderian) basement to the southeast. The Cape Ray Fault merges with the Cabot Fault so that Notre Dame subzone rocks do not extend far into the Cabot Strait area. Linear magnetic anomalies extending from the Port-aux-Basques subzone in southwestern Newfoundland to the Aspy terrane of Cape Breton Island are inferred to be related to magnetic mafic orthogneissic plutons in Aspy/Port-aux-Basques/Exploits (Ganderian) basement rock. Several elliptical magnetic halos in the Cabot Strait appear to be caused by Silurian-Devonian plutons like those in the Burgeo Batholith of southern Newfoundland. The Aspy-Bras d'Or terrane boundary is located north of the Ingonish magnetic anomaly. The latter anomaly, a prominent feature of the Cabot Strait, was resolved into five



components representing Late Neoproterozoic dioritic and granodioritic plutons of the Bras d'Or terrane and the Ingonish Island Rhyolite. The Bras d'Or terrane can be traced to the Grey River area in southern Newfoundland. The boundary with Avalonia is located south of the Bras d'Or terrane. (*GS4; Thurs. Poster*)

Structural and metamorphic evolution of the Key Anacon Zn-Pb-Cu-Ag deposit, Bathurst Mining Camp, Canada

Zulu, J.D-S., McFarlane, C.R.M. and Lentz, D.R., Department of Geology, University of New Brunswick, Fredericton, NB E3B 5A3, d4ln8@unb.ca

The textural and mineralogical evolution of the metamorphosed Key Anacon VMS has been determined by reconstructing the P-T-D evolution of the rocks. This work incorporates textural and mineralogical analyses of the sulfides and silicate assemblages, which have been used to infer portions of the D₁/M₁, D₂/M₂, and M₃ history of the Ordovician rocks. The upper-greenschist to amphibolite-facies rocks record ductile deformation microtextures preserved as aligned inclusions in garnet. Isoclinal to tight F₁ and F₂ microfolds relate to the ductile deformation stage during regional metamorphism. D₂ initiated crustal thickening, growth of garnet-bearing metapelitic assemblages, and then followed by exhumation. Garnet in the metapelites display compositional zoning, and records a series of growth and resorption stages, with an early formed core preserving S₁ fabric elements, and an lower-Ca overgrowth synchronous with S₂ development (M₂). Absolute timing of fabric development and garnet growth was established by dating monazite aligned in the internal (to garnet) foliation and the external D₂ schistosity.

P-T estimates using sphalerite-arsenopyrite geothermobarometer suggest an average pressure of 4.1 kbar and temperature of 400 °C (M₁). Metamorphic conditions for garnet-bearing metapelites estimated using THERMOCALC v.3.21 returned an average temperature of 536 ±11 °C at 2.5 kbar, whereas garnet-biotite pair calibrations yield temperatures of 530 °C. The P-T conditions of growth of the garnet core from forward modeling using THERIAK-DOMINO v01.08.09 (based on XRF-derived isochemical sections and compositional isopleths for the garnet cores), give temperature of 437 °C and pressure of 0.6 kbar. Successive P-T estimates from the first outer-core garnet annulus through to the rim were calculated to infer a P-T path followed by the rocks during their tectonic history. Peak metamorphic conditions of the garnet rim returned temperature estimate of 570 °C and pressure of 2.5 kbar and during this stage, pyrite recrystallization and plastic deformation predominated. The P-T path suggests prograde burial of the rocks during D₂ regional metamorphism with attainment of peak pressure (4.1 kbar) at a temperature of 524 °C, whereas peak temperature conditions occurred during the exhumation stage. The third metamorphic event (M₃) overprints earlier M₁ and M₂ assemblages and is due to the intrusion of the Devonian Pabineau Granite. This is characterized by annealing in pyrite and other silicate assemblages, suggesting that conditions during this episode were predominated by thermal metamorphism.

This work has integrated observations from both the sulfide and silicate assemblages to build a better understanding of the role of deformation and metamorphism in controlling the structural and mineralogical evolution of Key Anacon. (*SS10; Thurs. 9:20*)



Author Index

Index des auteurs

– A –

Abdu, Yassir SY1-P, SS18
 Abou-Aly, Salma SS16, SS16-P
 Abramov, Oleg GS3
 Adekanmbi, Olusola H. GS6
 Adelani, Pius O. SS5-P
 Adetunji, Ademola SS2
 Adibpour, Mojgan SS9-P
 Afanasiev, Valentin P. SS4
 Albrecht-Schmitt, Thomas E. SS5, SS5-P
 Alexandre, Paul SY1
 Alexandrov, Vitaly SS5-P
 Ali, Genevieve SS13-P, SS14, SS14-P
 Alimohammadi, Masoumeh SS23, SS23-P
 Alirezai, Saeed SS23, SS23-P
 Allard, Thierry SY1, SS5
 Amati, Lisa SY3
 Ames, Doreen E. SS9, SS9-P, GS2
 Amorim, H'elio S. SY2-P
 Andersen, Dale T. SS17
 Anderson, Alan J. SY2-P
 Anderson, J. SS16-P
 Anderson, Melissa O. SY2
 Anderson, Scott D. SS3
 Anderson-Trocme, Luke SS17
 Andre-Mayer, Anne-Sylvie GS2-P
 Andreozzi, Giovanni B. SY1-P
 Annesley, Irvine R. SS5
 Ansdell, Kevin M. SS5, SS6, SS6-P, SS21
 Applin, Daniel M. SS18-P
 Armitage, Al SS5
 Armstrong, Derek K. SS13, SS13-P
 Aseri, Abdullah SY2
 Ashton, Ken E. SS5, SS5-P, SS9
 Asselin, Esther SS13
 Asta, Mark SS5-P
 Atkinson, Nigel GS6-P

– B –

Backeberg, Nils R. GS4-P
 Badgerow, Charles J. SY1-P
 Bailes, Alan H. SS7, SS10
 Bajpai, R. K. GS1
 Baker, Don R. SY2, GS3
 Bakker, Ronald SS23
 Balan, Etienne SY1
 Balboni, Enrica SS5
 Baldwin, Geoffrey J. SS1-P
 Balint, Michael B. SY3
 Ballantine, Nancy G. SY2-P

Bamburak, James D. SS13, SS13-P
 Banerjee, Neil R. SS17, SS18
 Bank, Charly SS21, GS7-P
 Banks, Christopher SS13-P
 Barnes, Sarah-Jane SS8, SS9, SS23
 Barnett, Peter J. GS6-P
 Barnett, Robert L. SS9
 Barr, Erik SS17
 Barr, Sandra M. GS4-P
 Bates, Kerry SS13
 Battler, Melissa M. SS17
 Beakhouse, Gary P. SS3
 Beard, Charlie SS1
 Beaudoin, Georges SS5, SS7, SS9, SS12, SS23
 Beauregard, Michael A. SS1
 Beausoleil, Yvette Y. L. SS4
 Becker, Udo SS5
 Bécu, Valérie SS7, SS9, SS9-P
 Bédard, Jean H. SS1, SS2-P, SS3, SS8, SS17
 Bédard, Normand SS7
 Behnia, Pouran SS19, GS7
 Bekker, Andrey SS2, SS9, GS3-P
 Bell, Jeffrey J. SS14
 Bell III, James SS17, SS18
 Bellatreccia, Fabio SY1
 Bellefroid, Eric SY4
 Belley, Philippe M. SY1
 Bellucci, Jeremy SS5
 Benitez, Leila SS4, SS4-P
 Berard, Genevieve SS17
 Berman, Robert G. SS1, SS11
 Bernier, Claude SS7
 Bethune, Kathryn M. SS1, SS5, GS4
 Bezard, Rachel GS2
 Biczok, John SS3
 Bingham-Koslowski, Nikole SS13
 Bleeker, Wouter SS3, GS3
 Blichert-Toft, Janne GS3
 Bobrowsky, Peter T. SS21
 Bogdan, Terrance S. SS5
 Boggs, Katherine J.E. SS19
 Boiocchi, Massimo SY1
 Boivin, Alex SS17
 Bollmann, Trevor SS3
 Bonham, Oliver J.H. SS21
 Borhanzadeh, Fariba SS23
 Borisenko, Alexander S. SS2-P
 Bosi, Ferdinando SY1-P
 Bosman, Sean SS5
 Botcharnikov, Roman SY2

Author Index

Index des auteurs



Boulding, Richard GS5-P
 Boulerice, Alexandre R. SS5
 Bourke, Alexandre SS12
 Boutroy, Emilie SS23
 Bown, Todd SS16-P
 Boyce, Joseph M. SS16-P
 Boyce, W. Douglas SY3
 Braid, James A. SS11
 Brancourt, Juliette SS14-P
 Breker, John S. GS3-P
 Brenan, James M. SS9, SS9-P
 Brest, Jessica SS5
 Brett, Carlton E. SY3
 Broster, Bruce E. SS21
 Brown, Julie L. SS20
 Brown, Peter G. SS18
 Brunton, Frank R. SS13-P
 Bryden, Colin D. SS18
 Bryksin, Alexey SS2-P
 Brzozowski, Matthew GS1-P
 Buatois, Luis A. SY3, SS13-P, GS5-P
 Buchan, Kenneth L. SS11
 Buchanan, Chris SS1
 Buckwalter-Davis, Martha J. SS20
 Buhlmann, Eckart SS16
 Burns, Michael G.G. SY2
 Burns, Peter C. SY1, SS5, SS5-P
 Bynoe, Laurisha SY2

– C –

Cafagna, Fabio SS9-P
 Calas, Georges SY1, SS5
 Camacho, Alfredo SS4, GS3
 Cámara, Fernando SY1
 Campbell, D. Calvin SS16
 Campbell, Janet E. GS6
 Card, Colin SS5
 Carlson, Anders GS4
 Carlucci, Jesse R. SY3
 Caro, Guillaume GS3
 Caron, Jean-Bernard SY3
 Carr, Sharon D. GS3
 Carson, Christopher J. SY2
 Carson, Heather J. E. SS9
 Casey, William H. SY1-P, SS5
 Castonguay, Sebastien SY4, SS3
 Caté, Antoine V. SS7, SS7-P
 Cates, Nicole L. GS3
 Cayer, Alain GS6-P
 Cempirek, Jan SY2

Chabanole, Luc E. SS13-P
 Chacko, Thomas SS2, GS2
 Chafe, Alex SS6
 Chakhmouradian, Anton R. SY2-P, SS4, SS6, SS6
 Charbonneau, Rémi GS6-P
 Che, Xudong SY2
 Chen, Ning SS5
 Chew, Dave SY4
 Chi, Guoxiang SS5, SS5-P
 Chow, Nancy SS13
 Chu, Ka SY1-P
 Chudy, Thomas C. GS2
 Clark, Christine M. SY1-P
 Cleven, Nathan R. SS11
 Cloutis, Edward A. SS16-P, SS17, SS18, SS18-P
 Cocks, Robin M. SS11-P
 Colmont, Marie GS1-P
 Conceicao, Herbert GS3
 Conly, Andrew G. SS3-P
 Cooke, David SS23
 Cookenboo, Harrison O. SS4, SS4-P
 Copeland, Dave A. SS7-P
 Corkery, M. Timothy SS9, SS9-P, SS21
 Cormier, Laurent SY1, SS5
 Corrales, L. Rene SS5
 Corrigan, David SS2
 Corriveau, Louise SS23
 Côté, Jocelyn SS7
 Cotroneo, Sarina SS15
 Coulson, Ian M. SS6-P, GS2
 Cousens, Brian L. SS1, GS2
 Couture, Réjean SS21
 Cox, Grant M. SY4
 Craig, M. A. SS16-P
 Cramer, Christopher J. SS5
 Craven, Jim SS3-P
 Creaser, Robert SS1, SS23
 Creighton, Steven SS4, SS6
 Cremades, Ana SY2
 Crosta, Alvaro SS16
 Cuggy, Michael B. SY3
 Cutts, Jamie A. GS3
 Cymes, Brittany A. SY1-P

– D –

Dahn, Dustin SS11
 Dale, Janis E. SS14-P, GS5-P
 Dalsin, Mallory L. SS6
 Danesh, Donya GS6
 Danyushevsky, Leonid L. SS1



Author Index

Index des auteurs

Daoudene, Yannick SS2-P
Darbyshire, Fiona A. SS2-P, SS3
Dare, Sarah A.S. SS9, SS23
Davidson, Scott SS15, SS20
Davis, Donald W. SY2, SS11, GS3
Davis, William J. SS1, SS2, SS23
Day, Stephen SS12-P
De Moura, Odulio J.M. SY2-P
De Vito, Caterina SY1
Dean, Bethany SS4
Dehler, Sonya A. GS4-P
del Campo, Adolfo SY2
Delaye, Jean-Marc SS5
Della Ventura, Giancarlo SY1
Dell'Oro, Trent SS1
Delpech, Emilie SS2
Demski, Matthew W. SY3, SS13
Denham, Miles E. SS5
Deniset, Ian SS3-P
Deptuck, Mark E. SS16
Dera, Przemek SS18-P
Devine, Christine A. SS7, SS7-P
DeWolfe, Michelle Y. GS2
Dipple, Gregory M. SS15, GS3
Dittrich, Thomas SY2-P
Dobrzanski, Edward P. SY3, SS13
Donaldson, Colin H. SS8
Dongas, Jessica SS20
Dordevic, Mladen M. SS19
Dostal, Jaroslav GS2
Drljepan, Matea GS6
Droser, Mary L. SY3
Dubé, Benoît SS3, SS7, SS7-P, SS23
Duff, Jason SS3
Duff, Shamus SS7, SS7-P
Dufréchou, Grégory SS2-P
Duguet, Manuel SS3, GS4
Duke, M. John M. SS18
Duke, Norman A. SS9
Duley, Walter SS18
Dunlop, Matthew SS9
Dupuis, Nicole SS11
Durand, Cyril SS10
Duso, Greg GS6
Dutrow, Barbara A. SY1
Dzik, Ewa A. SS5
Dzubak, Allison SS5

– E –

Eary, Ted SS20

Easton, R. Michael SY4, GS3
Eggie, Lauren SS13
Eglington, Bruce E. SS2
Eglington, Bruce M. SS11
EIMF SS4
Einali, Morteza SS23
El Basbas, Aziz GS2-P
Elgr, Rastislav SS13-P
Elias, Robert J. SS13
Ellery, Alex SS17
Elliott, Rylan SS6-P
Elliott, William S. SY1-P
Ene, Vlad-Victor SS4
Engelbert, Margaret S. SS7
English, Carolyn B. SS14
Enkin, Randy SS23
Escayola, Monica SY4
Evans, Dave SS11
Evans, R. James SY1
Ewing, Rodney C. SS5, SS5-P

– F –

Fagan, Andrew J. SS10
Falck, Hendrick SY2, SS12-P, SS19
Färber, Gunnar GS1
Faure, Stéphane GS4
Fayek, Mostafa SY1, SS2, SS5, SS5-P
Fayol, Noémie SS23
Fedortchouk, Yana SS4, SS4-P
Fein, Jeremy B. SS5-P
Feng, Yonggang SS6, SS6-P
Fenton, Mark M. GS6-P
Fenwick, Lindsay SS20
Ferguson, Ian J. SS2, SS3-P, SS14
Ferris, Kaitlyn K. SS22
Fillmore, Julie A. GS2
Finch, Adrian A. SS8
Fischer, Reinhard X. SY1
Flemming, Roberta L. .. SS4, SS16, SS16-P, SS17, SS18, SS20
Fonseca, M.A. SY2
Ford, Ken L. SS5
Forslund, Nathan SS23
Fortin, Danielle SS15
Fortin, Marc-Antoine GS3
Foster, David A. SY1
Fournelle, John SS6
Fourny, Anaïs SS8-P
Franchuk, Anatoliy SS9
Francis, Don SS8
Francis, Raymond SS16, SS16-P

Author Index

Index des auteurs



Franklin, James T. SS3
 Frederiksen, Andrew W. SS2-P, SS3, SS3-P
 Frempong, Victoria E. SS20
 French, Jason E. SS17
 Fresia, Bastien SS12
 Frezzotti, Maria Luce SS4
 Friedman, Richard M. SS2, SS8
 Friske, Peter W.G. SS5
 From, Richard GS4-P
 Frost, B. Ronald SY2-P
 Fuchs, Sebastian SS5

– G –

Gadas, Radek SY2-P
 Gagliardi, Laura SS5
 Gagné, Olivier C. GS1
 Gagné, Simon SS7, SS7-P
 Gagnon, Joel E. GS1, GS1-P, GS2-P
 Gaidies, Fred GS2
 Galiová Vašíňová, Michaela SY2-P
 Galley, Alan G. SS7, SS10
 Galloway, Jennifer M. SS13
 Galois, Laurence SY1, SS5
 Gao, Cunhai GS6
 Gault, Andrew G. SS5, SS15, SS20
 Gebarski, Ben SS5
 Ghasemzadeh-Barvarz, Massoud SS12
 Ghent, Edward D. GS2-P
 Ghorbani, Mohammad Ali SS23-P
 Gibson, H. Daniel SS2
 Gibson, Harold L. Plenary, SS7, SS2, SS3, SS7, GS4
 Gilbert, H. Paul SS3, SS9, SS9-P
 Gilbert, Meagan M. SS13-P
 Gilbert, Sarah SS1
 Gill, Shannon B. SS7-P
 Giraldo, Katherine GS4
 Gladney, Evan SS11
 Gleeson, Sarah A. SS1, SS19
 Glendenning, Michael W.P. GS2-P
 Glombick, Paul SS13-P, SS16-P
 Goncalves, Philippe SS10
 Good, David SS9, SS9-P, GS1, GS1-P
 Gordey, Steve SS19
 Goutier, Jean SS2-P, SS3, SS7-P
 Greenberger, Rebecca SS17
 Greenfield, Anne-Marie R. GS2-P
 Greenough, John D. SS8-P
 Gregory, Daniel SS1
 Grew, Edward S. SY1, SY2
 Grice, Joel D. SY1

Groat, Lee A. SY1, SY2, SS6, SS10, SS23-P, GS1, GS2
 Grobe, Matt SS13-P
 Groulier, Pierre-Arthur GS2-P
 Groves, D.I. SS8
 Guha, Jayanta SS7
 Guilmette, Carl GS2
 Guimaraes, F. SS7-P
 Guitreau, Martin GS3
 Guo, Wang SS5-P
 Guo, Xiaofeng SS5-P
 Guoxiang, Chi SS5
 Gurzhiy, Vladislav V. SS5
 Gutzmer, Jens SY2-P
 Guzelaydin, Enis SY1-P

– H –

Haddad, Emile SS17
 Hagemann, Steffen SY2-P
 Hahn, Katherine E. SS1
 Haidl, Fran M. SS13-P
 Haixia, Chu SS5
 Hall, Douglas C. SY2
 Halpin, Kimberley SS6
 Halverson, Galen P. SY4
 Hamilton, Brett M. SS1
 Hanchar, John M. SS6
 Hanley, J. Jacob SY1-P, SS4
 Hannington, Mark SS7, SS7-P
 Hansen, Jeremy SS16, SS16-P
 Haring, Monika SY1
 Harper, Charlie T. SS6, SS6-P
 Harper, David A.T. SS11-P
 Harrington, James M. SS15, SS20
 Harris, Jeff R. SS1, SS19, GS7
 Harris, Jeff W. SS4
 Harris, Lyal B. SS2-P, SS3, SS17
 Harris, Rebecca SS17
 Harrison, Anna L. SS15, GS3
 Harrison, Tanya N. SS16-P
 Hastie, Evan C.G. GS2-P
 Hatcher, Joseph SS13
 Hathway, Ben SS13-P
 Hattori, Keiko H. SS3, SS5, SS12
 Havránek, Vladimír SY1-P
 Hawthorne, Frank C. SY1, SY1-P, SS18, GS1
 Hay, Duncan SS13-P
 Hayes, Ben SS1
 Hayward, Nathan SS23
 Heaman, Larry M. SS2
 Hébert, Réjean GS2



Author Index

Index des auteurs

Heggie, Geoff SS9
Heimann, Adriana SS10
Henry, Christopher D. GS2
Henry, Darrell J. SY1
Herd, Christopher D.K. SS18
Hertwig, Andreas SY1
Hetherington, Callum J. SY2-P
Hibbard, James SY4
Hicken, Anna K. GS6
Hicock, Stephen R. GS6-P
Hiebert, Russel S. SS9
Hiesinger, H. SS18
Higgins, John A. SY4
Hilchie, Luke SS4
Hindemith, Marisa SS10
Hlousek, Jan SS5-P
Hnatyshin, Daniel SS1
Hobbs, David T. SS5
Hodych, Joseph P. SS11
Hoffman, Paul F. Plenary, SY4
Holdsworth, David W. SS18
Hollings, Peter SS9, SS23
Holtz, François SY2
Hopkins, David G. GS3-P
Hopkins, Michelle D. GS3
Hou, Zengqian SS23-P
Houlé, Michel G. SS3, SS9, SS9-P
Howarth, Lani N. SS23
Hryciuk, Matthew SS1, SS8
Hu, Shuxian SS5
Hubeny, J. Bradford GS6
Hudak, George J. SS2, SS7
Hughes, John M. SY1
Hughes, Nigel C. SY3
Hunt, Emma J. SS8
Hunt, Lucy SS4
Husdal, Tomas SY2-P
Hynes, Andrew SS11

– I –

Ibrahim, Mahdia SS18
Ihlen, Peter M. SS12
Indares, Aphrodite SS10
Izawa, Matthew R.M. SS16-P, SS18, SS18-P

– J –

Jackson, Simon E. SS10
Jackson, Valerie A. SS2
Jackson-Brown, Sarah SS9
Jamieson, Heather E. SS5, SS6, SS15, SS20

Janousek, Vojtech SY2
Janser, Brian W. SS7
Járóka, Tom GS1-P
Jeanneret, Pauline SS10
Jébrak, Michel SS2, SS23, GS2-P, GS4
Jefferson, Charlie W. SS5, GS7
Jensen, Gavin K.S. SS13-P
Jiang, Dazhi SY2
Jin, Jisuo SY3, SS11-P, SS13
Jirsa, Mark A. SS2
Johan, Zdenek SY2-P
Johnson, Brent C. SS15, SS20
Johnson, Justin SS9
Johnson, Keith K. SS21
Johnson, Rene L. SS5
Johnston, Stephen T. SS2, SS11
Jollivet, Patrick SS5
Jones, Alan G. SS2, SS3-P
Jørgensen, Taus R.C. GS2
Jouffret, Laurent J. SS5, SS5-P
Jugo, Pedro J. SS9-P, GS2
Juhin, Amélie SY1

– K –

Kamber, Balz S. SS1, SS1-P, SS3
Kamenetsky, Vadim S. SS4
Ke, Xiaoxing SY2
Kelimu, Wahid SS14-P
Keller, Greg GS7
Kellett, Dawn A. SS1, GS3-P
Kenward, Paul A. GS3
Keppie, D. Fraser SS19
Kidston, Joseph SS13
Kimmig, Julien SY3
Kirkham, Garth D. SS21
Kissin, Stephen A. SS18, SS23
Kjarsgaard, Ingrid SS7, SS7-P
Knox, Bernadette SS9
Kodors, Charles GS6
Koeman, Elizabeth C. SS5
Koiter, Alexander J. SS14
Kontak, Daniel J. SY1-P, SY2, SS1, SS1-P, SS3, SS6, SS9, SS9-P, SS12, SS23, GS2
Kopylova, Maya G. SS4, SS6
Kotzer, Tom SS12
Kovrugin, Vadim SS5, GS1-P
Krapez, Bryan SS13
Krejsek, Stepan SY2
Kremer, Paul D. SY2
Kressall, Ryan D. SS4

Author Index

Index des auteurs



Kristiansen, Roy SY1
 Krivovichev, Sergey V. SY1, SS5, GS1-P
 Krueger, Andrea M. GS6
 Kuma, Jerry S. SS20
 Kunzmann, Marcus SY4
 Kynicky, Jindrich SY2
 Kyser, Kurt T. SY1, SY2, SS23

– L –

Laarman, Jordan E. SS9
 Lafond, Guy SS14-P
 Lafrance, Benoît SS7
 Lafrance, Bruno SS7, GS4
 Lafrance, Sacha GS2-P
 Laidlow, Allison M. SS5
 Lalonde, Erik SS7
 Lam, Judy SS7
 Lange, Karina SS20
 Langenberg, Willem SS20
 Lapenskie, Kathryn D. SY3
 Laramée, Myra L. SS22
 Large, Ross R. SS1
 LaRocque, Armand GS7
 Larson, Kyle GS4-P
 Lavoie, Denis SS13, SS13-P
 Layne, Graham D. SS7
 Layton-Matthews, Dan GS6
 Le Corre, L. SS18
 Le Heron, Danie SY4
 Lebedev, Vladimir I. SS2-P
 LeBlanc, William K.G. SS5
 Leblon, Brigitte GS7
 Lee, James K.W. GS3
 Lee, Sharon K.Y. GS7
 Legault, Marc SS7
 LeGault, T. SS5
 Legrow, Paul SS7
 Lens, Christoph SY1-P
 Lenton, Mitchell GS7
 Lentz, David R. SY2, SS10, GS7
 Lesage, Guillaume GS2
 Lesbros, Marion SS5
 Leshner, C. Michael SS3, SS8, SS9, GS2
 Lett, Ray E. GS6
 Léveillé, Richard J. SY1
 Leverett, Peter GS1
 Lewis, Adam R. GS3-P
 Li, Chusi SS9
 Li, Sheng SS14
 Li, Zenghua SS5

Liang, Rong SS5-P
 Lightfoot, Peter C. SS9
 Lima, Alexandre M.C. SY2-P, SS7-P
 Lin, Shoufa SY2, SS3, SS9-P, SS11
 Lindsay, Matthew B.J. SS15
 Ling, Victor SS16-P
 Linnen, Robert L. SY2, SS3, SS9, SS9-P, SS16, SS23-P, GS1, GS1-P
 Liu, Cenwei SS14-P
 Liu, Xiaoming SS5
 Liu, Yi SS5-P
 Llorens, Isabelle SS5
 Lobb, David A. SS13-P, SS14, SS14-P
 Lode, Stefanie SS7
 Lodge, Robert W.D. SS2, SS3
 London, David SY2
 Londry, Kathleen L. SS15, SS20
 Long, Darrel G.F. SS1
 Longstaffe, Fred J. SY1
 Lulin, Jean-Marc SS2
 Lussier, Aaron J. SY1-P, SS5

– M –

Ma, Chi SY1
 Maas, Roland SY2
 Macdonald, Francis A. SY4
 MacDonald, William D. SS16
 Macek, Ivo GS1-P
 MacHattie, Trevor G. GS4-P
 MacInnis, Linette M. SS9-P
 MacLachlan, Kate K. SS21
 MacNeil, Laura GS1
 MacTavish, Allan SS9
 Maginn, Edward SS5-P
 Magna, Tomas SY2
 Magnus, Seamus J. GS4
 Maier, Wolfgang D. SS3, SS8
 Makvandi, Sheida SS12
 Malo, Michel SS3, SS7
 Maloof, Adam C. SY4
 Maneta, Victoria SY2
 Mángano, M. Gabriela SY3, GS5-P
 Mann, P. SS18
 Manor, Matthew J. SS9
 Marcelli, Augusto SY1
 Maresch, Walter V. SY1
 Mariano, Anthony N. SS6
 Marion, Cassandra L. SS16, SS16-P
 Marquer, Didier SS10
 Marshall, Dan D. SS2



Author Index

Index des auteurs

Martel, Edith SS19
Martin, Robert F. SY1
Martin, Ryan SS3
Martinez, Nicholas SS5-P
Mate, David SS4
Mathieu, Jordan SS1-P
McAndrews, John H. GS6
McCarron, Travis GS2
McCarthy, Francine M.G. GS6
McCausland, Phil J.A. SS11-P, SS18
McClenaghan, M. Beth GS6, SS12, GS6
McClenaghan, Sean H. SS7
McCracken, Alexander D. SS13, SS13-P
McCutcheon, Jenine GS3
McDonald, Andrew M. SY1, SY2, SS12
McDowell, K GS2
McEwan, Brian GS4
McEwen, Alfred S. SS16-P
McFarlane, Christopher R.M. SY2, SS3, SS5, SS10
McGrail, Brendan T. SS5
McKay, Kirk GS6-P
McKechnie, Christine L. SS5
McKeough, Michelle SS10
McLean, Hayley SS4
McLeish, Duncan F. SS2
McLeod, Joe SS3-P
McLintock, Kyle GS4
McMartin, Isabelle SS23
McNicoll, Vicki J. SY4, SS3, SS7, SS7-P, SS9, SS9-P, SS23, GS3-P
McWhirter, Brittany R. SS13-P, SS14-P
Mealin, Caroline A. SS8, SS9-P
Medig, Kirsti P.R. SS2
Meghji, Imran SS9-P
Mendes, L. U.D.S. SY2-P
Mendoza, Fabio GS4
Mentré, Olivier GS1-P
Menzies, John GS6
Mercadier, Julien SS5
Mercier-Langevin, Patrick SS3, SS7, SS7-P
Méric, Julien SS9, SS23
Metsaranta, Riku T. SS3, SS9
Meurer, William P. SS8
Mihychuk, MaryAnn SS20, SS22
Milidragovic, Dejan SS8
Millar, Robert SS5
Miller, James D. SS8
Miller, Nathan R. SY4
Millonig, Leo J. SS23-P
Minarik, William SY4

Miro, Pere SS5
Mitchell, Roger H. SY1, SS6
Modreski, Peter J. SY2-P
Mogk, David W. SY1
Mojzsis, Stephen J. GS3
Monecke, Thomas SS7, SS7-P
Montreuil, Jean-François SS23
Moore, Bronwyn T. SS6
Moore, Lindsay C. SS3-P
Moore, Meghan A. SS6
Moorhead, James SS7
Morden, Robert SS1
Morin, Guillaume SS5
Morris, Evan SS14-P
Mortensen, Jim K. SS2
Morton, Ronald L. SS7
Mouhksil, Abdelali GS2-P
Muehlenbachs, Karlis SS4
Mueller, Paul A. SY1
Muir, Sarah L. SS18-P
Müller, Axel SY2, SS12
Mumin, A. Hamid SY2-P, SS23
Murphy, J. Brendan SS11
Murphy, Linda A. SS22
Murphy, Timothy GS1

– N –

Na, Chongzheng SS5
Nadeau, Leopold SS1
Nair, R GS2
Najem, Tarek SS15
Nathues, A. SS18
Navrotsky, Alexandra SY1-P, SS5, SS5-P, SS6
Nekvasil, Hanna SY1
Nelson, Anna-Gay D. SS5-P
Nguyen, Maurice K. GS6-P
Nguyen, Son T. SS20
Nichols, Katie SS4
Nicklin, Ian GS1-P
Nicolas, Michelle P.B. SS13, SS13-P
Nixon, Graham T. SS9
Normand, Charles SS5, SS5-P
Normandeau, Philippe X. SS23
Noronha, F. SY2-P
Novák, Milan SY1-P, SY2, SY2-P, GS1-P
Nowlan, Godfrey S. SS13

– O –

Oberti, Roberta SY1
O'Brien, Darren O. SS23-P

Author Index

Index des auteurs



O'Brien, Joshua J. SS10
 Oh, George N. SS5-P
 Ohlin, C. André SS5
 Ohnenstetter, Daniel GS2-P
 Ola, Oyekunle B. SS3-P
 Olinger, Danielle A. SS6-P
 Oliveira, A. SS7-P
 Ootes, Luke SS2, SS12-P, SS19
 Osinski, Gordon R. SS16, SS16-P, SS17, SS18
 Osovetskii, Boris M. SS4
 Oswald, William SS3
 Othmane, Guillaume SS5
 Ouellette, Robert Falcon SS22
 Owens, Phillip N. SS14, SS14-P

– P –

Pagé, Philippe SS9
 Palomba, E. SS18
 Pana, Dinu SS13-P
 Pandur, Krisztina SS6, SS6-P
 Papoutsas, Angeliki GS2
 Paradis, Suzanne SS10
 Park, Sulgiye SS5-P
 Parsons, Michael B. SS5, SS20
 Partin, Camille A. SS2
 Pathak, Vamdev GS2
 Patil, S.K. GS2
 Pattison, David R.M. SS1, SS10, GS2
 Paulen, Roger C. GS6
 Pavlova, Galina G. SS2-P
 Pawley, Steven M. GS6-P
 Pearson, D. Graham SS4, SS18
 Pearson, John G. SS6, SS6-P
 Peck, Dave C. SS9
 Pedersen, Per K. SS13-P
 Pehrsson, Sally J. SS1, SS2, SS11
 Pei, Junling GS6
 Pelkey, Robert SS13
 Pell, Jennifer SY3, SS4
 Pellegrini, Kristi L. , SS5, SS5-P
 Pe-Piper, Georgia GS2
 Percival, John A. SS1, SS3
 Peterson, Ronald C. SY1, SS17, GS1
 Petzold, Halya SS14-P
 Peugeot, Sylvain SS5
 Pezzotta, Federico SY2-P
 Phillip, William A. SS5-P
 Pickersgill, Annemarie E. SS16, SS16-P
 Pieczka, Adam SY1
 Pierce, Kelly SS12-P, SS19

Piercey, Glenn SS7
 Piercey, Stephen J. SS7, SS7-P
 Pierre, Samuel GS4
 Pietrus, Erik SS13
 Pilchin, Arkady SS7-P
 Pilchin, Marina SS7-P
 Pilgrim, Larry SS7
 Pilote, Jean-Luc SS7
 Pinti, Daniele L. SS12
 Piper, David GS2
 Pires, Fernando R.M. SY2, SY2-P
 Pittman, Nathan GS2
 Plasil, Jakub SS5, SS5-P
 Poirier, Andre SY4
 Poirier, Glenn SY1
 Polat, Ali GS2-P
 Pompilio, L. SS18
 Pothier, Hayley SS13
 Potter, Eric G. SS12, SS23
 Poulin, Rémy S. SS12
 Power, Ian M. SS15, GS3
 Power, Michael J. SS12
 Pratt, Brian R. SY3, SS13-P
 Prince, John SS13, GS3-P
 Prior, Glen SS13-P
 Prokopiev, Ilya R. SS2-P
 Pruden, Greg SS22
 Purdy, Colin J.K. SS6

– Q –

Qadi, Ala SS17
 Quesada, Cecilio SS11
 Quigley, Tom O. SS7
 Quirt, David H. SS5, SS10

– R –

Radica, Francesco SY1
 Rainbird, Robert H. SS2, SS13, SS19, GS3-P, GS7
 Raisuddin, Intesar GS7-P
 Ramaekers, Paul SS2
 Rani, Nishi GS1
 Rasmussen, Chistian M.Ø. SS11-P
 Rasmussen, Kirsten SS19
 Ratcliffe, Laura GS4
 Rayner, Nicole M. SS1, SS9-P
 Read, George H. SS4
 Reddy, V. SS18
 Reguir, Ekaterina P. SY2-P, SS4, SS6
 Reichelt, Raymond A.S. SS21
 Reid, Kyle D. SS5



Author Index

Index des auteurs

Renaut, Robin W. SS13-P
Renock, Devon SS5
Reusser, Dana SY1-P
Rhede, Dieter SY2-P
Richards, Jeremy P. SS23, SS23-P
Rios, Debora C. GS3
Ripley, Edward M. SS9
Robinson Settee, Helen SS22
Robson, Sean P. SY3
Rodrigues, B.C. SS7-P
Rodriguez, Miguel Ángel SY2
Rogers, Daen SS10
Rogers, Neil SY1-P, GS3-P
Roper, Adam J. GS1
Rosa, Maria de Lourdes S. GS3
Rose, Catherine V. SY4
Ross, Martin GS6
Ross, Pierre-Simon SS7, SS12
Rossman, George R. SY1
Rowe, Christen D. GS4-P
Rowe, Ralph SY1
Rowins, Stephen M. SS23
Roy, Gilles GS4
Roy, Heather GS6
Rubingh, Kate E. GS4
Rudisill, Tracy S. SS5
Rudkin, David M. SY3, SY3
Rudnick, Roberta L. SS5
Ruffet, Gilles SS2-P
Russell, Hazen SS1
Russell, J. Kelly SS4, GS2-P
Ryan, Anne Marie SS21

– S –

Sabouri, Mehdi SS23
Sack, Patrick J. SS1
Sader, Jamil GS6
Sadigh, Babak SS5-P
Saini-Eidukat, Bernhardt GS3-P
Samson, Iain SS6, SS6-P, SS9, SS9-P, GS1, GS1-P, GS2-P
Sanborn-Barrie, Mary SS1, SS2
Sánchez-Muñoz, Luis SY2, SY2-P
Sandmann, Dirk SS2-P
Santos, Edilton José dos SS6-P
Santos, Ivanara P.L. GS3
Sanz, Jesús SY2
Sapers, H. M. SS16-P
Sappin, Anne-Aurélie SS3
Savoie, Armand SS7
Schertl, Hans-Peter SY1

Schindler, Michael SY1
Schmidt, Mariek E. SS18
Schmitt, Douglas SS16-P
Schneider, Chris SS13-P
Schneider, David I. SS3, SS11
Schrag, Dan P. SY4
Schulz, Bernhard SY2-P
Schulze, Daniel J. SS4
Schumann, Dirk SS5, SS17
Scoates, James S. SS1, SS8, SS8-P, SS9
Scott Smith, Barbara H. SS4
Sealey, Heather N. SS20
Sears, S. Kelly SS17
Seifert, Thomas SY2-P, SS2-P, GS1-P
Sejkora, Jiri SS5-P
Sélo, Madeleine SS5
Sexton, Alan SS5
Shabaga, Brandi M. SS5-P
Shahabi-far, Maryam SS9 GS1
Shahkarami, Setareh GS5-P
Shales, Adam SS12
Shannon, Robert D. SY1
Sharpe, Ryan W. SS5
Sheehan, Peter M. SS11-P
Shelat, Yask GS7
Sheng, Li SS13-P
Sherriff, Barbara L. SS15, SS20
Shinkle, David A. SS9
Shipley, Scott T. SS19
Shirose, Yohei SY2-P
Shrivastava, J.P. GS1, GS2
Shvareva, Tatiana Y. SS5, SS5-P
Siab Ghodsi, A.Ali GS5-P
Sidhu, R. SS6
Silva, Liliane F. SY2, SY2-P
Simard, Patrice SS7
Simms, Darren H. SS7
Simonetti, Antonio SS5
Sinclair, Katherine SS22
Skanderbeg, Brian GS4
Škoda, Radek SY1-P, SY2-P, SS5-P
Skulski, Tom SY4, SS3
Skvortsova, Valeriya L. SS4-P
Slater, Greg SS17
Smith, Evan M. SS4, SS6
Smoke, Renata SS9
Snook, Ben SY2
Snyder, David SS2-P
Sobrados, Isabel SY2
Sokolova, Elena SY1

Author Index

Index des auteurs



Solferino, Giulio F. D. SS18-P
 Solgadi, Fabien GS2-P
 Solomon, Jonathan M. SS5-P
 Somarin, Ali K. SS12, SS23
 Sorba, Chad SS12
 Sosseinejad, Somayeh SS13-P
 Southam, Gordon SS15, GS3
 Souza Neto, João Aauto SS6-P
 Spencer, E.A. SS6
 Spezia, Riccardo SS5
 Spry, Paul G. SS10
 Šrein, Vladimír SY2-P
 Stachel, Thomas SS4
 Stanley, Cliff SS21
 Steffen, Ashley L. GS3-P
 Stern, Richard A. SS1, SS2, SS4
 Stevenson, Ross SY4, SS2
 Stewart, Lori A. SY3, SS13
 Stewart, R. Craig GS2
 St-Onge, Denis SY4
 St-Onge, Marc R. SS2
 Stott, Greg M. SS2, SS3
 Strauss, Justin V. SY4
 Stromberg, Jessica M. SS17
 Su, Grant SS20
 Sunley, Sean SS14-P
 Swart, Peter K. SY4
 Swetlow, Jerry SS14-P
 Swisher, Robert E. SY3
 Sylvester, Paul J. SY4, SS2, SS18
 Syme, Eric C. SS2
 Szymanowski, Jennifer E. S. SS5-P

– T –

Tait, Kimberly T. SY1-P, SS17, SS18, SS18-P, GS1-P
 Tananaev, Ivan G. SS5
 Tant, Connor SS14-P
 Taranovic, Valentina SS9-P
 Tavakoli, Amir H. SS5-P
 Taylor, Bruce SS10
 Teale, Graham S. SS10
 Teller, James T. Public Lecture
 Théou-Hubert, Lucie SY4
 Therrien, Steven J. SS3-P
 Theyer, Peter SS9-P
 Thibault, Yves SY2
 Thompson, Deborah P. SY3
 Thomson, Danielle M. SS13, GS3-P
 Thorkelson, Derek J. SS2

Thurston, Phillips C. SS3
 Tiessen, Kevin H.D. SS14
 Timmermans, Ann C. GS2
 Timofeev, Alexander SS6
 Tinkham, Douglas K. SS7, SS10, GS2
 Tiwari, Surya SS5-P
 Tokaryk, Tim GS5-P
 Tomes, Heidi GS1-P
 Tomkins, Andrew G. SS10
 Toni, David C. SS3-P, SS14
 Tornabene, Livio L. SS16, SS16-P
 Törö, Balázs SS13-P
 Totenhagen, Cabin F. SS7
 Trail, Dustin GS3
 Trap, Pierre SS10
 Tremblay, Alain SS2-P
 Tretiakova, Irina G. SS2-P
 Trommelen, Michelle S. GS6
 Tschirhart, Victoria GS7
 Tsujita, Cameron SS13
 Turchiaro, Francesco SS9-P
 Turner, Elizabeth C. SS1, SS1-P, SS2, SS19
 Turner, Katlyn M. SS5-P
 Turton, Charles L. GS6
 Tweedale, Fergus SY1-P

– U –

Uehara, Seiichiro SY2-P
 Umoh, Joseph SS18
 Ushakov, Sergey V. SS5, SS6
 Utting, Dan J. GS6-P
 Uvarova, Yulia SY1

– V –

Vaillancourt, Christine SS3
 Vali, Hojatollah SS5, SS17
 Van der Flier-Keller, Eileen E. SS21
 Van der Lee, Suzan SS2-P, SS3
 van Drongelen, Katrina D. SS18, SS18-P
 van Nostrand, Tim S. SS2
 van Staal, Cees SY4, GS3-P
 Van Tendeloo, Gustaaf SY2
 VanDine, Doug SS21
 Varela, Maria Eugenia SS18
 Veksler, Ilya V. SS4
 Venturi, Chantal SS8-P
 Verwimp, J. GS2
 Vlaisavljeivch, Bess SS5
 Volik, Olena GS6
 Vyravský, Jakub SY2-P



Author Index

Index des auteurs

– W –

Wach, Grant D. SS13
 Waldron, John W.F. SS11, GS4
 Walker, Sarah M. SS5
 Wall, Corey J. SS8
 Wall, Frances SY2
 Wallace, Christine SS5
 Wang, Chenshan GS2
 Wang, Rui W-R. SS23-P
 Wang, Xisheng GS6
 Wanvik, Jan Egil SS12
 Wartman, Jacob SS7
 Waters, Joan E. GS6-P
 Watson, David SS12-P
 Watson, Neil SS13
 Webster, Ewan R. GS2
 Weis, Dominique SS1, SS8-P
 Weisener, Christopher G. SS15
 Weiss, Jill SS13-P
 Weiss, Trevor L.C. SS4
 Welch, Mark D. SY1
 Weston, Ryan L. SS9
 Westrop, Stephen R. SY3
 Whalen, Joseph B. SS2, SS11
 Wheadon, Benjamin J. SS13
 Whelan, Shaunaugh C. SS1
 White, Chris E. GS4-P
 White, Joseph C. GS4
 White, Shawna E. GS4
 Whyte, Lyle SS17
 Williams, Peter A. SY1, GS1
 Williams-Jones, Anthony E. SS5
 Williamson, Ben SY2
 Williamson, Nicole SS1
 Wilson, Mark A. SY3
 Wilson, Siobhan A. SS15, GS3
 Wing, Boswell A. SS1, SS8, SS9
 Wirth, Richard SY2-P, SS4
 Wise, Michael A. SY2
 Witzke, Thomas GS1
 Wodicka, Natasha SS1, SS2
 Wolczanski, Heather E. GS3
 Wolfe, Robin GS7-P
 Wolfe, Rohan SS23
 Wood, Bradley D. GS6
 Wood, Chase GS4
 Wooden, Joseph L. SY1
 Woulfe, Justine SY2
 Wylie, Ernest M. SS5-P

– X –

Xiao, Wenjiao SS11
 Xie, Wei SS16-P

– Y –

Yanful, Ernest K. SS20
 Yang, Chao SS13-P
 Yang, Jingsui SS4
 Yang, Panseok SY2-P, SS4, SS6
 Yang, Xue-Ming SS9, SS9-P
 Yang, Zhiming SS23-P
 Yergeau, David SS7
 Young, Graham A. SY3, SS13
 Young, Michael D. SS1
 Yuan, Ke SS5

– Z –

Zagorevski, Alexandre SY4
 Zagorsky, Victor SY2-P
 Zamora, Felix GS3-P
 Zaporozan, Taras SS2-P, SS14
 Zema, Michele SY1
 Zhang, Fuxiang SS5-P
 Zhang, Jian SS3
 Zhang, Liya SS13-P
 Zhang, Shunxin SY3
 Zhang, Xi-guang SY3
 Zhang, Zhihai SS4, SS4-P
 Zhanjiu, Wen SS5-P
 Zhehong, Gan SY2
 Zhou, Xiaohui SS3
 Zsámboki, Louis GS4-P
 Zulu, Joseph D.S. SS10



Thank you to our Sponsors / Merci aux commanditaires

PLATINUM / PLATINE (\$15,000+)



GOLD / OR (\$10,000+)



SILVER / ARGENT (\$5,000+)



Natural Resources
Canada

Ressources naturelles
Canada



UNIVERSITY
OF MANITOBA

Clayton H. Riddell Faculty of
Environment, Earth, and Resources

BRONZE (\$2,000+)



IRON / FER (\$1,000+)



Manitoba Prospectors and
Developers Association



SUPPORTER / PARTISAN (<\$1,000)



Thank You to Supporters of the Winnipeg 2013 Organizing Committee
Merci aux bienfaiteurs du comité organisateur



Fredericton 2014

GAC[®]-MAC

Illuminating the past for 175 years



Fredericton2014.ca

AGC[®]-AMC

Éclairant le passé depuis 175 ans

Join us in Fredericton for the Annual Meeting of the Geological Association of Canada and Mineralogical Association of Canada. A diverse and enticing scientific program is being developed that will include a MAC-sponsored short course on cathodoluminescence and GAC-sponsored workshops on remote sensing and structural geology of ore deposits. Field trips will allow participants to experience first-hand the breathtaking scenery of the east coast while exploring the geological complexity of the Appalachian Orogen. Come celebrate 175 years of geoscience discovery and experience Maritime hospitality at its finest!

Joignez-vous aux collègues à Fredericton à l'occasion de l'Assemblée annuelle de l'Association géologique du Canada (AGC) et de l'Association minéralogique du Canada (AMC). Le programme d'activités scientifiques varié et alléchant en cours de développement comprendra un cours intensif sur la cathodoluminescence parrainé par l'AMC ainsi que des ateliers sur la télédétection et la géologie structurale des gisements minéraux parrainés par l'AGC. Des excursions de terrain permettront aux participants de goûter le paysage à couper le souffle de la côte Est, tout en explorant la complexité géologique de l'orogène des Appalaches. Venez commémorer 175 ans de découvertes géoscientifiques au Nouveau-Brunswick et profiter de l'hospitalité des Maritimes!

May 21-23, 2014

University of New Brunswick



Du 21 au 23 mai, 2014

Université du Nouveau-Brunswick

